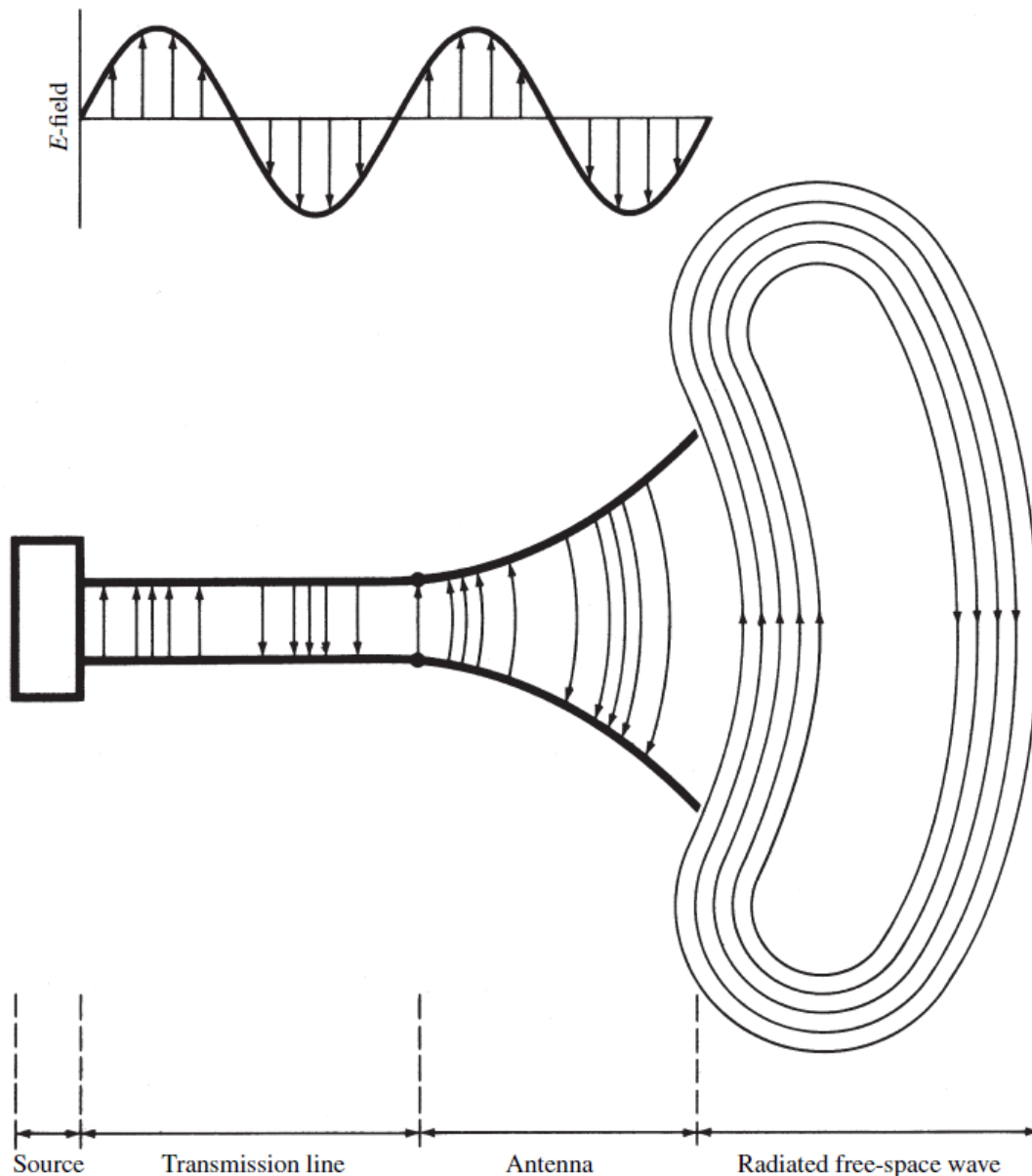


## ANTENNA FUNDAMENTALS

An antenna is defined as a metallic device (as a rod or wire) for radiating or receiving radio waves, or an aerial as a means for radiating or receiving radio waves. In other words, the antenna is the transitional structure between free-space and a guiding device, as shown in Figure 1.1. The guiding device or transmission line may take the form of a coaxial line or a hollow pipe (waveguide), and it is used to transport electromagnetic energy from the transmitting source to the antenna, or from the antenna to the receiver.



**Figure 1.1** Antenna as a transition device.

A transmission-line Thevenin equivalent of the antenna system of Figure 1.1 in the transmitting mode is shown in Figure 1.2 where the source is represented by an ideal generator, the transmission line is represented by a line with characteristic impedance  $Z_c$ , and the antenna is represented by a load  $Z_A$  [ $Z_A = (R_L + R_r) + jX_A$ ] connected to the transmission line.

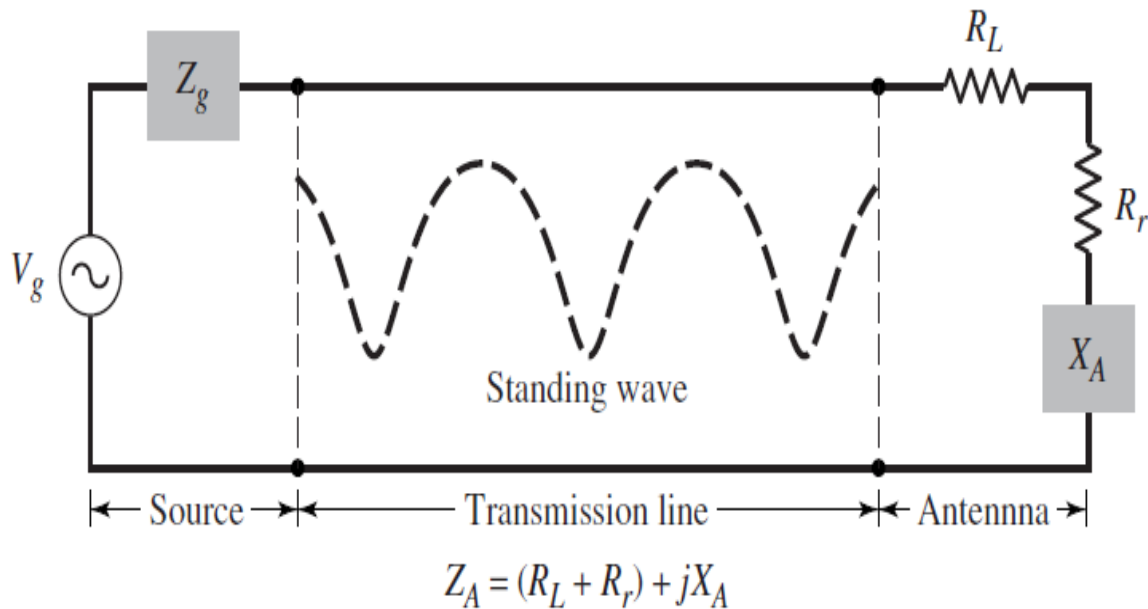


**Figure 1.2** Transmission-line Thevenin equivalent of antenna in transmitting mode.

The load resistance  $R_L$  is used to represent the conduction and dielectric losses associated with the antenna structure while  $R_r$ , referred to as the radiation resistance, is used to represent radiation by the antenna. The reactance  $X_A$  is used to represent the imaginary part of the impedance associated with radiation by the antenna.

## 1.2 TYPES OF ANTENNAS

### 1.2.1 Wire Antennas

Wire antennas are seen virtually everywhere—on automobiles, buildings, ships, aircraft, spacecraft, and so on. There are various shapes of wire antennas such as a straight wire (dipole), loop, and helix which are shown in Figure 1.3. Loop antennas need not only be circular. The circular loop is the most common because of its simplicity in construction.

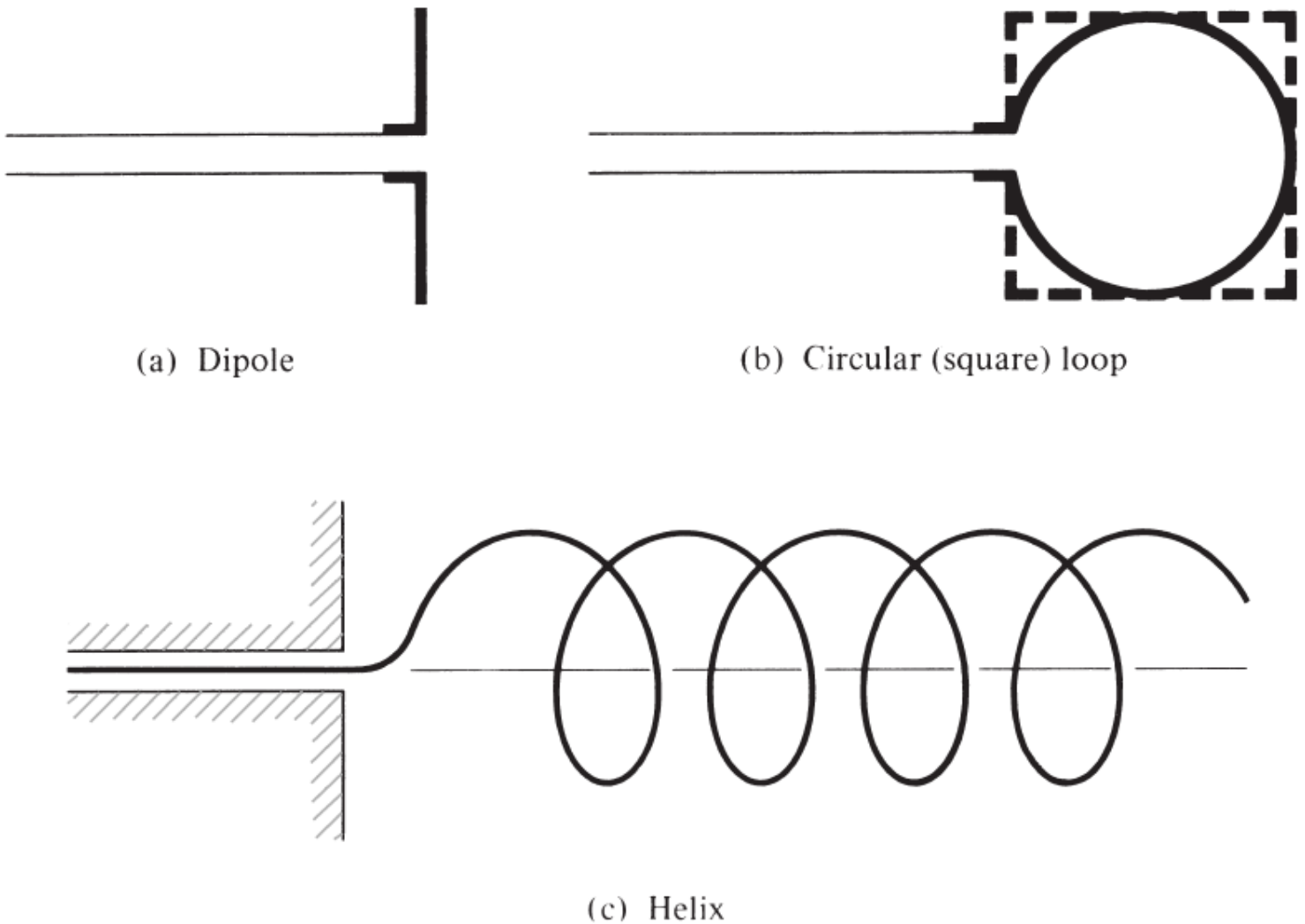
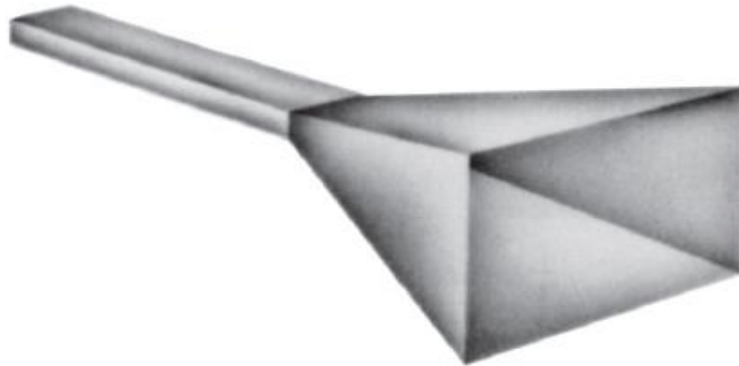


**Figure 1.3** Wire antenna configurations.

### 1.2.2 Aperture Antennas

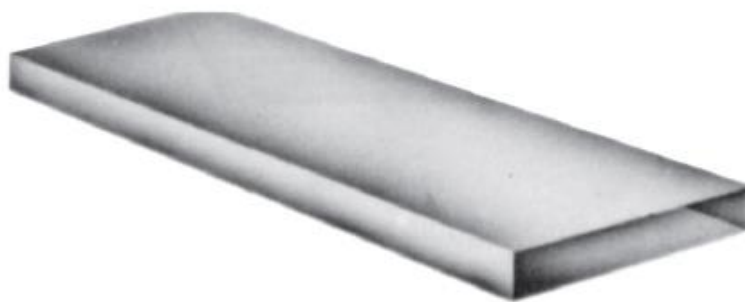
Some forms of aperture antennas are shown in Figure 1.4. Antennas of this type are very useful for aircraft and spacecraft applications, because they can be very conveniently flush-mounted on the skin of the aircraft or spacecraft. In addition, they can be covered with a dielectric material to protect them from hazardous conditions of the environment.



(a) Pyramidal horn



(b) Conical horn

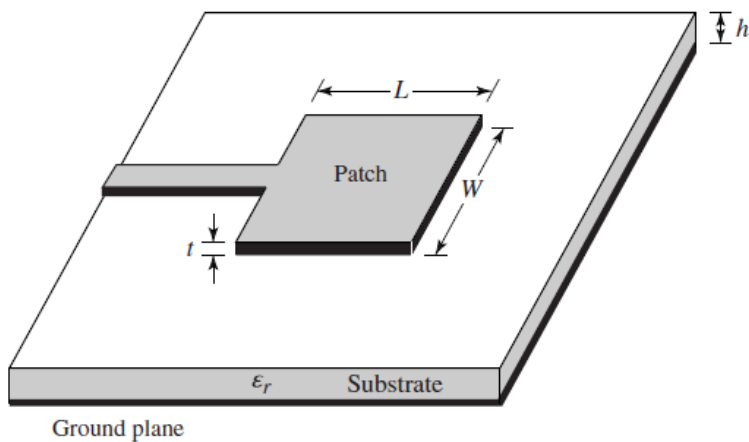


(c) Rectangular waveguide

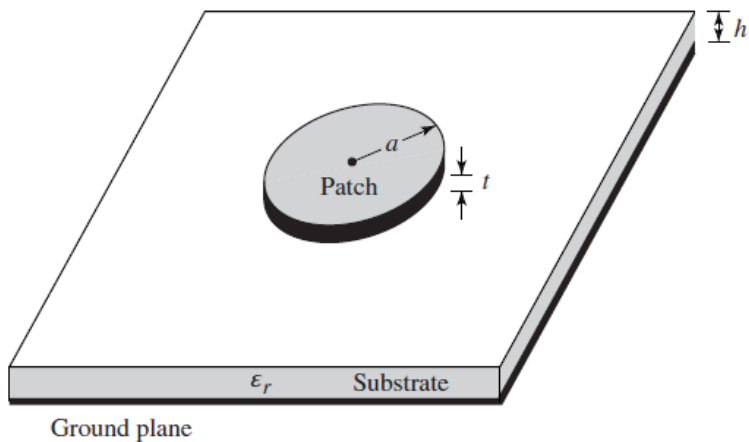
**Figure 1.4** Aperture antenna configurations.

### 1.2.3 Microstrip Antennas

Microstrip antennas became very popular in the 1970s primarily for spaceborne applications. These antennas consist of a metallic patch on a grounded substrate. The metallic patch can take many different configurations. However, the rectangular and circular patches, shown in Figure 1.5, are the most popular because of ease of analysis and fabrication, and their attractive radiation characteristics, especially low cross-polarization radiation. The microstrip antennas are low profile, conformable to planar and nonplanar surfaces, simple and inexpensive to fabricate using modern printed-circuit technology, mechanically robust when mounted on rigid surfaces, and very versatile in terms of resonant frequency, polarization, pattern, and impedance. These antennas can be mounted on the surface of high-performance aircraft, spacecraft, satellites, missiles, cars, and even mobile devices.



(a) Rectangular

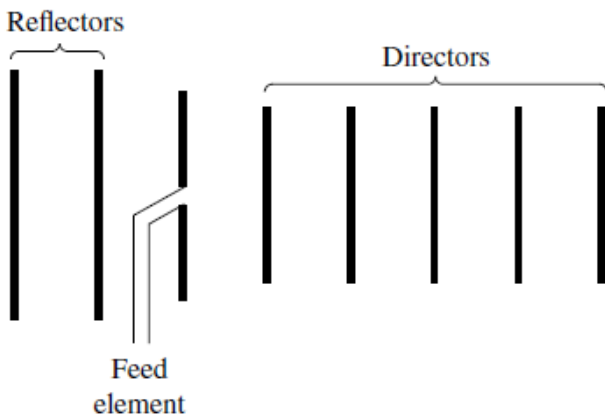


(b) Circular

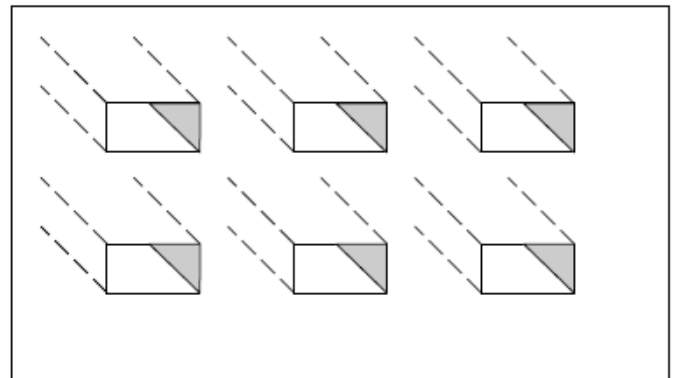
**Figure 1.5** Rectangular and circular microstrip (patch) antennas.

### 1.2.4 Array Antennas

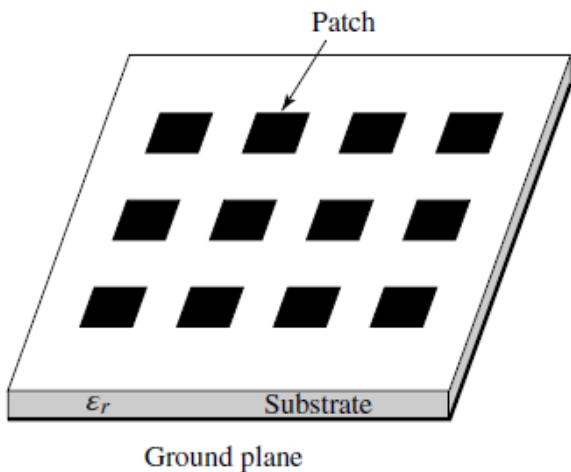
Many applications require radiation characteristics that may not be achievable by a single element. However, a group of radiating elements in an electrical and geometrical arrangement (an array) will result in the desired radiation characteristics. The arrangement of the array may be such that the radiation from the elements adds up to give a radiation maximum in a particular direction or directions, minimum in others, or otherwise as desired. Typical examples of arrays are shown in Figure 1.6. Usually the term array is reserved for an arrangement in which the individual radiators are separate as shown in Figures 1.6(a–c). However, the same term is also used to describe an assembly of radiators mounted on a continuous structure, shown in Figure 1.6(d).



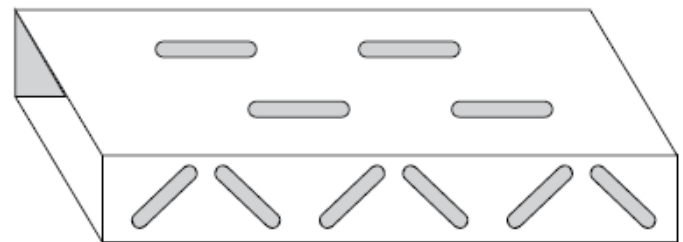
(a) Yagi-Uda array



(b) Aperture array



(c) Microstrip patch array



(d) Slotted-waveguide array

**Figure 1.6** Typical wire, aperture, and microstrip array configurations.

### 1.2.5 Reflector Antennas

The exploration of outer space has resulted in the need to communicate over great distances. These antennas were used in order to transmit and receive signals that had to travel millions of kilometers. A parabolic reflector shown in Figures 1.7(a) and (b). Antennas of this type have been built with diameters of 305 m or even larger. Such large dimensions are needed to achieve the high gain required to transmit or receive signals over very large distances. Another form of a reflector, although not as common as the parabolic, is the corner reflector, shown in Figure 1.7(c).

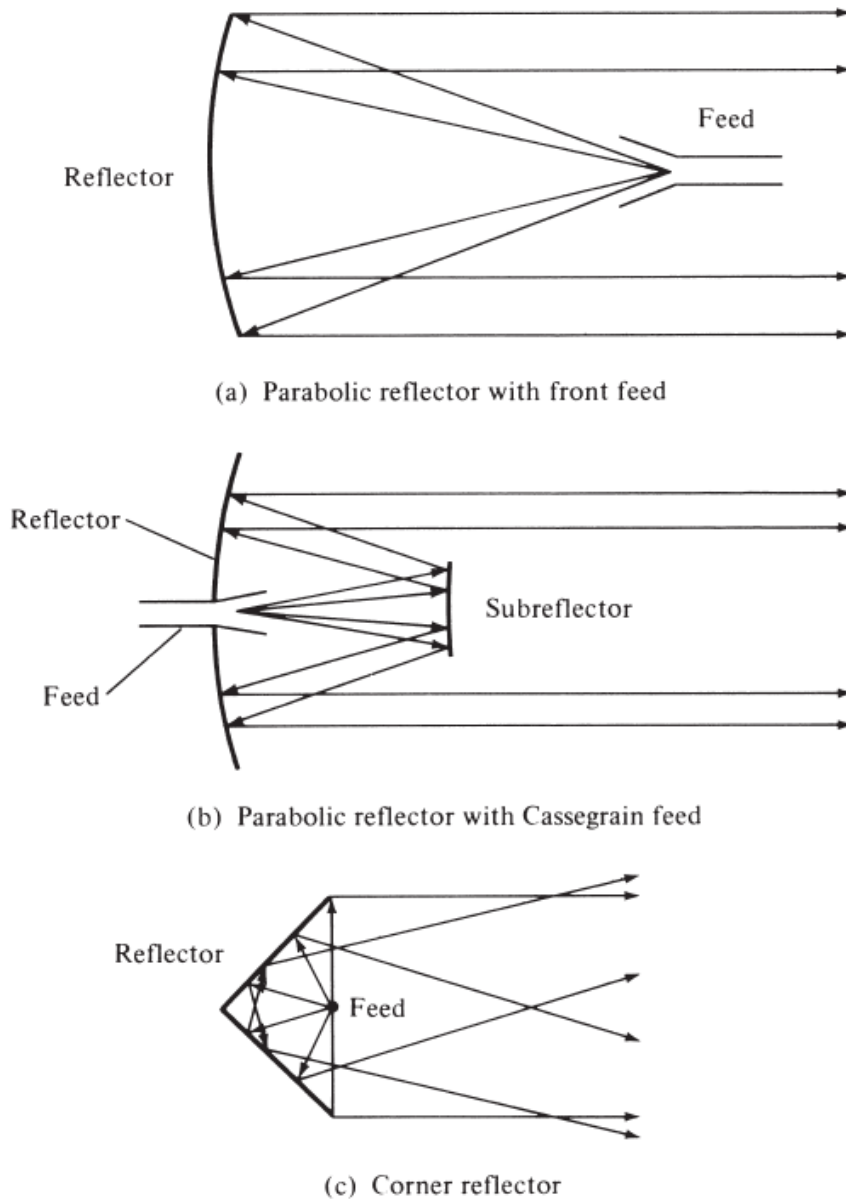


**Figure 1.7** Typical reflector configurations.

### 1.2.6 Lens Antennas

Lenses are primarily used to collimate incident divergent energy to prevent it from spreading in undesired directions. Lens antennas are classified according to the material from which they are constructed, or according to their geometrical shape. Some forms are shown in Figure 1.8. The diameter of the lens is usually many wavelengths, thus, their dimensions and weight become exceedingly large at lower frequencies.

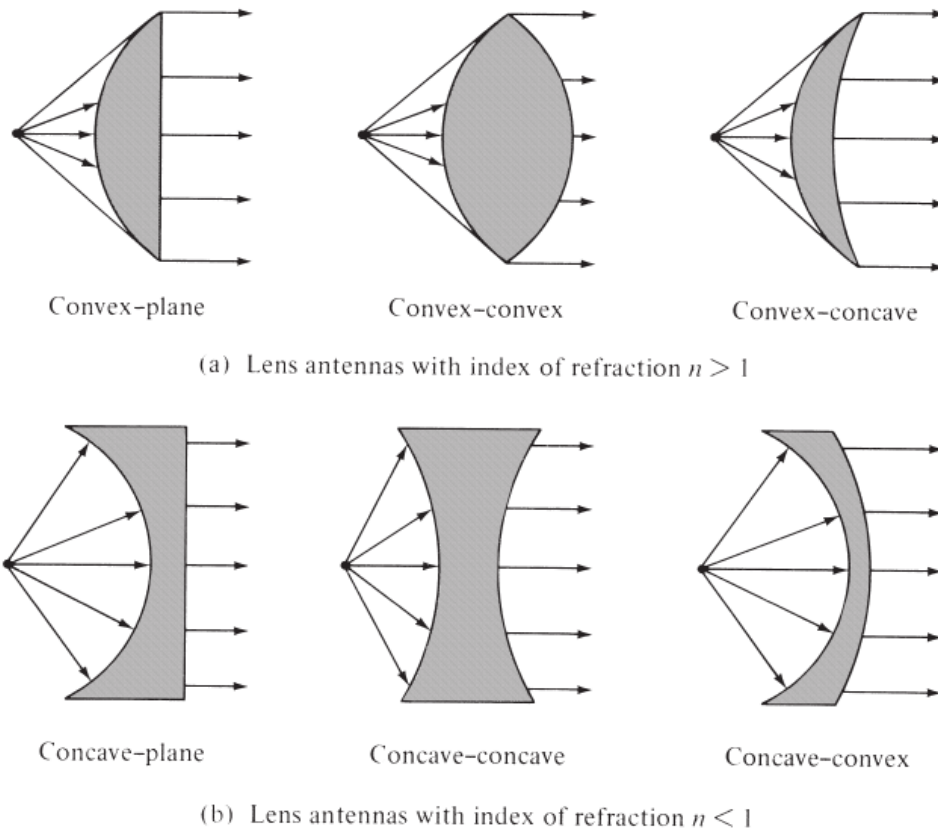


**Figure 1.8** Typical lens antenna configurations. (SOURCE: L. V. Blake, *Antennas*, Wiley, New York, 1966).

## 1.3 RADIATION MECHANISM

### 1.3.1 Single Wire

Conducting wires are material whose prominent characteristic is the motion of electric charges and the creation of current. Let us assume that an electric volume charge density, represented by  $q_v$  (coulombs/m<sup>3</sup>), is distributed uniformly in a circular wire of cross-sectional area  $A$  and volume  $V$ , as shown in Figure 1.9. The total charge  $Q$  within volume  $V$  is moving in the  $z$  direction with a uniform velocity  $v_z$  (meters/sec). It can be shown that the current density  $J_z$  (amperes/m<sup>2</sup>) over the cross section of the wire is given by

$$J_z = q_v v_z \quad (1-1a)$$

If the wire is made of an ideal electric conductor, the current density  $J_s$  (amperes/m) resides on the surface of the wire and it is given by

$$J_s = q_s v_z \quad (1-1b)$$

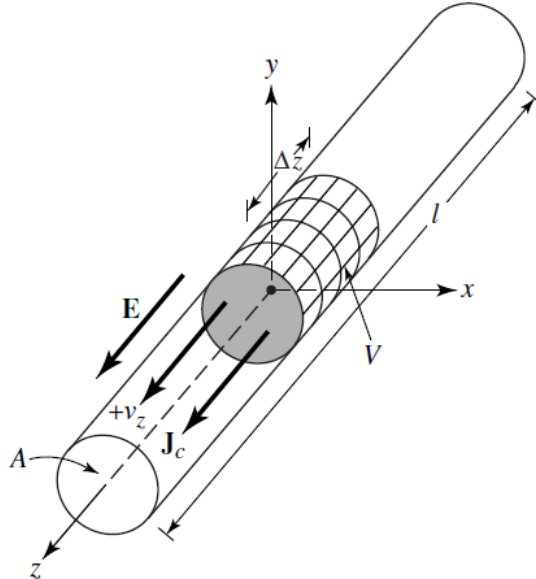


**Figure 1.9** Charge uniformly distributed in a circular cross section cylinder wire.

where  $q_s$  (coulombs/m<sup>2</sup>) is the surface charge density. If the wire is very thin (ideally zero radius), then the current in the wire can be represented by

$$I_z = q_l v_z \quad (1-1c)$$

where  $q_l$  (coulombs/m) is the charge per unit length.

Instead of examining all three current densities, we will primarily concentrate on the very thin wire. The conclusions apply to all three. If the current is time varying, then the derivative of the current of (1-1c) can be written as

$$\frac{dI_z}{dt} = q_l \frac{dv_z}{dt} = q_l a_z \quad (1-2)$$

where  $dv_z/dt = a_z$  (meters/sec<sup>2</sup>) is the acceleration. If the wire is of length  $l$ , then (1-2) can be written as

$$l \frac{dI_z}{dt} = l q_l \frac{dv_z}{dt} = l q_l a_z \quad (1-3)$$

Equation (1-3) is the basic relation between current and charge, and it also serves as the fundamental relation of electromagnetic radiation. It simply states that ***to create radiation, there must be a time-varying current or an acceleration (or deceleration) of charge.*** We usually refer to currents in time-harmonic applications while charge is most often mentioned in transients. To create charge acceleration (or deceleration) the wire must be curved, bent, discontinuous, or terminated. **Periodic charge acceleration (or deceleration) or time-varying current is also created when charge is oscillating in a time-harmonic motion, as shown in Figure 1.17 for a  $\lambda/2$  dipole.** Therefore:

1. If a charge is not moving, current is not created and there is no radiation.
2. If charge is moving with a uniform velocity:
  - a. There is no radiation if the wire is straight, and infinite in extent.
  - b. There is radiation if the wire is curved, bent, discontinuous, terminated, or truncated, as shown in Figure 1.10.
3. If charge is oscillating in a time-motion, it radiates even if the wire is straight.

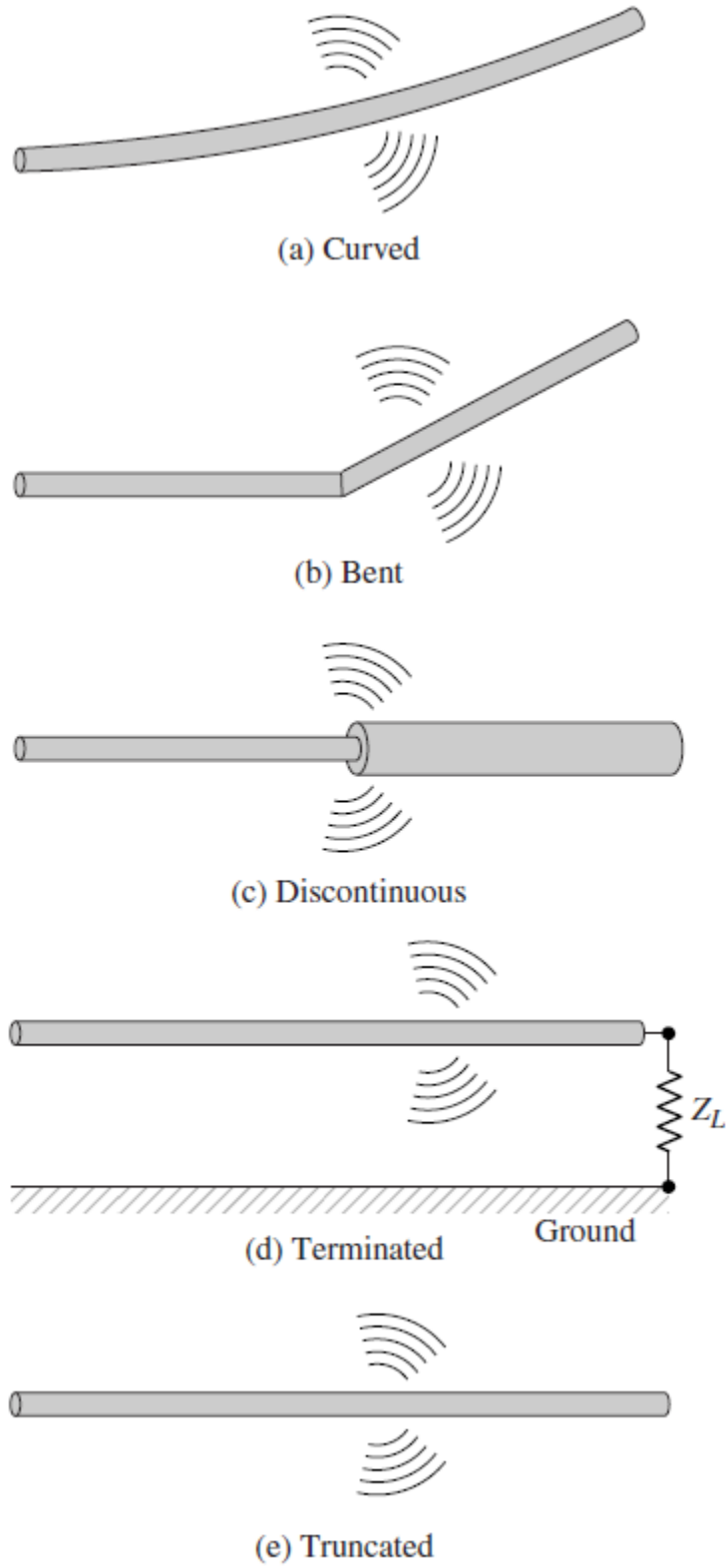


**Figure 1.10** Wire configurations for radiation.

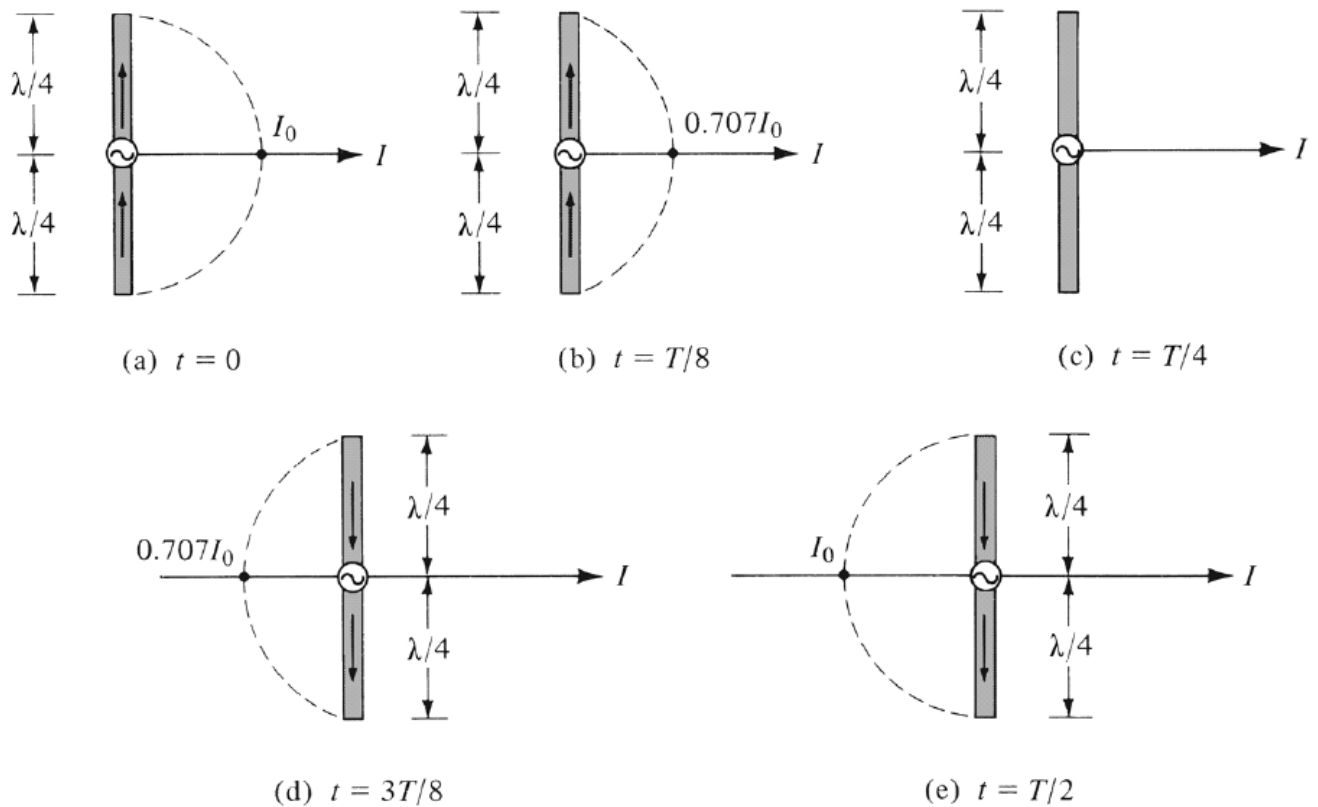


**Figure 1.17** Current distribution on a  $\lambda/2$  wire antenna for different times.

### 1.3.2 Two-Wires

Let us consider a voltage source connected to a two-conductor transmission line which is connected to an antenna. This is shown in Figure 1.11(a). Applying a voltage across the two-conductor transmission line creates an electric field between the conductors. The electric field has associated with it electric lines of force which are tangent to the electric field at each point and their strength is proportional to the electric field intensity. The electric lines of force have a tendency to act on the free electrons (easily detachable from the atoms) associated with each conductor and force them to be displaced. The movement of the charges creates a current that in turn creates a magnetic field intensity. Associated with the magnetic field intensity are magnetic lines of force which are tangent to the magnetic field.

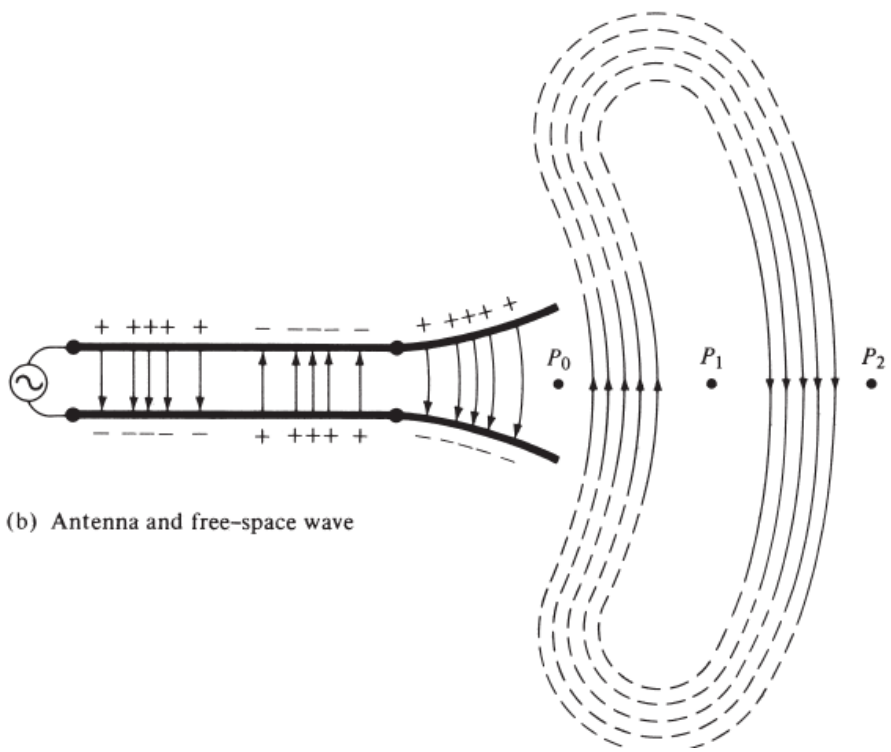
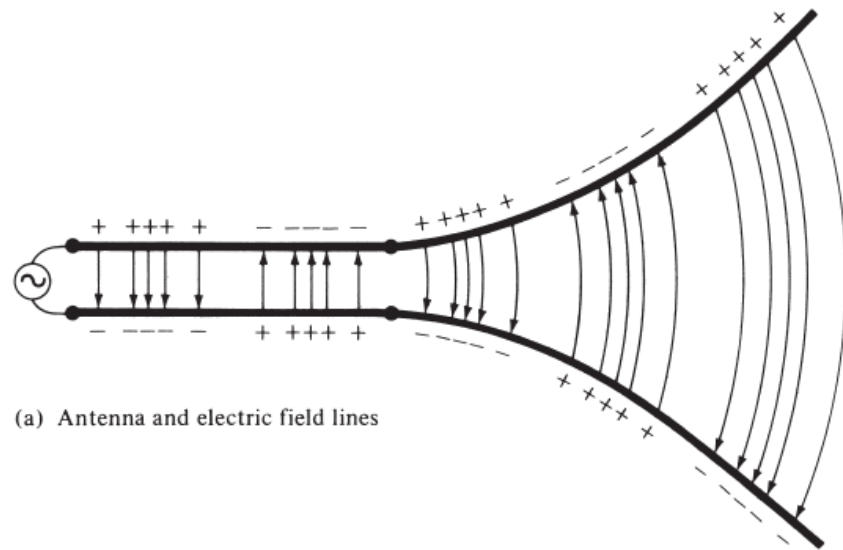


**Figure 1.11** Source, transmission line, antenna, and detachment of electric field lines.

We have accepted that electric field lines start on positive charges and end on negative charges. They also can start on a positive charge and end at infinity, start at infinity and end on a negative charge, or form closed loops neither starting or ending on any charge. Magnetic field lines always form closed loops encircling current-carrying conductors because physically there are no magnetic charges. In some mathematical formulations, it is often convenient to introduce equivalent magnetic charges and magnetic currents to draw a parallel between solutions involving electric and magnetic sources.

The electric field lines drawn between the two conductors help to exhibit the distribution of charge. If we assume that the voltage source is sinusoidal, we expect the electric field between the conductors to also be sinusoidal with a period equal to that of the applied source. The relative magnitude of the electric field intensity is indicated by the density (bunching) of the lines of force with the arrows showing the relative direction (positive or negative). The creation of time-varying electric and magnetic fields between the conductors forms electromagnetic waves which travel along the transmission line, as shown in Figure 1.11(a). The electromagnetic waves enter the antenna and have associated with them electric charges and corresponding currents. If we remove part of the antenna structure, as shown in Figure 1.11(b), free-space waves can be formed by “connecting” the open ends of the electric lines (shown dashed). The free-space waves are also periodic but a constant phase point  $P_0$  moves outwardly with the speed of light and travels a distance of  $\lambda/2$  (to  $P_1$ ) in the time of one-half of a period.

# Fundamental Parameters of Antennas

## RADIATION PATTERN

An antenna *radiation pattern* or *antenna pattern* is defined as “*a mathematical function or a graphical representation of the radiation properties of the antenna as a function of space coordinates.*” In most cases, the radiation pattern is *determined in the far-field region* and is represented as a function of the directional coordinates. *Radiation properties include power flux density, radiation intensity, field strength, directivity, phase or polarization.*” The radiation property of most concern is the two or three-dimensional spatial distribution of radiated energy as a function of the observer’s position along a path or surface of constant radius. *A convenient set of coordinates is shown in Figure 2.1.*

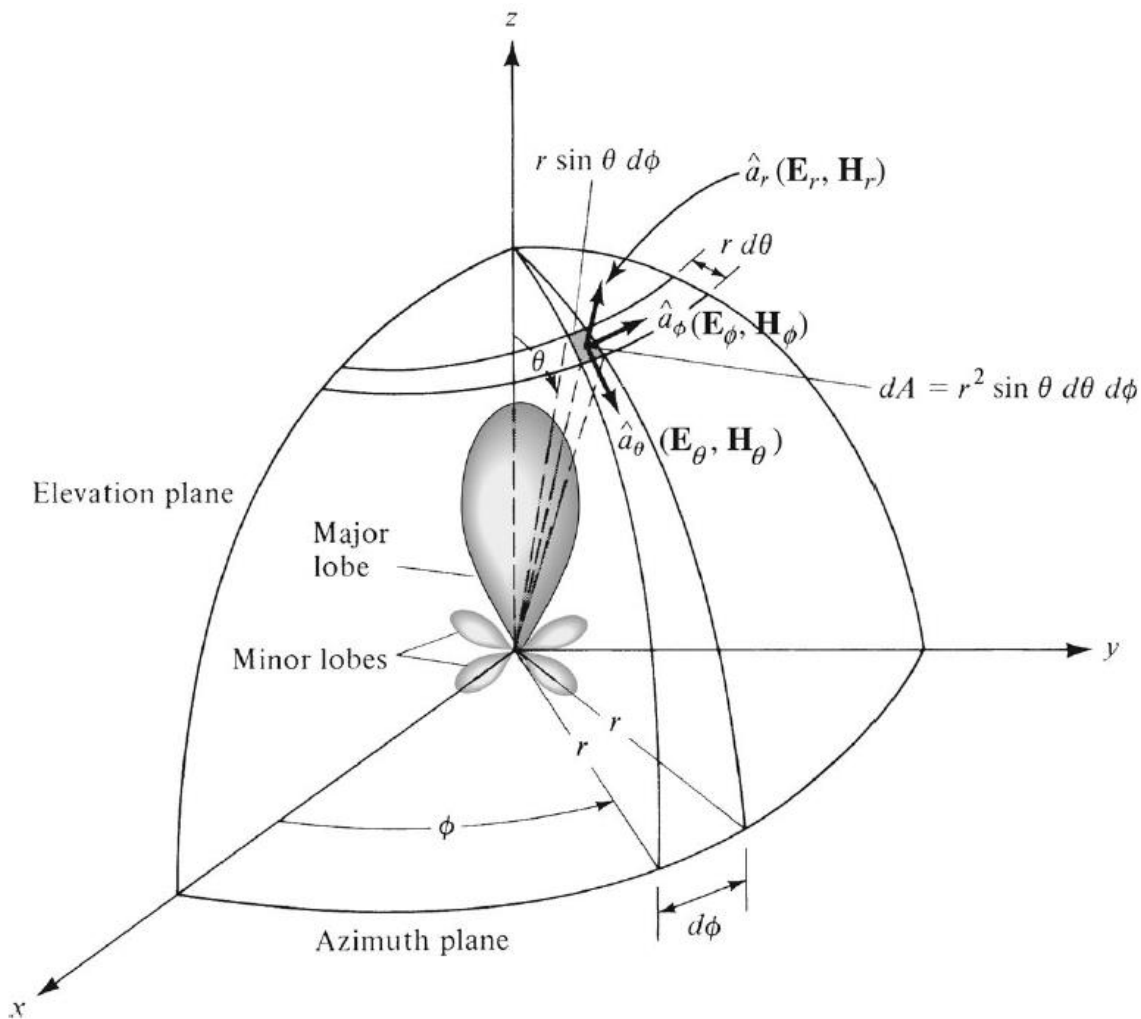


Figure 2.1 Coordinate system for antenna analysis.

A trace of the received electric (magnetic) field at a constant radius is called the amplitude field pattern. On the other hand, a graph of the spatial variation of the power density along a constant radius is called an amplitude power pattern.

Often the *field* and *power* patterns are **normalized with respect to their maximum value, yielding normalized field and power patterns**. Also, the power pattern is usually **plotted on a logarithmic scale or more commonly in decibels (dB)**. This *scale is usually desirable because a logarithmic scale can accentuate in more details those parts of the pattern that have very low values, which later we will refer to as minor lobes*. For an antenna, the

- a. field pattern (in linear scale)** typically represents a plot of the magnitude of the electric or magnetic field as a function of the angular space.
- b. power pattern (in linear scale)** typically represents a plot of the square of the magnitude of the electric or magnetic field as a function of the angular space.
- c. power pattern (in dB)** represents the magnitude of the electric or magnetic field, in decibels, as a function of the angular space.

To demonstrate this, the two-dimensional normalized field pattern (plotted in linear scale), power pattern (plotted in linear scale), and power pattern (plotted on a logarithmic dB scale) of a 10-element linear antenna array of isotropic sources, with a spacing of  $d = 0.25\lambda$  between the elements, are shown in Figure 2.2. In this and subsequent patterns, the plus (+) and minus (-) signs in the lobes indicate the relative polarization (positive or negative) of the amplitude between the various lobes, which changes (alternates) as the nulls are crossed. To find the points where the pattern achieves its half-power (-3 dB points), relative to the maximum value of the pattern, you set the value of the

- a. field pattern at 0.707 value of its maximum, as shown in Figure 2.2(a)**
- b. power pattern (in a linear scale) at its 0.5 value of its maximum, as shown in Figure 2.2(b)**
- c. power pattern (in dB) at -3 dB value of its maximum, as shown in Figure 2.2(c).**

All three patterns yield the same angular separation between the two half-power points, **38.64°**, on their respective patterns, referred to as **HPBW** and illustrated in Figure 2.2. This is discussed in detail in Section 2.5.

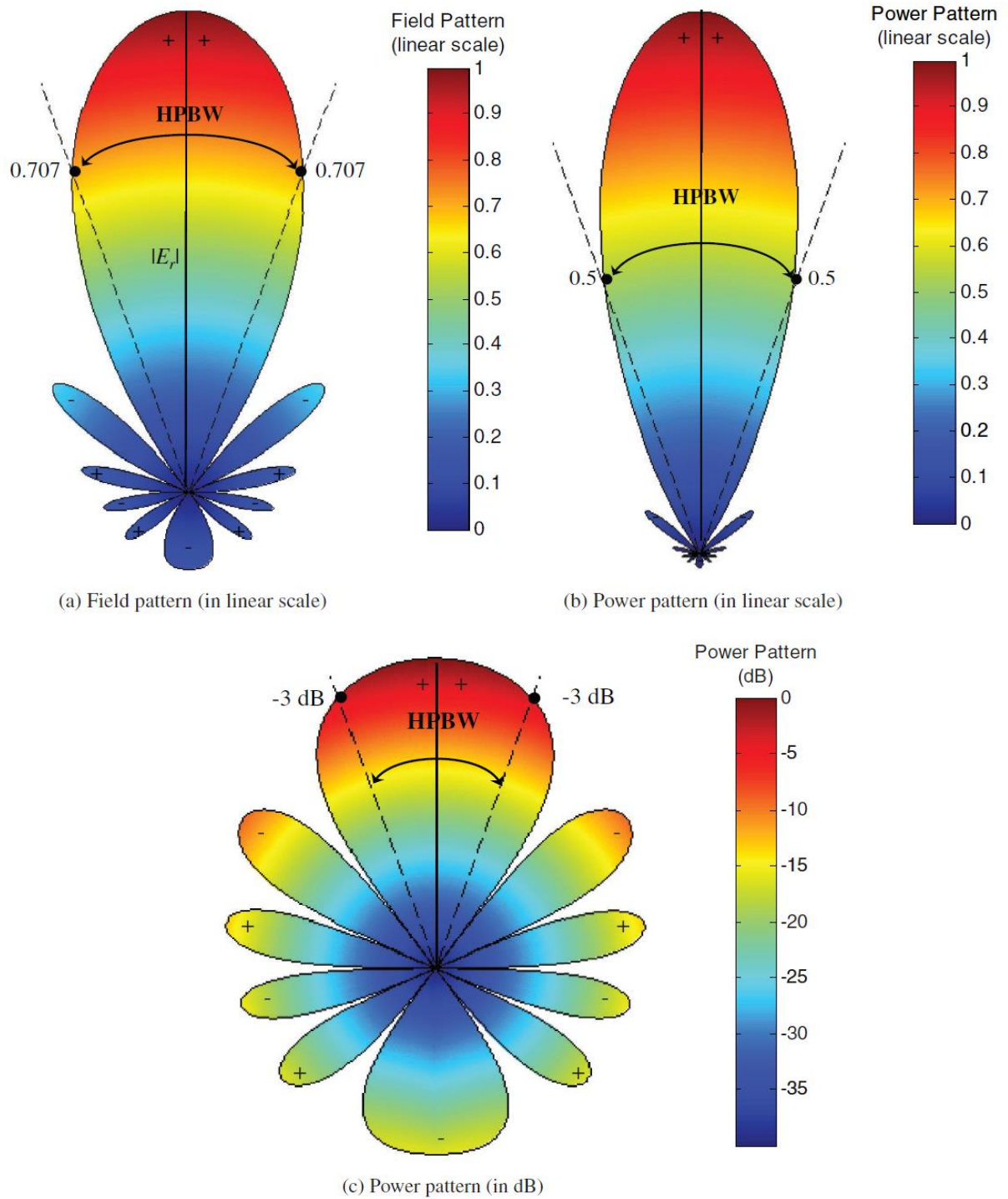


**Figure 2.2** Two-dimensional normalized *field* pattern (*linear scale*), *power* pattern (*linear scale*), and *power* pattern (*in dB*) of a 10-element linear array with a spacing of  $d = 0.25\lambda$ .

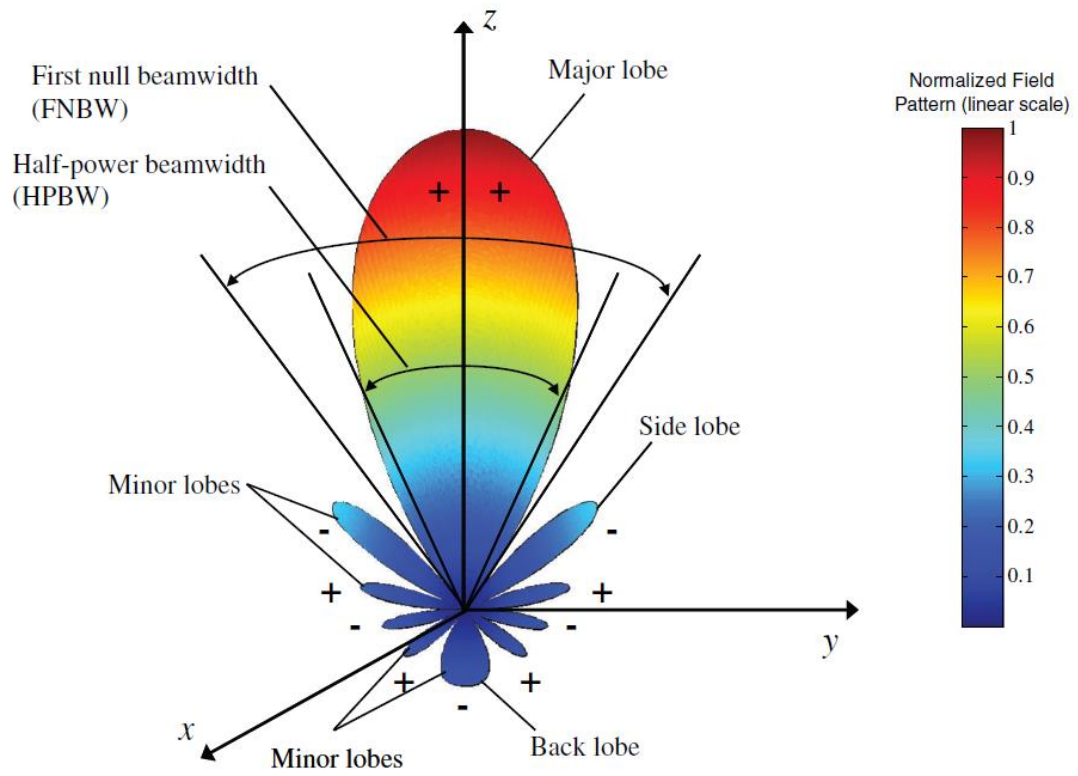
**In practice**, the three-dimensional pattern is measured and recorded in a series of two-dimensional patterns. However, for most practical applications, **a few plots of the pattern as a function of  $\theta$  for some particular values of  $\phi$ , plus a few plots as a function of  $\phi$  for some particular values of  $\theta$ , give most of the useful and needed information.**

## **Radiation Pattern Lobes**

Various parts of a radiation pattern are referred to as *lobes*, **which may be subclassified into major or main, minor, side, and back lobes.**

A *radiation lobe* is a **“portion of the radiation pattern bounded by regions of relatively weak radiation intensity.”** Figure 2.3(a) **demonstrates a symmetrical three-dimensional polar pattern with a number of radiation lobes.** Some are of **greater radiation intensity than others**, but all are classified as lobes. Figure 2.3(b) illustrates a linear two-dimensional pattern [one plane of Figure 2.3(a)] where the same pattern characteristics are indicated.

A *major lobe* (also called **main beam**) is defined as **“the radiation lobe containing the direction of maximum radiation.”** In Figure 2.3 the major lobe is pointing in the  $\theta = 0$  direction. In some antennas, such as split-beam antennas, there may exist more than one major lobe. A *minor lobe* is **any lobe except a major lobe.** In Figures 2.3(a) and (b) all the lobes with the exception of the major can be classified as minor lobes. A *side lobe* is “a radiation lobe in any direction other than the intended lobe. A *back lobe* is “a radiation lobe whose axis makes an angle of approximately  $180^\circ$  with respect to the beam of an antenna.” Usually it refers to a minor lobe that occupies the hemisphere in a direction opposite to that of the major (main) lobe.



(a)

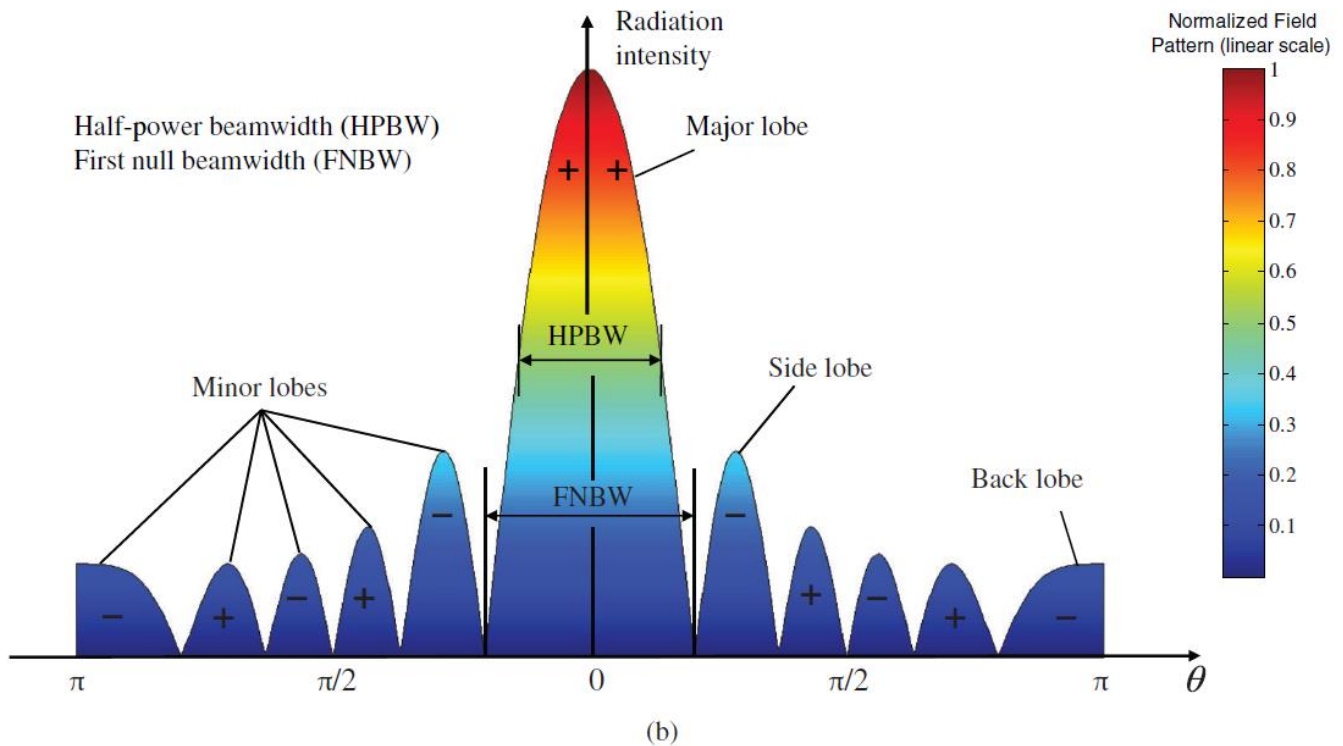


**Figure 2.3** (a) Radiation lobes and beamwidths of an antenna amplitude pattern in polar form. (b) Linear plot of power pattern and its associated lobes and beamwidths.

Minor lobes usually represent radiation in undesired directions, and they should be minimized. Side lobes are normally the largest of the minor lobes. The level of minor lobes is usually expressed as a ratio of the power density in the lobe in question to that of the major lobe. This ratio is often termed the side lobe ratio or side lobe level. Side lobe levels of  $-20$  dB or smaller are usually not desirable in most applications. Attainment of a side lobe level smaller than  $-30$  dB usually requires very careful design and construction. In most radar systems, low side lobe ratios are very important to minimize false target indications through the side lobes.

A normalized three-dimensional far-field amplitude pattern, plotted on a linear scale, of a 10-element linear antenna array of isotropic sources with a spacing of  $d = 0.25\lambda$  and progressive phase shift  $\beta = -0.6\pi$ , between the elements is shown in Figure 2.4. It is evident that this pattern has one major lobe, five minor lobes and one back lobe. The level of the side lobe is about  $-9$  dB relative to the maximum.

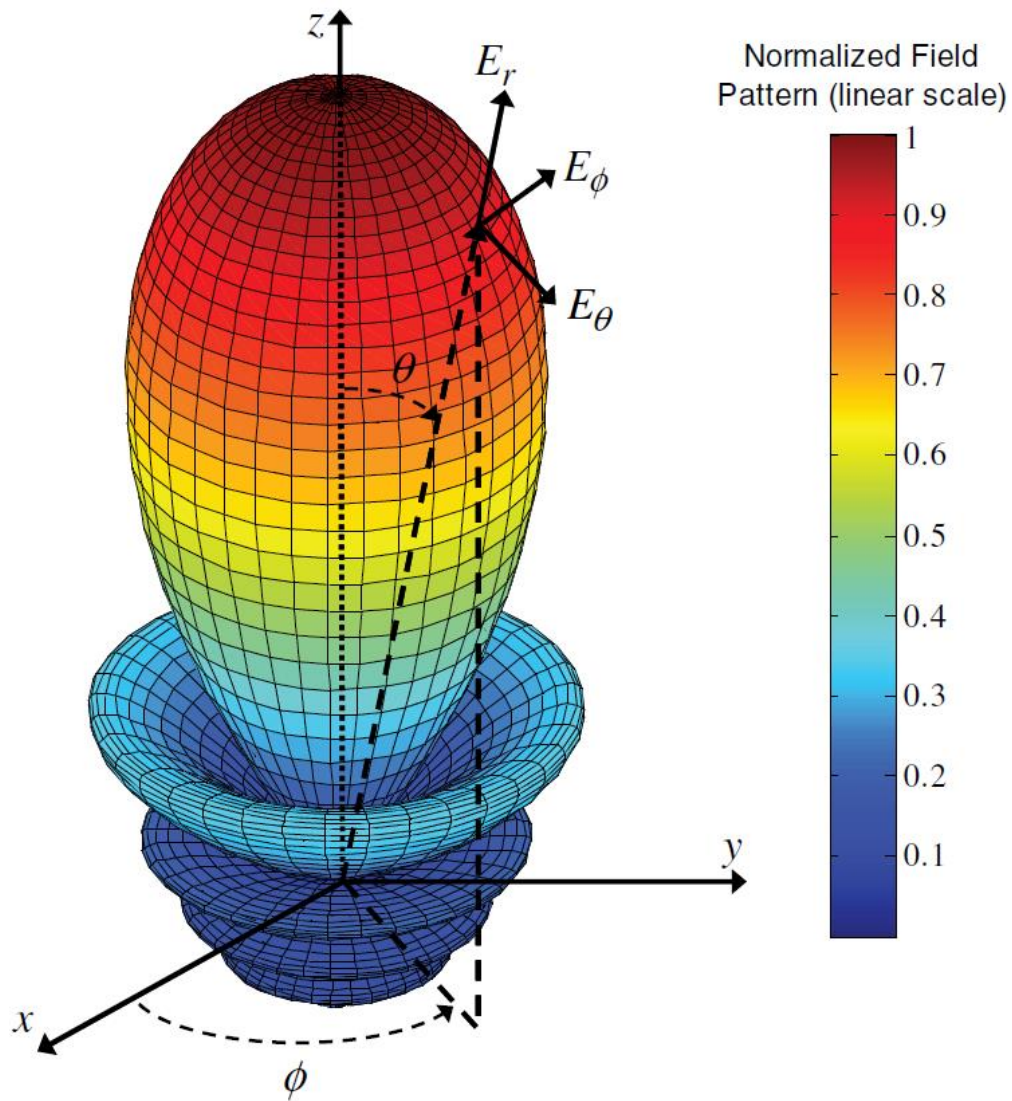


**Figure 2.4** Normalized three-dimensional amplitude *field* pattern (*in linear scale*) of a 10-element linear array antenna with a uniform spacing of  $d = 0.25\lambda$  and progressive phase shift  $\beta = -0.6\pi$  between the elements.

## Isotropic, Directional, and Omnidirectional Patterns

An *isotropic* radiator is defined as “a hypothetical lossless antenna having equal radiation in all directions.” Although it is ideal and not physically realizable, it is often taken as a reference for expressing the directive properties of actual antennas. A *directional* antenna is one “having the property of radiating or receiving electromagnetic waves more effectively in some directions than in others. This term is usually applied to an antenna whose maximum directivity is significantly greater than that of a half-wave dipole.” Examples of antennas with directional radiation patterns are shown in Figures 2.5 and 2.6. It is seen that the pattern in Figure 2.6 is nondirectional in the azimuth plane [ $f(\phi), \theta = \pi/2$ ] and directional in the elevation plane [ $g(\theta), \phi = \text{constant}$ ]. This type of a pattern is designated as *omnidirectional*, and it is defined as one “having an essentially nondirectional pattern in a given plane (in this case in azimuth) and a directional pattern in any orthogonal plane (in this case in elevation).” An *omnidirectional* pattern is then a special type of a *directional* pattern.

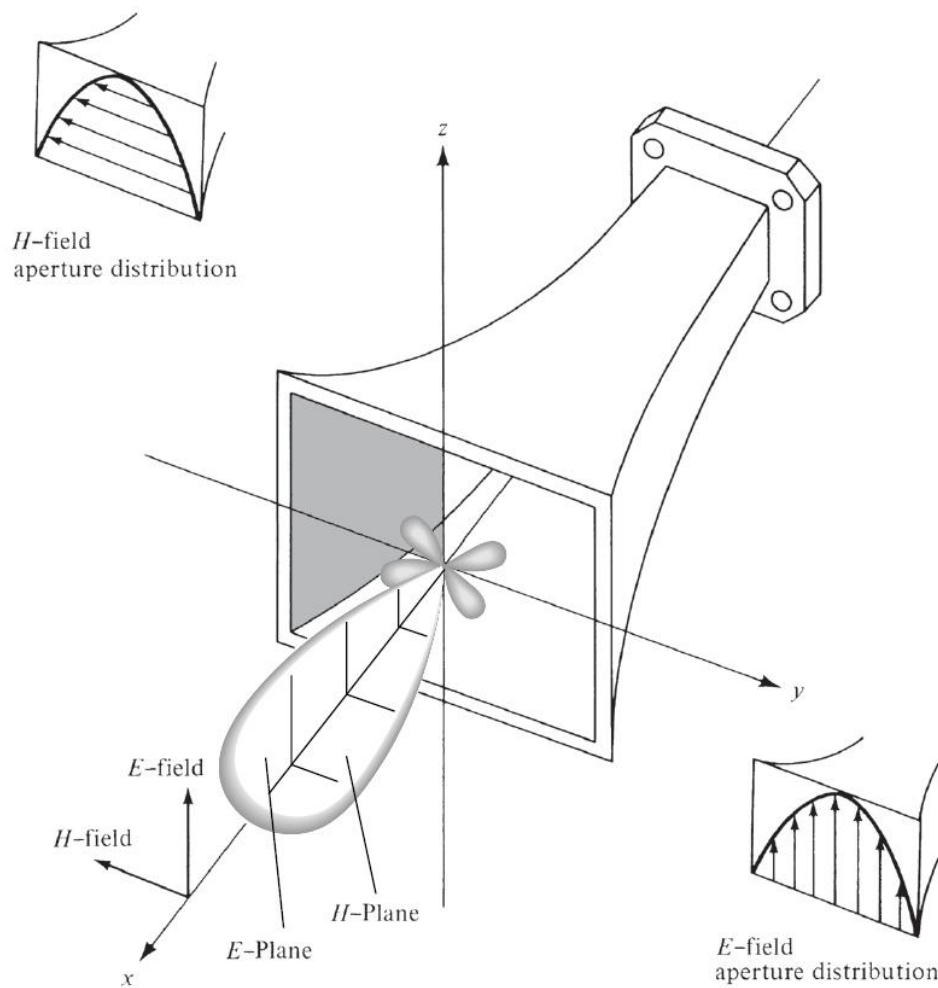


**Figure 2.5** Principal E- and H-plane patterns for a pyramidal horn antenna.

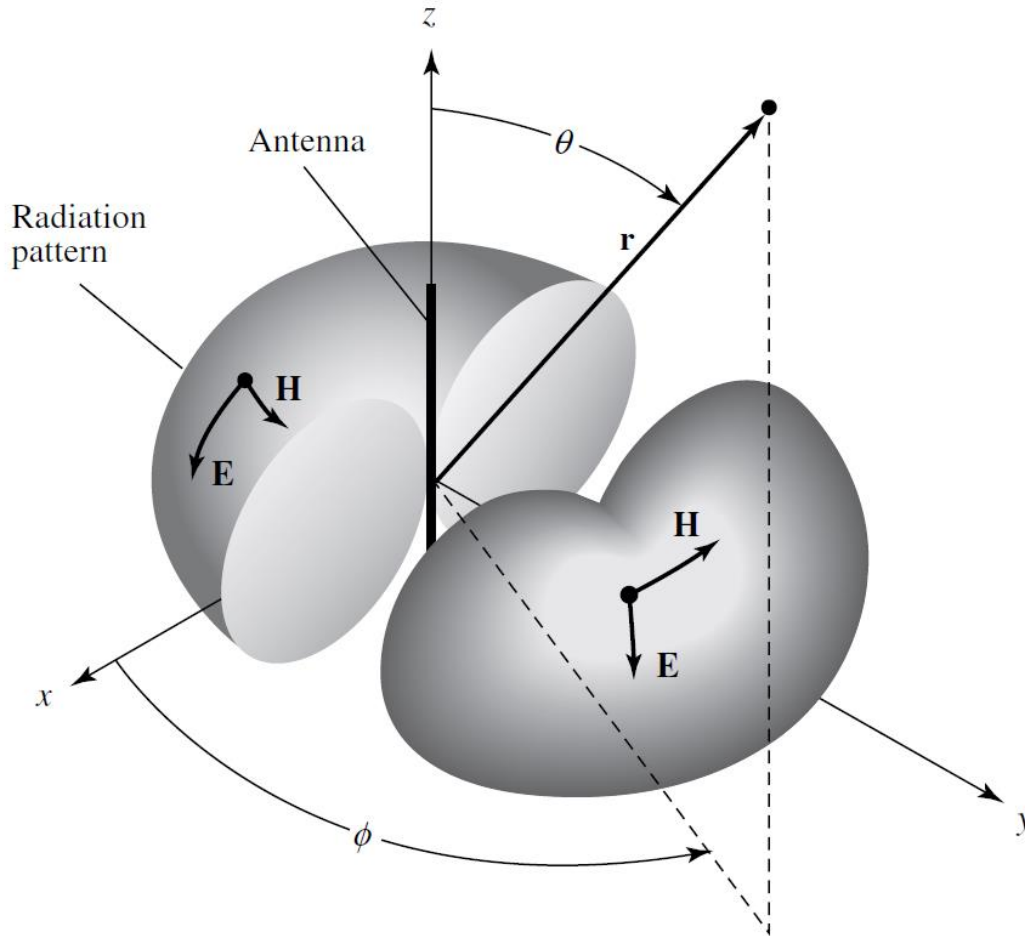


**Figure 2.6** Omnidirectional antenna pattern.

### 2.2.3 Principal Patterns

For a linearly polarized antenna, performance is often described in terms of its principal  $E$ - and  $H$ -plane patterns. The  $E$ -plane is defined as “the plane containing the electric-field vector and the direction of maximum radiation,” and the  $H$ -plane as “the plane containing the magnetic-field vector and the direction of maximum radiation.” Although it is very difficult to illustrate the principal patterns without considering a specific example, it is the usual practice to orient most antennas so that at least one of the principal plane patterns coincide with one of the geometrical principal planes. An illustration is shown in Figure 2.5. For this example, the  $x$ - $z$  plane (elevation plane;  $\phi = 0$ ) is the principal  $E$ -plane and the  $x$ - $y$  plane (azimuthal plane;  $\theta = \pi/2$ ) is the principal  $H$ -plane. Other coordinate orientations can be selected.

The omnidirectional pattern of Figure 2.6 has an infinite number of principal  $E$ -planes (elevation planes;  $\phi = \phi_c$ ) and one principal  $H$ -plane (azimuthal plane;  $\theta = 90^\circ$ ).

## 2.2.4 Field Regions

The space surrounding an antenna is usually subdivided into three regions:

- (a) reactive near-field,
  - (b) radiating near-field (Fresnel) and
  - (c) far-field (Fraunhofer) regions
- as shown in Figure 2.7.

These regions are so designated to identify the field structure in each. Although no abrupt changes in the field configurations are noted as the boundaries are crossed, there are distinct differences among them. The boundaries separating these regions are not unique, although various criteria have been established and are commonly used to identify the regions.

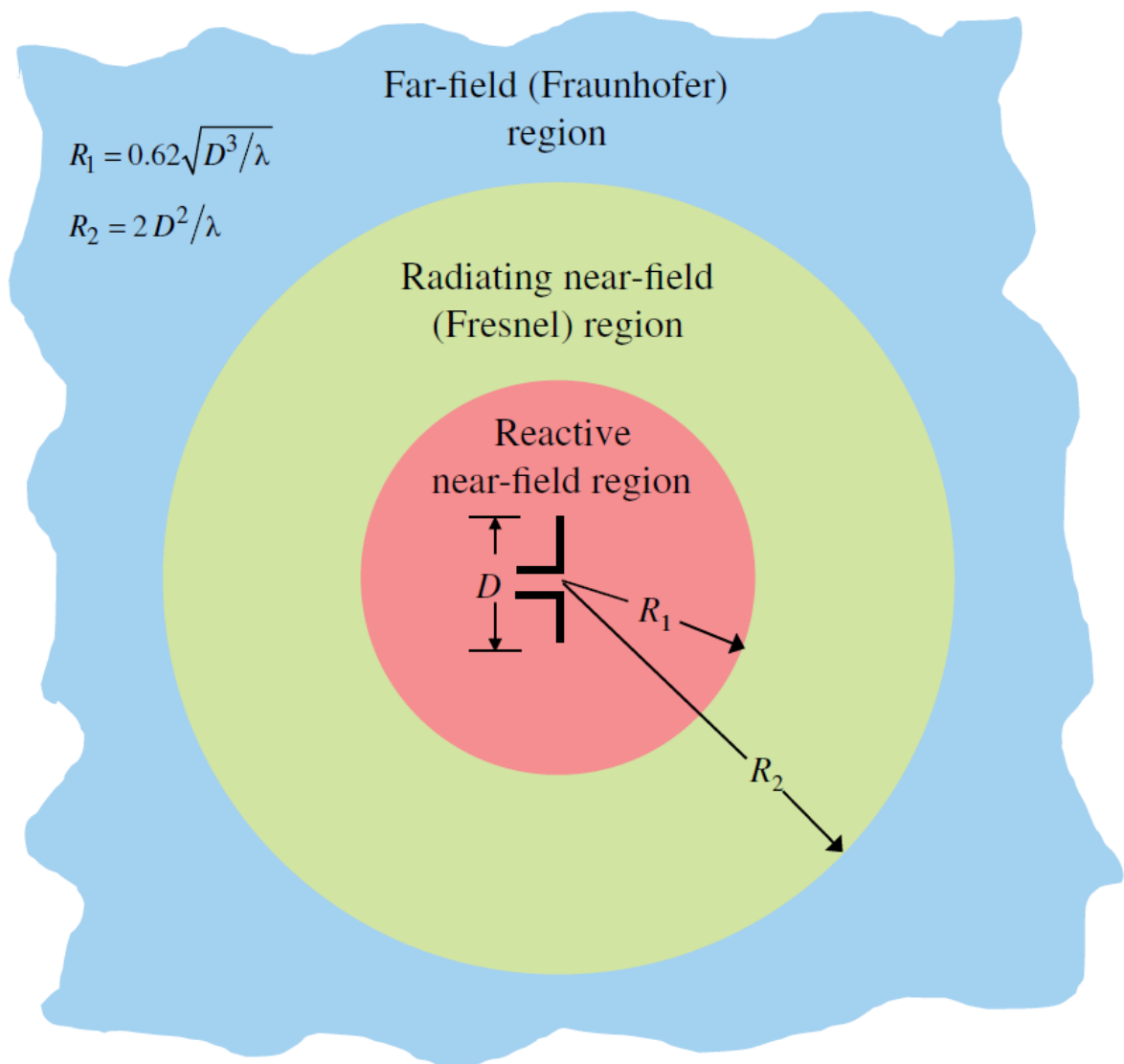


**Figure 2.7** Field regions of an antenna.

**Reactive near-field region** is defined as “that portion of the near-field region immediately surrounding the antenna wherein the reactive field predominates.” For most antennas, the outer boundary of this region is commonly taken to exist at a distance  $R < 0.62\sqrt{D^3\lambda}$

from the antenna surface, where  $\lambda$  is the wavelength and  $D$  is the largest dimension of the antenna.

“For a very short dipole, or equivalent radiator, the outer boundary is commonly taken to exist at a distance  $\lambda/2\pi$  from the antenna surface.”

**Radiating near-field (Fresnel) region** is defined as “that region of the field of an antenna between the reactive near-field region and the far-field region wherein radiation fields predominate and wherein the angular field distribution is dependent upon the distance from the antenna. If the antenna has a maximum dimension that is not large compared to the wavelength, this region may not exist.” For an antenna focused at infinity, the radiating near-field region is sometimes referred to as *the Fresnel region* on the **basis of analogy to optical terminology**. If the antenna has a maximum overall dimension which is very small compared to the wavelength, this field region may not exist.”

The inner boundary is taken to be the distance

$$R \geq 0.62\sqrt{D^3\lambda}$$

and the outer boundary the distance

$$R < 2D^2\lambda$$

where  $D$  is the largest\* dimension of the antenna.

This criterion is based on a *maximum phase error of  $\pi/8$* . In this region the field pattern is, in general, a function of the radial distance and the radial field component may be appreciable.

**Far-field (Fraunhofer) region** is defined as “that region of the field of an antenna where the angular field distribution is essentially independent of the distance from the antenna.” If the antenna has a maximum<sup>†</sup> overall dimension  $D$ , the far-field region is commonly taken to exist at distances greater than  $2D^2\lambda$  from the antenna,  $\lambda$  being the wavelength. The far-field patterns of certain antennas, such as multibeam reflector antennas, are sensitive to variations in phase over their apertures. For these antennas  $2D^2\lambda$  may be inadequate. In physical media, if the antenna has a maximum overall dimension,  $D$ , which is large compared to  $\pi/\gamma$ , the far-field region can be taken to begin approximately at a distance equal to  $|\gamma|D^2/\pi$  from the antenna,  $\gamma$  being the propagation constant in the medium.

\*To be valid,  $D$  must also be large compared to the wavelength ( $D > \lambda$ ).

†To be valid,  $D$  must also be large compared to the wavelength ( $D > \lambda$ ).

For an antenna focused at infinity, the far-field region is sometimes referred to as **the Fraunhofer region on the basis of analogy to optical terminology.** In this region, the field components are essentially transverse and the angular distribution is independent of the radial distance where the measurements are made. The inner boundary is taken to be the radial distance  $R = 2D^2/\lambda$  and the outer one at **infinity**.

The amplitude pattern of an antenna, as the observation distance is varied from the reactive near field to the far field, **changes in shape because of variations of the fields, both magnitude and phase.** A typical progression of the shape of an antenna, with the largest dimension  $D$ , is shown in Figure 2.8.

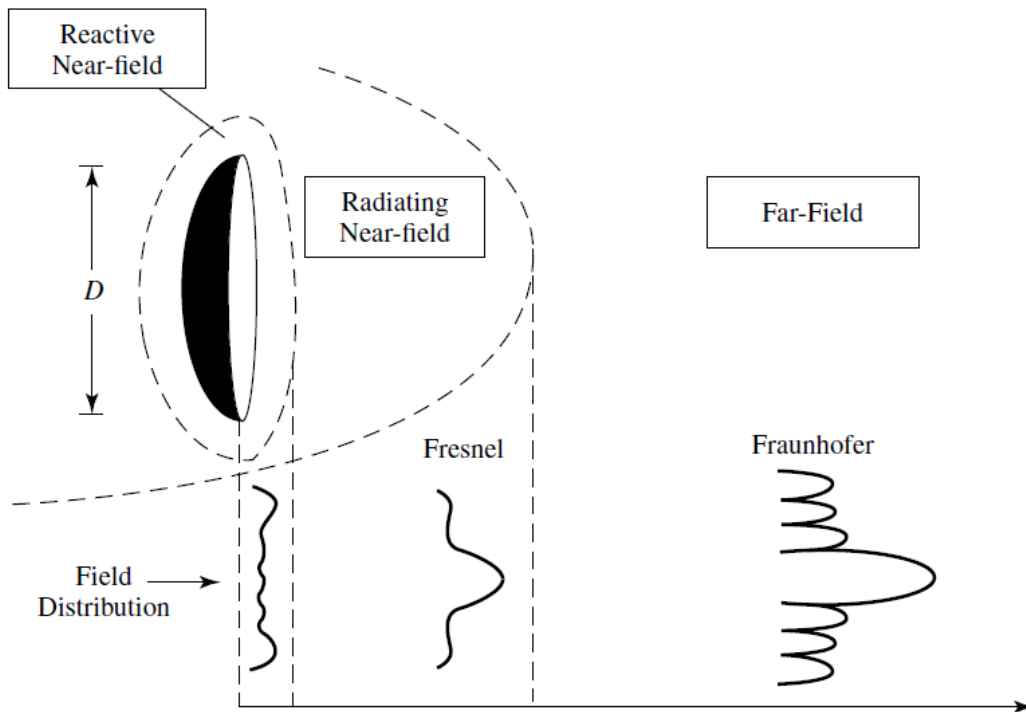


**Figure 2.8** Typical changes of antenna amplitude pattern shape from reactive near field toward the far field.

It is apparent that in the reactive near-field region the pattern is more spread out and nearly uniform, with slight variations. As the observation is moved to the radiating near-field region (Fresnel), the pattern begins to smooth and form lobes. In the far-field region (Fraunhofer), the pattern is well formed, usually consisting of few minor lobes and one, or more, major lobes.

## 2.2.5 Radian and Steradian

The measure of a plane angle is a radian. One radian is defined as the plane angle with its vertex at the center of a circle of radius  $r$  that is subtended by an arc whose length is  $r$ . A graphical illustration is shown in Figure 2.10(a). Since the circumference of a circle of radius  $r$  is  $C = 2\pi r$ , there are  $2\pi$  rad ( $2\pi/r$ ) in a full circle.

The measure of a solid angle is a steradian. One steradian is defined as the solid angle with its vertex at the center of a sphere of radius  $r$  that is subtended by a spherical surface area equal to that of a square with each side of length  $r$ . A graphical illustration is shown in Figure 2.10(b). Since the area of a sphere of radius  $r$  is  $A = 4\pi r^2$ , there are  $4\pi$  sr ( $4\pi r^2/r^2$ ) in a closed sphere.

The infinitesimal area  $dA$  on the surface of a sphere of radius  $r$ , shown in Figure 2.1, is given by

$$dA = r^2 \sin \theta d\theta d\phi \quad (\text{m}^2) \quad (2-1)$$

Therefore, the element of solid angle  $d\Omega$  of a sphere can be written as

$$d\Omega = \frac{dA}{r^2} = \sin \theta d\theta d\phi \quad (\text{sr}) \quad (2-2)$$

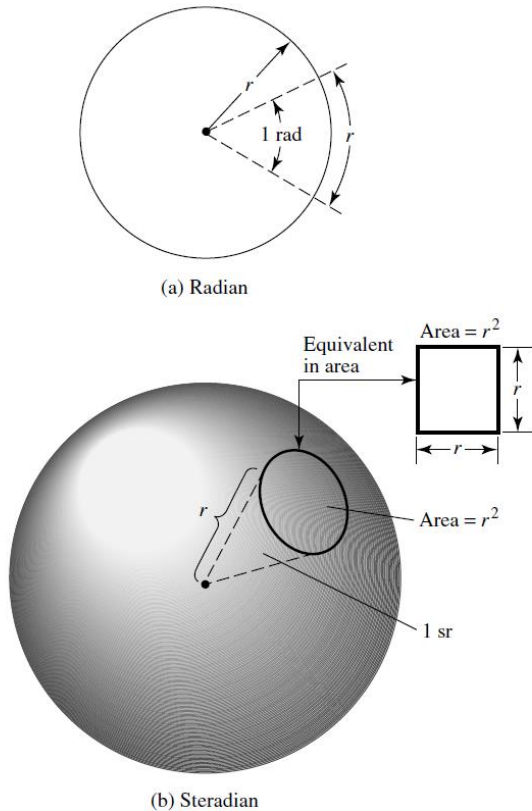


Figure 2.10 Geometrical arrangements for defining a radian and a steradian.

### Example 2.1

For a sphere of radius  $r$ , find the solid angle  $\Omega_A$  (in square radians or steradians) of a spherical cap on the surface of the sphere over the north-pole region defined by spherical angles of  $0 \leq \theta \leq 30^\circ, 0 \leq \phi \leq 360^\circ$ . Refer to Figures 2.1 and 2.10. Do this

- exactly.
- using  $\Omega_A \approx \Delta\Theta_1 \cdot \Delta\Theta_2$ , where  $\Delta\Theta_1$  and  $\Delta\Theta_2$  are two perpendicular angular separations of the spherical cap passing through the north pole.

Compare the two.

*Solution:*

- Using (2-2), we can write that

$$\begin{aligned}\Omega_A &= \int_0^{360^\circ} \int_0^{30^\circ} d\Omega = \int_0^{2\pi} \int_0^{\pi/6} \sin \theta \, d\theta \, d\phi = \int_0^{2\pi} d\phi \int_0^{\pi/6} \sin \theta \, d\theta \\ &= 2\pi [-\cos \theta]_0^{\pi/6} = 2\pi [-0.867 + 1] = 2\pi(0.133) = 0.83566\end{aligned}$$

$$\text{b. } \Omega_A \approx \Delta\Theta_1 \cdot \Delta\Theta_2 \underbrace{\overset{\Delta\Theta_1 = \Delta\Theta_2}{=}}_{=} (\Delta\Theta_1)^2 = \frac{\pi}{3} \left(\frac{\pi}{3}\right) = \frac{\pi^2}{9} = 1.09662$$

It is apparent that the approximate beam solid angle is about 31.23% in error.

## 2.2.4 Field Regions

The space surrounding an antenna is usually subdivided into three regions:

- a- reactive near-field,
- b- radiating near-field (Fresnel) and
- c- far-field (Fraunhofer) regions

as shown in Figure 2.7.

These regions are so designated to identify the field structure in each. **Although no abrupt changes in the field configurations are noted as the boundaries are crossed, there are distinct differences among them.** The boundaries separating these regions are not unique, although various criteria have been established and are commonly used to identify the regions.

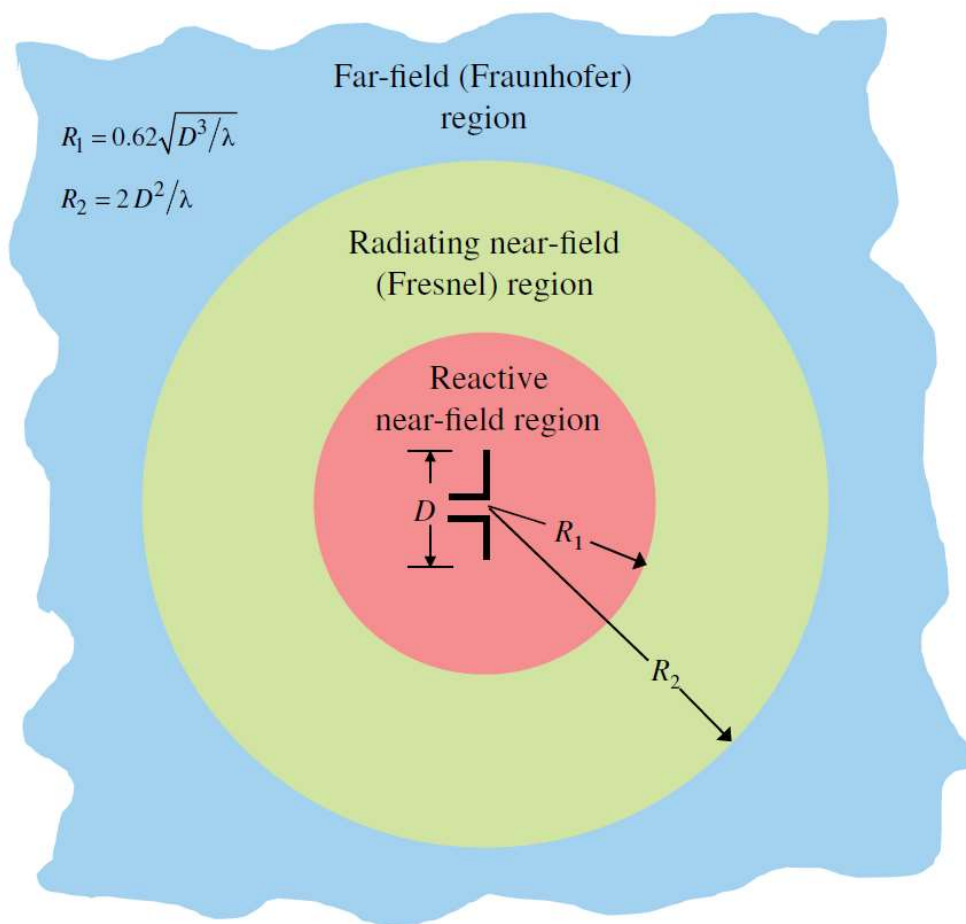


Figure 2.7 Field regions of an antenna.

**1- Reactive near-field region** is defined as “that portion of the near-field region immediately surrounding the antenna wherein the reactive field predominates.” For most antennas, the outer boundary of this region is commonly taken to exist at a distance  $R < 0.62\sqrt{D^3/\lambda}$

from the antenna surface, where

$\lambda$  : is the wavelength and

$D$  : is the largest dimension of the antenna.

“For a very short dipole, or equivalent radiator, the outer boundary is commonly taken to exist at a distance  $\lambda/2\pi$  from the antenna surface.”

- 2- **Radiating near-field (Fresnel) region** is defined as “that region of the field of an antenna between the reactive near-field region and the far-field region wherein radiation fields predominate and wherein the angular field distribution is dependent upon the distance from the antenna. If the antenna has a maximum dimension that is not large compared to the wavelength, this region may not exist.” For an antenna focused at infinity, the radiating near-field region is sometimes referred to as **the Fresnel region** on the **basis of analogy to optical terminology**. If the antenna has a maximum overall dimension which is very small compared to the wavelength, this field region may not exist.”

The inner boundary is taken to be the distance

$$R \geq 0.62\sqrt{D^3/\lambda}$$

and the outer boundary the distance

$$R < 2D^2/\lambda$$

where  $D$  is the largest\* dimension of the antenna.

This criterion is based on a **maximum phase error of  $\pi/8$** . In this region the field pattern is, in general, a function of the radial distance and the radial field component may be appreciable.

- 3- **Far-field (Fraunhofer) region** is defined as “that region of the field of an antenna where the angular field distribution is essentially independent of the distance from the antenna. If the antenna has a maximum<sup>†</sup> overall dimension  $D$ , the far-field region is commonly taken to exist at distances greater than  $2D^2/\lambda$  from the antenna,  $\lambda$  being the wavelength. The far-field patterns of certain antennas, such as multibeam reflector antennas, are sensitive to variations in phase over their apertures. For these antennas  $2D^2/\lambda$  may be inadequate. In physical media, if the antenna has a maximum overall dimension,  $D$ , which is large compared to  $\pi/\gamma$ , the far-field region can be taken to begin approximately at a distance equal to  $|\gamma|D^2/\pi$  from the antenna,  $\gamma$  being the propagation constant in the medium.

\*To be valid,  $D$  must also be large compared to the wavelength ( $D > \lambda$ ).

†To be valid,  $D$  must also be large compared to the wavelength ( $D > \lambda$ ).

For an antenna focused at infinity, the far-field region is sometimes referred to as **the Fraunhofer region on the basis of analogy to optical terminology**.” In this region, the field components are essentially transverse and the angular distribution is independent of the radial distance where the measurements are made. The inner boundary is taken to be the radial distance  $R = 2D^2/\lambda$  and the outer one at **infinity**.

The amplitude pattern of an antenna, as the observation distance is varied from the reactive near field to the far field, **changes in shape because of variations of the fields, both magnitude and phase.** A typical progression of the shape of an antenna, with the largest dimension  $D$ , is shown in Figure 2.8.

It is apparent that in the reactive near-field region the pattern is more spread out and nearly uniform, with slight variations. As the observation is moved to the radiating near-field region (Fresnel), the pattern begins to smooth and form lobes. In the far-field region (Fraunhofer), the pattern is well formed, usually consisting of few minor lobes and one, or more, major lobes.

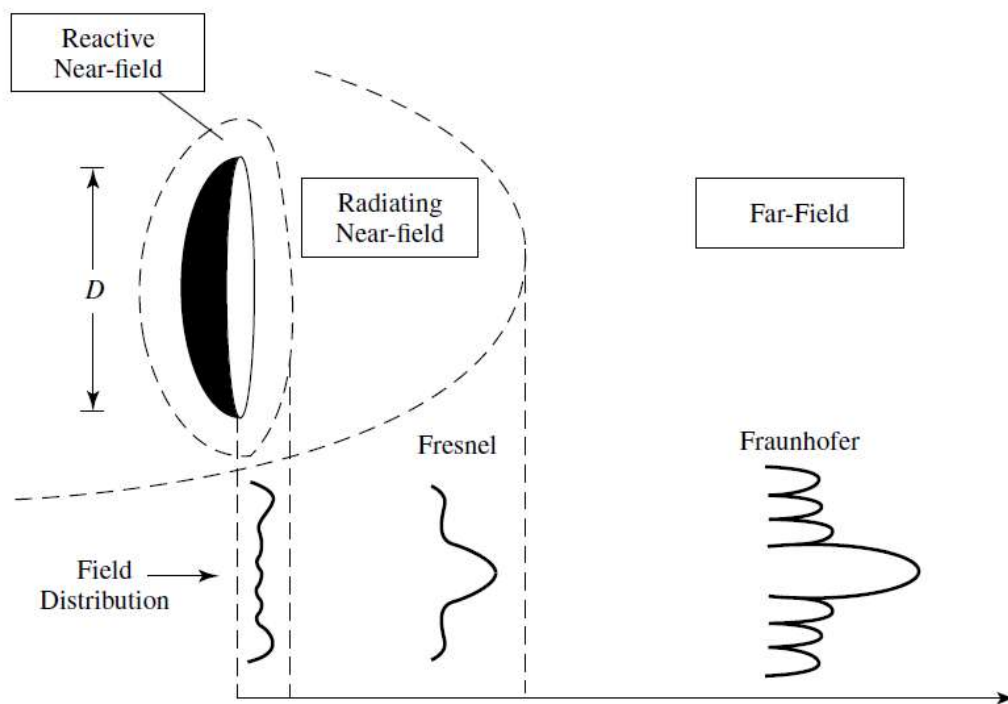


**Figure 2.8** Typical changes of antenna amplitude pattern shape from reactive near field toward the far field.

## 2.2.5 Radian and Steradian

*The measure of a plane angle is a radian. One radian is defined as the plane angle with its vertex at the center of a circle of radius  $r$  that is subtended by an arc whose length is  $r$ .* A graphical illustration is shown in Figure 2.10(a). *Since the circumference of a circle of radius  $r$  is  $C = 2\pi r$ , there are  $2\pi$  rad ( $2\pi/r$ ) in a full circle.*

*The measure of a solid angle is a steradian. One steradian is defined as the solid angle with its vertex at the center of a sphere of radius  $r$  that is subtended by a spherical surface area equal to that of a square with each side of length  $r$ .* A graphical illustration

is shown in Figure 2.10(b). Since the area of a sphere of radius  $r$  is  $A = 4\pi r^2$ , there are  $4\pi$  sr ( $4\pi r^2/r^2$ ) in a closed sphere.

The infinitesimal area  $dA$  on the surface of a sphere of radius  $r$ , shown in Figure 2.1, is given by

$$dA = r^2 \sin \theta d\theta d\phi \quad (\text{m}^2) \quad (2-1)$$

Therefore, the element of solid angle  $d\Omega$  of a sphere can be written as

$$d\Omega = \frac{dA}{r^2} = \sin \theta d\theta d\phi \quad (\text{sr}) \quad (2-2)$$

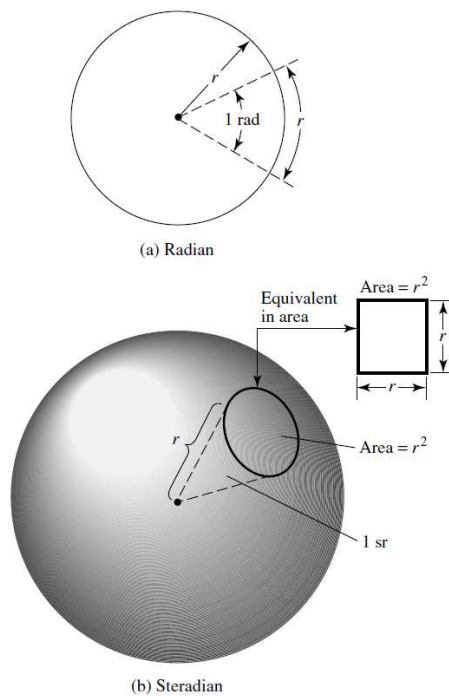


Figure 2.10 Geometrical arrangements for defining a radian and a steradian.

### Example 2.1

For a sphere of radius  $r$ , find the solid angle  $\Omega_A$  (in square radians or steradians) of a spherical cap on the surface of the sphere over the north-pole region defined by spherical angles of  $0 \leq \theta \leq 30^\circ, 0 \leq \phi \leq 360^\circ$ . Refer to Figures 2.1 and 2.10. Do this

- exactly.
- using  $\Omega_A \approx \Delta\Theta_1 \cdot \Delta\Theta_2$ , where  $\Delta\Theta_1$  and  $\Delta\Theta_2$  are two perpendicular angular separations of the spherical cap passing through the north pole.

Compare the two.

*Solution:*

- Using (2-2), we can write that

$$\begin{aligned}\Omega_A &= \int_0^{360^\circ} \int_0^{30^\circ} d\Omega = \int_0^{2\pi} \int_0^{\pi/6} \sin\theta \, d\theta \, d\phi = \int_0^{2\pi} d\phi \int_0^{\pi/6} \sin\theta \, d\theta \\ &= 2\pi[-\cos\theta]_0^{\pi/6} = 2\pi[-0.867 + 1] = 2\pi(0.133) = 0.83566\end{aligned}$$

$$\text{b. } \Omega_A \approx \Delta\Theta_1 \cdot \Delta\Theta_2 \underbrace{\Delta\Theta_1 = \Delta\Theta_2}_{=} (\Delta\Theta_1)^2 = \frac{\pi}{3} \left(\frac{\pi}{3}\right) = \frac{\pi^2}{9} = 1.09662$$

It is apparent that the approximate beam solid angle is about 31.23% in error.

## 2.3 RADIATION POWER DENSITY

Electromagnetic waves are used to transport information through a wireless medium or a guiding structure, from one point to the other. **It is then natural to assume that power and energy are associated with electromagnetic fields.** The quantity used to describe the power associated with an electromagnetic wave is *the instantaneous Poynting vector* defined as

$$\mathcal{W} = \mathcal{E} \times \mathcal{H} \quad (2-3)$$

$\mathcal{W}$  = instantaneous Poynting vector (W/m<sup>2</sup>)

$\mathcal{E}$  = instantaneous electric-field intensity (V/m)

$\mathcal{H}$  = instantaneous magnetic-field intensity (A/m)

Note that script letters are used to denote instantaneous fields and quantities, while roman letters are used to represent their complex counterparts. ***Since the Poynting vector***

is a power density, the total power crossing a closed surface can be obtained by integrating the normal component of the Poynting vector over the entire surface. In equation form

$$\mathcal{P} = \oint_S \mathcal{W} \cdot ds = \oint_S \mathcal{W} \cdot \hat{\mathbf{n}} da \quad (2-4)$$

$\mathcal{P}$  = instantaneous total power (W)

$\hat{\mathbf{n}}$  = unit vector normal to the surface

$da$  = infinitesimal area of the closed surface (m<sup>2</sup>)

For applications of time-varying fields, it is often more desirable to find the average power density which is obtained by integrating the instantaneous Poynting vector over one period and dividing by the period. For time-harmonic variations of the form  $e^{j\omega t}$ , we define the complex fields  $\mathbf{E}$  and  $\mathbf{H}$  which are related to their instantaneous counterparts  $\mathcal{E}$  and  $\mathcal{H}$  by

which are related to their instantaneous counterparts  $\mathcal{E}$  and  $\mathcal{H}$  by

$$\mathcal{E}(x, y, z; t) = \text{Re}[\mathbf{E}(x, y, z)e^{j\omega t}] \quad (2-5)$$

$$\mathcal{H}(x, y, z; t) = \text{Re}[\mathbf{H}(x, y, z)e^{j\omega t}] \quad (2-6)$$

Using the definitions of (2-5) and (2-6) and the identity  $\text{Re}[\mathbf{E}e^{j\omega t}] = \frac{1}{2}[\mathbf{E}e^{j\omega t} + \mathbf{E}^*e^{-j\omega t}]$ , (2-3) can be written as (the instantaneous Poynting vector)

$$\mathcal{W} = \mathcal{E} \times \mathcal{H} = \frac{1}{2}\text{Re}[\mathbf{E} \times \mathbf{H}^*] + \frac{1}{2}\text{Re}[\mathbf{E} \times \mathbf{H}e^{j2\omega t}] \quad (2-7)$$

The first term of (2-7) is not a function of time, and the time variations of the second are twice the given frequency. The time average Poynting vector (average power density) can be written as

$$\mathbf{W}_{\text{av}}(x, y, z) = [\mathcal{W}(x, y, z; t)]_{\text{av}} = \frac{1}{2}\text{Re}[\mathbf{E} \times \mathbf{H}^*] \quad (\text{W/m}^2) \quad (2-8)$$

The  $\frac{1}{2}$  factor appears in (2-7) and (2-8) because the  $\mathbf{E}$  and  $\mathbf{H}$  fields represent peak values, and it should be omitted for RMS values. A close observation of (2-8) may raise a question. If the real part of  $(\mathbf{E} \times \mathbf{H}^*)/2$  represents the average (real) power density, what does the imaginary part of the same quantity represent? At this point it will be very natural to assume that the imaginary part must represent the reactive (stored)

power density associated with the electromagnetic fields. In later chapters, it will be shown that the power density associated with the electromagnetic fields of an antenna in its far-field region is predominately real and will be referred to as *radiation density*. Based upon the definition of (2-8), the average power radiated by an antenna (radiated power) can be written as

$$\begin{aligned}
 P_{\text{rad}} = P_{\text{av}} &= \iint_S \mathbf{W}_{\text{rad}} \cdot d\mathbf{s} = \iint_S \mathbf{W}_{\text{av}} \cdot \hat{\mathbf{n}} da \\
 &= \frac{1}{2} \iint_S \text{Re}(\mathbf{E} \times \mathbf{H}^*) \cdot d\mathbf{s}
 \end{aligned}
 \tag{2-9}$$

The power pattern of the antenna, whose definition was discussed in Section 2.2, is just a measure, as a function of direction, of the average power density radiated by the antenna. The observations are usually made on a large sphere of constant radius extending into the far field. In practice, absolute power patterns are usually not desired. However, the performance of the antenna is measured in terms of the gain (to be discussed in a subsequent section) and in terms of relative power patterns. Three-dimensional patterns cannot be measured, but they can be constructed with a number of two dimensional cuts.

### Example 2.2

The radial component of the radiated power density of an antenna is given by

$$\mathbf{W}_{\text{rad}} = \hat{\mathbf{a}}_r W_r = \hat{\mathbf{a}}_r A_0 \frac{\sin \theta}{r^2} \quad (\text{W/m}^2)$$

where  $A_0$  is the peak value of the power density,  $\theta$  is the usual spherical coordinate, and  $\hat{\mathbf{a}}_r$  is the radial unit vector. Determine the total radiated power.

*Solution:* For a closed surface, a sphere of radius  $r$  is chosen. To find the total radiated power, the radial component of the power density is integrated over its surface. Thus

$$\begin{aligned} P_{\text{rad}} &= \oiint_S \mathbf{W}_{\text{rad}} \cdot \hat{\mathbf{n}} \, da \\ &= \int_0^{2\pi} \int_0^\pi \left( \hat{\mathbf{a}}_r A_0 \frac{\sin \theta}{r^2} \right) \cdot (\hat{\mathbf{a}}_r r^2 \sin \theta \, d\theta \, d\phi) = \pi^2 A_0 \quad (\text{W}) \end{aligned}$$

A three-dimensional normalized plot of the average power density at a distance of  $r = 1$  m is shown in Figure 2.6.

**An isotropic radiator** is *an ideal source that radiates equally in all directions*. Although it does not exist in practice, it provides a convenient isotropic reference with which to compare other antennas. Because of its symmetric radiation, its Poynting vector will not be a function of the spherical coordinate angles  $\theta$  and  $\phi$ . In addition, it will have only a radial component. **Thus the total power radiated by it is given by**

$$P_{\text{rad}} = \oiint_S \mathbf{W}_0 \cdot d\mathbf{s} = \int_0^{2\pi} \int_0^\pi [\hat{\mathbf{a}}_r W_0(r)] \cdot [\hat{\mathbf{a}}_r r^2 \sin \theta \, d\theta \, d\phi] = 4\pi r^2 W_0 \quad (2-10)$$

and the power density by which is uniformly distributed over the surface of a sphere of radius  $r$ .

$$\mathbf{W}_0 = \hat{\mathbf{a}}_r W_0 = \hat{\mathbf{a}}_r \left( \frac{P_{\text{rad}}}{4\pi r^2} \right) \quad (\text{W/m}^2) \quad (2-11)$$

## 2.4 RADIATION INTENSITY

Radiation intensity in a given direction is defined as “the power radiated from an antenna per unit solid angle.” The radiation intensity is a far-field parameter, and it can be obtained by simply multiplying the radiation density by the square of the distance. In mathematical form it is expressed as

$$U = r^2 W_{\text{rad}} \quad (2-12)$$

where

$U$  = radiation intensity (W/unit solid angle)

$W_{\text{rad}}$  = radiation density (W/m<sup>2</sup>)

The radiation intensity is also related to the far-zone electric field of an antenna, referring to Figure 2.4, by

$$\begin{aligned} U(\theta, \phi) &= \frac{r^2}{2\eta} |\mathbf{E}(r, \theta, \phi)|^2 \simeq \frac{r^2}{2\eta} [ |E_{\theta}(r, \theta, \phi)|^2 + |E_{\phi}(r, \theta, \phi)|^2 ] \\ &\simeq \frac{1}{2\eta} [ |E_{\theta}^{\circ}(\theta, \phi)|^2 + |E_{\phi}^{\circ}(\theta, \phi)|^2 ] \end{aligned} \quad (2-12a)$$

Where

$\mathbf{E}(r, \theta, \phi)$  = far-zone electric-field intensity of the antenna =  $\mathbf{E}^{\circ}(\theta, \phi) \frac{e^{-jkr}}{r}$

$E_{\theta}, E_{\phi}$  = far-zone electric-field components of the antenna

$\eta$  = intrinsic impedance of the medium

The radial electric-field component ( $Er$ ) is assumed, if present, to be small in the far zone. Thus the power pattern is also a measure of the radiation intensity. The total power is obtained by integrating the radiation intensity, as given by (2-12), over the entire solid angle of  $4\pi$ . Thus

$$P_{\text{rad}} = \oint_{\Omega} U d\Omega = \int_0^{2\pi} \int_0^{\pi} U \sin \theta d\theta d\phi \quad (2-13)$$

where  $d\Omega = \text{element of solid angle} = \sin\theta d\theta d\phi$ .

For an isotropic source  $U$  will be independent of the angles  $\theta$  and  $\phi$ , as was the case for  $W_{\text{rad}}$ . Thus (2-13) can be written as

$$P_{\text{rad}} = \oint_{\Omega} U_0 d\Omega = U_0 \oint_{\Omega} d\Omega = 4\pi U_0 \quad (2-14)$$

### Example 2.3

For the problem of Example 2.2, find the total radiated power using (2-13).

*Solution:* Using (2-12)

$$U = r^2 W_{\text{rad}} = A_0 \sin \theta$$

and by (2-13)

$$P_{\text{rad}} = \int_0^{2\pi} \int_0^{\pi} U \sin \theta d\theta d\phi = A_0 \int_0^{2\pi} \int_0^{\pi} \sin^2 \theta d\theta d\phi = \pi^2 A_0$$

which is the same as that obtained in Example 2.2. A three-dimensional plot of the relative radiation intensity is also represented by Figure 2.6.

or the radiation intensity of an isotropic source as

$$U_0 = \frac{P_{\text{rad}}}{4\pi} \quad (2-15)$$

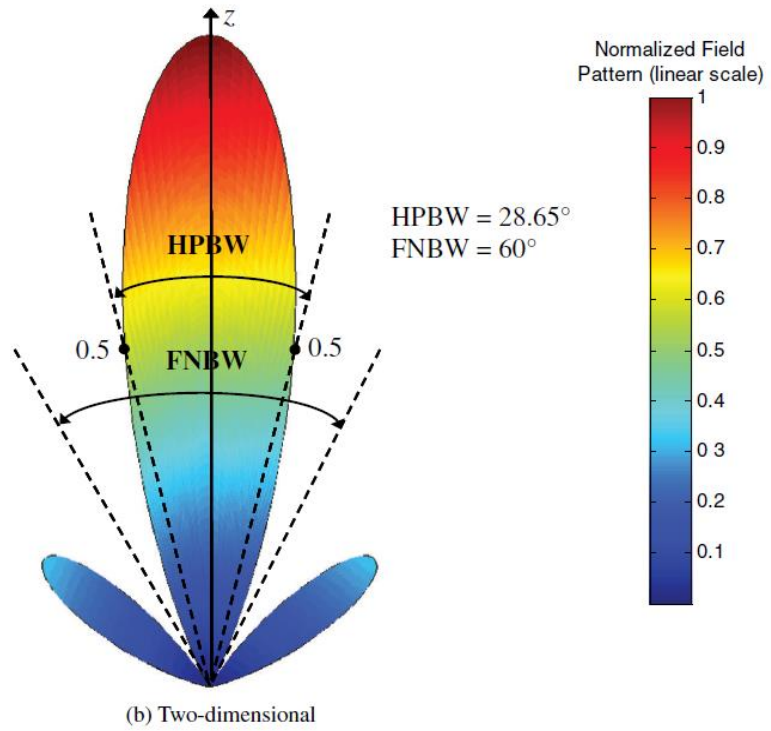
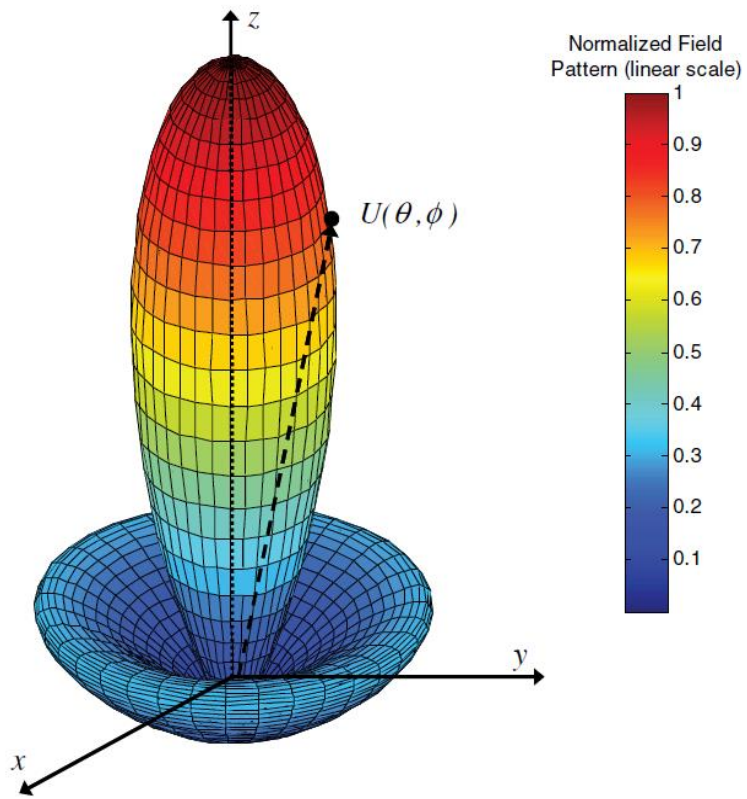


Figure 2.11 Three- and two-dimensional power patterns (in linear scale) of  $U(\theta) = \cos^2(\theta) \cos^2(3\theta)$ .

## 2.5 BEAMWIDTH

Associated with the pattern of an antenna is a parameter designated as *beamwidth*. The *beamwidth* of a pattern is defined as the angular separation between two identical points on opposite side of the pattern maximum.

In an antenna pattern, there are a number of beamwidths. One of the most widely used beamwidths is

- **The Half-Power Beamwidth (HPBW)**, which is defined by IEEE as: “In a plane containing the direction of the maximum of a beam, the angle between the two directions in which the radiation intensity is one-half value of the beam.” This is demonstrated in Figure 2.2.
- Another important beamwidth is the angular separation between the first nulls of the pattern, and it is referred to as the *First-Null Beamwidth (FNBW)*.
- Both the *HPBW* and *FNBW* are demonstrated for the pattern in Figure 2.11 for the pattern of Example 2.4.
- Other beamwidths are those where the pattern is  $-10$  dB from the maximum, or any other value.
- However, in practice, **the term *beamwidth*, with no other identification, usually refers to HPBW.**
  - The beamwidth of an antenna is a very important figure of merit and often is used as a trade-off between it and the side lobe level; that is, as the beamwidth decreases, the side lobe increases and vice versa.
  - In addition, the beamwidth of the antenna is also used to describe the resolution capabilities of the antenna to distinguish between two adjacent radiating sources or radar targets.
  - The most common resolution criterion states that *the resolution capability of an antenna to distinguish between two sources is equal to half the first-null beamwidth (FNBW/2), which is usually used to approximate the half-power beamwidth (HPBW) [5], [6].* That is, two sources separated by angular distances equal or greater than  $FNBW/2 \approx HPBW$  of an antenna with a uniform distribution **can be resolved**. If the separation is smaller, then the antenna will tend to smooth the angular separation distance.

### Example 2.4

The normalized radiation intensity of an antenna is represented by

$$U(\theta) = \cos^2(\theta) \cos^2(3\theta), \quad (0 \leq \theta \leq 90^\circ, \quad 0^\circ \leq \phi \leq 360^\circ)$$

The three- and two-dimensional plots of this, plotted in a linear scale, are shown in Figure 2.11. Find the

- half-power beamwidth HPBW (in radians and degrees)
- first-null beamwidth FNBW (in radians and degrees)

*Solution:*

- Since the  $U(\theta)$  represents the *power* pattern, to find the half-power beamwidth you set the function equal to half of its maximum, or

$$U(\theta)|_{\theta=\theta_h} = \cos^2(\theta) \cos^2(3\theta)|_{\theta=\theta_h} = 0.5 \Rightarrow \cos \theta_h \cos 3\theta_h = 0.707$$
$$\theta_h = \cos^{-1} \left( \frac{0.707}{\cos 3\theta_h} \right)$$

Since this is an equation with transcendental functions, it can be solved iteratively. After a few iterations, it is found that

$$\theta_h \approx 0.25 \text{ radians} = 14.325^\circ$$

Since the function  $U(\theta)$  is symmetrical about the maximum at  $\theta = 0$ , then the HPBW is

$$\text{HPBW} = 2\theta_h \approx 0.50 \text{ radians} = 28.65^\circ$$

- To find the first-null beamwidth (FNBW), you set the  $U(\theta)$  equal to zero, or

$$U(\theta)|_{\theta=\theta_n} = \cos^2(\theta) \cos^2(3\theta)|_{\theta=\theta_n} = 0$$

This leads to two solutions for  $\theta_n$ .

$$\cos \theta_n = 0 \Rightarrow \theta_n = \cos^{-1}(0) = \frac{\pi}{2} \text{ radians} = 90^\circ$$

$$\cos 3\theta_n = 0 \Rightarrow \theta_n = \frac{1}{3} \cos^{-1}(0) = \frac{\pi}{6} \text{ radians} = 30^\circ$$

The one with the smallest value leads to the FNBW. Again, because of the symmetry of the pattern, the FNBW is

$$\text{FNBW} = 2\theta_n = \frac{\pi}{3} \text{ radians} = 60^\circ$$

## 2.6 DIRECTIVITY

Basically **the term *directivity*** in the new 1983 version **has been used to replace** the term *directive gain* of the old 1973 version. Therefore *directivity of an antenna* **defined as** “the ratio of the radiation intensity in a given direction from the antenna to the radiation intensity averaged over all directions. The average radiation intensity is equal to the total power radiated by the antenna divided by  $4\pi$ . If the direction is not specified, the direction of maximum radiation intensity is implied.” Stated more simply, the directivity of a nonisotropic source is equal to the ratio of its radiation intensity in a given direction over that of an isotropic source. In mathematical form, using (2-15), it can be written as

$$D = \frac{U}{U_0} = \frac{4\pi U}{P_{\text{rad}}} \quad (2-16)$$

If the direction is not specified, it implies the direction of maximum radiation intensity (maximum directivity) expressed as

$$D_{\text{max}} = D_0 = \frac{U|_{\text{max}}}{U_0} = \frac{U_{\text{max}}}{U_0} = \frac{4\pi U_{\text{max}}}{P_{\text{rad}}} \quad (2-16a)$$

$D$  = directivity (dimensionless)

$D_0$  = maximum directivity (dimensionless)

$U$  = radiation intensity (W/unit solid angle)

$U_{\text{max}}$  = maximum radiation intensity (W/unit solid angle)

$U_0$  = radiation intensity of isotropic source (W/unit solid angle)

$P_{\text{rad}}$  = total radiated power (W)

**For an isotropic source, it is very obvious from (2-16) or (2-16a) that the directivity is unity since  $U$ ,  $U_{\text{max}}$ , and  $U_0$  are all equal to each other.**

For antennas with **orthogonal polarization components**, we define the *partial directivity of an antenna for a given polarization in a given direction* as “*that part of the radiation intensity corresponding to a given polarization divided by the total radiation intensity averaged over all directions.*” With this definition for the partial directivity, then **in a given direction** “*the total directivity is the sum of the partial directivities for any two orthogonal polarizations.*” For a spherical coordinate system, the total maximum directivity  $D_0$  for the orthogonal  $\theta$  and  $\phi$  components of an antenna can be written as

$$D_0 = D_\theta + D_\phi \quad (2-17)$$

while the partial directivities  $D_\theta$  and  $D_\phi$  are expressed as

$$D_\theta = \frac{4\pi U_\theta}{(P_{\text{rad}})_\theta + (P_{\text{rad}})_\phi} \quad (2-17a)$$

$$D_\phi = \frac{4\pi U_\phi}{(P_{\text{rad}})_\theta + (P_{\text{rad}})_\phi} \quad (2-17b)$$

**where**

$U_\theta$  = radiation intensity in a given direction contained in  $\theta$  field component

$U_\phi$  = radiation intensity in a given direction contained in  $\phi$  field component

$(P_{\text{rad}})_\theta$  = radiated power in all directions contained in  $\theta$  field component

$(P_{\text{rad}})_\phi$  = radiated power in all directions contained in  $\phi$  field component

### Example 2.5

As an illustration, find the maximum directivity of the antenna whose radiation intensity is that of Example 2.2. Write an expression for the directivity as a function of the directional angles  $\theta$  and  $\phi$ .

*Solution:* The radiation intensity is given by

$$U = r^2 W_{\text{rad}} = A_0 \sin \theta$$

The maximum radiation is directed along  $\theta = \pi/2$ . Thus

$$U_{\text{max}} = A_0$$

In Example 2.2 it was found that

$$P_{\text{rad}} = \pi^2 A_0$$

Using (2-16a), we find that the maximum directivity is equal to

$$D_0 = \frac{4\pi U_{\text{max}}}{P_{\text{rad}}} = \frac{4}{\pi} = 1.27$$

Since the radiation intensity is only a function of  $\theta$ , the directivity as a function of the directional angles is represented by

$$D = D_0 \sin \theta = 1.27 \sin \theta$$

Before proceeding with a more general discussion of directivity, it may be proper at this time to consider another example, compute its directivity, compare it with that of the previous example, and comment on what it actually represents. This may give the reader a better understanding and appreciation of the directivity.

### Example 2.6

The radial component of the radiated power density of an infinitesimal linear dipole of length  $l \ll \lambda$  is given by

$$W_{\text{av}} = \hat{\mathbf{a}}_r W_r = \hat{\mathbf{a}}_r A_0 \frac{\sin^2 \theta}{r^2} \quad (\text{W/m}^2)$$

where  $A_0$  is the peak value of the power density,  $\theta$  is the usual spherical coordinate, and  $\hat{\mathbf{a}}_r$  is the radial unit vector. Determine the maximum directivity of the antenna and express the directivity as a function of the directional angles  $\theta$  and  $\phi$ .

*Solution:* The radiation intensity is given by

$$U = r^2 W_r = A_0 \sin^2 \theta$$

The maximum radiation is directed along  $\theta = \pi/2$ . Thus

$$U_{\text{max}} = A_0$$

The total radiated power is given by

$$P_{\text{rad}} = \oiint_{\Omega} U d\Omega = A_0 \int_0^{2\pi} \int_0^{\pi} \sin^2 \theta \sin \theta d\theta d\phi = A_0 \left( \frac{8\pi}{3} \right)$$

Using (2-16a), we find that the maximum directivity is equal to

$$D_0 = \frac{4\pi U_{\text{max}}}{P_{\text{rad}}} = \frac{4\pi A_0}{\frac{8\pi}{3}(A_0)} = \frac{3}{2}$$

which is greater than 1.27 found in Example 2.5. Thus the directivity is represented by

$$D = D_0 \sin^2 \theta = 1.5 \sin^2 \theta$$

At this time, it will be proper to comment on the results of Examples 2.5 and 2.6. To better understand the discussion, we have plotted in Figure 2.12 the relative radiation intensities of Example 2.5 ( $U = A_0 \sin \theta$ ) and Example 2.6 ( $U = A_0 \sin^2 \theta$ ) where  $A_0$  was set equal to unity. We see that both patterns are omnidirectional but that of Example 2.6 has more directional characteristics (is narrower) in the elevation plane. **Since the directivity is a “figure of merit” describing how well the radiator directs energy in a certain direction, it should be convincing from Figure 2.12 that the directivity of Example 2.6 should be higher than that of Example 2.5.**

To demonstrate the significance of directivity, let us consider another example; in particular, let us examine the directivity of a half-wavelength dipole ( $l = \lambda/2$ ), which is derived in Section 4.6 of Chapter 4 and can be approximated by

$$D = D_0 \sin^3 \theta = 1.67 \sin^3 \theta \quad (2-18)$$

since it can be shown that [see Figure 4.12(b)]

$$\sin^3 \theta \simeq \left[ \frac{\cos \left( \frac{\pi}{2} \cos \theta \right)}{\sin \theta} \right]^2 \quad (2-18a)$$

where  $\theta$  is measured from the axis along the length of the dipole. The values represented by (2-18) and those of an isotropic source ( $D=1$ ) are plotted two- and three-dimensionally in Figure 2.13(a, b). For the three-dimensional graphical representation of Figure 2.13(b), at each observation point only the largest value of the two directivities is plotted. It is apparent that when

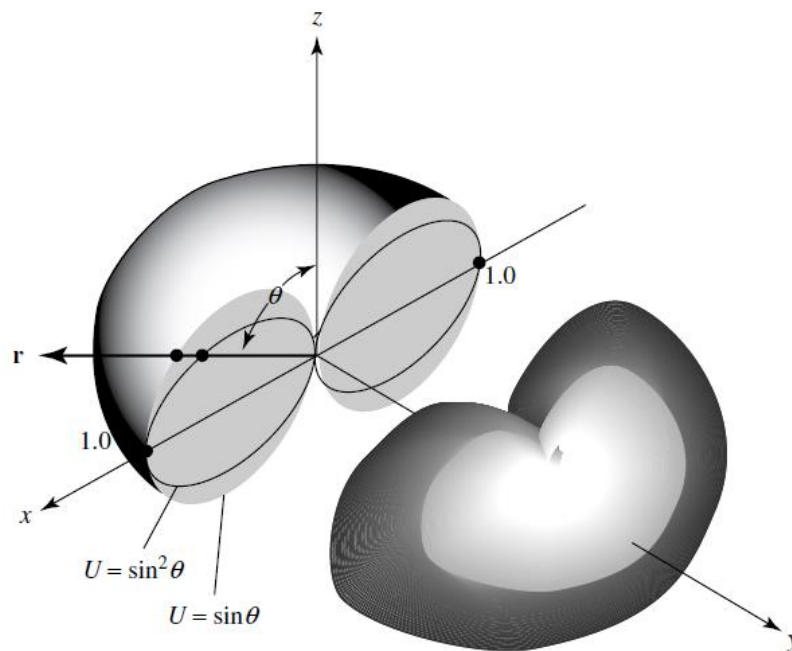


**Figure 2.12** Three-dimensional radiation intensity patterns. (SOURCE: P. Lorrain and D. R. Corson, *Electromagnetic Fields and Waves*, 2nd ed., W. H. Freeman and Co. Copyright © 1970).

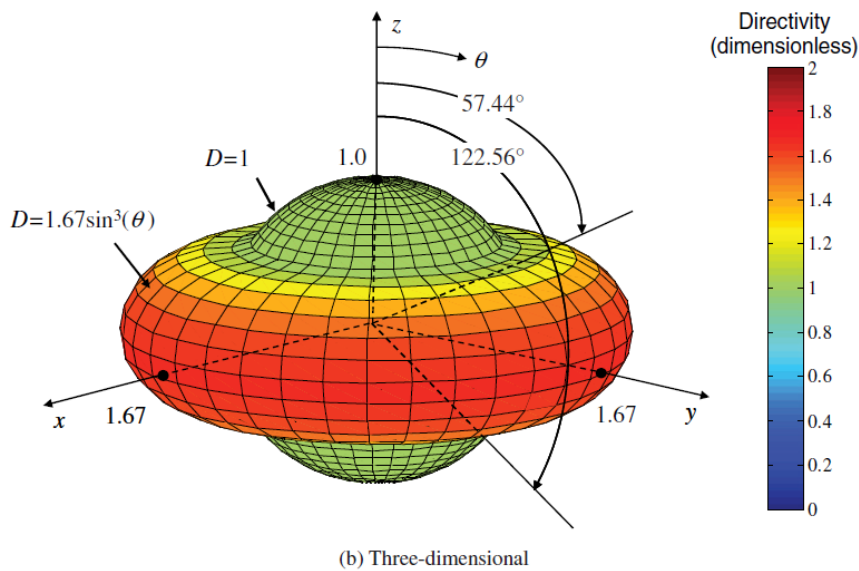
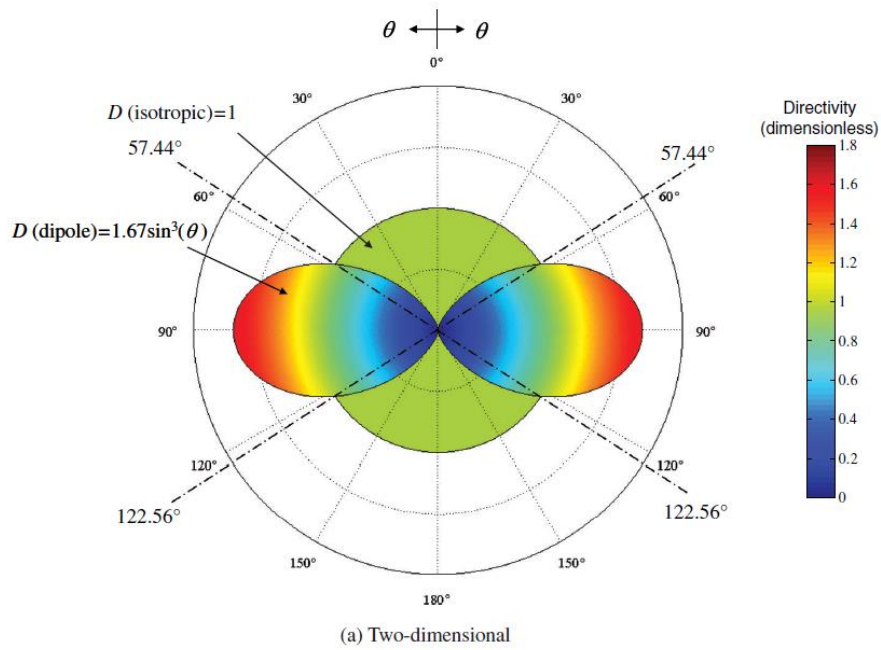


**Figure 2.13** Two- and three-dimensional directivity patterns of a  $\lambda/2$  dipole. (SOURCE: C. A. Balanis, "Antenna Theory: A Review." *Proc. IEEE*, Vol. 80, No. 1, January 1992. © 1992 IEEE).

$\sin^{-1}(1/1.67)^{1/3} = 57.44^\circ < \theta < 122.56^\circ$ , the dipole radiator **has greater directivity (greater intensity concentration) in those directions than that of an isotropic source.** Outside this range of angles, the isotropic radiator has higher directivity (more intense radiation). The maximum directivity of the dipole (relative to the isotropic radiator) occurs when  $\theta = \pi/2$ , and it is 1.67 (or 2.23 dB) more intense than that of the isotropic radiator (with the same radiated power).

The directivity of an isotropic source is unity since its power is radiated equally well in all directions. *For all other sources, the maximum directivity will always be greater than unity, and it is a relative “figure of merit” which gives an indication of the directional properties of the antenna as compared with those of an isotropic source.* In equation form, this is indicated in (2-16a). The directivity can be smaller than unity; in fact it can be equal to zero. For Examples 2.5 and 2.6, the directivity is equal to zero in the  $\theta = 0$  direction. *The values of directivity will be equal to or greater than zero and equal to or less than the maximum directivity ( $0 \leq D \leq D_0$ ).*

A more general expression for the directivity can be developed to include sources with radiation patterns that may be functions of both spherical coordinate angles  $\theta$  and  $\phi$ . In the previous examples we considered intensities that were represented by only one coordinate angle  $\theta$ , in order not to obscure the fundamental concepts by the mathematical details. So it may now be proper, since the basic definitions have been illustrated by simple examples, to formulate the more general expressions.

Let the radiation intensity of an antenna be of the form

$$U = B_0 F(\theta, \phi) \simeq \frac{1}{2\eta} \left[ |E_\theta^0(\theta, \phi)|^2 + |E_\phi^0(\theta, \phi)|^2 \right] \quad (2-19)$$

where  $B_0$  is a constant, and  $E_\theta^0$  and  $E_\phi^0$  are the antenna's far-zone electric-field components. The maximum value of (2-19) is given by

$$U_{\max} = B_0 F(\theta, \phi)|_{\max} = B_0 F_{\max}(\theta, \phi) \quad (2-19a)$$

The total radiated power is found using

$$P_{\text{rad}} = \oiint_{\Omega} U(\theta, \phi) d\Omega = B_0 \int_0^{2\pi} \int_0^\pi F(\theta, \phi) \sin \theta d\theta d\phi \quad (2-20)$$

We now write the general expression for the directivity and maximum directivity using (2-16) and (2-16a), respectively, as

$$D(\theta, \phi) = 4\pi \frac{F(\theta, \phi)}{\int_0^{2\pi} \int_0^\pi F(\theta, \phi) \sin \theta d\theta d\phi} \quad (2-21)$$

$$D_0 = 4\pi \frac{F(\theta, \phi)|_{\max}}{\int_0^{2\pi} \int_0^\pi F(\theta, \phi) \sin \theta \, d\theta \, d\phi} \quad (2-22)$$

Dividing by  $F(\theta, \phi)|_{\max}$  merely normalizes the radiation intensity  $F(\theta, \phi)$ , and it makes its maximum value unity.

*The beam solid angle  $\Omega_A$  is defined as the solid angle through which all the power of the antenna would flow if its radiation intensity is constant (and equal to the maximum value of  $U$ ) for all angles within  $\Omega_A$*

$$D_0 = \frac{4\pi}{\left[ \int_0^{2\pi} \int_0^\pi F(\theta, \phi) \sin \theta \, d\theta \, d\phi \right] / F(\theta, \phi)|_{\max}} = \frac{4\pi}{\Omega_A} \quad (2-23)$$

where  $\Omega_A$  is the beam solid angle, and it is given by

$$\Omega_A = \frac{1}{F(\theta, \phi)|_{\max}} \int_0^{2\pi} \int_0^\pi F(\theta, \phi) \sin \theta \, d\theta \, d\phi = \int_0^{2\pi} \int_0^\pi F_n(\theta, \phi) \sin \theta \, d\theta \, d\phi \quad (2-24)$$

$$F_n(\theta, \phi) = \frac{F(\theta, \phi)}{F(\theta, \phi)|_{\max}} \quad (2-25)$$

### Example 2.7

The radiation intensity of the major lobe of many antennas can be adequately represented by

$$U = B_0 \cos^4 \theta$$

where  $B_0$  is the maximum radiation intensity. The radiation intensity exists only in the upper hemisphere ( $0 \leq \theta \leq \pi/2$ ,  $0 \leq \phi \leq 2\pi$ ), and it is shown in Figure 2.15.

Find the

- beam solid angle; exact and approximate.
- maximum directivity; exact using (2-23) and approximate using (2-26).

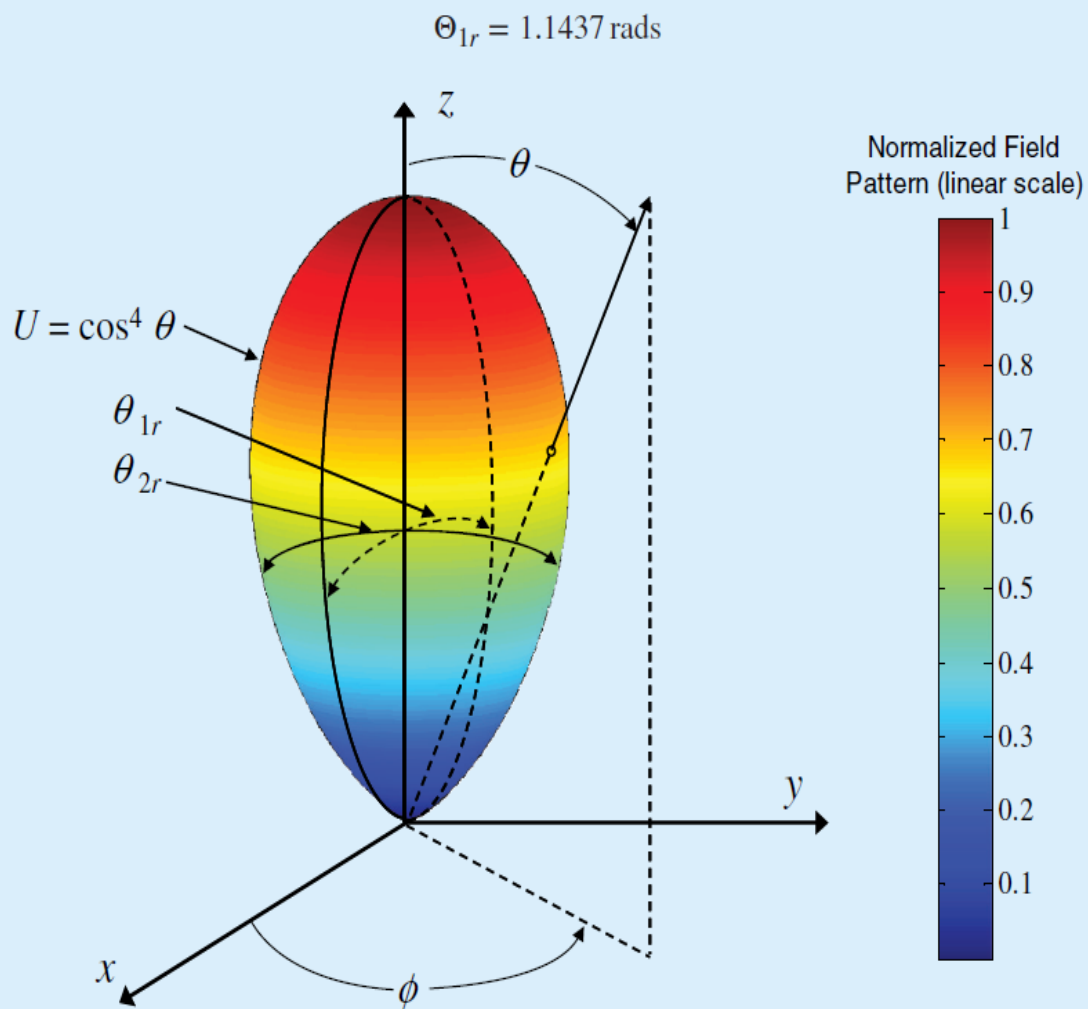


Figure 2.15 Radiation intensity pattern of the form  $U = \cos^4 \theta$  in the upper hemisphere.

Since the pattern is independent of the  $\phi$  coordinate, the beamwidth in the other plane is also equal to

$$\Theta_{2r} = 1.1437 \text{ rads}$$

a. *Beam solid angle*  $\Omega_A$ :

Exact: Using (2-24), (2-25)

$$\begin{aligned}\Omega_A &= \int_0^{360^\circ} \int_0^{90^\circ} \cos^4 \theta \, d\Omega = \int_0^{2\pi} \int_0^{\pi/2} \cos^4 \theta \sin \theta \, d\theta \, d\phi \\ &= \int_0^{2\pi} d\phi \int_0^{\pi/2} \cos^4 \theta \sin \theta \, d\theta \\ &= 2\pi \int_0^{\pi/2} \cos^4 \theta \sin \theta \, d\theta = \frac{2\pi}{5} \text{ steradians}\end{aligned}$$

Approximate: Using (2-26a)

$$\Omega_A \approx \Theta_{1r} \Theta_{2r} = 1.1437(1.1437) = (1.1437)^2 = 1.308 \text{ steradians}$$

b. *Directivity*  $D_0$ :

$$\text{Exact: } D_0 = \frac{4\pi}{\Omega_A} = \frac{4\pi(5)}{2\pi} = 10 \text{ (dimensionless)} = 10 \text{ dB}$$

The same exact answer is obtained using (2-16a).

$$\text{Approximate: } D_0 \approx \frac{4\pi}{\Omega_A} = \frac{4\pi}{1.308} = 9.61 \text{ (dimensionless)} = 9.83 \text{ dB}$$

The exact maximum directivity is 10 and its approximate value, using (2-26), is 9.61. Even better approximations can be obtained if the patterns have much narrower beamwidths, which will be demonstrated later in this section.

Many times it is desirable to express the directivity in decibels (dB) instead of dimensionless quantities. The expressions for converting the dimensionless quantities of directivity and maximum directivity to decibels (dB) are

$$D(\text{dB}) = 10 \log_{10}[D(\text{dimensionless})] \quad (2-28a)$$

$$D_0(\text{dB}) = 10 \log_{10}[D_0(\text{dimensionless})] \quad (2-28b)$$

## 2.8 ANTENNA EFFICIENCY

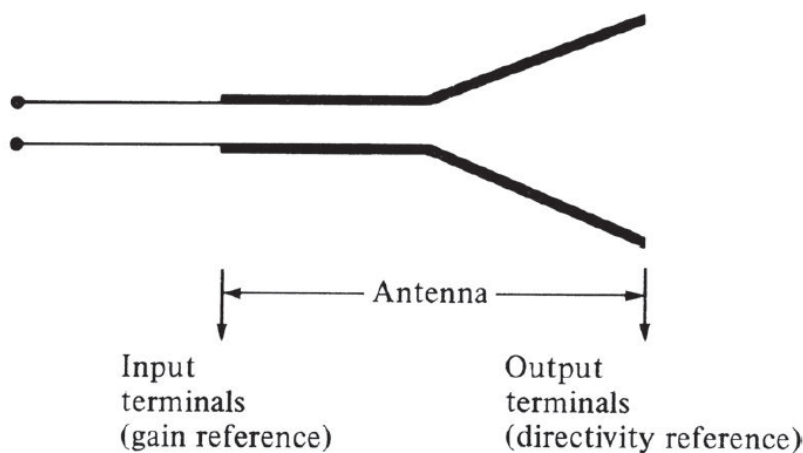
Associated with an antenna are a number of efficiencies and can be defined using Figure 2.22. The total antenna efficiency  $e_0$  is used to take into account losses at the input terminals and within the structure of the antenna. Such losses may be due, referring to Figure 2.22(b), to

1. reflections because of the mismatch between the transmission line and the antenna
2.  $I^2R$  losses (conduction and dielectric)

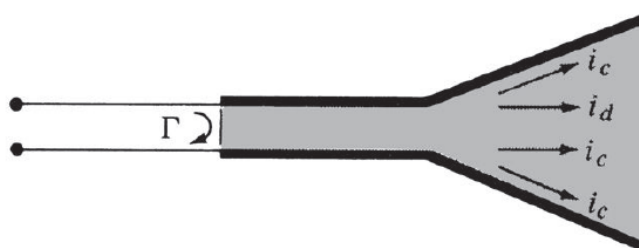
In general, the overall efficiency can be written as

$$e_0 = e_r e_c e_d$$

(2-44)



(a) Antenna reference terminals



(b) Reflection, conduction, and dielectric losses

**Figure 2.22** Reference terminals and losses of an antenna.

**Where:**

$e_0 =$  total efficiency (dimensionless)

$e_r =$  reflection (mismatch) efficiency =  $(1 - |\Gamma|^2)$  (dimensionless)

$e_c =$  conduction efficiency (dimensionless)

$e_d =$  dielectric efficiency (dimensionless)

$\Gamma =$  voltage reflection coefficient at the input terminals of the antenna

[ $\Gamma = (Z_{in} - Z_0)/(Z_{in} + Z_0)$  where  $Z_{in} =$  antenna input impedance,  $Z_0 =$  characteristic impedance of the transmission line]

$$\text{VSWR} = \text{voltage standing wave ratio} = \frac{1 + |\Gamma|}{1 - |\Gamma|}$$

Usually  $e_c$  and  $e_d$  are very difficult to compute, but they can be determined experimentally. Even by measurements they cannot be separated, and it is usually more convenient to write (2-44) as

$$e_0 = e_r e_{cd} = e_{cd}(1 - |\Gamma|^2) \quad (2-45)$$

where  $e_{cd} = e_c e_d =$  antenna radiation efficiency, which is used to relate the gain and directivity.

## 2.9 GAIN, REALIZED GAIN

Another useful figure-of-merit describing the performance of an antenna is the gain. Although the gain of the antenna is closely related to the directivity, it is a measure that takes into account the efficiency of the antenna as well as its directional capabilities. Remember that directivity is a measure that describes only the directional properties of the antenna, and it is therefore controlled only by the pattern.

Gain of an antenna (in a given direction) is defined as “the ratio of the intensity, in a given direction, to the radiation intensity that would be obtained if the power accepted by the antenna were radiated isotropically. The radiation intensity corresponding to the isotropically radiated power is equal to the power accepted (input) by the antenna divided by  $4\pi$ .” In equation form this can be expressed as

$$\text{Gain} = 4\pi \frac{\text{radiation intensity}}{\text{total input (accepted) power}} = 4\pi \frac{U(\theta, \phi)}{P_{in}} \quad (\text{dimensionless}) \quad (2-46)$$

In most cases we deal with relative gain, which is defined as “the ratio of the power gain in a given direction to the power gain of a reference antenna in its referenced direction.”

- The power input must be the same for both antennas.
- The reference antenna is usually a dipole, horn, or any other antenna whose gain can be calculated or it is known.
- In most cases, however, the reference antenna is a lossless isotropic source. Thus

$$G = \frac{4\pi U(\theta, \phi)}{P_{in}(\text{lossless isotropic source})} \quad (\text{dimensionless}) \quad (2-46a)$$

When the direction is not stated, the power gain is usually taken in the direction of maximum radiation.

Referring to Figure 2.22(a), we can write that the total radiated power ( $P_{rad}$ ) is related to the total input power ( $P_{in}$ ) by

$$P_{rad} = e_{cd} P_{in} \quad (2-47)$$

where  $e_{cd}$  is the antenna radiation efficiency (dimensionless) which is defined in (2-44), (2-45) and Section 2.14 by (2-90). According to the IEEE Standards, “gain does not include losses arising from impedance mismatches (reflection losses) and polarization mismatches (losses).”

In this edition of the book we define two gains; one, referred to as gain ( $G$ ), and the other, referred to as realized gain ( $G_{re}$ ), that also takes into account the reflection/mismatch losses represented in both (2-44) and (2-45).

Using (2-47) reduces (2-46a) to

$$G(\theta, \phi) = e_{cd} \left[ 4\pi \frac{U(\theta, \phi)}{P_{rad}} \right] \quad (2-48)$$

which is related to the directivity of (2-16) and (2-21) by

$$G(\theta, \phi) = e_{cd}D(\theta, \phi) \quad (2-49)$$

In a similar manner, **the maximum value of the gain is related to the maximum directivity** of (2-16a) and (2-23) by

$$G_0 = G(\theta, \phi)|_{\max} = e_{cd}D(\theta, \phi)|_{\max} = e_{cd}D_0 \quad (2-49a)$$

**While (2-47) does take into account the losses of the antenna element itself, it does not take into account the losses when the antenna element is connected to a transmission line, as shown in Figure 2.22.** These connection losses are usually referred to as **reflections (mismatch) losses**, and they are taken into account by introducing a **reflection (mismatch) efficiency  $e_r$** , which is related to the reflection coefficient as represented in (2-45) or  $e_r = (1 - |\Gamma|^2)$ . Thus, we can introduce a **realized gain  $G_{re}$**  that takes into account the reflection/mismatch losses (**due to the connection of the antenna element to the transmission line**), and it can be written as

$$\begin{aligned} G_{re}(\theta, \phi) &= e_r G(\theta, \phi) = (1 - |\Gamma|^2)G(\theta, \phi) \\ &= e_r e_{cd}D(\theta, \phi) = e_o D(\theta, \phi) \end{aligned} \quad (2-49b)$$

where  $e_o$  is the overall efficiency as defined in (2-44), (2-45). **Similarly, the maximum realized gain  $G_{re0}$  of (2-49a) is related to the maximum directivity  $D_0$  by**

$$\begin{aligned} G_{re0} &= G_{re}(\theta, \phi)|_{\max} = e_r G(\theta, \phi)|_{\max} = (1 - |\Gamma|^2)G(\theta, \phi)|_{\max} \\ &= e_r e_{cd}D(\theta, \phi)|_{\max} = e_o D(\theta, \phi)|_{\max} = e_o D_0 \end{aligned} \quad (2-49c)$$

If the antenna is matched to the transmission line, that is, the antenna input impedance  $Z_{in}$  is equal to the characteristic impedance  $Z_c$  of the line ( $|\Gamma| = 0$ ), then the two gains are equal ( $G_{re} = G$ ).

As was done with the directivity, we can define the partial gain of an antenna for a given polarization in a given direction as “that part of the radiation intensity corresponding to a given polarization divided by the total radiation intensity that would be obtained if the power accepted by the antenna were radiated isotropically.” With this definition for the partial gain, then, in a given direction, “the total gain is the sum of the partial gains for any two orthogonal polarizations.” For a spherical coordinate system, the total maximum gain  $G_0$  for the orthogonal  $\theta$  and  $\phi$  components of an antenna can be written, in a similar form as was the maximum directivity in (2-17)–(2-17b), as

$$G_0 = G_\theta + G_\phi \quad (2-50)$$

while the partial gains  $G_\theta$  and  $G_\phi$  are expressed as

$$G_\theta = \frac{4\pi U_\theta}{P_{in}} \quad (2-50a)$$

$$G_\phi = \frac{4\pi U_\phi}{P_{in}} \quad (2-50b)$$

where

$U_\theta$  = radiation intensity in a given direction contained in  $E_\theta$  field component

$U_\phi$  = radiation intensity in a given direction contained in  $E_\phi$  field component

$P_{in}$  = total input (accepted) power

In practice, whenever the term “gain” is used, it usually refers to the *maximum gain* as defined by (2-49a) or (2-49c).

Usually the gain is given in terms of decibels, instead of the dimensionless quantity of (2-49a). The conversion formula is

$$G_0(\text{dB}) = 10 \log_{10}[e_{cd} D_0 \text{ (dimensionless)}] \quad (2-52)$$

### Example 2.10

A lossless resonant half-wavelength dipole antenna, with input impedance of 73 ohms, is connected to a transmission line whose characteristic impedance is 50 ohms. Assuming that the pattern of the antenna is given approximately by

$$U = B_0 \sin^3 \theta$$

find the maximum realized gain of this antenna.

*Solution:* Let us first compute the maximum directivity of the antenna. For this

$$U|_{\max} = U_{\max} = B_0$$

$$P_{\text{rad}} = \int_0^{2\pi} \int_0^{\pi} U(\theta, \phi) \sin \theta \, d\theta \, d\phi = 2\pi B_0 \int_0^{\pi} \sin^4 \theta \, d\theta = B_0 \left( \frac{3\pi^2}{4} \right)$$

$$D_0 = 4\pi \frac{U_{\max}}{P_{\text{rad}}} = \frac{16}{3\pi} = 1.697$$

Since the antenna was stated to be lossless, then the radiation efficiency  $e_{cd} = 1$ .

Thus, the total maximum gain is equal to

$$G_0 = e_{cd} D_0 = 1(1.697) = 1.697$$

$$G_0(\text{dB}) = 10 \log_{10}(1.697) = 2.297$$

which is identical to the directivity because the antenna is lossless.

There is another loss factor which is not taken into account in the gain. That is the loss due to reflection or mismatch losses between the antenna (load) and the transmission line. This loss is accounted for by the reflection efficiency of (2-44) or (2-45), and it is equal to

$$e_r = (1 - |\Gamma|^2) = \left( 1 - \left| \frac{73 - 50}{73 + 50} \right|^2 \right) = 0.965$$

$$e_r(\text{dB}) = 10 \log_{10}(0.965) = -0.155$$

Therefore the overall efficiency is

$$e_0 = e_r e_{cd} = 0.965$$

$$e_0(\text{dB}) = -0.155$$

Thus, the overall losses are equal to 0.155 dB. The maximum realized gain is equal to

$$G_{re0} = e_0 D_0 = 0.965(1.697) = 1.6376$$

$$G_{re0}(\text{dB}) = 10 \log_{10}(1.6376) = 2.142$$

The gain in dB can also be obtained by converting the directivity and radiation efficiency in dB and then adding them. Thus,

$$e_{cd}(\text{dB}) = 10 \log_{10}(1.0) = 0$$

$$D_0(\text{dB}) = 10 \log_{10}(1.697) = 2.297$$

$$G_0(\text{dB}) = e_{cd}(\text{dB}) + D_0(\text{dB}) = 2.297$$

which is the same as obtained previously. The same procedure can be used for the realized gain.

## 2.10 BEAM EFFICIENCY

Another parameter that is frequently used to judge the quality of transmitting and receiving antennas is **the beam efficiency**. For an antenna with its major lobe directed along the  $z$ -axis ( $\theta = 0$ ), as shown in Figure 2.1(a), the beam efficiency (BE) is defined by

$$\text{BE} = \frac{\text{power transmitted (received) within cone angle } \theta_1}{\text{power transmitted (received) by the antenna}} \text{ (dimensionless)} \quad (2-53)$$

where  $\theta_1$  is the half-angle of the cone within which the percentage of the total power is to be found. Equation (2-53) can be written as

$$\text{BE} = \frac{\int_0^{2\pi} \int_0^{\theta_1} U(\theta, \phi) \sin \theta \, d\theta \, d\phi}{\int_0^{2\pi} \int_0^{\pi} U(\theta, \phi) \sin \theta \, d\theta \, d\phi} \quad (2-54)$$

If  $\theta_1$  is chosen as **the angle where the first null or minimum occurs** (see Figure 2.1), **then the beam efficiency will indicate the amount of power in the major lobe compared to the total power.** A very high beam efficiency (between the nulls or minima), usually in the high 90s, is necessary for antennas used in radiometry, astronomy, radar, and other applications where received signals through the minor lobes must be minimized. The beam efficiencies of some typical rectangular and circular aperture antennas will be discussed in Chapter 12.

## 2.11 BANDWIDTH

**The bandwidth of an antenna** is defined as “**the range of frequencies within which the performance of the antenna, with respect to some characteristic, conforms to a specified standard.**” The bandwidth can be considered to be the range of frequencies, on either side of a center frequency (usually the resonance frequency for a

dipole), where the antenna characteristics (such as input impedance, pattern, beamwidth, polarization, side lobe level, gain, beam direction, radiation efficiency) are within an acceptable value of those at the center frequency.

- For **broadband antennas**, the bandwidth is usually expressed as the ratio of the upper-to-lower frequencies of acceptable operation. For example, a 10:1 bandwidth indicates that the upper frequency is 10 times greater than the lower.
- For **narrowband antennas**, the bandwidth is expressed as a percentage of the frequency difference (upper minus lower) over the center frequency of the bandwidth. For example, a 5% bandwidth indicates that the frequency range of acceptable operation is 5% of the bandwidth center frequency.
- Because the characteristics (**input impedance, pattern, gain, polarization, etc.**) of an antenna do not necessarily vary in the same manner or are even critically affected by the frequency, there is no unique characterization of the bandwidth.
- **The specifications are set in each case to meet the needs of the particular application.**
- Usually there is a distinction made between **pattern and input impedance variations**. Accordingly, **pattern bandwidth and impedance bandwidth** are used to emphasize this distinction.
- Associated with **pattern bandwidth** are gain, side lobe level, beamwidth, polarization, and beam direction.
- while input impedance and radiation efficiency are related to **impedance bandwidth**.
- For example, the pattern of a linear dipole with overall length less than a half-wavelength ( $l < \lambda/2$ ) is basically insensitive to frequency.
- The limiting factor for this antenna is **its impedance**, and **its bandwidth can be formulated in terms of the  $Q$ .**
- The  $Q$  of antennas or arrays with dimensions large compared to the wavelength, excluding superdirective designs, is near unity. Therefore, the **bandwidth** is usually formulated in terms of **beamwidth, side lobe level, and pattern characteristics**.
- For **intermediate length antennas**, the bandwidth may be limited by either pattern or impedance variations, depending upon the particular application. For these antennas, a 2:1 bandwidth indicates a good design.

## 2.10 BEAM EFFICIENCY

Another parameter that is frequently used to judge the quality of transmitting and receiving antennas is **the beam efficiency**. For an antenna with its major lobe directed along the  $z$ -axis ( $\theta = 0$ ), as shown in Figure 2.1(a), the beam efficiency (BE) is defined by

$$\text{BE} = \frac{\text{power transmitted (received) within cone angle } \theta_1}{\text{power transmitted (received) by the antenna}} \text{ (dimensionless)} \quad (2-53)$$

where  $\theta_1$  is the half-angle of the cone within which the percentage of the total power is to be found. Equation (2-53) can be written as

$$\text{BE} = \frac{\int_0^{2\pi} \int_0^{\theta_1} U(\theta, \phi) \sin \theta \, d\theta \, d\phi}{\int_0^{2\pi} \int_0^{\pi} U(\theta, \phi) \sin \theta \, d\theta \, d\phi} \quad (2-54)$$

If  $\theta_1$  is chosen as **the angle where the first null or minimum occurs** (see Figure 2.1), **then the beam efficiency will indicate the amount of power in the major lobe compared to the total power.** A very high beam efficiency (between the nulls or minima), usually in the high 90s, is necessary for antennas used in radiometry, astronomy, radar, and other applications where received signals through the minor lobes must be minimized. The beam efficiencies of some typical rectangular and circular aperture antennas will be discussed in Chapter 12.

## 2.11 BANDWIDTH

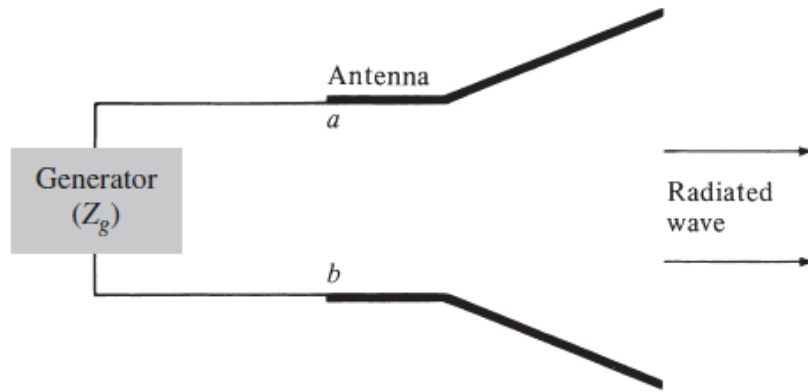
**The bandwidth of an antenna** is defined as “**the range of frequencies within which the performance of the antenna, with respect to some characteristic, conforms to a specified standard.**” The bandwidth can be considered to be **the range of frequencies, on either side of a center frequency (usually the resonance frequency for a**

dipole), where the antenna characteristics (such as input impedance, pattern, beamwidth, polarization, side lobe level, gain, beam direction, radiation efficiency) are within an acceptable value of those at the center frequency.

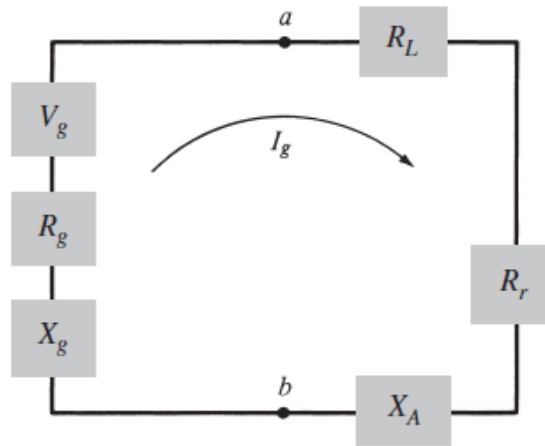
- For ***broadband antennas***, the bandwidth is usually expressed as the ratio of the upper-to-lower frequencies of acceptable operation. For example, a **10:1 bandwidth indicates that the upper frequency is 10 times greater than the lower.**
- For *narrowband antennas*, the bandwidth is expressed as a percentage of the frequency difference (upper minus lower) over the center frequency of the bandwidth. For example, a 5% bandwidth indicates that the frequency range of acceptable operation is 5% of the bandwidth center frequency.
- Because the characteristics (**input impedance, pattern, gain, polarization, etc.**) of an antenna do not necessarily vary in the same manner or are even critically affected by the frequency, there is no unique characterization of the bandwidth.
- **The specifications are set in each case to meet the needs of the particular application.**
- Usually there is a distinction made between **pattern and input impedance variations.** Accordingly, *pattern bandwidth* and *impedance bandwidth* are used to emphasize this distinction.
- Associated with *pattern bandwidth* are gain, side lobe level, beamwidth, polarization, and beam direction.
- while input impedance and radiation efficiency are related to impedance bandwidth.

## 2.13 INPUT IMPEDANCE

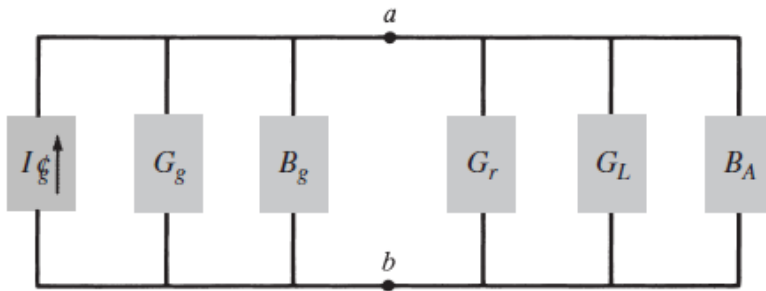
*Input impedance* is defined as “**the impedance presented by an antenna at its terminals or the ratio of the voltage to current at a pair of terminals or the ratio of the appropriate components of the electric to magnetic fields at a point.**” In this section we are primarily interested in the input impedance at a pair of terminals which are the input terminals of the antenna. In Figure 2.27(a) these terminals are designated as  $a - b$ .



(a) Antenna in transmitting mode



(b) Thevenin equivalent



(c) Norton equivalent

**Figure 2.27** Transmitting antenna and its equivalent circuits.

The ratio of the voltage to current at these terminals, with no load attached, defines the impedance of the antenna as

$$Z_A = R_A + jX_A \quad (2-72)$$

where

$Z_A$  = antenna impedance at terminals  $a-b$  (ohms)

$R_A$  = antenna resistance at terminals  $a-b$  (ohms)

$X_A$  = antenna reactance at terminals  $a-b$  (ohms)

In general, the resistive part of (2-72) consists of two components; that is

$$R_A = R_r + R_L \quad (2-73)$$

where

$R_r$  = radiation resistance of the antenna

$R_L$  = loss resistance of the antenna

The radiation resistance will be considered in more detail in later chapters, and it will be illustrated with examples.

If we assume that the antenna is attached to a generator with internal impedance

$$Z_g = R_g + jX_g \quad (2-74)$$

where

$R_g$  = resistance of generator impedance (ohms)

$X_g$  = reactance of generator impedance (ohms)

and the antenna is used in the transmitting mode, we can represent the antenna and generator by an equivalent circuit shown in Figure 2.27(b). To find the amount of power

delivered to  $R_r$  for radiation and the amount dissipated in  $R_L$  as heat ( $I^2 R_L/2$ ), we first find the current developed within the loop which is given by

$$I_g = \frac{V_g}{Z_t} = \frac{V_g}{Z_A + Z_g} = \frac{V_g}{(R_r + R_L + R_g) + j(X_A + X_g)} \quad (A) \quad (2-75)$$

and its magnitude by

$$|I_g| = \frac{|V_g|}{[(R_r + R_L + R_g)^2 + (X_A + X_g)^2]^{1/2}} \quad (2-75a)$$

where  $V_g$  is the peak generator voltage. The power delivered to the antenna for radiation is given by

$$P_r = \frac{1}{2} |I_g|^2 R_r = \frac{|V_g|^2}{2} \left[ \frac{R_r}{(R_r + R_L + R_g)^2 + (X_A + X_g)^2} \right] \quad (W) \quad (2-76)$$

and that dissipated as heat by

$$P_L = \frac{1}{2} |I_g|^2 R_L = \frac{|V_g|^2}{2} \left[ \frac{R_L}{(R_r + R_L + R_g)^2 + (X_A + X_g)^2} \right] \quad (W) \quad (2-77)$$

The remaining power is dissipated as heat on the internal resistance  $R_g$  of the generator, and it is given by

$$P_g = \frac{|V_g|^2}{2} \left[ \frac{R_g}{(R_r + R_L + R_g)^2 + (X_A + X_g)^2} \right] \quad (W) \quad (2-78)$$

The maximum power delivered to the antenna occurs when we have conjugate matching; that is when

$$R_r + R_L = R_g \quad (2-79)$$

$$X_A = -X_g \quad (2-80)$$

For this case

$$P_r = \frac{|V_g|^2}{2} \left[ \frac{R_r}{4(R_r + R_L)^2} \right] = \frac{|V_g|^2}{8} \left[ \frac{R_r}{(R_r + R_L)^2} \right] \quad (2-81)$$

$$P_L = \frac{|V_g|^2}{8} \left[ \frac{R_L}{(R_r + R_L)^2} \right] \quad (2-82)$$

$$P_g = \frac{|V_g|^2}{8} \left[ \frac{R_g}{(R_r + R_L)^2} \right] = \frac{|V_g|^2}{8} \left[ \frac{1}{R_r + R_L} \right] = \frac{|V_g|^2}{8R_g} \quad (2-83)$$

**Q1]** A hypothetical isotropic antenna is radiating in free-space. At a distance of 100 m from the antenna, the total electric field ( $\mathbf{E}_\theta$ ) is measured to be 5 V/m. Find the

- (a) power density ( $\mathbf{W}_{\text{rad}}$ ),  
 (b) power radiated ( $\mathbf{P}_{\text{rad}}$ ).

**Solution:**

$$(a) \quad \underline{W}_{\text{rad}} = \frac{1}{2}[\underline{E} \times \underline{H}^*] = \frac{E^2}{2\eta} \hat{a}_r = \frac{5^2 \hat{a}_r}{2(120\pi)} = 0.03315 \hat{a}_r \text{ watts/m}^2$$

$$(b) \quad P_{\text{rad}} = \oint_S W_{\text{rad}} dS = \int_0^{2\pi} \int_0^\pi (0.03315) (r^2 \sin\theta d\theta d\phi)$$

$$= \int_0^{2\pi} \int_0^\pi (0.03315) (100)^2 \sin\theta d\theta d\phi$$

$$= 2\pi (0.03315) (100)^2 \int_0^\pi \sin\theta d\theta = 2\pi (0.03315) (100)^2 \cdot 2$$

$$= 4165.75 \text{ watts}$$

**Q2]** The maximum radiation intensity of a 90% efficiency antenna is 200 mW/unit solid angle. Find the directivity and gain (dimensionless and in dB) when the:

- (a) input power is 125.66 mW,  
 (b) radiated power is 125.66 mW.

**Solution:**

Radiated power = input power X efficiency.

$$(a) \quad D_0 = \frac{4\pi U_{\text{max}}}{P_{\text{rad}}} = \frac{4\pi (200 \times 10^{-3})}{0.9 (125.66 \times 10^{-3})} = 22.22 = 13.47 \text{ dB}$$

$$G_0 = \epsilon_x \cdot D_0 = 0.9 (22.22) = 20 = 13.01 \text{ dB}$$

$$(b) \quad D_0 = \frac{4\pi U_{\text{max}}}{P_{\text{rad}}} = \frac{4\pi (200 \times 10^{-3})}{(125.66 \times 10^{-3})} = 20 = 13.01 \text{ dB}$$

$$G_0 = \epsilon_x \cdot D_0 = 0.9 \cdot (20) = 18 = 12.55 \text{ dB}$$

**Q3]** The normalized radiation intensity of a given antenna is given by  $U(\theta) = B_0 \cos^3(\theta)$ . If the total radiated power is equal to 10 Watts. Determine; (a) the maximum power density at a distance of 1km, (b) directivity and (c) gain.

$$U = B_0 \cos^3 \theta$$

$$(a) P_{rad} = \int_0^{2\pi} \int_0^{\pi/2} U \sin \theta d\theta d\phi = B_0 \int_0^{2\pi} \int_0^{\pi/2} \cos^3 \theta \sin \theta d\theta d\phi$$

$$= 2\pi B_0 \int_0^{\pi/2} \cos^3 \theta \sin \theta d\theta$$

$$P_{rad} = 2\pi B_0 \left( -\frac{\cos^4 \theta}{4} \right) \Big|_0^{\pi/2} = \frac{\pi}{2} B_0 = 10 \Rightarrow B_0 = \frac{20}{\pi} = 6.3662$$

$$U = 6.3662 \cos^3 \theta$$

$$W = \frac{U}{r^2} = \frac{6.3662}{r^2} \cos^3 \theta = \frac{6.3662}{(10^3)^2} \cdot \cos^3 \theta = 6.3662 \times 10^{-6} \cos^3 \theta$$

$$W|_{max} = 6.3662 \times 10^{-6} \cos^3 \theta \Big|_{max} = 6.3662 \times 10^{-6} \text{ Watts/m}^2$$

$$(b) D_0 = \frac{4\pi U_{max}}{P_{rad}} = \frac{4\pi (6.3662)}{10} = 8 = 9 \text{ dB}$$

$$(c) G_0 = e_t D_0 = 8 = 9 \text{ dB}$$

**Q4]** The normalized radiation intensity of a given antenna is  $U(\theta, \phi) = \sin \theta \sin \phi$ . The intensity exists only in the  $0 \leq \theta \leq \pi$ ,  $0 \leq \phi \leq \pi$  region, and it is zero elsewhere. Find the:  
 (a) exact directivity (dimensionless and in dB).  
 (b) azimuthal and elevation plane half-power beamwidths (in degrees).

$$D_0 = \frac{4\pi U_{max}}{P_{rad}}$$

$$(a) U = \sin \theta \sin \phi \quad \text{for } 0 \leq \theta \leq \pi, \quad 0 \leq \phi \leq \pi$$

$$U|_{max} = 1 \quad \text{and it occurs when } \theta = \phi = \pi/2.$$

$$P_{rad} = \int_0^{\pi} \int_0^{\pi} U \sin \theta d\theta d\phi = \int_0^{\pi} \sin \phi d\phi \int_0^{\pi} \sin^2 \theta d\theta = 2 \left( \frac{\pi}{2} \right) = \pi$$

$$\text{Thus } D_0 = \frac{4\pi (1)}{\pi} = 4 = 6.02 \text{ dB}$$

The half-power beamwidths are equal to

$$\text{HPBW (az.)} = 2 [90^\circ - \sin^{-1}(1/2)] = 2 (90^\circ - 30^\circ) = 120^\circ$$

$$\text{HPBW (el.)} = 2 [90^\circ - \sin^{-1}(1/2)] = 2 (90^\circ - 30^\circ) = 120^\circ$$

**In the azimuthal plane ( $\theta=90^\circ$ ) and in the elevation plane ( $\phi=90^\circ$ )**

**Q5]** In target-search ground-mapping radars it is desirable to have echo power received from a target, of constant cross section, to be independent of its range. For one such application, the desirable radiation intensity of the antenna is given by

$$U(\theta, \phi) = \left\{ \begin{array}{ll} 1 & 0^\circ \leq \theta \leq 20^\circ \\ 0.342 \csc(\theta) & 20^\circ \leq \theta \leq 60^\circ \\ 0 & 60^\circ \leq \theta \leq 180^\circ \end{array} \right\} \quad 0^\circ \leq \phi \leq 360^\circ$$

Find the directivity (in dB) using the exact formula.

**Solution:**

$$U(\theta, \phi) = \left\{ \begin{array}{ll} 1 & 0^\circ \leq \theta \leq 20^\circ \\ 0.342 \csc(\theta) & 20^\circ \leq \theta \leq 60^\circ \\ 0 & 60^\circ \leq \theta \leq 180^\circ \end{array} \right\} \quad 0^\circ \leq \phi \leq 360^\circ$$

$$P_{\text{rad}} = \int_0^{2\pi} \int_0^\pi U(\theta, \phi) \sin\theta \, d\theta \, d\phi = 2\pi \left[ \int_0^{20^\circ} \sin\theta \, d\theta + \int_{20^\circ}^{60^\circ} 0.342 \csc(\theta) \times \right.$$

$$\left. \sin\theta \, d\theta \right] = 2\pi \left\{ -\cos\theta \Big|_0^{\pi/9} + 0.342 \cdot \theta \Big|_{\pi/9}^{\pi/3} \right\}$$

$$= 2\pi \left\{ [-\cos(\frac{\pi}{9}) + 1] + 0.342 \left( \frac{\pi}{3} - \frac{\pi}{9} \right) \right\}$$

$$= 2\pi \left\{ [-0.93969 + 1] + 0.342 \pi \left( \frac{2}{9} \right) \right\}$$

$$= 2\pi \left\{ 0.06031 + 0.23876 \right\} = 1.87912$$

$$D_0 = \frac{4\pi U_{\text{max}}}{P_{\text{rad}}} = \frac{4\pi (1)}{1.87912} = 6.68737 = 8.25255 \text{ dB.}$$

**Q6]** The radiation intensity of an antenna is given by

$$U(\theta, \phi) = \cos^4 \theta \sin^2 \phi$$

for  $0 \leq \theta \leq \pi/2$  and  $0 \leq \phi \leq 2\pi$  (i.e., in the upper half-space). It is zero in the lower half-space. Find the:

- (a) exact directivity (dimensionless and in dB),  
 (b) elevation plane half-power beamwidth (in degrees).

**Solution:**

$$(a) \quad P_{\text{rad}} = \int_0^{2\pi} \int_0^{\pi} U(\theta, \phi) \sin \theta \, d\theta \, d\phi = \int_0^{2\pi} \sin^2 \phi \, d\phi \cdot \int_0^{\pi/2} \cos^4 \theta \sin \theta \, d\theta$$

$$= (\pi) \left(\frac{1}{5}\right) = \frac{\pi}{5}.$$

$$U_{\text{max}} = U(\theta=0^\circ, \phi=\pi/2) = 1.$$

$$D_0 = \frac{4\pi U_{\text{max}}}{P_{\text{rad}}} = \frac{4\pi}{(\pi/5)} = 20 = 13.0 \text{ dB}$$

(b) Elevation Plane:  $\theta$  varies,  $\phi$  fixed

→ choose  $\phi = \pi/2$ .

$$U(\theta, \phi=\pi/2) = \cos^4 \theta, \quad 0 \leq \theta \leq \pi/2.$$

$$\cos^4 \left[ \frac{\text{HPBW}(\text{el.})}{2} \right] = \frac{1}{2}$$

$$\text{HPBW}(\text{el.}) = 2 \cdot \cos^{-1} \{ \sqrt{0.5} \} = 65.5^\circ.$$

**Q7]** An antenna (1-m long dipole antenna is driven by a 150 MHz source) with a radiation resistance of 73 ohms, a loss resistance of 0.625 ohms, and a reactance of 42.5 ohms is connected to a generator with open-circuit voltage of 100 V and internal impedance of 50 ohms.

- Draw the equivalent circuit
- Determine the power supplied by the generator
- Determine the power radiated by the antenna
- the radiation efficiency of the antenna.

2-46  $f = 150 \text{ MHz}$ ,  $\lambda = 2 \text{ m}$   
 $\Rightarrow$  1 m dipole is  $\frac{\lambda}{2}$  in electrical length  
 $\Rightarrow R_r = 73 \Omega$ ,  $Z_{in} = 73 + j42.5 \Omega$

a.  $I_{ant} = \frac{V_s}{50 + 73 + 0.625 + j42.5} = 0.765 \angle -18.97^\circ \text{ A}$

b.  $P_{dissip} = P_{Loss} = \frac{1}{2} |I_{ant}|^2 R_{Loss} = 189 \text{ mW}$

c.  $P_{rad} = \frac{1}{2} |I_{ant}|^2 R_r = 21.36 \text{ W}$

d.  $e_{cd} = \frac{R_r}{R_r + R_{Loss}} = \frac{73 \times 100}{73 + 0.625} = 99 \%$

**Q8]** The E-field pattern of an antenna, varies as follows:

$$E = \begin{cases} 1 & 0^\circ \leq \theta \leq 45^\circ \\ 0 & 45^\circ < \theta \leq 90^\circ \\ \frac{1}{2} & 90^\circ < \theta \leq 180^\circ \end{cases}$$

- What is the directivity of this antenna?
- What is the radiation resistance of the antenna if the electric field at 200 m from it is equal to 10 V/m (rms) for  $\theta = 0^\circ$  and the terminal current is 5 A (rms)?

(a)  $U = \frac{r^2 E^2}{2\eta}$

$$U_{\max} = \frac{r^2}{\eta}$$

since the values of the E-field and current are given in rms values, then:

$$P_{\text{rad}} = \frac{r^2}{\eta} \int_0^{2\pi} d\phi \left[ \int_0^{45^\circ} \sin\theta d\theta + \int_{90^\circ}^{180^\circ} \frac{1}{4} \sin\theta d\theta \right]$$

$$= \frac{r^2}{\eta} [2\pi] \left[ -\cos\theta \Big|_0^{45^\circ} + \frac{1}{4} (-\cos\theta) \Big|_{90^\circ}^{180^\circ} \right]$$

$$= \frac{2r^2\pi}{\eta} \left[ -\cos 45^\circ + \cos 0^\circ - \frac{1}{4} \cos 180^\circ + \frac{1}{4} \cos 90^\circ \right]$$

$$P_{\text{rad}} = 0.54289 \frac{2\pi r^2}{\eta}$$

$$D = \frac{4\pi U_{\max}}{P_{\text{rad}}} = \frac{4\pi \frac{r^2}{\eta}}{0.54289 (2\pi) r^2 / \eta} = 3.684$$

(b) When the field is equal to 10 V/m, for  $\theta = 0^\circ$ .

$$\Rightarrow E = \begin{cases} 10 \text{ V/m} & 0 < \theta \leq 45^\circ \\ 0 & 45^\circ < \theta \leq 90^\circ \\ \frac{1}{2} \times 10 \text{ V/m} & 90^\circ < \theta \leq 180^\circ \end{cases}$$

$$P_{\text{rad}} = \frac{r^2}{\eta} \left[ \int_0^{2\pi} \left\{ \int_0^{45^\circ} |E|^2 \sin\theta d\theta + \int_{90^\circ}^{180^\circ} |E|^2 \sin\theta d\theta \right\} d\phi \right]$$

$$P_{\text{rad}} = r^2 (0.54289) \left( \frac{2\pi}{\eta} \right) |10|^2 = 36,193$$

$$P_{\text{rad}} = \frac{1}{2} |I|^2 R_r = |I_{\text{rms}}|^2 R_r$$

$$\Rightarrow R_r = \frac{36,193}{|I_{\text{rms}}|^2} = \frac{36,193}{25} = 1,447.72$$

**Q9-** Find the half-power beamwidth (HPBW) and first-null beamwidth (FNBW), *in radians and degrees*, for the following normalized radiation intensities:

$$\left. \begin{array}{ll} \text{(a) } U(\theta) = \cos \theta & \text{(b) } U(\theta) = \cos^2 \theta \\ \text{(c) } U(\theta) = \cos(2\theta) & \text{(d) } U(\theta) = \cos^2(2\theta) \\ \text{(e) } U(\theta) = \cos(3\theta) & \text{(f) } U(\theta) = \cos^2(3\theta) \end{array} \right\} (0 \leq \theta \leq 90^\circ, 0 \leq \phi \leq 360^\circ)$$

**Then plot the radiation intensity for each case.**

**Q10-** The normalized radiation intensity of a given antenna is given by

$$\begin{array}{ll} \text{(a) } U = \sin \theta \sin \phi & \text{(b) } U = \sin \theta \sin^2 \phi \\ \text{(c) } U = \sin \theta \sin^3 \phi & \text{(d) } U = \sin^2 \theta \sin \phi \\ \text{(e) } U = \sin^2 \theta \sin^2 \phi & \text{(f) } U = \sin^2 \theta \sin^3 \phi \end{array}$$

The intensity exists only in the  $0 \leq \theta \leq \pi, 0 \leq \phi \leq \pi$  region, and it is zero elsewhere. Find the

- (a) exact directivity (*dimensionless and in dB*).
- (b) azimuthal and elevation plane half-power beamwidths (in degrees).

**(c) plot the radiation intensity in yz-plane and xy-plane for each case.**

**Q11-** The *normalized radiation intensity* radiated by an antenna is given by

$$U(\theta, \phi) = \begin{cases} \sin \theta \cos^2 \phi & 0^\circ \leq \theta \leq 180^\circ \\ & 90^\circ \leq \theta \leq 270^\circ \\ 0 & \text{Elsewhere} \end{cases}$$

The maximum of the radiation intensity occurs towards  $\theta = 90^\circ$  and  $\phi = 180^\circ$ . Find the:

- (a) *Exact* maximum directivity (*dimensionless and in dB*).
- (b) Half-power beamwidth (*in degrees*) in the principal azimuth (horizontal) plane.
- (c) Half-power beamwidth (*in degrees*) in the principal elevation (vertical) plane.

**(d) plot the radiation intensity in xz-plane and xy-plane.**

**Q12-** The maximum gain of a horn antenna is +20 dB, while the gain of its first sidelobe is -15 dB. What is the difference in gain between the maximum and first sidelobe:

- (a) in dB
- (b) as a ratio of the field intensities.

## Radiation Integrals and Auxiliary Potential Functions

In the analysis of radiation problems, the usual procedure is to specify the sources ( $\mathbf{J}$  and  $\mathbf{M}$ ) and then require the fields ( $\mathbf{E}$  and  $\mathbf{H}$ ) radiated by the sources. A common practice in the analysis procedure is to introduce auxiliary functions, known as *vector potentials*, which will aid in the solution of the problems. The most common vector potential functions are the  $\mathbf{A}$  (magnetic vector potential) and  $\mathbf{F}$  (electric vector potential). Another pair is the Hertz potentials  $\mathbf{\Pi}_e$  and  $\mathbf{\Pi}_h$ . *Although the electric and magnetic field intensities ( $\mathbf{E}$  and  $\mathbf{H}$ ) represent physically measurable quantities, among most engineers the potentials are strictly mathematical tools.* The introduction of the potentials often simplifies the solution even though it may require determination of additional functions. While it is possible to determine the  $\mathbf{E}$  and  $\mathbf{H}$  fields directly from the source-current densities  $\mathbf{J}$  and  $\mathbf{M}$ , as shown in Figure 3.1, it is usually much simpler to find the auxiliary potential functions first and then determine the  $\mathbf{E}$  and  $\mathbf{H}$ . This two-step procedure is also shown in Figure 3.1.

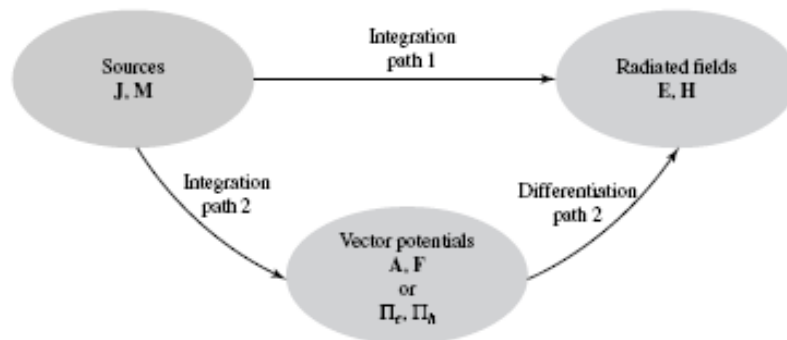


Figure 3.1 Block diagram for computing fields radiated by electric and magnetic sources.

### The Vector Potential $\mathbf{A}$ For An Electric Current Source $\mathbf{J}$

The vector potential  $\mathbf{A}$  is useful in solving the EM field due to a given harmonic electric current  $\mathbf{J}$ . The magnetic flux  $\mathbf{B}$  is always solenoidal; that is,  $\nabla \cdot \mathbf{B} = 0$ . Therefore, it can be represented as the curl of another vector because it obeys the vector identity

$$\nabla \cdot \nabla \times \mathbf{A} = 0 \quad (3-1)$$

where  $\mathbf{A}$  is an arbitrary vector. Thus we define

$$\mathbf{B}_A = \mu \mathbf{H}_A = \nabla \times \mathbf{A} \quad (3-2) \quad \text{Or} \quad \mathbf{H}_A = \frac{1}{\mu} \nabla \times \mathbf{A} \quad (3-2a)$$

where subscript  $A$  indicates the field due to the  $\mathbf{A}$  potential. Substituting (3-2a) into Maxwell's curl equation

$$\nabla \times \mathbf{E}_A = -j\omega \mu \mathbf{H}_A \quad (3-3) \quad \nabla \times \mathbf{E}_A = -j\omega \mu \mathbf{H}_A = -j\omega \nabla \times \mathbf{A} \quad (3-4)$$

$$\nabla \times [\mathbf{E}_A + j\omega \mathbf{A}] = 0 \quad (3-5)$$

From the vector identity

$$\nabla \times (-\nabla \phi_e) = 0 \quad (3-6)$$

From Eqs 3 to 5 it follows

$$\mathbf{E}_A + j\omega\mathbf{A} = -\nabla\phi_e$$

(3-7)

$$\mathbf{E}_A = -\nabla\phi_e - j\omega\mathbf{A}$$

(3-7a)

The scalar function  $\phi_e$  represents an arbitrary electric scalar potential which is a function of position.

Taking the curl of both sides of (3-2) and using the vector identity, it can be shown that (See Balanis, Antenna Theory and Design):

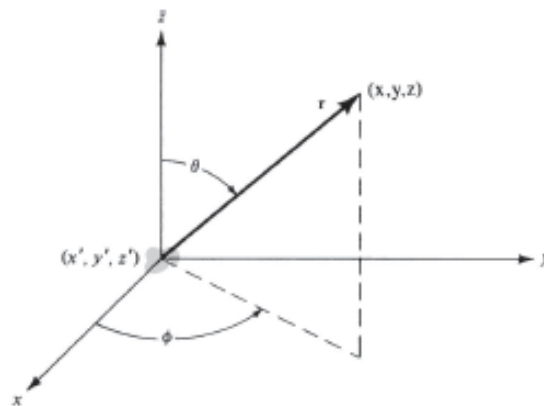
$$\mathbf{E}_A = -\nabla\phi_e - j\omega\mathbf{A} = -j\omega\mathbf{A} - j\frac{1}{\omega\mu\epsilon}\nabla(\nabla \cdot \mathbf{A})$$

(3-15)

Once  $\mathbf{A}$  is known,  $\mathbf{H}_A$  can be found from (3-2a) and  $\mathbf{E}_A$  from (3-15).  $\mathbf{E}_A$  can just as easily be found from Maxwell's equation with  $\mathbf{J} = 0$ . It will be shown later how to find  $\mathbf{A}$  in terms of the current density  $\mathbf{J}$ .

### ELECTRIC AND MAGNETIC FIELDS FOR ELECTRIC ( $\mathbf{J}$ ) AND MAGNETIC ( $\mathbf{M}$ ) CURRENT SOURCES

In the previous two sections we have developed equations that can be used to find the electric and magnetic fields generated by an electric current source  $\mathbf{J}$  and a magnetic current source  $\mathbf{M}$ . The procedure requires that the auxiliary potential functions  $\mathbf{A}$  and  $\mathbf{F}$  generated, respectively, by  $\mathbf{J}$  and  $\mathbf{M}$  are found first. In turn, the corresponding electric and magnetic fields are then determined ( $\mathbf{E}_A, \mathbf{H}_A$  due to  $\mathbf{A}$  and  $\mathbf{E}_F, \mathbf{H}_F$  due to  $\mathbf{F}$ ). The total fields are then obtained by the superposition of the individual fields due to  $\mathbf{A}$  and  $\mathbf{F}$  ( $\mathbf{J}$  and  $\mathbf{M}$ ).



(a) Source at origin

#### Summary

1. Specify  $\mathbf{J}$  and  $\mathbf{M}$  (electric and magnetic current density sources).
2. a. Find  $\mathbf{A}$  (due to  $\mathbf{J}$ ) using

$$\mathbf{A} = \frac{\mu}{4\pi} \iiint_V \mathbf{J} \frac{e^{-jkR}}{R} dv'$$

(3-27)

which is a solution of the inhomogeneous vector wave equation.

- b. Find  $\mathbf{F}$  (due to  $\mathbf{M}$ ) using

$$\mathbf{F} = \frac{\epsilon}{4\pi} \iiint_V \mathbf{M} \frac{e^{-jkR}}{R} dv'$$

(3-28)

## SOLUTION OF THE INHOMOGENEOUS VECTOR POTENTIAL WAVE EQUATION

Assume that a source with current density  $J_z$ , which in the limit is an infinitesimal source, is placed at the origin of a  $x, y, z$  coordinate system, as shown in Figure 3.2(a). Since the current density is directed along the  $z$ -axis ( $J_z$ ), only an  $A_z$  component will exist. Thus we can write ( note that  $J_z=0$  at the observation point)

$$\nabla^2 A_z + k^2 A_z = 0 \quad (3-32)$$

It can be shown that the solution of this equation is:

$$A = \frac{\mu}{4\pi} \iiint_V \mathbf{J} \frac{e^{-jkr}}{r} dV \quad (3-48)$$

Note the vectors  $\mathbf{A}$  and  $\mathbf{J}$  have the same components.

After finding  $A$  the radiated field components can be found as :

*Far-Field Region*

$$\left. \begin{array}{l} E_r \simeq 0 \\ E_\theta \simeq -j\omega A_\theta \\ E_\phi \simeq -j\omega A_\phi \end{array} \right\} \Rightarrow \mathbf{E}_A \simeq -j\omega \mathbf{A} \quad (3-58a)$$

(for the  $\theta$  and  $\phi$  components only  
since  $E_r \simeq 0$ )

$$\left. \begin{array}{l} H_r \simeq 0 \\ H_\theta \simeq +j\frac{\omega}{\eta} A_\phi = -\frac{E_\phi}{\eta} \\ H_\phi \simeq -j\frac{\omega}{\eta} A_\theta = +\frac{E_\theta}{\eta} \end{array} \right\} \Rightarrow \mathbf{H}_A \simeq \frac{\hat{\mathbf{a}}_r}{\eta} \times \mathbf{E}_A = -j\frac{\omega}{\eta} \hat{\mathbf{a}}_r \times \mathbf{A} \quad (3-58b)$$

(for the  $\theta$  and  $\phi$  components only  
since  $H_r \simeq 0$ )

## Chapter 4; Linear Wire Antennas

Wire antennas, linear or curved, are some of the oldest, simplest, cheapest, and in many cases the most versatile for many applications.

### INFINITESIMAL DIPOLE

An infinitesimal linear wire ( $l \ll \lambda$ ) is positioned symmetrically at the origin of the coordinate system and oriented along the  $z$  axis, as shown in Figure 4.1(a). Although infinitesimal dipoles are not very practical, they are used to represent capacitor-plate (also referred to as *top-hat-loaded*) antennas. In addition, they are utilized as building blocks of more complex geometries. The end plates are used to provide capacitive loading in order to maintain the current on the dipole nearly uniform. Since the end plates are assumed to be small, their radiation is usually negligible. The wire, in addition to being very small ( $l \ll \lambda$ ), is very thin ( $a \ll \lambda$ ). The spatial variation of the current is assumed to be constant and given by ( with  $I_0$  constant) :

$$\mathbf{I}(z') = \hat{\mathbf{a}}_z I_0 \quad (4-1)$$

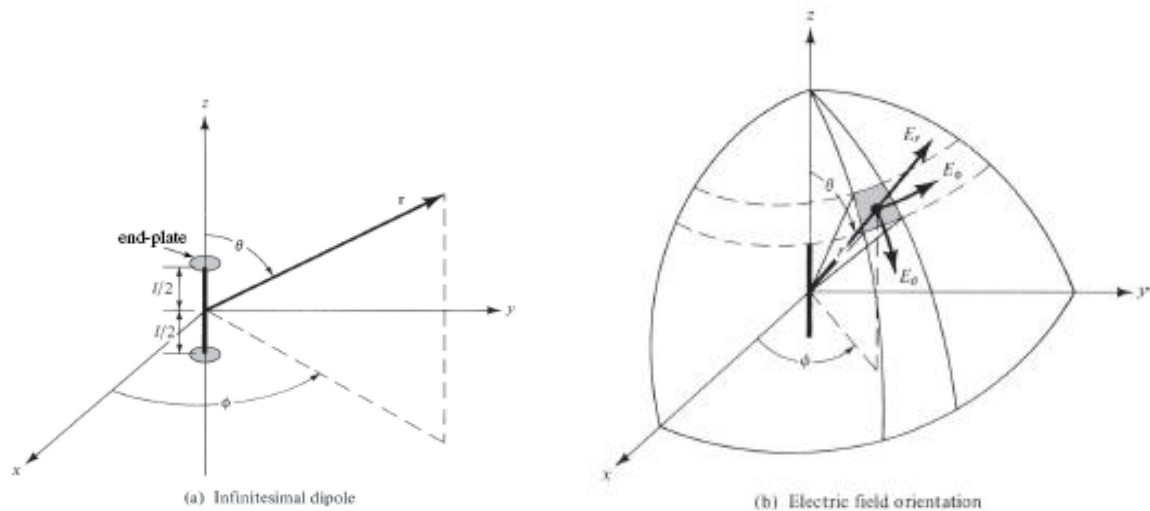


**Figure 4.1** Geometrical arrangement of an infinitesimal dipole and its associated electric-field components on a spherical surface.

Since the source only carries an electric current  $\mathbf{I}_e, \mathbf{I}_m$  and the potential function  $F$  are zero. To find  $\mathbf{A}$  we write

$$\mathbf{A}(x, y, z) = \frac{\mu}{4\pi} \int_C \mathbf{I}_e(x', y', z') \frac{e^{-jkR}}{R} dl' \quad (4-2)$$

where  $(x, y, z)$  represent the observation point coordinates,  $(x', y', z')$  represent the coordinates of the source,  $R$  is the distance from any point on the source to the observation point, and path  $C$  is along the length of the source. For the problem of Figure 4.1

$$\mathbf{I}_e(x', y', z') = \hat{\mathbf{a}}_z I_0 \quad (4-3a)$$

$$x' = y' = z' = 0 \text{ (infinitesimal dipole)} \quad (4-3b)$$

$$\begin{aligned} R &= \sqrt{(x-x')^2 + (y-y')^2 + (z-z')^2} = \sqrt{x^2 + y^2 + z^2} \\ &= r = \text{constant} \end{aligned} \quad (4-3c)$$

$$dl' = dz' \quad (4-3d)$$

so we can write (4-2) as

$$\mathbf{A}(x, y, z) = \hat{\mathbf{a}}_z \frac{\mu I_0}{4\pi r} e^{-jkr} \int_{-l/2}^{+l/2} dz' = \hat{\mathbf{a}}_z \frac{\mu I_0 l}{4\pi r} e^{-jkr} \quad (4-4)$$

The next step of the procedure is to find  $\mathbf{H}_A$  using (3-2a) and then  $\mathbf{E}_A$  using (3-15) or (3-10) with  $\mathbf{J} = 0$ . To do this, it is often much simpler to transform (4-4) from rectangular to spherical components and then use (3-2a) and (3-15) or (3-10) in spherical coordinates to find  $\mathbf{H}$  and  $\mathbf{E}$ .

The transformation between rectangular and spherical components is given, in matrix form, by (VII-12a) (see Appendix VII)

$$\begin{bmatrix} A_r \\ A_\theta \\ A_\phi \end{bmatrix} = \begin{bmatrix} \sin \theta \cos \phi & \sin \theta \sin \phi & \cos \theta \\ \cos \theta \cos \phi & \cos \theta \sin \phi & -\sin \theta \\ -\sin \phi & \cos \phi & 0 \end{bmatrix} \begin{bmatrix} A_x \\ A_y \\ A_z \end{bmatrix} \quad (4-5)$$

For this problem,  $A_x = A_y = 0$ , so (4-5) using (4-4) reduces to

$$A_r = A_z \cos \theta = \frac{\mu I_0 l e^{-jkr}}{4\pi r} \cos \theta \quad (4-6a)$$

$$A_\theta = -A_z \sin \theta = -\frac{\mu I_0 l e^{-jkr}}{4\pi r} \sin \theta \quad (4-6b)$$

$$A_\phi = 0 \quad (4-6c)$$

Using the symmetry of the problem (no  $\phi$  variations), (3-2a) can be expanded in spherical coordinates and written in simplified form as

$$\mathbf{H} = \hat{\mathbf{a}}_\phi \frac{1}{\mu r} \left[ \frac{\partial}{\partial r}(rA_\theta) - \frac{\partial A_r}{\partial \theta} \right] \quad (4-7)$$

Substituting (4-6a)–(4-6c) into (4-7) reduces it to

$$H_r = H_\theta = 0 \quad (4-8a)$$

$$H_\phi = j \frac{k I_0 l \sin \theta}{4\pi r} \left[ 1 + \frac{1}{jkr} \right] e^{-jkr} \quad (4-8b)$$

The electric field  $\mathbf{E}$  can now be found using (3-15) or (3-10) with  $\mathbf{J} = 0$ . That is,

$$\mathbf{E} = \mathbf{E}_A = -j\omega \mathbf{A} - j \frac{1}{\omega \mu \epsilon} \nabla(\nabla \cdot \mathbf{A}) = \frac{1}{j\omega \epsilon} \nabla \times \mathbf{H} \quad (4-9)$$

Substituting (4-6a)–(4-6c) or (4-8a)–(4-8b) into (4-9) reduces it to

$$E_r = \eta \frac{I_0 l \cos \theta}{2\pi r^2} \left[ 1 + \frac{1}{jkr} \right] e^{-jkr} \quad (4-10a)$$

$$E_\theta = j\eta \frac{kI_0 l \sin \theta}{4\pi r} \left[ 1 + \frac{1}{jkr} - \frac{1}{(kr)^2} \right] e^{-jkr} \quad (4-10b)$$

$$E_\phi = 0 \quad (4-10c)$$

The **E**- and **H**-field components are valid everywhere, except on the source itself, and they are sketched in Figure 4.1(b) on the surface of a sphere of radius  $r$ . It is a straightforward exercise to verify Equations (4-10a)–(4-10c), and this is left as an exercise to the reader (Prob. 4.14).

#### 4.2.2 Power Density and Radiation Resistance

For a lossless antenna, the real part of the input impedance was designated as radiation resistance. It is through the mechanism of the radiation resistance that power is transferred from the guided wave to the free-space wave. To find the input resistance for a lossless antenna, the Poynting vector is formed in terms of the **E**- and **H**-fields radiated by the antenna. By integrating the Poynting vector over a closed surface (usually a sphere of constant radius), the total power radiated by the antenna is found. The real part of it is related to the input resistance.

For the infinitesimal dipole, the complex Poynting vector can be written using (4-8a)–(4-8b) and (4-10a)–(4-10c) as

$$\begin{aligned} \mathbf{W} &= \frac{1}{2}(\mathbf{E} \times \mathbf{H}^*) = \frac{1}{2}(\hat{\mathbf{a}}_r E_r + \hat{\mathbf{a}}_\theta E_\theta) \times (\hat{\mathbf{a}}_\phi H_\phi^*) \\ &= \frac{1}{2}(\hat{\mathbf{a}}_r E_\theta H_\phi^* - \hat{\mathbf{a}}_\theta E_r H_\phi^*) \end{aligned} \quad (4-11)$$

whose radial  $W_r$  and transverse  $W_\theta$  components are given, respectively, by

$$W_r = \frac{\eta}{8} \left| \frac{I_0 l}{\lambda} \right|^2 \frac{\sin^2 \theta}{r^2} \left[ 1 - j \frac{1}{(kr)^3} \right] \quad (4-12a)$$

$$W_\theta = j\eta \frac{k|I_0 l|^2 \cos \theta \sin \theta}{16\pi^2 r^3} \left[ 1 + \frac{1}{(kr)^2} \right] \quad (4-12b)$$

The complex power moving in the radial direction is obtained by integrating (4-11)–(4-12b) over a closed sphere of radius  $r$ . Thus it can be written as

$$P = \oiint_S \mathbf{W} \cdot d\mathbf{s} = \int_0^{2\pi} \int_0^\pi (\hat{\mathbf{a}}_r W_r + \hat{\mathbf{a}}_\theta W_\theta) \cdot \hat{\mathbf{a}}_r r^2 \sin \theta \, d\theta \, d\phi \quad (4-13)$$

which reduces to

$$P = \int_0^{2\pi} \int_0^\pi W_r r^2 \sin \theta \, d\theta \, d\phi = \eta \frac{\pi}{3} \left| \frac{I_0 l}{\lambda} \right|^2 \left[ 1 - j \frac{1}{(kr)^3} \right] \quad (4-14)$$

The transverse component  $W_\theta$  of the power density does not contribute to the integral. Thus (4-14) does not represent the total complex power radiated by the antenna. Since  $W_\theta$ , as given by (4-12b), is purely imaginary, it will not contribute to any real radiated power. However, it does contribute to the imaginary (reactive) power which along with the second term of (4-14) can be used to determine the total reactive power of the antenna. *The reactive power density, which is most dominant for small values of  $kr$ , has both radial and transverse components. It merely changes between outward and inward directions to form a standing wave at a rate of twice per cycle. It also moves in the transverse direction as suggested by (4-12b).*

Equation (4-13), which gives the real and imaginary power that is moving outwardly, can also be written as

$$P = \frac{1}{2} \iint_S \mathbf{E} \times \mathbf{H}^* \cdot d\mathbf{s} = \eta \left( \frac{\pi}{3} \right) \left| \frac{I_0 l}{\lambda} \right|^2 \left[ 1 - j \frac{1}{(kr)^3} \right]$$

$$= P_{\text{rad}} + j2\omega(\tilde{W}_m - \tilde{W}_e) \quad (4-15)$$

where

$P$  = power (in radial direction)

$P_{\text{rad}}$  = time-average power radiated

$\tilde{W}_m$  = time-average magnetic energy density (in radial direction)

$\tilde{W}_e$  = time-average electric energy density (in radial direction)

$2\omega(\tilde{W}_m - \tilde{W}_e)$  = time-average imaginary (reactive) power (in radial direction)

From (4-14)

$$P_{\text{rad}} = \eta \left( \frac{\pi}{3} \right) \left| \frac{I_0 l}{\lambda} \right|^2 \quad (4-16)$$

and

$$2\omega(\tilde{W}_m - \tilde{W}_e) = -\eta \left( \frac{\pi}{3} \right) \left| \frac{I_0 l}{\lambda} \right|^2 \frac{1}{(kr)^3} \quad (4-17)$$

It is clear from (4-17) that the radial electric energy must be larger than the radial magnetic energy. For large values of  $kr$  ( $kr \gg 1$  or  $r \gg \lambda$ ), the reactive power diminishes and vanishes when  $kr = \infty$ .

Since the antenna radiates its real power through the radiation resistance, for the infinitesimal dipole it is found by equating (4-16) to

$$P_{\text{rad}} = \eta \left( \frac{\pi}{3} \right) \left| \frac{I_0 l}{\lambda} \right|^2 = \frac{1}{2} |I_0|^2 R_r \quad (4-18)$$

where  $R_r$  is the radiation resistance. Equation (4-18) reduces to

$$R_r = \eta \left( \frac{2\pi}{3} \right) \left( \frac{l}{\lambda} \right)^2 = 80\pi^2 \left( \frac{l}{\lambda} \right)^2 \quad (4-19)$$

for a free-space medium ( $\eta \approx 120\pi$ ). It should be pointed out that the radiation resistance of (4-19) represents the total radiation resistance since (4-12b) does not contribute to it.

For a wire antenna to be classified as an infinitesimal dipole, its overall length must be very small (usually  $l \leq \lambda/50$ ).

#### Example 4.1

Find the radiation resistance of an infinitesimal dipole whose overall length is  $l = \lambda/50$ .

*Solution:* Using (4-19)

$$R_r = 80\pi^2 \left( \frac{l}{\lambda} \right)^2 = 80\pi^2 \left( \frac{1}{50} \right)^2 = 0.316 \text{ ohms}$$

Since the radiation resistance of an infinitesimal dipole is about 0.3 ohms, it will present a very large mismatch when connected to practical transmission lines, many of which have characteristic impedances of 50 or 75 ohms. The reflection efficiency ( $e_r$ ) and hence the overall efficiency ( $e_0$ ) will be very small.

#### 4.2.4 Near-Field ( $kr \ll 1$ ) Region

An inspection of (4-8a)–(4-8b) and (4-10a)–(4-10c) reveals that for  $kr \ll \lambda$  or  $r \ll \lambda/2\pi$  they can be reduced in much simpler form and can be approximated by

$$E_r \simeq -j\eta \frac{I_0 l e^{-jkr}}{2\pi k r^3} \cos \theta \quad (4-20a)$$

$$E_\theta \simeq -j\eta \frac{I_0 l e^{-jkr}}{4\pi k r^3} \sin \theta \quad (4-20b)$$

$$E_\phi = H_r = H_\theta = 0 \quad (4-20c)$$

$$H_\phi \simeq \frac{I_0 l e^{-jkr}}{4\pi r^2} \sin \theta \quad (4-20d)$$

#### 4.2.5 Intermediate-Field ( $kr > 1$ ) Region

As the values of  $kr$  begin to increase and become greater than unity, the terms that were dominant for  $kr \ll 1$  become smaller and eventually vanish. For moderate values of  $kr$  the **E**-field components lose their in-phase condition and approach time-phase quadrature. Since their magnitude is not the same, in general, they form a rotating vector whose extremity traces an ellipse. This is analogous to the polarization problem except that the vector rotates in a plane parallel to the direction of propagation and is usually referred to as the *cross field*. At these intermediate values of  $kr$ , the  $E_\theta$  and  $H_\phi$  components approach time-phase, which is an indication of the formation of time-average power flow in the outward (radial) direction (radiation phenomenon).

As the values of  $kr$  become moderate ( $kr > 1$ ), the field expressions can be approximated again but in a different form. In contrast to the region where  $kr \ll 1$ , the first term within the brackets in (4-8b) and (4-10a) becomes more dominant and the second term can be neglected. The same is true for (4-10b) where the second and third terms become less dominant than the first. Thus we can write for  $kr > 1$

$$E_r \simeq \eta \frac{I_0 l e^{-jkr}}{2\pi r^2} \cos \theta \quad (4-23a)$$

$$E_\theta \simeq j\eta \frac{kI_0 l e^{-jkr}}{4\pi r} \sin \theta \quad (4-23b)$$

$$E_\phi = H_r = H_\theta = 0 \quad (4-23c)$$

$$H_\phi \simeq j \frac{kI_0 l e^{-jkr}}{4\pi r} \sin \theta \quad (4-23d)$$

#### 4.2.6 Far-Field ( $kr \gg 1$ ) Region

Since (4-23a)–(4-23d) are valid only for values of  $kr > 1$  ( $r > \lambda$ ), then  $E_r$  will be smaller than  $E_\theta$  because  $E_r$  is inversely proportional to  $r^2$  where  $E_\theta$  is inversely proportional to  $r$ . In a region where  $kr \gg 1$ , (4-23a)–(4-23d) can be simplified and approximated by

$$E_\theta \simeq j\eta \frac{kI_0 l e^{-jkr}}{4\pi r} \sin \theta \quad (4-26a)$$

$$E_r \simeq E_\phi = H_r = H_\theta = 0 \quad (4-26b)$$

$$H_\phi \simeq j \frac{kI_0 l e^{-jkr}}{4\pi r} \sin \theta \quad (4-26c)$$

The ratio of  $E_\theta$  to  $H_\phi$  is equal to

$$Z_w = \frac{E_\theta}{H_\phi} \simeq \eta \quad (4-27)$$

where

$Z_w$  = wave impedance

$\eta$  = intrinsic impedance ( $377 \simeq 120\pi$  ohms for free-space)

The **E**- and **H**-field components are perpendicular to each other, transverse to the radial direction of propagation, and the  $r$  variations are separable from those of  $\theta$  and  $\phi$ . The shape of the pattern is not a function of the radial distance  $r$ , and the fields form a Transverse ElectroMagnetic (TEM) wave whose wave impedance is equal to the intrinsic impedance of the medium.

#### 4.2.7 Directivity

The real power  $P_{\text{rad}}$  radiated by the dipole was found in Section 4.2.2, as given by (4-16). The same expression can be obtained by first forming the average power density, using (4-26a)–(4-26c). That is,

$$W_{av} = \frac{1}{2} \text{Re}(\mathbf{E} \times \mathbf{H}^*) = \hat{\mathbf{a}}_r \frac{1}{2\eta} |E_\theta|^2 = \hat{\mathbf{a}}_r \frac{\eta}{2} \left| \frac{kI_0 l}{4\pi} \right|^2 \frac{\sin^2 \theta}{r^2} \quad (4-28)$$

Integrating (4-28) over a closed sphere of radius  $r$  reduces it to (4-16).

Associated with the average power density of (4-28) is a radiation intensity  $U$  which is given by

$$U = r^2 W_{av} = \frac{\eta}{2} \left( \frac{kI_0 l}{4\pi} \right)^2 \sin^2 \theta = \frac{r^2}{2\eta} |E_\theta(r, \theta, \phi)|^2 \quad (4-29)$$

and it conforms with (2-12a). The normalized pattern of (4-29) is shown in Figure 4.3. The maximum value occurs at  $\theta = \pi/2$  and it is equal to

$$U_{\max} = \frac{\eta}{2} \left( \frac{kI_0 l}{4\pi} \right)^2 \quad (4-30)$$

Using (4-16) and (4-30), the directivity reduces to

$$D_0 = 4\pi \frac{U_{\max}}{P_{\text{rad}}} = \frac{3}{2} \quad (4-31)$$

and the maximum effective aperture to

$$A_{em} = \left( \frac{\lambda^2}{4\pi} \right) D_0 = \frac{3\lambda^2}{8\pi} \quad (4-32)$$

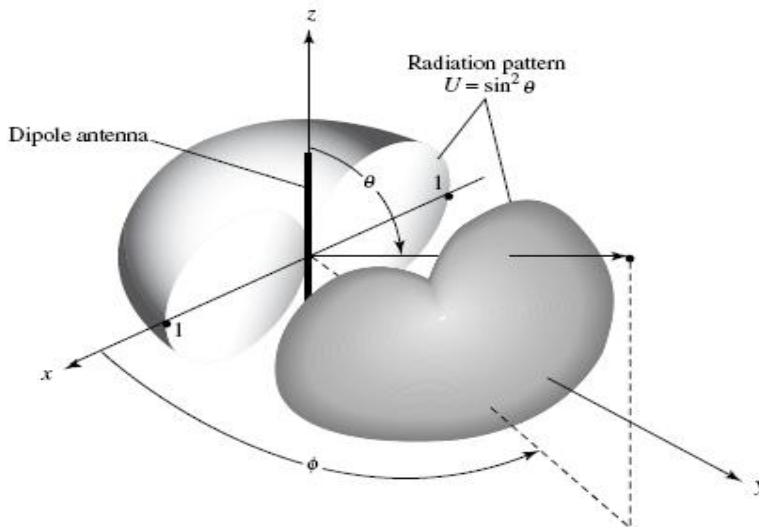


Figure 4.3 Three-dimensional radiation pattern of infinitesimal dipole.

Integrating the complex Poynting vector over a closed sphere, as was done in (4-13), results in the power (real and imaginary) directed in the radial direction. Any transverse components of power density, as given by (4-12b), will not be captured by the integration even though they are part of the overall power. *Because of this limitation, this method cannot be used to derive the input reactance of the antenna.* The procedure that can be used to derive the far-zone electric and magnetic fields radiated by an antenna, along with some of the most important parameters/figures of merit that are used to describe the performance of an antenna, are summarized in Table 4.1

**TABLE 4.1** Summary of Procedure to Determine the Far-Field Radiation Characteristics of an Antenna

1. Specify electric and/or magnetic current densities  $\mathbf{J}$ ,  $\mathbf{M}$  [physical or equivalent (see Chapter 3, Figure 3.1)]
2. Determine vector potential components  $A_\theta$ ,  $A_\phi$  and/or  $F_\theta$ ,  $F_\phi$  using (3-46)–(3-54) in far field
3. Find far-zone  $\mathbf{E}$  and  $\mathbf{H}$  radiated fields ( $E_\theta$ ,  $E_\phi$ ;  $H_\theta$ ,  $H_\phi$ ) using (3-58a)–(3-58b)
4. Form either
  - a.

$$\begin{aligned} W_{\text{rad}}(r, \theta, \phi) &= W_{\text{av}}(r, \theta, \phi) = \frac{1}{2} \text{Re}[\mathbf{E} \times \mathbf{H}^*] \\ &\simeq \frac{1}{2} \text{Re} [(\hat{a}_\theta E_\theta + \hat{a}_\phi E_\phi) \times (\hat{a}_\theta H_\theta^* + \hat{a}_\phi H_\phi^*)] \\ W_{\text{rad}}(r, \theta, \phi) &= \hat{a}_r \frac{1}{2} \left[ \frac{|E_\theta|^2 + |E_\phi|^2}{\eta} \right] = \hat{a}_r \frac{1}{r^2} |f(\theta, \phi)|^2 \end{aligned}$$

or

- b.  $U(\theta, \phi) = r^2 W_{\text{rad}}(r, \theta, \phi) = |f(\theta, \phi)|^2$

5. Determine either

- a.  $P_{\text{rad}} = \int_0^{2\pi} \int_0^\pi W_{\text{rad}}(r, \theta, \phi) r^2 \sin \theta \, d\theta \, d\phi$

or

- b.  $P_{\text{rad}} = \int_0^{2\pi} \int_0^\pi U(\theta, \phi) \sin \theta \, d\theta \, d\phi$

6. Find directivity using

$$\begin{aligned} D(\theta, \phi) &= \frac{U(\theta, \phi)}{U_0} = \frac{4\pi U(\theta, \phi)}{P_{\text{rad}}} \\ D_0 = D_{\text{max}} &= D(\theta, \phi)|_{\text{max}} = \frac{U(\theta, \phi)|_{\text{max}}}{U_0} = \frac{4\pi U(\theta, \phi)|_{\text{max}}}{P_{\text{rad}}} \end{aligned}$$

7. Form *normalized* power amplitude pattern:

$$P_n(\theta, \phi) = \frac{U(\theta, \phi)}{U_{\text{max}}}$$

8. Determine radiation and input resistance:

$$R_r = \frac{2P_{\text{rad}}}{|I_0|^2}; \quad R_{\text{in}} = \frac{R_r}{\sin^2\left(\frac{kl}{2}\right)}$$

9. Determine maximum effective area

### 4.3 SMALL DIPOLE

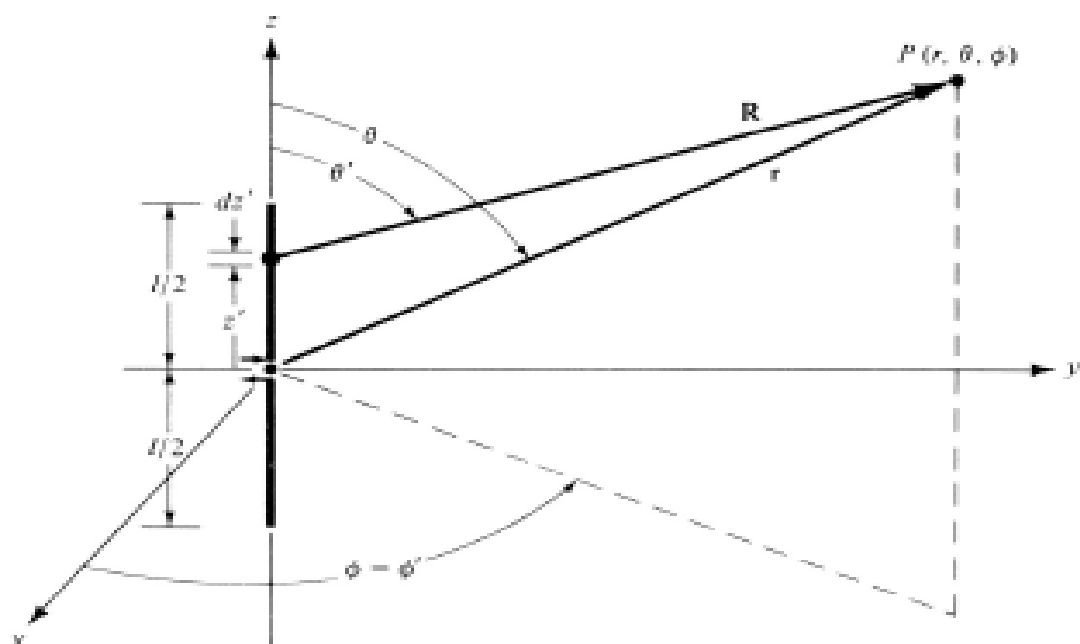
The creation of the current distribution on a thin wire was discussed in Section 1.4, and it was illustrated with some examples in Fig. 1.16. The radiation properties of an infinitesimal dipole, which is usually taken to have a length  $l \leq \lambda/50$ , were discussed in the previous section. Its current distribution was assumed to be constant. Although a constant current distribution is not realizable (other than top-hat-loaded elements), it is a mathematical quantity that is used to represent actual current distributions of antennas that have been incremented into many small lengths.

A better approximation of the current distribution of wire antennas, whose lengths are usually  $\lambda/50 < l \leq \lambda/10$ , is the triangular variation of Fig. 1.16(a). The sinusoidal variations of Fig. 1.16(b)–(c) are more accurate representations of the current distribution of any length wire antenna.

The most convenient geometrical arrangement for the analysis of a dipole is usually to have it positioned symmetrically about the origin with its length directed along the  $z$ -axis, as shown in Fig. 4.4(a). This is not necessary, but it is usually the most convenient. The current distribution of a small dipole ( $\lambda/50 < l \leq \lambda/10$ ) is shown in Fig. 4.4(b), and it is given by

$$\mathbf{I}_e(x', y', z') = \begin{cases} \hat{\mathbf{a}}_z I_0 \left(1 - \frac{2z'}{l}\right), & 0 \leq z' \leq l/2 \\ \hat{\mathbf{a}}_z I_0 \left(1 + \frac{2z'}{l}\right), & -l/2 \leq z' \leq 0 \end{cases} \quad (4-33)$$

where  $I_0 = \text{constant}$ .



(a) Dipole and geometry

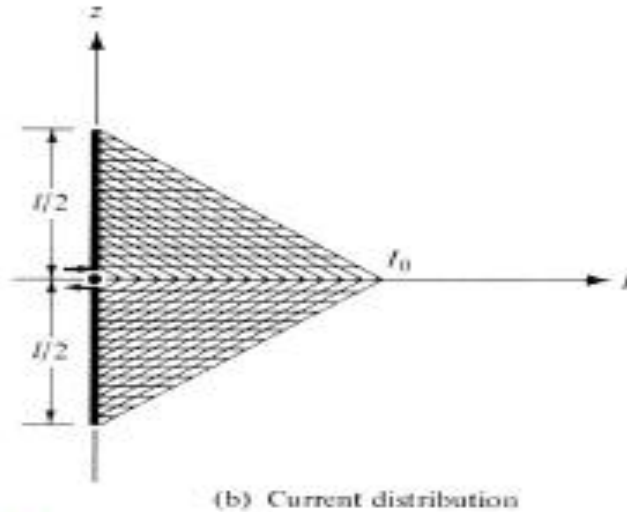


**Figure 4.4** Geometrical arrangement of dipole and current distribution.

Following the procedure established in the previous section, the vector potential of (4-2) can be written using (4-33) as

$$\begin{aligned} \mathbf{A}(x, y, z) = \frac{\mu}{4\pi} \left[ \hat{\mathbf{a}}_z \int_{-l/2}^0 I_0 \left( 1 + \frac{2z'}{l} \right) \frac{e^{-jkR}}{R} dz' \right. \\ \left. + \hat{\mathbf{a}}_z \int_0^{l/2} I_0 \left( 1 - \frac{2z'}{l} \right) \frac{e^{-jkR}}{R} dz' \right] \end{aligned} \quad (4-34)$$

Because the overall length of the dipole is very small (usually  $l \leq \lambda/10$ ), the values of  $R$  for different values of  $z'$  along the length of the wire ( $-l/2 \leq z' \leq l/2$ ),  $R$  can be approximated by  $R \approx r$  throughout the integration path. The maximum phase error in (4-34) by allowing  $R = r$  for  $\lambda/50 < l \leq \lambda/10$ , will be  $kl/2 = \pi/10$  rad =  $18^\circ$  for  $l = \lambda/10$ . Smaller values will occur for the other lengths. This amount of phase error is usually negligible and has very little effect on the overall radiation characteristics. Performing the integration, (4-34) reduces to

$$\mathbf{A} = \hat{\mathbf{a}}_z A_z = \hat{\mathbf{a}}_z \frac{1}{2} \left[ \frac{\mu I_0 l e^{-jkr}}{4\pi r} \right] \quad (4-35)$$

which is one-half of that obtained in the previous section for the infinitesimal dipole and given by (4-4).

The potential function given by (4-35) becomes a more accurate as  $kr \rightarrow \infty$ . This is the region of practical interest, and it is called the *far-field* region. Since the potential function for the triangular distribution is **1/2** of that for the constant (uniform) current distribution, the corresponding fields of the former are one-half of the latter. Thus we can write the **E**- and **H**-fields radiated by a small dipole as

$$\left. \begin{aligned} E_{\theta} &\approx j\eta \frac{kI_0 l e^{-jkr}}{8\pi r} \sin \theta & (4-36a) \\ E_r &\approx E_{\phi} = H_r = H_{\theta} = 0 & (4-36b) \\ H_{\phi} &\approx j \frac{kI_0 l e^{-jkr}}{8\pi r} \sin \theta & (4-36c) \end{aligned} \right\} kr \gg 1$$

with the wave impedance equal, as before, to (4-27).

Since the directivity of an antenna is controlled by the relative shape of the field or power pattern, the directivity, and maximum effective area of this antenna are the same as the ones with the constant current distribution given by (4-31) and (4-32), respectively.

The radiation resistance of the antenna is strongly dependent upon the current distribution. Using the same procedure for the infinitesimal dipole, it can be shown that for the small dipole its radiated power is **1/4** of (4-18). Thus the radiation resistance reduces to

$$R_r = \frac{2P_{\text{rad}}}{|I_0|^2} = 20\pi^2 \left(\frac{l}{\lambda}\right)^2 \quad (4-37)$$

which is also one-fourth ( **1/4** ) of that obtained for the infinitesimal dipole as given by (4-19). Their relative patterns (shapes) are the same and are shown in Fig. 4.3.

#### 4.4 REGION SEPARATION

It is desirable to separate the space surrounding an antenna into three regions; namely, the *reactive near-field*, *radiating near-field (Fresnel)* and the *far-field (Fraunhofer)*. Approximations can be made, for the far-field (Fraunhofer) region, which is of the most practical interest. So it will be very important to understand their implications upon the solution.

It is difficult to perform the integration of

$$\mathbf{A}(x, y, z) = \frac{\mu}{4\pi} \int_C \mathbf{I}_e(x', y', z') \frac{e^{-jkR}}{R} dl' \quad (4-38)$$

Where

$$R = \sqrt{(x - x')^2 + (y - y')^2 + (z - z')^2} \quad (4-38a)$$

The length  $R$  is defined as the distance from any point on the source to the observation point. The integral of (4-38) was used to solve for the fields of infinitesimal and small dipoles in Sections 4.1 and 4.2. However in the

first case (infinitesimal dipole)  $R = r$  and in the second case (small dipole)  $R$  was approximated by  $r$  ( $R \approx r$ ) because the length of the dipole was restricted to be  $l \leq \lambda/10$ . The major simplification of (4-38) will be in the approximation of  $R$ .

A very thin dipole of finite length  $l$  is symmetrically positioned about the origin with its length directed along the  $z$ -axis, as shown in Fig.4.5(a). Because the wire is assumed to be very thin ( $x' = y' = 0$ ), we can write (4-38) as

$$R = \sqrt{(x - x')^2 + (y - y')^2 + (z - z')^2} = \sqrt{x^2 + y^2 + (z - z')^2} \quad (4-39)$$

Which be written as

$$R = \sqrt{(x^2 + y^2 + z^2) + (-2zz' + z'^2)} = \sqrt{r^2 + (-2rz' \cos \theta + z'^2)} \quad (4-40)$$

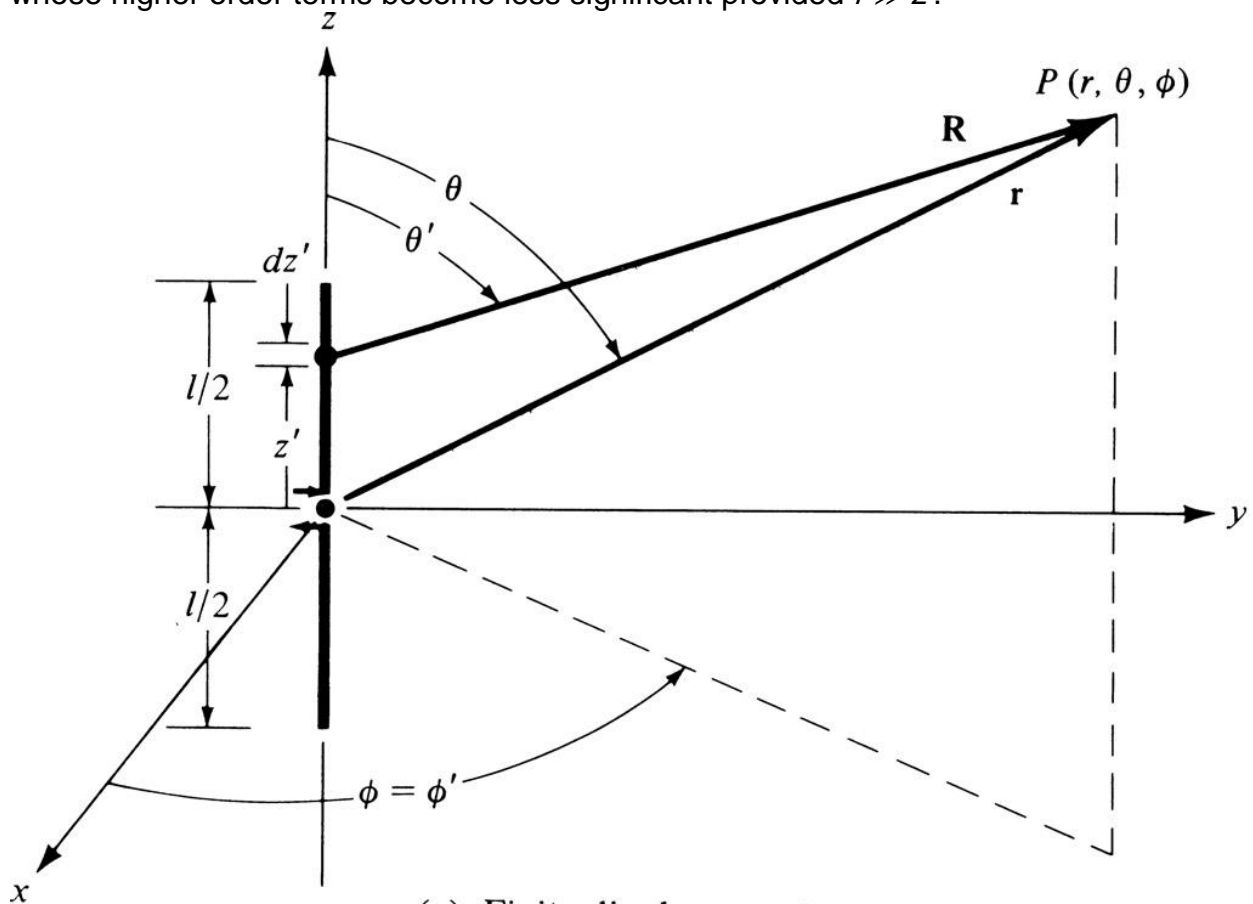
$$r^2 = x^2 + y^2 + z^2 \quad (4-40a)$$

$$z = r \cos \theta \quad (4-40b)$$

Using the binomial expansion, we can write (4-40) in a series as

$$R = r - z' \cos \theta + \frac{1}{r} \left( \frac{z'^2}{2} \sin^2 \theta \right) + \frac{1}{r^2} \left( \frac{z'^3}{2} \cos \theta \sin^2 \theta \right) + \dots \quad (4-41)$$

whose higher order terms become less significant provided  $r \gg z'$ .



(a) Finite dipole geometry



$$\frac{k(z')^2}{2r} \leq \frac{\pi}{8} \quad (4-44)$$

which for  $-l/2 \leq z' \leq l/2$  reduces to

$$r \geq 2 \left( \frac{l^2}{\lambda} \right) \quad (4-45)$$

Equation (4-45) means that for a maximum phase error  $\leq \pi/8$  rad (22.5°),  $r$  must equal or be greater than  $2L^2/\lambda$  where  $L$  is the largest dimension of the antenna. The usual simplification for the far-field region is to approximate the  $R$  in the exponential ( $e^{-jkR}$ ) of (4-38) by (4-42) and the  $R$  in the denominator of (4-38) by  $R \simeq r$ . These simplifications are designated as the far-field approximations and are usually denoted in the literature as *Far-field Approximations*

$$\begin{aligned} R &\simeq r - z' \cos \theta && \text{for phase terms} \\ R &\simeq r && \text{for amplitude terms} \end{aligned} \quad (4-46)$$

provided  $r$  satisfies (4-45).

It may be advisable to illustrate the approximation (4-46) geometrically. For  $R \simeq r - z' \cos \theta$ , where  $\theta$  is the angle measured from the  $z$ -axis, the radial vectors  $\mathbf{R}$  and  $\mathbf{r}$  must be parallel to each other, as shown in Fig. 4.5(b). For any other antenna whose maximum dimension is  $D$ , the approximation of (4-46) is valid provided the observations are made at a distance

$$r \geq 2 \frac{D^2}{\lambda} \quad (4-47)$$

For an aperture antenna the maximum dimension is taken to be its diagonal. For most practical antennas, whose overall length is large compared to the wavelength, these are adequate approximations. Allowing  $R$  to have a value of  $R = 4D^2/\lambda$  gives better results.

### Example 4.3

For an antenna with an overall length  $l = 5\lambda$ , the observations are made at  $r = 60\lambda$ . Find the errors in phase and amplitude using (4-46).

*Solution:* For  $\theta = 90^\circ$ ,  $z' = 2.5\lambda$ , and  $r = 60\lambda$ , (4-40) reduces to

$$R_1 = \lambda \sqrt{(60)^2 + (2.5)^2} = 60.052\lambda$$

and (4-46) to

$$R_2 = r = 60\lambda$$

Therefore the phase difference is

$$\Delta\phi = k\Delta R = \frac{2\pi}{\lambda}(R_1 - R_2) = 2\pi(0.052) = 0.327 \text{ rad} = 18.74^\circ$$

which is an appreciable fraction ( $\simeq \frac{1}{20}$ ) of a full period (360°).

The difference of the inverse values of  $R$  is

$$\frac{1}{R_2} - \frac{1}{R_1} = \frac{1}{\lambda} \left( \frac{1}{60} - \frac{1}{60.052} \right) = \frac{1.44 \times 10^{-5}}{\lambda}$$

which should always be a very small value in amplitude.

## 4.5 FINITE LENGTH DIPOLE

The former techniques can also be used to analyze linear dipoles of any length. For simplicity it is assumed here that the dipole has a negligible diameter (provided the diameter  $\ll \lambda$ ).

### 4.5.1 Current Distribution

For a very thin dipole (ideally zero diameter), the current distribution can be written, to a good approximation, as

$$\mathbf{I}_e(x' = 0, y' = 0, z') = \begin{cases} \hat{\mathbf{a}}_z I_0 \sin \left[ k \left( \frac{l}{2} - z' \right) \right], & 0 \leq z' \leq l/2 \\ \hat{\mathbf{a}}_z I_0 \sin \left[ k \left( \frac{l}{2} + z' \right) \right], & -l/2 \leq z' \leq 0 \end{cases} \quad (4-56)$$

This distribution assumes that the antenna is *center-fed and the current vanishes at the end points* ( $z' = \pm l/2$ ). Experimentally, the current in a center-fed wire antenna has sinusoidal form with nulls at the end points. For  $l = \lambda/2$  and  $\lambda/2 < l < \lambda$  the current distribution of (4-56) is shown plotted in Figs. 1.16(b) and 1.12(c), respectively. The geometry of the antenna is that shown in Fig. 4.5.

### 4.5.2 Radiated Fields: Element Factor, Space Factor, and Pattern

The finite dipole antenna of Figure 4.5 is subdivided into a number of infinitesimal dipoles of length  $\Delta z'$ . As the number of subdivisions is increased, each infinitesimal dipole approaches a length  $dz'$ . For an infinitesimal dipole of length  $dz'$  positioned along the  $z$ -axis at  $z'$ , the electric and magnetic field components in the far field are given, using (4-26a)–(4-26c), as

$$dE_\theta \approx j\eta \frac{kl_e(x', y', z')e^{-jkR}}{4\pi R} \sin \theta dz' \quad (4-57a)$$

$$dE_r \approx dE_\phi = dH_r = dH_\theta = 0 \quad (4-57b)$$

$$dH_\phi \approx j \frac{kl_e(x', y', z')e^{-jkR}}{4\pi R} \sin \theta dz' \quad (4-57c)$$

where  $R$  is given by (4-39) or (4-40).

Using the far-field approximations given by (4-46), (4-57a) can be written as

$$dE_\theta \approx j\eta \frac{kl_e(x', y', z')e^{-jkr}}{4\pi r} \sin \theta e^{+jkz' \cos \theta} dz' \quad (4-58)$$

Summing the contributions from all the infinitesimal elements, the integral reduces to

$$E_\theta = \int_{-l/2}^{+l/2} dE_\theta = j\eta \frac{ke^{-jkr}}{4\pi r} \sin \theta \left[ \int_{-l/2}^{+l/2} I_e(x', y', z') e^{+jkz' \cos \theta} dz' \right] \quad (4-58a)$$

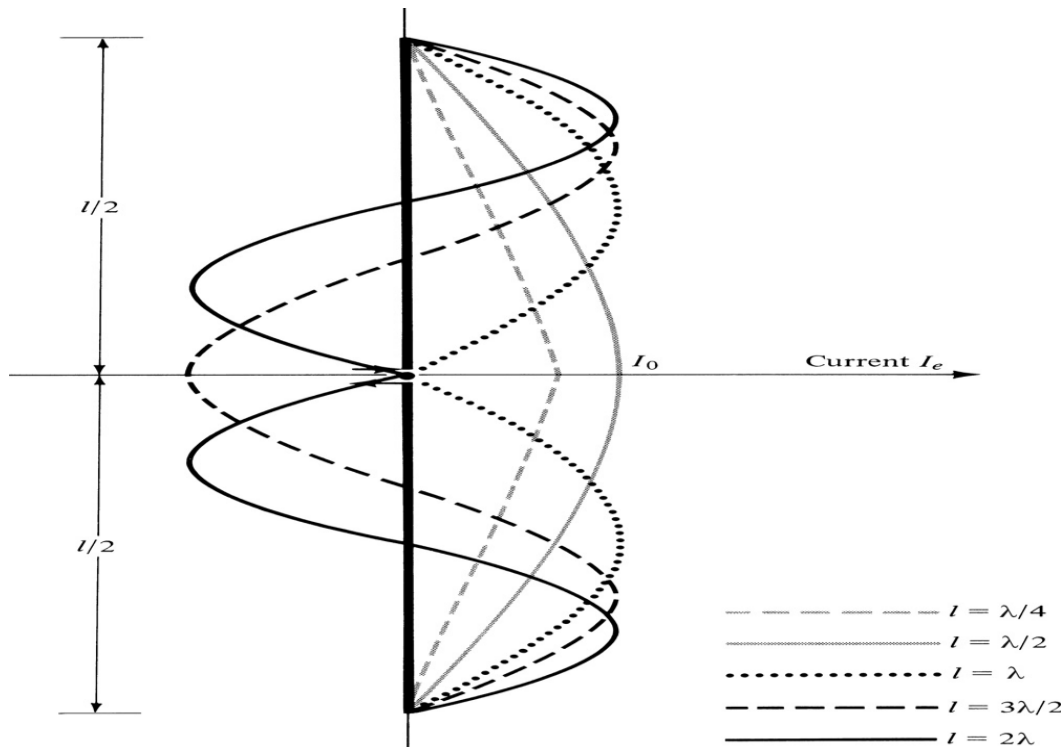


**Figure 4.8** Current distributions along the length of a linear wire antenna.

For the current distribution of (4-56), (4-58a) can be written as

$$E_{\theta} \approx j\eta \frac{kI_0 e^{-jkr}}{4\pi r} \sin \theta \left\{ \int_{-l/2}^0 \sin \left[ k \left( \frac{l}{2} + z' \right) \right] e^{+jkz' \cos \theta} dz' + \int_0^{+l/2} \sin \left[ k \left( \frac{l}{2} - z' \right) \right] e^{+jkz' \cos \theta} dz' \right\} \quad (4-60)$$

After performing the integration, it can be shown that

$$E_{\theta} \approx j\eta \frac{I_0 e^{-jkr}}{2\pi r} \left[ \frac{\cos \left( \frac{kl}{2} \cos \theta \right) - \cos \left( \frac{kl}{2} \right)}{\sin \theta} \right] \quad (4-62a)$$

And  $H_{\phi} = E_{\theta} / \eta$

### 4.5.3 Power Density, Radiation Intensity, and Radiation Resistance

For the dipole, the average Poynting vector can be written as

$$\begin{aligned} W_{av} &= \frac{1}{2} \text{Re}[\mathbf{E} \times \mathbf{H}^*] = \frac{1}{2} \text{Re}[\hat{a}_{\theta} E_{\theta} \times \hat{a}_{\phi} H_{\phi}^*] = \frac{1}{2} \text{Re} \left[ \hat{a}_{\theta} E_{\theta} \times \hat{a}_{\phi} \frac{E_{\theta}^*}{\eta} \right] \\ W_{av} &= \hat{a}_r W_{av} = \hat{a}_r \frac{1}{2\eta} |E_{\theta}|^2 = \hat{a}_r \eta \frac{|I_0|^2}{8\pi^2 r^2} \left[ \frac{\cos \left( \frac{kl}{2} \cos \theta \right) - \cos \left( \frac{kl}{2} \right)}{\sin \theta} \right]^2 \end{aligned} \quad (4-63)$$

And the radiation intensity is  $U = W_{av} r^2$  (4-64)

The normalized (to 0 dB) elevation power patterns, as given by (4-64) for  $l = \lambda/4, \lambda/2, 3\lambda/4,$  and  $\lambda$  are shown plotted in Figure 4.6. The current distribution of each is given by (4-56). The power patterns for an infinitesimal dipole  $l \ll \lambda$  ( $U \sim \sin^2 \theta$ ) is also included for comparison. As the length of the antenna increases, the beam becomes narrower. Because of that, the directivity should also increase with length. It is found that the 3-dB beamwidth of each is equal to

$l \ll \lambda$	3-dB beamwidth = $90^\circ$	(4-65)
$l = \lambda/4$	3-dB beamwidth = $87^\circ$	
$l = \lambda/2$	3-dB beamwidth = $78^\circ$	
$l = 3\lambda/4$	3-dB beamwidth = $64^\circ$	
$l = \lambda$	3-dB beamwidth = $47.8^\circ$	

As the length of the dipole increases beyond one wavelength ( $l > \lambda$ ), the number of lobes begin to increase. The normalized power pattern for a dipole with  $l = 1.25\lambda$  is shown in Fig. 4.7. In Fig. 4.7(a) the 3-D pattern in color is illustrated, while in Fig. 4.7(b) the 2-D (elevation pattern) in color is depicted. For the 3-D illustration, a  $90^\circ$  angular section of the pattern has been omitted to illustrate the elevation plane directional pattern variations. The current distribution for the dipoles with  $l = \lambda/4, \lambda/2, \lambda, 3\lambda/2,$  and  $2\lambda$ , as given by (4-56), is shown in Fig. 4.8.

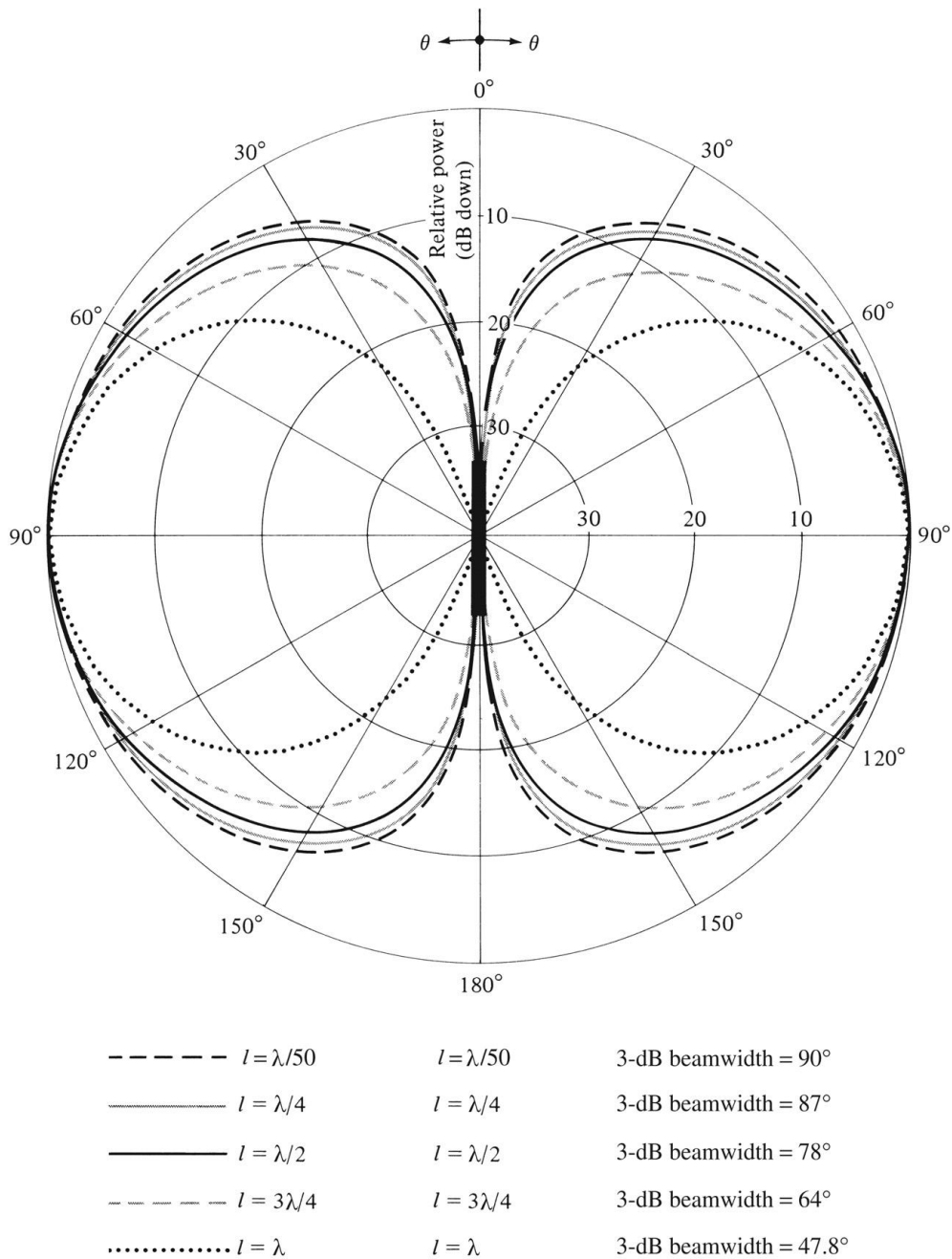


**Figure 4.6** Elevation plane amplitude patterns for a thin dipole with sinusoidal current distribution ( $l = \lambda/50, \lambda/4, \lambda/2, 3\lambda/4, \lambda$ ).

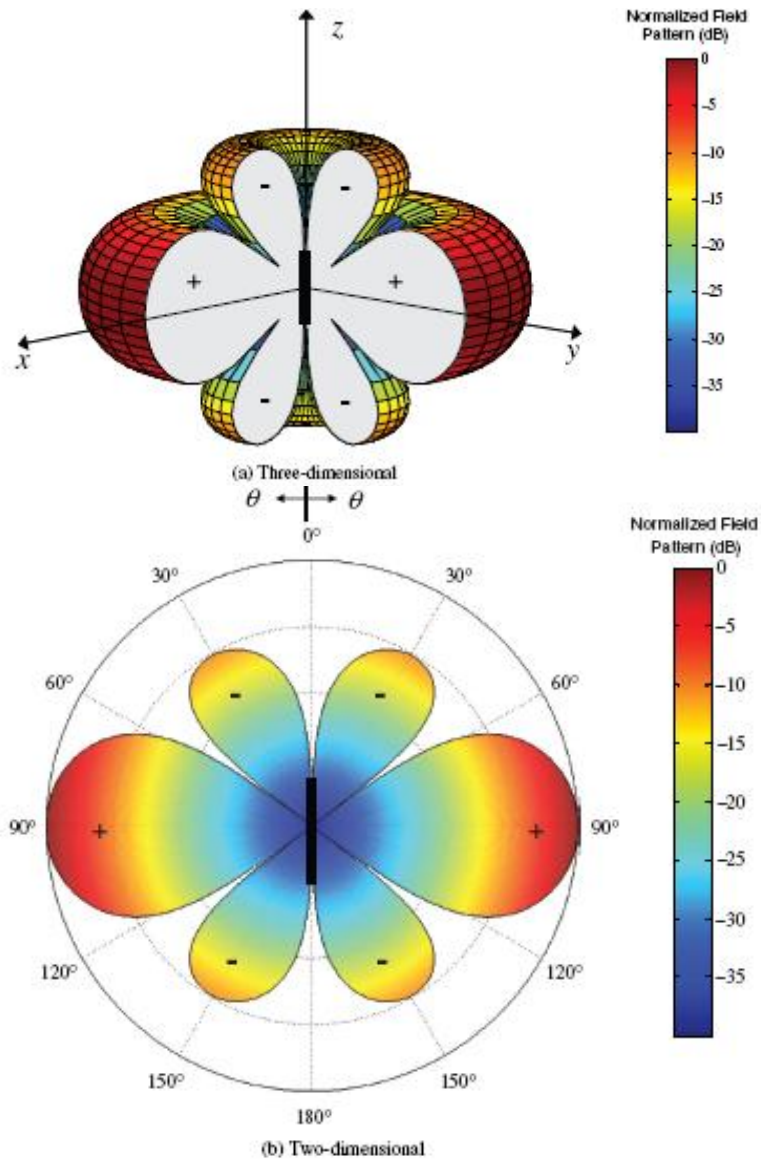


**Figure 4.7** 3-D and 2-D amplitude patterns for a thin dipole of  $l = 1.25\lambda$  and sinusoidal current distribution.

To find the total power radiated, the average Poynting vector of (4-63) is integrated over a sphere of radius  $r$ . Thus

$$\begin{aligned}
 P_{\text{rad}} &= \int_0^{2\pi} \int_0^\pi W_{\text{av}} r^2 \sin \theta \, d\theta \, d\phi \\
 &= \eta \frac{|I_0|^2}{4\pi} \int_0^\pi \frac{\left[ \cos\left(\frac{kl}{2} \cos \theta\right) - \cos\left(\frac{kl}{2}\right) \right]^2}{\sin \theta} \, d\theta \qquad (4-67)
 \end{aligned}$$

#### 4.5.4 Directivity

Figure 4.6, shows that as the radiation pattern of a dipole becomes more directional as its length increases. When the overall length is greater than one wavelength, the number of lobes increases and the antenna loses its directional properties. The parameter that is used as a “figure of merit” for the directional properties of the antenna is the directivity. The directivity

$$D_0 = 4\pi \frac{F(\theta, \phi)|_{\max}}{\int_0^{2\pi} \int_0^\pi F(\theta, \phi) \sin \theta \, d\theta \, d\phi} \quad (4-71)$$

where  $F(\theta, \phi)$  is related to the radiation intensity  $U$  by (2-19), or

$$U = B_0 F(\theta, \phi) \quad (4-72)$$

From (4-64), the dipole antenna of length  $l$  has

$$F(\theta, \phi) = F(\theta) = \left[ \frac{\cos\left(\frac{kl}{2} \cos \theta\right) - \cos\left(\frac{kl}{2}\right)}{\sin \theta} \right]^2 \quad (4-73)$$

It can be shown that

$$D_0 = \frac{2F(\theta)|_{\max}}{Q} \quad (4-75)$$

$$Q = \{C + \ln(kl) - C_i(kl) + \frac{1}{2} \sin(kl)[S_i(2kl) - 2S_i(kl)] + \frac{1}{2} \cos(kl)[C + \ln(kl/2) + C_i(2kl) - 2C_i(kl)]\} \quad (4-75a)$$

## 4.6 HALF-WAVELENGTH DIPOLE

One of the most commonly used antennas is the half-wavelength ( $l = \lambda/2$ ) dipole. Because its radiation resistance is 73 ohms, which is very near the 50-ohm or 75-ohm characteristic impedances of some transmission lines, its matching to the line is simplified especially at resonance. Because of its wide acceptance in practice, we will examine in a little more detail its radiation characteristics.

The electric and magnetic field components of a half-wavelength dipole can be obtained from (4-62a) and (4-62b) by letting  $l = \lambda/2$

$$E_\theta \approx j\eta \frac{I_0 e^{-jkr}}{2\pi r} \left[ \frac{\cos\left(\frac{\pi}{2} \cos \theta\right)}{\sin \theta} \right] \quad (4-84)$$

And  $H_\phi = E_\theta / \eta$

In turn, the time-average power density and radiation intensity can be written, respectively, as

$$W_{av} = \eta \frac{|I_0|^2}{8\pi^2 r^2} \left[ \frac{\cos\left(\frac{\pi}{2} \cos \theta\right)}{\sin \theta} \right]^2 \approx \eta \frac{|I_0|^2}{8\pi^2 r^2} \sin^3 \theta \quad (4-86)$$

And  $U = r^2 W_{av}$

whose two-dimensional pattern is shown plotted in Figure 4.6 while the three-dimensional pattern is depicted in Figure 4.12a. For the 3-D pattern of Fig. 4.12a, a  $90^\circ$  angular sector has been removed to illustrate the figure-eight elevation plane pattern variations.

The radiation intensity of the  $\lambda/2$  dipole can be approximated by, as represented in (4-87); that is,  $U \sim \sin^3 \theta$ .

The total power radiated can be obtained as a special case of (4-67), or

$$P_{rad} = \eta \frac{|I_0|^2}{4\pi} \int_0^\pi \frac{\cos^2 \left( \frac{\pi}{2} \cos \theta \right)}{\sin \theta} d\theta \quad (4-88)$$

$$D_0 = 4\pi \frac{U_{max}}{P_{rad}} = 4\pi \frac{U|_{\theta=\pi/2}}{P_{rad}} = \frac{4}{C_{in}(2\pi)} = \frac{4}{2.435} \approx 1.643 \quad (4-91)$$

The corresponding maximum effective area is equal to

$$A_{em} = \frac{\lambda^2}{4\pi} D_0 = \frac{\lambda^2}{4\pi} (1.643) \approx 0.13\lambda^2 \quad (4-92)$$

and the radiation resistance, for a free-space medium ( $\eta \approx 120\pi$ ), is given by

$$R_r = \frac{2P_{rad}}{|I_0|^2} = \frac{\eta}{4\pi} C_{in}(2\pi) = 30(2.435) \approx 73 \quad (4-93)$$

The radiation resistance of (4-93) is also the radiation resistance at the input terminals (input resistance) since the current maximum for a dipole of  $l = \lambda/2$  occurs at the input terminals (see Fig. 4.8). As it will be shown in Chapter 8, the imaginary part (reactance) associated with the input impedance of a dipole is a function of its length (for  $l = \lambda/2$ , it is equal to  $j42.5$ ). Thus the total input impedance for  $l = \lambda/2$  is equal to

$$Z_{in} = 73 + j42.5 \quad (4-93a)$$

To reduce the imaginary part of the input impedance to zero, the antenna is matched or reduced in length until the reactance vanishes. The latter is most commonly used in practice for  $\lambda/2$  dipoles.

## The $\lambda/4$ Monopole

In practice, a wide use has been made of a quarter-wavelength monopole ( $l = \lambda/4$ ) mounted above a ground plane, and fed by a coaxial line, as shown in Fig. 4.22(a). For analysis purposes, a  $\lambda/4$  image is introduced and it forms the  $\lambda/2$  equivalent of Fig. 4.22(b). It should be emphasized that the  $\lambda/2$  equivalent of Fig. 4.22(b) gives the correct field values for the actual system of Fig. 4.22(a) only above the interface ( $z \geq 0, 0 \leq \theta \leq \pi/2$ ). Thus, the far-zone E and H fields for the  $\lambda/4$  monopole above the ground plane are given, respectively, by (4-84) and (4-85).

$$E_{\theta} \simeq j\eta \frac{I_0 e^{-jkr}}{2\pi r} \left[ \frac{\cos\left(\frac{\pi}{2} \cos\theta\right)}{\sin\theta} \right] \quad (4-84)$$

$$H_{\phi} \simeq j \frac{I_0 e^{-jkr}}{2\pi r} \left[ \frac{\cos\left(\frac{\pi}{2} \cos\theta\right)}{\sin\theta} \right] \quad (4-85)$$

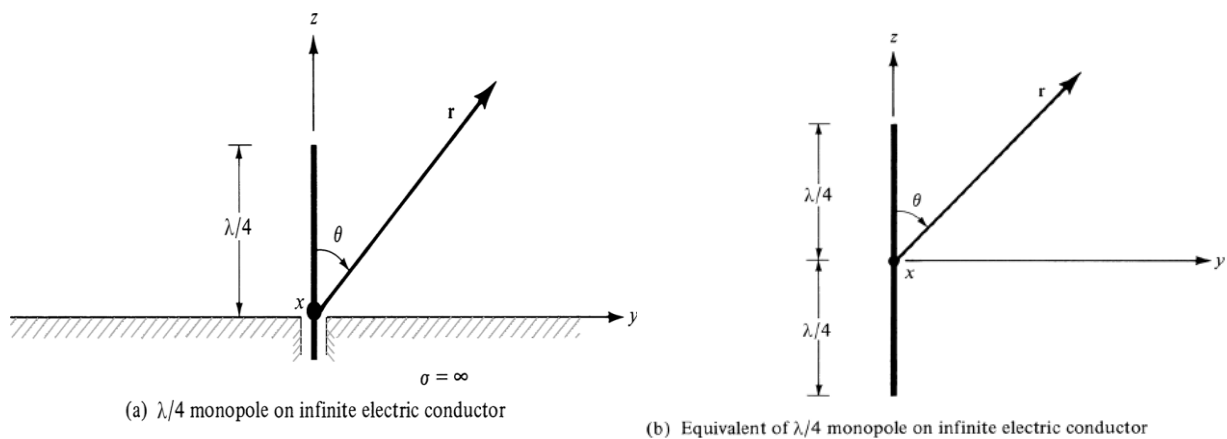


Figure 4.22 Quarter-wavelength monopole on an infinite perfect electric conductor.

From the discussions of the resistance of an infinitesimal dipole above a ground plane, it follows that the input impedance of a  $\lambda/4$  monopole above a ground plane is equal to one-half that of an isolated  $\lambda/2$  dipole. Thus, referred to the current maximum, the input impedance  $Z_{im}$  is given by

$$Z_{im} \text{ (monopole)} = \frac{1}{2} Z_{im} \text{ (dipole)} = \frac{1}{2} [73 + j42.5] = 36.5 + j21.25 \quad (4-106)$$

where  $73 + j42.5$  is the input impedance (and also the impedance referred to the current maximum) of a  $\lambda/2$  dipole as given by (4-93a).

## Summary of Important Formulas for the center-fed dipoles (far-field region)

**TABLE 4.3** Summary of Important Parameters and Associated Formulas and Equation Numbers for a Dipole in the Far Field

Parameter	Formula	Equation Number
<i>Infinitesimal Dipole</i> ( $l \leq \lambda/50$ )		
Normalized power pattern	$U = (E_{\theta n})^2 = C_0 \sin^2 \theta$	(4-29)
Radiation resistance $R_r$	$R_r = \eta \left(\frac{2\pi}{3}\right) \left(\frac{l}{\lambda}\right)^2 = 80\pi^2 \left(\frac{l}{\lambda}\right)^2$	(4-19)
Input resistance $R_{in}$	$R_{in} = R_r = \eta \left(\frac{2\pi}{3}\right) \left(\frac{l}{\lambda}\right)^2 = 80\pi^2 \left(\frac{l}{\lambda}\right)^2$	(4-19)
Wave impedance $Z_w$	$Z_w = \frac{E_{\theta}}{H_{\phi}} \simeq \eta = 377 \text{ ohms}$	
Directivity $D_0$	$D_0 = \frac{3}{2} = 1.761 \text{ dB}$	(4-31)
Maximum effective area $A_{em}$	$A_{em} = \frac{3\lambda^2}{8\pi}$	(4-32)
Half-power beamwidth	HPBW = 90°	(4-65)
<i>Small Dipole</i> ( $\lambda/50 < l \leq \lambda/10$ )		
Normalized power pattern	$U = (E_{\theta n})^2 = C_1 \sin^2 \theta$	(4-36a)
Radiation resistance $R_r$	$R_r = 20\pi^2 \left(\frac{l}{\lambda}\right)^2$	(4-37)
Input resistance $R_{in}$	$R_{in} = R_r = 20\pi^2 \left(\frac{l}{\lambda}\right)^2$	(4-37)
Wave impedance $Z_w$	$Z_w = \frac{E_{\theta}}{H_{\phi}} \simeq \eta = 377 \text{ ohms}$	(4-36a), (4-36c)
Directivity $D_0$	$D_0 = \frac{3}{2} = 1.761 \text{ dB}$	
Maximum effective area $A_{em}$	$A_{em} = \frac{3\lambda^2}{8\pi}$	
Half-power beamwidth	HPBW = 90°	(4-65)
<i>Half Wavelength Dipole</i> ( $l = \lambda/2$ )		
Normalized power pattern	$U = (E_{\theta n})^2 = C_2 \left[ \frac{\cos\left(\frac{\pi}{2} \cos \theta\right)}{\sin \theta} \right]^2 \simeq C_2 \sin^3 \theta$	(4-87)
Radiation resistance $R_r$	$R_r = \frac{\eta}{4\pi} C_{in}(2\pi) \simeq 73 \text{ ohms}$	(4-93)
Input impedance $Z_{in}$	$Z_{in} = 73 + j42.5$	(4-93a)
Directivity $D_0$	$D_0 = \frac{4}{C_{in}(2\pi)} \simeq 1.643 = 2.156 \text{ dB}$	(4-91)
Half-power beamwidth	HPBW = 78°	(4-65)

**Quarter-Wavelength Monopole**  
( $l = \lambda/4$ )

Normalized power pattern  $U = (E_{\theta n})^2 = C_2 \left[ \frac{\cos\left(\frac{\pi}{2} \cos\theta\right)}{\sin\theta} \right]^2 \approx C_2 \sin^3\theta$  (4-87)

Radiation resistance  $R_r$   $R_r = \frac{\eta}{8\pi} C_{in}(2\pi) \approx 36.5$  ohms (4-106)

Input resistance  $R_{in}$   $R_{in} = R_r = \frac{\eta}{8\pi} C_{in}(2\pi) \approx 36.5$  ohms (4-106)

Input impedance  $Z_{in}$   $Z_{in} = 36.5 + j21.25$  (4-106)

Wave impedance  $Z_w$   $Z_w = \frac{E_{\theta}}{H_{\phi}} \approx \eta = 377$  ohms

Directivity  $D_0$   $D_0 = 3.286 = 5.167$  dB

=====

**Solved Questions**

**Q1.** A horizontal infinitesimal electric dipole of constant current  $I_0$  is placed symmetrically about the origin and directed along the  $x$ -axis. Derive the (a) far-zone fields radiated by the dipole, (b) directivity of the antenna.

4-1. a.

$$\sin\psi = \sqrt{1 - \cos^2\psi} = \sqrt{1 - |\hat{a}_x \cdot \hat{a}_r|^2}$$

$$= \sqrt{1 - (\sin\theta \cos\phi)^2}$$

In far-zone fields

$$E_{\psi} \approx j\eta \frac{k I_0 l e^{-jkr}}{4\pi r} \cdot \sin\psi = j\eta \frac{k I_0 l e^{-jkr}}{4\pi r} \sqrt{1 - (\sin\theta \cos\phi)^2}$$

$$H_{\psi} \approx j \frac{k I_0 l e^{-jkr}}{4\pi r} \cdot \sin\psi = \frac{E_{\psi}}{\eta}$$

b.

$$U = U_0 (1 - \sin^2\theta \cos^2\phi)$$

$$\therefore \text{Prod} = U_0 \int_0^{2\pi} \int_0^{\pi} (1 - \sin^2\theta \cos^2\phi) \cdot \sin\theta d\theta d\phi = U_0 \cdot \frac{8\pi}{3}$$

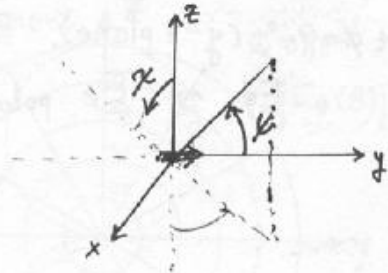
$$D_0 = \frac{4\pi \cdot U_0}{U_0 \cdot \frac{8\pi}{3}} = \frac{3}{2} = 1.5$$

**Q.2.** Repeat Problem 4.1 for a horizontal infinitesimal electric dipole directed along the  $y$ -axis.

4-2.

$$a. \sin\psi = \sqrt{1 - \cos^2\psi} = \sqrt{1 - |\hat{a}_y \cdot \hat{a}_r|^2}$$

$$= \sqrt{1 - \sin^2\theta \cdot \sin^2\phi}$$



In far-zone fields

$$E_{\psi} \approx j\eta \frac{k I_0 l e^{-jkr}}{4\pi r} \cdot \sin\psi = j\eta \frac{k I_0 l e^{-jkr}}{4\pi r} \cdot \sqrt{1 - \sin^2\theta \cdot \sin^2\phi}$$

$$H_{\psi} \approx \frac{E_{\psi}}{\eta} = j \frac{k I_0 l e^{-jkr}}{4\pi r} \sqrt{1 - \sin^2\theta \cdot \sin^2\phi}$$

b.  $U = U_0 (1 - \sin^2\theta \sin^2\phi)$

$$P_{rad} = U_0 \int_0^{2\pi} \int_0^{\pi} (1 - \sin^2\theta \cdot \sin^2\phi) \sin\theta d\theta d\phi = U_0 \int_0^{2\pi} \left[ \int_0^{\pi} \sin\theta - \sin^3\theta \cdot \sin^2\phi d\theta \right] d\phi$$

$$= U_0 \left[ \int_0^{2\pi} 2 d\phi - \frac{4}{3} \int_0^{2\pi} \sin^2\phi d\phi \right] = U_0 \left[ 4\pi - \frac{4}{3}\pi \right] = \frac{8}{3}\pi \cdot U_0$$

$$D_0 = \frac{4\pi \cdot U_0}{U_0 \cdot \frac{8\pi}{3}} = \frac{3}{2} = 1.5$$

=====  
**Q.3.** A thin linear dipole of length  $l$  is placed symmetrically about the  $Z$ -axis. Find the far-zone spherical  $E$  and  $H$  components radiated by the dipole whose current distribution can be approximated by:

$$(a) \underline{I}_z(z') = \begin{cases} I_0 \left(1 + \frac{z'}{l}\right), & -\frac{l}{2} < z' < 0 \\ I_0 \left(1 - \frac{z'}{l}\right), & 0 < z' < \frac{l}{2} \end{cases}$$

$$\underline{A}(r) \approx \hat{a}_z \frac{\mu}{4\pi} \frac{e^{-jkr}}{r} \int_{-l/2}^{l/2} I_z(z') e^{jk \hat{a}_r \cdot \vec{r}'} dz'$$

$$= \hat{a}_z \frac{\mu}{4\pi} \frac{e^{-jkr}}{r} \int_{-l/2}^{l/2} \left(1 - 2 \frac{|z'|}{l}\right) e^{jkz' \cos\theta} dz'$$

$$= \hat{a}_z \frac{\mu}{4\pi} \frac{e^{-jkr}}{r} \left\{ l \frac{\sin\left(\frac{kl}{2} \cos\theta\right)}{\left(\frac{kl}{2} \cos\theta\right)} - 2 \int_{-l/2}^{l/2} \frac{|z'|}{l} e^{jkz' \cos\theta} dz' \right\}$$

$$\int_{-l/2}^{l/2} \frac{|z'|}{l} e^{jkz' \cos\theta} dz' = \int_0^{l/2} \frac{z'}{l} e^{jkz' \cos\theta} dz' - \int_{-l/2}^0 \frac{z'}{l} e^{jkz' \cos\theta} dz'$$

$$\begin{aligned}
 &= \int_0^{l/2} \frac{z'}{l} e^{jkz' \cos \theta} dz' + \int_0^{l/2} \frac{z'}{l} e^{-jkz' \cos \theta} dz' \\
 &= 2 \int_0^{l/2} \frac{z'}{l} \cos[kz' \cos \theta] dz' = \frac{l}{2} \int_0^1 \cos\left[\frac{kl}{2} \xi \cos \theta\right] d\xi \\
 &= \frac{l}{2} \left\{ \frac{\sin\left(\frac{kl}{2} \cos \theta\right)}{\frac{kl}{2} \cos \theta} + \frac{\cos\left(\frac{kl}{2} \cos \theta\right) - 1}{\left(\frac{kl}{2} \cos \theta\right)^2} \right\}
 \end{aligned}$$

$$\therefore \underline{A}(\vec{r}) = \hat{a}_z \frac{\mu l}{4\pi} \frac{e^{-jkr}}{r} \left\{ \frac{1 - \cos\left(\frac{kl}{2} \cos \theta\right)}{\left(\frac{kl}{2} \cos \theta\right)^2} \right\}$$

$$A_\theta = \hat{a}_\theta \cdot \underline{A} = -\frac{\mu l}{4\pi} \frac{e^{-jkr}}{r} \sin \theta \left\{ \frac{1 - \cos\left(\frac{kl}{2} \cos \theta\right)}{\left(\frac{kl}{2} \cos \theta\right)^2} \right\}$$

$$A_\phi = \hat{a}_\phi \cdot \underline{A} = 0$$

In the far-zone  $E_r \approx 0$

$$E_\theta \approx j\omega\mu \frac{l}{4\pi} \frac{e^{-jkr}}{r} \sin \theta \left\{ \frac{1 - \cos\left(\frac{kl}{2} \cos \theta\right)}{\left(\frac{kl}{2} \cos \theta\right)^2} \right\}$$

$$E_\phi = H_r = H_\theta = 0, \quad \text{and} \quad H_\phi = E_\theta / \eta$$

$$(b) I_z(z') = I_0 \cos\left(\frac{\pi}{l} z'\right), \quad -l/2 \leq z' \leq l/2$$

$$\begin{aligned}
 E_\theta &= j\eta \frac{k e^{-jkr}}{4\pi r} \sin \theta \left[ \int_{-l/2}^{l/2} I(z') e^{jkz' \cos \theta} dz' \right] \\
 E_\theta &= j\eta \frac{k e^{-jkr}}{4\pi r} \sin \theta \cdot I_0 \int_{-l/2}^{l/2} \cos\left(\frac{\pi z'}{l}\right) e^{jkz' \cos \theta} dz'
 \end{aligned}$$

let  $a = jk \cos \theta$  and  $b = \frac{\pi}{l}$ , use following integral formula

$$\int \cos bz e^{az} dz = \frac{e^{az} (a \cos bz + b \sin bz)}{a^2 + b^2}$$

$$E_\theta = j\eta \frac{k e^{-jkr}}{4\pi r} \sin \theta \cdot I_0 \cdot \left\{ \frac{e^{jkz' \cos \theta}}{\left(\frac{\pi}{l}\right)^2 - k^2 \cos^2 \theta} \left[ jk \cos \theta \cos \frac{\pi z'}{l} + \frac{\pi}{l} \sin \frac{\pi z'}{l} \right] \right\}_{-l/2}^{l/2}$$

$$= j\eta \frac{k e^{-jkr}}{4\pi r} \sin \theta \cdot I_0 \left[ \frac{e^{jk \cdot l/2 \cos \theta}}{\left(\frac{\pi}{l}\right)^2 - k^2 \cos^2 \theta} \frac{\pi}{l} + \frac{e^{-jk \cdot l/2 \cos \theta}}{\left(\frac{\pi}{l}\right)^2 - k^2 \cos^2 \theta} \frac{\pi}{l} \right]$$

$$E_\theta = j\eta \frac{I_0 k e^{-jkr}}{4\pi r} \sin \theta \cdot \frac{\pi}{l} \cdot \frac{2 \cos\left(\frac{kl}{2} \cos \theta\right)}{\left(\frac{\pi}{l}\right)^2 - k^2 \cos^2 \theta} = j\eta \frac{I_0 e^{-jkr}}{2\pi r} \cdot \frac{\cos\left(\frac{\pi}{2} \cos \theta\right)}{\sin \theta}$$

$$H_\phi = j \frac{I_0 k e^{-jkr}}{4\pi r} \sin \theta \cdot \frac{\pi}{l} \cdot \frac{2 \cos\left(\frac{kl}{2} \cos \theta\right)}{\left(\frac{\pi}{l}\right)^2 - k^2 \cos^2 \theta} = j \frac{I_0 e^{-jkr}}{2\pi r} \frac{\cos\left(\frac{\pi}{2} \cos \theta\right)}{\sin \theta}$$

$$(c) I_z(z') = I_0 \cos^2 \left( \frac{\pi}{l} z' \right), \quad -l/2 \leq z' \leq l/2$$

$$(c) E_\theta = j\eta \frac{k e^{-jkr}}{4\pi r} \sin\theta \left[ \int_{-l/2}^{l/2} I_0 \cos^2 \left( \frac{\pi}{l} z' \right) e^{jkz' \cos\theta} dz' \right]$$

let  $a = jk \cos\theta$  and  $b = \frac{\pi}{l}$ , use the following integral formula

$$\int \cos^2 bz \cdot e^{az} dz = \frac{e^{az}}{2a} + \frac{e^{az}}{a^2 + 4b^2} \left( \frac{a}{2} \cos 2bz + b \sin 2bz \right)$$

$$E_\theta = j\eta \frac{k e^{-jkr}}{4\pi r} \sin\theta \cdot I_0 \left\{ \frac{e^{jkz' \cos\theta}}{jk \cos\theta} + \frac{e^{jkz' \cos\theta}}{\left(\frac{2\pi}{l}\right)^2 - k^2 \cos^2\theta} \left( \frac{jk \cos\theta}{2} \cos \frac{2\pi}{l} z' + \frac{\pi}{l} \sin \frac{2\pi}{l} z' \right) \right\}_{-l/2}^{l/2}$$

$$= j\eta \frac{k e^{-jkr}}{4\pi r} \sin\theta \cdot I_0 \left\{ \frac{\sin\left(\frac{kl}{2} \cos\theta\right)}{k \cos\theta} + k \cos\theta \frac{\sin\left(\frac{kl}{2} \cos\theta\right)}{\left(\frac{2\pi}{l}\right)^2 - k^2 \cos^2\theta} \right\}$$

$$H_\phi = j \frac{k e^{-jkr}}{4\pi r} \sin\theta I_0 \left\{ \frac{\sin\left(\frac{kl}{2} \cos\theta\right)}{k \cos\theta} + k \cos\theta \frac{\sin\left(\frac{kl}{2} \cos\theta\right)}{\left(\frac{2\pi}{l}\right)^2 - k^2 \cos^2\theta} \right\}$$

#### Q4

The radiation field of a particular antenna is given by:

$$\mathbf{E} = \hat{\mathbf{a}}_\theta j\omega\mu k \sin\theta \frac{I_0 A_1 e^{-jkr}}{4\pi r} + \hat{\mathbf{a}}_\phi \omega\mu \sin\theta \frac{I_0 A_2 e^{-jkr}}{2\pi r}$$

The values  $A_1$  and  $A_2$  depend on the antenna geometry. Obtain an expression for the radiation resistance. What is the polarization of the antenna?

$$W_{av} = \frac{1}{2\eta} (|E_\theta|^2 + |E_\phi|^2) = \frac{1}{2\eta} \left[ \frac{\omega^2 \mu^2 \sin^2\theta}{16\pi^2 r^2} I_0^2 (k^2 A_1^2 + 4A_2^2) \right]$$

$$P_{rad} = \frac{1}{2\eta} \frac{\omega^2 \mu^2 I_0^2}{16\pi^2} \left[ \int_0^{2\pi} \int_0^\pi \sin^3\theta d\theta d\phi \right] [k^2 A_1^2 + 4A_2^2]$$

$$P_{rad} = \frac{\omega^2 \mu^2 I_0^2 (k^2 A_1^2 + 4A_2^2)}{12\pi\eta}, \quad \left( \int_0^{2\pi} \int_0^\pi \sin^3\theta d\theta d\phi = \frac{8\pi}{3} \right)$$

$$\Rightarrow R_{rad} = \frac{2P_{rad}}{I_0^2} = \frac{\omega^2 \mu^2 (k^2 A_1^2 + 4A_2^2)}{6\pi\eta}$$

Elliptical polarization since

$$\vec{E}(t) = \frac{-\omega\mu k \sin\theta}{4\pi r} I_0 A_1 \sin(\omega t - kr) \hat{\mathbf{a}}_\theta + \frac{\omega\mu k \sin\theta}{2\pi r} I_0 A_2 \cos(\omega t - kr) \hat{\mathbf{a}}_\phi$$

**Q5]** A  $\lambda/2$  dipole situated with its center at the origin radiates a time-averaged power of 600 W at a frequency of 300 MHz. A second  $\lambda/2$  dipole is placed with its center at a point  $P(r, \theta, \phi)$ , where  $r = 200$  m,  $\theta = 90^\circ$ ,  $\phi = 40^\circ$ . Its axis is parallel to that of the transmitting antenna. What is the available power at the terminals of the second (receiving) dipole?



$$\text{At } f = 300 \text{ MHz, } \lambda = \frac{c}{f} = 1 \text{ m}$$

$$\Rightarrow \frac{2D^2}{\lambda} = \frac{2\left(\frac{\lambda}{2}\right)^2}{\lambda} = 0.5 \text{ m}$$

$r = 200 \text{ m} \gg 0.5 \text{ m}$

$$P_r = \left(\frac{\lambda}{4\pi r}\right)^2 G_{\text{Tot}} G_{\text{or}} = \left(\frac{\lambda}{4\pi r}\right)^2 D_{\text{ot}} D_{\text{or}}$$

Now since  $D_{\text{ot}} = D_{\text{or}} = 1.643$  for  $\frac{\lambda}{2}$  dipole. ← for lossless antenna

$$P_r = \left(\frac{1}{4\pi \cdot 200}\right)^2 (1.643)(1.643) \quad W = 0.2 \text{ mW}$$

**Q6]** A  $\lambda/2$  dipole is radiating into free-space. The coordinate system is defined so that the origin is at the center of the dipole and the  $z$ -axis is aligned with the dipole. Input power to the dipole is 100 W. The overall efficiency is 50%, find the power density (in  $\text{W/m}^2$ ) at  $r = 500$  m,  $\theta = 60^\circ$ ,  $\phi = 0^\circ$ .

The time average power density ( $W_{\text{av}} = \frac{1}{2} \frac{|E|^2}{\eta}$ )

$$W_{\text{av}} = \eta \frac{|I_0|^2}{8\pi^2 r^2} \left[ \frac{\cos^2\left(\frac{\pi}{2} \cos\theta\right)}{\sin^2\theta} \right], \quad P_{\text{rad}} = \eta \frac{|I_0|^2}{4\pi} \int_0^\pi \frac{\cos^2\left(\frac{\pi}{2} \cos\theta\right)}{\sin^2\theta} d\theta$$

$$P_{\text{rad}} = \frac{1}{2} R_{\text{rad}} |I_0|^2, \quad R_{\text{rad}} = \frac{\eta}{4\pi} [\gamma + \ln(2\pi) - C_2(2\pi)] = 30 [0.5772 + 1.838 + 0.02]$$

$$R_{\text{rad}} = 73.0523.$$

$$P_{\text{rad}} = (0.5 \cdot 100) = 50 \text{ watts.} \quad 50 = \frac{1}{2} (73.0523) |I_0|^2$$

$$|I_0|^2 = 1.36888.$$

$$\text{At } r = 500 \text{ m, } \theta = 60^\circ, \phi = 0^\circ$$

$$W_{\text{av}} = 120 \pi \cdot \frac{1.36888}{8\pi^2 (500)^2} \cdot \left[ \frac{\cos^2\left(\frac{\pi}{2} \cos 60^\circ\right)}{\sin^2 60^\circ} \right]$$

$$= 15 \cdot \frac{1.36888}{\pi \cdot 25 \times 10^4} \cdot (0.6667)$$

$$= 1.743 \times 10^{-5} \text{ Watts/m}^2.$$

**Q7]** A 3-cm long dipole carries a phasor current  $I_0 = 10e^{j60^\circ}$  A. Assuming that  $\lambda = 5$  cm, determine the E- and H-fields at 10 cm away from the dipole and at  $\theta = 45^\circ$ .

$$\begin{aligned}
 & l = 3 \text{ cm}, \lambda = 5 \text{ cm}, I = 10e^{j60^\circ} \\
 & r > \frac{2D^2}{\lambda} = \frac{2 \times 3^2}{5} = \frac{18}{5} = 3.6 \text{ cm} \Rightarrow 10 \text{ cm is in the far field.} \\
 & \frac{l}{\lambda} = \frac{3}{5} = 0.6 \Rightarrow \text{length of dipole is finite, } \frac{kl}{2} = \pi \cdot \frac{l}{\lambda} = 0.6\pi \\
 & E_\theta \approx j\eta \frac{I_0 e^{-jkr}}{2\pi r} \left[ \frac{\cos\left(\frac{kl}{2} \cos\theta\right) - \cos\left(\frac{kl}{2}\right)}{\sin\theta} \right] = j\eta \frac{I_0 e^{-jkr}}{2\pi r} \left[ \frac{\cos(0.6\pi \cos\theta) + 0.309}{\sin\theta} \right] \\
 & H_\phi \approx \frac{E_\theta}{\eta}, \quad \left( \left. \frac{\cos(0.6\pi \cos 45^\circ) + 0.309}{\sin 45^\circ} \right|_{\theta=45^\circ} = 0.7703 \right) \\
 & e^{-jkr} \Rightarrow kr = \frac{2\pi}{\lambda} r = \frac{2\pi}{5} \cdot 10 = 4\pi = 12.5663 \text{ rad} \\
 & \Rightarrow E_\theta = j 120\pi \cdot \frac{I_0 e^{j60^\circ} \cdot e^{-j4\pi}}{2\pi (0.1 \text{ m})} \cdot (0.7703) = 4620 e^{j11.52} \\
 & |E_\theta| = 4620 \text{ V/m}, |H_\phi| = \frac{4620}{120\pi} = 12.25 \text{ Ampere}
 \end{aligned}$$

**Q8]** A satellite S transmits an e.m. wave, at 10 GHz, via its transmitting antenna. The satellite which is at a distance of  $3.7 \times 10^7$  m from the earth surface, radiates 10 W from its antenna whose directivity is 50 dB. Determine the magnitude of the E-field at earth surface.

$$\begin{aligned}
 & P_{\text{rad}} = 10 \text{ Watt}, r = 3.7 \times 10^7 \text{ m}, D_0 = 50 \text{ dB} \Rightarrow 10^5 \\
 & a. D_0 = \frac{4\pi U_{\text{max}}}{P_{\text{rad}}} = \frac{4\pi \cdot r^2 |E|^2}{2\eta \cdot 10} = 10^5, \quad (\text{Since } U_{\text{max}} = \frac{\gamma^2 E_{\text{max}}^2}{2\eta}; \eta = 120\pi) \\
 & \Rightarrow E^2 = \frac{10^5 \times 2 \times 120\pi \times 10}{4\pi (3.7 \times 10^7)^2} = 4.4 \times 10^{-8} \\
 & E = 2 \times 10^{-4} \text{ V/m}
 \end{aligned}$$

**Q9]** A base-station in a mobile system has a lossless antenna of a maximum gain of 16 dB and works at 1,900 MHz. Assuming the input power to the antenna is 8 watts, what is the:

(a) maximum radiated power density (in watts/cm<sup>2</sup>) at a distance of 100 m from the base station.

(b) maximum power received at 100m by a mobile telephone whose antenna is a lossless  $\lambda/4$  vertical monopole. Assume the  $\lambda/4$  monopole is mounted on an infinite ground plane.

**Q10]** The half-wavelength dipole has an input impedance of  $(73+j42.5)$  Ohm. Determine its equivalent capacitor and resistance, then find the VSWR when it is connected to a 50 Ohm feed line.

3.  $l = \lambda/2, Z_c = 50 \text{ ohms}$

$$Z_{in} = 73 + j42.5, Y_{in} = \frac{1}{Z_{in}} = \frac{1}{73 + j42.5} \cdot \frac{73 - j42.5}{73 - j42.5}$$

$$Y_{in} = 0.01023 - j0.0059563 = (10.23 - j5.9563) \times 10^{-3} = G_{in} - jB_{in}$$

$$B_{in} = \omega C_{in} = 2\pi f C_{in} \Rightarrow C_{in} = \frac{B_{in}}{2\pi f} = \frac{5.9563 \times 10^{-3}}{2\pi \cdot (10 \times 10^8)} = 0.947997 \times 10^{-12}$$

$$\therefore C_{in} = 0.947997 \text{ pF}$$

$$G_{in} = 10.23 \times 10^{-3}$$

$$R_{in} = \frac{1}{G_{in}} = 97.75, \Gamma_{in} = \frac{R_{in} - Z_c}{R_{in} + Z_c} = \frac{97.75 - 50}{97.75 + 50} = 0.3232$$

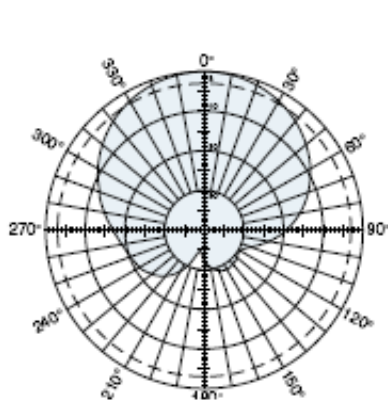
$$VSWR = \frac{1 + |\Gamma_{in}|}{1 - |\Gamma_{in}|} = \frac{1 + 0.3232}{1 - 0.3232} = 1.955$$



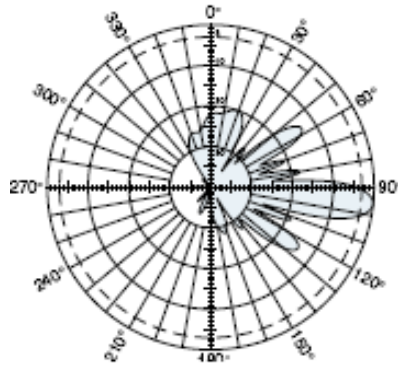
Examples of external and embedded/internal antennas in commercial cellular and CB radios.



Triangular array of dipoles used as a sectoral antenna in base-station antenna for mobile communication.



Horizontal pattern  
±45°- polarization



Vertical pattern  
±45°- polarization  
6° electrical downtilt



**Specifications:**

Frequency range	806–960 MHz
Gain	2 x 16.5 dBi (806–880 MHz) 2 x 17 dBi (880–960 MHz)
Impedance	50 ohms
VSWR	< 1.5:1 (806–880 MHz) < 1.3:1 (880–960 MHz)
Intermodulation (2x20w)	IM3: <-150dBc
Front-to-back ratio	>30 dB (co-polar)

## Friis Transmission Equation

The Friis Transmission Equation relates the power received to the power transmitted between two antennas separated by a distance  $R > 2D^2/\lambda$ , where  $D$  is the largest dimension of either antenna. Referring to Fig.2.31, let us assume that the transmitting antenna is initially isotropic. If the input power at the terminals of the transmitting antenna is  $P_t$ , then its isotropic power density  $W_0$  at distance  $R$  from the antenna is

$$W_0 = e_t \frac{P_t}{4\pi R^2} \quad (2-113)$$

where  $e_t$  is the radiation efficiency of the transmitting antenna. For a nonisotropic transmitting antenna, the power density of (2-113) in the direction  $\theta_t, \phi_t$  can be written as

$$W_t = \frac{P_t G_t(\theta_t, \phi_t)}{4\pi R^2} = e_t \frac{P_t D_t(\theta_t, \phi_t)}{4\pi R^2} \quad (2-114)$$

where  $G_t(\theta_t, \phi_t)$  is the gain and  $D_t(\theta_t, \phi_t)$  is the directivity of the transmitting antenna in the direction  $\theta_t, \phi_t$ . Since the effective area  $A_r$  of the receiving antenna is related to its efficiency  $e_r$  and directivity  $D_r$  by

$$A_r = e_r D_r(\theta_r, \phi_r) \left( \frac{\lambda^2}{4\pi} \right) \quad (2-115)$$

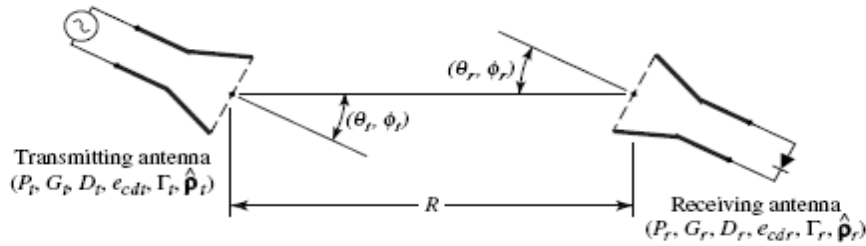


**Figure 2.31** Geometrical orientation of transmitting and receiving antennas for Friis transmission equation.

the amount of power  $P_r$  collected by the receiving antenna can be written, using (2-114) and (2-115), as

$$P_r = e_r D_r(\theta_r, \phi_r) \frac{\lambda^2}{4\pi} W_t = e_t e_r \frac{\lambda^2 D_t(\theta_t, \phi_t) D_r(\theta_r, \phi_r) P_t}{(4\pi R)^2} |\hat{p}_t \cdot \hat{p}_r|^2 \quad (2-116)$$

or the ratio of the received to the input power as

$$\frac{P_r}{P_t} = e_t e_r \frac{\lambda^2 D_t(\theta_t, \phi_t) D_r(\theta_r, \phi_r)}{(4\pi R)^2} \quad (2-117)$$

The  $P_r$  based on (2-117) assumes that the transmitting and receiving antennas are matched to their respective lines or loads (reflection efficiencies are unity) and the polarization of the receiving antenna is matched to the impinging wave (polarization efficiency is unity). Then

$$\frac{P_r}{P_t} = e_{cdt} e_{cdr} (1 - |\Gamma_t|^2) (1 - |\Gamma_r|^2) \left( \frac{\lambda}{4\pi R} \right)^2 D_t(\theta_t, \phi_t) D_r(\theta_r, \phi_r) |\hat{p}_t \cdot \hat{p}_r|^2 \quad (2-118)$$

### Example 2.16

Two *lossless* X-band (8.2–12.4 GHz) horn antennas are separated by a distance of  $100\lambda$ . The reflection coefficients at the terminals of the transmitting and receiving antennas are 0.1 and 0.2, respectively. The maximum directivities of the transmitting and receiving antennas (over isotropic) are 16 dB and 20 dB, respectively. Assuming that the input power in the lossless transmission line connected to the transmitting antenna is 2 W, and the antennas are aligned for maximum radiation between them and are polarization-matched, find the power delivered to the load of the receiver.

*Solution:* For this problem

$$e_{cdt} = e_{cdr} = 1 \text{ because the antennas are lossless.}$$

$$|\hat{\rho}_t \cdot \hat{\rho}_r|^2 = 1 \text{ because the antennas are polarization-matched}$$

$$\left. \begin{array}{l} D_t = D_{0t} \\ D_r = D_{0r} \end{array} \right\} \text{ because the antennas are aligned for} \\ \text{maximum radiation between them}$$

$$D_{0t} = 16 \text{ dB} \Rightarrow 39.81 \text{ (dimensionless)}$$

$$D_{0r} = 20 \text{ dB} \Rightarrow 100 \text{ (dimensionless)}$$

Using (2-118), we can write

$$\begin{aligned} P_r &= [1 - (0.1)^2][1 - (0.2)^2][\lambda/4\pi(100\lambda)]^2(39.81)(100)(2) \\ &= 4.777 \text{ mW} \end{aligned}$$

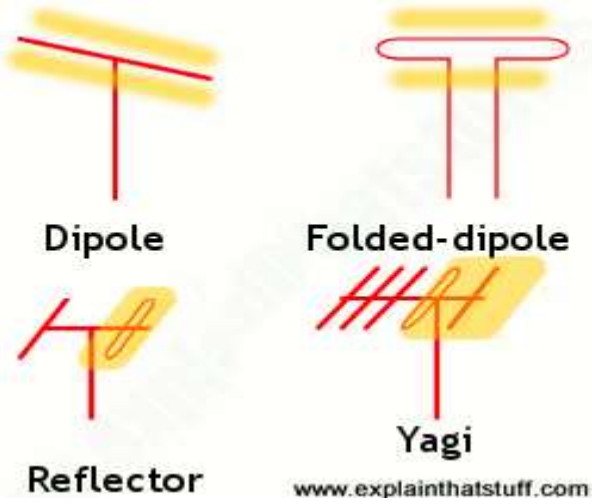
For reflection and polarization-matched antennas aligned for maximum directional radiation and reception, (2-118) reduces to

$$\frac{P_r}{P_t} = \left( \frac{\lambda}{4\pi R} \right)^2 G_{0t} G_{0r} \quad (2-119)$$

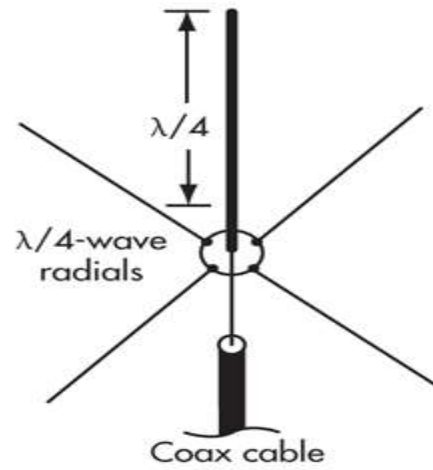
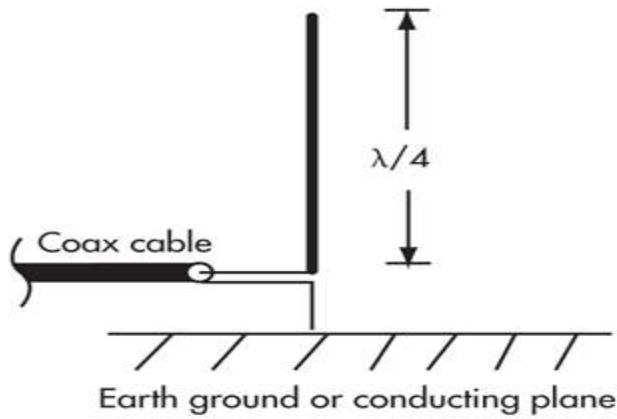
Equations (2-117), (2-118), or (2-119) are known as the ***Friis Transmission Equation***, and it relates the power  $P_r$  (delivered to the receiver load) to the input power of the transmitting antenna  $P_t$ . The term  $(\lambda/4\pi R)^2$  is called the ***free-space loss factor***, and it takes into account the losses due to the spherical spreading of the energy by the antenna.

**Q1]** In a long-range microwave communication system operating at 9 GHz, the transmitting and receiving antennas are identical, and they are separated by 10,000 m. To meet the signal-to-noise ratio of the receiver, the received power must be at least 10  $\mu\text{W}$ . Assuming the two antennas are aligned for maximum reception to each other, including being polarization matched, what should the gains (in dB) of the transmitting and receiving antennas be when the input power to the transmitting antenna is 10 W?

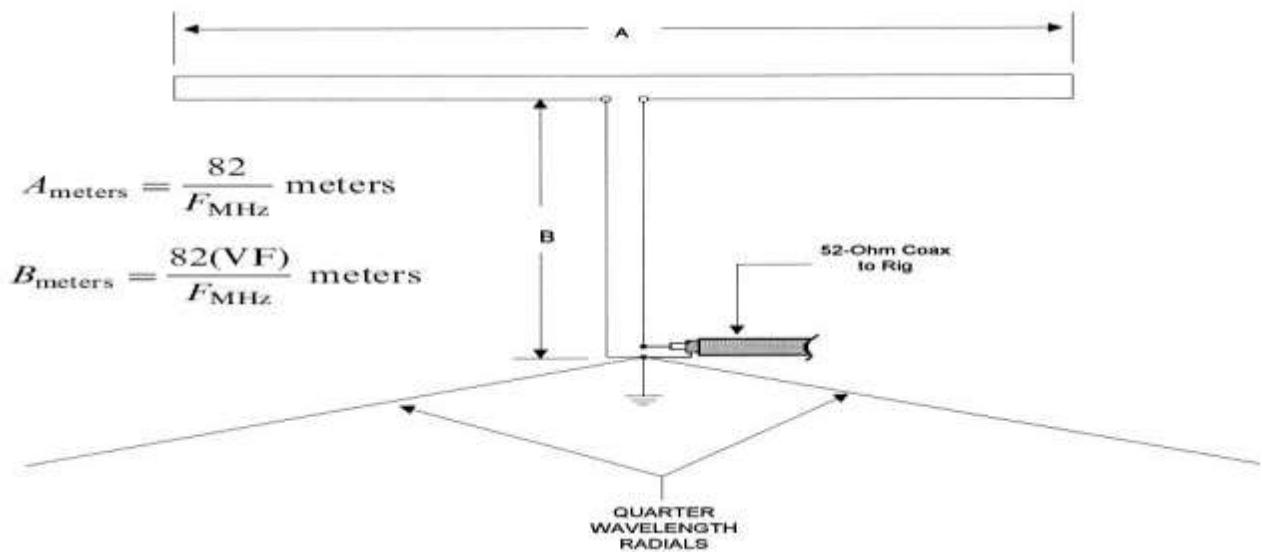
**Q2]** A communication system, operating at 100 MHz, uses two identical  $\lambda/2$  vertical lossless dipole antennas as transmitting and receiving elements separated by 10 km. In order for the signal to be detected by the receiver, the power level at the receiver terminals must be at least 1  $\mu\text{W}$ . Each antenna is connected to the transmitter and receiver by a lossless 50- $\Omega$  transmission line. Assuming the antennas are polarization-matched and are aligned so that the maximum intensity of one is directed toward the maximum radiation intensity of the other, determine the minimum transmitter power so that the signal will be detected by the receiver.



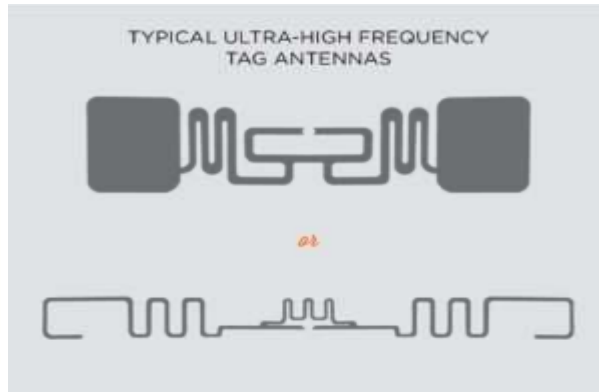
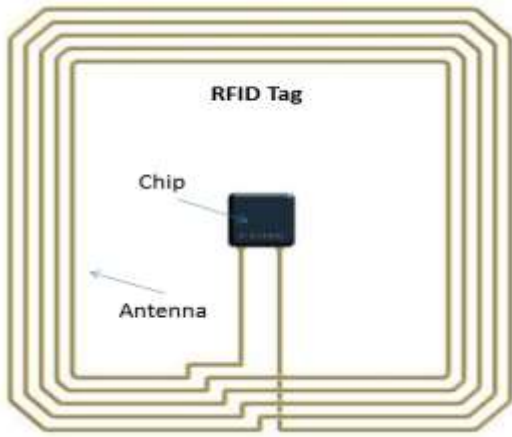
The Yagi Antenna (VHF & HF)



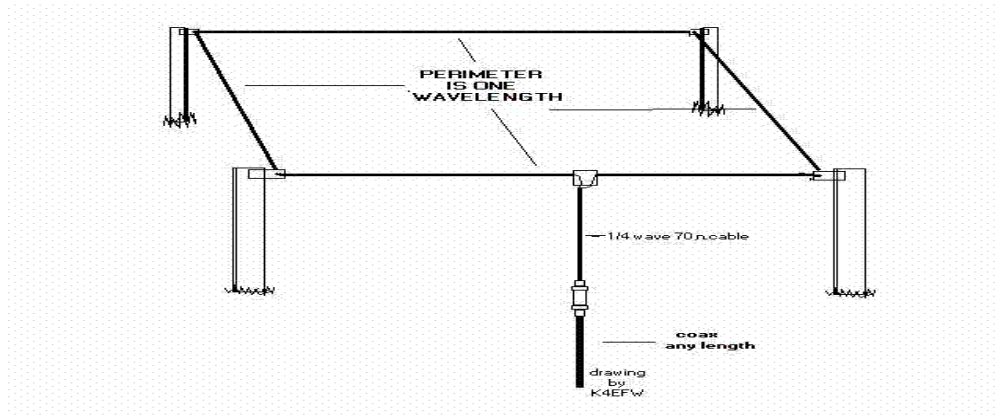
Monopole antenna over ground or conducting plane      Monopole antenna over 4 wires



The Folded Dipole Antenna



**The RFID (Radio Frequency Identification Device) Loop and Dipole Antennas**



**Loop Antennas ( VHF )**

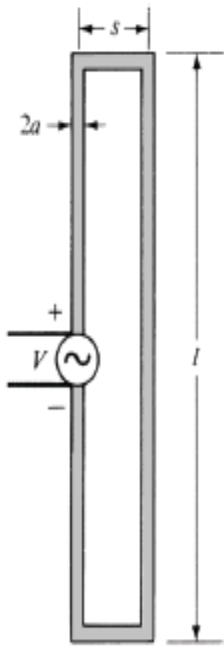


**The Helical antenna**

## The FOLDED DIPOLE

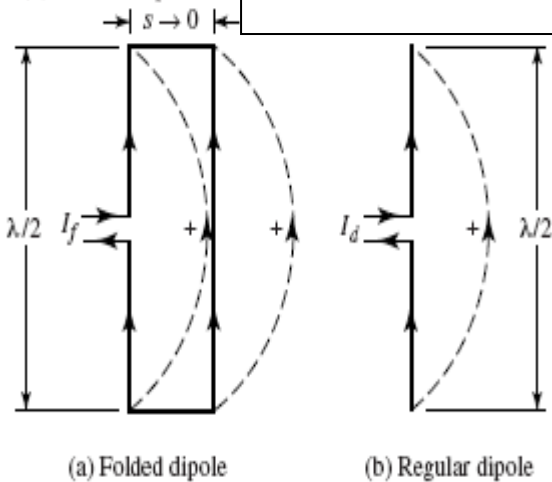
To achieve good directional pattern characteristics and good matching to practical coaxial lines with 50- or 75-ohm impedances, the length of a single wire element is usually chosen to be  $\lambda/4 \leq l < \lambda$ . The most widely used dipole is that whose overall length is  $l \approx \lambda/2$ , and which has an input impedance of  $Z_{in} \approx 73 + j42.5$  and directivity of  $D_o \approx 1.643$ .

In practice, there are other very common transmission lines whose characteristic impedance is much higher than 50 or 75 ohms. For example, a “twin-lead” transmission line (usually two parallel wires separated by about 8mm and embedded in a low-loss plastic material used for support and spacing) is widely used for TV applications and has a characteristic impedance of about 300 ohms.



To provide good matching characteristics, variations of the single dipole element must be used. One simple geometry that can achieve this is a folded wire which forms a very thin ( $s \ll \lambda$ ) rectangular loop as shown in Figure . When ( $s < \lambda$ ), is known as a *folded dipole* and it serves as a step-up impedance transformer (approximately by a factor of 4 when  $l = \lambda/2$ ) of the single-element impedance. Thus when  $l = \lambda/2$  and the antenna is resonant, impedances on the order of about 300 ohms can be achieved, and it would be ideal for connections to “twin-lead” transmission lines.

$$Z_f = 4 Z_d = 4 \times 73 = 292 \approx 300 \text{ Ohm}$$



when  $I_f$  is the current of the folded dipole and  $I_d$  is the current of the ordinary dipole, the input power of the two dipoles are identical, or

$$P_f \equiv \frac{1}{2} I_f^2 Z_f = P_d \equiv \frac{1}{2} I_d^2 Z_d$$

Which means

$$Z_f = 4 Z_d$$

## Loop Antennas

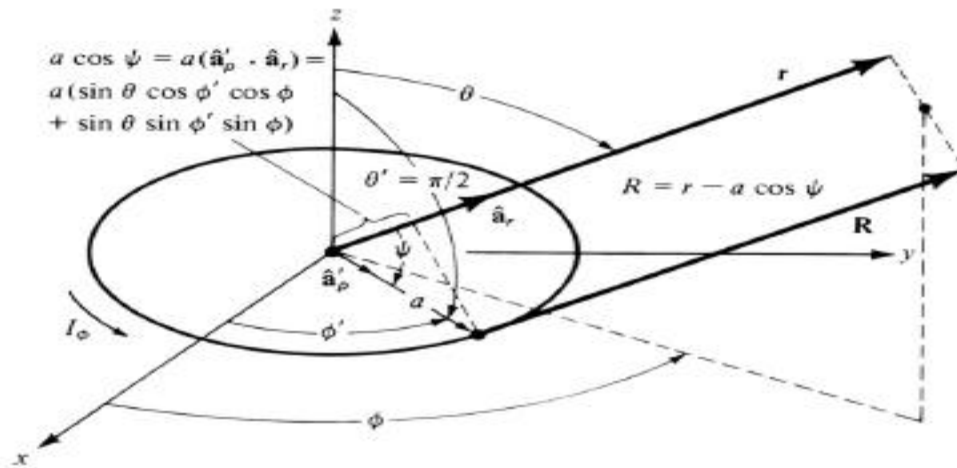
Loop antennas are simple, inexpensive, and very versatile type of antennas. Loop antennas take many different forms such as a rectangle, square, triangle, ellipse, circle, and many other configurations.

Because of the simplicity in analysis and construction, the circular loop is the most popular and has received the widest attention. The small loop (circular or square) is equivalent to an infinitesimal magnetic dipole whose axis is perpendicular to the plane of the loop. That is, the fields radiated by an electrically small circular or square loop are of the same mathematical form as those radiated by an infinitesimal magnetic dipole.

Loop antennas are usually classified into two categories, electrically small and electrically large. Electrically small antennas are those whose overall length (circumference) is usually less than about  $(C < 0.1 \lambda)$ . However, electrically large loops are those whose circumference is about  $(C \sim \lambda)$ . Most of the applications of loop antennas are in the HF (3–30 MHz), VHF (30–300 MHz), and UHF (300–3,000 MHz) bands.

### SMALL CIRCULAR LOOP

Consider a small loop antenna on the  $x$ - $y$  plane, at  $z = 0$ , as shown in the Figure. The wire is assumed to be very thin and the current is constant along the wire,  $I_\phi = I_0$ . This type of current distribution is accurate only for a very small circumference.



(b) Geometry for far-field observations

$$\left. \begin{aligned} H_\theta &\simeq -\frac{k^2 a^2 I_0 e^{-jkr}}{4r} \sin \theta = -\frac{\pi S I_0 e^{-jkr}}{\lambda^2 r} \sin \theta \\ E_\phi &\simeq \eta \frac{k^2 a^2 I_0 e^{-jkr}}{4r} \sin \theta = \eta \frac{\pi S I_0 e^{-jkr}}{\lambda^2 r} \sin \theta \end{aligned} \right\} kr \gg 1$$

$$H_r \simeq H_\phi = E_r = E_\theta = 0$$

The far-field components of the small circular loop antenna of radius  $a$ .  
 $S = \pi a^2$   
 is the area of the loop.

$$D_0 = 4\pi \frac{U_{\max}}{P_{\text{rad}}} = \frac{3}{2}$$

$$A_{em} = \left(\frac{\lambda^2}{4\pi}\right) D_0 = \frac{3\lambda^2}{8\pi}$$

When the radius of the loop is relatively large and the current can be considered constant along the loop, then the far-field components will be

$$E_r \simeq E_\theta = 0$$

$$E_\phi \simeq \frac{ak\eta I_0 e^{-jkr}}{2r} J_1(ka \sin \theta)$$

$$H_r \simeq H_\theta = 0$$

$$H_\phi \simeq -\frac{E_\phi}{\eta} = -\frac{akI_0 e^{-jkr}}{2r} J_1(ka \sin \theta)$$

$$r \gg a$$

$$I = \text{constant}$$

$$U = r^2 W_r = \frac{(a\omega\mu)^2 |I_0|^2}{8\eta} J_1^2(ka \sin \theta)$$

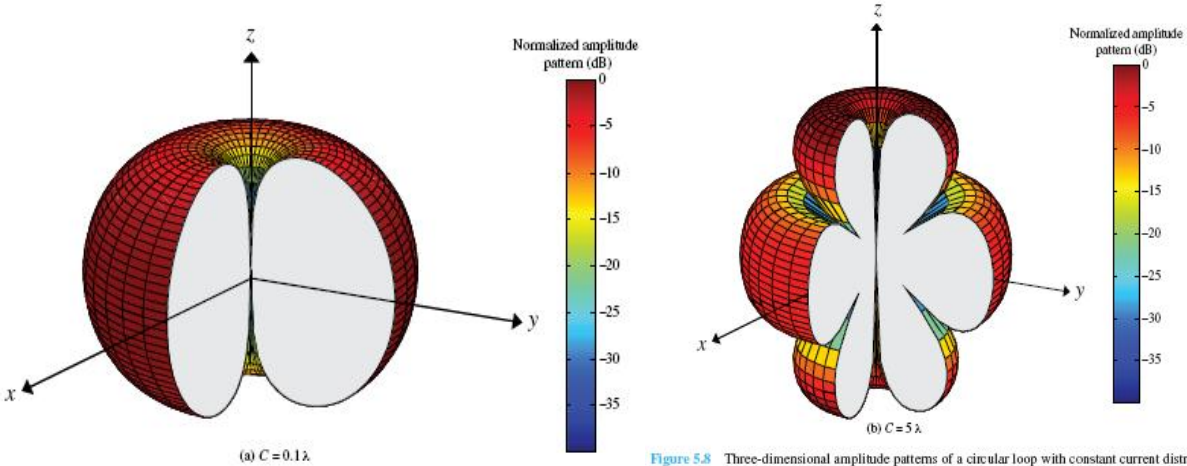


Figure 5.8 Three-dimensional amplitude patterns of a circular loop with constant current distribution.

A horizontal, lossless, one-turn circular loop of circumference  $C = \lambda$ , with a nonuniform current distribution, is radiating in free space. The far-field pattern of the antenna can be approximated by

$$E_\phi \simeq C_0 \cos^2 \theta \frac{e^{-jkr}}{r} \left. \begin{array}{l} 0^\circ \leq \theta \leq 90^\circ \\ 0^\circ \leq \phi \leq 360^\circ \end{array} \right\}$$

where  $C_0$  is a constant and  $\theta$  is measured from the normal to the plane/area of the loop. Determine the

- (a) Maximum exact directivity (*dimensionless and in dB*).
- (b) *Approximate* input impedance of the loop.
- (c) Input *reflection coefficient* when the antenna is connected to a balanced “twin-lead” transmission line with a characteristic impedance of 300 ohms.
- (d) *Maximum gain* of the loop (*dimensionless and in dB*).

## Array Antennas

Usually the radiation pattern of a single element is relatively wide, and each element provides low values of directivity and gain. In many applications, antennas with very directive characteristics (very high gains) are required to meet long distance communications. This can only be accomplished by increasing the electrical size of the antenna.

Enlarging the dimensions of a single element often leads to more directive characteristics. Another way to enlarge the dimensions of the antenna, without necessarily increasing the element size, is to form a group of elements in an electrical and geometrical configuration. This new antenna is referred to as an **array**. In most cases, the elements of an array are identical as this is convenient, simpler, and more practical. The individual elements of an array may be of any form (wires, apertures, etc.).

The total field of the array is determined by the vector addition of the fields radiated by the individual elements. To provide very directive patterns, it is necessary that the fields from the elements of the array interfere constructively (add) in the desired directions and interfere destructively (cancel each other) in the remaining space. Ideally this can be accomplished, but practically it is only approached. In an array of identical elements, there are at least five controls that can be used to shape the overall pattern of the antenna. These are:

1. the geometrical configuration of the overall array (linear, circular, rectangular, spherical, etc.),
2. the relative displacement between the elements,
3. the excitation amplitude of the individual elements,
4. the excitation phase of the individual elements,
5. the relative pattern of the individual elements.

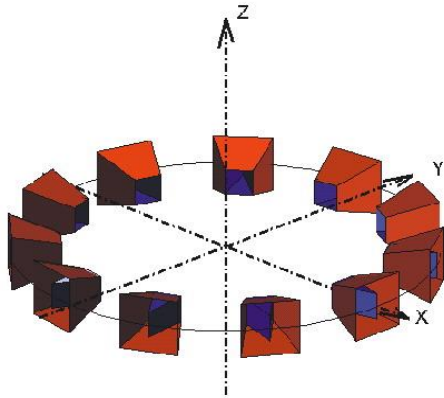
The simplest and one of the most practical arrays is formed by placing the elements along a line. We will start with the simplest example of a two-element array.

### Two-Element Array

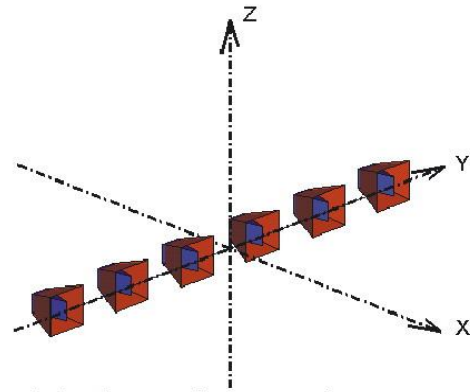
Assume that the two element antenna is an array of two infinitesimal horizontal dipoles positioned along the  $z$ -axis, as shown in Fig. 6.1(a). The total field radiated by the two elements, *assuming no coupling between the elements*, is equal to the sum of the two and in the  $y$ - $z$  plane it is given by

$$\mathbf{E}_t = \mathbf{E}_1 + \mathbf{E}_2 = \hat{\mathbf{a}}_{\theta} j\eta \frac{kI_0 l}{4\pi} \left\{ \frac{e^{-j[kr_1 - (\beta/2)]}}{r_1} \cos \theta_1 + \frac{e^{-j[kr_2 + (\beta/2)]}}{r_2} \cos \theta_2 \right\} \quad (6-1)$$

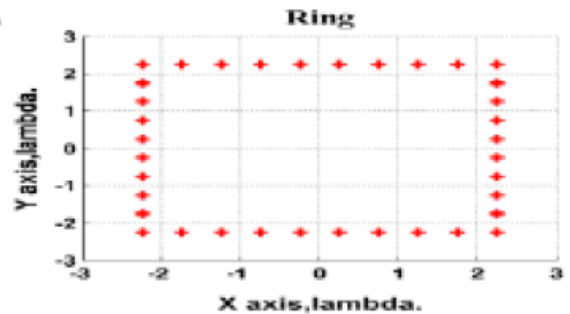
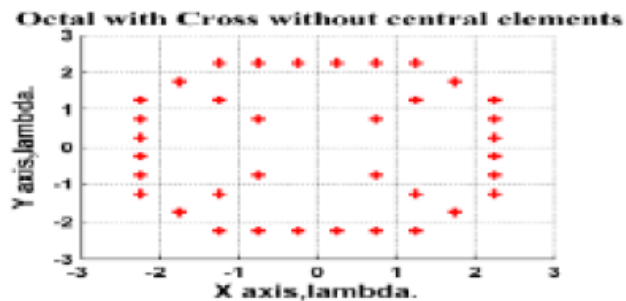
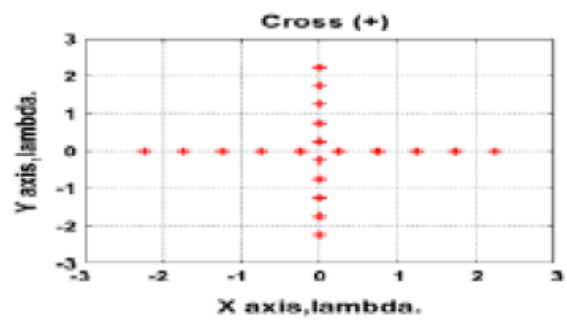
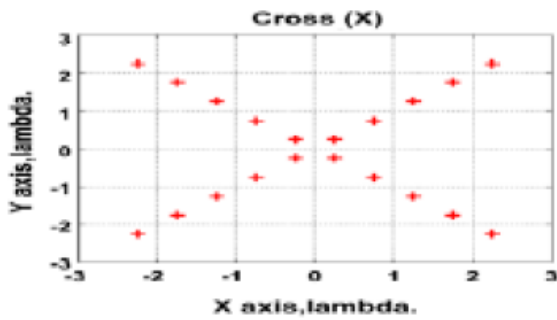
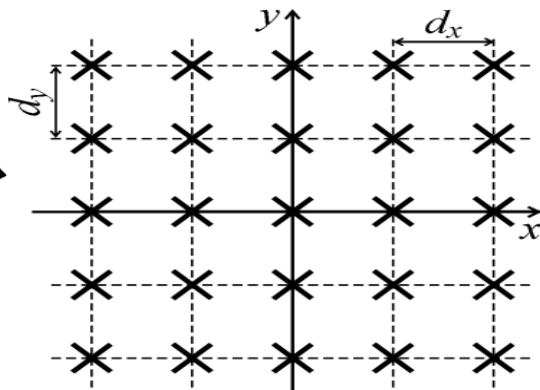
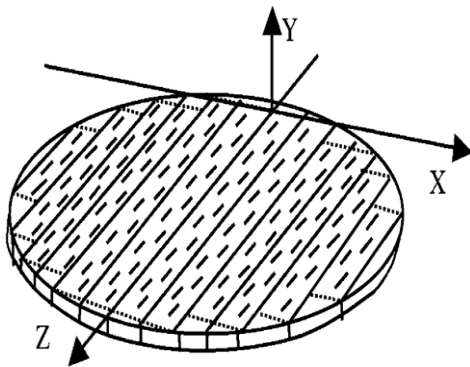
where  $\beta$  is the difference in phase excitation between the elements. The magnitude excitation of the radiators is identical. In the far-field region, the following approximations can be made



Uniform Circular Array (UCA)



Uniform Linera Array (ULA)



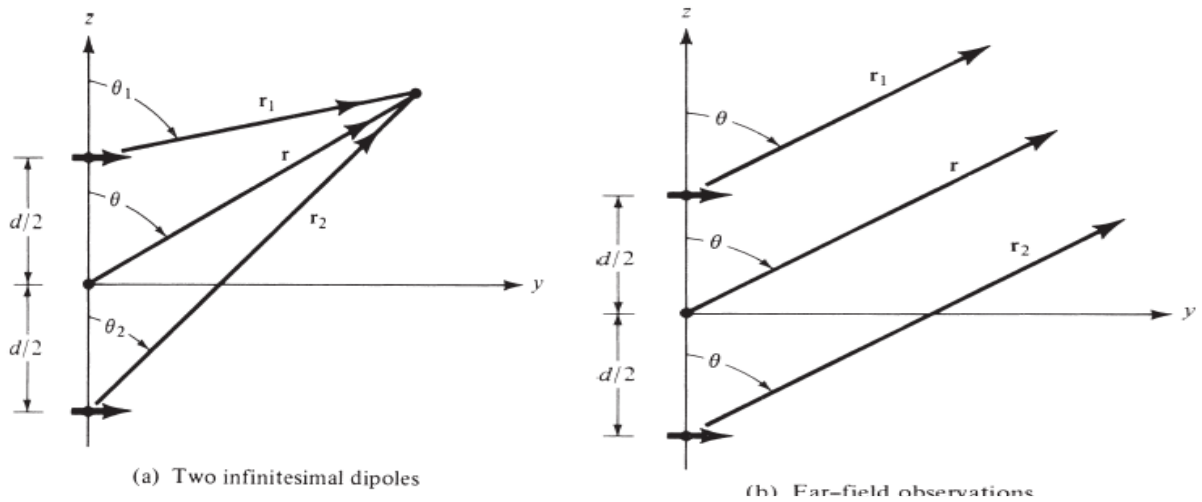


Fig. 6-1 Geometry of a two-element array positioned along the z-axis.

$$\theta_1 \simeq \theta_2 \simeq \theta \quad (6-2a)$$

$$\left. \begin{aligned} r_1 &\simeq r - \frac{d}{2} \cos \theta \\ r_2 &\simeq r + \frac{d}{2} \cos \theta \end{aligned} \right\} \text{for phase variations} \quad (6-2b)$$

$$r_1 \simeq r_2 \simeq r \quad \text{for amplitude variations} \quad (6-2c)$$

Then Eq. 6-1 can be written as

$$\mathbf{E}_t = \hat{\mathbf{a}}_{\theta} j\eta \frac{kI_0 l e^{-jkr}}{4\pi r} \cos \theta \left[ e^{+j(kd \cos \theta + \beta)/2} + e^{-j(kd \cos \theta + \beta)/2} \right]$$

$$\mathbf{E}_t = \hat{\mathbf{a}}_{\theta} j\eta \frac{kI_0 l e^{-jkr}}{4\pi r} \cos \theta \left\{ 2 \cos \left[ \frac{1}{2}(kd \cos \theta + \beta) \right] \right\} \quad (6-3)$$

Equation (6-3) shows that the total field of the array is equal to the field of a single element positioned at the origin multiplied by a factor which is called the **array factor**. Thus for the two-element array of constant amplitude, the array factor is given by

$$AF = 2 \cos \left[ \frac{1}{2}(kd \cos \theta + \beta) \right] \quad (6-4)$$

And its normalized version is

$$(AF)_n = \cos \left[ \frac{1}{2}(kd \cos \theta + \beta) \right] \quad (6-4a)$$

The array factor is a function of the array geometry and the excitation phase. By varying the separation  $d$  and/or the phase  $\beta$  between the elements, the array factor and of the total field of the array can be controlled.

It has been illustrated that the far-zone field of a uniform two-element array of identical elements is equal to the *product of the field of a single element, at a selected reference point (usually the origin), and the array factor of that array.* That is,

$$\mathbf{E}(\text{total}) = [\mathbf{E}(\text{single element at reference point})] \times [\text{array factor}] \quad (6-5)$$

This is referred to as *pattern multiplication* for arrays of identical elements. It is also valid for arrays with any number of identical elements which do not necessarily have identical magnitudes, phases, and/or spacings between them.

Each array has its own array factor. The array factor, is a function of the number of elements, their geometrical arrangement, their relative magnitudes, their relative phases, and their spacings. The array factor is usually derived using the point-source array, then the total field of the actual array is obtained by the use of (6-5). Each point-source is assumed to have the amplitude, phase, and location of the corresponding element it is replacing.

In order to synthesize the total pattern of an array, the designer is not only required to select the proper radiating elements but the geometry (positioning) and excitation of the individual elements.

### Example 6.1

Given the array of Fig. 6.1(a) and (b), find the nulls of the total field when  $d = \lambda/4$  and: (a)  $\beta=0$ , (b)  $\beta=\pi/2$ , (c)  $\beta= -\pi/2$ .

**Solution: (a)  $\beta=0$ ,**

In this case  $kd=2\pi/\lambda \times \lambda/4 = \pi/2$ , then Eq. 6-4-a becomes

$$E_{tn} = \cos \theta \cos \left( \frac{\pi}{4} \cos \theta \right)$$

The nulls are obtained by setting the total field equal to zero, or  $E_{tn}=0$ ,

$$E_{tn} = \cos \theta \cos \left( \frac{\pi}{4} \cos \theta \right) |_{\theta=\theta_n} = 0$$

which means that the product of two terms is equal to zero, then

either  $\cos \theta_n = 0 \Rightarrow \theta_n = 90^\circ$ , or

$$\cos \left( \frac{\pi}{4} \cos \theta_n \right) = 0 \Rightarrow \frac{\pi}{4} \cos \theta_n = \frac{\pi}{2}, -\frac{\pi}{2} \Rightarrow \theta_n = \text{does not exist}$$

The only null occurs at  $\theta = 90^\circ$  and is due to the pattern of the individual elements. The array factor does not contribute any additional nulls since there is not enough separation between the elements to introduce a phase difference of  $180^\circ$  between the elements, for any observation angle.

**Solution: (a)  $\beta=\pi/2$ ,**

In this case  $kd=2\pi/\lambda \times \lambda/4 = \pi/2$ , then Eq. 6-4-a becomes

$$E_{tn} = \cos \theta \cos \left[ \frac{\pi}{4} (\cos \theta + 1) \right]$$

The nulls are obtained by setting the total field equal to zero, or  $E_{tn}=0$ ,

$$E_{tn} = \cos \theta \cos \left[ \frac{\pi}{4} (\cos \theta + 1) \right] |_{\theta=\theta_n} = 0$$

which means that the product of two terms is equal to zero, then

either  $\cos \theta_n = 0 \Rightarrow \theta_n = 90^\circ$ , or

$$\cos \left[ \frac{\pi}{4} (\cos \theta + 1) \right] |_{\theta=\theta_n} = 0 \Rightarrow \frac{\pi}{4} (\cos \theta_n + 1) = \frac{\pi}{2} \Rightarrow \theta_n = 0^\circ$$

$$\Rightarrow \frac{\pi}{4} (\cos \theta_n + 1) = -\frac{\pi}{2} \Rightarrow \theta_n = \text{does not exist}$$

The nulls of the array occur at  $\theta = 90^\circ$  and  $0^\circ$ . The null at  $0^\circ$  is introduced by the arrangement of the elements (array factor). This can also be shown by physical reasoning, as shown in Fig. 6.2(a). The element in the negative  $z$ -axis has an initial phase lag of  $90^\circ$  relative to the other element. As the wave from that element travels toward the positive  $z$ -axis ( $\theta = 0^\circ$  direction), it undergoes an additional  $90^\circ$  phase retardation when it arrives at the other element on the positive  $z$ -axis. Thus there is a total of  $180^\circ$  phase difference between the waves of the two elements when travel is toward the positive  $z$ -axis ( $\theta = 0^\circ$ ). The waves of the two elements are in phase when they travel in the negative  $z$ -axis ( $\theta = 180^\circ$ ), as shown in Fig.6.2(b).

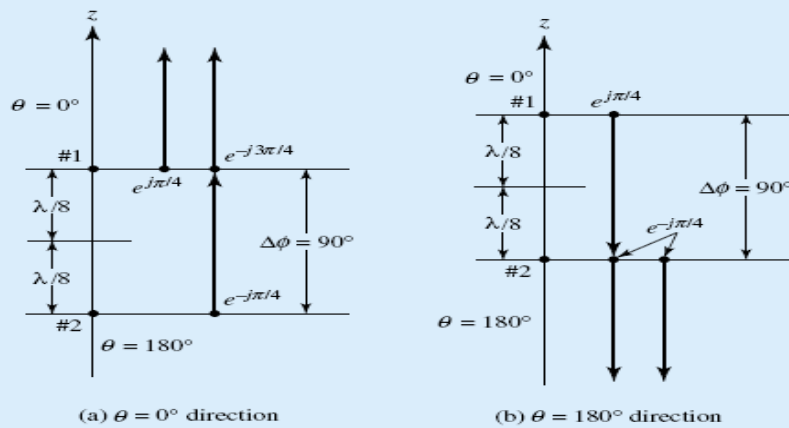


**Figure 6.2** Phase accumulation for two-element array for null formation toward  $\theta = 0^\circ$  and  $180^\circ$ .

c.  $\beta = -\frac{\pi}{2}$

The normalized field is given by

$$E_{tn} = \cos \theta \cos \left[ \frac{\pi}{4} (\cos \theta - 1) \right]$$

and the nulls by

$$E_{tn} = \cos \theta \cos \left[ \frac{\pi}{4} (\cos \theta - 1) \right] |_{\theta=\theta_n} = 0$$

Thus

$$\cos \theta_n = 0 \Rightarrow \theta_n = 90^\circ$$

and

$$\cos \left[ \frac{\pi}{4} (\cos \theta_n - 1) \right] = 0 \Rightarrow \frac{\pi}{4} (\cos \theta_n - 1) = \frac{\pi}{2} \Rightarrow \theta_n = \text{does not exist}$$

and

$$\Rightarrow \frac{\pi}{4} (\cos \theta_n - 1) = -\frac{\pi}{2} \Rightarrow \theta_n = 180^\circ$$

The nulls occur at  $90^\circ$  and  $180^\circ$ . The element at the positive  $z$ -axis has a phase lag of  $90^\circ$  relative to the other, and the phase difference is  $180^\circ$  when travel is restricted toward the negative  $z$ -axis. There is no phase difference when the waves travel toward the positive  $z$ -axis. A diagram similar to that of Fig. 6.2 can be used to illustrate this case.

The normalized patterns of the single element, the array factor, and the total array for each of the above array examples are shown in Fig. 6.3, 6.4(a), and 6.4(b). In each figure, the total pattern of the array is obtained by multiplying the pattern of the single element by that of the array factor. *In each case, the pattern is normalized to its own maximum.* Since the array factor for the example of Fig. 6.3 is nearly isotropic (within 3 dB), the element pattern and the total pattern are almost identical in shape. The largest magnitude difference between the two is about 3 dB, and for each case it occurs toward the direction along which the phases of the two elements are in phase quadrature ( $90^\circ$  out of phase). For Fig. 6.3 this occurs along  $\theta = 0^\circ$  while for Fig.6.4(a,b) this occurs along  $\theta = 90^\circ$ . Because the array factor for Fig.6.4(a) is of cardioid form, its corresponding element and total patterns are considerably different. In the total pattern, the null at  $\theta = 90^\circ$  is due to the element pattern while that toward  $\theta = 0^\circ$  is due to the array factor. Similar results are displayed in Fig. 6.4(b).

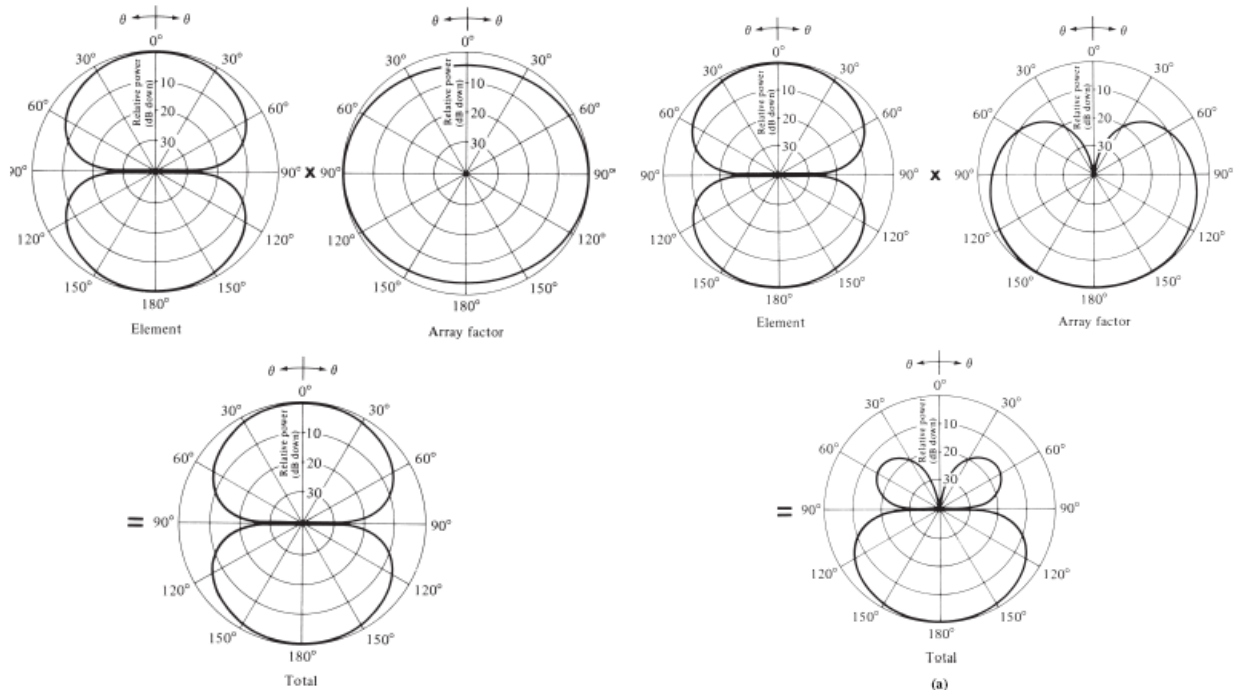


**Fig.6.3** Element, array factor, and total field Patterns of a 2-element array ( $\beta = 0^\circ$ ,  $d = \lambda/4$ ).

**Fig.6.4-a** Element, array factor, and total field Patterns of a 2-element array ( $\beta = 90^\circ$ ,  $d = \lambda/4$ ).

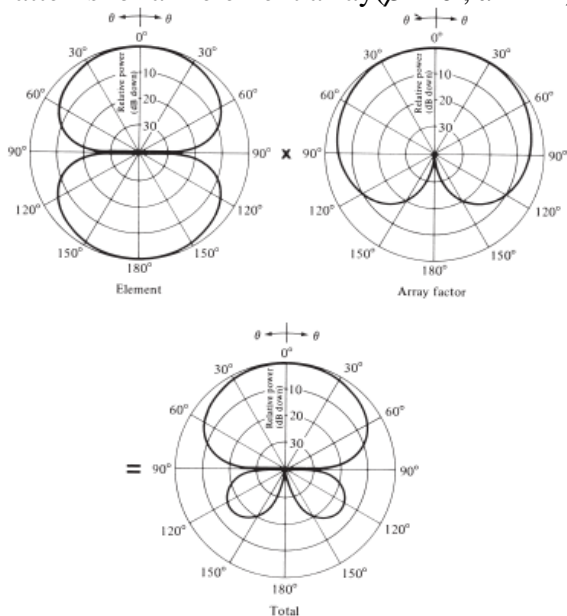
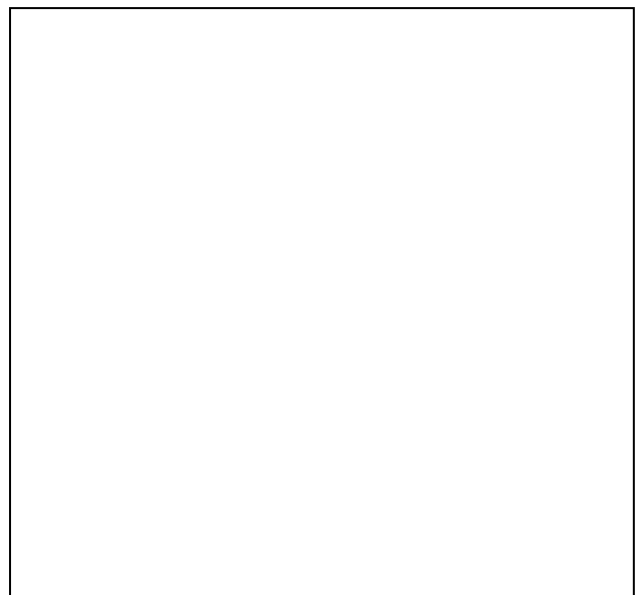


**Fig.6.4-b** ( $\beta = -90^\circ$ ,  $d = \lambda/4$ ).



### Example 6.2

Consider an array of two identical infinitesimal dipoles oriented as shown in Figs.6.1(a) and (b). For a separation  $d$  and phase excitation difference  $\beta$  between the elements, find the angles of observation where the nulls of the array occur. The magnitude excitation of the elements is the same.

*Solution:* The normalized total field of the array is given by (6-3) as

$$E_{\text{tot}} = \cos \theta \cos\left[\frac{1}{2}(kd \cos \theta + \beta)\right]$$

To find the nulls, the field is set equal to zero, or

$$E_{\text{tot}} = \cos \theta \cos\left[\frac{1}{2}(kd \cos \theta + \beta)\right]_{\theta=\theta_n} = 0$$

$$\cos \theta_n = 0 \Rightarrow \theta_n = 90^\circ$$

Thus  
and

$$\begin{aligned} \cos\left[\frac{1}{2}(kd \cos \theta_n + \beta)\right] = 0 &\Rightarrow \frac{1}{2}(kd \cos \theta_n + \beta) = \pm\left(\frac{2n+1}{2}\right)\pi \\ &\Rightarrow \theta_n = \cos^{-1}\left(\frac{\lambda}{2\pi d}[-\beta \pm (2n+1)\pi]\right), \\ &n = 0, 1, 2, \dots \end{aligned}$$

The null at  $\theta = 90^\circ$  is attributed to the pattern of the individual elements of the array while the remaining ones are due to the formation of the array. For no phase difference between the elements ( $\beta = 0$ ), the separation  $d$  must be equal or greater than half a wavelength ( $d \geq \lambda/2$ ) in order for at least one null, due to the array, to occur.

### N-ELEMENT LINEAR ARRAY: UNIFORM AMPLITUDE AND SPACING

Now let us generalize the method to include  $N$  elements. Referring to the geometry of Figure 6.5(a), assume that all the elements have identical amplitudes but each succeeding element has a  $\beta$  progressive phase lead current excitation relative to the preceding one ( $\beta$  represents the phase by which the current in each element leads the current of the preceding element). *An array of identical elements all of identical magnitude and each with a progressive phase is referred to as a uniform array.* The array factor can be obtained by considering the elements to be point sources. If the actual elements are not isotropic sources, the total field can be formed by multiplying the array factor of the isotropic sources by the field of a single element. This is the pattern multiplication rule of (6-5), and it applies only for arrays of identical elements.

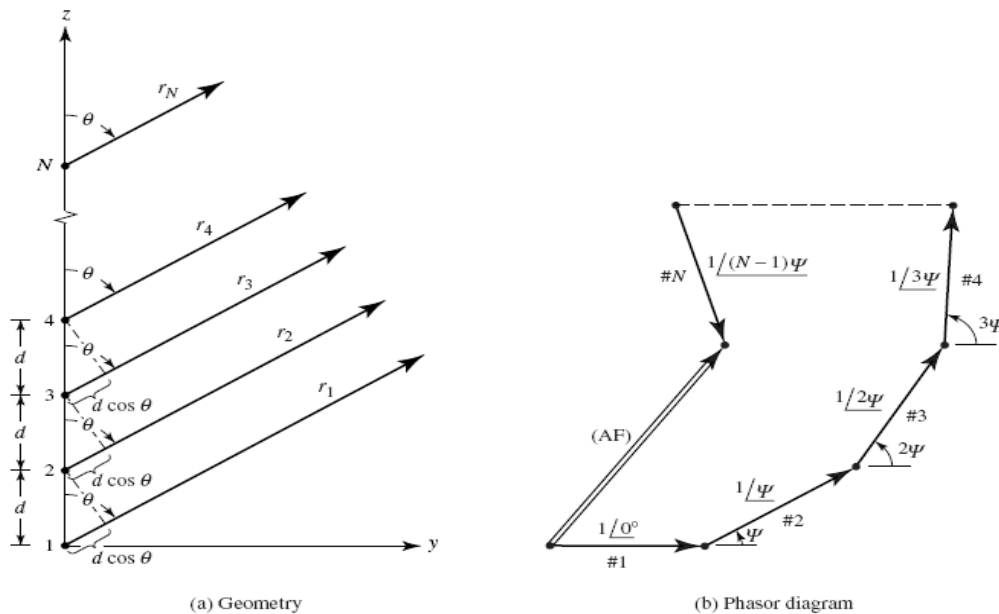


**Figure 6.5** Far-field geometry and phasor diagram of  $N$ -element array of isotropic sources positioned along the  $z$ -axis.

The array factor is given by

$$AF = 1 + e^{+j(kd \cos \theta + \beta)} + e^{+j2(kd \cos \theta + \beta)} + \dots + e^{j(N-1)(kd \cos \theta + \beta)}$$

$$AF = \sum_{n=1}^N e^{j(n-1)(kd \cos \theta + \beta)} \quad (6-6)$$

Which can be written as

$$AF = \sum_{n=1}^N e^{j(n-1)\psi} \quad (6-7)$$

$$\text{where } \psi = kd \cos \theta + \beta \quad (6-7a)$$

Since the total array factor for the uniform array is a summation of exponentials, it can be represented by the vector sum of  $N$  phasors each of unit amplitude and progressive phase  $\psi$  relative to the previous one. Graphically this is illustrated by the phasor diagram in Fig. 6.5(b). It is apparent from the phasor diagram that the amplitude and phase of the AF can be controlled in uniform arrays by properly selecting the relative phase  $\psi$  between the elements; in nonuniform arrays, the amplitude as well as the phase can be used to control the formation and distribution of the total array factor.

The array factor of (6-7) can also be expressed in an alternate, compact and closed form whose functions and their distributions are more recognizable. This is accomplished as follows.

Multiplying both sides of (6-7) by  $e^{j\psi}$ , it can be written as

$$(AF)e^{j\psi} = e^{j\psi} + e^{j2\psi} + e^{j3\psi} + \dots + e^{j(N-1)\psi} + e^{jN\psi} \quad (6-8)$$

Subtracting (6-7) from (6-8) reduces to

$$AF(e^{j\psi} - 1) = (-1 + e^{jN\psi}) \quad (6-9)$$

which can also be written as

$$\begin{aligned} AF &= \left[ \frac{e^{jN\psi} - 1}{e^{j\psi} - 1} \right] = e^{j[(N-1)/2]\psi} \left[ \frac{e^{j(N/2)\psi} - e^{-j(N/2)\psi}}{e^{j(1/2)\psi} - e^{-j(1/2)\psi}} \right] \\ &= e^{j[(N-1)/2]\psi} \left[ \frac{\sin\left(\frac{N}{2}\psi\right)}{\sin\left(\frac{1}{2}\psi\right)} \right] \end{aligned} \quad (6-10)$$

If the reference point is the physical center of the array, the array factor of (6-10) reduces to

$$AF = \left[ \frac{\sin\left(\frac{N}{2}\psi\right)}{\sin\left(\frac{1}{2}\psi\right)} \right] \quad (6-10a)$$

For small values of  $\psi$ , the above expression can be approximated by

$$AF \simeq \left[ \frac{\sin\left(\frac{N}{2}\psi\right)}{\frac{\psi}{2}} \right] \quad (6-10b)$$

The maximum value of (6-10a) or (6-10b) is equal to  $N$ . To normalize the array factors so that the maximum value of each is equal to unity, (6-10a) and (6-10b) are written in normalized form as

$$(AF)_n = \frac{1}{N} \left[ \frac{\sin\left(\frac{N}{2}\psi\right)}{\sin\left(\frac{1}{2}\psi\right)} \right] \quad (6-10c)$$

Which can be approximated to

$$(AF)_n \simeq \left[ \frac{\sin\left(\frac{N}{2}\psi\right)}{\frac{N}{2}\psi} \right] \quad (6-10d)$$

To find **the nulls** of the array, (6-10c) or (6-10d) is set equal to zero. That is,

$$\sin\left(\frac{N}{2}\psi\right) = 0 \Rightarrow \frac{N}{2}\psi|_{\theta=\theta_n} = \pm n\pi \Rightarrow \theta_n = \cos^{-1}\left[\frac{\lambda}{2\pi d}\left(-\beta \pm \frac{2n\pi}{N}\right)\right]$$

$$n = 1, 2, 3, \dots \quad (6-11)$$

$$n \neq N, 2N, 3N, \dots \text{ with (6-10c)}$$

For  $n = N, 2N, 3N, \dots$ , (6-10c) attains its maximum values because it reduces to a  $\sin(0)/0$  form. The values of  $n$  determine the order of the nulls (first, second, etc.). For a zero to exist, the argument of the arccosine cannot exceed unity. Thus the number of nulls that can exist will be a function of the element separation  $d$  and the phase excitation difference  $\beta$ .

The **maximum values** of (6-10c) occur when

$$\frac{\psi}{2} = \frac{1}{2}(kd \cos \theta + \beta)|_{\theta=\theta_m} = \pm m\pi \Rightarrow \theta_m = \cos^{-1}\left[\frac{\lambda}{2\pi d}(-\beta \pm 2m\pi)\right]$$

$$m = 0, 1, 2, \dots \quad (6-12)$$

The array factor of (6-10d) has only one maximum and occurs when  $m = 0$  in (6-12). That is,

$$\theta_m = \cos^{-1}\left(\frac{\lambda\beta}{2\pi d}\right) \quad (6-13)$$

which is the observation angle that makes  $\psi = 0$ .

The **3-dB point** for the array factor of (6-10d) occurs when

$$\frac{N}{2}\psi = \frac{N}{2}(kd \cos \theta + \beta)|_{\theta=\theta_h} = \pm 1.391$$

$$\Rightarrow \theta_h = \cos^{-1}\left[\frac{\lambda}{2\pi d}\left(-\beta \pm \frac{2.782}{N}\right)\right] \quad (6-14)$$

Which can also be written as

$$\theta_h = \frac{\pi}{2} - \sin^{-1}\left[\frac{\lambda}{2\pi d}\left(-\beta \pm \frac{2.782}{N}\right)\right] \quad (6-14a)$$

For large values of  $d$  ( $d \gg \lambda$ ), it reduces to

$$\theta_h \simeq \left[\frac{\pi}{2} - \frac{\lambda}{2\pi d}\left(-\beta \pm \frac{2.782}{N}\right)\right] \quad (6-14b)$$

The **half-power beamwidth**  $\Theta_h$  can be found once the angles of the first maximum ( $\theta_m$ ) and the 3dB point ( $\theta_h$ ) are determined. For a symmetrical pattern

$$\Theta_h = 2|\theta_m - \theta_h| \quad (6-14c)$$

The **secondary maxima** (maxima of minor lobes) which occur *approximately* when the numerator of (6-10d) attains its maximum value. That is,

$$\sin\left(\frac{N}{2}\psi\right) = \sin\left[\frac{N}{2}(kd \cos \theta + \beta)\right]|_{\theta=\theta_s} \simeq \pm 1 \Rightarrow \frac{N}{2}(kd \cos \theta + \beta)|_{\theta=\theta_s}$$

$$\simeq \pm \left(\frac{2s+1}{2}\right)\pi \Rightarrow \theta_s \simeq \cos^{-1}\left\{\frac{\lambda}{2\pi d}\left[-\beta \pm \left(\frac{2s+1}{N}\right)\pi\right]\right\},$$

$$s = 1, 2, 3, \dots \quad (6-15)$$

Which can also be written as

$$\theta_s \simeq \frac{\pi}{2} - \sin^{-1} \left\{ \frac{\lambda}{2\pi d} \left[ -\beta \pm \left( \frac{2s+1}{N} \right) \pi \right] \right\}, \quad s = 1, 2, 3, \dots \quad (6-15a)$$

For large values of  $d$  ( $d \gg \lambda$ ), it reduces to

$$\theta_s \simeq \frac{\pi}{2} - \frac{\lambda}{2\pi d} \left[ -\beta \pm \left( \frac{2s+1}{N} \right) \pi \right], \quad s = 1, 2, 3, \dots \quad (6-15b)$$

The maximum of the first minor lobe of (6-10c) occurs *approximately* when

$$\frac{N}{2}\psi = \frac{N}{2}(kd \cos \theta + \beta)|_{\theta=\theta_s} \simeq \pm \left( \frac{3\pi}{2} \right) \quad (6-16)$$

Or when

$$\theta_s = \cos^{-1} \left\{ \frac{\lambda}{2\pi d} \left[ -\beta \pm \frac{3\pi}{N} \right] \right\} \quad (6-16a)$$

At that point, the magnitude of (6-10d) reduces to

$$(\text{AF})_n \simeq \left[ \frac{\sin \left( \frac{N}{2}\psi \right)}{\frac{N}{2}\psi} \right]_{\theta=\theta_s, s=1} = \frac{2}{3\pi} = 0.212 \quad (6-17)$$

Which in dB is equal to

$$(\text{AF})_n = 20 \log_{10} \left( \frac{2}{3\pi} \right) = -13.46 \text{ dB} \quad (6-17a)$$

Thus the maximum of the first minor lobe of the array factor of (6-10d) is 13.46 dB down from the maximum at the major lobe. More accurate expressions for the angle, beamwidth, and magnitude of first minor lobe of the array factor of (6-10d) can be obtained.

### Broadside Array

In many applications it is desirable to have the maximum radiation of an array directed normal to the array axis [broadside;  $\theta_0 = 90^\circ$  of Fig. 6.5(a)]. To optimize the design, the maxima of the single element and of the array factor should both be directed toward  $\theta_0 = 90^\circ$ . The requirements of the single elements can be accomplished by proper choice of the radiators, and those of the array factor by the proper separation and excitation of the individual radiators. In this section, the requirements that allow the array factor to “radiate” efficiently broadside will be developed.

Referring to (6-10c) or (6-10d), the first maximum of the array factor occurs when

$$\psi = kd \cos \theta + \beta = 0 \quad (6-18)$$

Since it is desired to have the first maximum directed toward  $\theta_0 = 90^\circ$ , then

$$\psi = kd \cos \theta + \beta|_{\theta=90^\circ} = \beta = 0 \quad (6-18a)$$

Thus to have the maximum of the array factor of a uniform linear array directed broadside to the axis of the array, it is necessary that all the elements have the same phase excitation (in addition to the same amplitude excitation). The separation between the elements can be of any value. To ensure that there are no principal maxima in other directions, which are referred to as *grating lobes*, the

separation between the elements should not be equal to multiples of a wavelength ( $d \neq n\lambda$ ,  $n = 1, 2, 3, \dots$ ) when  $\beta = 0$ . If  $d = n\lambda$ ,  $n = 1, 2, 3, \dots$  and  $\beta = 0$ , then

$$\psi = kd \cos \theta + \beta \Big|_{\substack{\beta=0 \\ n=1,2,3,\dots}}^{d=n\lambda} = 2\pi n \cos \theta \Big|_{\theta=0^\circ, 180^\circ} = \pm 2n\pi \quad (6-19)$$

This value of  $\psi$  when substituted in (6-10c) makes the array factor attain its maximum value. Thus for a uniform array with  $\beta = 0$  and  $d = n\lambda$ , in addition to having the maxima of the array factor directed broadside ( $\theta = 90^\circ$ ) to the axis of the array, there are additional maxima directed along the axis ( $\theta_0 = 0^\circ, 180^\circ$ ) of the array (end-fire radiation).

One of the objectives in many designs is to avoid multiple maxima, in addition to the main maximum, which are referred to as *grating lobes*. Often it may be required to select the largest spacing between the elements but with no grating lobes. *To avoid any grating lobe, the largest spacing between the elements should be less than one wavelength ( $d_{\max} < \lambda$ ).*

To illustrate the method, the 3-D array factor of a 10-element ( $N = 10$ ) uniform array with  $\beta = 0$  and  $d = \lambda/4$  is shown plotted in Figure 6.6(a). A  $90^\circ$  angular sector has been removed for better view of the pattern distribution in the elevation plane. The only maximum occurs at broadside ( $\theta = 90^\circ$ ). To form a comparison, the three-dimensional pattern of the same array but with  $d = \lambda$  is also plotted in Figure 6.6(b). For this pattern, in addition to the maximum at  $\theta = 90^\circ$ , there are additional maxima directed toward  $\theta_0 = 0^\circ, 180^\circ$ . The corresponding two-dimensional patterns of Figures 6.6(a,b) are shown in Fig. 6.7.

If the spacing between the elements is chosen between  $\lambda < d < 2\lambda$ , then the maximum of Figure 6.6 toward  $\theta_0 = 0^\circ$  shifts toward the angular region  $0^\circ < \theta < 90^\circ$  while the maximum toward  $\theta_0 = 180^\circ$  shifts toward  $90^\circ < \theta < 180^\circ$ . When  $d = 2\lambda$ , there are maxima toward  $0^\circ, 60^\circ, 90^\circ, 120^\circ$  and  $180^\circ$ .

In Tables 6.1 and 6.2 the expressions for the nulls, maxima, half-power points, minor lobe maxima, and beamwidths for broadside arrays have been listed. They are derived from (6-10c)–(6-16a).

NULLS	$\theta_n = \cos^{-1} \left( \pm \frac{n \lambda}{N d} \right)$ $n = 1, 2, 3, \dots$ $n \neq N, 2N, 3N, \dots$
MAXIMA	$\theta_m = \cos^{-1} \left( \pm \frac{m\lambda}{d} \right)$ $m = 0, 1, 2, \dots$
HALF-POWER POINTS	$\theta_h \simeq \cos^{-1} \left( \pm \frac{1.391\lambda}{\pi N d} \right)$ $\pi d/\lambda \ll 1$
MINOR LOBE MAXIMA	$\theta_s \simeq \cos^{-1} \left[ \pm \frac{\lambda}{2d} \left( \frac{2s+1}{N} \right) \right]$ $s = 1, 2, 3, \dots$ $\pi d/\lambda \ll 1$

TABLE 6.1 Nulls, Maxima, Half-Power Points, and Minor Lobe Maxima for Uniform Amplitude Broadside Arrays

**TABLE 6.2** Beamwidths for Uniform Amplitude Broadside Arrays

FIRST-NULL BEAMWIDTH (FNBW)	$\Theta_n = 2 \left[ \frac{\pi}{2} - \cos^{-1} \left( \frac{\lambda}{Nd} \right) \right]$
HALF-POWER BEAMWIDTH (HPBW)	$\Theta_h \simeq 2 \left[ \frac{\pi}{2} - \cos^{-1} \left( \frac{1.391\lambda}{\pi Nd} \right) \right]$ $\pi d/\lambda \ll 1$
FIRST SIDE LOBE BEAMWIDTH (FSLBW)	$\Theta_s \simeq 2 \left[ \frac{\pi}{2} - \cos^{-1} \left( \frac{3\lambda}{2dN} \right) \right]$ $\pi d/\lambda \ll 1$

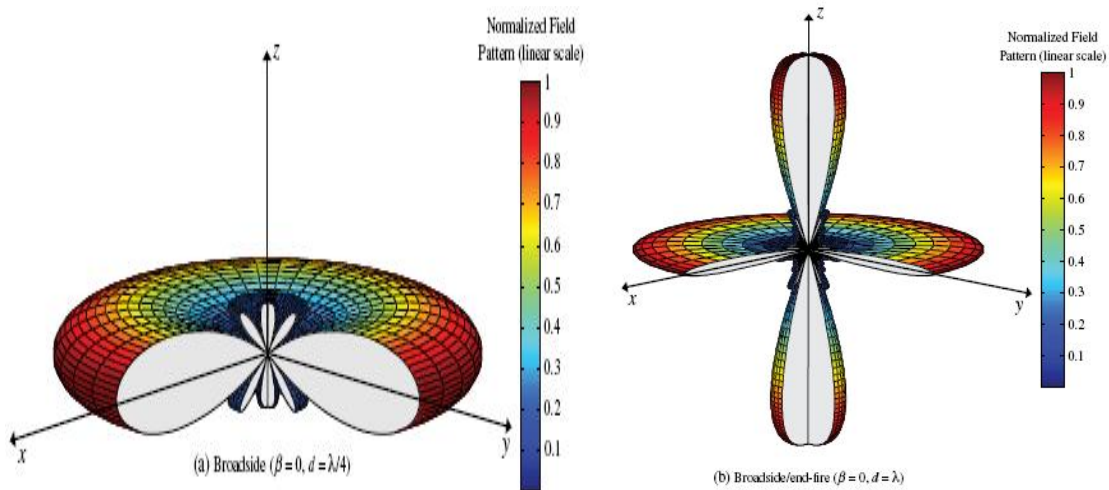


**Figure 6** Three-dimensional amplitude patterns for broadside array (left), and broadside/end-fire array (right) with ( $N = 10$ ).

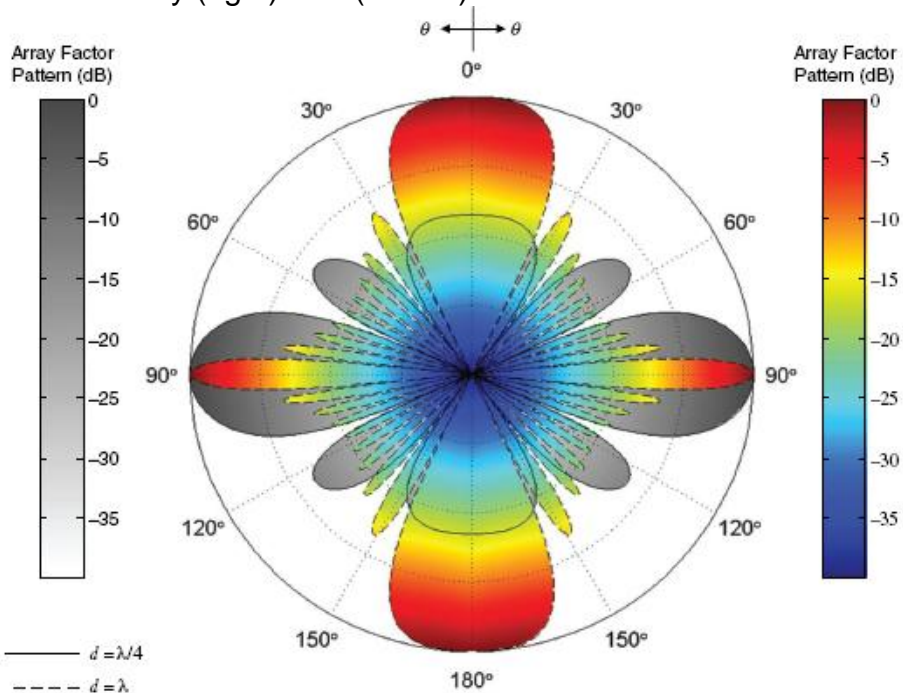


**Figure 6.7** Array factor patterns of a 10-element uniform amplitude broadside array ( $N = 10, \beta = 0$ ).

### 6.3.2 Ordinary End-Fire Array

Instead of having the maximum radiation broadside to the axis of the array, it may be desirable to direct it along the axis of the array (end-fire). It may be necessary that the array radiates toward only one direction (either  $\theta_0 = 0^\circ$  or  $180^\circ$  of Fig. 6.5).

To direct the first maximum toward  $\theta_0 = 0^\circ$ ,

$$\psi = kd \cos \theta + \beta|_{\theta=0^\circ} = kd + \beta = 0 \Rightarrow \beta = -kd \quad (6-20a)$$

If the first maximum is desired toward  $\theta_0 = 180^\circ$ , then

$$\psi = kd \cos \theta + \beta|_{\theta=180^\circ} = -kd + \beta = 0 \Rightarrow \beta = kd \quad (6-20b)$$

Thus end-fire radiation is accomplished when  $\beta = -kd$  (for  $\theta_0 = 0^\circ$ ) or  $\beta = kd$  (for  $\theta_0 = 180^\circ$ ).

If the element separation is  $d = \lambda/2$ , end-fire radiation exists simultaneously in both directions ( $\theta_0 = 0^\circ$  and  $\theta_0 = 180^\circ$ ). If the element spacing is a multiple of a wavelength ( $d = n\lambda$ ,  $n = 1, 2, 3, \dots$ ), then in addition to having end-fire radiation in both directions, there also exist maxima in the broadside directions. Thus for  $d = n\lambda$ ,  $n = 1, 2, 3, \dots$  there exist four maxima; two in the broadside directions and two along the axis of the array. *To have only one end-fire maximum and to avoid any grating lobes, the maximum spacing between the elements should be less than  $d_{\max} < \lambda/2$ .*

The three-dimensional radiation patterns of a 10-element ( $N = 10$ ) array with  $d = \lambda/4$ ,  $\beta = +kd$  are plotted in Figure 6.8. When  $\beta = -kd$ , the maximum is directed along  $\theta_0 = 0^\circ$  and the 3-D pattern is shown in Fig. 6.8(a). However, when  $\beta = +kd$ , the maximum is oriented toward  $\theta_0 = 180^\circ$ , and the 3D pattern is shown in Fig. 6.8(b). The 2D patterns of Figs. 6.8(a,b) are shown in Figure 6.9. To form a comparison, the array factor of the same array ( $N = 10$ ) but with  $d = \lambda$  and  $\beta = -kd$  has been calculated. Its pattern is identical to that of a broadside array with  $N = 10$ ,  $d = \lambda$ , and it is shown plotted in Fig. 6.7. It is seen that there are four maxima; two broadside and two along the axis of the array.

The expressions for the nulls, maxima, half-power points, minor lobe maxima, and beamwidths, as applied to ordinary end-fire arrays, are listed in Tables 6.3 and 6.4.

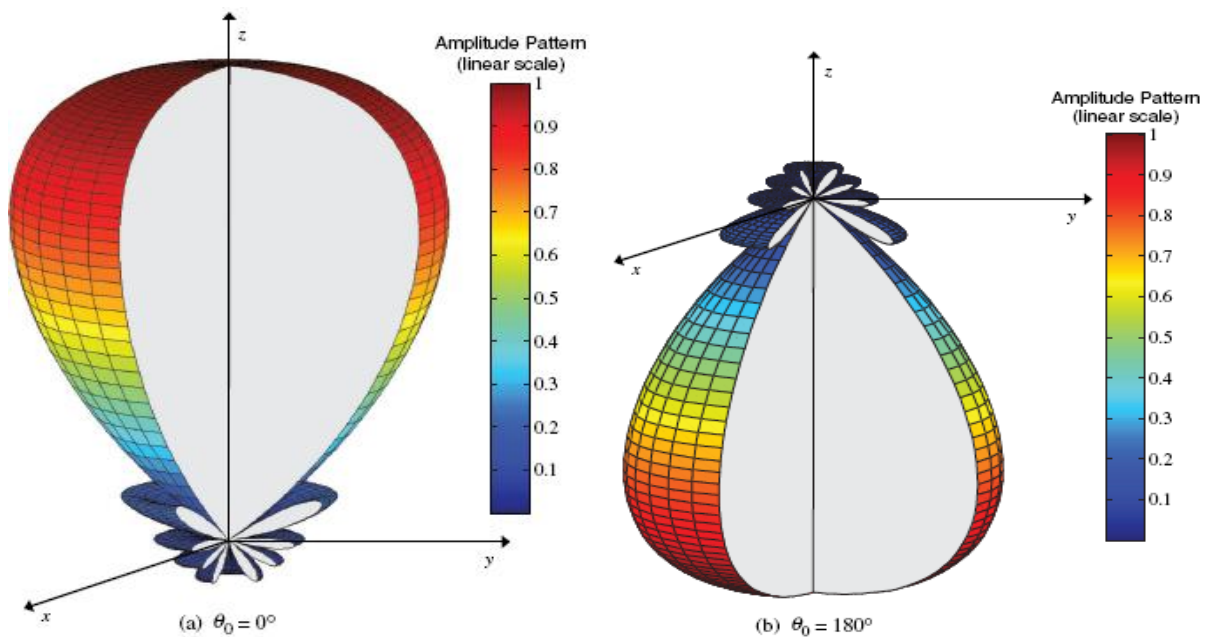


**Fig. 6.8** 3D amplitude patterns for end-fire arrays toward  $\theta_0 = 0^\circ$  and  $180^\circ$  ( $N=10, d=\lambda/4$ ).

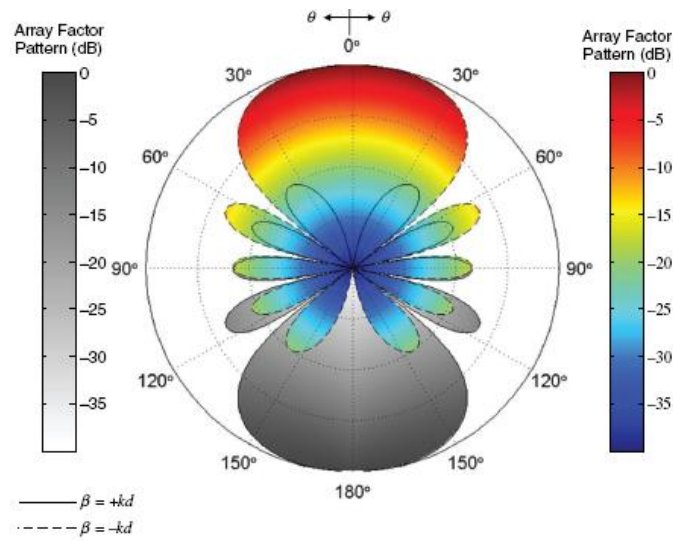


**Figure 6.9** Array factor patterns of a 10-element uniform amplitude end-fire array ( $N = 10, d = \lambda/4$ ).

NULLS	$\theta_n = \cos^{-1} \left( 1 - \frac{n\lambda}{Nd} \right)$ $n = 1, 2, 3, \dots$ $n \neq N, 2N, 3N, \dots$
MAXIMA	$\theta_m = \cos^{-1} \left( 1 - \frac{m\lambda}{d} \right)$ $m = 0, 1, 2, \dots$
HALF-POWER POINTS	$\theta_h \simeq \cos^{-1} \left( 1 - \frac{1.391\lambda}{\pi dN} \right)$ $\pi d/\lambda \ll 1$
MINOR LOBE MAXIMA	$\theta_s \simeq \cos^{-1} \left[ 1 - \frac{(2s+1)\lambda}{2Nd} \right]$ $s = 1, 2, 3, \dots$ $\pi d/\lambda \ll 1$

**TABLE 6.3** Nulls, Maxima, Half-Power Points, and Minor Lobe Maxima for Uniform Amplitude Ordinary End-Fire Arrays

**TABLE 6.4** Beamwidths for Uniform Amplitude Ordinary End-Fire Arrays

FIRST-NULLS BEAMWIDTH (FNBW)	$\Theta_n = 2 \cos^{-1} \left( 1 - \frac{\lambda}{Nd} \right)$
HALF-POWER BEAMWIDTH (HPBW)	$\Theta_h \simeq 2 \cos^{-1} \left( 1 - \frac{1.391\lambda}{\pi dN} \right)$ $\pi d/\lambda \ll 1$
FIRST SIDE LOBE BEAMWIDTH (FSLBW)	$\Theta_s \simeq 2 \cos^{-1} \left( 1 - \frac{3\lambda}{2Nd} \right)$ $\pi d/\lambda \ll 1$

### 6.3.3 Phased (Scanning) Array

In the previous two sections it was shown how to direct the major radiation from an array, by controlling the phase excitation between the elements, in directions normal (broadside) and along the axis (end fire) of the array. It is then

logical to assume that the maximum radiation can be oriented in any direction to form a scanning array. The procedure is similar to that of the previous two sections.

Let us assume that the maximum radiation of the array is required to be oriented at an angle  $\theta$  ( $0^\circ \leq \theta \leq 180^\circ$ ). To accomplish this, the phase excitation  $\beta$  between the elements must be adjusted so that

$$\psi = kd \cos \theta + \beta \Big|_{\theta=\theta_0} = kd \cos \theta_0 + \beta = 0 \Rightarrow \beta = -kd \cos \theta_0 \quad (6-21)$$

Thus by controlling the progressive phase difference between the elements, the maximum radiation can be squinted in any desired direction to form a scanning array. This is the basic principle of electronic scanning phased array operation. Since in phased array technology the scanning must be continuous, the system should be capable of continuously varying the progressive phase between the elements. In practice, this is accomplished electronically by the use of ferrite or diode phase shifters. For ferrite phase shifters, the phase shift is controlled by the magnetic field within the ferrite, which in turn is controlled by the amount of current flowing through a coil around the phase shifter.

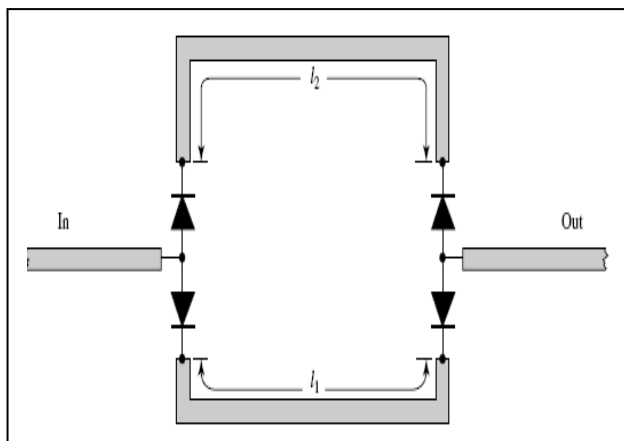


Figure 6.10 shows an *incremental switched-line PIN-diode phase shifter*. This design is simple, straightforward, lightweight, and high speed. The lines of lengths  $l_1$  and  $l_2$  are switched on and off by controlling the bias of the PIN diodes, using two single-pole double-throw switches. The differential phase shift, provided by switching on and off the two paths, is given by  $\Delta\phi = k(l_2 - l_1)$

## 6.4 N-ELEMENT LINEAR ARRAY: DIRECTIVITY

Here we investigate the directivity of the broadside and end-fire arrays. The directivity represents a figure of merit on the operation of the system.

### 6.4.1 Broadside Array

As a result of the criteria for broadside radiation given by (6-18a), the array factor for this form of the array reduces to

$$(AF)_n = \frac{1}{N} \left[ \frac{\sin\left(\frac{N}{2}kd \cos \theta\right)}{\sin\left(\frac{1}{2}kd \cos \theta\right)} \right] \quad (6-38)$$

which for a small spacing between the elements ( $d \ll \lambda$ ) can be approximated by

$$(AF)_n \approx \left[ \frac{\sin\left(\frac{N}{2}kd \cos \theta\right)}{\left(\frac{N}{2}kd \cos \theta\right)} \right] \quad (6-38a)$$

The radiation intensity can be written as:

$$U(\theta) = [(AF)_n]^2 = \left[ \frac{\sin\left(\frac{N}{2}kd \cos \theta\right)}{\frac{N}{2}kd \cos \theta} \right]^2 = \left[ \frac{\sin(Z)}{Z} \right]^2 \quad (6-39)$$

$$Z = \frac{N}{2}kd \cos \theta \quad (6-39a)$$

The directivity can be obtained using (6-32)  $D_0 = \frac{4\pi U_{\max}}{P_{\text{rad}}} = \frac{U_{\max}}{U_0}$  where  $U_{\max}$  of (6-39) is equal to unity ( $U_{\max} = 1$ ) and it occurs at  $\theta = 90^\circ$ . The average value  $U_0$  of the intensity reduces to

$$\begin{aligned} U_0 &= \frac{1}{4\pi} P_{\text{rad}} = \frac{1}{2} \int_0^\pi \left[ \frac{\sin(Z)}{Z} \right]^2 \sin \theta \, d\theta \\ &= \frac{1}{2} \int_0^\pi \left[ \frac{\sin\left(\frac{N}{2}kd \cos \theta\right)}{\frac{N}{2}kd \cos \theta} \right]^2 \sin \theta \, d\theta \end{aligned} \quad (6-40)$$

By making a change of variable, that is

$$Z = \frac{N}{2}kd \cos \theta \quad (6-40a)$$

$$dZ = -\frac{N}{2}kd \sin \theta \, d\theta \quad (6-40b)$$

(6-40) can be written as

$$U_0 = -\frac{1}{Nkd} \int_{+Nkd/2}^{-Nkd/2} \left[ \frac{\sin Z}{Z} \right]^2 dZ = \frac{1}{Nkd} \int_{-Nkd/2}^{+Nkd/2} \left[ \frac{\sin Z}{Z} \right]^2 dZ \quad (6-41)$$

For a large array ( $Nkd/2 \rightarrow \text{large}$ ), then (6-41) can be approximated by extending the limits to infinity. That is,

$$U_0 = \frac{1}{Nkd} \int_{-Nkd/2}^{+Nkd/2} \left[ \frac{\sin Z}{Z} \right]^2 dZ \approx \frac{1}{Nkd} \int_{-\infty}^{+\infty} \left[ \frac{\sin Z}{Z} \right]^2 dZ \quad (6-41a)$$

Since

$$\int_{-\infty}^{+\infty} \left[ \frac{\sin(Z)}{Z} \right]^2 dZ = \pi \quad (6-41b)$$

(6-41a) reduces to

$$U_0 \approx \frac{\pi}{Nkd} \quad (6-41c)$$

The directivity of (6-32) can now be written as

$$D_0 = \frac{U_{\max}}{U_0} \approx \frac{Nkd}{\pi} = 2N \left( \frac{d}{\lambda} \right) \quad (6-42)$$

Using  $L = (N - 1)d$  (6-43)

where  $L$  is the overall length of the array, (6-42) can be expressed as

$$D_0 \approx 2N \left( \frac{d}{\lambda} \right) \approx 2 \left( 1 + \frac{L}{d} \right) \left( \frac{d}{\lambda} \right) \quad (6-44)$$

which for a large array ( $L \gg d$ ) reduces to

$$D_0 \approx 2N \left( \frac{d}{\lambda} \right) = 2 \left( 1 + \frac{L}{d} \right) \left( \frac{d}{\lambda} \right) \stackrel{L \gg d}{\approx} 2 \left( \frac{L}{\lambda} \right) \quad (6-44a)$$

### Example 6.3

Given a linear, broadside, uniform array of 10 isotropic elements ( $N = 10$ ) with a separation of  $\lambda/4$  ( $d = \lambda/4$ ) between the elements, find the directivity of the array.

*Solution:* Using (6-44a)

$$D_0 \approx 2N \left( \frac{d}{\lambda} \right) = 5 \text{ (dimensionless)} = 10 \log_{10}(5) = 6.99 \text{ dB}$$

## 6.4.2 Ordinary End-Fire Array

For an end-fire array, with the maximum radiation in the  $\theta_0 = 0^\circ$  direction, the array factor is given by

$$(AF)_n = \left[ \frac{\sin \left[ \frac{N}{2} kd(\cos \theta - 1) \right]}{N \sin \left[ \frac{1}{2} kd(\cos \theta - 1) \right]} \right] \quad (6-45)$$

which, for a small spacing between the elements ( $d \ll \lambda$ ), can be approximated by

$$(AF)_n \approx \left[ \frac{\sin \left[ \frac{N}{2} kd(\cos \theta - 1) \right]}{\left[ \frac{N}{2} kd(\cos \theta - 1) \right]} \right] \quad (6-45a)$$

The corresponding radiation intensity can be written as

$$U(\theta) = [(AF)_n]^2 = \left[ \frac{\sin \left[ \frac{N}{2} kd(\cos \theta - 1) \right]}{\frac{N}{2} kd(\cos \theta - 1)} \right]^2 = \left[ \frac{\sin(Z)}{Z} \right]^2 \quad (6-46)$$

$$Z = \frac{N}{2} kd(\cos \theta - 1) \quad (6-46a)$$

whose maximum value is unity ( $U_{\max} = 1$ ) and it occurs at  $\theta = 0^\circ$ . The average value of the radiation intensity is given by

$$\begin{aligned} U_0 &= \frac{1}{4\pi} \int_0^{2\pi} \int_0^\pi \left[ \frac{\sin \left[ \frac{N}{2} kd(\cos \theta - 1) \right]}{\frac{N}{2} kd(\cos \theta - 1)} \right]^2 \sin \theta \, d\theta \, d\phi \\ &= \frac{1}{2} \int_0^\pi \left[ \frac{\sin \left[ \frac{N}{2} kd(\cos \theta - 1) \right]}{\frac{N}{2} kd(\cos \theta - 1)} \right]^2 \sin \theta \, d\theta \end{aligned} \quad (6-47)$$

By letting

$$Z = \frac{N}{2} kd(\cos \theta - 1) \quad (6-47a)$$

$$dZ = -\frac{N}{2} kd \sin \theta \, d\theta \quad (6-47b)$$

(6-47) can be written as

$$U_0 = -\frac{1}{Nkd} \int_0^{-Nkd} \left[ \frac{\sin(Z)}{Z} \right]^2 dZ = \frac{1}{Nkd} \int_0^{Nkd} \left[ \frac{\sin(Z)}{Z} \right]^2 dZ \quad (6-48)$$

For a large array ( $Nkd \rightarrow \text{large}$ ), (6-48) can be approximated by extending the limits to infinity. That is,

$$U_0 = \frac{1}{Nkd} \int_0^{Nkd} \left[ \frac{\sin(Z)}{Z} \right]^2 dZ \approx \frac{1}{Nkd} \int_0^\infty \left[ \frac{\sin(Z)}{Z} \right]^2 dZ \quad (6-48a)$$

Using (6-41b) reduces (6-48a) to

$$U_0 \approx \frac{\pi}{2Nkd} \quad (6-48b)$$

and the directivity to

$$D_0 = \frac{U_{\max}}{U_0} \approx \frac{2Nkd}{\pi} = 4N \left( \frac{d}{\lambda} \right) \quad (6-49)$$

Another form of (6-49), using (6-43), is

$$D_0 \approx 4N \left( \frac{d}{\lambda} \right) = 4 \left( 1 + \frac{L}{d} \right) \left( \frac{d}{\lambda} \right) \quad (6-49a)$$

which for a large array ( $L \gg d$ ) reduces to

$$D_0 \approx 4N \left( \frac{d}{\lambda} \right) = 4 \left( 1 + \frac{L}{d} \right) \left( \frac{d}{\lambda} \right) \stackrel{L \gg d}{\approx} 4 \left( \frac{L}{\lambda} \right) \quad (6-49b)$$

It should be noted that **the directivity of the end-fire array, as given by (6-49)–(6-49b), is twice that for the broadside array as given by (6-42) – (6-44a).**

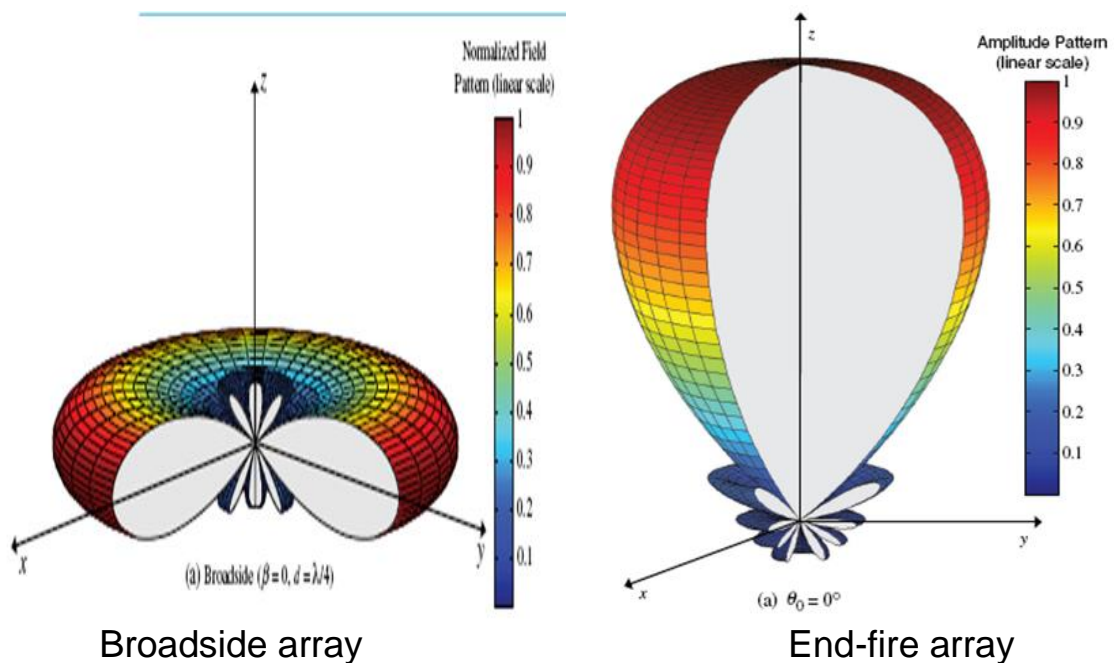
#### Example 6.4

Given a linear, end-fire, uniform array of 10 elements ( $N = 10$ ) with a separation of  $\lambda/4$  ( $d = \lambda/4$ ) between the elements, find the directivity of the array factor. This array is identical to the broadside array of Example 6.3.

*Solution:* Using (6-49)

$$D_0 \approx 4N \left( \frac{d}{\lambda} \right) = 10 \text{ (dimensionless)} = 10 \log_{10}(10) = 10 \text{ dB}$$

This value for the directivity ( $D_0 = 10$ ) is approximate, based on the validity of (6-48a). However, it compares very favorably with the value of  $D_0 = 10.05$  obtained by numerically integrating (6-45) using the **Directivity** computer program of Chapter 2.



## 6.5 DESIGN PROCEDURE

In the design of any antenna system, the most important design parameters are usually the **number of elements  $N$** , **spacing between the elements  $d$** , excitation (**amplitude and phase**), **half-power beamwidth  $HPBW$** , **directivity  $D_o$** , and **side lobe level**. In a design procedure some of these parameters are specified and the others are then determined.

The parameters that are specified and those that are determined vary among designs. For a uniform array, the side lobe is always approximately  $-13.5$  dB. The order in which the other parameters are specified and determined varies among designs. For each of the uniform linear arrays that have been discussed, equations and some graphs have been presented which can be used to determine the half-power beamwidth and directivity, once the number of elements and spacing (or the total length of the array) are specified. In fact, some of the equations have been boxed or listed in tables. This may be considered more of an analysis procedure. The other approach is to specify the half-power beamwidth or directivity and to determine most of the other parameters. This can be viewed more as a design approach, and can be accomplished to a large extent with equations or graphs that have been presented. More exact values can be obtained, if necessary, using iterative or numerical methods.

### Example 6.6

Design a uniform linear scanning array whose maximum of the array factor is  $30^\circ$  from the axis of the array ( $\theta_0 = 30^\circ$ ). The desired half-power beamwidth is  $2^\circ$  while the spacing between the elements is  $\lambda/4$ . Determine the excitation of the elements (amplitude and phase), length of the array (in wavelengths), number of elements, and directivity (in dB).

*Solution:* Since the desired design is a uniform linear scanning array, the amplitude excitation is uniform. However, the progressive phase between the elements is, using (6-21)

$$\beta = -kd \cos \theta_0 = -\frac{2\pi}{\lambda} \left( \frac{\lambda}{4} \right) \cos(30^\circ) = -1.36 \text{ radians} = -77.94^\circ$$

The length of the array is obtained using an iterative procedure of (6-22) or its graphical solu-

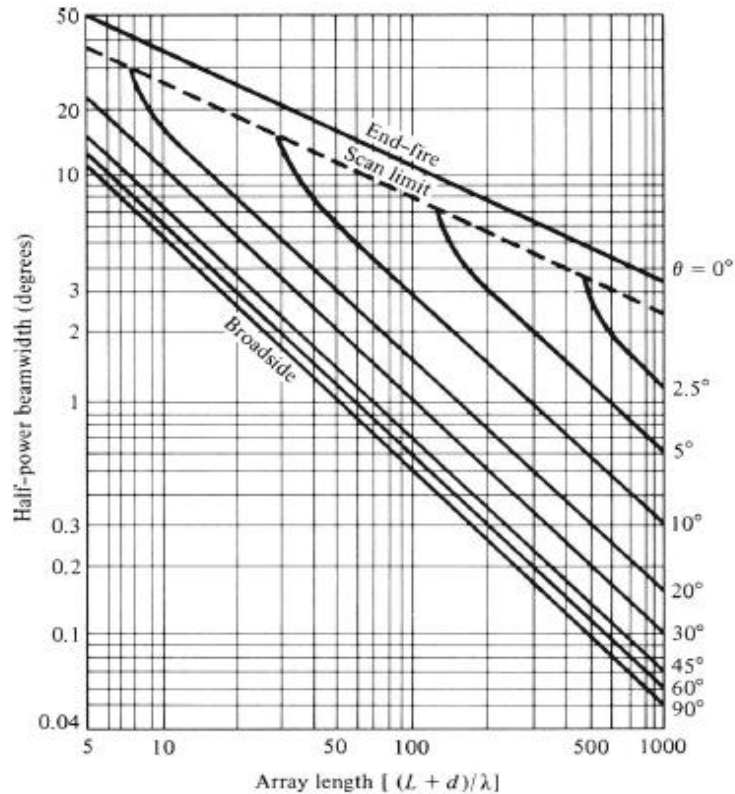


**Figure 6.12** Half-power beamwidth for broadside, ordinary end-fire, and scanning uniform linear arrays. (SOURCE: R. S. Elliott, "Beamwidth and Directivity of Large Scanning Arrays," First of Two Parts, *The Microwave Journal*, December 1963).

tion of Figure 6.12. Using the graph of Figure 6.12 for a scan angle of  $30^\circ$  and  $2^\circ$  half-power beamwidth, the approximate length plus one spacing ( $L + d$ ) of the array is  $50\lambda$ . For the  $50\lambda$  length plus one spacing dimension from Figure 6.12 and  $30^\circ$  scan angle, (6-22) leads to a half-power beamwidth of  $2.03^\circ$ , which is very close to the desired value of  $2^\circ$ . Therefore, the length of the array for a spacing of  $\lambda/4$  is  $49.75\lambda$ .

Since the length of the array is  $49.75\lambda$  and the spacing between the elements is  $\lambda/4$ , the total number of elements is

$$N = \frac{L}{d} + 1 = \left( \frac{L + d}{d} \right) = \frac{50}{1/4} = 200$$

The directivity of the array is obtained using the radiation intensity and the computer program **Directivity** of Chapter 2, and it is equal to 100.72 or 20.03 dB.

## 6.6 N-ELEMENT LINEAR ARRAY: THREE-DIMENSIONAL CHARACTERISTICS

Up to now, the 2-D array factor of an  $N$ -element linear array has been investigated. Although in practice only 2-D patterns can be measured, a collection of them can be used to reconstruct the 3-D characteristics of an array. It would then be instructive to examine the 3-D patterns of an array of elements. Emphasis will be placed on the array factor.

### 6.6.1 N-Elements Along Z-Axis

A linear array of  $N$  isotropic elements are positioned along the  $z$ -axis and are separated by a distance  $d$ , as shown in Fig. 6.5(a). The amplitude excitation of each element is  $an$  and there exists a

progressive phase excitation  $\beta$  between the elements. For far-field observations, the array factor can be written according to (6-6) as

$$AF = \sum_{n=1}^N a_n e^{j(n-1)(kd \cos \gamma + \beta)} = \sum_{n=1}^N a_n e^{j(n-1)\psi} \quad (6-52)$$

$$\psi = kd \cos \gamma + \beta \quad (6-52a)$$

where the  $a_n$ 's are the amplitude excitation coefficients and  $\gamma$  is the angle between the axis of the array (z-axis) and the radial vector from the origin to the observation point.

In general, the angle  $\gamma$  can be obtained from the dot product of a unit vector along the axis of the array with a unit vector directed toward the observation point. For the geometry of Figure 6.5(a)

$$\cos \gamma = \hat{a}_z \cdot \hat{a}_r = \hat{a}_z \cdot (\hat{a}_x \sin \theta \cos \phi + \hat{a}_y \sin \theta \sin \phi + \hat{a}_z \cos \theta) = \cos \theta \Rightarrow \gamma = \theta \quad (6-53)$$

Thus (6-52) along with (6-53) is identical to (6-6), because the system of Fig. 6.5(a) possesses a symmetry around the z-axis (no  $\phi$  variations). This is not the case when the elements are placed along any of the other axes, as will be shown next.

### 6.6.2 N-Elements Along X- or Y-Axis

Let us consider an array of  $N$  isotropic elements along the x-axis, as shown in Fig. 6.16. The far-zone array factor for this array is identical in form to that of Fig. 6.5(a) except for the phase factor  $\psi$ . For this geometry

$$\cos \gamma = \hat{a}_x \cdot \hat{a}_r = \hat{a}_x \cdot (\hat{a}_x \sin \theta \cos \phi + \hat{a}_y \sin \theta \sin \phi + \hat{a}_z \cos \theta) = \sin \theta \cos \phi \quad (6-54)$$

$$\cos \gamma = \sin \theta \cos \phi \Rightarrow \gamma = \cos^{-1}(\sin \theta \cos \phi) \quad (6-54a)$$

The array factor of this array is also given by (6-52) but with  $\gamma$  defined by (6-54a). For this system, the array factor is a function of both angles ( $\theta$  and  $\phi$ ).

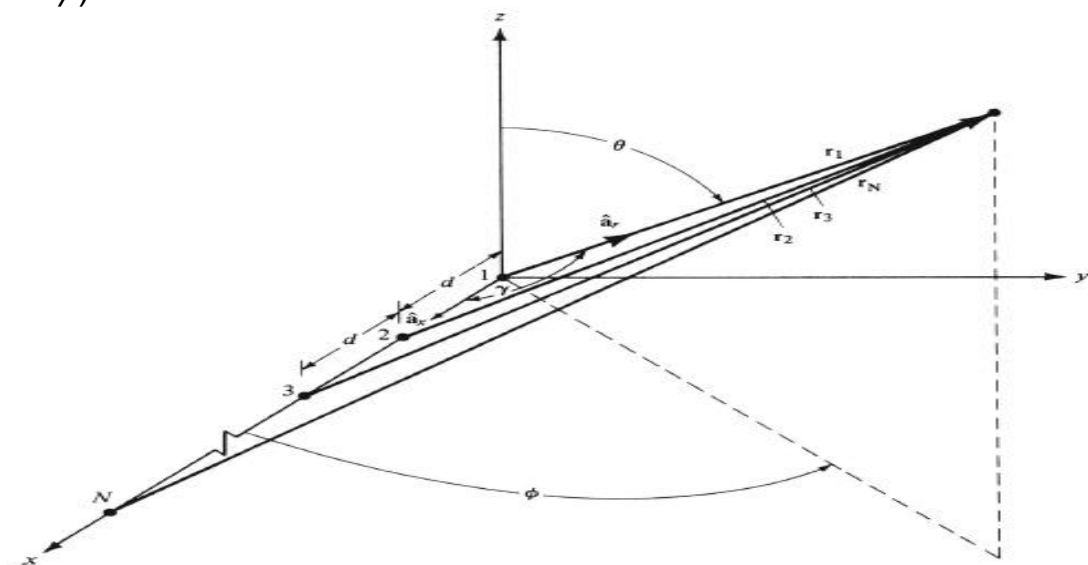


Figure 6.16 Linear array of  $N$  isotropic elements positioned along the x-axis.

In a similar manner, the array factor for  $N$  isotropic elements placed along the  $y$ -axis is that of (6-52) but with  $\gamma$  defined by

$$\cos \gamma = \hat{\mathbf{a}}_y \cdot \hat{\mathbf{a}}_r = \sin \theta \sin \phi \Rightarrow \gamma = \cos^{-1}(\sin \theta \sin \phi) \quad (6-55)$$

Physically placing the elements along the  $z$ -,  $x$ -, or  $y$ -axis does not change the characteristics of the array. Numerically they yield identical patterns even though their mathematical forms are different.

**Example 6.7**

Two half-wavelength dipole ( $l = \lambda/2$ ) are positioned along the  $x$ -axis and are separated by a distance  $d$ , as shown in Figure 6.17. The lengths of the dipoles are parallel to the  $z$ -axis. Find the total field of the array. Assume uniform amplitude excitation and a progressive phase difference of  $\beta$ .

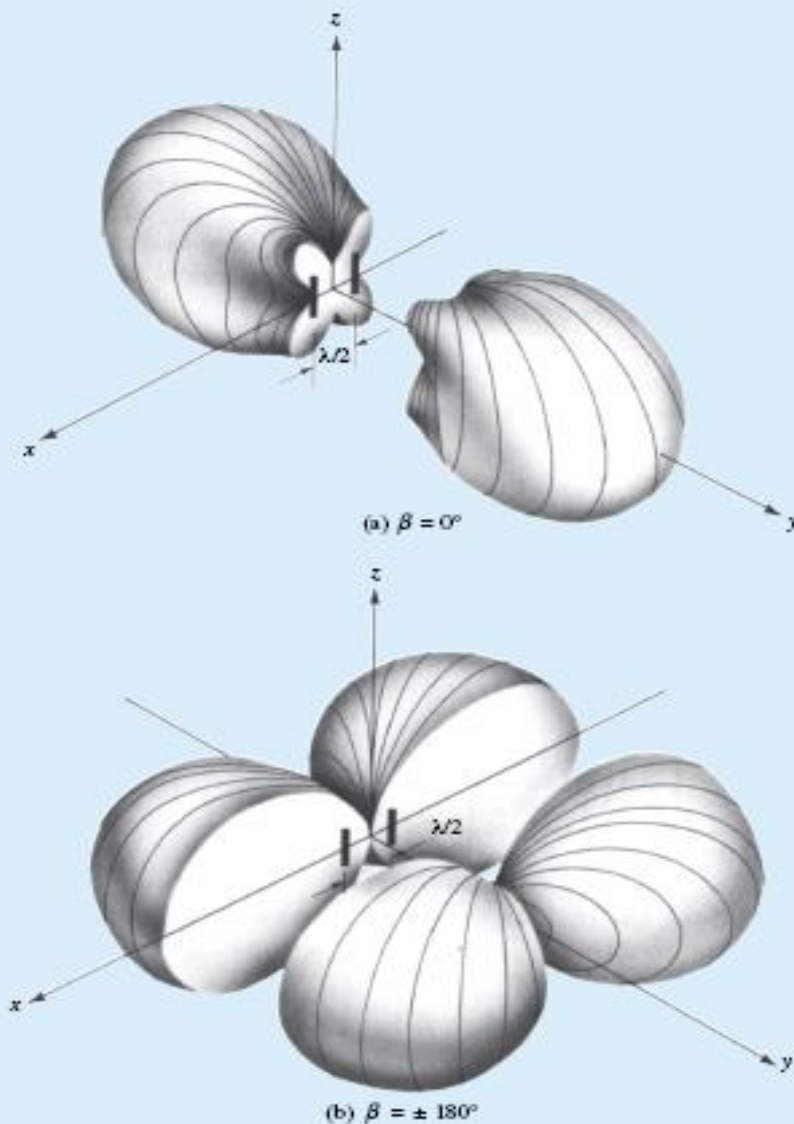


**Figure 6.17** Three-dimensional patterns for two  $\lambda/2$  dipoles spaced  $\lambda/2$ . (SOURCE: P. Lorrain and D. R. Corson, *Electromagnetic Fields and Waves*, 2nd ed., W. H. Freeman and Co., Copyright (©) 1970).

*Solution:* The field pattern of a single element placed at the origin is given by (4-84) as

$$E_{\theta} = j\eta \frac{I_0 e^{-jkr}}{2\pi r} \left[ \frac{\cos\left(\frac{\pi}{2} \cos\theta\right)}{\sin\theta} \right]$$

Using (6-52), (6-54a), and (6-10c), the array factor can be written as

$$(\text{AF})_n = \frac{\sin(kd \sin\theta \cos\phi + \beta)}{2 \sin\left[\frac{1}{2}(kd \sin\theta \cos\phi + \beta)\right]}$$

The total field of the array is then given, using the pattern multiplication rule of (6-5), by

$$E_{\theta t} = E_{\theta} \cdot (\text{AF})_n = j\eta \frac{I_0 e^{-jkr} \cos\left(\frac{\pi}{2} \cos\theta\right)}{2\pi r \sin\theta} \left[ \frac{\sin(kd \sin\theta \cos\phi + \beta)}{2 \sin\left[\frac{1}{2}(kd \sin\theta \cos\phi + \beta)\right]} \right]$$

To illustrate the techniques, the three-dimensional patterns of the two-element array of Example 6.7 have been sketched in Figs. 6.17(a) and (b). For both, the element separation is  $\lambda/2$  ( $d = \lambda/2$ ). For the pattern of Fig. 6.17(a), the phase excitation between the elements is identical ( $\beta = 0$ ). In addition to the nulls in the  $\theta = 0^\circ$  direction, provided by the individual elements of the array, there are additional nulls along the x-axis ( $\theta = \pi/2$ ,  $\phi = 0$  and  $\phi = \pi$ ) provided by the formation of the array. The  $180^\circ$  phase difference required to form the nulls along the x-axis is a result of the separation of the elements [ $kd = (2\pi/\lambda)(\lambda/2) = \pi$ ].

To form a comparison, the three-dimensional pattern of the same array but with a  $180^\circ$  phase excitation ( $\beta = 180^\circ$ ) between the elements is sketched in Fig. 6.17(b). The overall pattern of this array is quite different from that shown in Fig. 6.17(a). In addition to the nulls along the z-axis ( $\theta = 0$ ) provided by the individual elements, there are nulls along the y-axis formed by the  $180^\circ$  excitation phase difference.

## 6.8 N-ELEMENT LINEAR ARRAY: UNIFORM SPACING, NONUNIFORM AMPLITUDE

The theory to analyze linear arrays with uniform spacing, uniform amplitude, and a progressive phase between the elements was introduced in the previous lectures. In this lecture, broadside arrays with uniform spacing but nonuniform amplitude distribution are considered. The binomial and Dolph-Tschebyscheff broadside arrays (also spelled Tchebyscheff or Chebyshev) will be analyzed.

*Of the three distributions (uniform, binomial, and Tschebyscheff), a uniform amplitude array yields the smallest half-power beamwidth. It is followed, in order, by the Dolph-Tschebyscheff and binomial arrays. In contrast, binomial arrays usually possess the smallest side lobes followed, in order, by the Dolph-Tschebyscheff and uniform arrays. As a matter of fact, binomial arrays with element spacing equal or less than  $\lambda/2$  have no side lobes. It is apparent that the designer must **compromise** between side lobe level and beamwidth.*

A criterion that can be used to judge the relative beamwidth and side lobe level of one design to another is the amplitude distribution (tapering) along the source. *It has been shown analytically that for a given side lobe level the Dolph-Tschebyscheff array produces the smallest beamwidth between the first nulls. Conversely, for a given beamwidth between the first nulls, the Dolph-Tschebyscheff design leads to the smallest possible side lobe level.*

Uniform arrays usually possess the largest directivity. However, superdirective (or super gain as most people refer to them) antennas possess directivities higher than those of a uniform array. Before introducing design methods for specific nonuniform amplitude distributions, let us first derive the array factor.

### 6.8.1 Array Factor

An array of an even number of isotropic elements  $2M$  (where  $M$  is an integer) is positioned symmetrically along the  $z$ -axis, as shown in Fig. 6.19(a). The separation between the elements is  $d$ , and  $M$  elements are placed on each side of the origin. Assuming that the amplitude excitation is symmetrical about the origin, the array factor for a nonuniform amplitude broadside array can be written as

$$\begin{aligned}
 (\text{AF})_{2M} &= a_1 e^{+j(1/2)kd \cos \theta} + a_2 e^{+j(3/2)kd \cos \theta} + \dots \\
 &\quad + a_M e^{+j[(2M-1)/2]kd \cos \theta} \\
 &\quad + a_1 e^{-j(1/2)kd \cos \theta} + a_2 e^{-j(3/2)kd \cos \theta} + \dots \\
 &\quad + a_M e^{-j[(2M-1)/2]kd \cos \theta} \\
 (\text{AF})_{2M} &= 2 \sum_{n=1}^M a_n \cos \left[ \frac{(2n-1)}{2} kd \cos \theta \right] \tag{6-59}
 \end{aligned}$$

Which in normalized form reduces to

$$(\text{AF})_{2M} = \sum_{n=1}^M a_n \cos \left[ \frac{(2n-1)}{2} kd \cos \theta \right] \tag{6-59a}$$

where  $a_n$ 's are the excitation coefficients of the array elements.

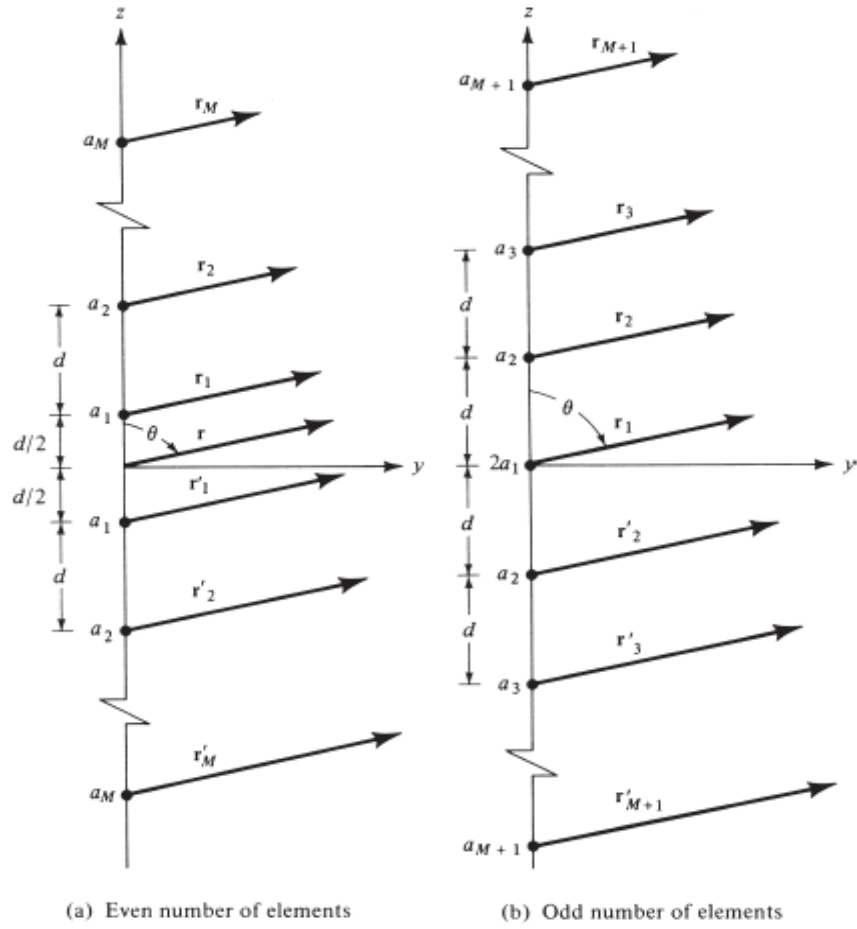


Figure 6.19 Nonuniform amplitude arrays of even and odd number of elements.

If the total number of isotropic elements of the array is odd  $2M + 1$  (where  $M$  is an integer), as shown in Fig. 6.19(b), the array factor can be written as

$$\begin{aligned}
 (\text{AF})_{2M+1} &= 2a_1 + a_2 e^{+jkd \cos \theta} + a_3 e^{j2kd \cos \theta} + \dots + a_{M+1} e^{jMkd \cos \theta} \\
 &\quad + a_2 e^{-jkd \cos \theta} + a_3 e^{-j2kd \cos \theta} + \dots + a_{M+1} e^{-jMkd \cos \theta} \\
 (\text{AF})_{2M+1} &= 2 \sum_{n=1}^{M+1} a_n \cos[(n-1)kd \cos \theta] \tag{6-60}
 \end{aligned}$$

Which in normalized form reduces to

$$(\text{AF})_{2M+1} = \sum_{n=1}^{M+1} a_n \cos[(n-1)kd \cos \theta] \tag{6-60a}$$

The amplitude excitation of the center element is  $2a_1$ .

Equations (6-59a) and (6-60a) can be written in normalized form as



### B. Design Procedure

For the binomial method, as for any other nonuniform array method, one of the requirements is the amplitude excitation coefficients for a given number of elements. This can be accomplished using either (6-62) or the Pascal triangle of (6-63) or extensions of it. Other figures of merit are the directivity, half-power beamwidth and side lobe level. It already has been stated that *binomial arrays do not exhibit any minor lobes provided the spacing between the elements is equal or less than one-half of a wavelength*. Unfortunately, closed-form expressions for the directivity and half-power beamwidth for binomial arrays of any spacing between the elements are not available. However, because the design using a  $\lambda/2$  spacing leads to a pattern with no minor lobes, approximate closed-form expressions for the half-power beamwidth and maximum directivity for the  $d = \lambda/2$  spacing only have been derived in terms of the numbers of elements or the length of the array, and they are given, respectively, by

$$\text{HPBW}(d = \lambda/2) \simeq \frac{1.06}{\sqrt{N-1}} = \frac{1.06}{\sqrt{2L/\lambda}} = \frac{0.75}{\sqrt{L/\lambda}} \quad (6-64)$$

$$D_0 = \frac{2}{\int_0^\pi \left[ \cos\left(\frac{\pi}{2} \cos\theta\right) \right]^{2(N-1)} \sin\theta \, d\theta} \quad (6-65)$$

$$D_0 = \frac{(2N-2)(2N-4) \cdots 2}{(2N-3)(2N-5) \cdots 1} \quad (6-65a)$$

$$D_0 \simeq 1.77\sqrt{N} = 1.77\sqrt{1+2L/\lambda} \quad (6-65b)$$

These expressions can be used effectively to design binomial arrays with a desired half-power beamwidth or directivity. The value of the directivity as obtained using (6-65) to (6-65b) can be compared with the value using the array factor and the computer program **Directivity** of Chapter 2.

To illustrate the method, the patterns of a 10-element binomial array ( $2M = 10$ ) with spacings between the elements of  $\lambda/4$ ,  $\lambda/2$ ,  $3\lambda/4$ , and  $\lambda$ , respectively, have been plotted in Fig. 6.20. The patterns are plotted using (6-61a) and (6-61c) with the coefficients of  $a_1 = 126$ ,  $a_2 = 84$ ,  $a_3 = 36$ ,  $a_4 = 9$ , and  $a_5 = 1$ . It is observed that there are no minor lobes for the arrays with spacings of  $\lambda/4$  and  $\lambda/2$  between the elements. While binomial arrays have very low level minor lobes, they exhibit larger beamwidths (compared to uniform and Dolph-Tschebyscheff designs). A major practical disadvantage of binomial arrays is the wide variations between the amplitudes of the different elements of an array, especially for an array with a large number of elements. This leads to very low efficiencies for the feed network, and it makes the method not very desirable in practice. For example, the relative amplitude coefficient of the end elements of a 10-element array is 1 while that of the center element is 126. Practically, it

would be difficult to obtain and maintain such large amplitude variations among the elements. They would also lead to very inefficient antenna systems. Because the magnitude distribution is monotonically decreasing from the center toward the edges and the magnitude of the extreme elements is negligible compared to those toward the center, a very low side lobe level is expected.

*Table 6.7 lists the maximum element spacing  $d_{\max}$  for the various linear and planar arrays, including binomial arrays, in order to maintain either one or two amplitude maxima.*

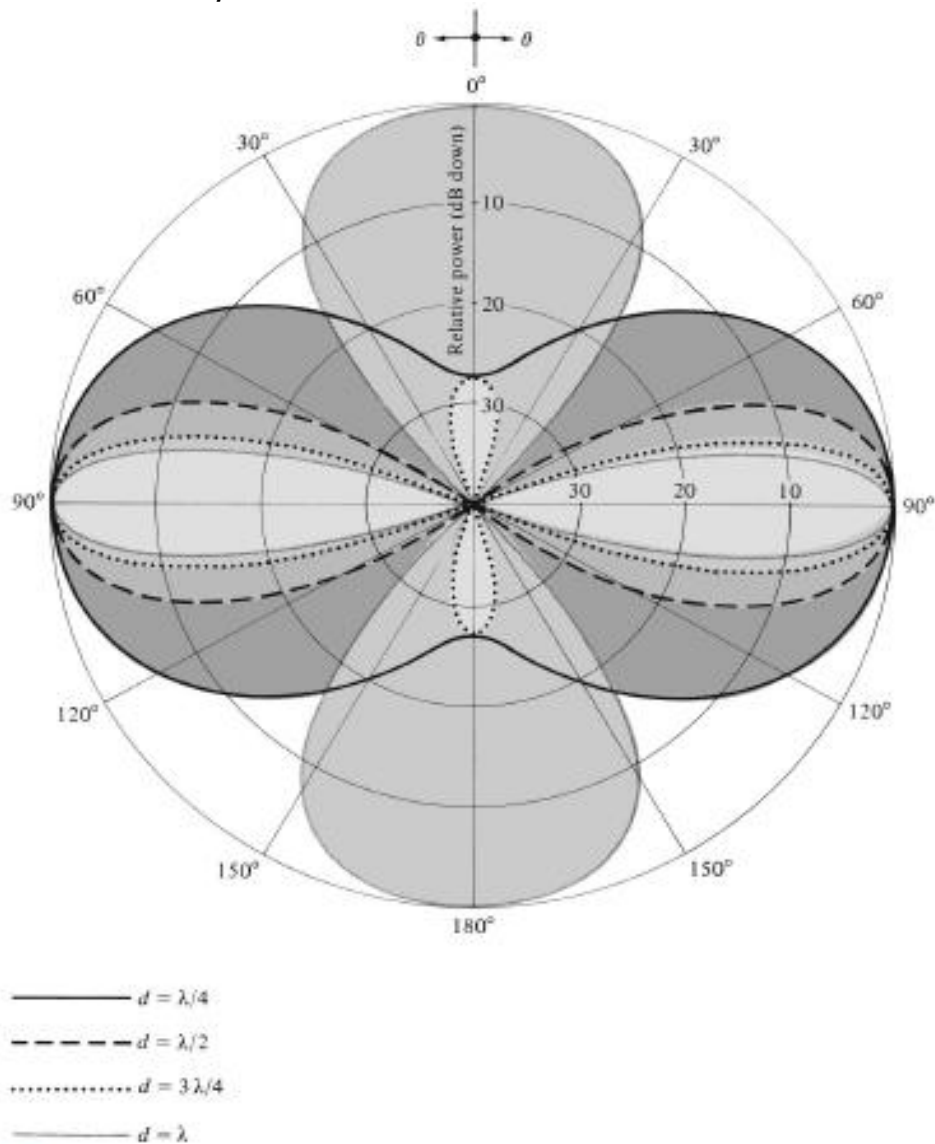


**Figure 6.20** Array factor power patterns for a 10-element broadside binomial array with  $N = 10$  and  $d = \lambda/4, \lambda/2, 3\lambda/4$ , and  $\lambda$ .

### Example 6.8

For a 10-element binomial array with a spacing of  $\lambda/2$  between the elements, whose amplitude pattern is displayed in Figure 6.20, determine the half-power beamwidth (in degrees) and the maximum directivity (in dB). Compare the answers with other available data.

*Solution:* Using (6-64), the half-power beamwidth is equal to

$$\text{HPBW} \simeq \frac{1.06}{\sqrt{10-1}} = \frac{1.06}{3} = 0.353 \text{ radians} = 20.23^\circ$$

The value obtained using the array factor, whose pattern is shown in Figure 6.20, is  $20.5^\circ$  which compares well with the approximate value.

Using (6-65a), the value of the directivity is equal for  $N = 10$

$$D_0 = 5.392 = 7.32 \text{ dB}$$

while the value obtained using (6-65b) is

$$D_0 = 1.77\sqrt{10} = 5.597 = 7.48 \text{ dB}$$

The value obtained using the array factor and the computer program **Directivity** is  $D_0 = 5.392$  (dimensionless) = 7.32 dB. These values compare favorably with each other.

**TABLE 6.7** Maximum Element Spacing  $d_{\text{max}}$  to Maintain Either One or Two Amplitude Maxima of a Linear Array

Array	Distribution	Type	Direction of Maximum	Element Spacing
Linear	Uniform	Broadside	$\theta_0 = 90^\circ$ only	$d_{\text{max}} < \lambda$
			$\theta_0 = 0^\circ, 90^\circ, 180^\circ$ simultaneously	$d = \lambda$
Linear	Uniform	Ordinary end-fire	$\theta_0 = 0^\circ$ only	$d_{\text{max}} < \lambda/2$
			$\theta_0 = 180^\circ$ only	$d_{\text{max}} < \lambda/2$
			$\theta_0 = 0^\circ, 90^\circ, 180^\circ$ simultaneously	$d = \lambda$
Linear	Uniform	Hansen-Woodyard end-fire	$\theta_0 = 0^\circ$ only	$d \simeq \lambda/4$
			$\theta_0 = 180^\circ$ only	$d \simeq \lambda/4$
Linear	Uniform	Scanning	$\theta_0 = \theta_{\text{max}}$ $0 < \theta_0 < 180^\circ$	$d_{\text{max}} < \lambda$
Linear	Nonuniform	Binomial	$\theta_0 = 90^\circ$ only	$d_{\text{max}} < \lambda$
			$\theta_0 = 0^\circ, 90^\circ, 180^\circ$ simultaneously	$d = \lambda$
Linear	Nonuniform	Dolph-Tschebyscheff	$\theta_0 = 90^\circ$ only	$d_{\text{max}} \leq \frac{\lambda}{\pi} \cos^{-1} \left( -\frac{1}{z_0} \right)$
			$\theta_0 = 0^\circ, 90^\circ, 180^\circ$ simultaneously	$d = \lambda$
Planar	Uniform	Planar	$\theta_0 = 0^\circ$ only	$d_{\text{max}} < \lambda$
			$\theta_0 = 0^\circ, 90^\circ$ and $180^\circ$ ; $\phi_0 = 0^\circ, 90^\circ, 180^\circ, 270^\circ$ simultaneously	$d = \lambda$

## 6.10 PLANAR ARRAY

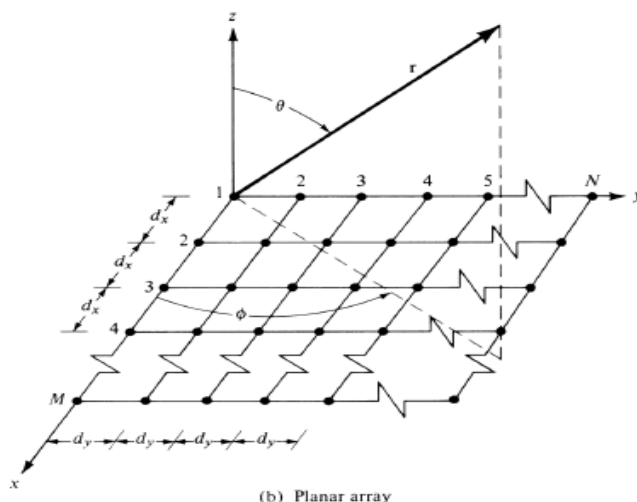
In addition to placing elements along a line (to form a linear array), individual radiators can be positioned along a rectangular grid to form a rectangular or planar array. Planar arrays provide additional variables which can be used to control and shape the pattern of the array. Planar arrays are more versatile and can provide more symmetrical patterns with lower side lobes. In addition, they can be used to scan the main beam of the antenna toward any point in space. Applications include tracking radar, search radar, remote sensing, communications, and many others.

### 6.10.1 Array Factor

To derive the array factor for a planar array, let us refer to Figure 6.30. If  $M$  elements are initially placed along the  $x$ -axis, as shown in Figure 6.30(a), the array factor of it can be written according to (6-52) and (6-54) as

$$AF = \sum_{m=1}^M I_{m1} e^{j(m-1)(kd_x \sin \theta \cos \phi + \beta_x)} \quad (6-87)$$

where  $I_{m1}$  is the excitation coefficient of each element. The spacing and progressive phase shift between the elements along the  $x$ -axis are represented, respectively, by  $d_x$  and  $\beta_x$ . If  $N$  such arrays are placed next to each other in the  $y$ -direction, a distance  $d_y$  apart and with a progressive phase  $\beta_y$ , a rectangular array will be formed as shown in Fig. 6.30(b). The array factor for the entire planar array can be written as



$$AF = \sum_{n=1}^N I_{1n} \left[ \sum_{m=1}^M I_{m1} e^{j(m-1)(kd_x \sin \theta \cos \phi + \beta_x)} \right] e^{j(n-1)(kd_y \sin \theta \sin \phi + \beta_y)} \quad (6-87a)$$

or

$$AF = S_{xm} S_{yn} \quad (6-88)$$

where

$$S_{xm} = \sum_{m=1}^M I_{m1} e^{j(m-1)(kd_x \sin \theta \cos \phi + \beta_x)} \quad (6-88a)$$

$$S_{yn} = \sum_{n=1}^N I_{1n} e^{j(n-1)(kd_y \sin \theta \sin \phi + \beta_y)} \quad (6-88b)$$

Equation (6-88) indicates that the pattern of a rectangular array is the product of the array factors of the arrays in the  $x$ - and  $y$ -directions.

If the amplitude excitation coefficients of the elements of the array in the  $y$ -direction are proportional to those along the  $x$ , the amplitude of the  $(m, n)$ th element can be written as

$$I_{mn} = I_{m1} I_{1n} \quad (6-89)$$

If in addition the amplitude excitation of the entire array is uniform ( $I_{mn} = I_0$ ), (6-87a) can be expressed as

$$AF = I_0 \sum_{m=1}^M e^{j(m-1)(kd_x \sin \theta \cos \phi + \beta_x)} \sum_{n=1}^N e^{j(n-1)(kd_y \sin \theta \sin \phi + \beta_y)} \quad (6-90)$$

According to (6-6), (6-10), and (6-10c), the normalized form of (6-90) can also be written as

$$AF_n(\theta, \phi) = \left\{ \frac{1}{M} \frac{\sin\left(\frac{M}{2}\psi_x\right)}{\sin\left(\frac{\psi_x}{2}\right)} \right\} \left\{ \frac{1}{N} \frac{\sin\left(\frac{N}{2}\psi_y\right)}{\sin\left(\frac{\psi_y}{2}\right)} \right\} \quad (6-91)$$

where

$$\psi_x = kd_x \sin \theta \cos \phi + \beta_x \quad (6-91a)$$

$$\psi_y = kd_y \sin \theta \sin \phi + \beta_y \quad (6-91b)$$

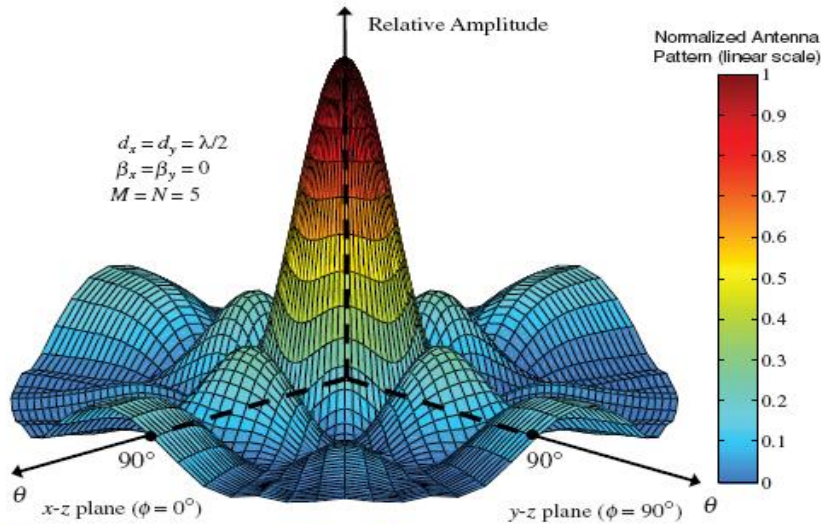


Figure 6.32 Three-dimensional antenna pattern of a planar array of isotropic elements with a spacing of  $d_x = d_y = \lambda/2$ , and equal amplitude and phase excitations.

## PROBLEMS ABOUT ARRAY ANTENNAS

- 6.1.** Three isotropic sources, with spacing  $d$  between them, are placed along the  $z$ -axis. The excitation coefficient of each outside element is unity while that of the center element is 2. For a spacing of  $d = \lambda/4$  between the elements, find the
- array factor
  - angles (in degrees) where the nulls of the pattern occur ( $0^\circ \leq \theta \leq 180^\circ$ )
  - angles (in degrees) where the maxima of the pattern occur ( $0^\circ \leq \theta \leq 180^\circ$ )
  - directivity using the computer program **Directivity** of Chapter 2.

6.1. a.  $E_t = E_1 + E_2 + E_3 = 2E_0 \frac{e^{-jkr}}{r} + E_0 \frac{e^{-jkr_1}}{r_1} + E_0 \frac{e^{-jkr_2}}{r_2}$

where the center element is placed at the origin. For far-field observations

$$\left. \begin{aligned} r_1 &\approx r - d \cos\theta \\ r_2 &\approx r + d \cos\theta \end{aligned} \right\} \text{for phase variations}$$

$$r_1 \approx r_2 \approx r \quad \text{for amplitude variations}$$

and  $E_t = E_0 \frac{e^{-jkr}}{r} \left\{ 2 + e^{jkd \cos\theta} + e^{-jkd \cos\theta} \right\}$

$$\approx E_0 \frac{e^{-jkr}}{r} \left\{ 2 \left[ 1 + \frac{1}{2} (e^{jkd \cos\theta} + e^{-jkd \cos\theta}) \right] \right\}$$

$$= E_0 \frac{e^{-jkr}}{r} \left\{ 2 [1 + \cos(kd \cos\theta)] \right\}$$

Computer Program

Directivity

$$U = \cos^4\left(\frac{\pi}{4} \cos\theta\right)$$

$$\text{At } d = \lambda/4$$

$$P_{\text{rad}} = 8.7119$$

$$D_0 = 1.44244$$

$$= 1.5910 \text{ dB}$$

$$kd = \frac{2\pi}{\lambda} \cdot \frac{\lambda}{4} = \frac{\pi}{2}$$

$$AF(\theta) = 4 \cos^2\left(\frac{\pi}{4} \cos\theta\right)$$

Thus the array factor is equal to

$$AF(\theta) = 2 [1 + \cos(kd \cos\theta)] = 4 \cos^2\left(\frac{kd}{2} \cos\theta\right)$$

which in normalized form can also be written as

$$AF(\theta)_n = 1 + \cos(kd \cos\theta) = 2 \cos^2\left(\frac{kd}{2} \cos\theta\right)$$

- b. The nulls of the pattern can be found using either of the above forms for the array factor. For example

One Form

$$AF(\theta) = 1 + \cos(kd \cos\theta_n) = 0$$

$$\cos(kd \cos\theta_n) = -1$$

$$kd \cos\theta_n = \cos^{-1}(-1) = n\pi, \quad n = \pm 1, \pm 3, \dots$$

$$\theta_n = \cos^{-1}\left(\frac{n\lambda}{2d}\right), \quad n = \pm 1, \pm 3, \pm 5, \dots$$

the other Form

$$2 \cos^2\left(\frac{kd}{2} \cos\theta_n\right) = 0$$

$$\frac{kd}{2} \cos\theta_n = \cos^{-1}(0) = \frac{n\pi}{2}, \quad n = \pm 1, \pm 3, \dots$$

$$\theta_n = \cos^{-1}\left(\frac{n\lambda}{2d}\right), \quad n = \pm 1, \pm 3, \dots$$

which are of identical form. Therefore both forms yield the same results. Thus for  $d = \lambda/4$

$$\theta_n = \cos^{-1}\left(\frac{n\lambda}{2d}\right)_{d=\lambda/4} = \cos^{-1}(2n), \quad n = \pm 1, \pm 3, \dots \Rightarrow \text{No nulls exist.}$$

C. Similarly the maxima of the pattern can be found using either of the two forms for the array factor. For example

6-1(Cont'd) One Form

$$AF(\theta) = 1 + \cos(kd \cos \theta_m) = 2$$

$$\cos(kd \cos \theta_m) = 1$$

$$kd \cos \theta_m = \cos^{-1}(1) = 2m\pi, m=0, \pm 1, \dots, \frac{kd}{2} \cos \theta_m = \cos^{-1}(\pm 1) = m\pi, m=0, \pm 1, \dots$$

$$\theta_m = \cos^{-1}\left(\frac{m\lambda}{d}\right), m=0, \pm 1, \pm 2, \dots, \theta_m = \cos^{-1}\left(\frac{m\lambda}{d}\right), m=0, \pm 1, \pm 2, \dots$$

which are of identical form. Therefore both yield the same results.

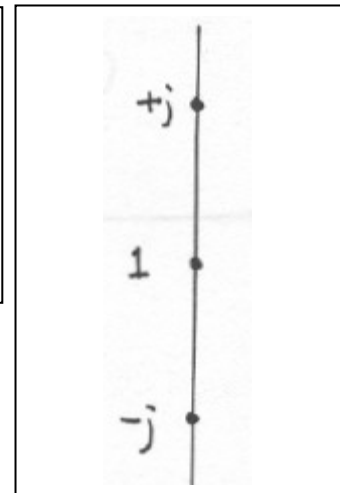
Thus for  $d = \lambda/4$ .

$$\theta_m = \cos^{-1}(4m), m=0, \pm 1, \pm 2, \dots \rightarrow$$

- $m=0: \theta_0 = \cos^{-1}(0) = 90^\circ$
  - $m=\pm 1: \theta_1 = \cos^{-1}(4) \Rightarrow$  Does not exist.
- The same is true for other values of  $m$  (i.e.  $m=\pm 2, \pm 3, \dots$ ). Therefore the only maxima occur at  $\theta = 90^\circ$

**6.3.** A three-element array of isotropic sources has the phase and magnitude relationships shown. The spacing between the elements is  $d = \lambda/2$ .

- (a) Find the array factor.
- (b) Find all the nulls.



a.  $AF = 1 + e^{j(kd \cos \theta + \pi/2)} + e^{-j(kd \cos \theta + \pi/2)}$

$$= 1 + 2 \cos(kd \cos \theta + \pi/2)$$

$$\therefore AF = 1 - 2 \sin(kd \cos \theta)$$

b. to find the nulls,

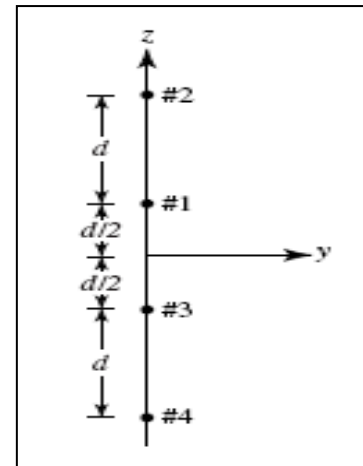
$$AF = 1 - 2 \sin(kd \cos \theta) = 0$$

$$2 \sin(kd \cos \theta) = 1, \pi \cos \theta = \sin^{-1}\left(\frac{1}{2}\right) = \frac{\pi}{6}, \frac{5\pi}{6}, \frac{13\pi}{6}, \dots$$

$$\cos \theta = \frac{1}{6}, \frac{5}{6}, \frac{13}{6}, \dots$$

$$\theta_{null} = 80.4^\circ, 33.6^\circ$$

**6.5.** Four isotropic sources are placed along the z-axis as shown. Assuming that the amplitudes of elements #1 and #2 are +1 and the amplitudes of elements #3 and #4 are -1 (or 180 degrees out of phase with #1 and #2), find  
 (a) the array factor in simplified form  
 (b) all the nulls when  $d = \lambda/2$



$$(a) E = \frac{e^{-jkr_2}}{r_2} + \frac{e^{-jkr_1}}{r_1} - \frac{e^{-jkr_3}}{r_3} - \frac{e^{-jkr_4}}{r_4}$$

$$= \frac{e^{-jkr}}{r} \left[ e^{jk\frac{3d}{2}\cos\theta} + e^{jk\frac{d}{2}\cos\theta} - e^{-jk\frac{d}{2}\cos\theta} - e^{-jk\frac{3d}{2}\cos\theta} \right]$$

$$r_1 = r - \frac{d}{2}\cos\theta, \quad r_2 = r - \frac{3d}{2}\cos\theta, \quad r_3 = r + \frac{d}{2}\cos\theta, \quad r_4 = r + \frac{3d}{2}\cos\theta$$

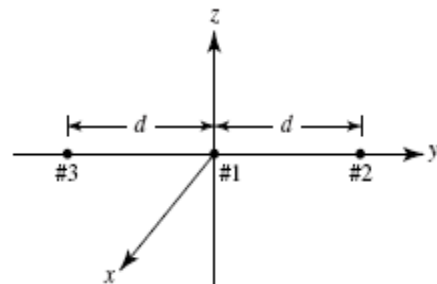
$$AF = 2j \left[ \sin\left(\frac{3kd}{2}\cos\theta\right) + \sin\left(\frac{kd}{2}\cos\theta\right) \right]$$

$$(b) \text{ let } x = kd\cos\theta, \quad y = \frac{kd}{2}\cos\theta \Rightarrow AF = 4j \left[ \sin(kd\cos\theta) \cos\left(\frac{kd}{2}\cos\theta\right) \right]$$

$$AF(d = \lambda/2) = 4j \left[ \sin(\pi\cos\theta) \cos\left(\frac{\pi}{2}\cos\theta\right) \right]$$

$$\therefore \theta_n = 0^\circ, 90^\circ, 180^\circ$$

**6.7.** Three isotropic elements of equal excitation phase are placed along the y-axis, as shown in the figure. If the relative amplitude of #1 is +2 and of #2 and #3 is +1, find a simplified expression for the three-dimensional unnormalized array factor.



$$E_{total} = \frac{e^{-jkr}}{r} \left[ 2 + e^{jkd\cos\psi} + e^{-jkd\cos\psi} \right]$$

$$= \frac{e^{-jkr}}{r} \left[ 2 + 2\cos(kd\cos\psi) \right]$$

$$\cos\psi = \hat{a}_y \cdot \hat{a}_r = \sin\theta \sin\phi$$

$$\text{So, } AF = 2 + 2\cos(kd\sin\theta\sin\phi)$$

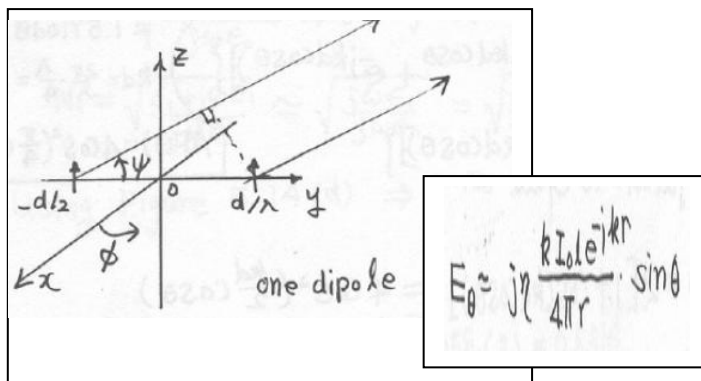
$$\text{or } AF = 2 \left[ 1 + \cos(kd\sin\theta\sin\phi) \right]$$

**6.2** Two very short dipoles (“infinitesimal”) of equal length are equidistant from the origin with their centers lying on the y-axis, and oriented parallel to the z-axis. They are excited with currents of equal amplitude. The current in dipole 1 (at  $y = -d/2$ ) leads the current in dipole 2 (at  $y = +d/2$ ) by  $90^\circ$  in phase. The spacing between dipoles is one quarter wavelength. To simplify the notation, let  $E_0$  equal the maximum magnitude of the far field at distance  $r$  due to either source alone.

(a) Derive expressions for the following six principal-plane patterns:

1.  $|E_\theta(\theta)|$  for  $\phi = 0^\circ$  ,
2.  $|E_\theta(\theta)|$  for  $\phi = 90^\circ$
3.  $|E_\theta(\phi)|$  for  $\theta = 90^\circ$  ,
4.  $|E_\phi(\theta)|$  for  $\phi = 0^\circ$
5.  $|E_\phi(\theta)|$  for  $\phi = 90^\circ$  ,
6.  $|E_\phi(\phi)|$  for  $\theta = 90^\circ$

(b) Sketch the six field patterns.



Array Factor:

$$(AF)_z = E_0 \left[ e^{j\frac{\pi}{2}} \cdot e^{-j\frac{\lambda}{8} \cdot \frac{2\pi}{\lambda} \cos\psi} + e^{+j\frac{\lambda}{8} \cdot \frac{2\pi}{\lambda} \cos\psi} \right]$$

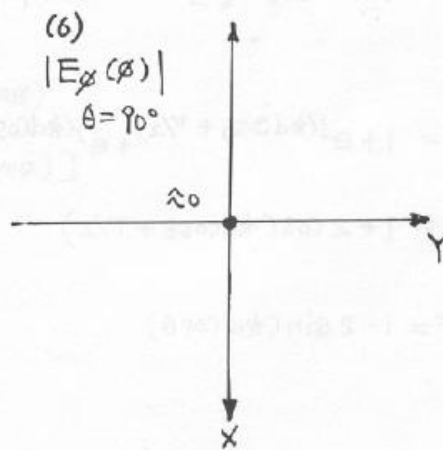
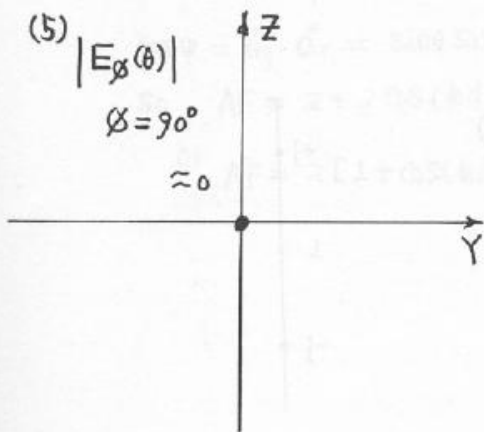
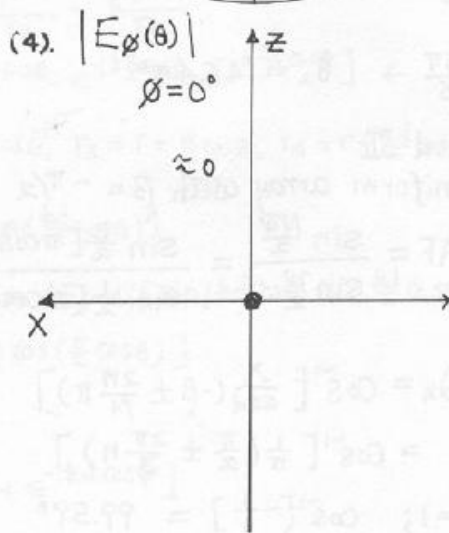
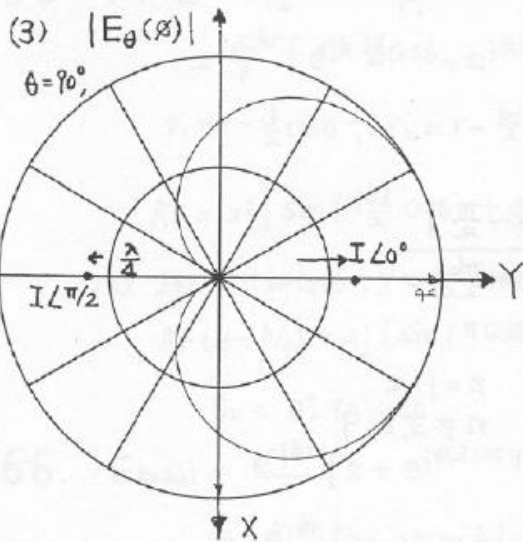
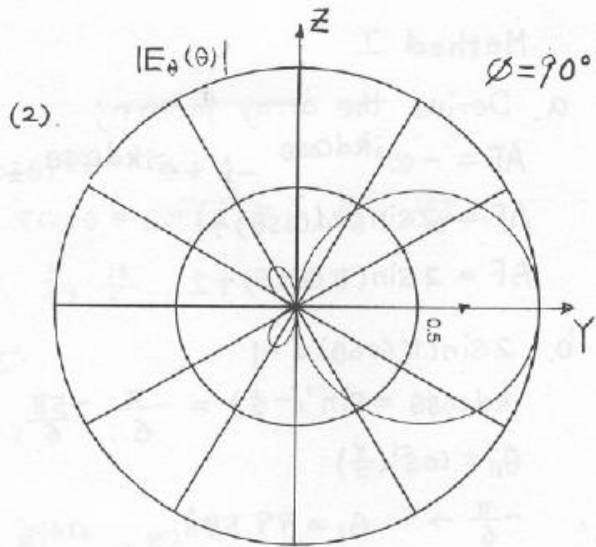
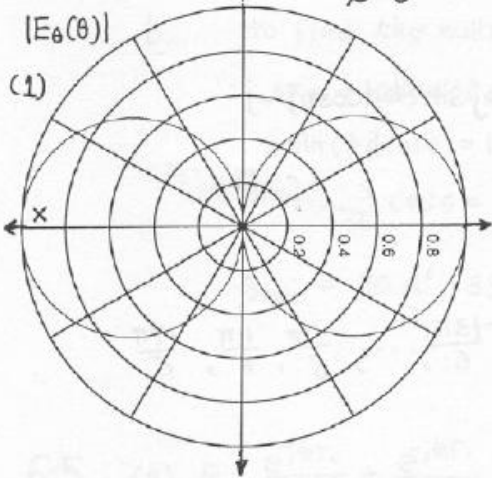
$$= E_0 e^{j\frac{\pi}{4}} \left[ e^{-j\frac{\pi}{4}(\cos\psi - 1)} + e^{j\frac{\pi}{4}(\cos\psi - 1)} \right]$$

$$= E_0 e^{j\frac{\pi}{4}} \cdot 2 \cdot \cos\left(\frac{\pi}{4}(\cos\psi - 1)\right) = E_0 e^{j\frac{\pi}{4}} \cdot 2 \cos\left(\frac{\pi}{4}(\sin\theta \sin\phi - 1)\right)$$

$(\hat{a}_y \cdot \hat{a}_r = \sin\theta \cdot \sin\phi = \cos\psi)$  At y-z plane,  $\phi = 90^\circ$

- a. (1)  $|E_\theta(\theta)| \propto \left| \sin\theta \cdot \cos\left(\frac{\pi}{4}\right) \right|$  , (x-z plane)  
 $\phi = 0^\circ$
- (2)  $|E_\theta(\theta)| \propto \left| \sin\theta \cdot \cos\left(\frac{\pi}{4}(\sin\theta - 1)\right) \right|$  , (y-z plane)  
 $\phi = 90^\circ$
- (3)  $|E_\theta(\phi)| \propto \left| \cos\left(\frac{\pi}{4}(\sin\phi - 1)\right) \right|$  , (x, y, plane)  
 $\theta = 90^\circ$
- (4)  $|E_\phi(\theta)|_{\phi=0^\circ} \propto 0$
- (5)  $|E_\phi(\theta)|_{\phi=90^\circ} \propto 0$
- (6)  $|E_\phi(\theta)|_{\theta=90^\circ} \propto 0$

6-2. (Cont'd)



- 6.13.** Design an ordinary end-fire uniform linear array with only one maximum so that its directivity is 20 dB (above isotropic). The spacing between the elements is  $\lambda/4$ , and its length is much greater than the spacing. Determine the
- number of elements,
  - overall length of the array (in wavelengths),
  - approximate half-power beamwidth (in degrees),
  - amplitude level (compared to the maximum of the major lobe) of the first minor lobe (in dB),
  - progressive phase shift between the elements (in degrees).

a.  $D_0 = 4N \left(\frac{d}{\lambda}\right)$

$$20 = 10 \log_{10} D_0 \text{ (dimensionless)} \Rightarrow D_0 \text{ (dimensionless)} = 10^2 = 100$$

$$100 = 4N \left(\frac{\lambda}{4\lambda}\right) = N \Rightarrow N = 100$$

b.  $L = 99 \left(\frac{\lambda}{4}\right) = \frac{99}{4} \lambda = 24.75 \lambda$

c.  $\Theta_{3dB} = \Theta_h = 2 \cos^{-1} \left( 1 - \frac{1.391 \lambda}{N d \pi} \right) \Big|_{n=100} = 2 \cos^{-1} \left( 1 - \frac{1.391 \lambda}{\pi \left(\frac{\lambda}{4}\right) 100} \right)$   
 $= 2 \cos^{-1} \left( 1 - \frac{1.391(4)}{100 \pi} \right) = 2 \cos^{-1} (1 - 0.01771) = 2 \cos^{-1} (0.98228)$

$$\Theta_h = 2(10.799^\circ) = 21.598^\circ \approx 21.6^\circ$$

d. Sidelobe (dB)  $\approx -13.5$  dB

e.  $\beta = \pm kd = \pm \frac{2\pi}{\lambda} \left(\frac{\lambda}{4}\right) = \pm \frac{\pi}{2} = \pm 90^\circ$

**6.20.** Show that in order for a uniform array of  $N$  elements not to have any minor lobes, the spacing and the progressive phase shift between the elements must be

(a)  $d = \lambda/N$ ,  $\beta = 0$  for a broadside array.

(b)  $d = \lambda/(2N)$ ,  $\beta = \pm kd$  for an ordinary end-fire array.

5.  $(AF)_n = \frac{\sin \left[ \frac{N}{2} (kd \cos \theta + \beta) \right]}{N \sin \left[ \frac{1}{2} (kd \cos \theta + \beta) \right]}$

a. For  $\beta = 0 \Rightarrow (AF)_n = \frac{\sin \left( \frac{N}{2} kd \cos \theta \right)}{N \sin \left( \frac{1}{2} kd \cos \theta \right)}$

In order for the array not to have any minor lobes, we can assume that its first null occurs at  $\theta = 0^\circ$  or  $180^\circ$ . Thus

$$(AF)_n = \frac{\sin \left( \frac{N}{2} kd \right)}{N \sin \left( \frac{1}{2} kd \right)} = 0 \Rightarrow \frac{N}{2} kd = \pi \Rightarrow d = \frac{2\pi}{kN} = \frac{\lambda}{N}$$

This assures that there are no minor lobes formed.

b. For  $\beta = kd$  the maximum occurs at  $\theta = 180^\circ$  and the array factor can be written as  $(AF)_n = \frac{\sin[\frac{N}{2}kd(\cos\theta + 1)]}{N \sin[\frac{1}{2}kd(\cos\theta + 1)]}$

In order for the array not to have any minor lobes, we can assume that the first null is formed at  $\theta = 0^\circ$ .

$$\text{Thus } \frac{N}{2}kd(\cos\theta + 1) \Big|_{\theta=0^\circ} = Nkd = \pi \Rightarrow d = \frac{\pi}{Nk} = \frac{\lambda}{2N}$$

**6.6.** A uniform linear broadside array of 4 elements are placed along the  $z$ -axis each a distance  $d$  apart.

(a) Write the normalized array factor in *simplified form*.

(b) For a separation of  $d = 3\lambda/8$  between the elements, determine the:

1. Approximate half-power beamwidth (*in degrees*).

2. Approximate directivity (*dimensionless and in dB*).

-----

**6.8.** Design a uniform broadside linear array of  $N$  elements placed along the  $z$ -axis with a uniform spacing  $d = \lambda/10$  between the elements. Determine the *closest integer number* of elements so that in the *elevation plane* the

(a) Half-power beamwidth of the array factor is approximately  $60^\circ$ .

(b) First-null beamwidth of the array factor is  $60^\circ$ .

-----

**6.9.** A uniform array of 3 elements is designed so that its maximum is directed toward broadside. The spacing between the elements is  $\lambda/2$ . For the array factor of the antenna, determine

(a) all the angles (*in degrees*) where the nulls will occur.

(b) all the angles (*in degrees*) where all the maxima will occur.

(c) the half-power beamwidth (*in degrees*).

(d) directivity (*dimensionless and in dB*).

(e) the *relative value (in dB)* of the magnitude of the array factor toward end-fire ( $\theta_0 = 0^\circ$ ) compared to that toward broadside ( $\theta_0 = 90^\circ$ ).

-----

**6.12.** Design a four-element ordinary end-fire array with the elements placed along the  $z$ -axis a distance  $d$  apart. For a spacing of  $d = \lambda/2$  between the elements find the

(a) progressive phase excitation between the elements to accomplish this

(b) angles (*in degrees*) where the nulls of the array factor occur

(c) angles (*in degrees*) where the maximum of the array factor occur

(d) beamwidth (*in degrees*) between the first nulls of the array factor.

### 6.8.3 Dolph-Tschebyscheff Array: Broadside

Another array, with many practical applications, is the *Dolph-Tschebyscheff array*. The design was originally introduced by Dolph and investigated afterward by others. It is primarily a compromise between uniform and binomial arrays. Its excitation coefficients are related to Tschebyscheff polynomials. A Dolph-Tschebyscheff array with no side lobes (or side lobes of  $-\infty$  dB) reduces to the binomial design. The excitation coefficients for this case, as obtained by both methods, would be identical.

#### A. Array Factor

Referring to (6-61a) and (6-61b), the array factor of an array of even or odd number of elements with symmetric amplitude excitation is nothing more than a summation of  $M$  or  $M + 1$  cosine terms. The largest harmonic of the cosine terms is one less than the total number of elements of the array. Each cosine term, whose argument is an integer times a fundamental frequency, can be rewritten as a series of cosine functions with the fundamental frequency as the argument. That is,

$$\begin{aligned}
 m = 0 \quad \cos(mu) &= 1 \\
 m = 1 \quad \cos(mu) &= \cos u \\
 m = 2 \quad \cos(mu) &= \cos(2u) = 2 \cos^2(u) - 1 \\
 m = 3 \quad \cos(mu) &= \cos(3u) = 4 \cos^3(u) - 3 \cos(u) \\
 m = 4 \quad \cos(mu) &= \cos(4u) = 8 \cos^4(u) - 8 \cos^2(u) + 1 \\
 m = 5 \quad \cos(mu) &= \cos(5u) = 16 \cos^5(u) - 20 \cos^3(u) + 5 \cos(u) \\
 m = 6 \quad \cos(mu) &= \cos(6u) = 32 \cos^6(u) - 48 \cos^4(u) + 18 \cos^2(u) - 1
 \end{aligned} \tag{6-66}$$

The above are obtained by the use of Euler's formula

$$[e^{ju}]^m = (\cos u + j \sin u)^m = e^{jmu} = \cos(mu) + j \sin(mu) \tag{6-67}$$

and the trigonometric identity  $\sin^2 u = 1 - \cos^2 u$ .

If we let

$$z = \cos u \tag{6-68}$$

$$u = \frac{\pi d}{\lambda} \cos \theta$$

(6-66) can be written as

$$\begin{aligned}
 m = 0 \quad \cos(mu) &= 1 = T_0(z) \\
 m = 1 \quad \cos(mu) &= z = T_1(z) \\
 m = 2 \quad \cos(mu) &= 2z^2 - 1 = T_2(z) \\
 m = 3 \quad \cos(mu) &= 4z^3 - 3z = T_3(z) \\
 m = 4 \quad \cos(mu) &= 8z^4 - 8z^2 + 1 = T_4(z) \\
 m = 5 \quad \cos(mu) &= 16z^5 - 20z^3 + 5z = T_5(z) \\
 m = 6 \quad \cos(mu) &= 32z^6 - 48z^4 + 18z^2 - 1 = T_6(z)
 \end{aligned} \tag{6-69}$$

and each is related to a Tschebyscheff (Chebyshev) polynomial  $T_m(z)$ . These relations between the cosine functions and the Tschebyscheff polynomials are valid only in the  $-1 \leq z \leq +1$  range.

Because  $|\cos(mu)| \leq 1$ , each Tschebyscheff polynomial is  $|T_m(z)| \leq 1$  for  $-1 \leq z \leq +1$ . For  $|z| > 1$ , the Tschebyscheff polynomials are related to the hyperbolic cosine functions.

The recursion formula for Tschebyscheff polynomials is

$$T_m(z) = 2zT_{m-1}(z) - T_{m-2}(z) \quad (6-70)$$

It can be used to find one Tschebyscheff polynomial if the polynomials of the previous two orders are known. Each polynomial can also be computed using

$$T_m(z) = \cos[m \cos^{-1}(z)] \quad -1 \leq z \leq +1 \quad (6-71a)$$

$$T_m(z) = \cosh[m \cosh^{-1}(z)]^\dagger \quad z < -1, z > +1 \quad (6-71b)$$

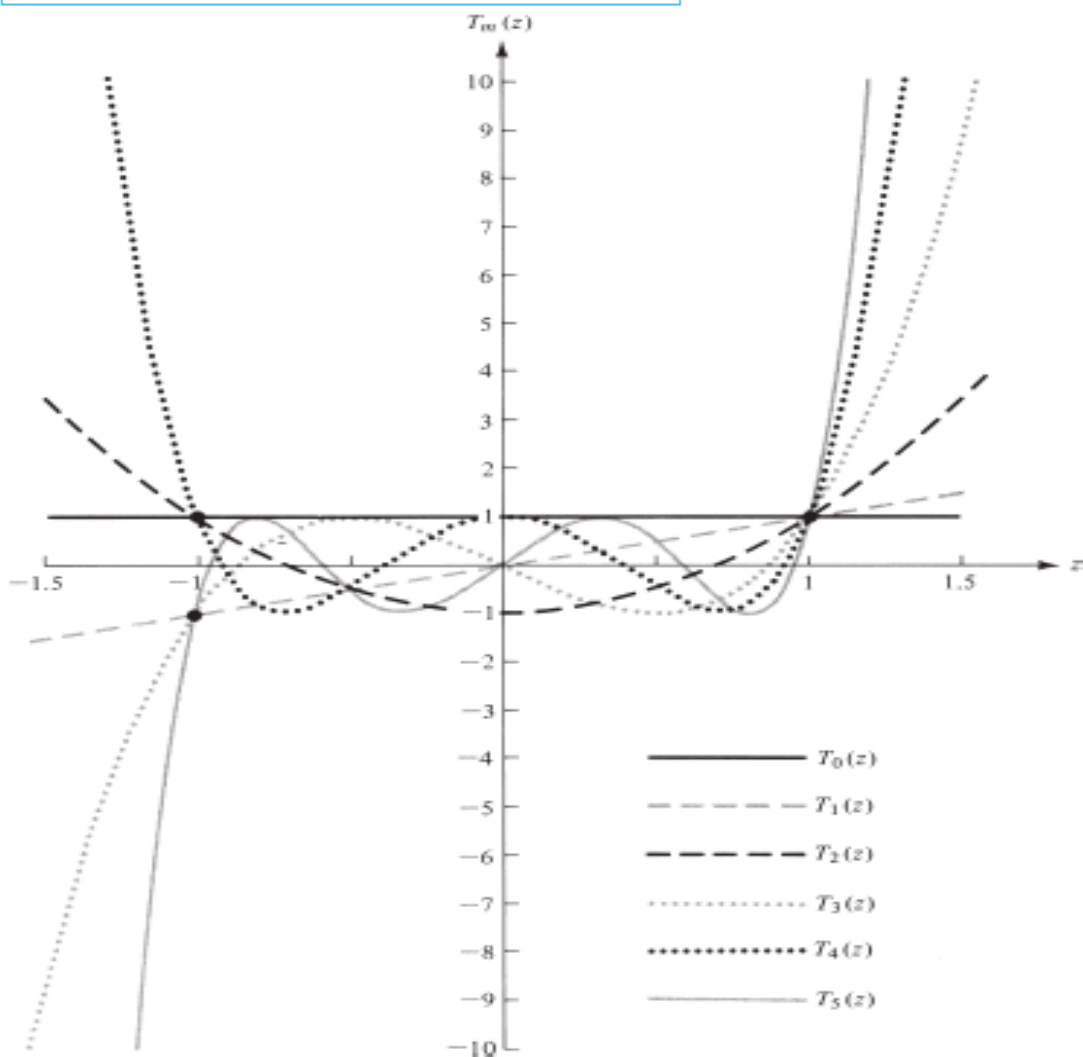


Figure 6.21 Tschebyscheff polynomials of orders zero through five.

In Fig. 6.21 the first six Tschebyscheff polynomials have been plotted. The following **properties of the polynomials** are of interest:

1. All polynomials, of any order, pass through the point (1, 1).
2. Within the range  $-1 \leq z \leq 1$ , the polynomials have values within  $-1$  to  $+1$ .
3. All roots occur within  $-1 \leq z \leq 1$ , and all maxima and minima have values of  $+1$  and  $-1$ , respectively.

Since the array factor of an even or odd number of elements is a summation of cosine terms whose form is the same as the Tschebyscheff polynomials, the unknown coefficients of the array factor can be determined by equating the series representing the cosine terms of the array factor to the appropriate Tschebyscheff polynomial. **The order of the polynomial should be one less than the total number of elements of the array.**

### **B. Array Design**

It is assumed that the number of elements, spacing between them, and ratio of major-to-minor lobe intensity ( $R_0$ ) are known. The requirements will be to determine the excitation coefficients and the array factor.

**Statement.** Design a broadside Dolph-Tschebyscheff array of  $2M$  or  $2M+1$  elements with spacing  $d$  between the elements. The side lobes are  $R_0$  dB below the maximum of the major lobe. Find the excitation coefficients and form the array factor.

#### **Procedure**

- a. Select the appropriate array factor as given by (6-61a) or (6-61b) (even or odd).
- b. Expand the array factor. Replace each  $\cos(mu)$  function ( $m=0,1,2, \dots$ ) by its appropriate series expansion found in (6-66).
- c. Determine the point  $z = z_0$  such that  $T_m(z_0) = R_0$  (voltage ratio). *The order  $m$  of the Tschebyscheff polynomial is always one less than the total number of elements.* The design procedure requires that the Tschebyscheff polynomial in the  $-1 \leq z \leq z_1$ , where  $z_1$  is the null nearest to  $z = +1$ , be used to represent the minor lobes of the array. The major lobe of the pattern is formed from the remaining part of the polynomial up to point  $z_0$  ( $z_1 < z \leq z_0$ ).
- d. Substitute

$$\cos(u) = \frac{z}{z_0} \quad (6-72)$$

in the array factor of step **b**. The  $\cos(u)$  is replaced by  $z/z_0$ , and not by  $z$ , so that (6-72) would be valid for  $|z| \leq |z_0|$ . At  $|z| = |z_0|$ , (6-72) attains its maximum value of unity.

e. Equate the array factor from step b, after substitution of (6-72), to a  $T_m(z)$  from (6-69). The  $T_m(z)$  chosen should be of order  $m$  where  $m$  is an integer equal to one less than the total number of elements of the designed array. This will allow the determination of the excitation coefficients  $a_n$ 's.

f. Write the array factor of (6-61a) or (6-61b) using the coefficients found in step e.

### Example 6.9

Design a broadside Dolph-Tschebyscheff array of 10 elements with spacing  $d$  between the elements and with a major-to-minor lobe ratio of 26 dB. Find the excitation coefficients and form the array factor.

*Solution:*

1. The array factor is given by (6-61a) and (6-61c). That is,

$$(AF)_{2M} = \sum_{n=1}^{M-1} a_n \cos[(2n-1)u]$$

$$u = \frac{\pi d}{\lambda} \cos \theta$$

2. When expanded, the array factor can be written as

$$(AF)_{10} = a_1 \cos(u) + a_2 \cos(3u) + a_3 \cos(5u) + a_4 \cos(7u) + a_5 \cos(9u)$$

Replace  $\cos(u)$ ,  $\cos(3u)$ ,  $\cos(5u)$ ,  $\cos(7u)$ , and  $\cos(9u)$  by their series expansions found in (6-66).

3.  $R_0$  (dB) = 26 =  $20 \log_{10}(R_0)$  or  $R_0$  (voltage ratio) = 20. Determine  $z_0$  by equating  $R_0$  to  $T_9(z_0)$ . Thus

$$R_0 = 20 = T_9(z_0) = \cosh[9 \cosh^{-1}(z_0)]$$

Or

$$z_0 = \cosh\left[\frac{1}{9} \cosh^{-1}(20)\right] = 1.0851$$

Another equation which can, in general, be used to find  $z_0$  and does not require hyperbolic functions is

$$z_0 = \frac{1}{2} \left[ \left( R_0 + \sqrt{R_0^2 - 1} \right)^{1/P} + \left( R_0 - \sqrt{R_0^2 - 1} \right)^{1/P} \right] \quad (6-73)$$

where  $P$  is an integer equal to one less than the number of array elements (in this case  $P = 9$ ).  $R_0 = H_0/H_1$  and  $z_0$  are identified in Figure 6.22.

4. Substitute

$$\cos(u) = \frac{z}{z_0} = \frac{z}{1.0851}$$

in the array factor found in step 2.

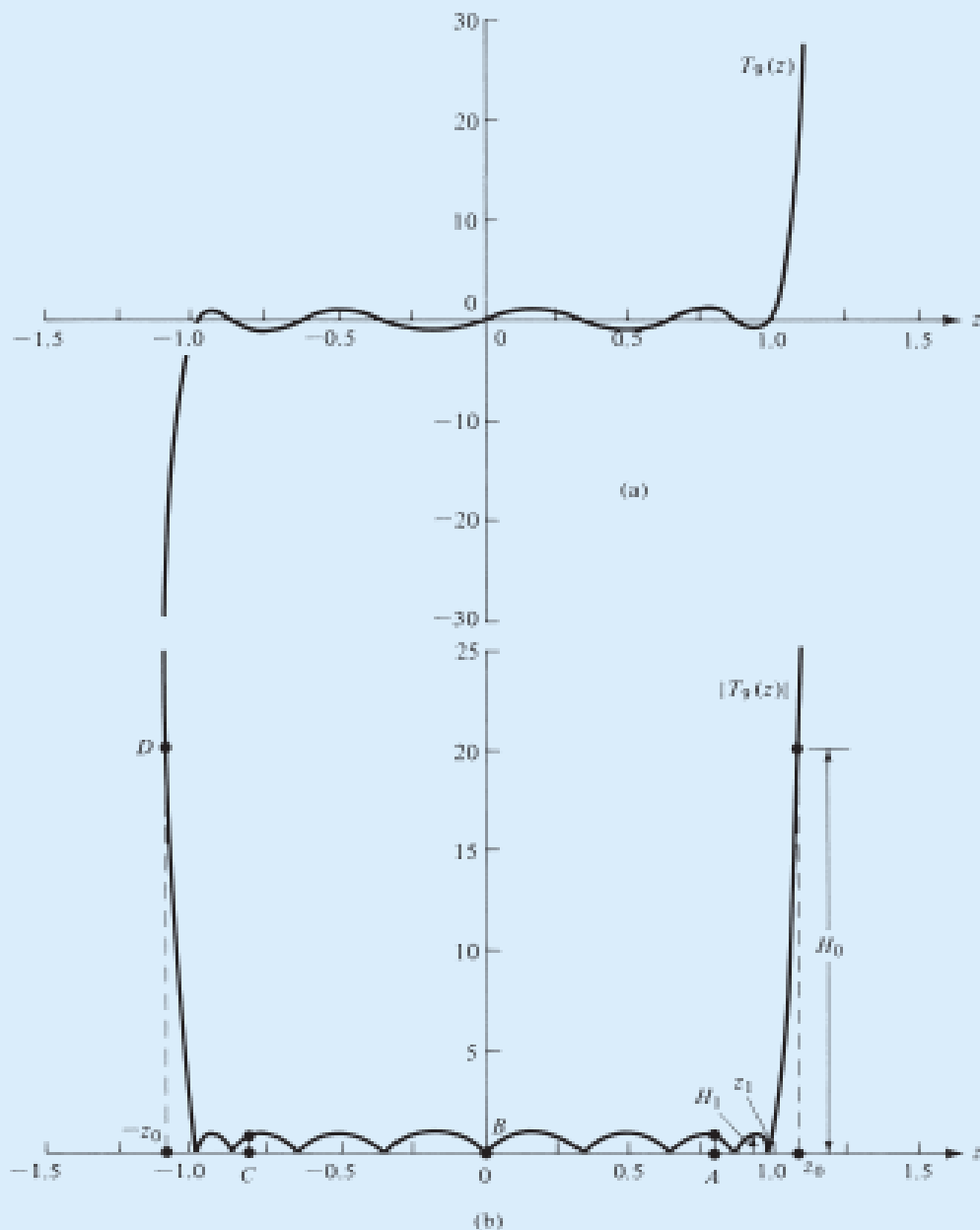


Figure 6.22 Tschebyscheff polynomial of order nine (a) amplitude (b) magnitude.

5. Equate the array factor of step 2, after the substitution from step 4, to  $T_9(z)$ . The polynomial  $T_9(z)$  is shown plotted in Figure 6.22. Thus

$$\begin{aligned}
 (AF)_{10} &= z[(a_1 - 3a_2 + 5a_3 - 7a_4 + 9a_5)/z_0] \\
 &+ z^3[(4a_2 - 20a_3 + 56a_4 - 120a_5)/z_0^3] \\
 &+ z^5[(16a_3 - 112a_4 + 432a_5)/z_0^5] \\
 &+ z^7[(64a_4 - 576a_5)/z_0^7] \\
 &+ z^9[(256a_5)/z_0^9] \\
 &= 9z - 120z^3 + 432z^5 - 576z^7 + 256z^9
 \end{aligned}$$

Matching similar terms allows the determination of the  $a_n$ 's. That is,

$$\begin{aligned} 256a_5/z_0^9 &= 256 & \Rightarrow a_5 &= 2.0860 \\ (64a_4 - 576a_5)/z_0^7 &= -576 & \Rightarrow a_4 &= 2.8308 \\ (16a_3 - 112a_4 + 432a_5)/z_0^5 &= 432 & \Rightarrow a_3 &= 4.1184 \\ (4a_2 - 20a_3 + 56a_4 - 120a_5)/z_0^3 &= -120 & \Rightarrow a_2 &= 5.2073 \\ (a_1 - 3a_2 + 5a_3 - 7a_4 + 9a_5)/z_0 &= 9 & \Rightarrow a_1 &= 5.8377 \end{aligned}$$

In normalized form, the  $a_n$  coefficients can be written as

$$\begin{aligned} a_5 &= 1 & a_5 &= 0.357 \\ a_4 &= 1.357 & a_4 &= 0.485 \\ a_3 &= 1.974 & \text{or} & a_3 = 0.706 \\ a_2 &= 2.496 & a_2 &= 0.890 \\ a_1 &= 2.798 & a_1 &= 1 \end{aligned}$$

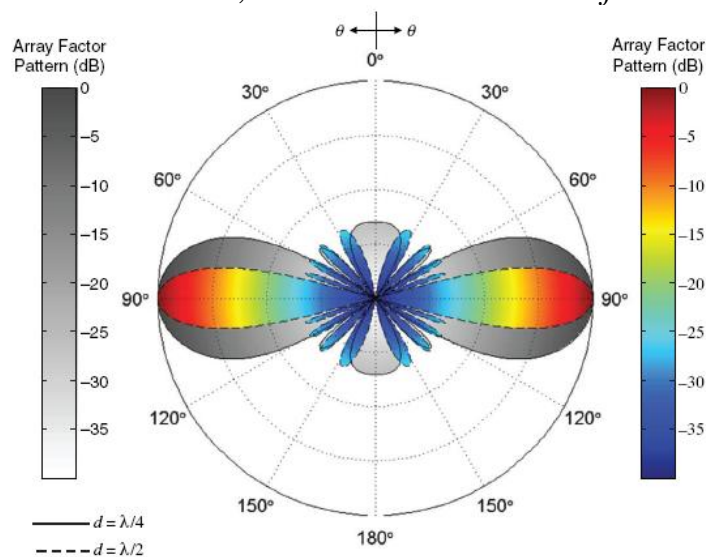
The first (left) set is normalized with respect to the amplitude of the elements at the edge while the other (right) is normalized with respect to the amplitude of the center element.

6. Using the first (left) set of normalized coefficients, the array factor can be written as

$$\begin{aligned} (AF)_{10} &= 2.798 \cos(u) + 2.496 \cos(3u) + 1.974 \cos(5u) \\ &+ 1.357 \cos(7u) + \cos(9u) \end{aligned}$$

where  $u = [(\pi d/\lambda) \cos \theta]$ .

The array factor patterns of Example 6.9 for  $d = \lambda/4$  and  $\lambda/2$  are shown plotted in Fig. 6.23. Since the spacing is less than  $\lambda$  ( $d < \lambda$ ), maxima exist only at broadside ( $\theta_0 = 90^\circ$ ). However when the spacing is equal to  $\lambda$  ( $d = \lambda$ ), two more maxima appear (one toward  $\theta_0 = 0^\circ$  and the other toward  $\theta_0 = 180^\circ$ ). For  $d = \lambda$  the array has four maxima, and it acts as an *end-fire* as well as a *broadside*



array. **Figure 6.23** Array factor power pattern of a  $N = 10$  element broadside Dolph-Tschebyscheff array.

Table 6.7 lists the maximum element spacing  $d_{\max}$  for the various arrays, including Dolph-Tschebyscheff arrays, in order to maintain one or two amplitude maxima.

Four isotropic sources are placed symmetrically along the  $z$ -axis a distance  $d$  apart. Design a binomial array. Find the

- (a) normalized excitation coefficients                      (b) array factor  
 (c) angles (in degrees) where the array factor nulls occur when  $d = 3\lambda/4$

6-26. The excitation coefficients of a 4-element binomial array are 1, 3, 3, 1  
 or

$$a. \quad \left. \begin{array}{l} a_1 = 3 \\ a_2 = 1 \end{array} \right\} N = 2M = 4 \Rightarrow M = 2$$

$$b. \quad (AF)_4 = \sum_{n=1}^{M=2} a_n \cos[(2n-1)u], \quad u = \frac{\pi d}{\lambda} \cos\theta, \quad \text{using (6-61a) and (6-61c).}$$

Thus

$$(AF)_4 = a_1 \cos(u) + a_2 \cos(3u) = 3 \cos\left(\frac{\pi d}{\lambda} \cos\theta\right) + \cos\left(\frac{3\pi d}{\lambda} \cos\theta\right)$$

which can also be written, using (6-66) for  $m=3$ , as

$$(AF)_4 = 3 \cos\left(\frac{\pi d}{\lambda}\right) + 4 \cos^3\left(\frac{\pi d}{\lambda} \cos\theta\right) - 3 \cos\left(\frac{\pi d}{\lambda} \cos\theta\right) = 4 \cos^3\left(\frac{\pi d}{\lambda} \cos\theta\right)$$

$$(AF)_4 = 4 \cos^3\left(\frac{\pi d}{\lambda} \cos\theta\right)$$

c. The nulls occur when

$$(AF)_4 = 4 \cos^3\left(\frac{\pi d}{\lambda} \cos\theta_n\right) = 0 \Rightarrow \frac{\pi d}{\lambda} \cos\theta_n = \cos^{-1}(0) = \pm \frac{(2n+1)\pi}{2}, \quad n=0, 1, 2, \dots$$

$$\text{or } \theta_n = \cos^{-1}\left[\pm \frac{(2n+1)\lambda}{2d}\right] \stackrel{d=3\lambda/4}{=} \cos^{-1}\left[\pm \frac{(2n+1)2}{3}\right], \quad n=0, 1, 2, \dots$$

$$n=0 : \theta_0 = \cos^{-1}\left(\pm \frac{2}{3}\right) = 48.19^\circ, 131.81^\circ$$

$$n=1 : \theta_1 = \cos^{-1}(\pm 2) = \text{Does not exist. The same holds for } n \geq 2.$$

Design a four-element binomial array of  $\lambda/2$  dipoles, placed symmetrically along the  $x$ -axis a distance  $d$  apart. The length of each dipole is parallel to the  $z$ -axis.

- (a) Find the normalized excitation coefficients.  
 (b) Write the array factor for all space.  
 (c) Write expressions for the  $E$ -fields for all space.

6-28. The excitation coefficients for a 4-element binomial array are 1, 3, 3, 1

$$a. \quad \text{or } a_1 = 3, a_2 = 1$$

b. Since the elements are placed along the  $x$ -axis

$$\cos\gamma = \hat{a}_x \cdot \hat{a}_r = \hat{a}_x \cdot (\hat{a}_x \sin\theta \cos\phi + \hat{a}_y \sin\theta \sin\phi + \hat{a}_z \cos\theta) = \sin\theta \cos\phi$$

The array factor for this array is similar to that of Problem 6.26. The

$$(AF)_4 = 3 \cos\left(\frac{\pi d}{\lambda} \sin\theta \cos\phi\right) + \cos\left(\frac{3\pi d}{\lambda} \sin\theta \cos\phi\right) = 4 \cos^3\left(\frac{\pi d}{\lambda} \sin\theta \cos\phi\right)$$

c. The total field is obtained using the pattern multiplication rule of (6-5) by multiplying the field of a single  $\lambda/2$  dipole, as given by (4-84), with the array factor above. Thus

$$E_\theta(\text{total}) = E_\theta(\text{single}) \times (AF) = j\eta \frac{I_0 e^{jkr}}{2\pi r} \cdot \frac{\cos\left(\frac{\pi}{2} \cos\theta\right)}{\sin\theta} \left[ 4 \cos^3\left(\frac{\pi d}{\lambda} \sin\theta \cos\phi\right) \right]$$

Design a four-element, -40 dB side lobe level Dolph-Tschebyscheff array of isotropic elements placed symmetrically about the z-axis. Find the  
 (a) amplitude excitation coefficients (b) array factor  
 (c) angles where the nulls occur for  $d = 3\lambda/4$ .

Solution:

Number of elements =  $2M = 4$ , then degree of polynomial =  $2M-1 = 3$ .

6-35. a.  $(AF)_4 = \sum_{n=1}^2 a_n \cos[(2n-1)\mu]$

$$= a_1 \cos(\mu) + a_2 \cos(3\mu) = a_1 \cos(\mu) + a_2 (4 \cos^3(\mu) - 3 \cos(\mu))$$

$$= (a_1 - 3a_2) \cos(\mu) + 4a_2 \cos^3(\mu)$$

Since  $m = 3$   $\cos(m\mu) = \cos(3\mu) = 4 \cos^3 \mu - 3 \cos \mu$

$$R_0 = 40 \text{ dB} \Rightarrow R_0 = 100$$

$$z_0 = \cosh\left[\frac{1}{3} \cosh^{-1}(100)\right] = 3.0095$$

Therefore  $(AF)_4 = (a_1 - 3a_2) \frac{z}{z_0} + 4a_2 \left(\frac{z}{z_0}\right)^3 = -3z + 4z^3 = T_3(z)$

$$\frac{4a_2}{(3.0095)^3} = 4 \Rightarrow a_2 = 27.257$$

$$\frac{a_1 - 3(27.257)}{(3.0095)} = -3 \Rightarrow a_1 = 72.742$$

$$\left. \begin{array}{l} a_1 = 2.668 \\ a_2 = 1 \end{array} \right\}$$

b.  $AF = 2.668 \cos \mu + \cos 3\mu$ ,  $\mu = \frac{\pi d}{\lambda} \cos \theta$

c.  $d = \frac{3\lambda}{4}$ ,  $\mu = \frac{3\pi}{4} \cos \theta$

$$AF = 2.668 \cos \mu + \cos 3\mu = 2.668 \cos \mu - 3 \cos \mu + 4 \cos^3 \mu$$

$$= -0.332 \cos \mu + 4 \cos^3 \mu = \cos\left(\frac{3\pi}{4} \cos \theta\right) \left[-0.332 + 4 \cos^2\left(\frac{3\pi}{4} \cos \theta\right)\right]$$

$$= \cos\left(\frac{3\pi}{4} \cos \theta\right) \left[1.668 + 2 \cos\left(\frac{3\pi}{2} \cos \theta\right)\right] = 0$$

$$\therefore \cos\left(\frac{3\pi}{4} \cos \theta_n\right) = 0 \text{ or } \frac{3\pi}{2} \cos \theta_n = \cos^{-1}(-0.834) = \begin{cases} 2.5571 \\ 3.7261 \end{cases}$$

$$\theta_n = \cos^{-1}\left(\frac{\pi}{2} \cdot \frac{4}{3\pi}\right) = 48.19^\circ$$

$$\theta_n = \cos^{-1}\left[\frac{2}{3\pi}(2.5571)\right] = 57.137^\circ$$

$$\theta_n = \cos^{-1}\left[\frac{2}{3\pi}(3.7261)\right] = 37.7487^\circ$$

Computer Result.  
 Directivity  
 $D_0 = 6.85 \text{ dB}$

Computer Program:  $a_1 = 72.742$ ,  $a_2 = 27.217 \Rightarrow$  Normalized  $a_2 = 1$ ,  $a_1 = 2.668$ .

Design a broadside uniform array, with its elements placed along the z axis, in order the directivity of the array factor is 33 dB (above isotropic). Assuming the spacing between the elements is  $\lambda/16$ , and it is very small compared to the overall length of the array, determine the:

- Closest number of integer elements to achieve this.
- Overall length of the array (in wavelengths).
- Half-power beamwidth (in degrees).
- Amplitude level (in dB) of the maximum of the first minor lobe compared to the maximum of the major lobe.

6-43. a.  $D_o = 2N \left( \frac{d}{\lambda} \right)$

$$D_o = 33 \text{ dB} = 10 \log_{10} D_o \text{ (dimensionless)}$$

$$3.3 = \log_{10} D_o \text{ (dimensionless)}$$

$$D_o \text{ (dimensionless)} = 10^{3.3} = 1,995.26$$

$$1995.26 = 2N \left( \frac{d}{\lambda} \right) = 2N \left( \frac{\lambda}{16\lambda} \right) = \frac{N}{8} \Rightarrow N = 15,962.1 \approx 15,962.$$

$$N = 15,962$$

b.  $L = (N-1)d = (15,962 - 1) \frac{\lambda}{16} = \frac{(15,961 \cdot \lambda)}{16} = 997.56 \lambda$

$$L = 997.56 \lambda$$

c.  $\Theta_h \approx 2 \left[ \frac{\pi}{2} - \cos^{-1} \left( \frac{1.391 \lambda}{\pi N d} \right) \right] = 2 \left[ 90^\circ - \cos^{-1} \left( \frac{1.391 (16) \lambda}{\pi (15,962) \lambda} \right) \right]$

$$\Theta_h \approx 2 [90^\circ - 89.9745^\circ] = 0.05086^\circ = 0.05086^\circ$$

d.  $-13.46 \approx -13.5 \text{ dB}$

Design a nonuniform amplitude broadside linear array of 5 elements. The total length of the array is  $2\lambda$ . To meet the sidelobe and half-power beamwidth specifications, the amplitude excitations of the elements must be that of a cosine on-a-pedestal distribution represented by

$$\text{Amplitude distribution} = 1 + \cos(\pi x_n / L)$$

where  $x_n$  is the position of the  $n$ th element (in terms of  $L$ ) measured from the center of the array. Determine the amplitude excitation coefficients  $a_n$ 's of the five elements. Assume uniform spacing between the elements and the end elements are located at the edges of the array length.

$$a_n = 1 + \cos \left( \frac{\pi x_n}{L} \right)$$

$$2a_1 = 1 + \cos \left( \frac{\pi x_1}{L} \right) = 1 + \cos(0) = 2 \Rightarrow a_1 = 1$$

$$a_2 = 1 + \cos \left( \frac{\pi x_2}{L} \right) \Big|_{x_2 = L/4} = 1 + \cos \left( \frac{\pi L}{4L} \right) = 1 + \cos \left( \frac{\pi}{4} \right) = 1.707$$

$$a_3 = 1 + \cos \left( \frac{\pi x_3}{L} \right) \Big|_{x_3 = L/2} = 1 + \cos \left( \frac{\pi}{2} \right) = 1.$$

$a_1=1, a_2=1.707, a_3=1, \dots$  element excitations:: 1 / 1.707 / 2 / 1.707 / 1

## Lecture Notes-15 BROAD BAND ANTENNAS

One of the main objectives in the design of an antenna is to increase its bandwidth. Typically, the response of an antenna, versus frequency, can be classified qualitatively into three categories: *narrowband*, *intermediate band*, and *wide band*. In Fig. 9.1, we exhibit four different dipole configurations, starting with the classic dipole in Fig. 9.1(a) and ending with the hemispherical dipole of Fig. 9.1(d). These dipoles can be qualitatively categorized into three groups; *narrowband*, *intermediate band*, and *wide band*. The same can be concluded for the geometries of the four monopole geometries of Fig. 9.2. Although in Fig. 9.1 and 9.2, the last two configurations (*d* in each) exhibit the most broadband characteristics, usually these geometries are not as convenient and economical for practical implementation. However, any derivatives of these geometries, especially two-dimensional types, are configurations that may be used to broadband the frequency characteristics.

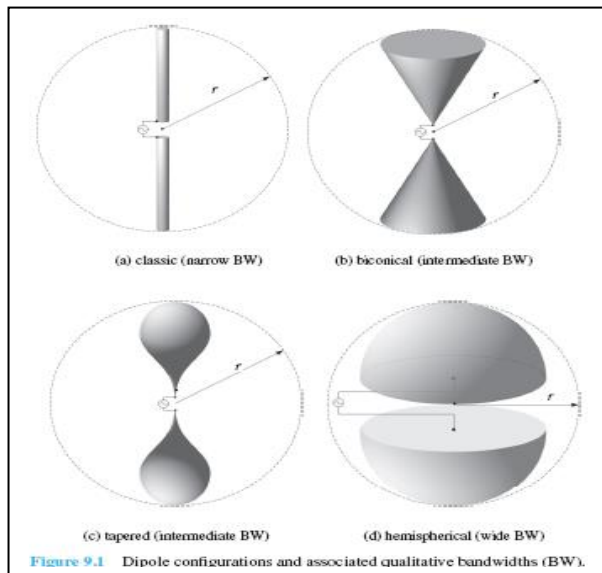


Figure 9.1 Dipole configurations and associated qualitative bandwidths (BW).

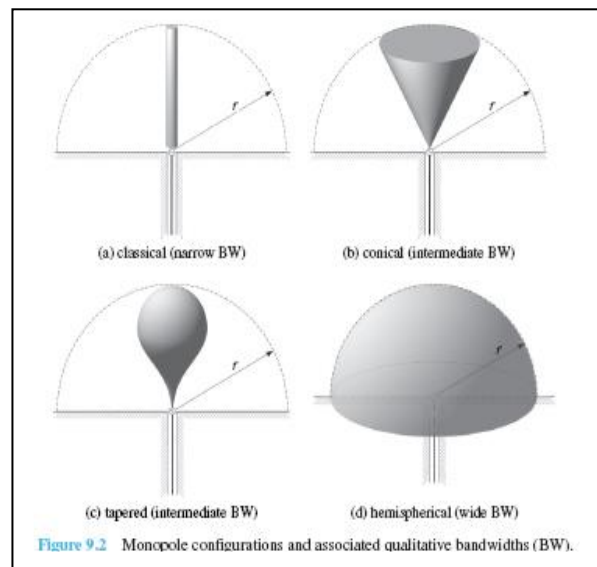


Figure 9.2 Monopole configurations and associated qualitative bandwidths (BW).

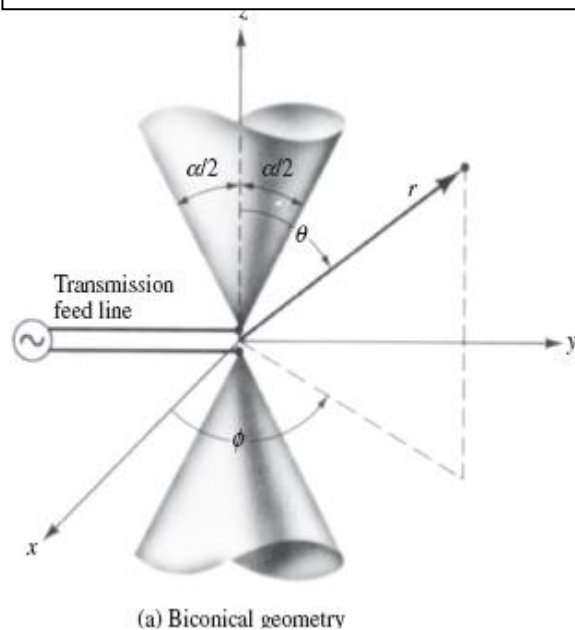
### 9.2 BICONICAL ANTENNA

The biconical antenna formed by placing two cones of infinite extent together, as shown in Fig. 9.3(a) is a simple design that can be used to achieve broadband characteristics. This can be thought to represent a uniformly tapered transmission line.

$$Z_c = Z_{in} = 120 \ln \left[ \cot \left( \frac{\alpha}{4} \right) \right]$$

$$R_r = \frac{2P_{rad}}{[I(0)]^2} = \frac{\eta}{\pi} \ln \left[ \cot \left( \frac{\alpha}{4} \right) \right]$$

If the cone is truncated, the results differs slightly



(a) Biconical geometry

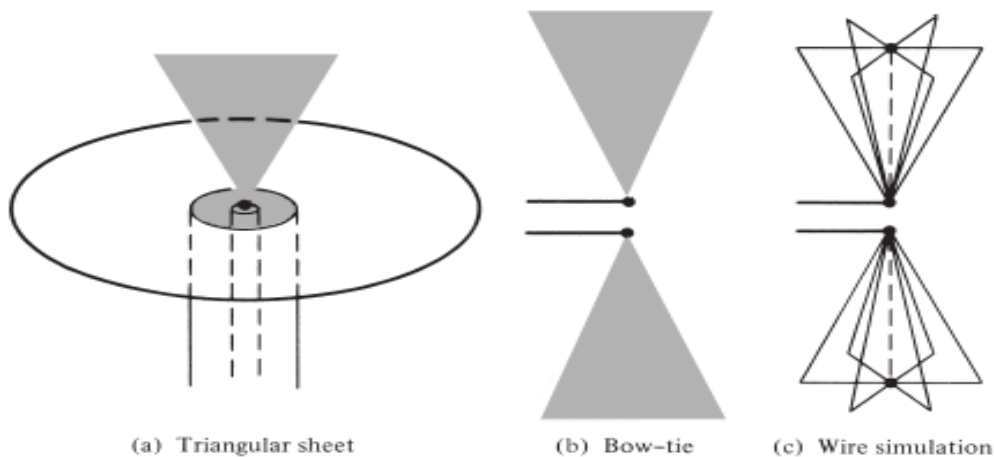


**Figure 9.6** Triangular sheet, bow-tie, and wire simulation of biconical antenna.

Geometrical approximations of the solid or shell conical unipole or biconical antenna are the triangular sheet and bow-tie antennas shown in Figs. 9.6(a, b), respectively, each fabricated from sheet metal. Each of these antennas can also be simulated by a wire along the periphery of its surface, which reduces significantly the weight and wind resistance of the structure. A biconical antenna of low-mass structures, multielement intersecting wire bow-ties were employed, see Fig. 9.6(c).

### 9.7 DISCONE AND CONICAL SKIRT MONOPOLE

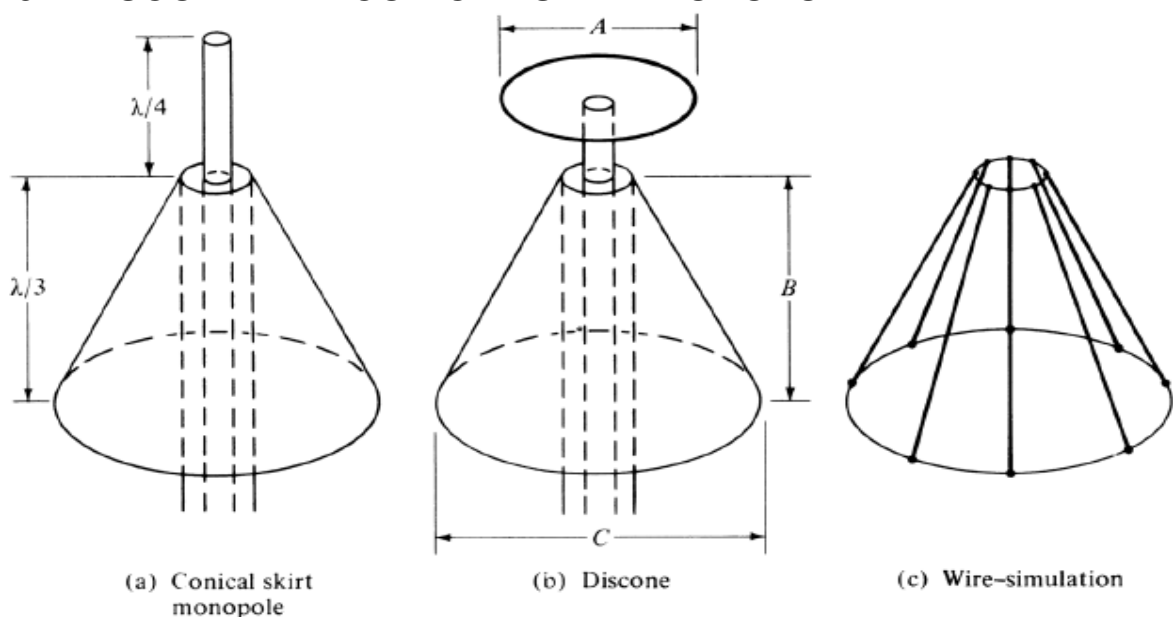


**Figure 9.24** Conical skirt monopole, discone, and wire-simulated cone surface.

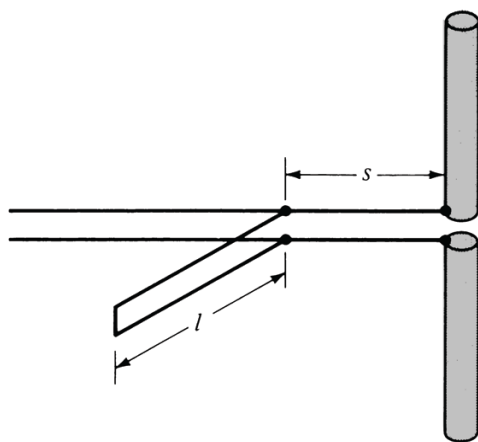
There are many variations to the basic geometrical configurations of cones and dipoles, to obtain broadband characteristics. Two other common radiators are the conical skirt monopole and the discone antenna shown in Figs. 9.24(a) and (b), respectively. For each antenna, the overall pattern is essentially the same as that of a linear dipole of length  $l < \lambda$  (i.e., a solid of revolution formed by the rotation of a figure-

eight) whereas in the horizontal (azimuthal) plane it is nearly omnidirectional. The polarization of each is vertical. Each antenna because of its simple mechanical design, ease of installation, and attractive broadband characteristics has wide applications in the VHF (30–300 MHz) and UHF (300 MHz–3 GHz) spectrum for broadcast, television, and communication applications.

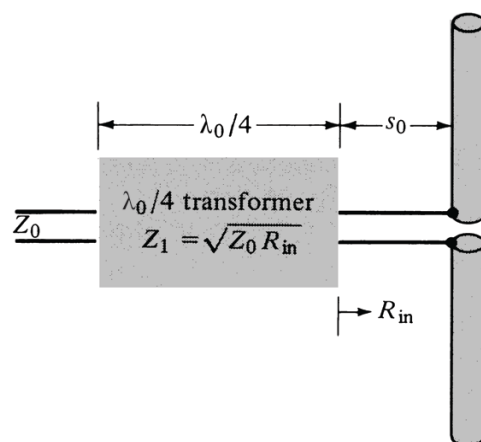
The discone antenna is formed by a disk and a cone. The disk is attached to the center conductor of the coaxial feed line, and it is perpendicular to its axis. The cone is connected at its apex to the outer shield of the coaxial line. In general, the impedance and pattern variations of a discone as a function of frequency are much less severe than those of a dipole of fixed length  $l$ . The frequency response is similar to a high-pass filter. Below an effective cutoff frequency it becomes inefficient, and it produces severe standing waves in the feed line. At cutoff, the slant height of the cone is approximately  $\lambda/4$ .

### 9.8 MATCHING TECHNIQUES

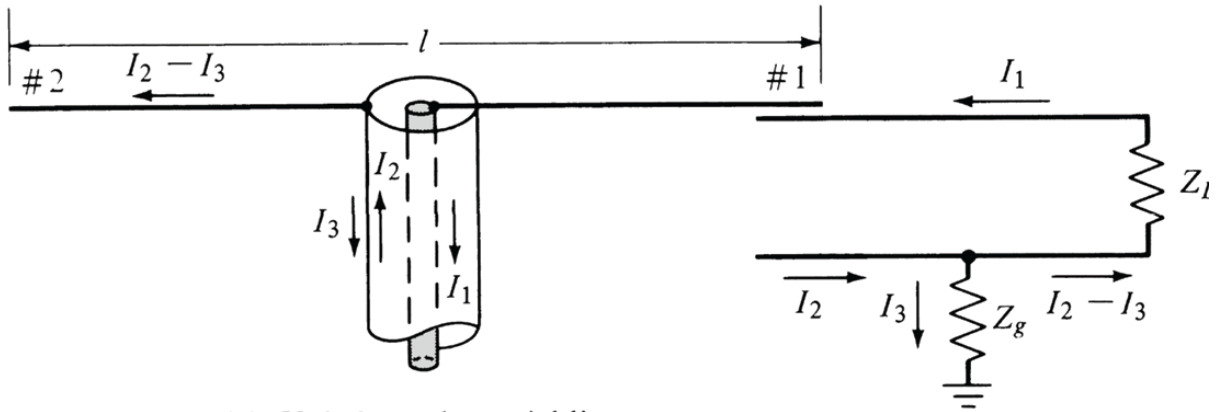
The operation of an antenna system over a frequency range is not completely dependent upon the frequency response of the antenna element itself but rather on the frequency characteristics of the transmission line–antenna element combination. The characteristic impedance of the transmission line is usually real whereas that of the antenna element is complex. Also the variation of each as a function of frequency is not the same. Thus efficient coupling-matching networks must be designed which attempt to couple-match the characteristics of the two devices over the desired frequency range.



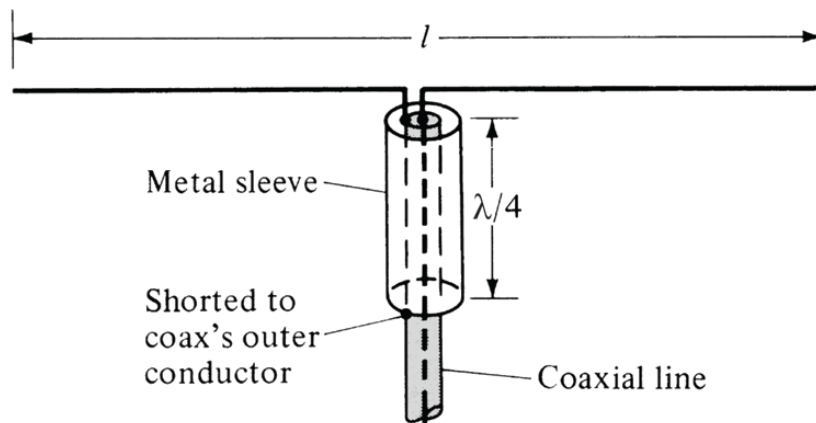
(a) Shunt matching



(b)  $\lambda_0/4$  transformer



(a) Unbalanced coaxial line



(b) Bazooka balun (1 : 1)

### Frequency Independent Antennas

Antenna characteristics such as impedance, pattern, polarization, and so forth, are invariant to a change of the physical size if a similar change is also made in the operating frequency or  $\lambda$ . For example, if *all* the physical dimensions are *reduced* by a factor of two, the performance of the antenna will remain unchanged if the operating frequency is *increased* by a factor of two. In other words, the performance is invariant if the electrical dimensions (size/ $\lambda$ ) remain unchanged. If the shape of the antenna were completely specified by angles, its performance would have to be independent of frequency. The infinite biconical dipole is one such structure.

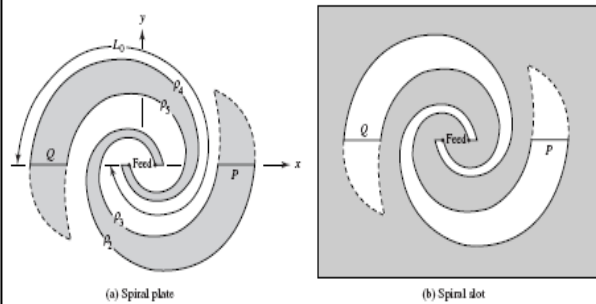


FIGURE 11.2 Spiral plate and slot antennas.

To make infinite structures more practical, the designs usually require that the current on the structure decrease with distance away from the input terminals. After a certain point the current is negligible, and the structure beyond that point to infinity can be truncated and removed. The lower cutoff frequency is that for which the current at the point of truncation becomes negligible. The upper cutoff is limited to

frequencies for which the dimensions of the feed transmission line cease to look like a “point” (usually about  $\lambda/8$  where  $\lambda$  is the wavelength at the highest desirable frequency). Practical bandwidths are on the order of about 40:1. Even higher ratios (i.e., 1,000:1) can be achieved in antenna design but they are not necessary, since they would far exceed the bandwidths of receivers and transmitters.

**Planar Spiral**

Has the form of wire or strip in the shape of two spirals as shown in Fig. 11.1.

**Log-Periodic antennas**

All the dimensions of the log-periodic array increase logarithmically as defined by the inverse of the geometric ratio  $\tau$

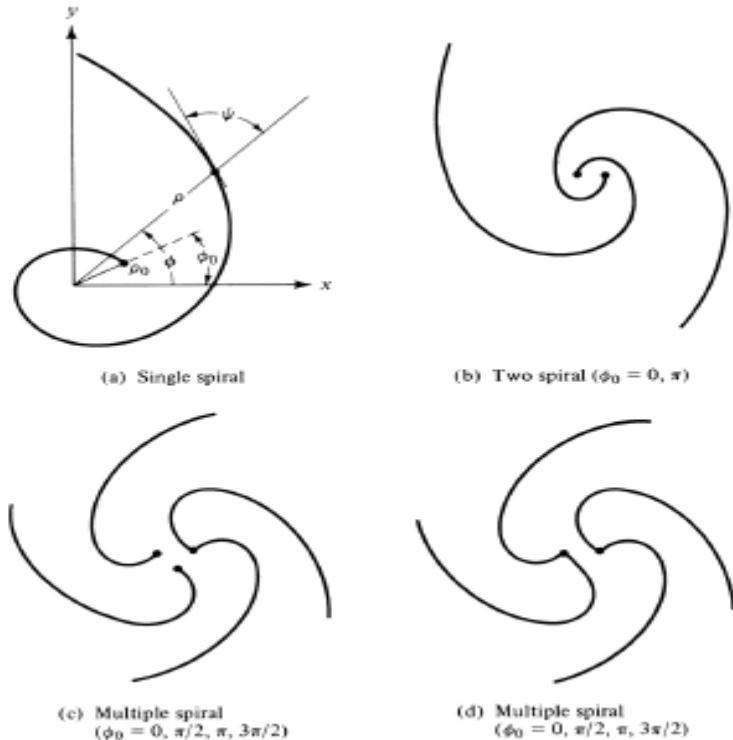
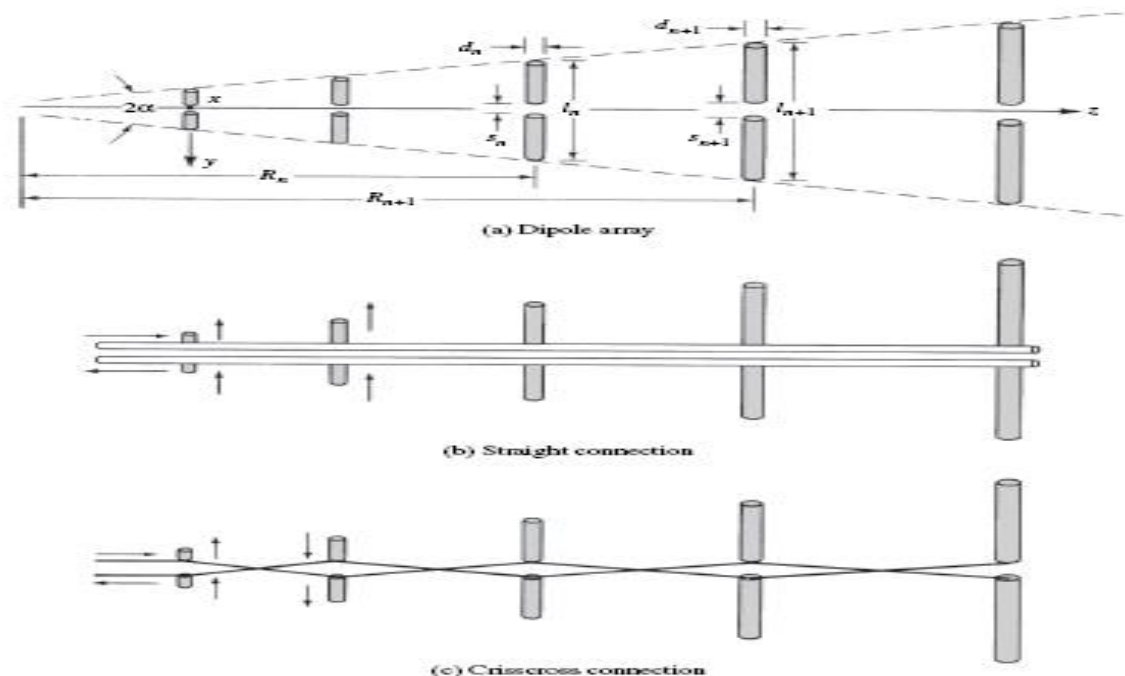
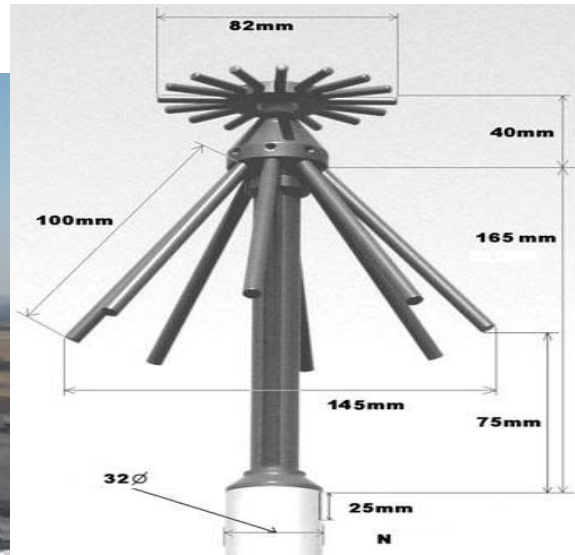


Figure 11.1 Spiral wire antennas.



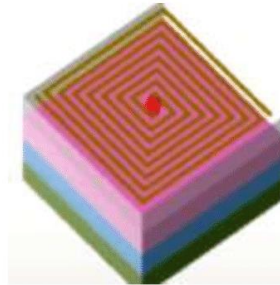
$$\frac{1}{\tau} = \frac{l_2}{l_1} = \frac{l_{n+1}}{l_n} = \frac{R_2}{R_1} = \frac{R_{n+1}}{R_n} = \frac{d_2}{d_1} = \frac{d_{n+1}}{d_n} = \frac{s_2}{s_1} = \frac{s_{n+1}}{s_n}$$



Discone Antennas; Continuous surface (left), rods (right).



(a) Log periodic Spiral



(b) Square Spiral



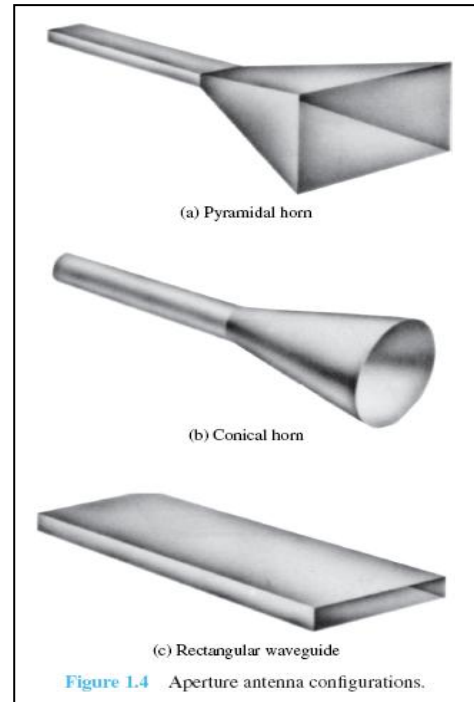
(c) Archimedian Spiral (2 arm)



(d) Archimedian Spiral (4 arm)



Aperture antennas are most common at microwave frequencies. The various geometrical configurations of an aperture antenna with some of the most popular ones are shown in Fig.1.4. They may take the form of a waveguide or a horn whose aperture may be square, rectangular, circular, elliptical, or any other configuration. Aperture antennas are very practical for space applications, because they can be flush mounted on the surface of the spacecraft or aircraft. Their opening can be covered with a dielectric material to protect them from environmental conditions. This type of mounting does not disturb the aerodynamic profile of the craft, which in high-speed applications is critical.



## 12.5 RECTANGULAR APERTURES

In practice, the rectangular aperture is probably the most common microwave antenna. Because of its configuration, the rectangular coordinate system is the most convenient system to express the fields at the aperture and to perform the integration. Shown in Fig. 12.6 are the three most common and convenient coordinate positions used for the solution of an aperture antenna. In Fig. 12.6(a) the aperture lies on the  $y$ - $z$  plane, in Fig. 12.6(b) on the  $x$ - $z$  plane, and in Fig. 12.6(c) on the  $x$ - $y$  plane. For a given field distribution, the analytical forms for the fields for each of the arrangements are not the same. However the computed values will be the same, since the physical problem is identical in all cases.

$$R \simeq r - r' \cos \psi \quad \text{for phase variations} \quad (12-5a)$$

$$R \simeq r \quad \text{for amplitude variations} \quad (12-5b)$$

The differential paths take the form of

$$\begin{aligned} r' \cos \psi &= \mathbf{r}' \cdot \hat{\mathbf{a}}_r = (\hat{\mathbf{a}}_y y' + \hat{\mathbf{a}}_z z') \cdot (\hat{\mathbf{a}}_x \sin \theta \cos \phi + \hat{\mathbf{a}}_y \sin \theta \sin \phi + \hat{\mathbf{a}}_z \cos \theta) \\ &= y' \sin \theta \sin \phi + z' \cos \theta \quad \text{[Figure 12.6(a)]} \end{aligned} \quad (12-15a)$$

$$\begin{aligned} r' \cos \psi &= \mathbf{r}' \cdot \hat{\mathbf{a}}_r = (\hat{\mathbf{a}}_x x' + \hat{\mathbf{a}}_z z') \cdot (\hat{\mathbf{a}}_x \sin \theta \cos \phi + \hat{\mathbf{a}}_y \sin \theta \sin \phi + \hat{\mathbf{a}}_z \cos \theta) \\ &= x' \sin \theta \cos \phi + z' \cos \theta \quad \text{[Figure 12.6(b)]} \end{aligned} \quad (12-15b)$$

$$\begin{aligned} r' \cos \psi &= \mathbf{r}' \cdot \hat{\mathbf{a}}_r = (\hat{\mathbf{a}}_x x' + \hat{\mathbf{a}}_y y') \cdot (\hat{\mathbf{a}}_x \sin \theta \cos \phi + \hat{\mathbf{a}}_y \sin \theta \sin \phi + \hat{\mathbf{a}}_z \cos \theta) \\ &= x' \sin \theta \cos \phi + y' \sin \theta \sin \phi \quad \text{[Figure 12.6(c)]} \end{aligned} \quad (12-15c)$$

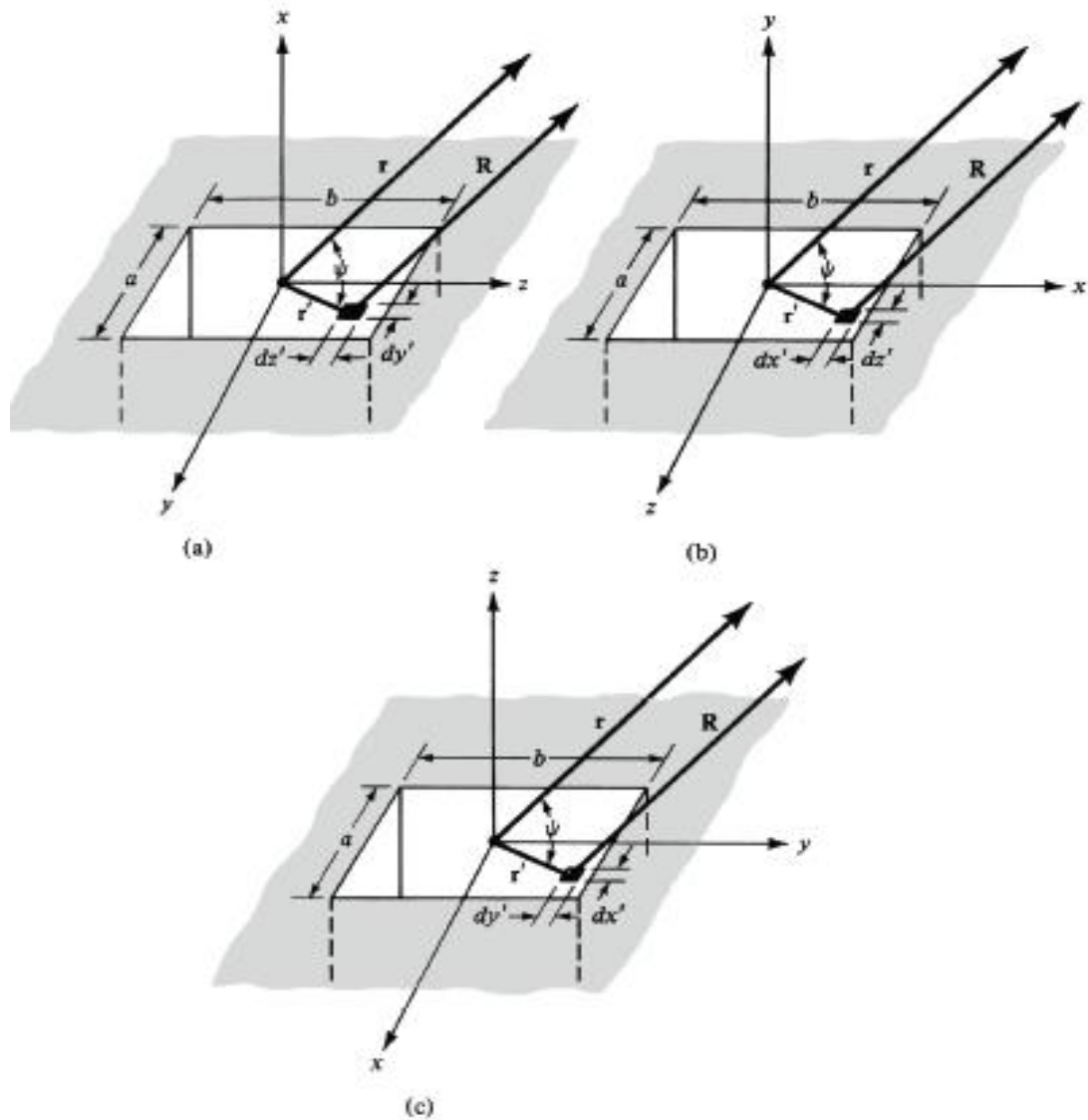


**Figure 12.6** Rectangular aperture positions for antenna system analysis.

and the differential areas are represented by

$$ds' = dy' dz' \quad [\text{Figure 12.6(a)}] \quad (12-16a)$$

$$ds' = dx' dz' \quad [\text{Figure 12.6(b)}] \quad (12-16b)$$

$$ds' = dx' dy' \quad [\text{Figure 12.6(c)}] \quad (12-16c)$$

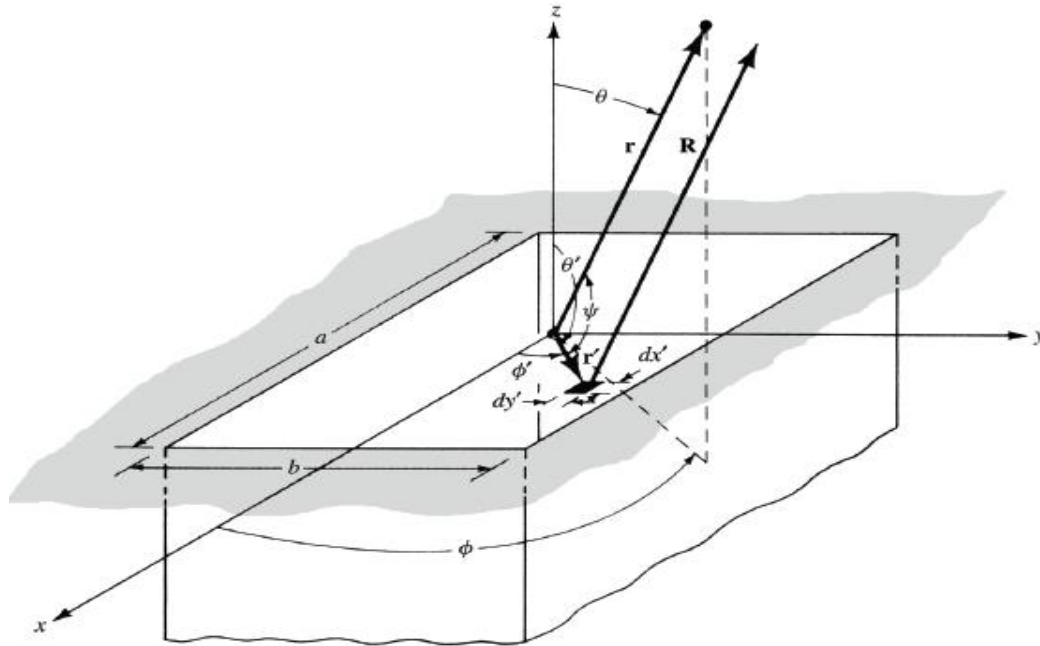


Figure 12.7 Rectangular aperture on an infinite electric ground plane.

### 12.5.1 Uniform Distribution on an Infinite Ground Plane

A rectangular aperture mounted on an infinite ground plane is shown in Fig. 12.7. To reduce the mathematical complexities, initially the field over the opening is assumed to be constant and given by

$$\mathbf{E}_a = \hat{\mathbf{a}}_y E_0 \quad -a/2 \leq x' \leq a/2, \quad -b/2 \leq y' \leq b/2 \quad (12-17)$$

where  $E_0$  is a constant. The task is to find the fields radiated by it, the pattern beamwidths, the side lobe levels of the pattern, and the directivity.

#### **B. Radiation Fields: Element and Space Factors**

The far-zone fields radiated by the aperture of Fig. 12.7 can be found by following the derivations in the text book *ANTENNA THEORY, ANALYSIS & DESIGN* 4th Ed. 2016 / Constantine A. Balanis

For the problem in Fig. 12.7, the  $E$ -plane pattern is on the  $y$ - $z$  plane ( $\phi = \pi/2$ ) and the  $H$ -plane is on the  $x$ - $z$  plane ( $\phi = 0$ ). Thus

#### **E-Plane ( $\phi = \pi/2$ )**

$$E_r = E_\phi = 0 \quad (12-24a)$$

$$E_\theta = j \frac{abkE_0 e^{-jkr}}{2\pi r} \left[ \frac{\sin\left(\frac{kb}{2} \sin\theta\right)}{\frac{kb}{2} \sin\theta} \right] \quad (12-24b)$$

#### **H-Plane ( $\phi=0$ )**

$$E_r = E_\theta = 0 \quad (12-25a)$$

$$E_\phi = j \frac{abkE_0 e^{-jkr}}{2\pi r} \left\{ \cos\theta \left[ \frac{\sin\left(\frac{ka}{2} \sin\theta\right)}{\frac{ka}{2} \sin\theta} \right] \right\} \quad (12-25b)$$

To demonstrate the techniques, three-dimensional patterns have been plotted in Figs. 12.8 and 12.9. The dimensions of the aperture are indicated in each figure. Multiple lobes appear, because the dimensions of the aperture are greater than one wavelength. The number of lobes increases as the dimensions increase. For the aperture whose dimensions are  $a = 3\lambda$  and  $b = 2\lambda$  (Fig. 12.8), there are a total of five lobes in the principal  $H$ -plane and three lobes in the principal  $E$ -plane. The pattern in the  $H$ -plane is only a function of the dimension  $a$  whereas that in the  $E$ -plane is only influenced by  $b$ . In the  $E$ -plane, the side lobe formed on each side of the major lobe is a result of  $\lambda < b \leq 2\lambda$ . In the  $H$ -plane, the first minor lobe on each side of the major lobe is formed when  $\lambda < a \leq 2\lambda$  and the second side lobe when  $2\lambda < a \leq 3\lambda$ . Additional lobes are formed when one or both of the aperture dimensions increase. This is illustrated in Fig. 12.9 for an aperture with  $a = b = 3\lambda$ .

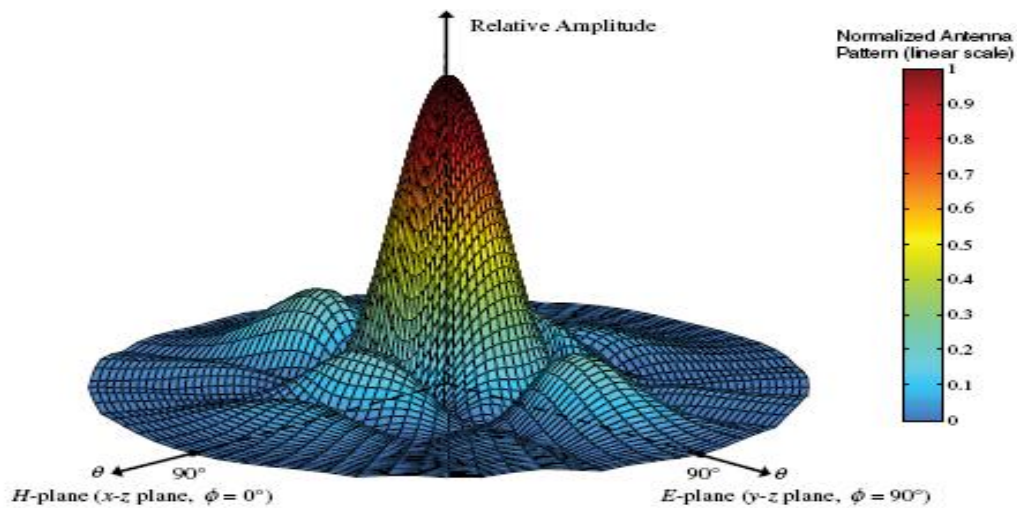


**Figure 12.8** Three-dimensional field pattern of a constant field rectangular aperture mounted on an infinite ground plane ( $a = 3\lambda, b = 2\lambda$ ).

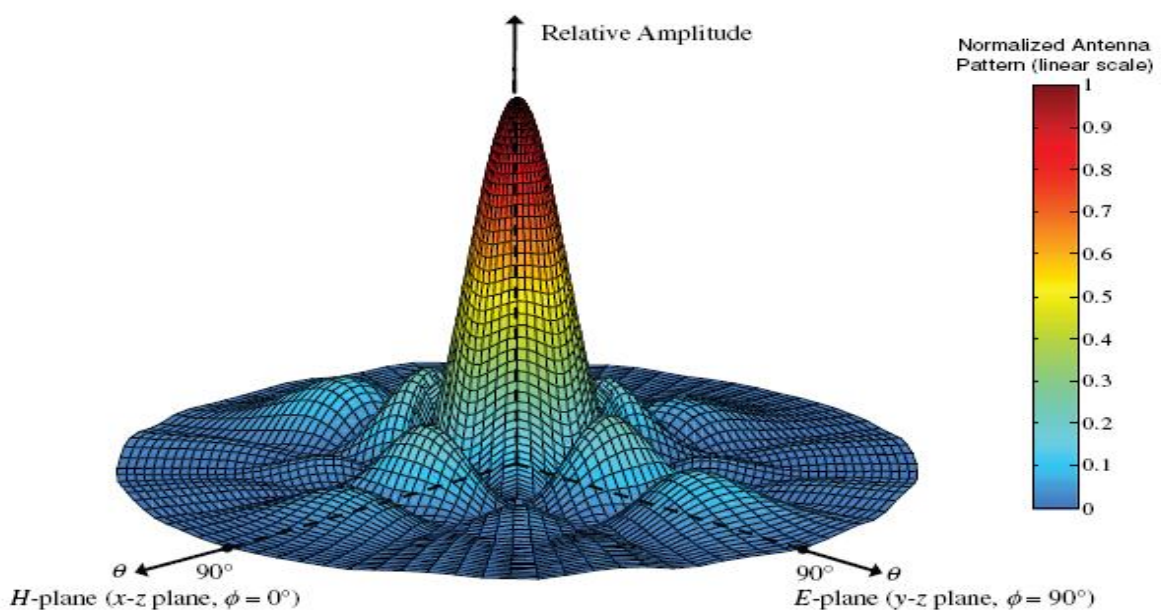


**Figure 12.9** Three-dimensional field pattern of a constant field square aperture mounted on an infinite ground plane ( $a = b = 3\lambda$ ).

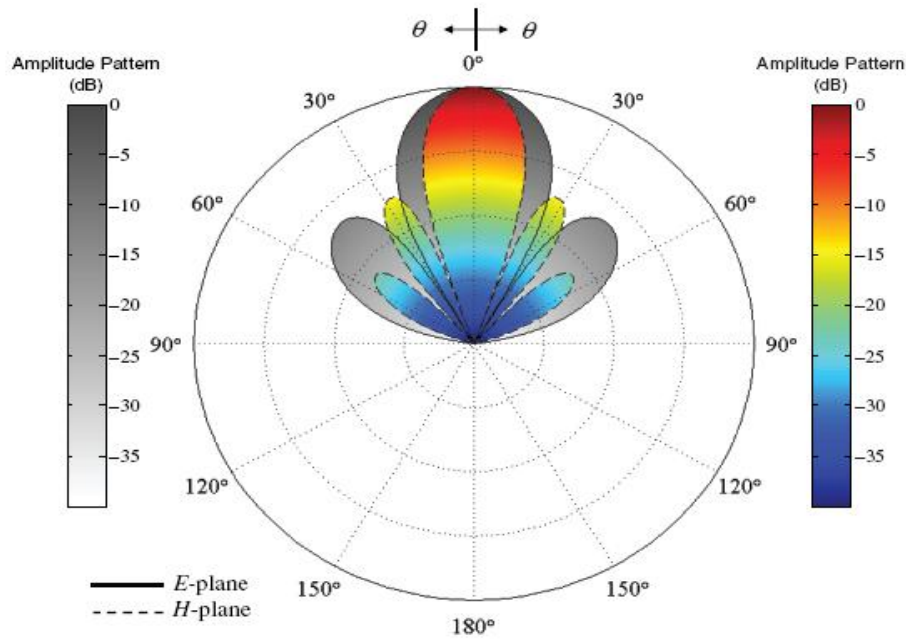


Figure 12.10 *E*- and *H*-plane amplitude patterns for uniform distribution aperture mounted on an infinite ground plane ( $a = 3\lambda, b = 2\lambda$ ).

The two-dimensional principal plane patterns for the aperture with  $a = 3\lambda$ ,  $b = 2\lambda$  are shown in Fig.12.10. For this, and for all other size apertures mounted on an infinite ground plane, the *H*-plane patterns along the ground plane vanish. This is dictated by the boundary conditions. The *E*-plane patterns, in general, do not have to vanish along the ground plane, unless the dimension of the aperture in that plane (in this case  $b$ ) is a multiple of a wavelength.

### C. Beamwidths

For the *E*-plane pattern given by (12-24b), the maximum radiation is directed along the  $z$ -axis ( $\theta = 0$ ). The nulls (zeros) occur when

$$\frac{kb}{2} \sin \theta|_{\theta=\theta_n} = n\pi, \quad n = 1, 2, 3, \dots \quad (12-26)$$

Or the angles at

$$\begin{aligned} \theta_n &= \sin^{-1} \left( \frac{2n\pi}{kb} \right) = \sin^{-1} \left( \frac{n\lambda}{b} \right) \text{ rad} \\ &= 57.3 \sin^{-1} \left( \frac{n\lambda}{b} \right) \text{ degrees}, \quad n = 1, 2, 3, \dots \end{aligned} \quad (12-26a)$$

If  $b \gg n\lambda$ , (12-26a) reduces approximately to

$$\theta_n \simeq \frac{n\lambda}{b} \text{ rad} = 57.3 \left( \frac{n\lambda}{b} \right) \text{ degrees}, \quad n = 1, 2, 3, \dots \quad (12-26b)$$

The total *beamwidth between nulls* is given by

$$\begin{aligned} \Theta_n &= 2\theta_n = 2 \sin^{-1} \left( \frac{n\lambda}{b} \right) \text{ rad} \\ &= 114.6 \sin^{-1} \left( \frac{n\lambda}{b} \right) \text{ degrees}, \quad n = 1, 2, 3, \dots \end{aligned} \quad (12-27)$$

or approximately (for large apertures,  $b \gg n\lambda$ ) by

$$\Theta_n \simeq \frac{2n\lambda}{b} \text{ rad} = 114.6 \left( \frac{n\lambda}{b} \right) \text{ degrees}, \quad n = 1, 2, 3, \dots \quad (12-27a)$$

The *first-null beamwidth* (FNBW) is obtained by letting  $n = 1$ .

The half-power point occurs when (see Appendix I)

$$\frac{kb}{2} \sin \theta |_{\theta=\theta_h} = 1.391 \quad (12-28)$$

or at an angle of

$$\begin{aligned} \theta_h &= \sin^{-1} \left( \frac{2.782}{kb} \right) = \sin^{-1} \left( \frac{0.443\lambda}{b} \right) \text{ rad} \\ &= 57.3 \sin^{-1} \left( \frac{0.443\lambda}{b} \right) \text{ degrees} \end{aligned} \quad (12-28a)$$

If  $b \gg 0.443\lambda$ , (12-28a) reduces approximately to

$$\theta_h \simeq \left( 0.443 \frac{\lambda}{b} \right) \text{ rad} = 25.38 \left( \frac{\lambda}{b} \right) \text{ degrees} \quad (12-28b)$$

Thus the total *half-power beamwidth* (HPBW) is given by

$$\Theta_h = 2\theta_h = 2 \sin^{-1} \left( \frac{0.443\lambda}{b} \right) \text{ rad} = 114.6 \sin^{-1} \left( \frac{0.443\lambda}{b} \right) \text{ degrees} \quad (12-29)$$

or approximately (when  $b \gg 0.443\lambda$ ) by

$$\Theta_h \simeq \left( 0.886 \frac{\lambda}{b} \right) \text{ rad} = 50.8 \left( \frac{\lambda}{b} \right) \text{ degrees} \quad (12-29a)$$

The maximum of the first side lobe occurs when (see Appendix I)

$$\theta_s \simeq 1.43 \left( \frac{\lambda}{b} \right) \text{ rad} = 81.9 \left( \frac{\lambda}{b} \right) \text{ degrees} \quad (12-30b)$$

#### **D. Side Lobe Level**

The maximum of (12-24b) at the first side lobe is given by (see Appendix I)

$$|E_\theta(\theta = \theta_s)| = \left| \frac{\sin(4.494)}{4.494} \right| = 0.217 = -13.26 \text{ dB} \quad (12-31)$$

A similar procedure can be followed to find the nulls, 3-dB points, beamwidth between nulls and 3-dB points, angle where the maximum of first side lobe occurs, and its magnitude at that point for the *H*-plane pattern of (12-25b). A comparison between the *E*- and *H*-plane patterns of (12-24b) and (12-25b) shows that they are similar in form except for the additional  $\cos \theta$  term that appears in (12-25b). An examination of the terms in (12-25b) reveals that the  $\cos \theta$  term is a much slower varying

function than the  $\sin(ka \sin \theta/2)/(ka \sin \theta/2)$  term, especially when  $a$  is large.

### E. Directivity

The directivity for the aperture can be found using (12-23a)–(12-23c), (12-13)–(12-13a), and (2-19)–(2-22). The analytical details using this procedure, especially the integration to compute the radiated power ( $P_{\text{rad}}$ ), are more cumbersome.

Because the aperture is mounted on an infinite ground plane, an alternate and much simpler method can be used to compute the radiated power. The average power density is first formed using the fields at the aperture, and it is then integrated over the physical bounds of the opening. The integration is confined to the physical bounds of the opening. Using Fig.12.7 and assuming that the magnetic field at the aperture is given by

$$\mathbf{H}_a = -\hat{\mathbf{a}}_x \frac{E_0}{\eta} \quad (12-34)$$

where  $\eta$  is the intrinsic impedance, the radiated power reduces to

$$P_{\text{rad}} = \iint_S \mathbf{W}_{\text{av}} \cdot d\mathbf{s} = \frac{|E_0|^2}{2\eta} \iint_{S_a} ds = ab \frac{|E_0|^2}{2\eta} \quad (12-35)$$

The maximum radiation intensity ( $U_{\text{max}}$ ), using the fields of (12-23a)–(12-23b), occurs toward  $\theta = 0^\circ$  and it is equal to

$$E_r = 0 \quad (12-23a)$$

$$E_\theta = j \frac{abkE_0 e^{-jkr}}{2\pi r} \left[ \sin \phi \left( \frac{\sin X}{X} \right) \left( \frac{\sin Y}{Y} \right) \right] \quad (12-23b)$$

$$U_{\text{max}} = \left( \frac{ab}{\lambda} \right)^2 \frac{|E_0|^2}{2\eta} \quad (12-36)$$

Thus the directivity is equal to

$$D_0 = \frac{4\pi U_{\text{max}}}{P_{\text{rad}}} = \frac{4\pi}{\lambda^2} ab = \frac{4\pi}{\lambda^2} A_p = \frac{4\pi}{\lambda^2} A_{em} \quad (12-37)$$

where

$A_p$  = physical area of the aperture

$A_{em}$  = maximum effective area of the aperture

Using the definition of (2-110), it is shown that *the physical and maximum effective areas of a constant distribution aperture are equal.*

The beamwidths, side lobe levels, and directivity of this and other apertures are summarized in Table 12.1.

TABLE 12.1 Equivalents, Fields, Beamwidths, Side Lobe Levels, and Directivities of Rectangular Apertures

	Uniform Distribution on Aperture on Ground Plane	Uniform Distribution Aperture in Free-Space	TE <sub>10</sub> -Mode Distribution Aperture on Ground Plane
Aperture distribution of tangential components (analytical)	$E_x = \hat{a}_y E_0 \begin{cases} -a/2 \leq x \leq a/2 \\ -b/2 \leq y \leq b/2 \end{cases}$	$E_x = \hat{a}_y E_0 \begin{cases} -a/2 \leq x \leq a/2 \\ -b/2 \leq y \leq b/2 \end{cases}$ $H_x = -\hat{a}_y \frac{E_0}{\eta}$	$E_x = \hat{a}_y E_0 \cos\left(\frac{\pi x}{a}\right) \begin{cases} -a/2 \leq x \leq a/2 \\ -b/2 \leq y \leq b/2 \end{cases}$
Aperture distribution of tangential components (graphical)			
Equivalent	$M_x = \begin{cases} -2\hat{n} \times E_x & -a/2 \leq x \leq a/2 \\ 0 & -b/2 \leq y \leq b/2 \\ & \text{elsewhere} \end{cases}$ $J_x = 0 \quad \text{everywhere}$	$M_x = -\hat{n} \times E_x \begin{cases} -a/2 \leq x \leq a/2 \\ -b/2 \leq y \leq b/2 \\ & \text{elsewhere} \end{cases}$ $J_x = \hat{n} \times H_x$ $M_y = J_y = 0 \quad \text{elsewhere}$	$M_x = \begin{cases} -2\hat{n} \times E_x & -a/2 \leq x \leq a/2 \\ 0 & -b/2 \leq y \leq b/2 \\ & \text{elsewhere} \end{cases}$ $J_x = 0 \quad \text{everywhere}$
Far-zone fields	$E_x = H_x = 0$ $E_\theta = C \sin\phi \frac{\sin X \sin Y}{X Y}$ $E_\phi = C \cos\theta \cos\phi \frac{\sin X \sin Y}{X Y}$ $H_\theta = -E_\phi/\eta$ $H_\phi = E_\theta/\eta$	$E_x = H_x = 0$ $E_\theta = \frac{C}{2} \sin\phi(1 + \cos\theta) \frac{\sin X \sin Y}{X Y}$ $E_\phi = \frac{C}{2} \cos\phi(1 + \cos\theta) \frac{\sin X \sin Y}{X Y}$ $H_\theta = -E_\phi/\eta$ $H_\phi = E_\theta/\eta$	$E_x = H_x = 0$ $E_\theta = -\frac{\pi}{2} C \sin\phi \frac{\cos X \sin Y}{(X)^2 - \left(\frac{\pi}{2}\right)^2}$ $E_\phi = -\frac{\pi}{2} C \cos\theta \cos\phi \frac{\cos X \sin Y}{(X)^2 - \left(\frac{\pi}{2}\right)^2}$ $H_\theta = -E_\phi/\eta$ $H_\phi = E_\theta/\eta$
	$X = \frac{ka}{2} \sin\theta \cos\phi$ $Y = \frac{kb}{2} \sin\theta \sin\phi$ $C = j \frac{abME_0 e^{-jkr}}{2\pi r}$		

Half-power beamwidth (degrees)	<i>E</i> -plane $b \gg \lambda$	$50.8 \frac{b}{\lambda}$	$50.8 \frac{b}{\lambda}$	$50.8 \frac{b}{\lambda}$
	<i>H</i> -plane $a \gg \lambda$	$50.8 \frac{a}{\lambda}$	$50.8 \frac{a}{\lambda}$	$50.8 \frac{a}{\lambda}$
First null beamwidth (degrees)	<i>E</i> -plane $b \gg \lambda$	$114.6 \frac{b}{\lambda}$	$114.6 \frac{b}{\lambda}$	$114.6 \frac{b}{\lambda}$
	<i>H</i> -plane $a \gg \lambda$	$114.6 \frac{a}{\lambda}$	$114.6 \frac{a}{\lambda}$	$171.9 \frac{a}{\lambda}$
First side lobe max. (to main max.) (dB)	<i>E</i> -plane	-13.26	-13.26	-13.26
	<i>H</i> -plane	-13.26 $a \gg \lambda$	-13.26 $a \gg \lambda$	-23 $a \gg \lambda$
Directivity $D_0$ (dimensionless)		$\frac{4\pi}{\lambda^2}(\text{area}) = 4\pi \left(\frac{ab}{\lambda^2}\right)$	$\frac{4\pi}{\lambda^2}(\text{area}) = 4\pi \left(\frac{ab}{\lambda^2}\right)$	$\frac{8}{\pi^2} \left[ 4\pi \left(\frac{ab}{\lambda^2}\right) \right] = 0.81 \left[ 4\pi \left(\frac{ab}{\lambda^2}\right) \right]$

### Example 12.2

A rectangular aperture with a constant field distribution, with  $a = 3\lambda$  and  $b = 2\lambda$ , is mounted on an infinite ground plane. Compute the

- FNBW in the  $E$ -plane
- HPBW in the  $E$ -plane
- FSLBW in the  $E$ -plane
- FSLMM in the  $E$ -plane
- directivity using (12-37)
- directivity using the computer program **Directivity** at the end of Chapter 2, the fields of (12-23a)–(12-23f), and the formulation of Section 12.4

### Solution

- a. Using (12-27)

$$\Theta_1 = 114.6 \sin^{-1}\left(\frac{1}{2}\right) = 114.6(0.524) = 60^\circ$$

- b. Using (12-29)

$$\Theta_h = 114.6 \sin^{-1}\left(\frac{0.443}{2}\right) = 114.6(0.223) = 25.6^\circ$$

- c. Using (12-30c)

$$\Theta_s = 2\theta_s = 114.6 \sin^{-1}\left(\frac{1.43}{2}\right) = 114.6(0.796) = 91.3^\circ$$

- d. Using (12-31)

$$|E_\theta|_{\theta=\theta_s} = 0.217 \simeq -13.26 \text{ dB}$$

- e. Using (12-37)

$$D_0 = 4\pi(3)(2) = 75.4 = 18.77 \text{ dB}$$

- f. Using the computer program at the end of Chapter 2

$$D_0 \simeq 80.4 = 19.05 \text{ dB}$$

The difference in directivity values using (12-37) and the computer program is not attributed to the accuracy of the numerical method. The main contributor is the aperture tangential magnetic field of (12-34), which was assumed to be related to the aperture tangential electric field by the intrinsic impedance. Although this is a good assumption for large size apertures, it is not exact. Therefore the directivity value computed using the computer program should be considered to be the more accurate.

## Lecture Notes-17 Aperture Antennas-2

### 12.5.3 TE<sub>10</sub>-Mode Distribution on an Infinite Ground Plane

In practice, a commonly used aperture antenna is that of a rectangular waveguide mounted on an infinite ground plane. At the opening, the field is usually approximated by the dominant TE<sub>10</sub>-mode. Thus

$$\mathbf{E}_a = \hat{\mathbf{a}}_y E_0 \cos\left(\frac{\pi}{a} x'\right) \begin{cases} -a/2 \leq x' \leq +a/2 \\ -b/2 \leq y' \leq +b/2 \end{cases} \quad (12-39)$$

#### A. Equivalent, Radiated Fields, Beamwidths, and Side Lobe Levels

Because the physical geometry of this antenna is identical to that of Fig.12.7, their equivalents and the procedure to analyze each one are identical.

The summary of its radiation characteristics is included in Table 12.1. The *E*-plane pattern of this aperture is identical in form (with the exception of a normalization factor) to the *E*-plane of the aperture of Section 12.5.1. This is expected, since the TE<sub>10</sub>-mode field distribution along the *E*-plane (*y*-*z* plane) is also a constant. That is not the case for the *H*-plane or at all other points removed from the principal planes. To demonstrate that, a three-dimensional pattern for the TE<sub>10</sub>-mode aperture with  $a = 3\lambda$ ,  $b = 2\lambda$  was computed and it is shown in Fig. 12.12. This pattern should be compared with that of Fig. 12.8.

The expressions for the beamwidths and side lobe level in the *E*-plane are identical to those given by (12-26)–(12-33). However those for the *H*-plane are more complex, and a simple procedure is not available. Computations for the HPBW, FNBW, FSLBW, FSLMM in the *E*- and *H*-planes were made, and they are shown graphically in Fig.12.13 and 12.14.

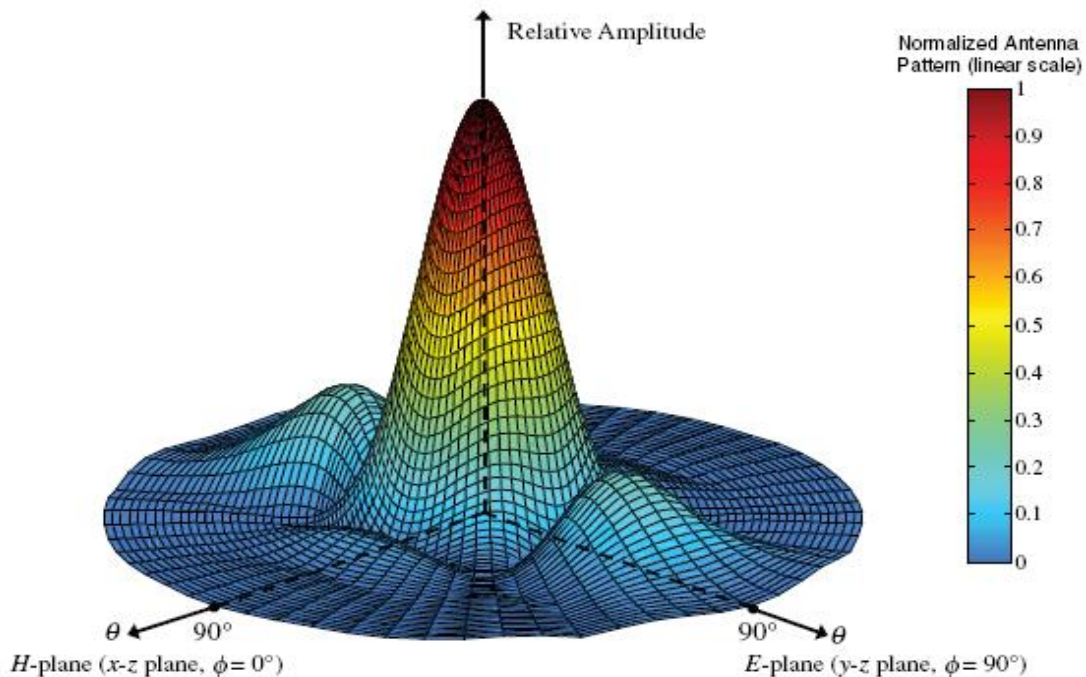


**Figure 12.12** Three-dimensional field pattern of a TE<sub>10</sub>-mode rectangular waveguide mounted on an infinite ground plane ( $a = 3\lambda$ ,  $b = 2\lambda$ ).

When the same aperture is not mounted on a ground plane, the far-zone fields do not have to be rederived but rather can be written by inspection. This is accomplished by introducing appropriately, in each of the field components ( $E_\theta$  and  $E_\phi$ ) of the fourth column of Table 12.1, a  $(1 + \cos \theta)/2$  factor, as is done for the fields of the two apertures in the second and third columns. This factor is appropriate when the  $z$ -axis is perpendicular to the plane of the aperture. Other similar factors will have to be used when either the  $x$ -axis or  $y$ -axis is perpendicular to the plane of the aperture.

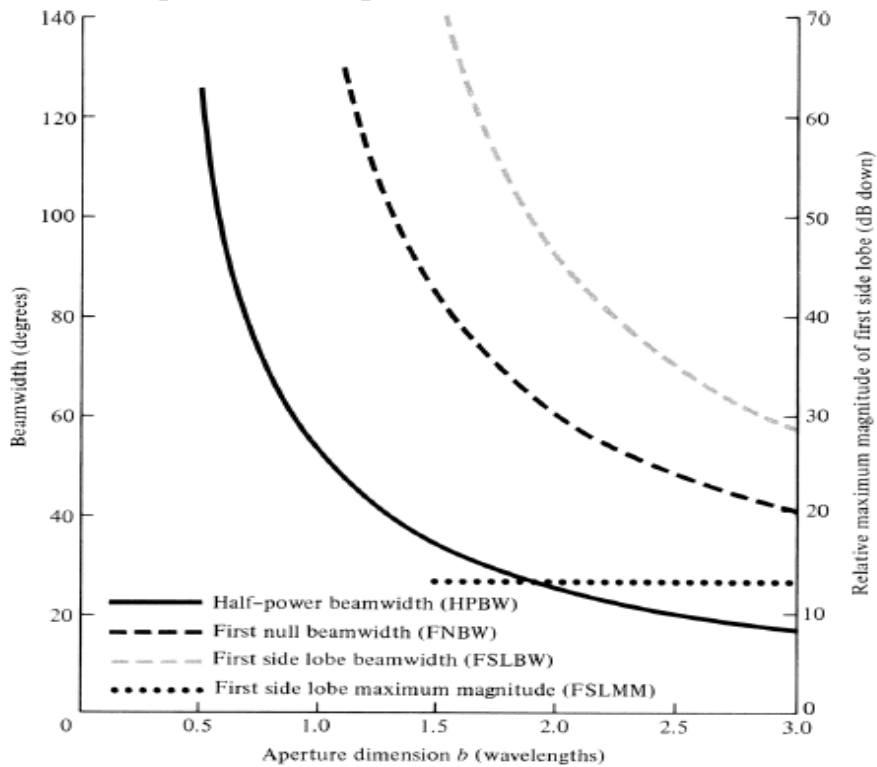


**Figure 12.13**  $E$ -plane beamwidths and first side lobe relative maximum magnitude for  $TE_{10}$ -mode rectangular waveguide mounted on an infinite ground plane.

### B. Directivity and Aperture Efficiency

The directivity of this aperture is found in the same manner as that of the uniform distribution aperture of Section 12.5.1. Using the aperture electric field of (12-39), and assuming that the aperture magnetic field is related to the electric field by the intrinsic impedance  $\eta$ , the radiated power can be written as

$$P_{\text{rad}} = \iint_S \mathbf{W}_{\text{av}} \cdot d\mathbf{s} = ab \frac{|E_0|^2}{4\eta} \quad (12-39a)$$

The maximum radiation intensity occurs at  $\theta = 0^\circ$ , and it is given by

$$U_{\text{max}} = \frac{8}{\pi^2} \left( \frac{ab}{\lambda} \right)^2 \frac{|E_0|^2}{4\eta} \quad (12-39b)$$

Thus the directivity is equal to

$$D_0 = \frac{8}{\pi^2} \left[ ab \left( \frac{4\pi}{\lambda^2} \right) \right] = 0.81 \left[ ab \left( \frac{4\pi}{\lambda^2} \right) \right] = 0.81 A_p \left( \frac{4\pi}{\lambda^2} \right) = A_{em} \left( \frac{4\pi}{\lambda^2} \right) \quad (12-39c)$$

In general, the maximum effective area  $A_{em}$  is related to the physical area  $A_p$  by

$$A_{em} = \varepsilon_{ap} A_p, \quad 0 \leq \varepsilon_{ap} \leq 1 \quad (12-40)$$

where  $\varepsilon_{ap}$  is the aperture efficiency. For this problem  $\varepsilon_{ap} = 8/\pi^2 \simeq 0.81$ . The aperture efficiency is a figure of merit which indicates how efficiently the physical area of the antenna is utilized. Typically, aperture antennas have aperture efficiencies from about 30% to 90%, horns from 35% to 80% (optimum gain horns have  $\varepsilon_{ap} \simeq 50\%$ ), and circular reflectors from 50% to 80%.

## 12.6 CIRCULAR APERTURES

A widely used microwave antenna is the circular aperture. One of the attractive features of this configuration is its simplicity in construction. In addition, closed form expressions for the fields of all the modes that can exist over the aperture can be obtained.

The procedure followed to determine the fields radiated by a circular aperture is identical to that of the rectangular, as summarized in Section 12.3. The primary differences lie in the formulation of the equivalent current densities ( $J_x, J_y, J_z, M_x, M_y, M_z$ ), the differential paths from the source to the observation point ( $r' \cos \psi$ ), and the differential area ( $ds'$ ). Before an example is considered, these differences will be reformulated for the circular aperture.

Because of the circular profile of the aperture, it is often convenient and desirable to adopt cylindrical coordinates for the solution of the fields. In most cases, therefore, the electric and magnetic field components over the circular opening will be known in cylindrical form; that is,  $E_\rho, E_\phi, E_z, H_\rho, H_\phi$ , and  $H_z$ . Thus the components of the equivalent current densities  $\mathbf{M}$ s and  $\mathbf{J}$ s would also be conveniently expressed in cylindrical form ( $M_\rho, M_\phi, M_z, J_\rho, J_\phi, J_z$ ). In addition, the required integration over the aperture to find  $N_\theta, N_\phi, L_\theta$ , and  $L_\phi$  of (12-12a)–(12-12d) should also be done in cylindrical coordinates. It is then desirable to reformulate  $r' \cos \psi$  and  $ds'$ , as given by (12-15a)–(12-16c).

The most convenient position for placing the aperture is that shown in Fig.12.16 (aperture on  $x$ - $y$  plane). The transformation between the rectangular and cylindrical components of  $\mathbf{J}_s$  is given by (see Appendix VII)

$$\begin{bmatrix} J_x \\ J_y \\ J_z \end{bmatrix} = \begin{bmatrix} \cos \phi' & -\sin \phi' & 0 \\ \sin \phi' & \cos \phi' & 0 \\ 0 & 0 & 1 \end{bmatrix} \begin{bmatrix} J_\rho \\ J_\phi \\ J_z \end{bmatrix} \quad (12-41a)$$

A similar transformation exists for the components of  $\mathbf{M}$ s. The rectangular and cylindrical coordinates are related by (see Appendix VII)

$$\begin{aligned} x' &= \rho' \cos \phi' \\ y' &= \rho' \sin \phi' \\ z' &= z' \end{aligned} \quad (12-41b)$$

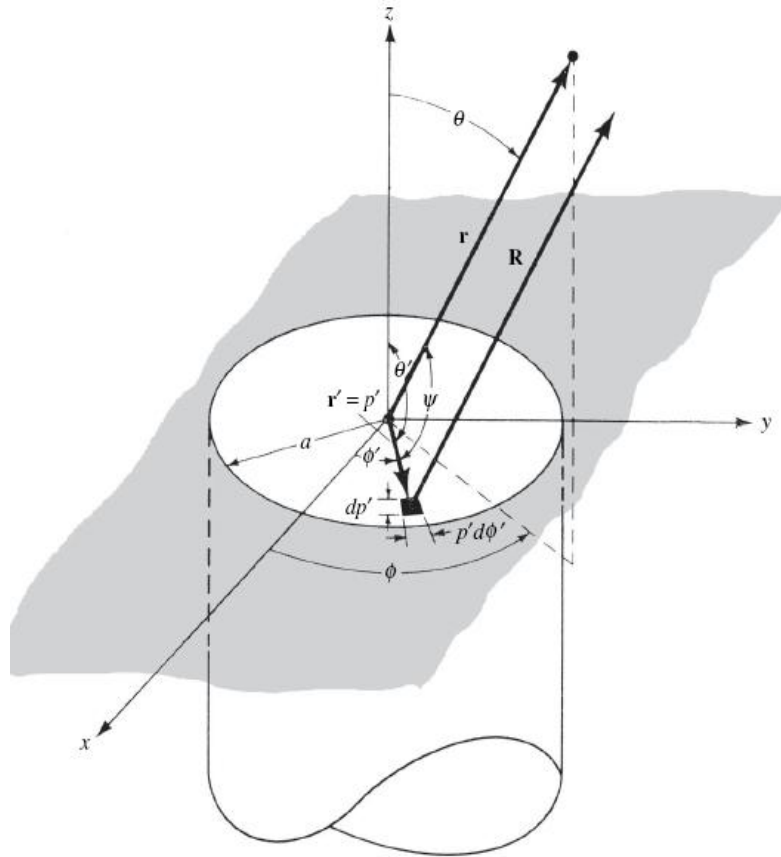


Figure 12.16 Circular aperture mounted on an infinite ground plane.

### 12.6.1 Uniform Distribution on an Infinite Ground Plane

To demonstrate the methods, the field radiated by a circular aperture mounted on an infinite ground plane will be formulated. To simplify the mathematical details, the field over the aperture is assumed to be constant and given by

$$\mathbf{E}_a = \hat{\mathbf{a}}_y E_0 \quad \rho' \leq a \quad (12-44)$$

where  $E_0$  is a constant.

The radiated fields are given by

$$E_r = 0 \quad (12-53a)$$

$$E_\theta = j \frac{ka^2 E_0 e^{-jkr}}{r} \left\{ \sin \phi \left[ \frac{J_1(ka \sin \theta)}{ka \sin \theta} \right] \right\} \quad (12-53b)$$

$$E_\phi = j \frac{ka^2 E_0 e^{-jkr}}{r} \left\{ \cos \theta \cos \phi \left[ \frac{J_1(ka \sin \theta)}{ka \sin \theta} \right] \right\} \quad (12-53c)$$

In the principal E- and H-planes, the electric field components simplify to

**E-Plane ( $\phi = \pi/2$ )**

$$E_r = E_\phi = 0 \quad (12-54a)$$

$$E_\theta = j \frac{ka^2 E_0 e^{-jkr}}{r} \left[ \frac{J_1(ka \sin \theta)}{ka \sin \theta} \right] \quad (12-54b)$$

**H-Plane ( $\phi = 0$ )**

$$E_r = E_\theta = 0 \quad (12-55a)$$

$$E_\phi = j \frac{ka^2 E_0 e^{-jkr}}{r} \left\{ \cos \theta \left[ \frac{J_1(ka \sin \theta)}{ka \sin \theta} \right] \right\} \quad (12-55b)$$

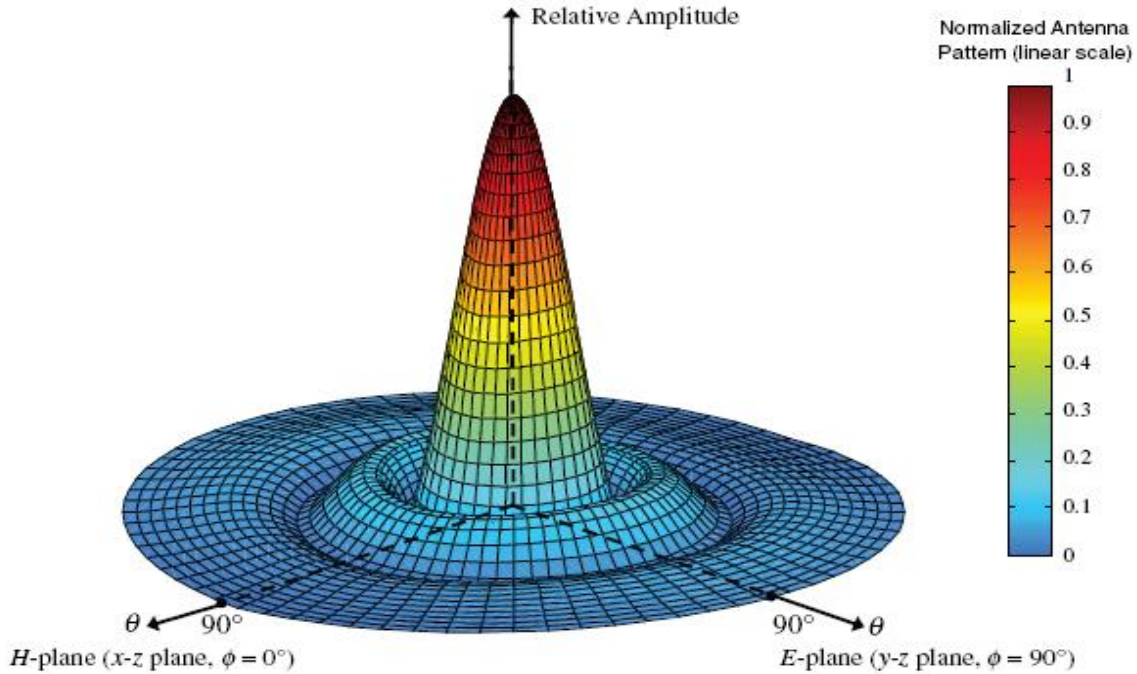


**Figure 12.17** Three-dimensional field pattern of a constant field circular aperture mounted on an infinite ground plane ( $a = 1.5\lambda$ ).

A three-dimensional pattern has been computed for the constant field circular aperture of  $a = 1.5\lambda$ , and it is shown in Fig. 12.17. The pattern of Fig.12.17 seems to be symmetrical. However closer observation, especially through the two-dimensional *E*- and *H*-plane patterns, will reveal that not to be the case. It does, however, possess characteristics that are almost symmetrical.

### **B. Beamwidth, Side Lobe Level, and Directivity**

Exact expressions for the beamwidths and side lobe levels cannot be obtained easily. However approximate expressions are available, and they are shown tabulated in Table 12.2. More exact data can be obtained by numerical methods.

**HPBW=29.2λ/a** degrees where *a* is the radius of the aperture

Since the field distribution over the aperture is constant, the directivity is given by

$$D_0 = \frac{4\pi}{\lambda^2} A_{em} = \frac{4\pi}{\lambda^2} A_p = \frac{4\pi}{\lambda^2} (\pi a^2) = \left( \frac{2\pi a}{\lambda} \right)^2 = \left( \frac{C}{\lambda} \right)^2 \quad (12-56)$$

since the maximum effective area  $A_{em}$  is equal to the physical area  $A_p$  of the aperture [as shown for the rectangular aperture in (12-37)].

A summary of the radiation parameters of this aperture is listed in Table 12.2.

### 12.6.2 TE<sub>11</sub>-Mode Distribution on an Infinite Ground Plane

A very practical antenna is a circular waveguide of radius  $a$  mounted on an infinite ground plane, as shown in Fig. 12.16. However, the field distribution over the aperture is usually that of the dominant TE<sub>11</sub>-mode for a circular waveguide given by

$$\left. \begin{aligned} E_\rho &= \frac{E_0}{\rho'} J_1 \left( \frac{\chi'_{11}}{a} \rho' \right) \sin \phi' \\ E_\phi &= E_0 \frac{\partial}{\partial \rho'} \left[ J_1 \left( \frac{\chi'_{11}}{a} \rho' \right) \right] \cos \phi' \\ E_z &= 0 \\ \chi'_{11} &= 1.841 \end{aligned} \right\} \quad (12-57)$$

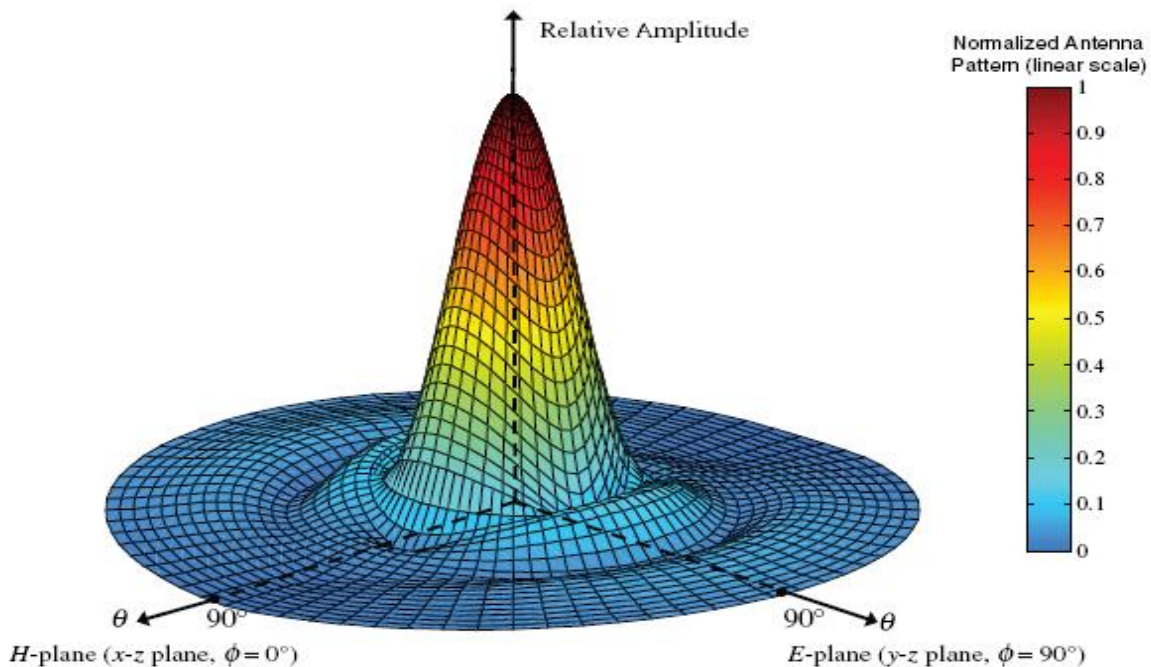


**Figure 12.18** Three-dimensional field pattern of a TE<sub>11</sub>-mode circular waveguide mounted on an infinite ground plane ( $a = 1.5\lambda$ ).

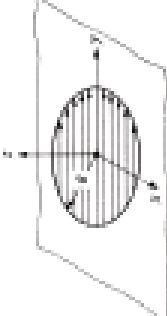
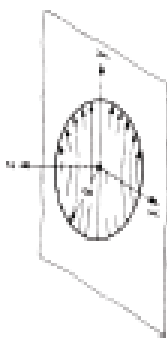
A summary of all the radiation characteristics is included in Table 12.2. When the same apertures of Table 12.2 are not mounted on a ground plane, the far-zone fields do not have to be rederived but rather can be written by inspection. This is accomplished by introducing appropriately, in each of the field components ( $E_\theta$  and  $E_\phi$ ) of the second and third columns of Table 12.2, a  $(1 + \cos \theta)/2$  factor, as was done for the fields of the two apertures in the second and third columns of Table 12.1.

**HPBW=29.2λ/a** degrees in the E-Plane

**HPBW=37 λ/a** degrees in the H-Plane

where  $a$  is the radius of the aperture.

TABLE 12.2 Equivalents, Fields, Beamwidths, Side Lobe Levels, and Directivities of Circular Apertures

	Uniform Distribution Aperture on Ground Plane	TE <sub>11</sub> -Mode Distribution Aperture on Ground Plane
Aperture distribution of tangential components (analytical)	$E_z = \hat{a}_y E_0 \quad \theta \leq \alpha$	$E_x = \hat{a}_x E_0 + \hat{a}_\phi E_\phi$ $E_y = E_0 J_1'(x'_{11} \rho/a) \sin \theta' / \rho \quad \theta' \leq \alpha$ $E_\phi = E_0 J_1'(x'_{11} \rho/a) \cos \theta' \quad x'_{11} = 1.841$ $r = \frac{\rho}{\sin \theta'}$
Aperture distribution of tangential components (graphical)		
Equivalent	$M_z = \begin{cases} -2\hat{a}_y \times E_0 & \theta \leq \alpha \\ 0 & \text{elsewhere} \end{cases}$ $J_z = 0 \quad \text{everywhere}$	$M_z = \begin{cases} -2\hat{a}_y \times E_0 & \theta' \leq \alpha \\ 0 & \text{elsewhere} \end{cases}$ $J_z = 0 \quad \text{everywhere}$
<i>Far-zone fields</i> $Z = ka \sin \theta$ $C_1 = j \frac{ka^2 E_0 e^{-jkr}}{r}$ $C_2 = j \frac{ka^2 E_0 J_1'(x'_{11}) e^{-jkr}}{r}$ $x'_{11} = 1.841$	$E_r = H_\theta = 0$ $E_\phi = jC_1 \sin \theta \frac{J_1(Z)}{Z}$ $E_\theta = jC_1 \cos \theta \cos \phi \frac{J_1(Z)}{Z}$ $H_\phi = -E_\theta / \eta$ $H_\theta = E_\phi / \eta$	$E_r = H_\theta = 0$ $E_\phi = C_2 \sin \theta \frac{J_1(Z)}{Z}$ $E_\theta = C_2 \cos \theta \cos \phi \frac{J_1'(Z)}{1 - (Z/x'_{11})^2}$ $H_\phi = -E_\theta / \eta$ $H_\theta = E_\phi / \eta$ $J_1'(Z) = J_0(Z) - J_1(Z)/Z$

Half-power beamwidth (degrees)	<i>E</i> -plane $a \gg \lambda$	$29.2 \frac{a}{\lambda}$	$29.2 \frac{a}{\lambda}$	$29.2 \frac{a}{\lambda}$
	<i>H</i> -plane $a \gg \lambda$	$29.2 \frac{a}{\lambda}$	$29.2 \frac{a}{\lambda}$	$27.0 \frac{a}{\lambda}$
First null beamwidth (degrees)	<i>E</i> -plane $a \gg \lambda$	$69.9 \frac{a}{\lambda}$	$69.9 \frac{a}{\lambda}$	$69.9 \frac{a}{\lambda}$
	<i>H</i> -plane $a \gg \lambda$	$69.9 \frac{a}{\lambda}$	$69.9 \frac{a}{\lambda}$	$98.0 \frac{a}{\lambda}$
First side lobe max. (to main max.) (dB)	<i>E</i> -plane	-17.6	-17.6	-17.6
	<i>H</i> -plane	-17.6	-17.6	-26.2
Directivity $D_0$ (dimensionless)		$\frac{4\pi}{\lambda^2}(\text{area}) = \frac{4\pi}{\lambda^2}(\pi a^2) = \left(\frac{2\pi a}{\lambda}\right)^2$		$0.836 \left(\frac{2\pi a}{\lambda}\right)^2 = 10.5\pi \left(\frac{a}{\lambda}\right)^2$

## 12.7 DESIGN CONSIDERATIONS

As is the case for arrays, aperture antennas can be designed to control their radiation characteristics. Typically the level of the minor lobes can be controlled by tapering the distribution across the aperture; the smoother the taper from the center of the aperture toward the edge, the lower the side lobe level and the larger the half-power beamwidth, and conversely. Therefore a very smooth taper, such as that represented by a binomial distribution or others, would result in very low side lobes but larger half-power beamwidths. In contrast, an abrupt distribution, such as that of uniform illumination, exhibits the smaller half-power beamwidth but the highest side lobe level (about - 13.5 dB). Therefore if it is desired to achieve simultaneously both a very low sidelobe level, as well as a small half-power beamwidth, a compromise has to be made. Typically an intermediate taper, such as that of a Tschebyscheff distribution or any other similar one, will have to be selected.

-----  
**12.15.** For the rectangular aperture of Section 12.5.1 with  $a = b = 3\lambda$ , compute the directivity using (12-37)

$$12-15. \quad a = b = 3\lambda \\ \text{Using (12-37), } D_o = \frac{4\pi}{\lambda^2} ab = 4\pi(3)^2 = 113.1 = 20.53 \text{ dB}$$

-----  
**12.28.** A uniform plane wave is incident upon an X-band rectangular waveguide, with dimensions of 2.286 cm and 1.016 cm, mounted on an infinite ground plane. Assuming the waveguide is operating in the dominant TE<sub>10</sub> mode (aperture efficiency=0.81), determine the maximum power that can be delivered to a matched load. The frequency is 10 GHz and the power density of the incident plane wave is  $10^{-4}$  watts/m<sup>2</sup>.

$$A_{em} = \frac{\lambda^2}{4\pi} \cdot D_o = \frac{\lambda^2}{4\pi} \left[ 0.81 \cdot a \cdot b \cdot \left( \frac{4\pi}{\lambda^2} \right) \right] = 0.81 ab$$

$$A_{em} = 0.81 \cdot (0.02286 \times 0.0106) = 0.81 \cdot (2.32257 \times 10^{-4}) \\ = 1.88 \times 10^{-4} \text{ m}^2$$

The maximum power that can be delivered to  
matched load

$$P_{max} = W_i \cdot A_{em} = (10^{-4} \text{ watts/m}^2) \cdot (1.88 \times 10^{-4} \text{ m}^2)$$

$$= 1.88 \times 10^{-8} \text{ watts} = 0.0188 \mu\text{Watts}$$

**12.26.** Two X-band (8.2–12.4 GHz) rectangular waveguides, each operating in the dominant TE<sub>10</sub>-mode, are used, respectively, as transmitting and receiving antennas in a long distance communication system. The dimensions of each waveguide are  $a = 2.286$  cm and  $b = 1.016$  cm and the center frequency of operation is 10 GHz. Assuming the waveguides are separated by 10 kilometers and they are positioned for maximum radiation and reception toward each other, and the radiated power is 1 watt, find the:

a- Incident power density at the receiving antenna

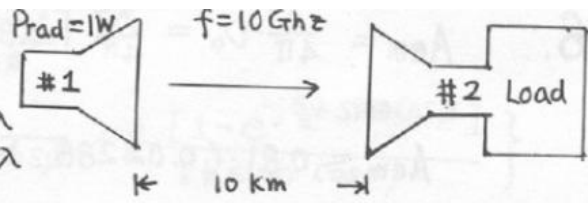
b- Maximum power that can be delivered to a matched load

Assume the antennas are lossless, are polarization matched, and each is mounted on an infinite ground plane

a.  $\lambda = \frac{3 \times 10^{10} \text{ cm/s}}{10 \times 10^9 \text{ Hz}} = 3 \text{ cm}$

$a = 0.9'' = 2.286 \text{ cm} = 0.762 \lambda$

$b = 0.4'' = 1.016 \text{ cm} = 0.339 \lambda$



Power density for isotropic source;

$$W_0 = \frac{P_{\text{rad}}}{4\pi R^2} = \frac{1 \text{ Watt}}{4\pi (10 \times 10^3)^2} = 7.96 \times 10^{-10} \text{ W/m}^2$$

Directivity from Table 12.1, 12.2.

$$D_0 = \frac{8}{\pi^2} \left[ \frac{4\pi}{\lambda^2} ab \right] = \frac{32}{\pi} (0.762)(0.339) = 2.63$$

Incident Power density

$$W_i = W_0 D_0 = (7.96 \times 10^{-10} \text{ W/m}^2)(2.63) \Rightarrow W_i = 2.09 \times 10^{-9} \text{ W/m}^2$$

b. The maximum power that can be delivered to a matched load.

$$A_{\text{em}} = \epsilon_{\text{ap}} A_p = 0.81 ab = 1.88 \times 10^{-4} \text{ m}^2$$

$$P_{\text{max}} = W_i A_{\text{em}} = (2.09 \times 10^{-9} \text{ W/m}^2)(1.88 \times 10^{-4} \text{ m}^2) = 3.94 \times 10^{-13} \text{ W}$$

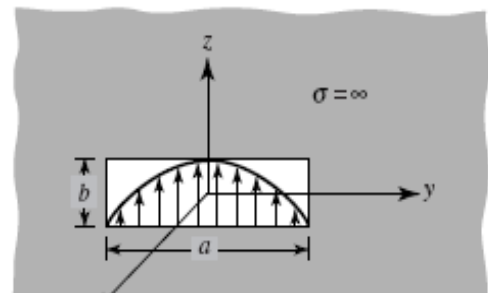
$$P_{\text{max}} = 3.94 \times 10^{-13} \text{ W}$$

**12.27.** The normalized far-zone electric field radiated in the  $E$ -plane ( $x$ - $z$  plane;  $\phi = 0^\circ$ ) by a waveguide aperture antenna of dimensions  $a$  and  $b$ , mounted on an infinite ground plane as shown in the figure, is given by

$$\mathbf{E} = -\hat{\mathbf{a}}_{\theta} j \frac{\omega \mu b I_0 e^{-jkr}}{4\pi r} \frac{\sin\left(\frac{kb}{2} \cos \theta\right)}{\frac{kb}{2} \cos \theta}$$

Determine in the  $E$ -plane the:

- The HPBW in the  $E$ -plane,
- The HPBW in the  $H$ -plane.



12.21. For the rectangular aperture of Section 12.5.3 (waveguide/mode TE<sub>10</sub>) with  $a = 3\lambda$ ,  $b = 2\lambda$ , compute the

- a- *E*-plane half-power beamwidth,      b- *H*-plane half-power beamwidth  
 c- *E*-plane first-null beamwidth,      d- *H*-plane first-null beamwidth  
 e- *E*-plane first side lobe maximum (relative to main maximum)  
 f- *H*-plane first side lobe maximum (relative to main maximum)

using the formulas of Table 12.1.

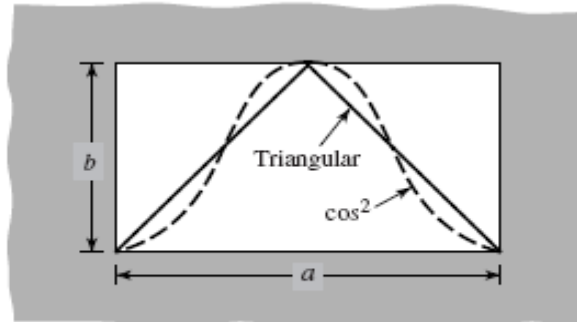
Solution:

- |  |   |
|--|---|
| a- HPBW = $50.8\lambda/b$ , (E-Plane)  | HPBW = $50.8 \times \lambda/2\lambda = 25.4^\circ$  |
| b- HPBW = $68.8\lambda/a$ , (H-Plane)  | HPBW = $68.8 \times \lambda/3\lambda = 22.93^\circ$ |
| c- NNBW = $114.6\lambda/b$ , (E-Plane) | NNBW = $114.6 \times \lambda/2\lambda = 57.3^\circ$ |
| d- NNBW = $171.9\lambda/a$ , (H-Plane) | NNBW = $171.9 \times \lambda/3\lambda = 57.3^\circ$ |
| e- -13.26 dB                           |   |
| f- -23 dB                              |   |

A rectangular aperture mounted on an infinite ground plane has aperture electric field distributions and corresponding efficiencies of

Field Distribution	Aperture Efficiency
(a) Triangular	75%
(b) Cosine square	66.67%

What are the corresponding directives (in dB) if the dimensions of the aperture are  $a = \lambda/2$  and  $b = \lambda/4$ ?



$$D_0 = \frac{4\pi}{\lambda^2} A_{em} = \frac{4\pi}{\lambda^2} \epsilon_{ap} A_p = \epsilon_{ap} \frac{4\pi}{\lambda^2} (ab)$$

$$D_0 = \epsilon_{ap} \frac{4\pi (ab)}{\lambda^2} = \epsilon_{ap} \frac{4\pi}{\lambda^2} \left(\frac{\lambda^2}{8}\right) = \epsilon_{ap} \frac{\pi}{2}$$

a. Triangular :  $\epsilon_{ap} = 75\% = 3/4$

$$D_0 = \frac{3}{4} \left(\frac{\pi}{2}\right) = 1.1781 = 0.7118 \text{ dB}$$

$$D_0 = 1.1781 = 0.7118 \text{ dB}$$

b. Cosine Square ;  $\epsilon_{ap} = 66.67\% = 2/3$

$$D_0 = \epsilon_{ap} \frac{\pi}{2} = \frac{2}{3} \left(\frac{\pi}{2}\right) = \frac{\pi}{3} = 1.0472 = 0.2 \text{ dB}$$

$$D_0 = 1.0472 = 0.2 \text{ dB}$$

## Lecture Notes-18

# Horn Antennas

### 13.1 INTRODUCTION

One of the simplest and the most widely used microwave antenna is the horn. Its existence and early use dates back to the late 1800s. Although neglected somewhat in the early 1900s, its revival began in the late 1930s from the interest in microwaves and waveguide transmission lines during the period of World War II. The horn is widely used as a **feed element** for large radio astronomy, satellite tracking, and communication dishes found installed throughout the world. In addition to its utility as a **feed for reflectors and lenses**, it is a common element of phased arrays and serves as a **universal standard for calibration and gain measurements** of other high-gain antennas. Its widespread applicability stems from its simplicity in construction, ease of excitation, versatility, large gain, and preferred overall performance.

An electromagnetic horn can take many different forms, four of which are shown in Fig. 13.1. The horn is nothing more than a hollow cylinder of different cross sections, which has been tapered (flared) to a larger opening. The type, direction, and amount of taper (flare) can have a profound effect on the overall performance of the element as a radiator.

### 13.2 E-PLANE SECTORAL HORN

The  $E$ -plane sectoral horn is one whose opening is flared in the direction of the  $E$ -field, and it is shown in Fig. 13.1(a).

#### 13.2.1 Aperture Fields

The horn can be treated as an aperture antenna. To find its radiation characteristics, the equivalent principle techniques developed in Chapter 12 can be utilized. To develop an exact equivalent of it, it is necessary that the tangential electric and magnetic field components over a closed surface are known. The closed surface that is usually selected is an infinite plane that coincides with the aperture of the horn. When the horn is not mounted on an infinite ground plane, the fields outside the aperture are not known and an exact equivalent cannot be formed. However, the usual approximation is to assume that the fields outside the aperture are zero, as was done for the aperture of Section 12.5.2.

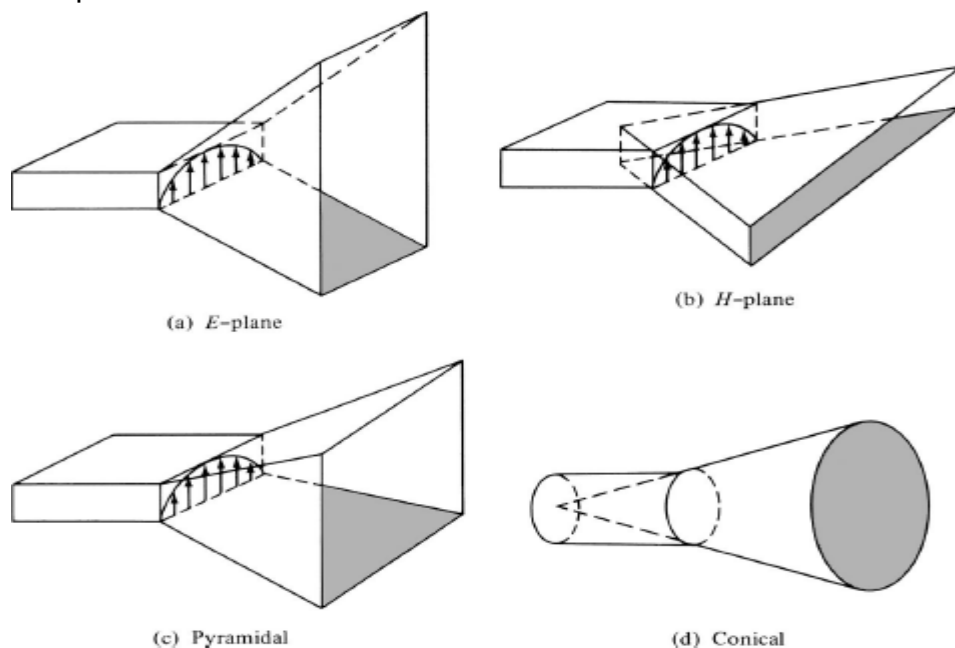


**Figure 13.1** Typical electromagnetic horn antenna configurations.

It can be shown that if the: **(1)** fields of the feed waveguide are those of its dominant TE<sub>10</sub> mode and **(2)** horn length is large compared to the aperture dimensions, the lowest order mode fields at the aperture of the horn are given by

$$E'_z = E'_x = H'_y = 0 \quad (13-1a)$$

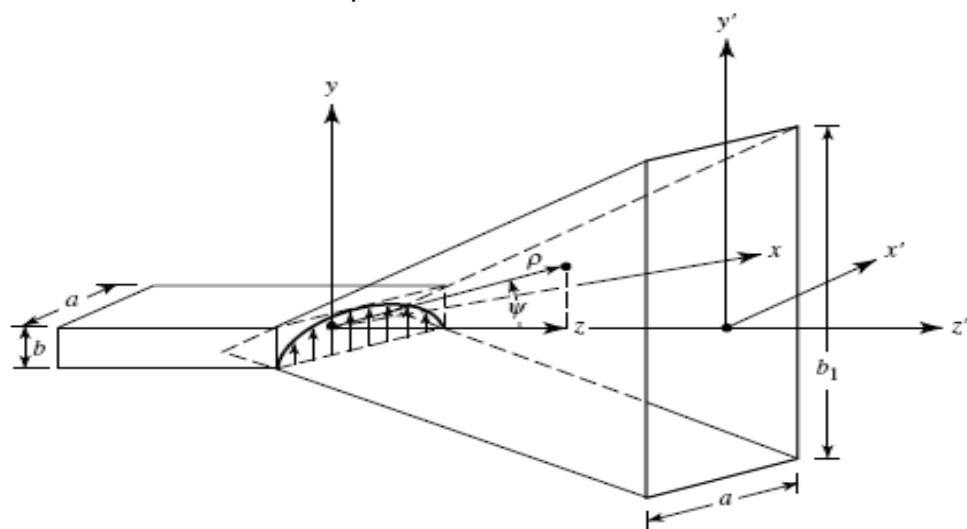
$$E'_y(x', y') \simeq E_1 \cos\left(\frac{\pi}{a}x'\right) e^{-j[ky'^2/(2\rho_1)]} \quad (13-1b)$$

$$H'_z(x', y') \simeq jE_1 \left(\frac{\pi}{kan\eta}\right) \sin\left(\frac{\pi}{a}x'\right) e^{-j[ky'^2/(2\rho_1)]} \quad (13-1c)$$

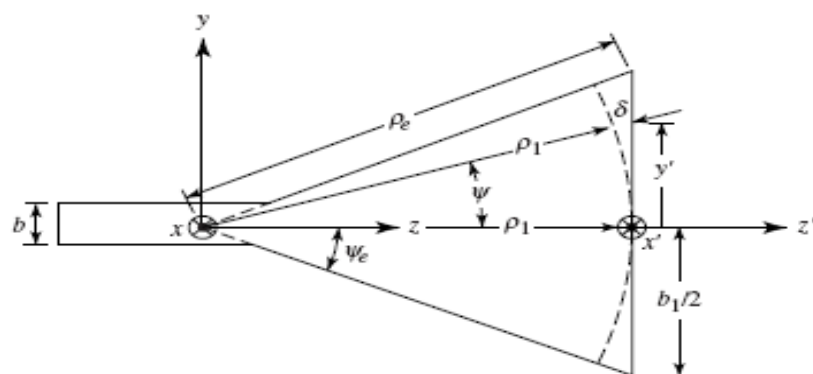
$$H'_x(x', y') \simeq -\frac{E_1}{\eta} \cos\left(\frac{\pi}{a}x'\right) e^{-j[ky'^2/(2\rho_1)]} \quad (13-1d)$$

$$\rho_1 = \rho_e \cos \psi_e \quad (13-1e)$$

where  $E_1$  is a constant. The primes are used to indicate the fields at the aperture of the horn. The expressions are similar to the fields of a TE<sub>10</sub>-mode for a rectangular waveguide with aperture dimensions of  $a$  and  $b_1$  ( $b_1 > a$ ). The only difference is the complex exponential term which is used here to represent the quadratic phase variations of the fields over the aperture of the horn.



(a) E-plane horn



(b) E-plane view

**Figure 13.2** E-plane horn and coordinate system.

The necessity of the quadratic phase term in (13-1b)–(13-1d) can be illustrated geometrically. Referring to Fig. 13.2(b), let us assume that at the imaginary apex of the horn (shown dashed) there exists a line source radiating cylindrical waves. As the waves travel in the outward radial direction, the constant phase fronts are cylindrical. At any point  $y'$  at the aperture of the horn, the phase of the field will not be the same as that at the origin ( $y' = 0$ ). The phase is different because the wave has traveled different distances from the apex to the aperture. The difference in path of travel, designated as  $\delta(y')$ , can be obtained by referring to Fig. 13.2(b). For any point  $y'$

$$[\rho_1 + \delta(y')]^2 = \rho_1^2 + (y')^2 \quad (13-2)$$

Or

$$\delta(y') = -\rho_1 + [\rho_1^2 + (y')^2]^{1/2} = -\rho_1 + \rho_1 \left[ 1 + \left( \frac{y'}{\rho_1} \right)^2 \right]^{1/2} \quad (13-2a)$$

which is referred to as the *spherical* phase term.

Using the binomial expansion and retaining only the first two terms of it, (13-2a) reduces to

$$\delta(y') \simeq -\rho_1 + \rho_1 \left[ 1 + \frac{1}{2} \left( \frac{y'}{\rho_1} \right)^2 \right] = \frac{1}{2} \left( \frac{y'^2}{\rho_1} \right) \quad (13-2b)$$

The quadratic phase variation for the fields of the dominant mode at the aperture of a horn antenna has been a standard for many years, and it yields in most practical cases very good results. It also leads to closed form expressions, in terms of sine and cosine Fresnel integrals, for the radiation characteristics (far-zone fields, directivity, etc.) of the horn.

### 13.2.2 Radiated Fields

The electric field components radiated by the horn can be given by

$$E_r=0 \quad (13-11a)$$

$$E_\theta = -j \frac{a \sqrt{\pi k \rho_1} E_1 e^{-jkr}}{8r} \times \left\{ e^{j(k_y^2 \rho_1 / 2k)} \sin \phi (1 + \cos \theta) \left[ \frac{\cos \left( \frac{k_x a}{2} \right)}{\left( \frac{k_x a}{2} \right)^2 - \left( \frac{\pi}{2} \right)^2} \right] F(t_1, t_2) \right\} \quad (13-11b)$$

$$E_\phi = -j \frac{a \sqrt{\pi k \rho_1} E_1 e^{-jkr}}{8r} \times \left\{ e^{j(k_y^2 \rho_1 / 2k)} \cos \phi (\cos \theta + 1) \left[ \frac{\cos \left( \frac{k_x a}{2} \right)}{\left( \frac{k_x a}{2} \right)^2 - \left( \frac{\pi}{2} \right)^2} \right] F(t_1, t_2) \right\} \quad (13-11c)$$

where  $t_1$ ,  $t_2$ ,  $k_x$ ,  $k_y$ , and  $F(t_1, t_2)$  are given, respectively, by (13-8a), (13-8b), (13-9a), (13-9b), and (13-9c). The corresponding **H**-field components are obtained using (12-10d)–(12-10f).

In the principal *E*- and *H*-planes, the electric field reduces to

**E-Plane ( $\phi = \pi/2$ )**

$$E_r = E_\phi = 0 \quad (13-12a)$$

$$E_\theta = -j \frac{a\sqrt{\pi k \rho_1} E_1 e^{-jkr}}{8r} \left\{ -e^{j(k\rho_1 \sin^2 \theta/2)} \left(\frac{2}{\pi}\right)^2 (1 + \cos \theta) F(t'_1, t'_2) \right\} \quad (13-12b)$$

$$t'_1 = \sqrt{\frac{k}{\pi \rho_1}} \left( -\frac{b_1}{2} - \rho_1 \sin \theta \right) \quad (13-12c)$$

$$t'_2 = \sqrt{\frac{k}{\pi \rho_1}} \left( +\frac{b_1}{2} - \rho_1 \sin \theta \right) \quad (13-12d)$$

**H-Plane ( $\phi = 0$ )**

$$E_r = E_\theta = 0 \quad (13-13a)$$

$$E_\phi = -j \frac{a\sqrt{\pi k \rho_1} E_1 e^{-jkr}}{8r} \left\{ (1 + \cos \theta) \left[ \frac{\cos\left(\frac{ka}{2} \sin \theta\right)}{\left(\frac{ka}{2} \sin \theta\right)^2 - \left(\frac{\pi}{2}\right)^2} \right] F(t''_1, t''_2) \right\} \quad (13-13b)$$

$$t''_1 = -\frac{b_1}{2} \sqrt{\frac{k}{\pi \rho_1}} \quad (13-13c)$$

$$t''_2 = +\frac{b_1}{2} \sqrt{\frac{k}{\pi \rho_1}} \quad (13-13d)$$

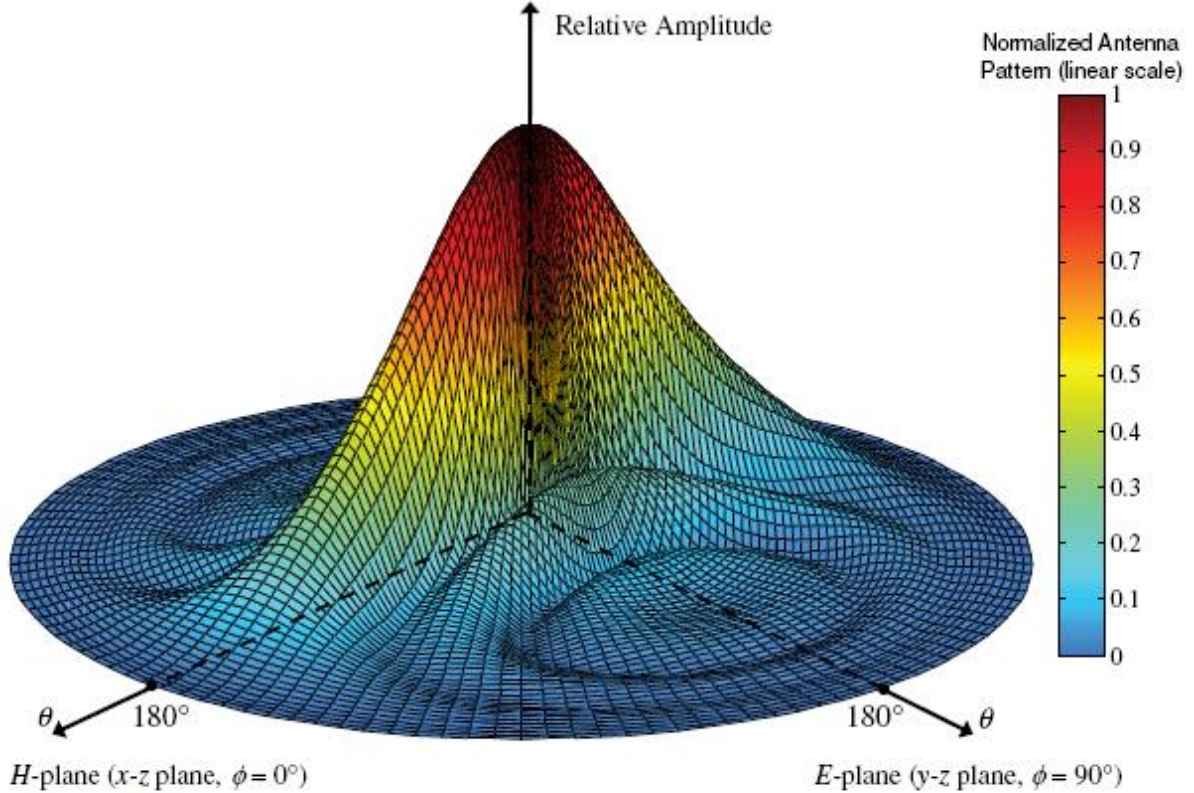


**Figure 13.3** Three-dimensional field pattern of *E*-plane sectoral horn ( $\rho_1 = 6\lambda$ ,  $b_1 = 2.75\lambda$ ,  $a = 0.5\lambda$ ).

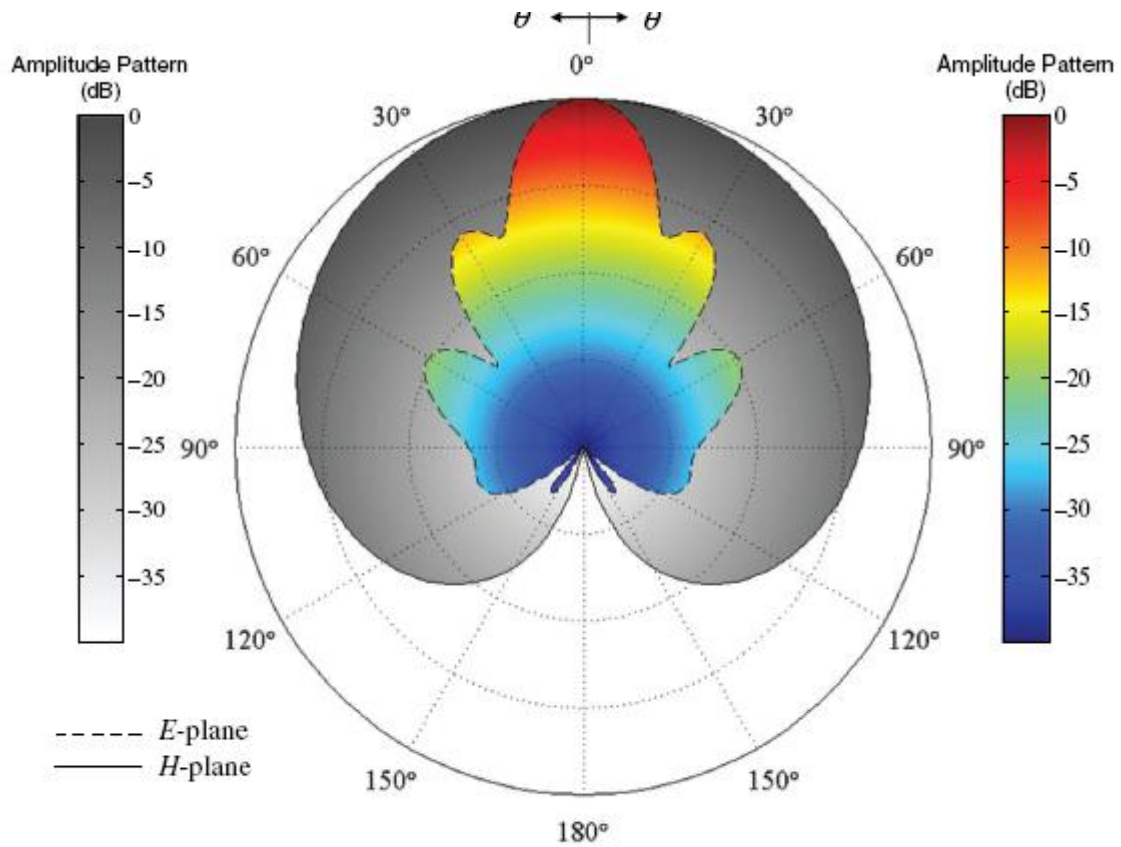


Figure 13.4 E- and H-plane patterns of an E-plane sectoral horn.

### 13.2.3 Directivity

The directivity is one of the parameters that is often used as a figure of merit to describe the performance of an antenna. To find the directivity, the maximum radiation is formed. That is,

$$U_{\max} = U(\theta, \phi)|_{\max} = \frac{r^2}{2\eta} |E|_{\max}^2 \quad (13-14)$$

For most horn antennas  $|E|_{\max}$  is directed nearly along the z-axis ( $\theta = 0^\circ$ ). Thus,

$$|E|_{\max} = \sqrt{|E_\theta|_{\max}^2 + |E_\phi|_{\max}^2} = \frac{2a\sqrt{\pi k\rho_1}}{\pi^2 r} |E_1| |F(t)| \quad (13-15)$$

$$U_{\max} = \frac{r^2}{2\eta} |E|_{\max}^2 = \frac{2a^2 k\rho_1}{\eta\pi^3} |E_1|^2 |F(t)|^2 = \frac{4a^2 \rho_1 |E_1|^2}{\eta\lambda\pi^2} |F(t)|^2 \quad (13-16)$$

$$P_{\text{rad}} = |E_1|^2 \frac{b_1 a}{4n} \quad (13-17a)$$

Using (13-16) and (13-17a), the directivity for the E-plane horn can be written as

$$\begin{aligned} D_E &= \frac{4\pi U_{\max}}{P_{\text{rad}}} = \frac{64a\rho_1}{\pi\lambda b_1} |F(t)|^2 \\ &= \frac{64a\rho_1}{\pi\lambda b_1} \left[ C^2 \left( \frac{b_1}{\sqrt{2\lambda\rho_1}} \right) + S^2 \left( \frac{b_1}{\sqrt{2\lambda\rho_1}} \right) \right] \end{aligned} \quad (13-18)$$

Where C and S are the cosine and sine integrals.

The directivity increases as the aperture increases till it reaches Max. then drops down due to the effect of the increasing phase error as can be seen in Fig. 13.7.

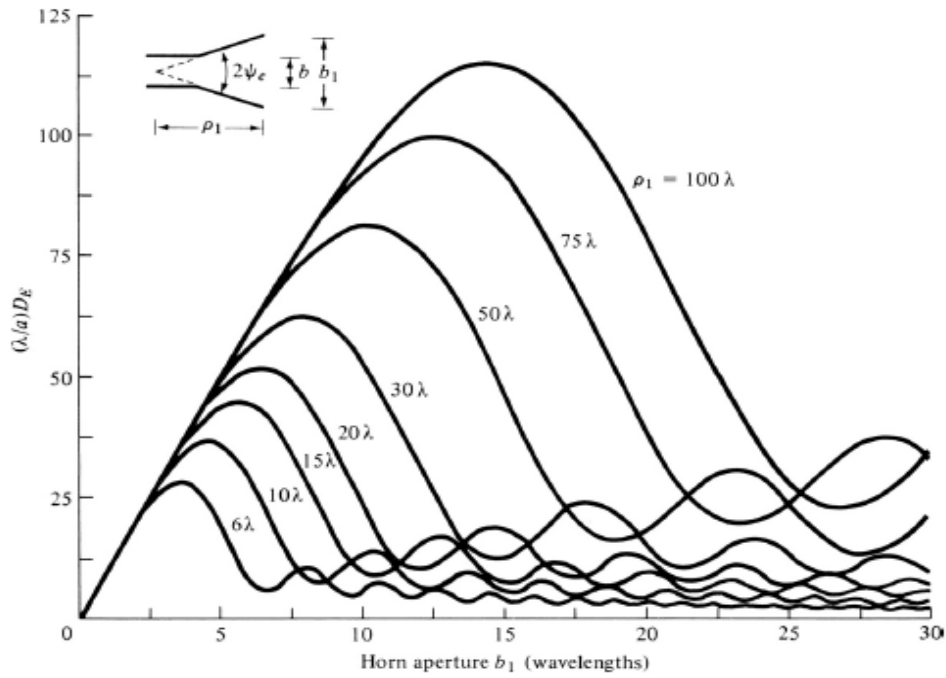


**Figure 13.7** Normalized directivity of  $E$ -plane sectoral horn as a function of aperture size and for different lengths.

Maximum directivity can be obtained when

$$b_1 \simeq \sqrt{2\lambda\rho_1} \quad (13-18a)$$

### 13.3H-PLANE SECTORAL HORN

Flaring the dimensions of a rectangular waveguide in the direction of the  $H$ -field, while keeping the other constant, forms an  $H$ -plane sectoral horn shown in Fig.13.1(b). The analysis procedure for this horn is similar to that for the  $E$ -plane horn, which was outlined in the previous section.

It can be shown that each optimum directivity occurs when

$$a_1 \simeq \sqrt{3\lambda\rho_2} \quad (13-39c)$$

Where  $a_1$  is the flared horn aperture size along and  $\rho_2$

## 13.4 PYRAMIDAL HORN

The most widely used horn is the one which is flared in both directions, as shown in Fig. 13.16. It is widely referred to as a pyramidal horn, and its radiation characteristics are essentially a combination of the  $E$ - and  $H$ -plane sectoral horns.

$$E'_y(x', y') = E_0 \cos\left(\frac{\pi x'}{a_1}\right) e^{-j[k(x'^2/\rho_2 + y'^2/\rho_1)/2]} \quad (13-41a)$$

$$H'_x(x', y') = -\frac{E_0}{\eta} \cos\left(\frac{\pi x'}{a_1}\right) e^{-j[k(x'^2/\rho_2 + y'^2/\rho_1)/2]} \quad (13-41b)$$

### 13.4.1 Aperture Fields, Equivalent, and Radiated Fields

To simplify the analysis and to maintain a modeling that leads to computations that have been shown to correlate well with experimental data, the tangential components of the  $E$ - and  $H$ -fields over the aperture of the horn are approximated by

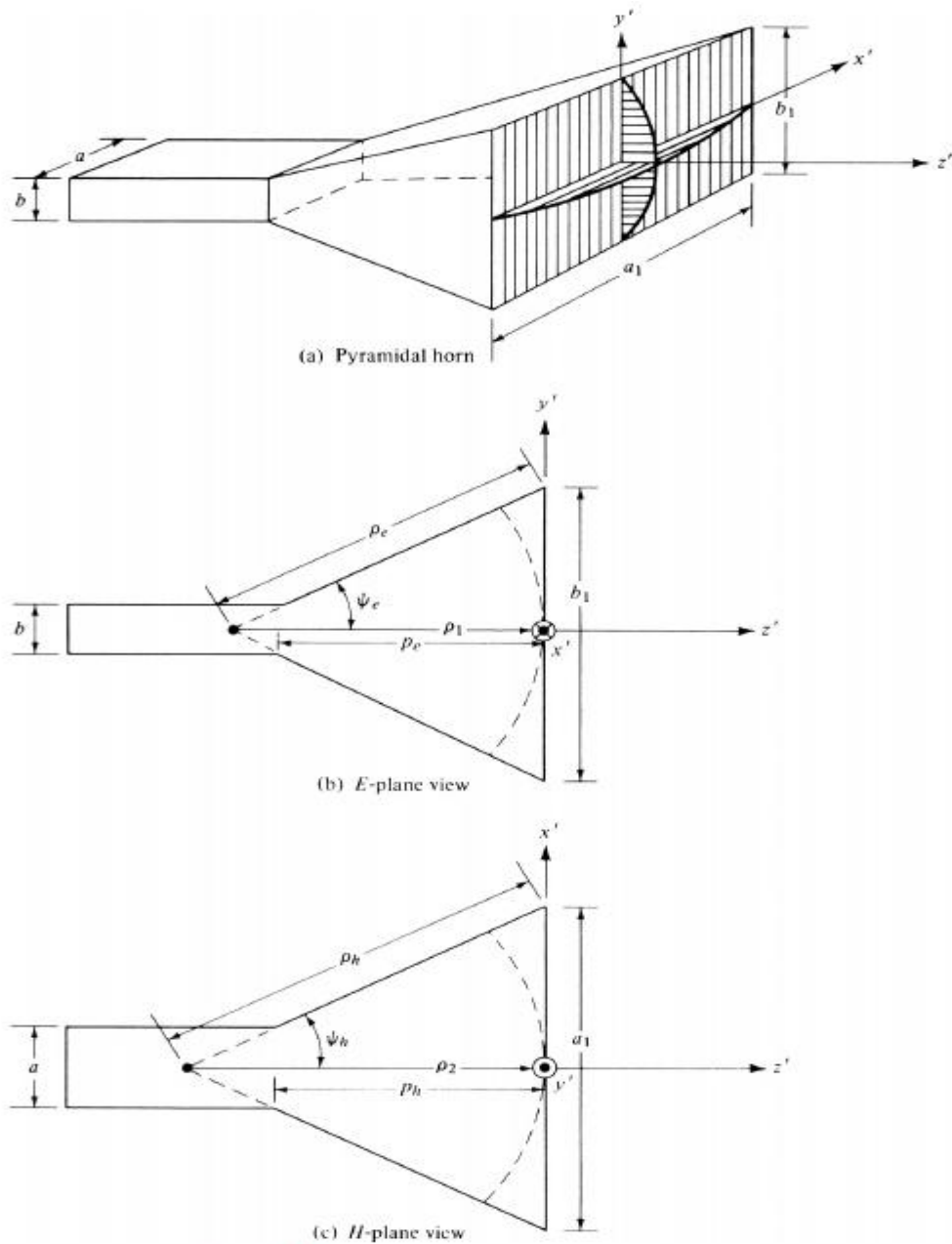


**Figure 13.16** Pyramidal horn and coordinate system.

Combining (13-43a)–(13-43d), the far-zone **E**- and **H**-field components of (12-10a)–(12-10c) reduce to

$$E_r = 0 \quad (13-46a)$$

$$\begin{aligned} E_\theta &= -j \frac{ke^{jkr}}{4\pi r} [L_\phi + \eta N_\theta] \\ &= j \frac{kE_0 e^{-jkr}}{4\pi r} [\sin \phi (1 + \cos \theta) I_1 I_2] \end{aligned} \quad (13-46b)$$

$$\begin{aligned} E_\phi &= +j \frac{ke^{-jkr}}{4\pi r} [L_\theta - \eta N_\phi] \\ &= j \frac{kE_0 e^{-jkr}}{4\pi r} [\cos \phi (\cos \theta + 1) I_1 I_2] \end{aligned} \quad (13-46c)$$

The fields radiated by a pyramidal horn, as given by (13-46a)–(13-46c), are valid for all angles of observation. An examination of these equations reveals that the principal  $E$ -plane pattern ( $\phi = \pi/2$ ) of a pyramidal horn, aside from a normalization factor, is identical to the  $E$ -plane pattern of an  $E$ -plane sectoral horn. Similarly the  $H$ -plane ( $\phi = 0$ ) is identical to that of an  $H$ -plane sectoral horn. Therefore the pattern of a pyramidal horn is very narrow in both principal planes and, in fact, in all planes. This is illustrated in Fig.13.17.

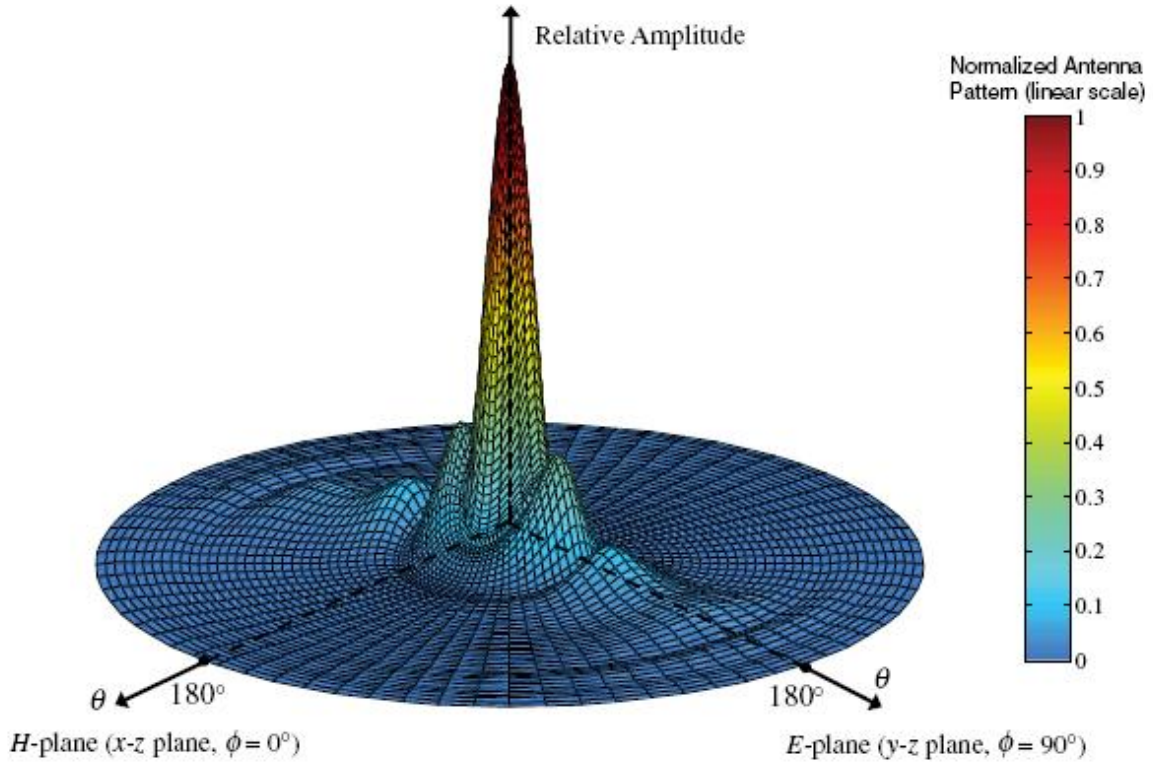


**Figure 13.17** Three-dimensional field pattern of a pyramidal horn ( $\rho_1 = \rho_2 = 6\lambda$ ,  $a_1 = 5.5\lambda$ ,  $b_1 = 2.75\lambda$ ,  $a = 0.5\lambda$ ,  $b = 0.25\lambda$ ).

1

### 3.4.2 Directivity

The directivity of the pyramidal configuration is vital to the antenna designer. It is a very simple exercise to show that  $|E_\theta|_{\max}$ ,  $|E_\phi|_{\max}$ , and in turn  $U_{\max}$  can be written, using (13-46b) and (13-46c), as

$$|E_\theta|_{\max} = |E_0 \sin \phi| \frac{\sqrt{\rho_1 \rho_2}}{r} \{ [C(u) - C(v)]^2 + [S(u) - S(v)]^2 \}^{1/2} \\ \times \left\{ C^2 \left( \frac{b_1}{\sqrt{2\lambda \rho_1}} \right) + S^2 \left( \frac{b_1}{\sqrt{2\lambda \rho_1}} \right) \right\}^{1/2} \quad (13-48a)$$

$$|E_\phi|_{\max} = |E_0 \cos \phi| \frac{\sqrt{\rho_1 \rho_2}}{r} \{ [C(u) - C(v)]^2 + [S(u) - S(v)]^2 \}^{1/2} \\ \times \left\{ C^2 \left( \frac{b_1}{\sqrt{2\lambda \rho_1}} \right) + S^2 \left( \frac{b_1}{\sqrt{2\lambda \rho_1}} \right) \right\}^{1/2} \quad (13-48b)$$

$$U_{\max} = \frac{r^2}{2\eta} |\mathbf{E}|_{\max}^2 = |E_0|^2 \frac{\rho_1 \rho_2}{2\eta} \{ [C(u) - C(v)]^2 + [S(u) - S(v)]^2 \} \\ \times \left\{ C^2 \left( \frac{b_1}{\sqrt{2\lambda \rho_1}} \right) + S^2 \left( \frac{b_1}{\sqrt{2\lambda \rho_1}} \right) \right\} \quad (13-48c)$$

$$P_{\text{rad}} = |E_0|^2 \frac{a_1 b_1}{4\eta} \quad (13-49)$$

the directivity of the pyramidal horn can be written as

$$D_p = \frac{4\pi U_{\text{max}}}{P_{\text{rad}}} = \frac{8\pi\rho_1\rho_2}{a_1 b_1} \{ [C(u) - C(v)]^2 + [S(u) - S(v)]^2 \} \times \left\{ C^2\left(\frac{b_1}{\sqrt{2\lambda\rho_1}}\right) + S^2\left(\frac{b_1}{\sqrt{2\lambda\rho_1}}\right) \right\} \quad (13-50)$$

which reduces to

$$D_p = \frac{\pi\lambda^2}{32ab} D_E D_H \quad (13-50a)$$

where  $D_E$  and  $D_H$  are the directivities of the  $E$ - and  $H$ -plane sectoral horns as given by (13-18) and (13-39), respectively. This is a well-known relationship and has been used extensively in the design of pyramidal horns.

The aperture dimensions of the optimum pyramidal horn can be given by:

$$a_1 = \sqrt{3\lambda\rho_2}$$

$$b_1 = \sqrt{2\lambda\rho_1}$$

While the gain can be given by

$$G_0 = \frac{1}{2} \frac{4\pi}{\lambda^2} (a_1 b_1)$$

### 13.5 CONICAL HORN

Another very practical microwave antenna is the conical horn shown in Fig.13.24 with a photo of one in Figure 13.25. While the pyramidal,  $E$ -, and  $H$ -plane sectoral horns are usually fed by a rectangular waveguide, the feed of a conical horn is often a circular waveguide. The modes within the horn are found by introducing a spherical coordinate system and are in terms of spherical Bessel functions and Legendre polynomials.

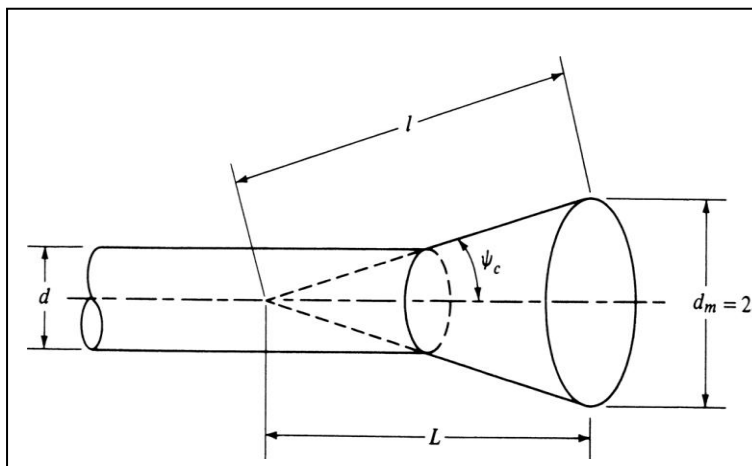


Figure 13.24 Geometry of the conical horn.



Fig. 13.25 Photo of an X-band conical horn ( $L = 7.147\lambda$ ,  $2\psi_c = 35^\circ$ ).

The optimum maximum directivity  $(D_c)_{opt}$  and axial length  $L$  based on the optimum horn

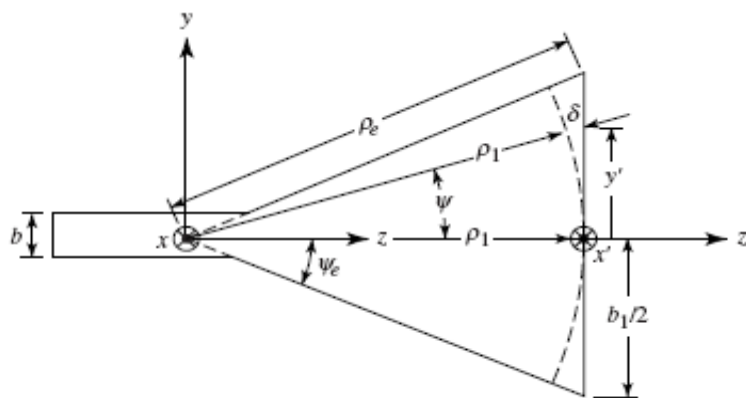
$$(D_c)_{opt} \approx 15.9749 \left( \frac{L}{\lambda} \right) + 1.7209 \quad (13-57a)$$

$$(D_c)_{opt} \approx 5.1572 \left( \frac{d_m}{\lambda} \right)^2 - 0.6451 \left( \frac{d_m}{\lambda} \right) + 1.3645 \quad (13-57b)$$

$$L \approx 0.3232 \left( \frac{d_m}{\lambda} \right)^2 - 0.0475 \left( \frac{d_m}{\lambda} \right) + 0.0052 \quad (13-57c)$$

Design an  $E$ -plane horn such that the maximum phase difference between two points at the aperture, (one at the center and the other at the edge) is  $120^\circ$ . Assuming that the maximum length along its wall ( $\rho_e$ ), measured from the aperture to its apex, is  $10\lambda$ , find the

- maximum total flare angle of the horn.
- largest dimension of the horn at the aperture.



(b)  $E$ -plane view

2. Using the geometry of Figure 13.2(b)

$$a. \quad \Phi_{max} = \frac{2\pi}{3} = k \delta_{max} = \frac{2\pi}{\lambda} (\rho_e - \rho_1) = \frac{2\pi}{\lambda} (\rho_e - \rho_e \cos \psi_e) = \frac{2\pi}{\lambda} \rho_e (1 - \cos \psi_e)$$

$$\frac{2\pi}{3} = \frac{2\pi}{\lambda} (10\lambda) (1 - \cos \psi_e) = 2\pi (10) (1 - \cos \psi_e) = 2\pi (10) [2\sin^2(\frac{\psi_e}{2})]$$

$$\sin^2 \frac{\psi_e}{2} = \frac{1}{3(20)} = \frac{1}{60} \Rightarrow \frac{\psi_e}{2} = \sin^{-1}(\frac{1}{\sqrt{20}}) = 7.418^\circ$$

$$\psi_e = 2(7.418^\circ) = 14.836^\circ, \quad 2\psi_e = 29.672^\circ$$

$$b. \quad \frac{b_1}{2} = \rho_e \sin \psi_e = 10\lambda \sin(14.836^\circ) = 2.56\lambda \Rightarrow b_1 = 5.12\lambda$$

$$c. \quad \rho_1 = \rho_e \cos \psi_e = 10\lambda \cos(14.836^\circ) = 9.667\lambda$$

Design a pyramidal horn antenna with optimum gain at a frequency of 10 GHz. The overall length of the antenna from the imaginary vertex of the horn to the center of the aperture is  $10\lambda$  and is nearly the same in both planes. Determine the

a- Aperture dimensions of the horn (in cm).

b- Gain of the antenna (in dB)

c- Aperture efficiency of the antenna (in %). Assume the reflection, conduction, and dielectric losses of the antenna are negligible.

d- Power delivered to a matched load when the incident power density is  $10\mu\text{W}/\text{m}^2$ .

13-18.

$$\lambda = \frac{30 \times 10^9}{10 \times 10^9} = 3 \text{ cm}$$

$$a. \quad a_1 \simeq \sqrt{3\lambda\rho} = \sqrt{3\lambda(10\lambda)} = \sqrt{30\lambda^2} = 5.477\lambda = 16.43 \text{ cm}$$

$$b_1 \simeq \sqrt{2\lambda\rho} = \sqrt{20\lambda^2} = 4.472\lambda = 13.416 \text{ cm}$$

$$b. \quad G_0 = \frac{1}{2} \frac{4\pi}{\lambda^2} (a_1 b_1) = \frac{1}{2} \frac{4\pi}{\lambda^2} (5.477\lambda)(4.472\lambda) = 153.89 = 21.87 \text{ dB}$$

$$c. \quad \epsilon_r \epsilon_{cd} \epsilon_{ap} = 1 \cdot 1 \cdot \epsilon_{ap} = \frac{1}{2}, \quad \epsilon_{ap} = \frac{1}{2} = 50\%$$

$$d. \quad A_{em} = \frac{\lambda^2}{4\pi} G_0 = \frac{3^2}{4\pi} (153.89) = 110.2156 \text{ cm}^2 = 110.2156 \times 10^{-4} \text{ m}^2$$

$$P_{rec} = W_i A_{em} = 10 \times 10^{-6} \times 110.2156 \times 10^{-4} = 1.102156 \times 10^{-10} = 11.02156 \times 10^{-8}$$

$$P_{rec} = 11.02156 \times 10^{-8} = 0.1102156 \mu \text{ Watts}$$

As part of a 10-GHz microwave communication system, a horn antenna that is said to have a directivity of 75 (dimensionless). The conduction and dielectric losses of the antenna are negligible, and the horn is polarization matched to the incoming signal. A standing wave meter indicates a voltage reflection coefficient of 0.1 at the antenna waveguide junction.

a- Calculate the maximum effective aperture of the horn.

b- If an impinging wave with a uniform power density of  $1 \mu\text{W}/\text{m}^2$  is incident upon the horn, what is the maximum power delivered to a load which is connected and matched to the lossless waveguide?

$$a. \quad A_{em} = (1 - |\Gamma|^2) \cdot \frac{\lambda^2}{4\pi} \cdot D_0 = 0.99 \cdot \frac{(0.03)^2}{4\pi} \cdot 75 = 5.317764 \times 10^{-3} \text{ m}^2$$

$$(f = 10 \text{ GHz} \rightarrow \lambda = 0.03 \text{ m})$$

$$A_{em} = 0.005317764 \text{ m}^2$$

$$b. \quad P_{max} = A_{em} \cdot W_i = (1 \times 10^{-6} \text{ watts/m}^2) \cdot (0.005317764) = 5.317 \times 10^{-9} \text{ Watts}$$

$$P_{max} = 5.317764 \times 10^{-9} \text{ Watts}$$

## LN-19 Microstrip Antennas

### 14.1 INTRODUCTION

In high-performance aircraft, spacecraft, satellite, and missile applications, where size, weight, cost, performance, ease of installation, and aerodynamic profile are constraints, low-profile antennas are required. Other applications like mobile radio and wireless communications need small and light antennas. To meet these requirements, microstrip antennas (patch antennas) can be used. These antennas are of low profile, conformable to planar and nonplanar surfaces, simple and inexpensive to manufacture using modern printed-circuit technology, mechanically robust when mounted on rigid surfaces, compatible with MMIC designs. Moreover, by adding loads between the patch and the ground plane, such as PIN and varactor diodes, adaptive elements with variable resonant frequency, impedance, polarization, and pattern can be designed.

Disadvantages of microstrip antennas are their low efficiency, low power, high  $Q$  (sometimes  $> 100$ ), poor polarization purity, poor scan performance, spurious feed radiation and very narrow frequency bandwidth, which is typically  $< \text{few}\%$ . In addition, microstrip antennas are rather large physically at VHF and possibly UHF frequencies.

#### 14.1.1 Basic Characteristics

Microstrip antennas were first presented in 1953 and patented in 1955, then received considerable attention in the 1970s. Microstrip antennas, as shown in Fig.14.1(a), consist of a very thin ( $t \ll \lambda_0$ , where  $\lambda_0$  is the free-space wavelength) metallic strip (patch) placed a small fraction of a wavelength ( $h \ll \lambda_0$ , usually  $0.003\lambda_0 \leq h \leq 0.05\lambda_0$ ) above a ground plane. The microstrip patch is designed so its pattern maximum is normal to the patch (broadside radiator). This is accomplished by properly choosing the mode (field configuration) of excitation beneath the patch.

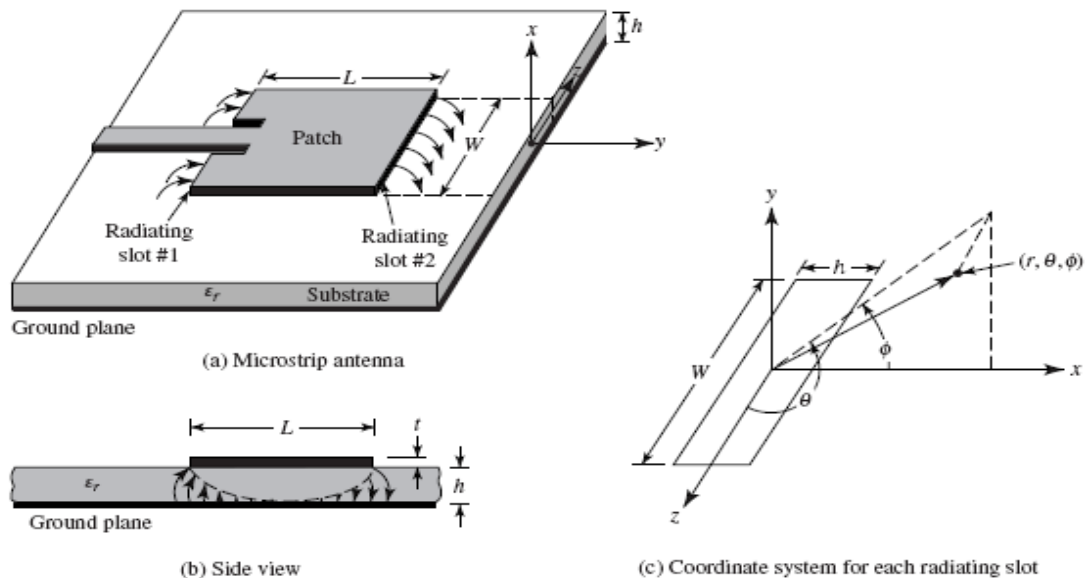


**Figure 14.1** Microstrip antenna and coordinate system.

For a rectangular patch, the length  $L$  of the element is usually  $\lambda_0/3 < L < \lambda_0/2$ . The strip (patch) and the ground plane are separated by a dielectric sheet (substrate), as shown in Figure 14.1(a).

The numerous substrates that are used in the design of microstrip antennas have dielectric constants in the range of  $2.2 \leq \epsilon_r \leq 12$ . The ones that are most desirable for good antenna performance are thick substrates whose dielectric constant is in the lower end of the range because they provide better efficiency, larger bandwidth, but

at the expense of larger element size. Thin substrates with higher dielectric constants are desirable for microwave circuitry because they require tightly bound fields to minimize undesired radiation and coupling, and lead to smaller element sizes; however, because of their greater losses, they are less efficient and have relatively smaller bandwidths.

The radiating elements and the feed lines are usually photoetched on the dielectric substrate. The radiating patch can have various shapes as illustrated in Fig.14.2. Square, rectangular, dipole (strip), and circular are the most common because of ease of analysis and fabrication, and attractive radiation characteristics especially low cross-polarization radiation. Microstrip dipoles are attractive because they inherently possess a large bandwidth and occupy less space, which makes them attractive for arrays.

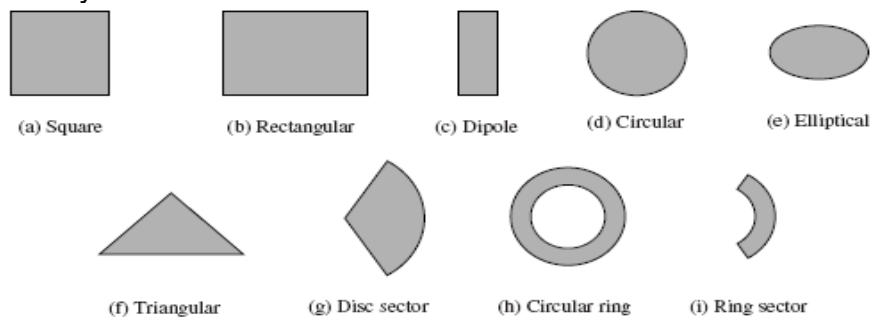


**Figure 14.2** Representative shapes of microstrip patch elements.

#### 14.1.2 Feeding Methods

There are many methods of feeding microstrip antennas as shown in Fig.14.3. The four most popular are the microstrip line, coaxial probe, aperture coupling, and proximity coupling. The microstrip feed line is also a conducting strip, usually of much smaller width compared to the patch. The microstrip-line feed is easy to fabricate, simple to match by controlling the inset position and rather simple to model. However as the substrate thickness increases, surface waves and spurious feed radiation increase, and thus limit the bandwidth (typically 2–5%).

Coaxial-line feeds, are also widely used. The coaxial probe feed is also easy to fabricate and match, and it has low spurious radiation. However, it also has narrow bandwidth and it is more difficult to model, especially for thick substrates ( $h > 0.02\lambda_0$ ). Both the microstrip feed line and the probe possess inherent asymmetries which generate higher order modes which produce cross-polarized radiation. To overcome these problems, noncontacting aperture-coupling feeds, as shown in Figs.14.3(c,d), have been introduced.

#### 14.1.3 Methods of Analysis

The common methods of analysis for microstrip antennas are; **1-** the *transmission-line*, **2-** the *cavity*, and **3-**the *full wave*. The transmission-line model is the easiest of all, it gives good physical insight, but is less accurate and it is more difficult to model coupling. The cavity model is more accurate but at the same time more complex. The full-wave models are very accurate, very versatile, and can treat single elements, finite and infinite arrays, stacked elements, arbitrary shaped elements, and coupling. However they are the most complex models and usually give less physical insight.

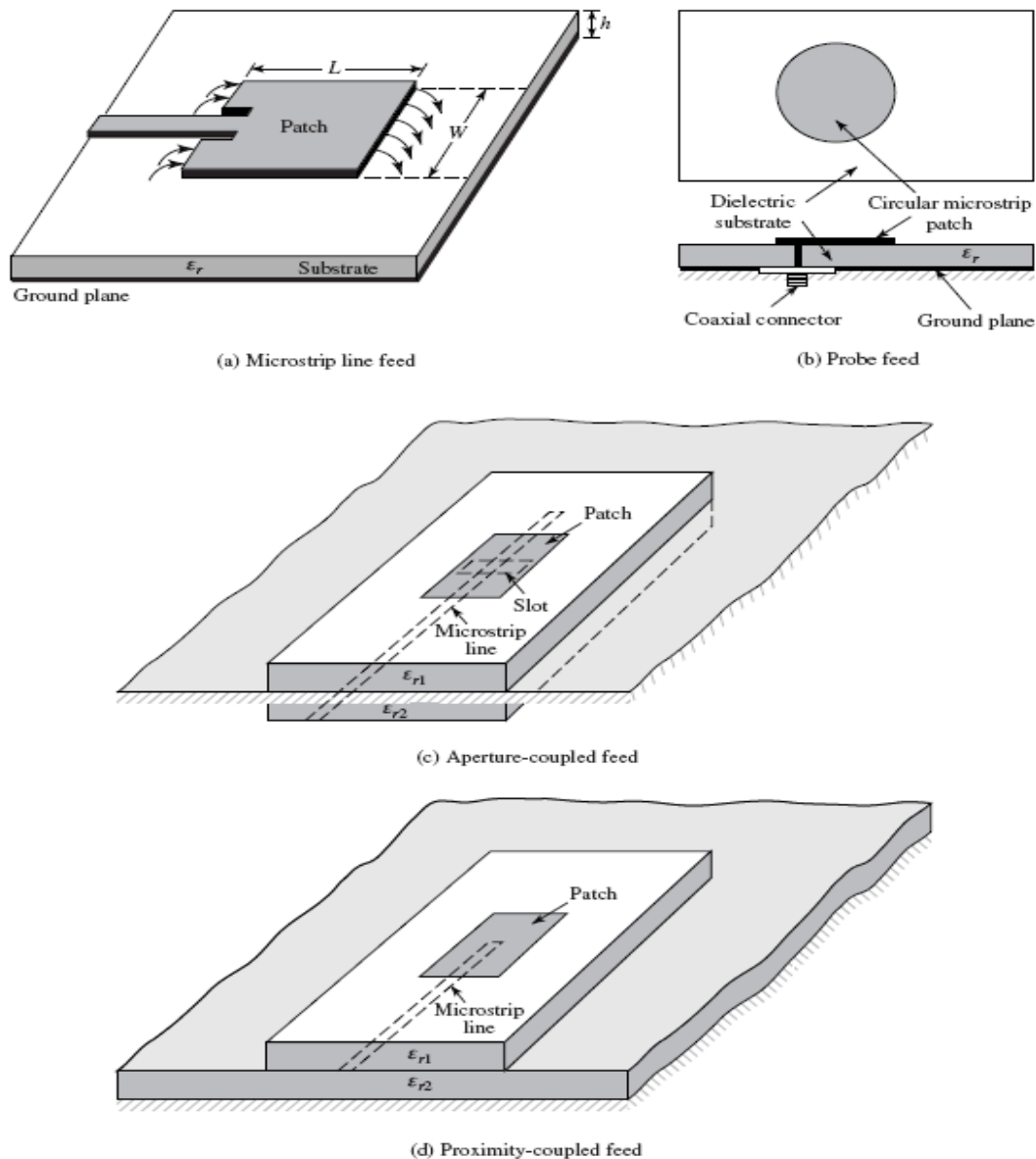


Figure 14.3 Typical feeds for microstrip antennas.

## 14.2 RECTANGULAR PATCH

The rectangular patch is the most widely used configuration. It is very easy to analyze using both the transmission-line and cavity models.

### 14.2.1 Transmission-Line Model

The rectangular microstrip antenna can be represented as an array of two *radiating* narrow apertures (slots), each of width  $W$  and height  $h$ , separated by a distance  $L$ . Basically the transmission-line model represents the microstrip antenna by two slots, separated by a low-impedance  $Z_c$  transmission line of length  $L$ .

#### A. Fringing Effects

Because the dimensions of the patch are finite along the length and width, the fields at the edges of the patch undergo fringing. This is illustrated along the length in Figs. 14.1(a,b) for the two radiating slots of the microstrip antenna. The same applies along the width. The amount of fringing is a function of the dimensions of the patch and the height of the substrate. For microstrip antennas  $L/h \gg 1$ , then fringing is reduced; however, it must be taken into account because it influences the resonant frequency of the antenna. The same applies for the width.

The effective dielectric constant can be given by

$$\epsilon_{\text{reff}} = \frac{\epsilon_r + 1}{2} + \frac{\epsilon_r - 1}{2} \left[ 1 + 12 \frac{h}{W} \right]^{-1/2} \quad (14-1)$$

*B. Effective Length, Resonant Frequency, and Effective Width*

Because of the fringing effects, electrically the patch of the microstrip antenna looks greater than its physical dimensions. For the principal *E*-plane (*xy*-plane), this is demonstrated in Fig. 14.7 where the dimensions of the patch along its length have been extended on each end by a distance  $\Delta L$ , which is a function of the effective dielectric constant  $\epsilon_{\text{reff}}$  and the width-to-height ratio ( $W/h$ ). A very popular and practical approximate relation for the normalized extension of the length is

$$\frac{\Delta L}{h} = 0.412 \frac{(\epsilon_{\text{reff}} + 0.3) \left( \frac{W}{h} + 0.264 \right)}{(\epsilon_{\text{reff}} - 0.258) \left( \frac{W}{h} + 0.8 \right)} \quad (14-2)$$

The width of the patch is given by

$$W = \frac{1}{2f_r \sqrt{\mu_0 \epsilon_0}} \sqrt{\frac{2}{\epsilon_r + 1}} = \frac{v_0}{2f_r} \sqrt{\frac{2}{\epsilon_r + 1}} \quad (14-6)$$

The actual length of the patch can now be determined by

$$L = \frac{1}{2f_r \sqrt{\epsilon_{\text{reff}}} \sqrt{\mu_0 \epsilon_0}} - 2\Delta L \quad (14-7)$$

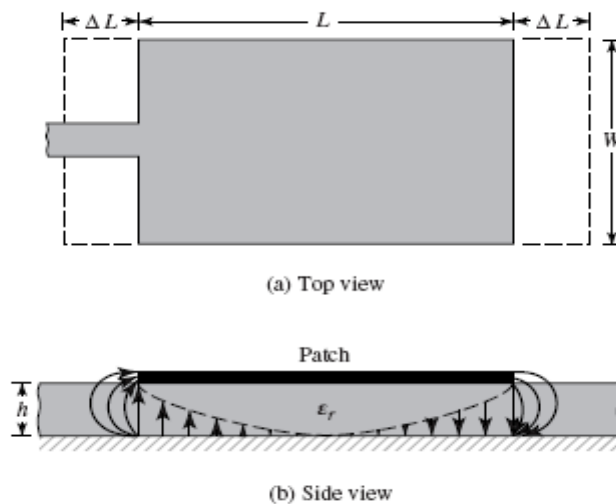


**Figure 14.7** Physical and effective lengths of rectangular microstrip patch.

Since the length of the patch has been extended by  $\Delta L$  on each side, the effective length of the patch is now ( $L = \lambda/2$  for dominant  $TM_{010}$  mode with no fringing)

$$L_{\text{eff}} = L + 2\Delta L \quad (14-3)$$

For the dominant  $TM_{010}$  mode, the resonant frequency of the microstrip antenna is a function of its length. Usually it is given by

$$(f_r)_{010} = \frac{1}{2L\sqrt{\epsilon_r}\sqrt{\mu_0\epsilon_0}} = \frac{v_0}{2L\sqrt{\epsilon_r}} \quad (14-4)$$

where  $v_0$  is the speed of light in free space. Since (14-4) does not account for fringing, it must be modified to include edge effects and should be computed using

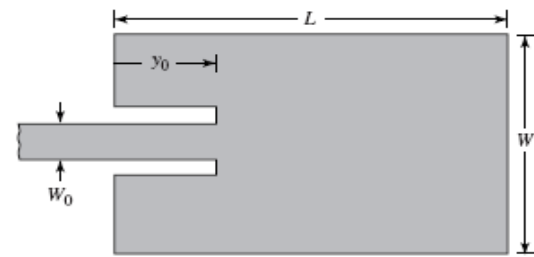
$$\begin{aligned} (f_{rc})_{010} &= \frac{1}{2L_{\text{eff}}\sqrt{\epsilon_{\text{reff}}}\sqrt{\mu_0\epsilon_0}} = \frac{1}{2(L + 2\Delta L)\sqrt{\epsilon_{\text{reff}}}\sqrt{\mu_0\epsilon_0}} \\ &= q \frac{1}{2L\sqrt{\epsilon_r}\sqrt{\mu_0\epsilon_0}} = q \frac{v_0}{2L\sqrt{\epsilon_r}} \end{aligned} \quad (14-5)$$

The  $q$  factor is called the *fringe factor* (length reduction factor). The designed resonant frequency, based on fringing, is lower as the patch looks longer.

### F. Matching Techniques

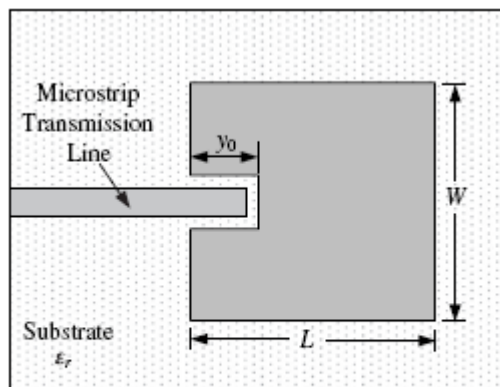
The resonant input resistance, is referenced at slot #1. However, it has been shown that the resonant input resistance can be changed by using an inset feed, recessed a distance  $y_0$  from slot #1, as shown in Fig.14.11(a). This technique can be used effectively to match the patch antenna using a microstrip-line feed when its characteristic impedance is known. The input resistance varies with the inset distance as given by Eq. 14-20a, where  $G_1$  and  $G_{12}$  are the slot conductance and mutual conductance respectively.

$$G_1 = \begin{cases} \frac{1}{90} \left(\frac{W}{\lambda_0}\right)^2 & W \ll \lambda_0 \\ \frac{1}{120} \left(\frac{W}{\lambda_0}\right) & W \gg \lambda_0 \end{cases} \quad (14-13)$$

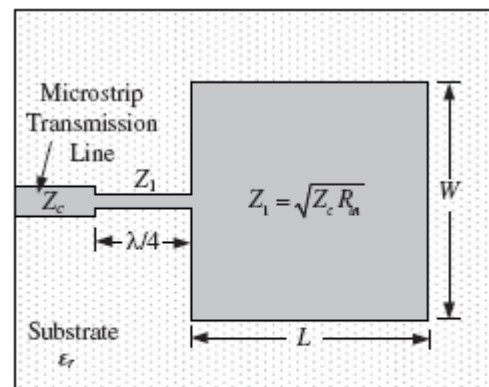


(a) Recessed microstrip-line feed

$$\begin{aligned} R_{in}(y = y_0) &= \frac{1}{2(G_1 \pm G_{12})} \cos^2\left(\frac{\pi}{L}y_0\right) \\ &= R_{in}(y = 0) \cos^2\left(\frac{\pi}{L}y_0\right) \end{aligned} \quad (14-20a)$$



(a) Coupled



(b)  $\lambda/4$  impedance transformer

**Figure 14.12** Alternate feeding techniques of microstrip antenna for impedance matching.

Fig. 14.12 shows two other alternative methods of matching with the patch antenna.

### C. Fields Radiated— $TM_{x010}$ Mode

To find the fields radiated by each slot, we follow a procedure similar to that used to analyze the aperture in Section 12.5.1. The total field is the sum of the two-element array with each element representing one of the two slots.

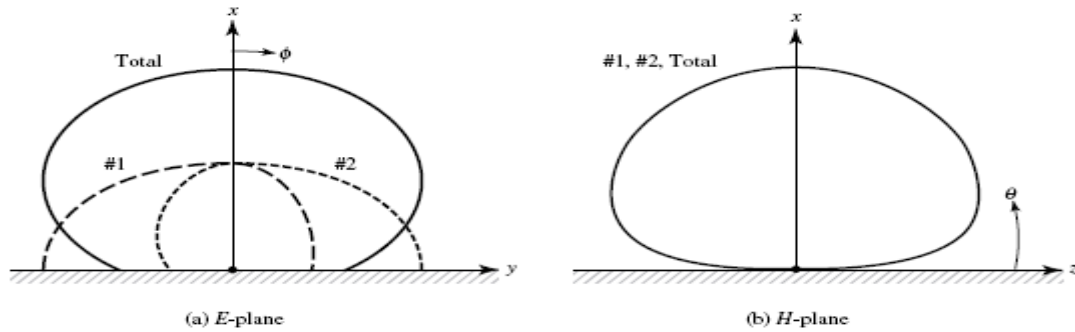


**Figure 14.19** Typical  $E$ - and  $H$ -plane patterns of each microstrip patch slot, and of the two together.

**$E$ -Plane ( $\theta = 90^\circ, 0^\circ \leq \phi \leq 90^\circ$  and  $270^\circ \leq \phi \leq 360^\circ$ )**

For the microstrip antenna, the  $x$ - $y$  plane ( $\theta = 90^\circ, 0^\circ \leq \phi \leq 90^\circ$  and  $270^\circ \leq \phi \leq 360^\circ$ ) is the principal  $E$ -plane. For this plane, the expressions for the radiated fields of (14-43)–(14-43b) reduce to

$$E_\phi^r = +j \frac{k_0 W V_0 e^{-jk_0 r}}{\pi r} \left\{ \frac{\sin\left(\frac{k_0 h}{2} \cos \phi\right)}{\frac{k_0 h}{2} \cos \phi} \right\} \cos\left(\frac{k_0 L_e}{2} \sin \phi\right) \quad (14-45)$$

**$H$ -Plane ( $\phi = 0^\circ, 0^\circ \leq \theta \leq 180^\circ$ )**

The principal  $H$ -plane of the microstrip antenna is the  $x$ - $z$  plane ( $\phi = 0^\circ, 0^\circ \leq \theta \leq 180^\circ$ ), and the expressions for the radiated fields of (14-43)–(14-43b) reduce to

$$E_\phi^r \simeq +j \frac{k_0 W V_0 e^{-jk_0 r}}{\pi r} \left\{ \sin \theta \frac{\sin\left(\frac{k_0 h}{2} \sin \theta\right) \sin\left(\frac{k_0 W}{2} \cos \theta\right)}{\frac{k_0 h}{2} \sin \theta \frac{k_0 W}{2} \cos \theta} \right\} \quad (14-46)$$

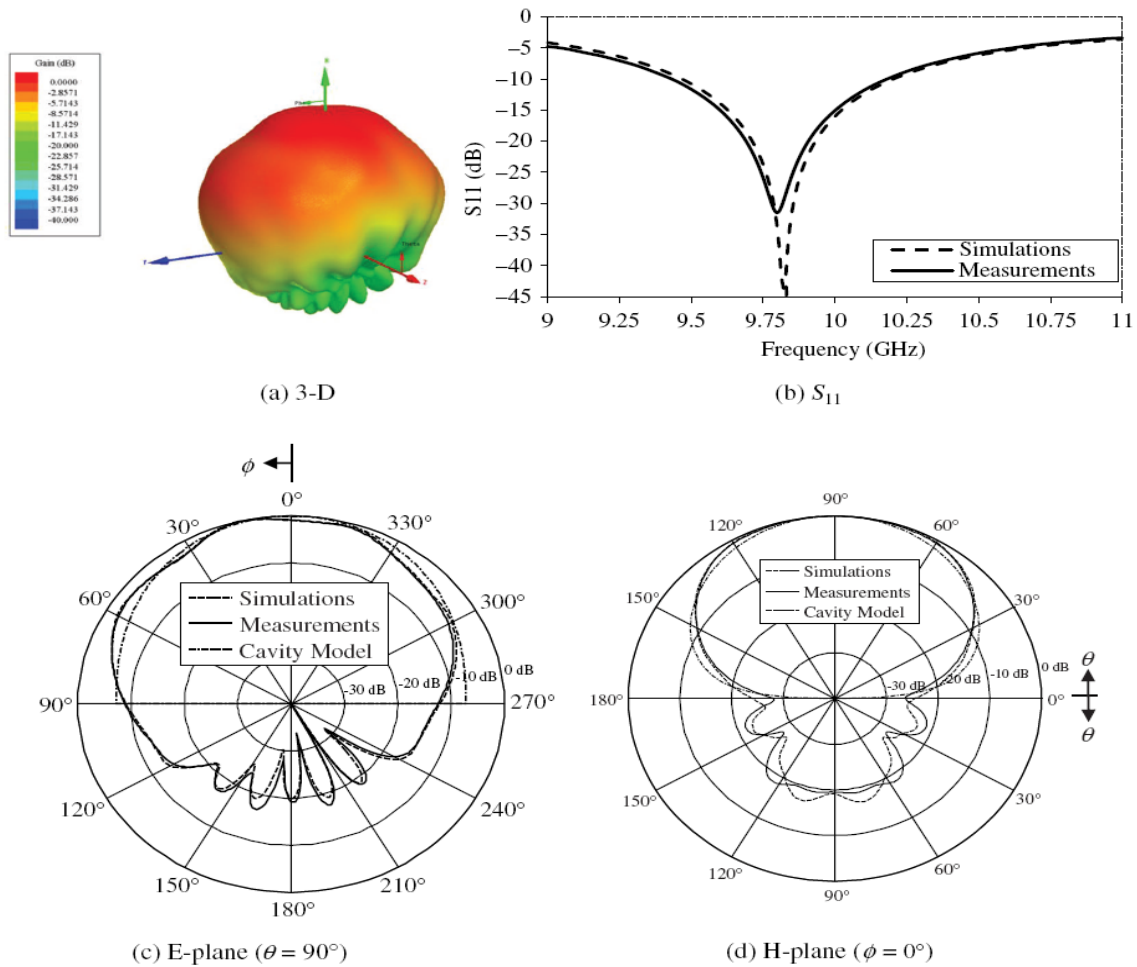


**Figure 14.21** Normalized 3D and 2D patterns and  $S_{11}$  of rectangular microstrip patch ( $L = 0.906$  cm,  $W = 1.186$  cm,  $h = 0.1588$  cm,  $y_0 = 0.203$  cm,  $\epsilon_r = 2.2$ ,  $f_0 = 9.8$  GHz).

**14.2.3 Directivity**

As for every other antenna, the directivity is one of the most important figures-of-merit whose definition is given by (2-16a) or

$$D_0 = \frac{U_{\max}}{U_0} = \frac{4\pi U_{\max}}{P_{\text{rad}}} \tag{14-50}$$

The directivity of one slot can be found, then the mutual conductance and array factor are taken into account to find the total directivity of the two slots. This is a long procedure.

Asymptotically the directivity of two slots (microstrip antenna) can be expressed as

$$D_2 = \begin{cases} 6.6(\text{dimensionless}) = 8.2 \text{ dB} & W \ll \lambda_0 \\ 8 \left( \frac{W}{\lambda_0} \right) & W \gg \lambda_0 \end{cases} \tag{14-57}$$

The directivity is not a strong function of the substrate height, as long as the height is maintained electrically small. About 2 dB difference is indicated between the directivity of one and two slots. A typical plot of the directivity of a patch for a fixed resonant frequency as a function of the substrate height ( $h/\lambda_0$ ), for two different dielectrics, is shown in Fig. 14.23.

-----

### Example 14.1

Design a rectangular microstrip antenna using a substrate (RT/duroid 5880) with dielectric constant of 2.2,  $h = 0.1588$  cm (0.0625 inches) so as to resonate at 10 GHz.

*Solution:* Using (14-6), the width  $W$  of the patch is

$$W = \frac{30}{2(10)} \sqrt{\frac{2}{2.2 + 1}} = 1.186 \text{ cm (0.467 in)}$$

The effective dielectric constant of the patch is found using (14-1), or

$$\epsilon_{\text{reff}} = \frac{2.2 + 1}{2} + \frac{2.2 - 1}{2} \left( 1 + 12 \frac{0.1588}{1.186} \right)^{-1/2} = 1.972$$

The extended incremental length of the patch  $\Delta L$  is, using (14-2)

$$\begin{aligned} \Delta L &= 0.1588(0.412) \frac{(1.972 + 0.3) \left( \frac{1.186}{0.1588} + 0.264 \right)}{(1.972 - 0.258) \left( \frac{1.186}{0.1588} + 0.8 \right)} \\ &= 0.081 \text{ cm (0.032 in)} \end{aligned}$$

The actual length  $L$  of the patch is found using (14-3), or

$$L = \frac{\lambda}{2} - 2\Delta L = \frac{30}{2(10)\sqrt{1.972}} - 2(0.081) = 0.906 \text{ cm (0.357 in)}$$

Finally the effective length is

$$L_e = L + 2\Delta L = \frac{\lambda}{2} = 1.068 \text{ cm (0.421 in)}$$

**Q 14.5** Design a rectangular microstrip patch with dimensions  $W$  and  $L$ , whose center frequency is 10 GHz. The dielectric constant of the substrate is 10.2 and the height of the substrate is 0.127 cm. Determine the physical dimensions  $W$  and  $L$  (in cm) of the patch, taking into account field fringing.

The relations used in the solution:

$$W = \frac{1}{2f_r \sqrt{\mu_0 \epsilon_0}} \sqrt{\frac{2}{\epsilon_r + 1}} = \frac{v_0}{2f_r} \sqrt{\frac{2}{\epsilon_r + 1}}$$

$$\epsilon_{\text{reff}} = \frac{\epsilon_r + 1}{2} + \frac{\epsilon_r - 1}{2} \left[ 1 + 12 \frac{h}{W} \right]^{-1/2}$$

$$\frac{\Delta L}{h} = 0.412 \frac{(\epsilon_{\text{reff}} + 0.3) \left( \frac{W}{h} + 0.264 \right)}{(\epsilon_{\text{reff}} - 0.258) \left( \frac{W}{h} + 0.8 \right)}$$

$$L = \frac{1}{2f_r \sqrt{\epsilon_{\text{reff}}} \sqrt{\mu_0 \epsilon_0}} - 2\Delta L$$

$$4-5. f_0 = 10 \text{ GHz}, \epsilon_r = 10.2, h = 0.05 \text{ in} = 0.127 \text{ cm}, W = \frac{30}{2 \cdot 10} \sqrt{\frac{2}{10.2 + 1}} = 0.634 \text{ cm}$$

$$\epsilon_{\text{reff}} = \frac{10.2 + 1}{2} + \frac{10.2 - 1}{2} \left[ 1 + 12 \left( \frac{0.127}{0.634} \right) \right]^{-1/2}, \frac{W}{h} = \frac{0.634}{0.127} = 4.992$$

$$= 8.093. \Delta L = (0.127)(0.412) \frac{(8.093 + 0.3) (4.992 + 0.264)}{(8.093 - 0.258) (4.992 + 0.8)} = 0.0509 \text{ cm}$$

$$L = \frac{30}{2(10)} \cdot \frac{1}{\sqrt{8.093}} - 2(0.0509) = 0.4255 \text{ cm},$$

$$W = 0.634 \text{ cm} = 0.2496 \text{ in} \\ L = 0.4255 \text{ cm} = 0.1675 \text{ in}$$

## LN -20 Reflector Antennas

### 15.1 INTRODUCTION

Reflector antennas have been in use since the discovery of electromagnetic wave propagation in 1888 by Hertz. World War II brought numerous radar applications which needed reflector antennas. Subsequent demands of reflectors for use in radio astronomy, microwave communication, and satellite tracking resulted in fast development of techniques to optimize the characteristics of reflector antennas. Reflector antennas take many geometrical configurations such as the plane, corner, and curved reflectors (especially the paraboloid), as shown in Fig. 15.1.

### 15.2 PLANE REFLECTOR

The simplest type of reflector is a plane reflector shown in Fig. 15.1(a). It has been clearly demonstrated that the polarization of the radiating source and its position relative to the reflecting surface can be used to control the radiating properties (pattern, impedance, directivity) of the overall system. Image theory has been used to analyze the radiating characteristics of such a system. Although the infinite dimensions of the plane reflector are idealized, the results can be used as approximations for electrically large surfaces.

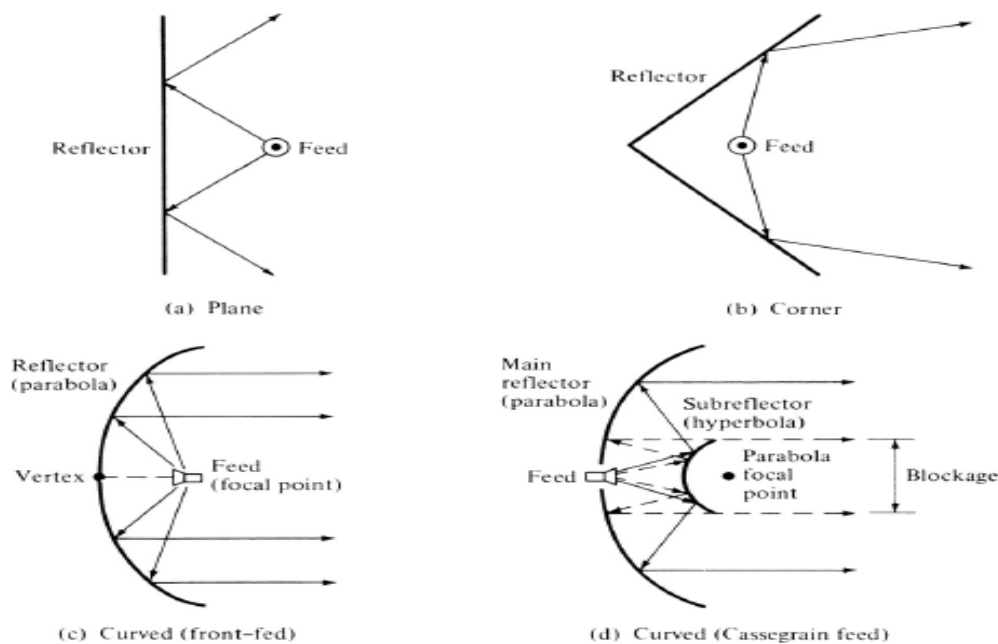


Figure 15.1 Geometrical configuration for some reflector systems.

### 15.3 CORNER REFLECTOR

To better collimate the energy in the forward direction, the shape of the plane reflector itself must be changed so as to prevent radiation in the back and side directions. One arrangement which accomplishes that consists of two plane reflectors joined so as to form a corner, as shown in Figs. 15.1(b) & 15.2(a), which is known as the corner reflector. Because of its simplicity in construction, it has many unique applications. The reflector is used as a passive target for radar or communication applications, where it will return the signal exactly in the same direction as it received it when its included angle is  $90^\circ$ . This is illustrated geometrically in Fig. 15.2(b).

In most practical applications, the included angle formed by the plates is usually  $90^\circ$ ; however other angles are sometimes used. To maintain a given system efficiency, the spacing between the vertex and the feed element must increase as the included angle of the reflector decreases, and vice versa. For reflectors with infinite sides, the gain increases as the included angle between the planes decreases. This, however, may not be true for finite size plates. However, since in practice the dimensions must be finite, guidelines on the size of the aperture ( $D_a$ ), length ( $l$ ), and height ( $h$ ) will be given.

The feed element for a corner reflector is almost always a dipole or an array of collinear dipoles placed parallel to the vertex a distance  $s$  away, as shown in a perspective view in Fig. 15.2(c).

Greater bandwidth is obtained when the feed elements are cylindrical or biconical dipoles instead of thin wires. In many applications, especially when the wavelength is large compared to tolerable physical dimensions, the surfaces of the corner reflector are frequently made of grid wires rather than solid sheet metal, as shown in Fig.15.2(d). One of the reasons for doing that is to reduce wind resistance and overall system weight. The spacing ( $g$ ) between wires is made a small fraction of a wavelength (usually  $g \leq \lambda/10$ ). For wires that are parallel to the length of the dipole, as is the case for the arrangement of Fig.15.2(d), the reflectivity of the grid-wire surface is as good as that of a solid surface.

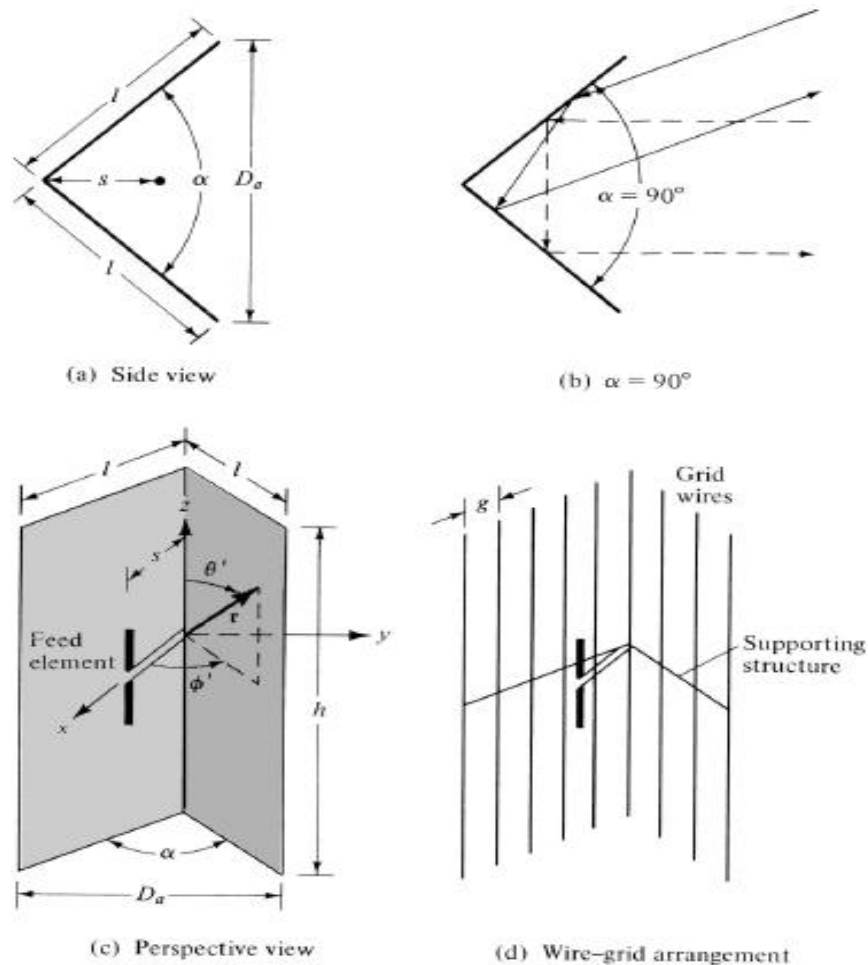


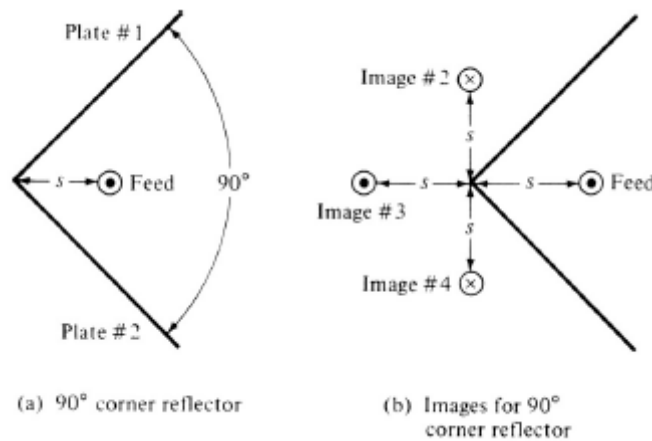
**Figure 15.2** Side and perspective views of solid and wire-grid corner reflectors.

In practice, the aperture of the corner reflector ( $D_a$ ) is usually made between one and two wavelengths ( $\lambda < D_a < 2\lambda$ ). The length of the sides of a  $90^\circ$  corner reflector is commonly taken to be about twice the distance from the vertex to the feed ( $l \approx 2s$ ). For reflectors with smaller included angles, the sides are made larger. The feed-to-vertex distance ( $s$ ) is usually taken to be between  $\lambda/3$  and  $2\lambda/3$  ( $\lambda/3 < s < 2\lambda/3$ ).

### 15.3.1 $90^\circ$ Corner Reflector

The first corner reflector to be analyzed is the one with an included angle of  $90^\circ$ . Because its radiation characteristics are the most attractive, it has become the most popular. Referring to the reflector of Figure 15.2(c) with its images in Figure 15.4(b), the total field of the system can be derived by summing the contributions from the feed and its images. Thus

$$\mathbf{E}(r, \theta, \phi) = \mathbf{E}_1(r_1, \theta, \phi) + \mathbf{E}_2(r_2, \theta, \phi) + \mathbf{E}_3(r_3, \theta, \phi) + \mathbf{E}_4(r_4, \theta, \phi) \quad (15-1)$$



$$\frac{E}{E_0} = AF(\theta, \phi) = 2[\cos(ks \sin \theta \cos \phi) - \cos(ks \sin \theta \sin \phi)] \quad (15-5)$$

Equation (15-5) represents not only the ratio of the total field to that of an isolated element at the origin but also the array factor of the entire reflector system. In the azimuthal plane ( $\theta = \pi/2$ ), Eq. (15-5) reduces to

$$\frac{E}{E_0} = AF(\theta = \pi/2, \phi) = 2[\cos(ks \cos \phi) - \cos(ks \sin \phi)] \quad (15-6)$$

Figure 15.5 shows the normalized patterns for an  $\alpha = 90^\circ$  corner reflector for spacings of  $s = 0.1\lambda$ ,  $0.7\lambda$ ,  $0.8\lambda$ ,  $0.9\lambda$ , and  $1.0\lambda$ . It is evident that for the small spacings the pattern consists of a single major lobe whereas multiple lobes appear for the larger spacings ( $s > 0.7\lambda$ ). For  $s = \lambda$  the pattern exhibits two lobes separated by a null along the  $\phi = 0^\circ$  axis.

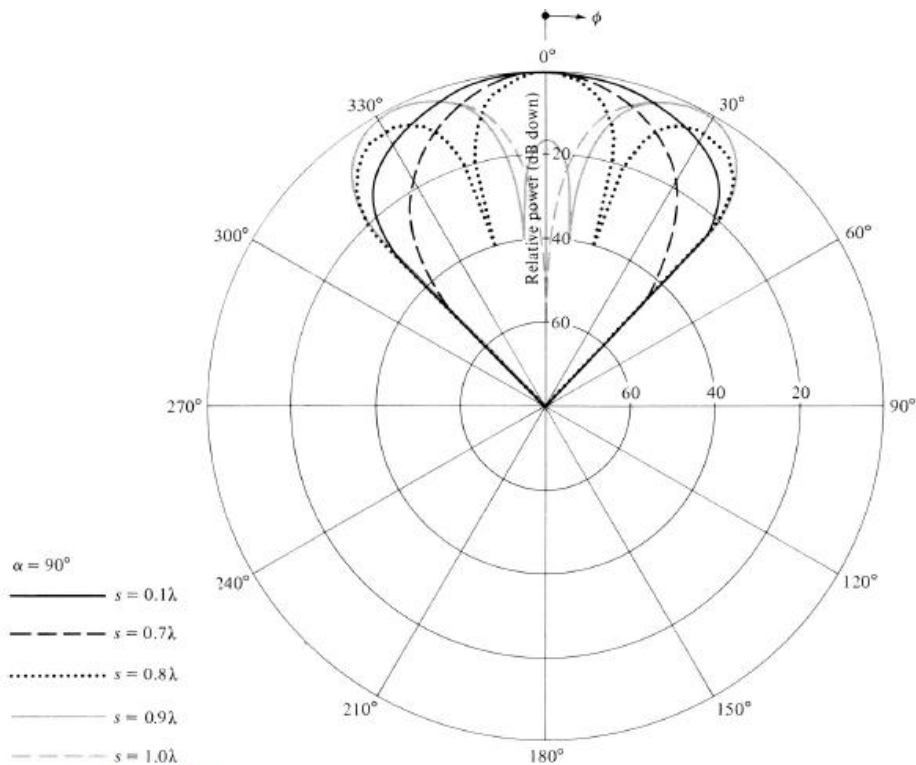


Figure 15.5 Normalized radiation amplitude patterns for  $\alpha = 90^\circ$  corner reflector.

## 15.4 PARABOLIC REFLECTOR

It has been shown by geometrical optics that if a beam of parallel rays is incident upon a reflector whose geometrical shape is a parabola, the radiation will converge (focus) at a spot which is known as the *focal point*. In the same manner, if a point source is placed at the focal point, the rays reflected by a parabolic reflector will emerge as a parallel beam. This is one form of the principle of reciprocity, and it is demonstrated geometrically in Fig. 15.1(c). The symmetrical point on the parabolic surface is known as the *vertex*. Rays that emerge in a parallel formation are usually said to be *collimated*.

Another arrangement that avoids placing the feed (transmitter and/or receiver) at the focal point is that shown in Fig. 15.1(d), and it is known as the *Cassegrain feed*. Through geometrical optics, Cassegrain, a famous astronomer (hence its name), showed that incident parallel rays can be focused to a point by utilizing two reflectors. To accomplish this, the main (primary) reflector must be a parabola, the secondary reflector (subreflector) a hyperbola, and the feed placed along the axis of the parabola usually at or near the vertex.

A parabolic reflector can take two different forms. One configuration is that of the parabolic right cylinder, shown in Fig. 15.8(a), whose energy is collimated at a line that is parallel to the axis of the cylinder through the focal point of the reflector. The most widely used feed for this type of a reflector is a linear dipole, a linear array, or a slotted waveguide. The other reflector configuration is that of Fig. 15.8(b) which is formed by rotating the parabola around its axis, and it is referred to as a *paraboloid* (parabola of revolution). A pyramidal or a conical horn has been widely utilized as a feed for this arrangement.

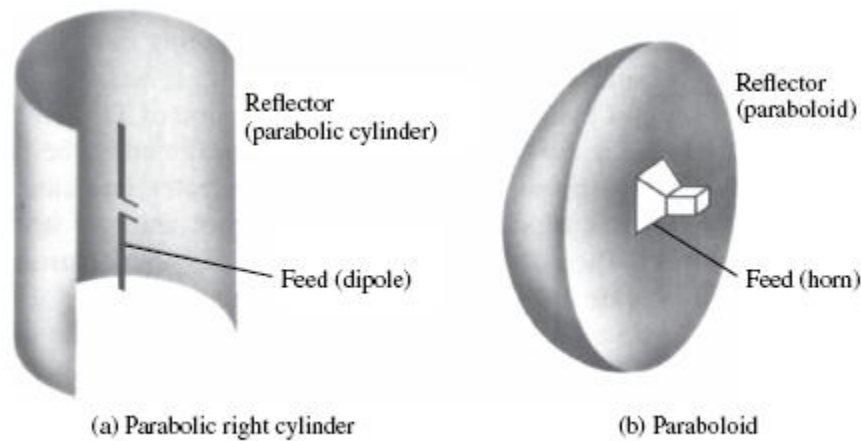


Figure 15.8 Parabolic right cylinder and paraboloid.

### 15.4.1 Front-Fed Parabolic Reflector

Parabolic cylinders have widely been used as high-gain apertures fed by line sources. The analysis of a parabolic cylinder (single curved) reflector is similar, but considerably simpler than that of a paraboloidal (double curved) reflector. The principal characteristics of aperture amplitude, phase, and polarization for a parabolic cylinder, as contrasted to those of a paraboloid, are as follows:

1. The amplitude taper, due to variations in distance from the feed to the surface of the reflector, is proportional to  $1/\rho$  in a cylinder compared to  $1/r^2$  in a paraboloid.
2. The focal region, where incident plane waves converge, is a line source for a cylinder and a point source for a paraboloid.
3. When the fields of the feed are linearly polarized parallel to the axis of the cylinder, no cross-polarized components are produced by the parabolic cylinder. That is not the case for a paraboloid.

Generally, parabolic cylinders, as compared to paraboloids, (1) are mechanically simpler to build, (2) provide larger aperture blockage, and (3) do not possess the attractive characteristics of a paraboloid.

#### A. Surface Geometry

The surface of a paraboloidal reflector is formed by rotating a parabola about its axis. Its surface must be a paraboloid of revolution so that rays emanating from the focus of the reflector are transformed into plane waves. The design is based on optical techniques, and it does not take into account any deformations (diffractions) from the rim of the reflector. Referring to Fig. 15.10 and choosing a plane perpendicular to the axis of the reflector through the focus, it follows that

$$OP + PQ = \text{constant} = 2f \quad (15-12)$$

Since

$$OP = r' \quad (15-13)$$

$$PQ = r' \cos \theta'$$

Eq. 15-12 can be written as

$$r'(1 + \cos \theta') = 2f \quad (15-14)$$

Or

$$r' = \frac{2f}{1 + \cos \theta'} = f \sec^2 \left( \frac{\theta'}{2} \right) \quad \theta \leq \theta_0 \quad (15-14a)$$

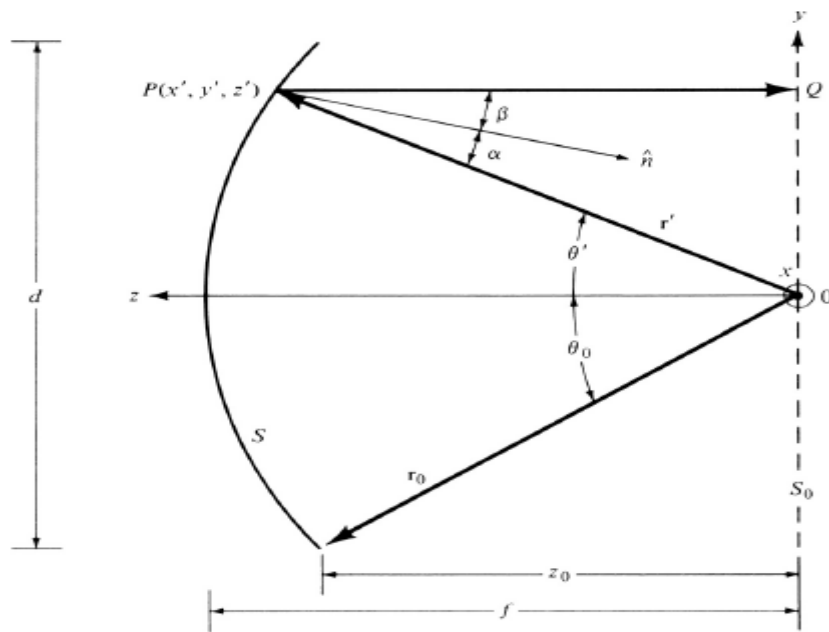


Figure 15.10 Two-dimensional configuration of a paraboloidal reflector.

The antenna directivity in the forward direction can be written as

$$D_0 = \left( \frac{\pi d}{\lambda} \right)^2 \left\{ \cot^2 \left( \frac{\theta_0}{2} \right) \left| \int_0^{\theta_0} \sqrt{G_f(\theta')} \tan \left( \frac{\theta'}{2} \right) d\theta' \right|^2 \right\} \quad (15-54)$$

Where  $G_f(\theta')$  is the gain function of the feed antenna.

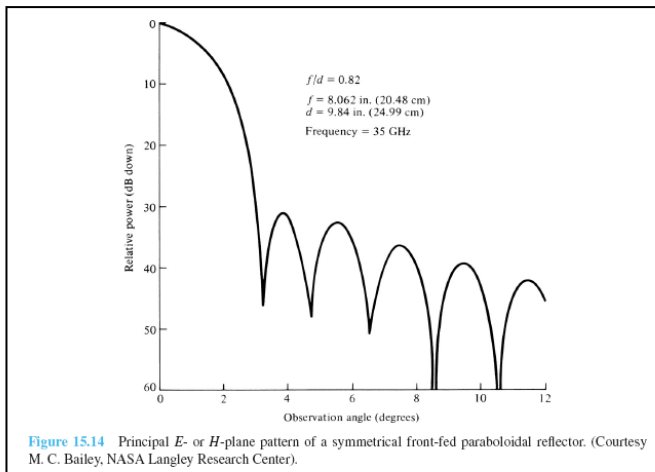


Figure 15.14 Principal E- or H-plane pattern of a symmetrical front-fed paraboloidal reflector. (Courtesy M. C. Bailey, NASA Langley Research Center).

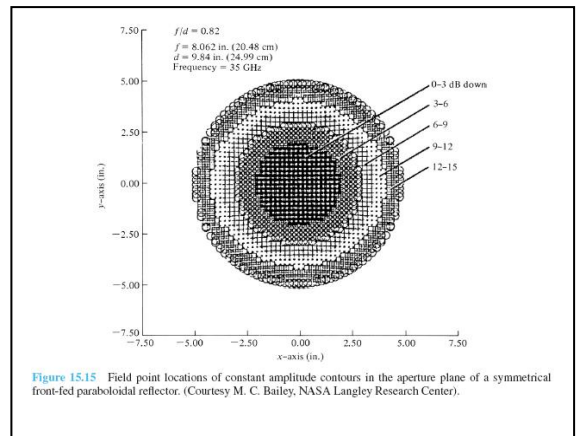


Figure 15.15 Field point locations of constant amplitude contours in the aperture plane of a symmetrical front-fed paraboloidal reflector. (Courtesy M. C. Bailey, NASA Langley Research Center).

1. A certain angular aperture or  $f/d$  ratio which leads to a maximum aperture efficiency, which is around 82–83%.
2. As the feed pattern becomes more directive the angular aperture of the reflector that leads to the maximum efficiency is smaller.

## Factors affecting parabolic reflector antenna gain

There are a number of factors that affect the parabolic antenna gain. These factors include the following:

- **Diameter of reflecting surface** The larger the diameter of the reflecting surface of the antenna the higher the parabolic reflector gain will be.
- **Operational wavelength:** The parabolic reflector antenna gain is dependent upon the reflector size in terms of wavelengths. Therefore, if the same reflector is used on two different frequencies, the gain will be different. It is inversely proportional to the wavelength being used.
- **Antenna efficiency:** The efficiency of the antenna has a significant effect on the overall parabolic reflector gain. Typical figures are between 50 and 70%. The efficiency varies as a result of a number of different factors which are detailed below.

## Parabolic reflector antenna gain

The parabolic antenna gain can easily be calculated from a knowledge of the diameter of the reflecting surface, the wavelength of the signal, and a knowledge or estimate of the efficiency of the antenna.

The parabolic reflector antenna gain is calculated as the gain over an isotropic source, i.e. relative to a source that radiates equally in all directions. This is a theoretical source that is used as the benchmark against which most antennas are compared. The standard formula for the parabolic reflector antenna gain is:

$$Gain (dB) = 10 \times \log_{10} k \left( \frac{\pi D}{\lambda} \right)^2$$

### Where:

G is the gain over an isotropic source in dB

k is the efficiency factor which is generally around 50% to 60%, i.e. 0.5 to 0.6

D is the diameter of the parabolic reflector in meters

$\lambda$  is the wavelength of the signal in meters

From this it can be seen that very large gains can be achieved if sufficiently large reflectors are used. However when the antenna has a very large gain, the beamwidth is also very small and the antenna requires very careful control over its position.

It can be seen that the parabolic reflector gain can be of the order of 50 dB for antennas that have a reflector diameter of a hundred wavelengths or more. Whilst antennas of this size would not be practicable for many antenna designs such as the Yagi, and many others, the parabolic reflector can be made very large in comparison to the wavelength and therefore it can achieve these enormous gain levels. More normal sizes for these antennas are a few wavelengths, but these are still able to provide very high levels of gain.

### **Parabolic reflector gain efficiency**

In the overall gain formula for the antenna, an efficiency factor is included. Typically this may be between 50 and 70% dependent upon the actual antenna.

The parabolic reflector antenna gain efficiency is dependent upon a variety of factors. These are all multiplied together to give the overall efficiency.

$$k = k_r k_t k_s k_b$$

***Radiation efficiency,  $k_r$ :*** The radiation efficiency is denoted as  $k_r$  above. It is governed by the resistive or Ohmic losses within the antenna. For most antennas this is high and close to unity. Therefore the radiation efficiency does not have a major effect on the parabolic reflector antenna gain and is normally ignored.

- ***Spillover Efficiency  $k_s$ :*** The spillover efficiency is denoted as  $k_s$  above. Any energy that spills over the edge of the reflector surface will reduce the efficiency and hence the parabolic reflector antenna gain. In the ideal case, the reflector surface needs to be equally and fully illuminated and none should spill over the

edge. In the real case this is not viable and some reduction in efficiency, and hence the antenna gain is experienced.

- **Aperture Taper Efficiency  $k_t$ :** The aperture taper efficiency is denoted as  $k_t$  above. It affects the antenna gain because the whole parabolic reflector needs to be properly illuminated for the optimum gain to be achieved. If parts of the surface are not optimally illuminated by the radiated energy from the radiator then the parabolic reflector gain will be reduced. The optimum performance is achieved when the centre is illuminated a little more than the edges.
- **Surface Error:** In order to provide the highest levels of parabolic reflector antenna gain, the surface must follow the parabolic contour as accurately as possible. Deviations from this will result in poor reflection accuracy.
- **Aperture Blockage:** The physical structure of the feed and other elements of the antenna often mask part of the reflector. This naturally reduces the efficiency and hence the antenna gain. This factor needs to be accommodated within the antenna gain calculation.

### **Parabolic antenna beamwidth calculation**

As the gain of the parabolic antenna, or any antenna, increases, so the beamwidth falls. It is possible to **estimate** the beamwidth reasonably accurately from the following formula.

$$\text{Beamwidth } \Psi = 70 \lambda/D$$

#### **Where:**

D is the diameter of the parabolic reflector

$\lambda$  is the wavelength of the signal

All dimensions must be in the same units for the calculation to be correct, e.g. both diameter and wavelength in meters, or both in feet, etc..



## LN-21 FRIIS and RADAR EQUATIONS

### 2.17 FRIIS TRANSMISSION EQUATION

The analysis and design of radar and communications systems often require the use of the *Friis Transmission Equation* and the *Radar Range Equation*.

#### 2.17.1 Friis Transmission Equation

The Friis Transmission Equation relates the power received to the power transmitted between two antennas separated by a distance  $R > 2D^2/\lambda$ , where  $D$  is the largest dimension of either antenna. Referring to Figure 2.31, let us assume that the transmitting antenna is initially isotropic. If the input power at the terminals of the transmitting antenna is  $P_t$ , then its isotropic power density  $W_0$  at distance  $R$  from the antenna is

$$W_0 = e_t \frac{P_t}{4\pi R^2} \quad (2-113)$$

where  $e_t$  is the radiation efficiency of the transmitting antenna. For a nonisotropic transmitting antenna, the power density of (2-113) in the direction  $\theta_t, \phi_t$  can be written as

$$W_t = \frac{P_t G_t(\theta_t, \phi_t)}{4\pi R^2} = e_t \frac{P_t D_t(\theta_t, \phi_t)}{4\pi R^2} \quad (2-114)$$

where  $G_t(\theta_t, \phi_t)$  is the gain and  $D_t(\theta_t, \phi_t)$  is the directivity of the transmitting antenna in the direction  $\theta_t, \phi_t$ . Since the effective area  $A_r$  of the receiving antenna is related to its efficiency  $e_r$  and directivity  $D_r$  by

$$A_r = e_r D_r(\theta_r, \phi_r) \left( \frac{\lambda^2}{4\pi} \right) \quad (2-115)$$

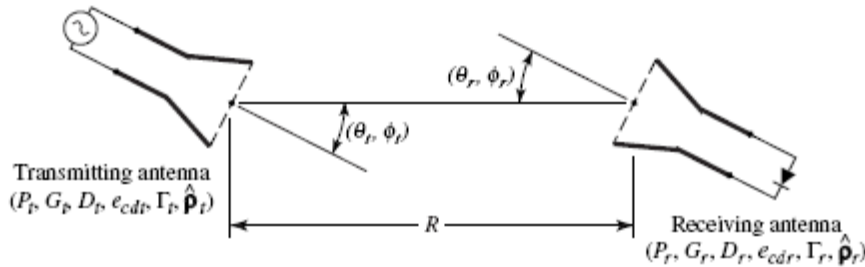


**Figure 2.31** Geometrical orientation of transmitting and receiving antennas for Friis transmission equation. the amount of power  $P_r$  collected by the receiving antenna can be written, using (2-114) and (2-115), as

$$P_r = e_r D_r(\theta_r, \phi_r) \frac{\lambda^2}{4\pi} W_t = e_t e_r \frac{\lambda^2 D_t(\theta_t, \phi_t) D_r(\theta_r, \phi_r) P_t}{(4\pi R)^2} |\hat{p}_t \cdot \hat{p}_r|^2 \quad (2-116)$$

or the ratio of the received to the input power as

$$\boxed{\frac{P_r}{P_t} = e_t e_r \frac{\lambda^2 D_t(\theta_t, \phi_t) D_r(\theta_r, \phi_r)}{(4\pi R)^2}} \quad (2-117)$$

The power received based on (2-117) assumes that the transmitting and receiving antennas are matched to their respective lines or loads (reflection efficiencies are unity) and the polarization of the receiving antenna is polarization-matched to the

impinging wave (polarization loss factor and polarization efficiency are unity). If these two factors are also included, then the ratio of the received to the input power of (2-117) is represented by

$$\frac{P_r}{P_t} = e_{cdt}e_{cdr}(1 - |\Gamma_t|^2)(1 - |\Gamma_r|^2)\left(\frac{\lambda}{4\pi R}\right)^2 D_t(\theta_t, \phi_t)D_r(\theta_r, \phi_r)|\hat{\rho}_t \cdot \hat{\rho}_r|^2 \quad (2-118)$$

For reflection and polarization-matched antennas aligned for maximum directional radiation and reception, (2-118) reduces to

$$\frac{P_r}{P_t} = \left(\frac{\lambda}{4\pi R}\right)^2 G_{0t}G_{0r} \quad (2-119)$$

Eqs. (2-117), (2-118), or (2-119) are known as the *Friis Transmission Equation*, and it relates the power  $P_r$  (delivered to the receiver load) to the input power of the transmitting antenna  $P_t$ . The term  $(\lambda/4\pi R)^2$  is called the *free-space loss factor*, and it takes into account the losses due to the spherical spreading of the energy by the antenna.

### Example 2.16

Two *lossless* X-band (8.2–12.4 GHz) horn antennas are separated by a distance of  $100\lambda$ . The reflection coefficients at the terminals of the transmitting and receiving antennas are 0.1 and 0.2, respectively. The maximum directivities of the transmitting and receiving antennas (over isotropic) are 16 dB and 20 dB, respectively. Assuming that the input power in the lossless transmission line connected to the transmitting antenna is 2 W, and the antennas are aligned for maximum radiation between them and are polarization-matched, find the power delivered to the load of the receiver.

*Solution:* For this problem

$$e_{cdt} = e_{cdr} = 1 \text{ because the antennas are lossless.}$$

$$|\hat{\rho}_t \cdot \hat{\rho}_r|^2 = 1 \text{ because the antennas are polarization-matched}$$

$$\left. \begin{array}{l} D_t = D_{0t} \\ D_r = D_{0r} \end{array} \right\} \text{ because the antennas are aligned for} \\ \text{maximum radiation between them}$$

$$D_{0t} = 16 \text{ dB} \Rightarrow 39.81 \text{ (dimensionless)}$$

$$D_{0r} = 20 \text{ dB} \Rightarrow 100 \text{ (dimensionless)}$$

Using (2-118), we can write

$$\begin{aligned} P_r &= [1 - (0.1)^2][1 - (0.2)^2][\lambda/4\pi(100\lambda)]^2(39.81)(100)(2) \\ &= 4.777 \text{ mW} \end{aligned}$$

### 2.17.2 Radar Range Equation

In radar application, the transmitted power is incident upon a target, as shown in Fig.2.32. The *radar cross section* or *echo area* ( $\sigma$ ) of a target which is defined as *the area intercepting that amount of power which, when scattered isotropically, produces at the receiver a density which is equal to that scattered by the actual target*. In equation form

$$\lim_{R \rightarrow \infty} \left[ \frac{\sigma W_i}{4\pi R^2} \right] = W_s \quad (2-120)$$

Or

$$\begin{aligned} \sigma &= \lim_{R \rightarrow \infty} \left[ 4\pi R^2 \frac{W_s}{W_i} \right] = \lim_{R \rightarrow \infty} \left[ 4\pi R^2 \frac{|\mathbf{E}^s|^2}{|\mathbf{E}^i|^2} \right] \\ &= \lim_{R \rightarrow \infty} \left[ 4\pi R^2 \frac{|\mathbf{H}^s|^2}{|\mathbf{H}^i|^2} \right] \end{aligned} \quad (2-120a)$$

Where

$\sigma$  = radar cross section or echo area (m<sup>2</sup>)

$R$  = observation distance from target (m)

$W_i$  = incident power density (W/m<sup>2</sup>)

$W_s$  = scattered power density (W/m<sup>2</sup>)

$\mathbf{E}^i$  ( $\mathbf{E}^s$ ) = incident (scattered) electric field (V/m)

$\mathbf{H}^i$  ( $\mathbf{H}^s$ ) = incident (scattered) magnetic field (A/m)

Using the definition of radar cross section, we can consider that the transmitted power incident upon the target is initially captured and then it is reradiated isotropically, insofar as the receiver is concerned. The amount of captured power  $P_c$  is obtained by multiplying the incident power density of (2-114) by the radar cross section  $\sigma$ , or

$$P_c = \sigma W_t = \sigma \frac{P_t G_t(\theta_t, \phi_t)}{4\pi R_1^2} = e_t \sigma \frac{P_t D_t(\theta_t, \phi_t)}{4\pi R_1^2} \quad (2-121)$$

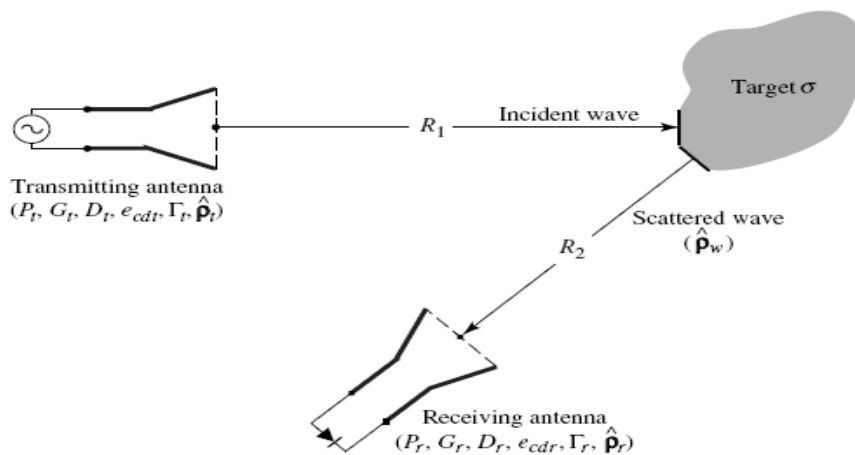


Figure 2.32 Geometrical arrangement of transmitter, target, and receiver for radar range equation.

The power captured by the target is reradiated isotropically, and the scattered power density can be written as

$$W_s = \frac{P_c}{4\pi R_2^2} = e_{cdt}\sigma \frac{P_t D_t(\theta_t, \phi_t)}{(4\pi R_1 R_2)^2} \quad (2-122)$$

The amount of power delivered to the receiver load is given by

$$P_r = A_r W_s = e_{cdt} e_{cdr} \sigma \frac{P_t D_t(\theta_t, \phi_t) D_r(\theta_r, \phi_r)}{4\pi} \left( \frac{\lambda}{4\pi R_1 R_2} \right)^2 \quad (2-123)$$

where  $A_r$  is the effective area of the receiving antenna as defined by (2-115).

Equ. (2-123) can be written as the ratio of the received power to the input power, or

$$\frac{P_r}{P_t} = e_{cdt} e_{cdr} \sigma \frac{D_t(\theta_t, \phi_t) D_r(\theta_r, \phi_r)}{4\pi} \left( \frac{\lambda}{4\pi R_1 R_2} \right)^2 \quad (2-124)$$

Expression (2-124) is used to relate the received power to the input power, and it takes into account only conduction-dielectric losses (radiation efficiency) of the transmitting and receiving antennas. It does not include reflection losses (reflection efficiency) and polarization losses (polarization loss factor or polarization efficiency). If these two losses are also included, then (2-124) must be expressed as

$$\frac{P_r}{P_t} = e_{cdt} e_{cdr} (1 - |\Gamma_t|^2) (1 - |\Gamma_r|^2) \sigma \frac{D_t(\theta_t, \phi_t) D_r(\theta_r, \phi_r)}{4\pi} \times \left( \frac{\lambda}{4\pi R_1 R_2} \right)^2 |\hat{\rho}_w \cdot \hat{\rho}_r|^2 \quad (2-125)$$

where

$\hat{\rho}_w$  = polarization unit vector of the scattered waves

$\hat{\rho}_r$  = polarization unit vector of the receiving antenna

For polarization-matched antennas aligned for maximum directional radiation and reception, (2-125) reduces to

$$\frac{P_r}{P_t} = \sigma \frac{G_{0t} G_{0r}}{4\pi} \left[ \frac{\lambda}{4\pi R_1 R_2} \right]^2 \quad (2-126)$$

Equ. (2-124), or (2-125) or (2-126) is known as the *Radar Range Equation*. It relates the power  $P_r$  (delivered to the receiver load) to the input power  $P_t$  transmitted by an antenna, after it has been scattered by a target with a radar cross section (echo area) of  $\sigma$ .

**How to maximize the ratio  $P_r/P_t$  ?**

Transmitting and receiving antennas operating at 1 GHz with gains of 20 and 15 dB, respectively, are separated by a distance of 1 km. Find the power delivered to the load when the input power is 150 mW. Assume the Polarization Loss Factor PLF = 1.

$$\frac{P_r}{P_t} = |\hat{p}_t \cdot \hat{p}_r|^2 \left(\frac{\lambda}{4\pi R}\right)^2 G_{ot} G_{or}$$

$$G_{ot} = 20 \text{ dB} \Rightarrow G_{ot} \text{ (power ratio)} = 10^2 = 100$$

$$G_{or} = 15 \text{ dB} \Rightarrow G_{or} \text{ (power ratio)} = 10^{1.5} = 31.623$$

$$f = 1 \text{ GHz} \Rightarrow \lambda = 0.3 \text{ meters}$$

$$R = 1 \times 10^3 \text{ meters}$$

$$\text{For } |\hat{p}_t \cdot \hat{p}_r|^2 = 1$$

$$P_r = \left(\frac{0.3}{4\pi \times 10^3}\right)^2 (100)(31.623)(150 \times 10^{-3}) = 270.344 \mu \text{ Watts}$$

Two lossless, polarization-matched antennas are aligned for maximum radiation between them, and are separated by a distance of  $50\lambda$ . The antennas are matched to their transmission lines and have directivities of 20 dB. Assuming that the power at the input terminals of the transmitting antenna is 10 W, find the power at the terminals of the receiving antenna.

$$\text{Lossless: } e_{cd} = 1, \text{ polarization matched: } |\hat{p}_w \cdot \hat{p}_a|^2 = 1,$$

$$\text{line matched: } (1 - |\Gamma|^2) = 1$$

$$D_o = 20 \text{ dB} = 10^2 = 100 = D_{or} = D_{ot}$$

$$P_r = P_t \left(\frac{\lambda}{4\pi R}\right)^2 D_{ot} D_{or} = 10 \left(\frac{\lambda}{4\pi \cdot 50\lambda}\right)^2 (100)(100) = 0.253 \text{ Watts}$$

$$P_r = 0.253 \text{ Watts}$$

A radar antenna, used for both transmitting and receiving, has a gain of 150 at its operating frequency of 5 GHz. It transmits 100 kW, and is aligned for maximum directional radiation and reception to a target 1000 km away having a radar cross section of  $3 \text{ m}^2$ . The received signal matches the polarization of the transmitted signal. Find the received power.

$$P_r = P_t \sigma \cdot \frac{G_{ot} \cdot G_{or}}{4\pi} \cdot \left[\frac{\lambda}{4\pi R_1 \cdot R_2}\right]^2, \quad \lambda = \frac{3 \times 10^8}{5 \times 10^9} = 0.06 \text{ m}$$

$$P_r = 10^5 \cdot (3) \cdot \frac{150^2}{4\pi} \cdot \left[\frac{0.06}{4\pi (10^6)}\right]^2$$

$$P_r = 1.22 \times 10^{-8} \text{ Watts}$$

A rectangular X-band horn, with aperture dimensions of 5.5 cm and 7.4 cm and a gain of 16.3 dB (over isotropic) at 10 GHz, is used to transmit and receive energy scattered from a perfectly conducting sphere of radius  $a = 5\lambda$ . Find the maximum scattered power delivered to the load when the distance between the horn and the sphere is (a)  $200\lambda$ , (b)  $500\lambda$ . Assume that the input power is 200 mW, and the radar cross section is equal to the geometrical cross section.

$$\sigma = \pi a^2 = 25\pi\lambda^2$$

$$G_{\text{ot}} = G_{\text{or}} = 16.3 \text{ dB} \Rightarrow G_{\text{ot}} (\text{power ratio}) = 10^{1.63} = 42.66$$

$$f = 10 \text{ GHz} \Rightarrow \lambda = 0.03 \text{ m}$$

$$\frac{P_r}{P_t} = \sigma \frac{G_{\text{ot}} \cdot G_{\text{or}}}{4\pi} \left( \frac{\lambda}{4\pi R_1 R_2} \right)^2$$

$$R_1 = R_2 = 200\lambda = 6 \text{ meters};$$

$$P_r = 25\pi\lambda^2 \cdot \frac{(42.66)^2}{4\pi} \cdot \left[ \frac{\lambda}{4\pi(200\lambda)^2} \right]^2 \cdot (0.2) = 9.00 \text{ n watts}$$

$$R_1 = R_2 = 500\lambda = 15 \text{ meters};$$

$$P_r = 0.23 \text{ n watts}$$

-----  
 In a long-range microwave communication system operating at 9 GHz, the transmitting and receiving antennas are identical, and they are separated by 10,000 m. To meet the signal-to noise ratio of the receiver, the received power must be at least  $10 \mu\text{W}$ . Assuming the two antennas are aligned for maximum reception to each other, including being polarization matched, what should the gains (in dB) of the transmitting and receiving antennas be when the input power to the transmitting antenna is 10 W ?

$$\frac{P_r}{P_t} = \left( \frac{\lambda}{4\pi R} \right)^2 \cdot G_{\text{ot}} \cdot G_{\text{or}}, \quad \lambda = \frac{3 \times 10^8}{9 \times 10^9} = \frac{3 \times 10^8}{90 \times 10^8} = \frac{1}{30}$$

$$R = 10,000 \text{ meter} = \frac{10,000}{1/30} \lambda = 3 \times 10^5 \lambda$$

$$\frac{P_r}{P_t} = \left[ \frac{\lambda}{4\pi(3 \times 10^5 \lambda)} \right]^2 \cdot G_0^2 = \frac{10 \times 10^{-6}}{10} = 10^{-6}$$

$$G_0^2 = 10^{-6} (4\pi \times 3 \times 10^5)^2$$

$$G_0 = 10^{-3} (4\pi \times 3 \times 10^5) = 12\pi \times 10^2 = 1200\pi$$

$$G_0 = 1200\pi = 3,769.91 = 10 \log_{10}(3,769.91) \text{ dB}$$

$$G_0 = 3,769.91 = 35.76 \text{ dB}$$

6.1 ANTENNAS LOCATED OVER A FLAT EARTH

The general features of the interference phenomena associated with antennas placed over the earth can be determined by studying the effects associated with antennas located above a flat earth. Figure 6.1 shows a transmitting antenna at height  $h_1$  and a receiving antenna at height  $h_2$ , with separation  $d$ . The figure also shows the direct ray and indirect or reflected ray that reach the receiving antenna. When the two path lengths  $R_1$  and  $R_2$  differ by an appropriate amount there may be either constructive or destructive interference at the receiving antenna.

With reference to Fig. 6.1, the field that reaches the receiving antenna directly will produce a voltage proportional to

$$f_1(\theta_1)f_2(\theta'_1) \frac{e^{-jk_0R_1}}{4\pi R_1}$$

where  $f_1$  and  $f_2$  are the radiation field strength patterns of the two antennas. The voltage produced by the indirect wave is proportional to

$$f_1(\theta_2)f_2(\theta'_2)\rho e^{j\phi} \frac{e^{-jk_0R_2}}{4\pi R_2}$$

where  $\rho e^{j\phi}$  is the reflection coefficient at the ground. In the usual situation  $h_1$  and  $h_2$  are very small compared with the separation  $d$ , so the angles  $\theta_1$ ,  $\theta_2$ ,  $\theta'_1$ ,  $\theta'_2$  are very small, and the antenna radiation patterns can be assumed constant over the range of angles involved. An exception would be the case when highly

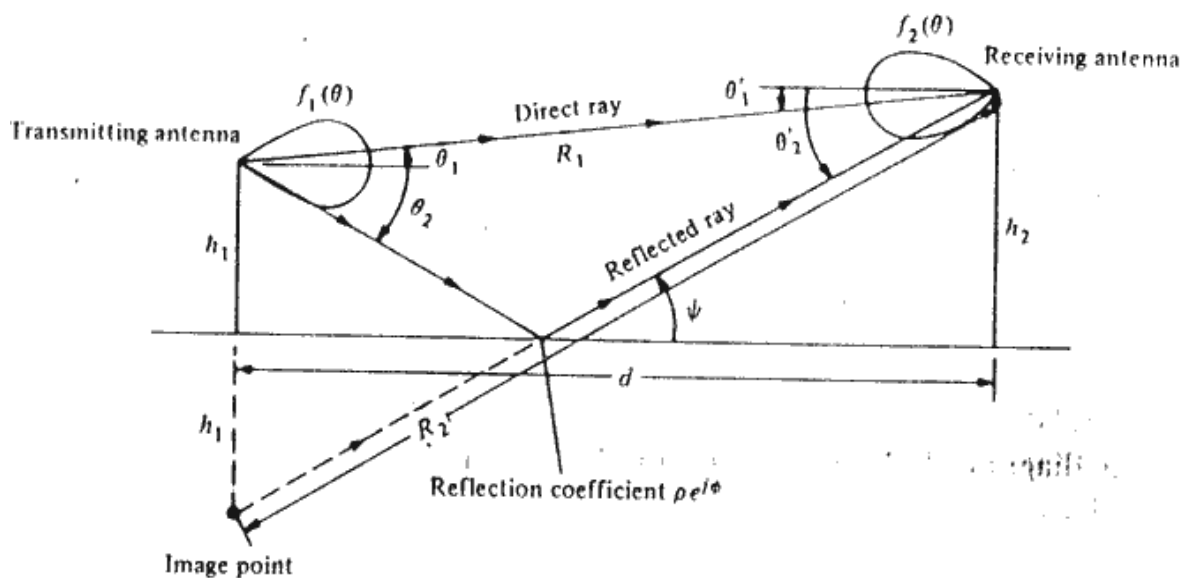


Figure 6.1 Illustration of direct and reflected rays.

directive antennas are used and  $h_2$  is large, such as occurs if the transmitting antenna is located on the ground and the receiving antenna is located aboard a high-flying aircraft. In this case very little power might be radiated toward the ground; that is  $f_1(\theta_2) \ll f_1(\theta_1)$ . The total received voltage will be proportional to (we use  $R_2 \approx R_1$  in the denominator)

$$\left| f_1(\theta_1)f_2(\theta'_1) \frac{e^{-jk_0R_1}}{4\pi R_1} \left[ 1 + \rho e^{j\phi} \frac{f_1(\theta_2)f_2(\theta'_2)}{f_1(\theta_1)f_2(\theta'_1)} e^{-jk_0(R_2-R_1)} \right] \right| = \left| f_1(\theta_1)f_2(\theta'_1) \frac{e^{-jk_0R_1}}{4\pi R_1} \right| F \quad (6.1)$$

The factor  $F$ , called the *path-gain factor*, shows how the field at the receiving antenna differs from the value it would have under free-space propagation conditions. When it can be assumed that  $f_1(\theta_2) \approx f_1(\theta_1)$  and  $f_2(\theta'_2) \approx f_2(\theta'_1)$ , then  $F$  can be expressed as

$$F = |1 + \rho e^{j\phi - jk_0(R_2-R_1)}| \quad (6.2)$$

The path-gain factor is the array factor associated with the antenna at height  $h_1$  and its image below the surface, with the relative excitation of the image antenna being  $\rho e^{j\phi}$ .

With reference to Fig. 6.1, it can be seen that  $R_1 = [d^2 + (h_2 - h_1)^2]^{1/2}$  and  $R_2 = [d^2 + (h_1 + h_2)^2]^{1/2}$ . When  $h_1$  and  $h_2$  are very small compared with  $d$ , a binomial expansion gives

$$R_1 \approx d + \frac{1}{2} \frac{(h_2 - h_1)^2}{d} \quad R_2 \approx d + \frac{1}{2} \frac{(h_2 + h_1)^2}{d}$$

from which we obtain

$$R_2 - R_1 = \frac{2h_1h_2}{d}$$

If  $\rho e^{j\phi}$  were equal to  $-1$  then

$$F = |1 - e^{-jk_0 2h_1h_2/d}| = 2 \left| \sin \frac{k_0 h_1 h_2}{d} \right| \quad (6.3)$$

This shows that interference effects can lead to a doubling of the field strength relative to its value under free-space conditions. With reference to Fig. 6.2 we let  $\psi_0$  be the elevation angle given by  $\tan \psi_0 = h_2/d$  so that Eq. (6.3) can be written as

$$F = 2|\sin(k_0 h_1 \tan \psi_0)| \quad (6.4)$$

The relationship expressed by Eq. (6.4) is usually plotted in the form of a coverage diagram showing the variation of  $F$  with  $h_2$  and  $d$ , that is, with  $\psi_0$ , for given values of  $h_1$  and  $\lambda_0$  expressed as a ratio  $h_1/\lambda_0$ . Note that  $F$  is a maximum when

$$\tan \psi_0 = \frac{1}{k_0 h_1} \left( \frac{\pi}{2} + n\pi \right) = \frac{\lambda_0}{h_1} \left( \frac{1}{4} + \frac{n}{2} \right) \quad n = 0, 1, 2, \dots \quad (6.5a)$$

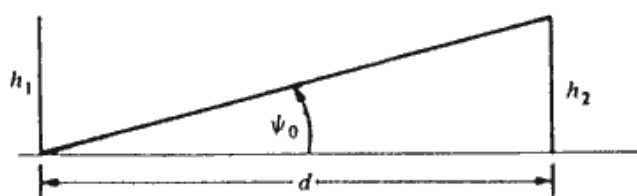


Figure 6.2 Elevation angle  $\psi_0$ .

and is a minimum when

$$\tan \psi_0 = \frac{\lambda_0 n}{h_1 2} \quad n = 0, 1, 2, \dots \quad (6.5b)$$

A coverage diagram is a plot of the relative field strength as a function of direction in space from the transmitting antenna. It is analogous to the field-strength radiation pattern of an antenna. In any coverage diagram the fixed parameters are the height  $h_1$  of the transmitting antenna and the wavelength  $\lambda_0$ . The distance  $d$  to the location of the receiving antenna and the height  $h_2$  of the receiving antenna are variable parameters, and each pair of values  $h_2, d$  determines a point in space. The coverage diagram is a plot of the curves  $F/r = \text{constant}$  in the  $h_2 d$  plane. In most situations the direct line-of-sight distance  $r$  between antennas is very nearly equal to the horizontal distance  $d$ . The various curves of  $F/r$  that are plotted are usually chosen to represent the same signal level that would be obtained at a distance of a multiple or a fractional multiple of a convenient free-space reference range  $r_f$ ; for example,  $F/r = m/r_f$  or  $F = mr/r_f \approx md/r_f$ , with  $m = 1, \sqrt{2}, 2, \dots$  or  $1/\sqrt{2}, 1/2, \dots$ . The difference in signal level between successive curves is then 3 dB. By using Eq. (6.3) we find that the constant signal level curves are given by (we assume that  $r \approx d$ )

$$F = 2 \left| \sin \frac{k_0 h_1 h_2}{d} \right| = m \frac{d}{d_f} \quad (6.6a)$$

when the reflection coefficient equals  $-1$ . For the flat-earth case it is more convenient to use Eq. (6.4) or (6.5) which gives

$$2|\sin k_0 h_1 \tan \psi_0| \approx 2|\sin k_0 h_1 \psi_0| = m \frac{d}{d_f} \quad (6.6b)$$

In this equation  $d$  can be treated as the radial coordinate and  $\psi_0$  as the angle coordinate in a polar-coordinate reference frame. However, note that since the vertical scale representing  $h_2$  is usually expanded relative to that for  $d$ , the angle  $\psi_0$  appears much larger than it actually is.

Whenever  $h_1 \gg \lambda_0$  and  $n$  is small,  $\tan \psi_0 \approx \psi_0$  and the above relations show that the lobe structure is very fine; i.e., the angular separation between lobes is very small. For example, if  $h_1 = 100\lambda_0$ , then the lobes are separated by  $\lambda_0/2h_1 = 1/200$  rad, or by approximately  $0.3^\circ$ . Figure 6.3 shows a typical coverage diagram. If  $r_f$  is the free-space range for a given received signal strength, then with interference taken into account the maximum range is  $2r_f$ , which corresponds to a horizontal distance  $d = 2r_f \cos \psi_0$ . For small values of  $\psi_0$

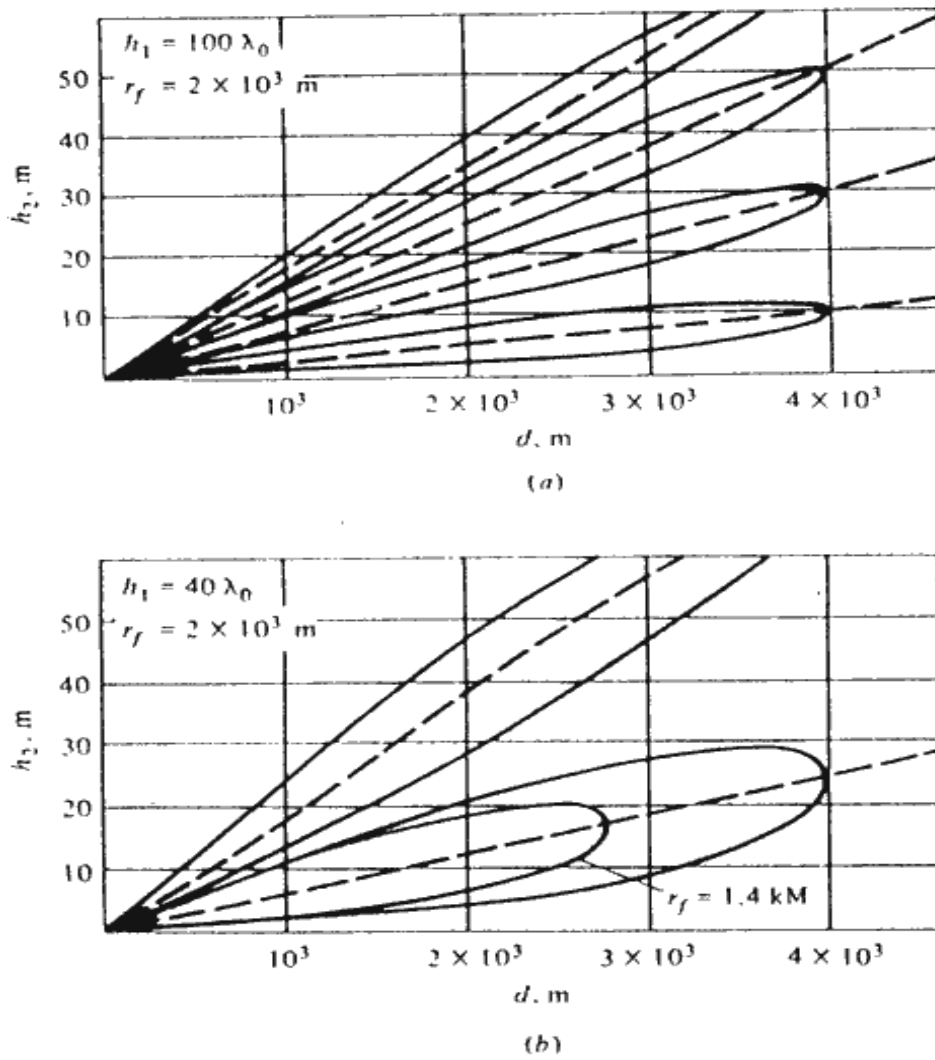


**Figure 6.3** Coverage diagrams for a flat earth with reflection coefficient equal to  $-1$ .

we have  $d \approx 2r_f$ . The curves corresponding to  $d = 2r_f \cos \psi_0$  appear as vertical lines in Fig. 6.3 because of the greatly expanded vertical scale. The coverage diagrams shown in Fig. 6.3 are plotted for a free-space propagation distance of 2 km. Any pair of values of  $h_2$  and  $d$  that lies on the curve describing a lobe represents a point in space where the received signal strength is the same as it would be at a distance of 2 km under free-space propagation conditions. The smaller lobe shown in Fig. 6.3b represents a constant signal level 3 dB greater than that of the larger lobe and comes from using  $m = \sqrt{2}$  in Eq. (6.6b).

When the coverage diagram has been plotted it is a simple matter to determine the field strength at the receiving antenna relative to the free-space value. For example, if the receiving antenna height is 10 m, Fig. 6.3b shows that the received signal strength at a distance of 3.2 km is the same as that at 2 km under free-space conditions. The same figure shows that by raising the antenna height to 25 m at a distance of 4 km a maximum signal level will be received. This signal level will be the same as that at 2 km with free-space propagation.

When the angle  $\psi_0$  is considerably below the first lobe maximum, Eq. (6.4)

can be approximated by  $2k_0 h_1 \psi_0$ , so

$$F = 2k_0 h_1 \psi_0 = \frac{2k_0 h_1 h_2}{d} \quad (6.7)$$

which makes the received signal voltage vary as the inverse square of the distance, thus reducing the maximum useful range quite severely.

The coverage diagrams shown in Fig. 6.3 are based on taking  $\rho = 1$ ,  $\phi = \pi$ . In practice this is a good approximation for the reflection coefficient for both horizontal and vertical polarization when the grazing angle  $\psi$  is small, say,  $1^\circ$  or less. When  $\psi$  is larger than  $1^\circ$ ,  $\rho e^{j\phi}$  may depart appreciably from  $-1$  for vertical polarization but may still be approximated by  $-1$  for horizontal polarization for values of  $\psi$  up to  $10^\circ$  or more.

The reflection coefficient  $\rho e^{j\phi}$  is given by the Fresnel expressions for the reflection coefficients for a plane TEM wave polarized with the electric field in the plane of incidence (vertical polarization) and for a wave polarized with the electric field perpendicular to the plane of incidence (horizontal polarization). The Fresnel reflection coefficients depend on the ground conductivity, permittivity, frequency, and angle of incidence. If the ground conductivity is  $\sigma$ , the permittivity  $\epsilon$  is  $\kappa\epsilon_0$ , and  $\psi$  is the grazing angle of incidence, then

$$\rho e^{j\phi} = \frac{(\kappa - j\chi) \sin \psi - \sqrt{(\kappa - j\chi) - \cos^2 \psi}}{(\kappa - j\chi) \sin \psi + \sqrt{(\kappa - j\chi) - \cos^2 \psi}} \quad \text{vertical polarization} \quad (6.8a)$$

$$\rho e^{j\phi} = \frac{\sin \psi - \sqrt{(\kappa - j\chi) - \cos^2 \psi}}{\sin \psi + \sqrt{(\kappa - j\chi) - \cos^2 \psi}} \quad \text{horizontal polarization} \quad (6.8b)$$

where  $\chi = \sigma/\omega\epsilon_0$ . Typical values for the dielectric constant  $\kappa$  are around 15, while the conductivity  $\sigma$  may range from  $10^{-3}$  to  $3 \times 10^{-2}$  S/m, with  $10^{-2}$  S/m being a typical value for flat prairie land. The conductivity of mountainous regions is much lower. In general,  $\kappa$  is smaller, around 6 or 7, for soil with poor conductivity and will increase up to about 30 for soil with a high conductivity.

Figure 6.4 shows the behavior of  $\rho$  and  $\phi$  as a function of the grazing angle  $\psi$ . Of particular significance is the Brewster angle effect for vertical polarization, which causes  $\rho$  to go through a minimum for values of  $\psi$  below about  $15^\circ$ . As  $\rho$  moves through the minimum with decreasing values of  $\psi$ , the phase angle  $\phi$  undergoes a rapid change from near  $0^\circ$  to  $180^\circ$ . This effect makes  $\rho e^{j\phi}$  nearly equal to  $-1$  for both vertical and horizontal polarizations when the grazing angle  $\psi$  approaches zero. For a perfectly conducting surface  $\rho e^{j\phi}$  would equal  $+1$  for vertical polarization. As the frequency  $\omega$  increases, the effect of a finite ground conductivity decreases, since the parameter  $\chi = \sigma/\omega\epsilon_0$  decreases. Thus for frequencies above 50 MHz, the ground behaves very nearly like a dielectric medium, since the displacement current  $j\omega\epsilon\mathbf{E}$  is then much larger than the conduction current  $\sigma\mathbf{E}$ . If the point of reflection occurs over water, particularly seawater, the reflection coefficient can be approximated by  $-1$  for horizontal

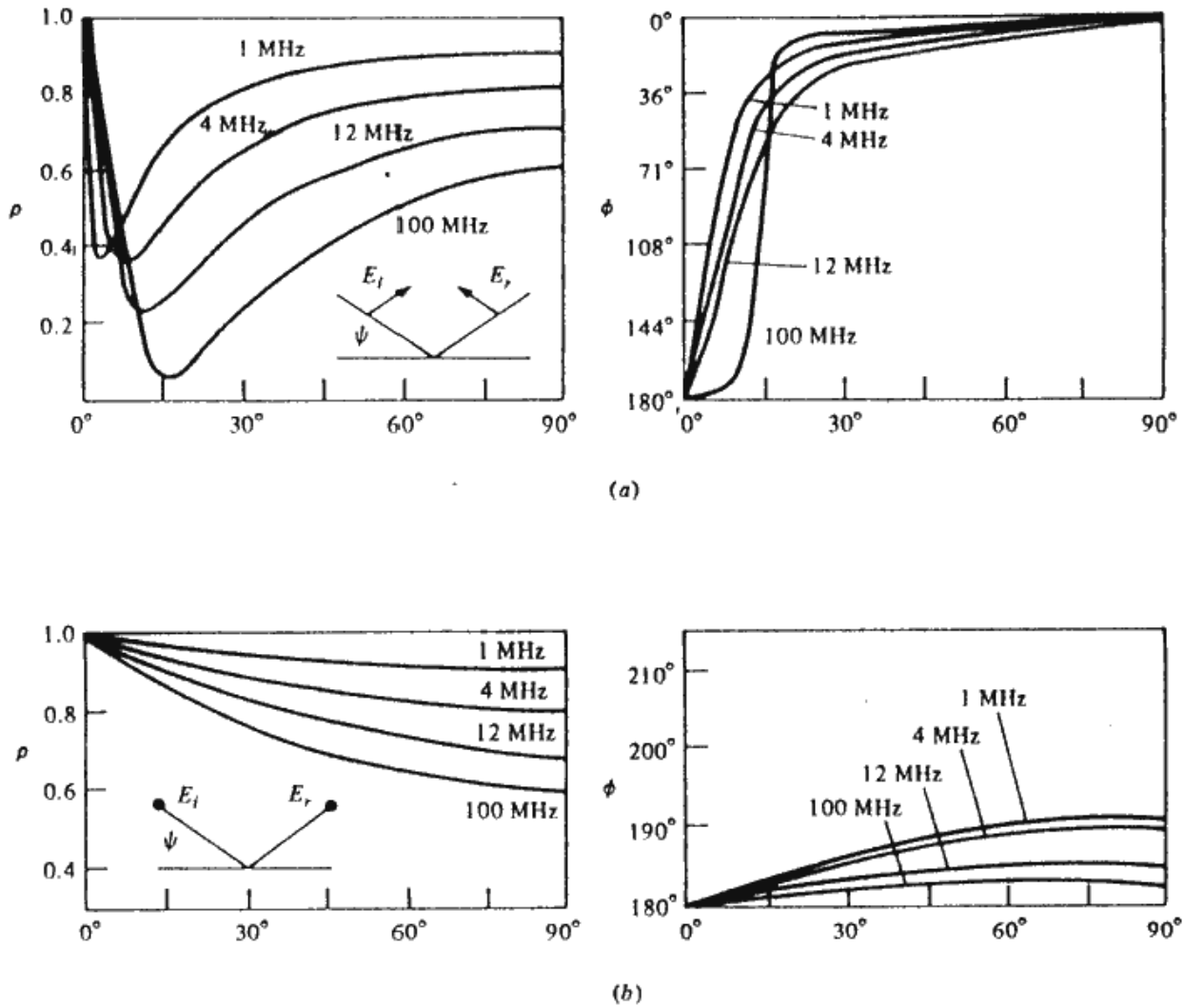


Figure 6.4 Typical reflection coefficients for the ground as a function of grazing angle  $\psi$ .  $\kappa = 15$ ,  $\sigma = 10^{-2}$  S/m. (a) Vertical polarization and (b) horizontal polarization.

polarization but may differ significantly from  $-1$  for vertical polarization, as reference to Fig. 6.5 shows. In the case of a rough sea the reflection coefficient could be quite small for either polarization.

Whenever the point of reflection occurs over a rough surface the field is scattered in a more diffuse manner, and the specular reflected component, and hence  $\rho$ , is reduced in value. A measure of the height of the surface irregularities that constitute a "rough surface" may be obtained by considering the effective wavelength of the incident wave in the direction perpendicular to the surface. If  $z$  is the coordinate perpendicular to the surface and  $x$  is the coordinate along the surface, the incident wave will have a propagation factor  $e^{jk_0z \sin \psi - jk_0x \cos \psi}$ . Thus in the vertical direction the effective wavelength  $\lambda_v$  is given by

$$\lambda_v = \frac{2\pi}{k_0 \sin \psi} = \frac{\lambda_0}{\sin \psi} \quad (6.9)$$

## 6.2 ANTENNAS LOCATED OVER A SPHERICAL EARTH

For antennas located over a spherical earth, with an effective radius  $a_e$  to account for standard refraction, it is quite tedious to derive the appropriate formulas for the interference effects. The complications that arise are due to a

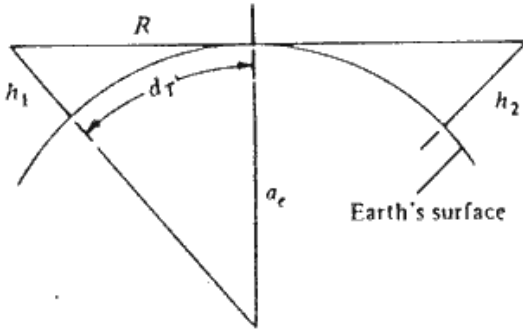


Figure 6.7 Illustration of horizontal range.

number of factors, including the difficulty of expressing the path-length difference between the direct ray and reflected ray in terms of the antenna heights  $h_1$  and  $h_2$  and horizontal distance  $d$  shown in Fig. 6.8. In addition, the grazing angle  $\psi$  relative to the tangent plane at the point of reflection must be determined in order to evaluate the reflection coefficient. Also for reflection from a spherical surface the rays in the reflected flux tube have a greater divergence than the rays in the incident flux tube, as pointed out in Sec. 4.5 and illustrated in Fig. 6.9. This increase in the divergence of the rays in a flux tube weakens the reflected field at the receiving antenna such that the appropriate expression for the path-gain factor  $F$  becomes

$$\begin{aligned} F &= |1 + D\rho e^{i\phi - ik_0 \Delta R}| \\ &= \{[1 + D\rho \cos(\phi - k_0 \Delta R)]^2 + [D\rho \sin(\phi - k_0 \Delta R)]^2\}^{1/2} \\ &= \left[ (1 + D\rho)^2 - 4D\rho \sin^2 \frac{\phi - k_0 \Delta R}{2} \right]^{1/2} \end{aligned} \quad (6.12)$$

where  $D$  is the ray-amplitude divergence factor and  $\Delta R$  is the path-length difference. [The divergence factor used here is the square root of that given by Eq. (4.59).]

An examination of Fig. 6.8 suggests that the relationships between the geometrical parameters describing the propagation paths would be relatively simple. This, unfortunately, is not the case. The known parameters are the two antenna heights  $h_1$  and  $h_2$  and the total range  $d$ . The point of reflection, which determines  $d_1$ ,  $d_2$ , the grazing angle  $\psi$ , and the divergence factor  $D$ , is governed by a cubic equation. The evaluation of the path-gain factor governing the interference region for a spherical earth has been systematized by the introduction of a set of parameters  $K$  and  $J$  that are functions of known parameters  $S$  and  $T$  related to the antenna heights and total range  $d$ . The relevant equations are given below without derivation and include formulas for the

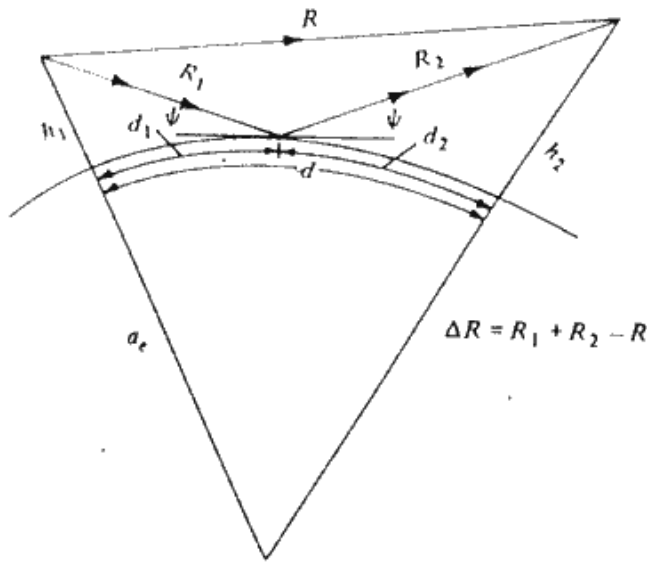


Figure 6.8 Reflection from a spherical earth.

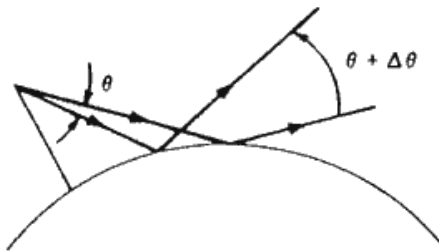


Figure 6.9 Illustration of ray divergence upon reflection from a spherical surface.

path-length difference  $\Delta R = R_1 + R_2 - R$  and the divergence factor  $D$ .†

$$\Delta R = \frac{2h_1h_2}{d} J(S, T) \quad (6.13)$$

$$\tan \psi = \frac{h_1 + h_2}{d} K(S, T) \quad (6.14)$$

$$D = \left[ 1 + \frac{4S_1S_2^2T}{S(1-S_2^2)(1+T)} \right]^{-1/2} \quad (6.15)$$

where  $S_1 = \frac{d_1}{\sqrt{2a_e h_1}}$

$$S_2 = \frac{d_2}{\sqrt{2a_e h_2}}$$

$$S = \frac{d}{\sqrt{2a_e h_1} + \sqrt{2a_e h_2}} = \frac{S_1 T + S_2}{1 + T}$$

$$T = \sqrt{h_1/h_2} < 1$$

$$J(S, T) = (1 - S_1^2)(1 - S_2^2)$$

$$K(S, T) = \frac{(1 - S_2^2) + T^2(1 - S_1^2)}{1 + T^2}$$

and  $d_1$ ,  $d_2$ ,  $d$ , and  $\psi$  are given in Fig. 6.8. Note that  $T$  must be chosen less than unity, so  $h_1$  is taken as the height of the lowest antenna. The above formulas show that  $\Delta R$  and  $D$  are functions of  $S_1$  and  $S_2$  and hence are functions of  $S$  and  $T$  only, since  $S_1$  and  $S_2$  are determined by given values of  $S$  and  $T$ . The range  $d_1$ , which determines  $d_2 = d - d_1$  and  $S_1$ ,  $S_2$ , may be found by solving the equations given below:

$$d_1 = \frac{d}{2} + p \cos\left(\frac{\Phi + \pi}{3}\right) \quad (6.16a)$$

where 
$$p = \frac{2}{\sqrt{3}} \left[ a_e(h_1 + h_2) + \frac{d^2}{4} \right]^{1/2} \quad (6.16b)$$

$$\Phi = \cos^{-1} \frac{2a_e(h_1 - h_2)d}{p^3} \quad h_1 \leq h_2 \quad (6.16c)$$

The phase angle of the reflected wave relative to that of the direct wave due to the path-length difference  $\Delta R$  only is given by

$$\begin{aligned} k_0 \Delta R &= \frac{2k_0 h_1 h_2}{d} (1 - S_1^2)(1 - S_2^2) \\ &= \frac{4\pi h_1^{3/2}}{\sqrt{2a_e \lambda_0}} \frac{h_2/h_1}{d/d_T} (1 - S_1^2)(1 - S_2^2) = \nu \zeta \pi \end{aligned} \quad (6.17a)$$

where 
$$\nu = \frac{4h_1^{3/2}}{\sqrt{2a_e \lambda_0}} = \frac{h_1^{3/2}}{1030\lambda_0} \quad (6.17b)$$

when  $h_1$  and  $\lambda_0$  are in meters, and

$$\zeta = \frac{h_2/h_1}{d/d_T} (1 - S_1^2)(1 - S_2^2) \quad (6.17c)$$

with  $d_T = \sqrt{2a_e h_1}$ . The parameter  $\zeta$  depends only on  $S$  and  $T$ .

If the reflection coefficient is assumed to be equal to  $-1$ , then the path-gain factor becomes

$$\begin{aligned} F &= \left[ (1 + D)^2 - 4D \cos^2 \frac{k_0 \Delta R}{2} \right]^{1/2} \\ &= \left[ (1 + D)^2 - 4D \cos^2 \left( \frac{\pi}{2} \nu \zeta \right) \right]^{1/2} \end{aligned} \quad (6.19)$$

For a spherical earth it is convenient to use the normalized coordinates  $h_2/h_1$  and  $d/d_T$ , where  $d_T = \sqrt{2a_e h_1}$ . The free-space reference range for a given coverage diagram is usually chosen as a suitable multiple of the horizontal range  $d_T$ . Hence a coverage diagram is a plot of

$$F = \left[ (1 + D)^2 - 4D \cos^2 \left( \frac{\pi}{2} \nu \zeta \right) \right]^{1/2} = m \frac{d}{d_T}$$

**Example 6.3 FM communication link** An FM transmitter has its antenna at a height  $h_2$  equal to 80 m. The antenna gain is 5, and the transmitter power is 500 W. The receiving antenna is at a height  $h_1$  equal to 10 m. The frequency of operation is 100 MHz. For this system  $\nu = 0.01$  and  $d_T = 4122\sqrt{10} = 13.03$  km, or  $\sqrt{2} \times 32.8 = 8.1$  mi. We wish to find the field strength in volts per meter at a distance of 8.1 mi from the transmitter. If we refer to Fig. 6.14 we see that at  $h_2/h_1 = 8$  and  $d = d_T$  the field strength is the same as it would be under free-space conditions at a distance of  $4d_T$ . The power density is

$$\frac{1}{2Z_0} |\mathbf{E}|^2 = \frac{P_t G}{4\pi(4d_T)^2}$$

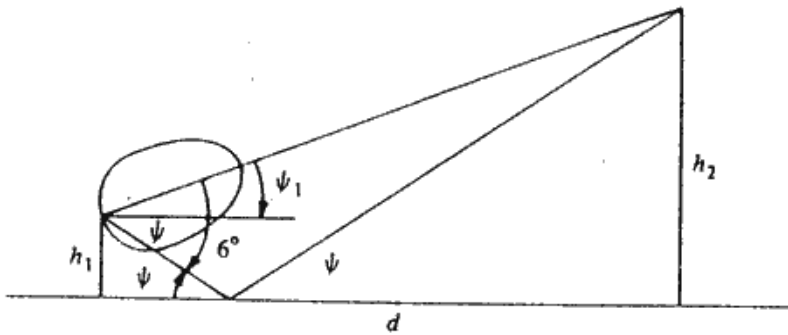


Figure 6.27 Illustration of effect of antenna pattern on the field incident on the ground.

Hence

$$|\mathbf{E}| = \left( \frac{Z_0 P_t G}{32\pi d_T^2} \right)^{1/2} = \left( \frac{120 \times 500 \times 5}{32 \times 1.3^2 \times 10^8} \right)^{1/2} = 7.4 \text{ mV/m}$$

At the receiving site the value of the path-gain factor is  $d_T/4d_T = 0.25$ .

**Example 6.4 Microwave communication link** In a microwave communication link the antennas are mounted on towers at a height of 35 m above the ground. The wavelength of operation is 10 cm. It is required to find the maximum distance  $d$  that can be used so that the signal level is not reduced below its free-space value. Thus a path-gain factor  $F$  equal to 1 is required. The parameter  $\nu$  is equal to  $h_1^{3/2}/1030\lambda_0 = 2.01$ . If we use the flat-earth interference formula [Eq. (6.3)] we have

$$F = 2 \left| \sin \left( \frac{\pi}{2} \nu \frac{h_2/h_1}{d/d_T} \right) \right| = 2 \left| \sin \pi \frac{d_T}{d} \right| = 1$$

and hence  $d = 6d_T$  in order to make  $F = 1$ . But since  $h_2 = h_1$  the maximum line-of-sight range is  $2d_T$ ; quite clearly the flat-earth interference formula is not applicable.

A coverage diagram for  $\nu = 2$  has not been included in this text. Thus we must use the formulas (6.14) to (6.17). Since  $h_2 = h_1$ , the parameters  $S_1$  and  $S_2$  are equal and  $T = 1$ ,  $S = d/2d_T = S_1$ . Hence the divergence factor  $D$  equals

$$D = \left[ 1 + \frac{d^2}{d_T^2(1 - d^2/4d_T^2)} \right]^{-1/2} = \frac{(1 - d^2/4d_T^2)^{1/2}}{(1 + 3d^2/4d_T^2)^{1/2}}$$

and

$$\zeta = \frac{h_2/h_1}{d/d_T} \left( 1 - \frac{d^2}{4d_T^2} \right)^2$$

When we equate the path-gain factor given by Eq. (6.19) to unity we obtain

$$\cos^2 \frac{\pi \nu \zeta}{2} = \frac{D + 2}{4}$$

This equation can be solved numerically, and it yields  $d = 1.36d_T$ ,  $D = 0.47$ , and  $\zeta = 0.21$ . Thus the maximum range is  $4122 \times 1.36\sqrt{35} = 33.16$  km. ■

## Radiowave Propagation

A complication that has not been included in the flat-earth interference formulas is the effect of the decrease in the index of refraction of the atmosphere with height above the surface.† At greater heights the less dense atmosphere results in a smaller index of refraction. This has the effect of causing the ray that leaves the antenna at a finite angle relative to the ground to curve or bend in a downward direction in accordance with Snell's law of refraction. The phenomenon of ray curvature may be readily understood by dividing the atmosphere into layers, with discrete values for the index of refraction in each layer, as shown in Fig. 6.6. For this staircase approximation to the continuous variation in the index of refraction, Snell's law gives

$$n_1 \sin \theta_1 = n_2 \sin \theta_2 = \cdots n_n \sin \theta_n = \cdots$$

Thus since each successive value of  $n_n$  is smaller than the preceding value, the angles  $\theta_n$  must increase and the ray curves in the downward direction. For propagation over a spherical earth this ray curvature extends the radio horizon beyond the geometrical horizon.

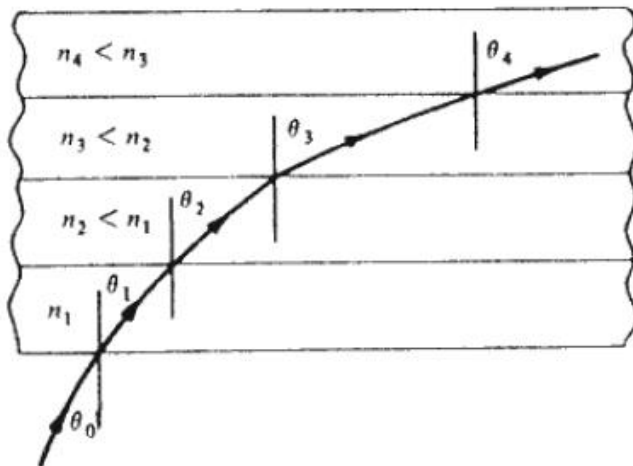


Figure 6.6 Illustration of ray curvature.

† The Rayleigh criterion allows for an obstruction with a height of  $\lambda_n/8$  leading to a maximum phase change of  $0.5\pi$ .

‡ The decrease in the refractive index with height is not always monotonic. Inversion layers leading to a phenomenon known as *ducting* can occur. Such effects are discussed in Sec. 6.12.

The effect of ray curvature can be taken into account in a simple way for propagation over a spherical earth by replacing the earth with an earth having a larger radius and considering the rays to propagate along straight lines, provided the index of refraction decreases linearly with height. By means of this artifice the height of any point on the ray above the surface of the earth remains the same. For propagation studies a standard index-of-refraction profile is commonly chosen such that it is equivalent to increasing the radius of the earth by a factor of 4/3. Thus the effective earth's radius  $a_e$  is chosen to be 5280 mi (8497 km). With reference to Fig. 6.7, it is seen that  $(h_1 + a_e)^2 = R^2 + a_e^2$ , so  $R^2 = 2h_1a_e + h_1^2 \approx 2h_1a_e$ . Since the antenna height  $h_1$  is small compared with the distance to the horizon, the slant distance  $R$  is nearly equal to the horizontal distance  $d_T$  to the horizon. Thus the distance to the horizon is given by  $d_T = (2h_1a_e)^{1/2}$ , and if  $d_T$  is expressed in miles and  $h_1$  in feet we have

$$d_T \text{ mi} = \sqrt{2h_1} \text{ ft} \quad (6.10)$$

The maximum line-of-sight distance in miles between two antennas at heights  $h_1$  and  $h_2$  ft above a spherical earth with standard refraction conditions is then readily seen to be given by

$$d_M = \sqrt{2h_1} + \sqrt{2h_2} \text{ mi} \quad (6.11)$$

The flat-earth interference formulas are generally not valid for distances approaching the maximum horizontal line-of-sight range. The exact distance over which the flat-earth formulas can be used depends on a number of factors, including wavelength. It is difficult to establish the range of validity without direct comparison with the interference effects based on using a spherical earth model. The evaluation of interference effects over a spherical earth is considerably more complex than that for a flat earth and is discussed in the next section.

$$d_{T \text{ (km)}} = 4.122 \sqrt{h_1}$$

where  $h_1$  is in meters

$$d_{m \text{ (km)}} = 4.122 \{ \sqrt{h_1} + \sqrt{h_2} \}$$

where  $h_1$  &  $h_2$  are in meters

## 6.2 ANTENNAS LOCATED OVER A SPHERICAL EARTH

For antennas located over a spherical earth, with an effective radius  $a_e$  to account for standard refraction, it is quite tedious to derive the appropriate formulas for the interference effects. The complications that arise are due to a

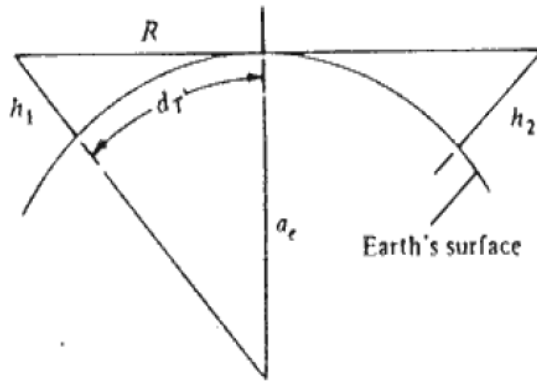


Figure 6.7 Illustration of horizontal range.

### 350 PROPAGATION

number of factors, including the difficulty of expressing the path-length difference between the direct ray and reflected ray in terms of the antenna heights  $h_1$  and  $h_2$  and horizontal distance  $d$  shown in Fig. 6.8. In addition, the grazing angle  $\psi$  relative to the tangent plane at the point of reflection must be determined in order to evaluate the reflection coefficient. Also for reflection from a spherical surface the rays in the reflected flux tube have a greater divergence than the rays in the incident flux tube, as pointed out in Sec. 4.5 and illustrated in Fig. 6.9. This increase in the divergence of the rays in a flux tube weakens the reflected field at the receiving antenna such that the appropriate expression for the path-gain factor  $F$  becomes

$$\begin{aligned}
 F &= |1 + D\rho e^{j\phi - jk_0 \Delta R}| \\
 &= \{[1 + D\rho \cos(\phi - k_0 \Delta R)]^2 + [D\rho \sin(\phi - k_0 \Delta R)]^2\}^{1/2} \\
 &= \left[ (1 + D\rho)^2 - 4D\rho \sin^2 \frac{\phi - k_0 \Delta R}{2} \right]^{1/2} \quad (6.12)
 \end{aligned}$$

where  $D$  is the ray-amplitude divergence factor and  $\Delta R$  is the path-length difference. [The divergence factor used here is the square root of that given by Eq. (4.59).]

An examination of Fig. 6.8 suggests that the relationships between the geometrical parameters describing the propagation paths would be relatively simple. This, unfortunately, is not the case. The known parameters are the two antenna heights  $h_1$  and  $h_2$  and the total range  $d$ . The point of reflection, which determines  $d_1$ ,  $d_2$ , the grazing angle  $\psi$ , and the divergence factor  $D$ , is governed by a cubic equation. The evaluation of the path-gain factor governing the interference region for a spherical earth has been systematized by the introduction of a set of parameters  $K$  and  $J$  that are functions of known parameters  $S$  and  $T$  related to the antenna heights and total range  $d$ . The relevant equations are given below without derivation and include formulas for the

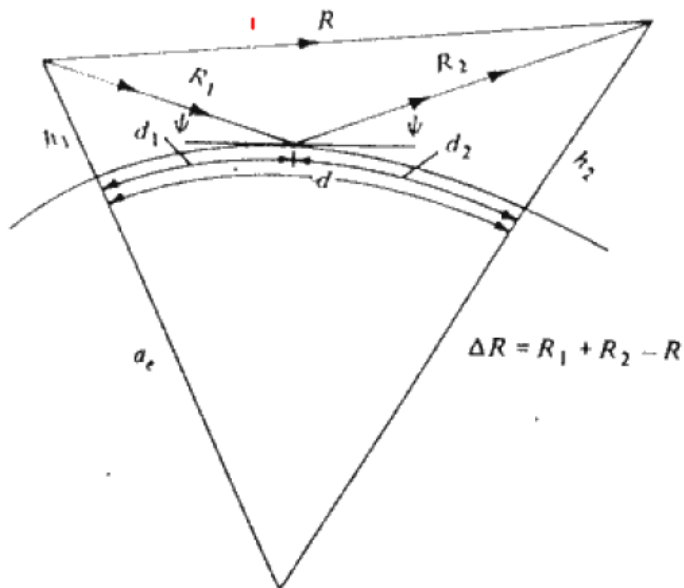


**Figure 6.8** Reflection from a spherical earth.



Figure 6.9 Illustration of ray divergence upon reflection from a spherical surface.

path-length difference  $\Delta R = R_1 + R_2 - R$  and the divergence factor  $D$ .†

$$\Delta R = \frac{2h_1 h_2}{d} J(S, T) \quad (6.13)$$

$$\tan \psi = \frac{h_1 + h_2}{d} K(S, T) \quad (6.14)$$

$$D = \left[ 1 + \frac{4S_1 S_2^2 T}{S(1 - S_2^2)(1 + T)} \right]^{-1/2} \quad (6.15)$$

where  $S_1 = \frac{d_1}{\sqrt{2a}h_1}$

$$S_2 = \frac{d_2}{\sqrt{2a}h_2}$$

$$S = \frac{d}{\sqrt{2a}h_1 + \sqrt{2a}h_2} = \frac{S_1 T + S_2}{1 + T}$$

$$T = \sqrt{h_1/h_2} < 1$$

$$J(S, T) = (1 - S_1^2)(1 - S_2^2)$$

$$K(S, T) = \frac{(1 - S_2^2) + T^2(1 - S_1^2)}{1 + T^2}$$

and  $d_1$ ,  $d_2$ ,  $d$ , and  $\psi$  are given in Fig. 6.8. Note that  $T$  must be chosen less than unity, so  $h_1$  is taken as the height of the lowest antenna. The above formulas show that  $\Delta R$  and  $D$  are functions of  $S_1$  and  $S_2$  and hence are functions of  $S$  and  $T$  only, since  $S_1$  and  $S_2$  are determined by given values of  $S$  and  $T$ . The range  $d_1$ , which determines  $d_2 = d - d_1$  and  $S_1$ ,  $S_2$ , may be found by solving the equations given below:

$$d_1 = \frac{d}{2} + p \cos\left(\frac{\Phi + \pi}{3}\right) \quad (6.16a)$$

†D. E. Kerr, *Propagation of Short Radio Waves*, McGraw-Hill Book Company, New York, 1951, Sec. 2.13. Note that we have interchanged  $h_1$ ,  $h_2$  and  $S_1$ ,  $S_2$ .

where 
$$p = \frac{2}{\sqrt{3}} \left[ a_e(h_1 + h_2) + \frac{d^2}{4} \right]^{1/2} \quad (6.16b)$$

$$\Phi = \cos^{-1} \frac{2a_e(h_1 - h_2)d}{p^3} \quad h_1 \leq h_2 \quad (6.16c)$$

The phase angle of the reflected wave relative to that of the direct wave due to the path-length difference  $\Delta R$  only is given by

$$\begin{aligned} k_0 \Delta R &= \frac{2k_0 h_1 h_2}{d} (1 - S_1^2)(1 - S_2^2) \\ &= \frac{4\pi h_1^{3/2}}{\sqrt{2a_e \lambda_0}} \frac{h_2/h_1}{d/d_T} (1 - S_1^2)(1 - S_2^2) = \nu \zeta \pi \end{aligned} \quad (6.17a)$$

where 
$$\nu = \frac{4h_1^{3/2}}{\sqrt{2a_e \lambda_0}} = \frac{h_1^{3/2}}{1030 \lambda_0} \quad (6.17b)$$

when  $h_1$  and  $\lambda_0$  are in meters, and

$$\zeta = \frac{h_2/h_1}{d/d_T} (1 - S_1^2)(1 - S_2^2) \quad (6.17c)$$

with  $d_T = \sqrt{2a_e h_1}$ . The parameter  $\zeta$  depends only on  $S$  and  $T$ .

If the reflection coefficient is assumed to be equal to  $-1$ , then the path-gain factor becomes

$$\begin{aligned} F &= \left[ (1 + D)^2 - 4D \cos^2 \frac{k_0 \Delta R}{2} \right]^{1/2} \\ &= \left[ (1 + D)^2 - 4D \cos^2 \left( \frac{\pi}{2} \nu \zeta \right) \right]^{1/2} \end{aligned} \quad (6.19)$$

For a spherical earth it is convenient to use the normalized coordinates  $h_2/h_1$  and  $d/d_T$ , where  $d_T = \sqrt{2a_e h_1}$ . The free-space reference range for a given coverage diagram is usually chosen as a suitable multiple of the horizontal range  $d_T$ . Hence a coverage diagram is a plot of

$$F = \left[ (1 + D)^2 - 4D \cos^2 \left( \frac{\pi}{2} \nu \zeta \right) \right]^{1/2} = m \frac{d}{d_T}$$

**Example 6.3 FM communication link** An FM transmitter has its antenna at a height  $h_2$  equal to 80 m. The antenna gain is 5, and the transmitter power is 500 W. The receiving antenna is at a height  $h_1$  equal to 10 m. The frequency of operation is 100 MHz. For this system  $\nu = 0.01$  and  $d_T = 4122\sqrt{10} = 13.03$  km, or  $\sqrt{2} \times 32.8 = 8.1$  mi. We wish to find the field strength in volts per meter at a distance of 8.1 mi from the transmitter. If we refer to Fig. 6.14 we see that at  $h_2/h_1 = 8$  and  $d = d_T$  the field strength is the same as it would be under free-space conditions at a distance of  $4d_T$ . The power density is

$$\frac{1}{2Z_0} |\mathbf{E}|^2 = \frac{P_t G}{4\pi(4d_T)^2}$$

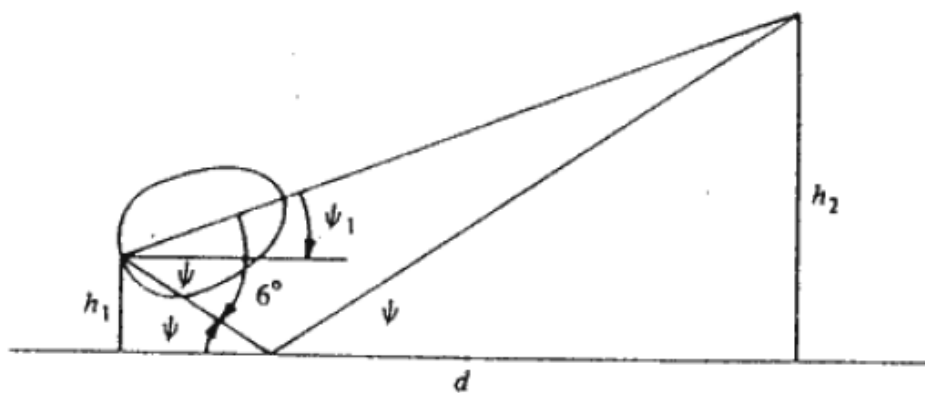


Figure 6.27 Illustration of effect of antenna pattern on the field incident on the ground.

Hence

$$|\mathbf{E}| = \left( \frac{Z_0 P_t G}{32\pi d_T^2} \right)^{1/2} = \left( \frac{120 \times 500 \times 5}{32 \times 1.3^2 \times 10^8} \right)^{1/2} = 7.4 \text{ mV/m}$$

At the receiving site the value of the path-gain factor is  $d_T/4d_T = 0.25$ .

**Example 6.4 Microwave communication link** In a microwave communication link the antennas are mounted on towers at a height of 35 m above the ground. The wavelength of operation is 10 cm. It is required to find the maximum distance  $d$  that can be used so that the signal level is not reduced below its free-space value. Thus a path-gain factor  $F$  equal to 1 is required. The parameter  $\nu$  is equal to  $h_1^{3/2}/1030\lambda_0 = 2.01$ . If we use the flat-earth interference formula [Eq. (6.3)] we have

$$F = 2 \left| \sin \left( \frac{\pi}{2} \nu \frac{h_2/h_1}{d/d_T} \right) \right| = 2 \left| \sin \pi \frac{d_T}{d} \right| = 1$$

and hence  $d = 6d_T$  in order to make  $F = 1$ . But since  $h_2 = h_1$  the maximum line-of-sight range is  $2d_T$ ; quite clearly the flat-earth interference formula is not applicable.

A coverage diagram for  $\nu = 2$  has not been included in this text. Thus we must use the formulas (6.14) to (6.17). Since  $h_2 = h_1$ , the parameters  $S_1$  and  $S_2$  are equal and  $T = 1$ ,  $S = d/2d_T = S_1$ . Hence the divergence factor  $D$  equals

$$D = \left[ 1 + \frac{d^2}{d_T^2(1 - d^2/4d_T^2)} \right]^{-1/2} = \frac{(1 - d^2/4d_T^2)^{1/2}}{(1 + 3d^2/4d_T^2)^{1/2}}$$

and

$$\zeta = \frac{h_2/h_1}{d/d_T} \left( 1 - \frac{d^2}{4d_T^2} \right)^2$$

When we equate the path-gain factor given by Eq. (6.19) to unity we obtain

$$\cos^2 \frac{\pi \nu \zeta}{2} = \frac{D + 2}{4}$$

This equation can be solved numerically, and it yields  $d = 1.36d_T$ ,  $D = 0.47$ , and  $\zeta = 0.21$ . Thus the maximum range is  $4122 \times 1.36\sqrt{35} = 33.16$  km. ■

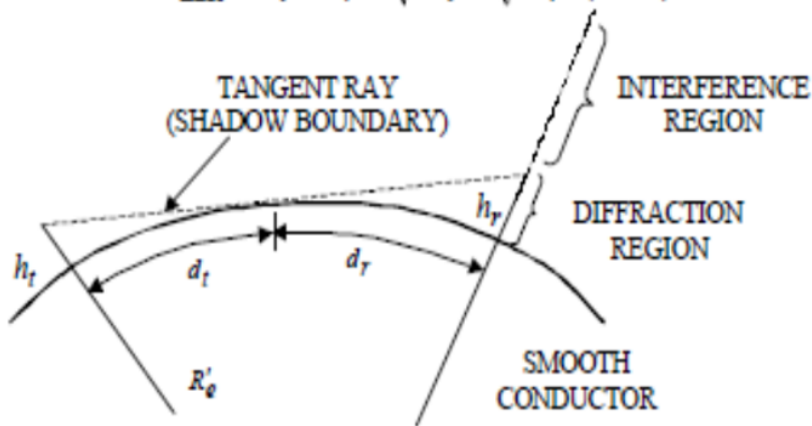
When the transmitter to receiver distance becomes too large the flat Earth approximation is no longer accurate. The curvature of the surface causes:

1. divergence of the power in the reflected wave in the interference region
2. diffracted wave in the shadow region (note that this is not the same as a ground wave)

The distance to the horizon is  $d_t = R_{RH} \approx \sqrt{2R_e' h_t}$  or, if  $h_t$  is in feet,  $d_t \approx \sqrt{2h_t}$  miles.

The maximum LOS distance between the transmit and receive antennas is

$$d_{\max} = d_t + d_r \approx \sqrt{2h_t} + \sqrt{2h_r} \text{ (miles)}$$



$$d_t^2 + R^2 = (R + h_t)^2$$

$$d_t \approx \sqrt{2R h_t}$$

$$R = 6370 \text{ km}$$

$$d_t \approx 3.57\sqrt{h_t}$$

$h_t$  in meters

$d_t$  in km

$d_t$  is called the

**Radio Horizon**

If refraction is considered

$$d_t \approx 4.11\sqrt{h_t}$$

Hence, the effective earth's radius factor,  $K$ , is defined as the factor that is multiplied by the actual earth's radius  $a$  to give the effective earth's radius. Thus  $k = a'/a$ . Due to earth's curvature and refraction of radio signal, each site must have a minimum elevation with respect to antenna height.

The value of  $k$  can be calculated for a given area based on refractivity gradient available from local chart. For standard atmosphere,  $k = 1.33 = 4/3$ . Higher values of  $k$  would mean a greater amount of bending of radio waves toward the earth's surface and consequently would result in extension of radio visibility. The value of radio horizon distance for a particular value of  $k$  is given by  $\sqrt{2k a h}$  where  $h$  is the antenna height.

$$k = 4/3$$

$$R_e = k * R = (4/3) * 6370 = 8493 \text{ km}$$

## LN-23 Propagation

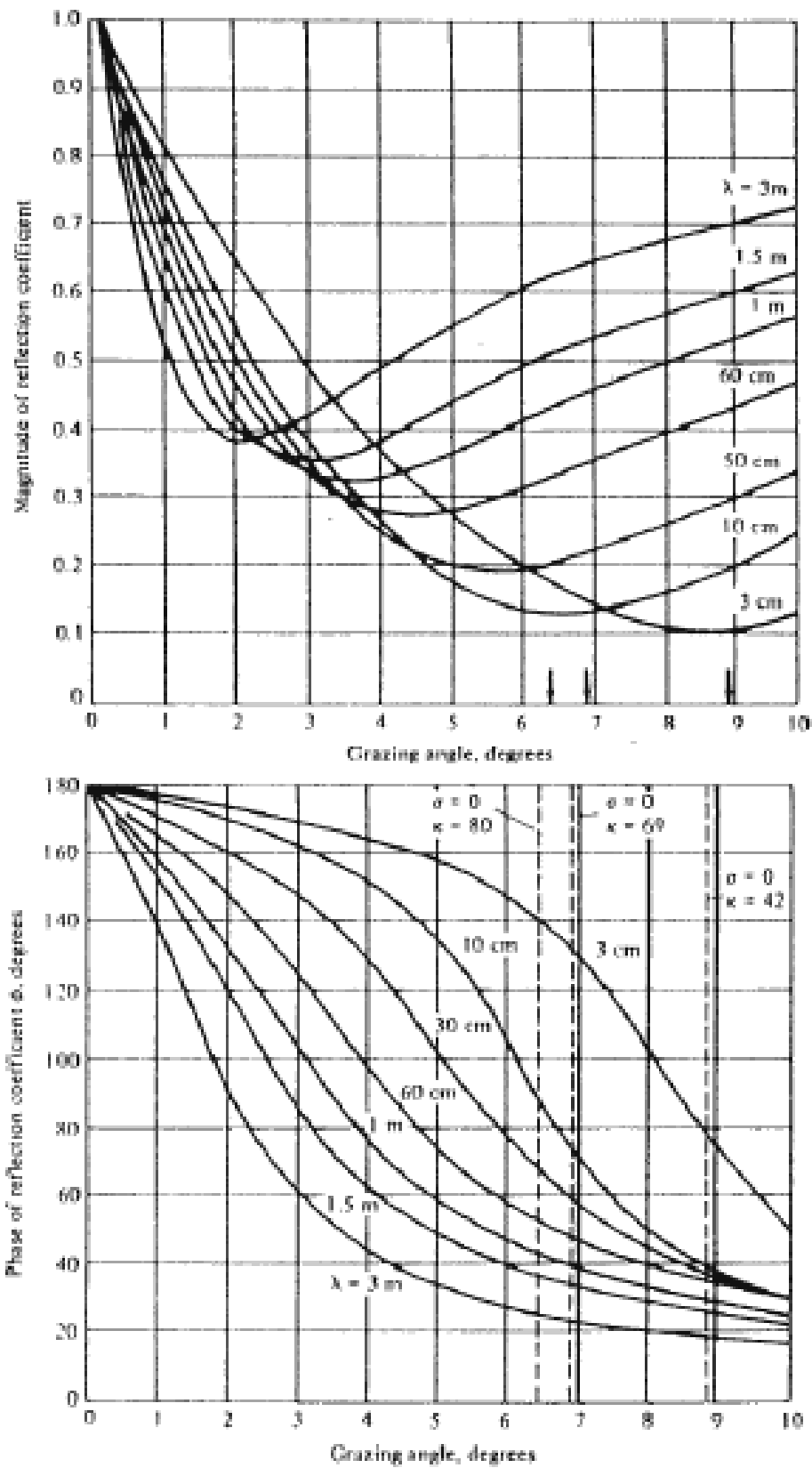


**Figure 6.5** Reflection coefficient for vertical polarization for seawater. The marked angles are the Brewster angles when the conductivity is zero. (From D. E. Kerr, *Propagation of Short Radio Waves*, McGraw-Hill Book Company, New York, 1951.)

When the grazing angle of incidence is small,  $\lambda_g$  will be large compared with  $\lambda_0$ , often by a factor of 10 to 100. If the point of reflection is raised by an amount  $\lambda_g/10$  the change in phase of the reflected wave reaching the receiving antenna will be  $(2k_0 \sin \psi)\lambda_g/10 = 0.4\pi$ . This may be regarded as being the boundary between what can be considered to be a rough surface and a smooth surface.† With this criterion the surface of generally flat land can be considered "smooth" whenever the surface irregularities have an average height variation of  $\lambda_g/10 \sin \psi$ . For example, with  $\lambda_0 = 1$  m and  $\psi = 1^\circ$ , we find that height variations of up to 6 m can still be regarded as a smooth surface. At the longer wavelengths most surfaces appear to be smooth, but at microwave frequencies most surfaces would be rough and the reflection coefficient would be smaller than that given by the Fresnel formulas.

A complication that has not been included in the flat-earth interference formulas is the effect of the decrease in the index of refraction of the atmosphere with height above the surface.‡ At greater heights the less dense atmosphere results in a smaller index of refraction. This has the effect of causing the ray that leaves the antenna at a finite angle relative to the ground to curve or bend in a downward direction in accordance with Snell's law of refraction. The phenomenon of ray curvature may be readily understood by dividing the atmosphere into layers, with discrete values for the index of refraction in each layer, as shown in Fig. 6.6. For this staircase approximation to the continuous variation in the index of refraction, Snell's law gives

$$n_1 \sin \theta_1 = n_2 \sin \theta_2 = \cdots n_n \sin \theta_n = \cdots$$

Thus since each successive value of  $n_n$  is smaller than the preceding value, the angles  $\theta_n$  must increase and the ray curves in the downward direction. For propagation over a spherical earth this ray curvature extends the radio horizon beyond the geometrical horizon.

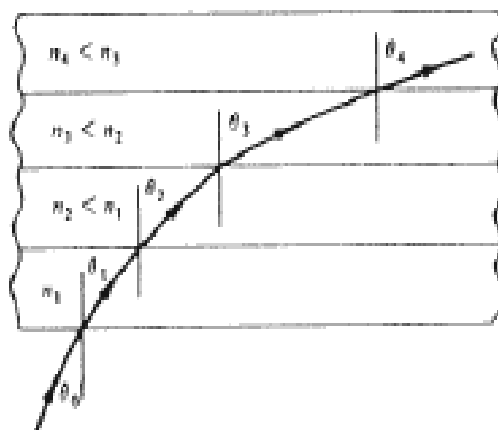


Figure 6.6 Illustration of ray curvature.

† The Rayleigh criterion allows for an obstruction with a height of  $\lambda_g/8$  leading to a maximum phase change of  $0.5\pi$ .

‡ The decrease in the refractive index with height is not always monotonic. Inversion layers leading to a phenomenon known as *ducting* can occur. Such effects are discussed in Sec. 6.12.

The effect of ray curvature can be taken into account in a simple way for propagation over a spherical earth by replacing the earth with an earth having a larger radius and considering the rays to propagate along straight lines, provided the index of refraction decreases linearly with height. By means of this artifice the height of any point on the ray above the surface of the earth remains the same. For propagation studies a standard index-of-refraction profile is commonly chosen such that it is equivalent to increasing the radius of the earth by a factor of 4/3. Thus the effective earth's radius  $a_e$  is chosen to be 5280 mi (8497 km). With reference to Fig. 6.7, it is seen that  $(h_1 + a_e)^2 = R^2 + a_e^2$ , so  $R^2 = 2h_1 a_e + h_1^2 = 2h_1 a_e$ . Since the antenna height  $h_1$  is small compared with the distance to the horizon, the slant distance  $R$  is nearly equal to the horizontal distance  $d_T$  to the horizon. Thus the distance to the horizon is given by  $d_T = (2h_1 a_e)^{1/2}$ , and if  $d_T$  is expressed in miles and  $h_1$  in feet we have

$$d_T \text{ mi} = \sqrt{2h_1 \text{ ft}} \quad (6.10)$$

The maximum line-of-sight distance in miles between two antennas at heights  $h_1$  and  $h_2$  ft above a spherical earth with standard refraction conditions is then readily seen to be given by

$$d_M = \sqrt{2h_1} + \sqrt{2h_2} \text{ mi} \quad (6.11)$$

The flat-earth interference formulas are generally not valid for distances approaching the maximum horizontal line-of-sight range. The exact distance over which the flat-earth formulas can be used depends on a number of factors, including wavelength. It is difficult to establish the range of validity without direct comparison with the interference effects based on using a spherical earth model. The evaluation of interference effects over a spherical earth is considerably more complex than that for a flat earth and is discussed in the next section.

$$d_{T \text{ (km)}} = 4.122 \sqrt{h_1} \quad \text{where } h_1 \text{ is in meters}$$

$$d_{M \text{ (km)}} = 4.122 \{ \sqrt{h_1} + \sqrt{h_2} \} \quad \text{where } h_1 \text{ \& } h_2 \text{ are in meters}$$

## Large Scale Propagation – Three Modes

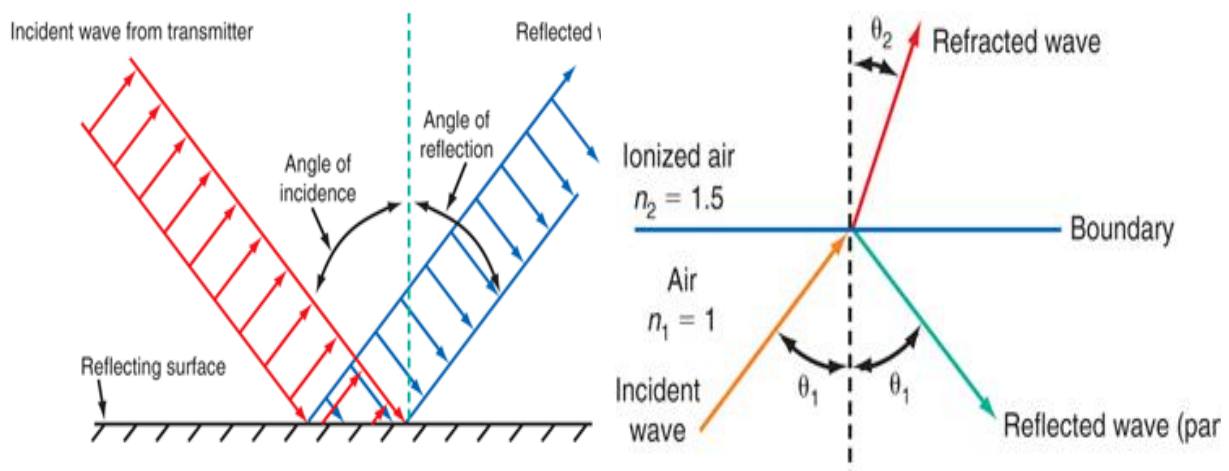
Large scale propagation is composed of three modes listed below in order of their dominance:

- **Reflection** – Energy reflects off large (relative to  $\lambda$ ) conductive objects.
- **Diffraction** – Bending of energy around objects.
- **Scattering** – Diffuse re-radiation of energy off rough, with respect to  $\lambda$  surfaces.

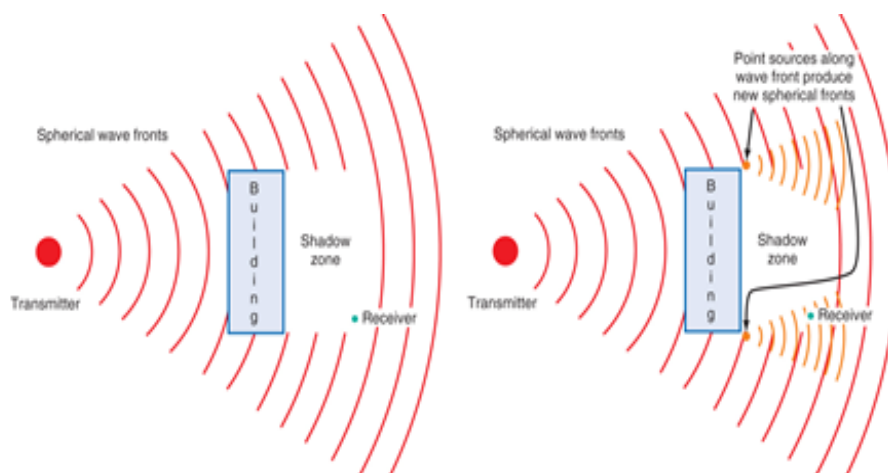
1. **Reflection** The angle of reflection is equal to the angle of incidence.

Reflection introduces a  $180^\circ$  phase shift in most cases.

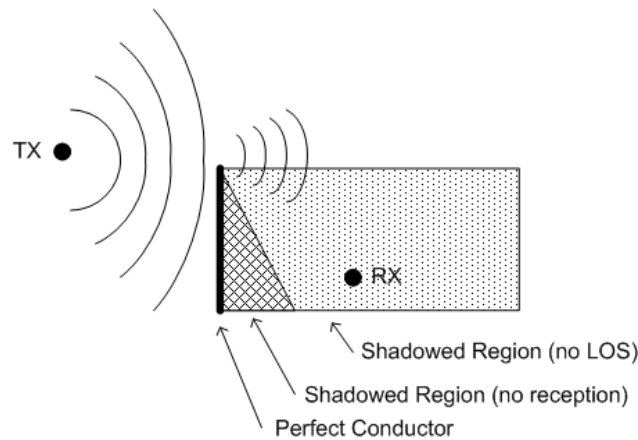
Refraction (with reflection): The radio wave is bent due to the changing in the index of refraction of the medium.



2. **Diffraction** Diffraction can be explained by Huygen's principle – all points on a wavefront serve as point sources for secondary wavefronts:

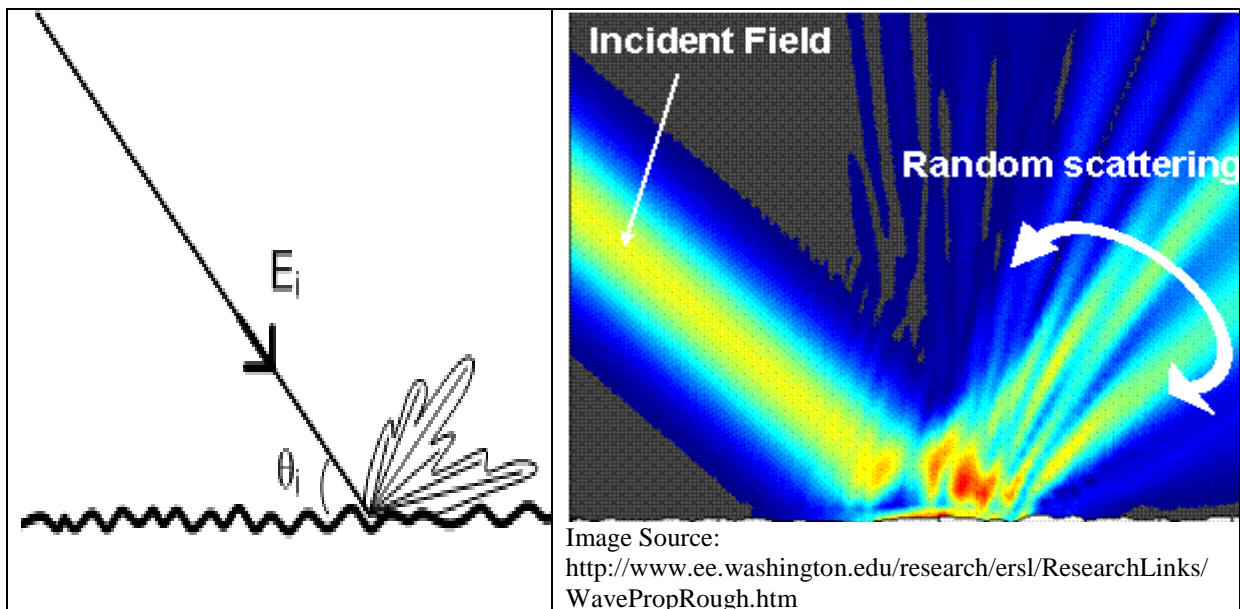


Consider a Transmitter and Receiver where an object is blocking the direct line-of-sight path between Tx and Rx. The signal can diffract around the object such that energy can get to the Rx even though it is shadowed.



**Note:** The more deeply the receiver is shadowed, the lower the received power. At some point, the receiver won't be able to receive any signal.

**3. Rough Surface Scattering** Sometimes called Diffuse Scattering or Diffuse Reflection, scattering happens when energy impacts a rough surface and is re-radiated in *numerous* directions.



So those are the basic modes of propagation. What happens when we add in a real earth and a real atmosphere?

The earth and the earth's atmosphere have the greatest impact on signals in the VLF – HF range (3 kHz – 30 MHz). It's not that the earth and atmosphere don't affect signals at higher frequencies (in fact, they do!) it's just at those

higher frequencies start to come into play and dominate the effects of the earth/atmosphere.

Let's look at what happens to these lower frequencies first before moving on to the higher frequencies.

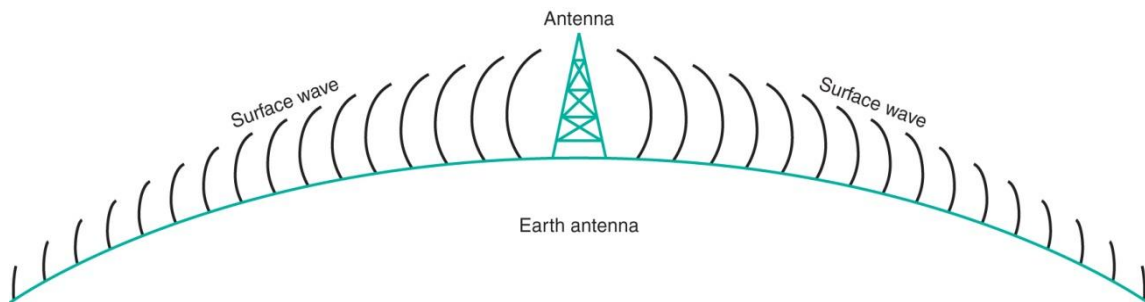
Radio Band	Frequency	Propagation Via
<a href="#">VLF</a> Very Low Frequency	3 - 30 <a href="#">kHz</a>	- Guided between the earth and the ionosphere
<a href="#">LF</a> Low Frequency	30 - 300 <a href="#">kHz</a>	- Guided between the earth and the ionosphere - Ground Waves
<a href="#">MF</a> Medium Frequency	0.3 - 3 <a href="#">MHz</a>	- Ground waves - E layer ionospheric refraction at night, when D layer absorption disappears
<a href="#">HF</a> High Frequency ( <a href="#">Short Wave</a> )	3 - 30 <a href="#">MHz</a>	- E layer ionospheric refraction - F layer ionospheric refraction
<a href="#">VHF</a> Very High Frequency	30 - 300 <a href="#">MHz</a>	- Line-of-sight
<a href="#">UHF</a> Ultra High Frequency	300 - 3000 <a href="#">MHz</a>	- Line-of-sight
<a href="#">SHF</a> Super High Frequency	3 - 30 <a href="#">GHz</a>	- Line-of-sight
<a href="#">EHF</a> Extremely High Frequency	30 - 300 <a href="#">GHz</a>	- Line-of-sight limited by absorption

For VLF-HF communications, there are two basic modes a radio wave travels from the transmitter to a receiving antenna:

- Ground wave
- Space wave
- Sky wave

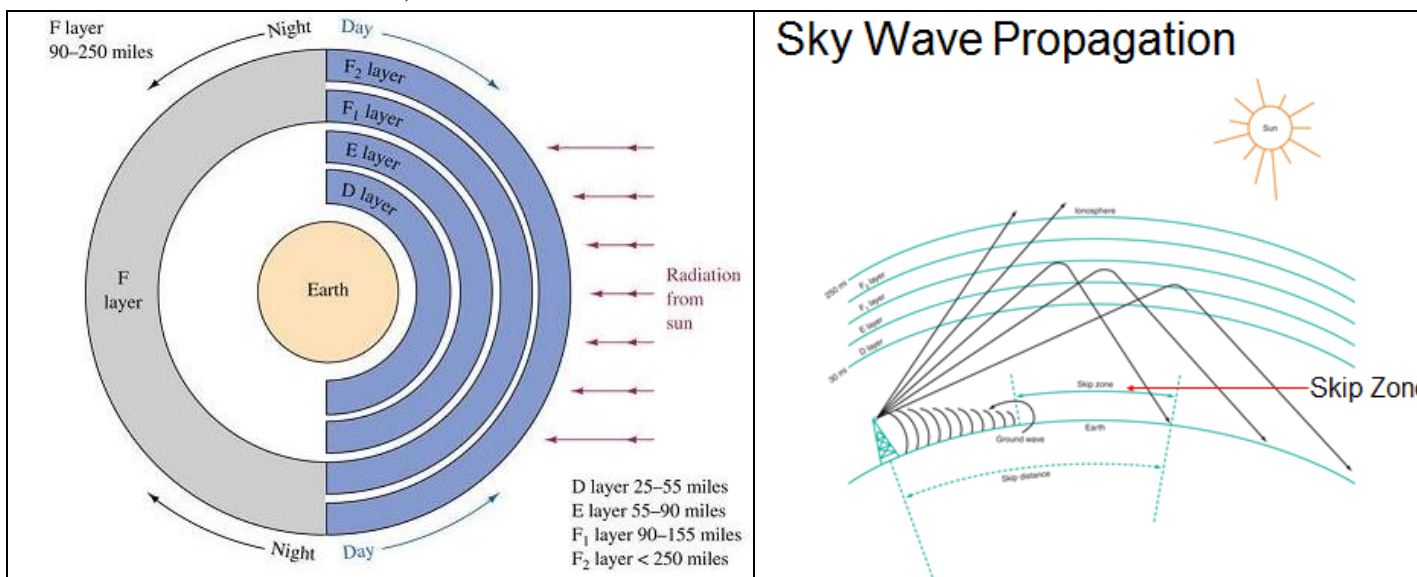
The **frequency** of the radio wave is the most important factor in determining the performance of each type of propagation.

**4. Ground Wave Propagation** A ground wave is a radio wave that travels along the earth's surface (also referred to as a **surface wave**). A ground wave must be vertically polarized for better propagation (lower losses since the ground is considered as poor conductor).



Lower frequencies travel efficiently as ground waves because they are **diffracted** by the surface of the earth. Ground waves thus follow the curvature of the earth and can travel beyond the horizon, for hundreds of miles. Ground wave propagation is strongest in the Low and Medium frequency ranges. Ground wave propagation constitutes the main signal path for signals in the frequency range from 30 kHz-3 MHz.

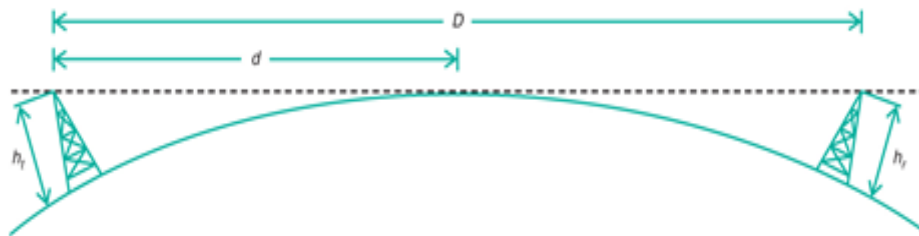
**5. Sky Wave Propagation** Sky waves are radiated by an antenna into the upper atmosphere where they are reflected back to earth. This bending is caused by refraction in the ionosphere. The air molecules of the ionosphere are subject to severe radiation from the sun. Ultraviolet radiation causes the molecules to **ionize**, or separate into charged particles, positive and negative ions. The ionosphere is composed of 3 layers, *D*, *E* and *F* (although *F* is subdivided into *F*<sub>1</sub> and *F*<sub>2</sub>).



The direction of reflection depends on the angle at which the radio wave enters the atmosphere and the different degrees of ionization of the layers, as well as the frequency of the transmission.

A receiver that lies between the end of the ground wave propagation and the first sky wave reflection will not receive the transmitted signal. This region is termed the *skip zone*.

**6. Space Wave Propagation** A **space wave** refers to the radio wave that travels directly in a straight line from the transmitting antenna (Line-of-sight). These waves are not refracted, and do not follow the curvature of the earth. The chief limitation of a space wave is that it is limited to **line-of-sight** distances. The range of space wave propagation is limited by the curvature of the earth and height of the antennas above the earth's surface.



If an antenna is at height  $h$ , the distance,  $d$ , to the radio horizon (which is the maximum range for space wave communications from that antenna) is given by the formula

$$d_{T (km)} = 4.122 \sqrt{h_1} \quad \text{where } h_1 \text{ is in meters}$$

In the picture below, where we have one antenna of height  $h_t$  and a second antenna of height  $h_r$ , the maximum separation at which they can still communicate by line-of-sight is

$$d_{m (km)} = 4.122 \{ \sqrt{h_1} + \sqrt{h_2} \} \quad \text{where } h_1 \text{ \& } h_2 \text{ are in meters}$$

### Example

What is the longest line-of-sight communication range between a transmitter whose transmitting antenna is 100 m high and a receiver whose receiving antenna is 10 m high?

### III. Log-Normal Model

The VLF – HF range of the frequency spectrum are mostly used for narrowband, long-distance communication. Most terrestrial wireless communications operate in the “sweet spot” of the wireless spectrum in the VHF and UHF bands. In this range, the earth and atmosphere play a far smaller role, and propagation becomes dominated by the *specific local environment*.

Let’s consider the following scenario. Suppose we convince the ECE Department to build a cell tower on the top of Rickover Hall, and you’re driving down McNair Road. The signal you receive will be a combination of Reflection, Diffraction, and Scattering, as shown in the image below. The problem is that we call it “mobile” radio for a reason: you want to be able to drive, move about the local environment, *and* communicate on your cell phone at the same time.



As you move about the environment, the three propagation modes will have an impact on the instantaneous received signal in different ways. In the example shown above, you receive a nice strong signal reflected from Mahan Hall, with a little bit of signal energy coming from diffraction off the back corner of Nimitz Library, along with some energy scattered by the clock tower. As you move towards Alumni hall, the direct line-of-sight signal to the tower will be

blocked, as will most of the strong reflected signals; diffraction is now the dominant mode. Conversely, if you moved towards Rickover, you would receive a nice strong line-of-sight signal from the tower, along with a strong reflection from the Northeast side of Nimitz as well as scattering from all the parked cars in the Triangle Lot.

So the question remains: Using your brand-new iPhone (or Samsung phone as the case may be), will your signal make it to the tower and will it have sufficient power to “close the link” and allow you communicate? Or will you suffer the fate of a cellular “dead zone”?

Clearly, the Friis Free Space equation is out, and the ground wave/sky wave effects are so small that they can be neglected. Although *numerous* sophisticated models exist (and are used to varying degrees in both commercial and military systems), by far the simplest and most common way to describe propagation in such an environment is the **Log-Normal** or **Log-Distance** model. This model is widely used to not only predict coverage for a particular mobile user, but also for predicting the interfering signal power that the mobile user will experience from other RF sources.

---

### Appendix A. Log-Normal Model.

First, a quick definition. We use the term *Path Loss* to denote the received signal power at a specific transmitter-receiver distance relative to the transmit power, or mathematically:

$$PL(d) = P_T - P_R(d) \quad [dB]$$

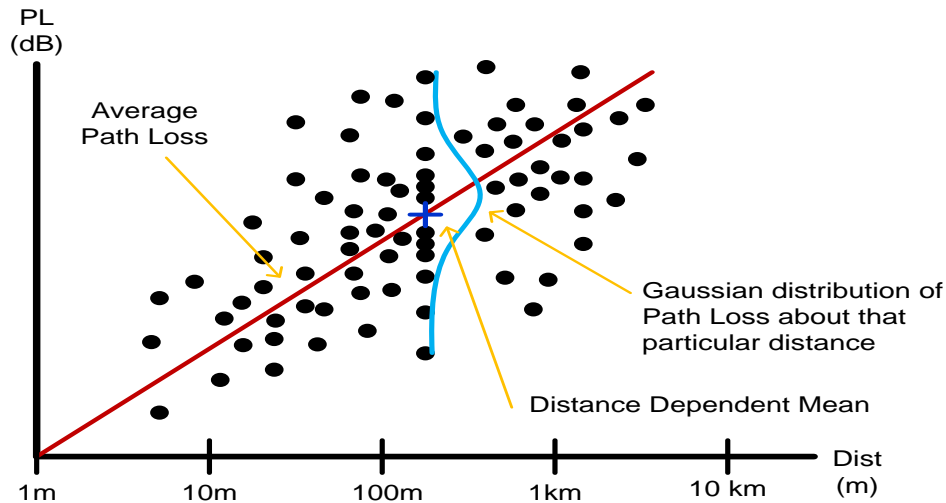
$P_T$             Is the transmitted power [dBm]

$P_R(d)$         Is the received power [dBm]

$d$                 Is the distance between transmitter and receiver [meters]

Over the years, wireless engineers have observed that *Average Path Loss for a particular environment* generally follows a  $d^n$  relationship, where the variable  $n$  is known as the Path Loss Exponent, and is *specific to that environment*. Researchers have also observed that when they made numerous measurements at a specific distance (but in different local environments), the variation in received signal power obeyed a “bell curve” distribution about the local mean (the “bell curve” is formally known as a “Normal” or “Gaussian” distribution).

Plotted on a log scale, the results look something like this:



We call this **Log-Normal Path Loss**. Average Path Loss obeys a linear relationship (straight line) on a log scale, and the variation in received power at that distance follows a normal distribution. The slope of the line is the Path Loss Exponent, and is determined experimentally for the particular scenario of interest.

Mathematically **Log-Normal Path Loss** is given by:

$$\bar{PL}(d) = PL(d_0) + 10n \log_{10} \left( \frac{d}{d_0} \right)$$

$\bar{PL}(d)$  Is the path loss at a distance  $d$  [dB]

$PL(d_0)$  Is the path loss at some close-in reference distance  $d_0$  ( $d_0 \ll d$ ).  
Can either be measured or calculated with the Friis Free Space equation.

$n$  Is the path loss exponent

**Note That:** Antenna gains, wavelength, etc. are embedded in the model ( $PL(d_0)$ , and  $n$ ) parameters. Changing the configuration means we will end up with *different* model parameters and *different* results.

## Free Space Loss

$$\frac{P_t}{P_r} = \frac{(4\pi d)^2}{\lambda^2} = \frac{(4\pi f d)^2}{c^2}$$

- Free space loss, ideal isotropic antenna
- $P_t$  = signal power at transmitting antenna
- $P_r$  = signal power at receiving antenna
- $\lambda$  = carrier wavelength,  
 $c$  = speed of light ( $\approx 3 \times 10^8$  m/s)
- $d$  = propagation distance between antennas  
where  $d$  and  $\lambda$  are in the same units (e.g., meters).

Free space loss equation can be recast:

$$\begin{aligned} L_{dB} &= 10 \log \frac{P_t}{P_r} = 20 \log \left( \frac{4\pi d}{\lambda} \right) \\ &= -20 \log(\lambda) + 20 \log(d) + 21.98 \text{ dB} \\ &= 20 \log \left( \frac{4\pi f d}{c} \right) = 20 \log(f) + 20 \log(d) - 147.56 \text{ dB} \end{aligned}$$

## Free space loss accounting for gain of antennas

$$\frac{P_t}{P_r} = \frac{(4\pi)^2 (d)^2}{G_r G_t \lambda^2} = \frac{(\lambda d)^2}{A_r A_t} = \frac{(c d)^2}{f^2 A_r A_t}$$

- $G_t$  = gain of transmitting antenna
- $G_r$  = gain of receiving antenna
- $A_t$  = effective area of transmitting antenna
- $A_r$  = effective area of receiving antenna

In the above formula, the powers correspond to that of the input signal at the transmitter and output at the receiver, respectively.

$$\begin{aligned} L_{dB} &= 20 \log(\lambda) + 20 \log(d) - 10 \log(A_t A_r) \\ &= -20 \log(f) + 20 \log(d) - 10 \log(A_t A_r) + 169.54 \text{ dB} \end{aligned}$$

For free-space environment the exponent  $n$  is equal 2 in the following equation:

$$\bar{P}L(d) = PL(d_0) + 10n \log_{10} \left( \frac{d}{d_0} \right)$$

Here the exponent  $n$  depends on the transmission environment

- o Urban vs suburban, medium-city vs large-city, obstructed vs unobstructed, indoors vs outdoors
- o Generally the values of  $n$  are between 2 and 4. Higher values means faster decay of the propagating signal.

### Fading

- Variation over time or distance of received signal power caused by changes in the transmission medium or path(s)
- In a fixed environment:
  - o Changes in atmospheric conditions
- In a mobile environment:
  - o Multipath propagation.

### Effects of Multipath Propagation

- Multiple copies of a signal may arrive at different phases
  - o If phases add destructively, the signal level relative to noise declines, making detection more difficult
- Intersymbol interference (ISI)
  - o One or more delayed copies of a pulse may arrive at the same time as the primary pulse for a subsequent bit.

### Types of Fading

- Fast fading
  - o Changes in signal strength in a short time period
- Slow fading
  - o Changes in signal strength in a short time period

- Flat fading
  - o Fluctuations proportionally equal over all frequency components
- Selective fading
  - o Different fluctuations for different frequencies
- Rayleigh fading
  - o Multiple indirect paths, but no dominant path such as LOS path
  - o Worst-case scenario
- Rician fading
  - o Multiple paths, but LOS path dominant
  - o Parametrized by K, ratio of power on dominant path to that on other paths

### Diversity Techniques

- Space diversity:
  - o Use multiple nearby antennas and combine received signals to obtain the desired signal.
  - o Use collocated multiple directional antennas
- Frequency diversity:
  - o Spreading out signal over a larger frequency bandwidth
  - o Spread spectrum
- Time diversity:
  - o Noise often occurs in bursts
  - o Spreading the data out over time spreads the errors and hence allows FEC techniques to work well
  - o TDM
  - o Interleaving

## 6.7 MICROWAVE AND MILLIMETER-WAVE PROPAGATION

In the microwave and millimeter-wave region where the frequency ranges from 1 GHz ( $\lambda_0 = 30$  cm) up to 300 GHz ( $\lambda_0 = 1$  mm) the ionosphere is transparent, since  $\omega$  is much greater than the plasma frequency  $\omega_p$  and the cyclotron frequency  $\omega_c$ . The propagation of waves in this frequency range is predominantly line-of-sight propagation. There will be interference phenomena from the ground-reflected wave, but it is not as pronounced as it is at lower frequencies because the roughness of the ground is much greater relative to the wavelengths involved. Thus the reflection from the ground is more diffuse with a weaker specular-reflected component. In those instances where a relatively smooth ground or water surface is present at the reflection point, the interference phenomena can be significant, and the interference pattern will exhibit a lobe structure with closely spaced lobes.

The most important factor to take into account at wavelengths of a few centimeters and shorter is attenuation and scattering by rain and snow, and for the millimeter-wave band attenuation, which can be very high, by fog, water vapor, and other gases in the atmosphere. In this section we will present an outline of the theory for predicting the attenuation and scattering by rain and also data on the attenuation caused by atmospheric gases. Other phenomena that affect the propagation of microwaves and millimeter waves are scattering by tropospheric irregularities in the index of refraction and ducting caused by inversions in the index-of-refraction profiles. The latter two topics are discussed in later sections of this chapter.

### Attenuation by Rain

Radio waves propagating through rain are attenuated because of absorption of power in the lossy dielectric medium represented by water. There is also some loss in the direct transmitted wave because of scattering of some energy out of the beam by the rain droplets. The scattering loss is usually small relative to the absorption loss. The theory for rain attenuation and scattering is based on the calculation of the absorption and scattering cross sections of a single raindrop. This calculation is straightforward for the case of a spherical droplet of water having a radius no larger than  $\lambda_0/10$ . In this situation the low-frequency Rayleigh scattering theory can be applied. Since the radius of raindrops ranges from a fraction of a millimeter up to several millimeters, the Rayleigh scattering theory is generally valid down to wavelengths of order 3 cm or somewhat less. The assumption of spherical droplets is not valid since raindrops take on an oblate spheroidal or flattened shape under the influence of aerodynamic forces and pressure forces as they fall. However, at the longer wavelengths an equivalent spherical radius can be assumed. At millimeter wavelengths it is important to consider the drop shape, and the determination of the cross sections is then much more difficult and laborious. However, with modern

Consider a spherical drop of water with a radius  $a$  much smaller than the wavelength of the incident plane wave, as shown in Fig. 6.46. The drop is characterized as a dielectric sphere with a complex dielectric constant  $\kappa = \kappa' - j\kappa''$ . The incident electric field is chosen as

$$\mathbf{E}_i = E_0 \mathbf{a}_z e^{-jk_0 x}$$

Over the extent of the drop the incident field is essentially uniform and equal to  $E_0 \mathbf{a}_z$ . The polarization produced in the drop is thus the same as would be produced in a dielectric sphere under the action of a uniform static electric field. This boundary value problem is readily solved (see Prob. 2.7) and shows

The incident power on the rain droplet undergoes the following types of attenuation:

1-power loss due to the fact that the rain droplet is a lossy dielectric

$$(\epsilon_r = \epsilon'_r - j \epsilon''_r).$$

2-power loss due to scattering of the incident ray to various other directions.

The overall losses will depend on the size of the rain drop relative to the wavelength, the density of the rain drops (rate of rain in mm/hour), and the frequency of the propagating wave.

distributions measured by ...

From the point of view of the communications engineer what is needed is a relatively simple formula relating specific attenuation to rain rate, frequency, and temperature. Fortunately such a formula exists, and it is of the form

$$A = aR^b \text{ dB/km} \quad (6.107)$$

where  $R$  is the rain rate in millimeters per hour and  $a$  and  $b$  are constants that depend on frequency and temperature of the rain. The temperature dependence is due to the variation of dielectric constant of water with temperature. A detailed review of the theory and experimental data has led to a compilation of the values of the two constants  $a$  and  $b$  by Olsen, Rodgers, and Hodge.† These authors established the following empirical formulas for the constants  $a$  and  $b$  at a temperature of 0°C:

$$a = G_a f^{E_a} \quad f \text{ in gigahertz} \quad (6.108a)$$

where	$G_a = 6.39 \times 10^{-5}$	$E_a = 2.03$	$f < 2.9 \text{ GHz}$
	$G_a = 4.21 \times 10^{-5}$	$E_a = 2.42$	$2.9 \text{ GHz} \leq f \leq 54 \text{ GHz}$
	$G_a = 4.09 \times 10^{-2}$	$E_a = 0.699$	$54 \text{ GHz} \leq f < 180 \text{ GHz}$
	$G_a = 3.38$	$E_a = -0.151$	$180 \text{ GHz} < f$

$$\text{and} \quad b = G_b f^{E_b} \quad f \text{ in gigahertz} \quad (6.108b)$$

where	$G_b = 0.851$	$E_b = 0.158$	$f < 8.5 \text{ GHz}$
	$G_b = 1.41$	$E_b = -0.0779$	$8.5 \text{ GHz} \leq f < 25 \text{ GHz}$
	$G_b = 2.63$	$E_b = -0.272$	$25 \text{ GHz} \leq f < 164 \text{ GHz}$
	$G_b = 0.616$	$E_b = 0.0126$	$164 \text{ GHz} \leq f$

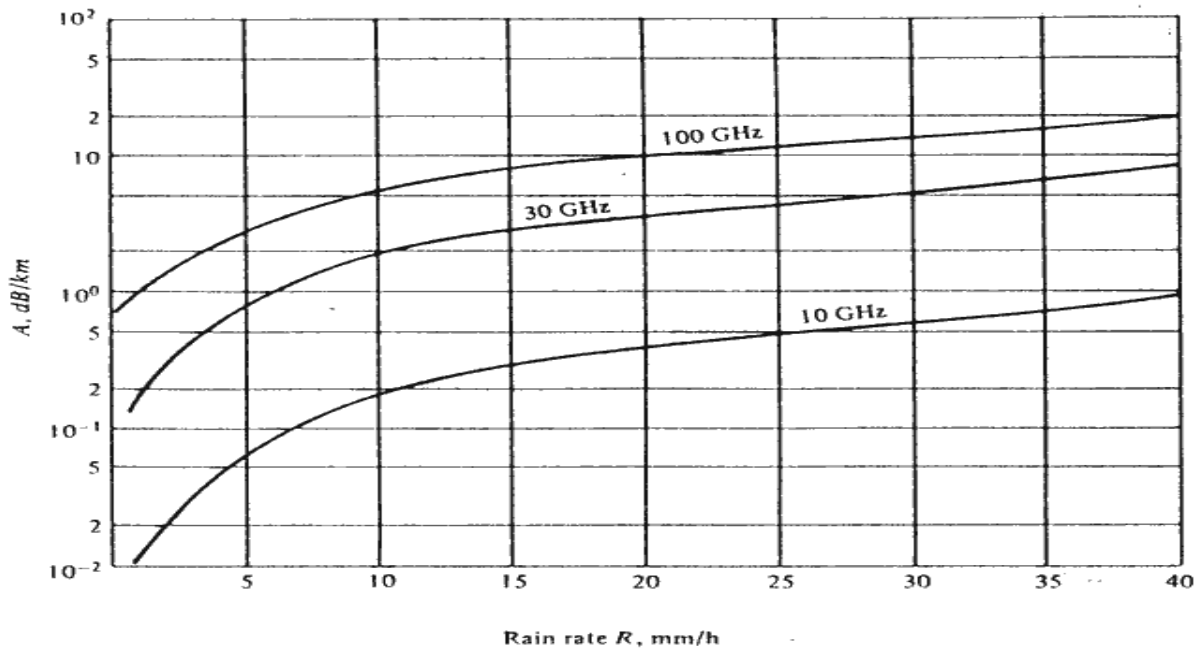


Figure 6.47 Attenuation by rain at 10, 30, and 100 GHz as a function of rain rate.

### Attenuation by Fog

The attenuation of microwaves and millimeter waves by fog is governed by the same fundamental equations as attenuation by rain. The main difference is that fog is a suspended mist of very small water droplets with radii in the range 0.01 to 0.05 mm. For frequencies below 300 GHz the attenuation by fog is essentially linearly proportional to the total water content per unit volume at any given frequency. The upper level for water content is around  $1 \text{ g/m}^3$ , with the content usually considerably less than this for most fogs. A concentration of  $0.032 \text{ g/m}^3$  corresponds to a fog that is characterized by an optical visibility of around 2000 ft. A concentration of  $0.32 \text{ g/m}^3$  corresponds to an optical visibility range of around 400 ft. The attenuation by fog in decibels per kilometer as a function of frequency is shown in Fig. 6.48 for the two concentration levels mentioned above. At a frequency of 300 GHz the attenuation in the more dense fog is still only about 1 dB/km. Hence, for communication link designs with sufficient signal margin built in to overcome the attenuation by rain, the attenuation by fog will not be the limiting factor.

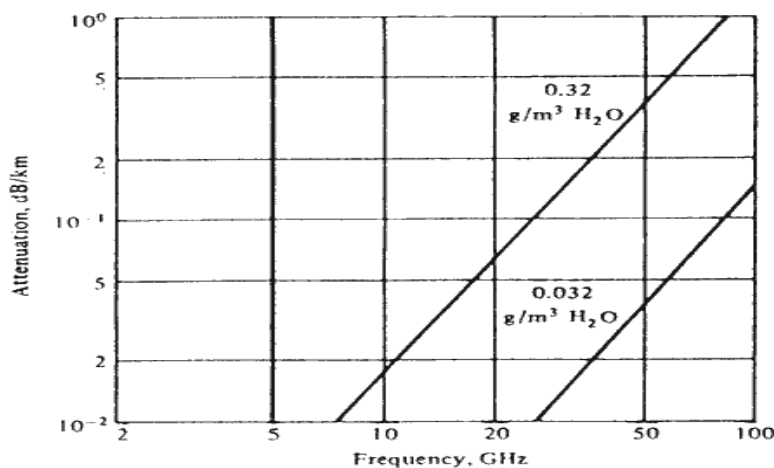


Figure 6.48 Attenuation in fog as a function of frequency for two different concentrations.

## Attenuation by Snow and Ice

When water solidifies into snow and ice crystals there is a significant change in the complex dielectric constant  $\kappa = \kappa' - j\kappa''$ . For ice,  $\kappa'$  is nearly constant and equal to 3.17 for temperatures from 0° to -30°C throughout the centimeter and millimeter wave bands. The imaginary part is very small, nearly independent of frequency in the microwave and millimeter wave bands, and drops from a value of approximately  $3.7 \times 10^{-3}$  at 0°C to  $5.2 \times 10^{-4}$  at -30°C.† The small value of the imaginary part indicates relatively little attenuation by dry ice crystals. However, snow and hail consist of a mixture of ice crystals and water in many instances, so the attenuation is strongly dependent on the meteorological conditions. Furthermore the shape of snow and ice crystals is so varied that the calculation of absorption by a single typical particle is a formidable task, if indeed a typical particle can even be defined.

## Attenuation by Atmospheric Gases

Uncondensed water vapor and oxygen both have various absorption lines in the centimeter and millimeter wave regions. Consequently, there are frequencies where high attenuation occurs and which are separated by windows or frequency bands where the attenuation is much lower. Figure 6.49 shows the attenuation by oxygen and water vapor (uncondensed) at 20°C at sea level. The water content is 1 percent water molecules, which is typical in temperate climates. At frequencies greater than 300 GHz the attenuation by oxygen is negligible relative to that of water vapor. There are strong water vapor absorption lines at  $\lambda_0 = 1.35$  cm and at 1.67 mm, as well as at shorter wavelengths. There is strong absorption by oxygen at  $\lambda_0 = 0.5$  and 0.25 cm. At  $\lambda_0 = 0.5$  cm, attenuation by oxygen alone exceeds 10 dB/km. The attenuation by oxygen and water vapor is additive. In those bands where the attenuation exceeds 10 dB/km the range over which communication can take place is severely restricted. By a proper choice of frequencies it is possible to achieve much less attenuation; for example, at  $\lambda_0 = 1.33$  mm the attenuation is less than 1 dB/km. For frequencies above 300 GHz the minimum attenuation is still large, 6 dB or more per kilometer, and places a great restriction on the

application of millimeter- and submillimeter-wave radiation for terrestrial line-of-sight paths. However, various specialized applications such as short-range secure communication systems and satellite-to-satellite links are suited to the use of millimeter-wavelength radiation. The short wavelengths involved allow very compact high-gain antennas to be used, and this can compensate for some of the attenuation loss.

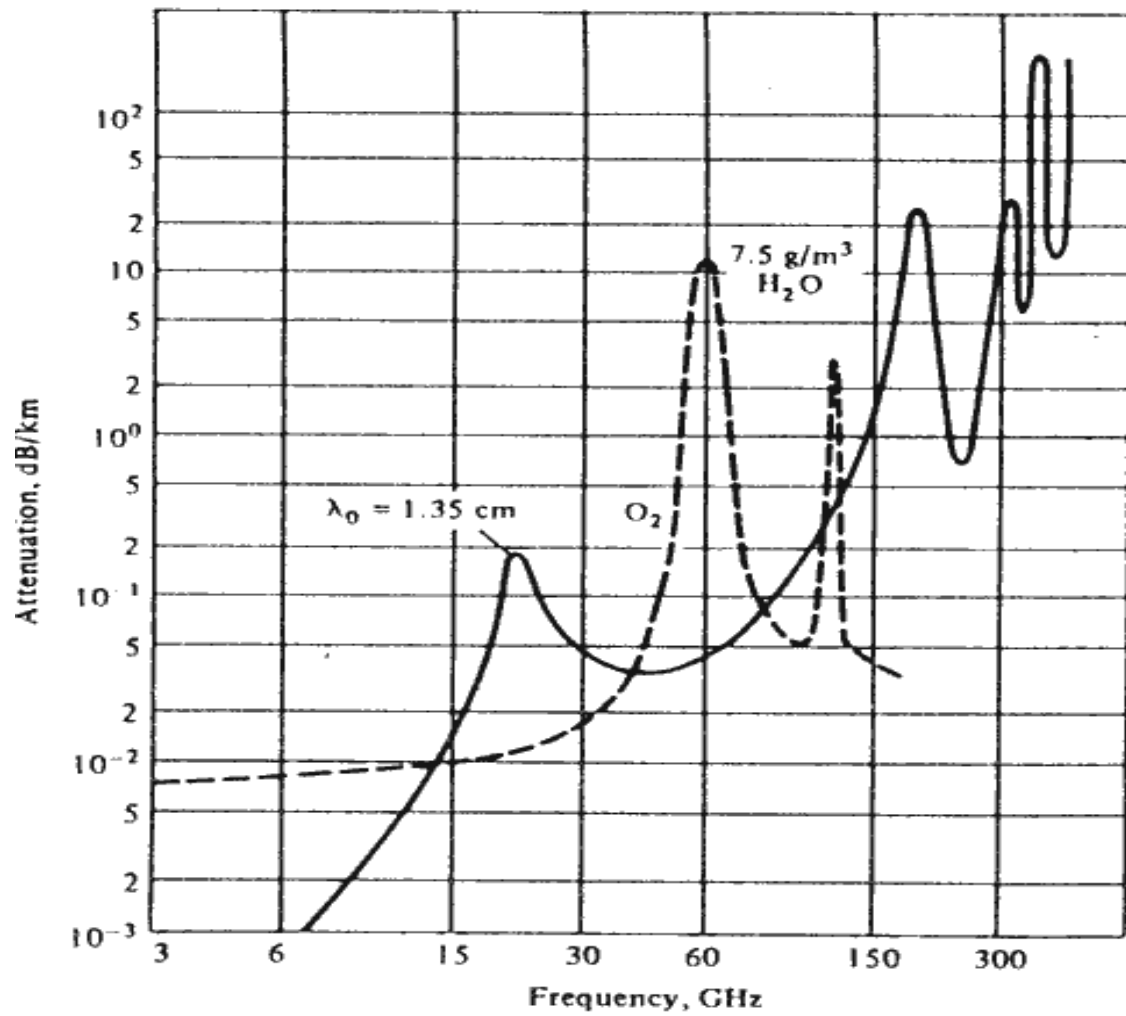


Figure 6.49 Attenuation by oxygen and water vapor at sea level.  $T = 20^\circ\text{C}$ . Water content is  $7.5 \text{ g/m}^3$ .

## 6.9 TROPOSPHERIC SCATTER PROPAGATION

An over-the-horizon tropospheric-scatter communication link is illustrated in Fig. 6.52. The two antenna beams overlap in a common volume located at considerable height above the surface of the earth (3 to 8 km). The scattering comes from the small random irregularities or fluctuations in the index of refraction of the atmosphere. These fluctuations are very weak, but when sufficiently high transmitted power is used a useful signal, in view of the large volume from which scattering occurs, is scattered in the direction of the receiving antenna. Tropospheric-scatter-propagation links operate in the frequency range of 200 MHz up to 10 GHz. Operation at lower frequencies is not attractive because of the cost of building antennas with sufficient gain. At higher frequencies the transmission loss becomes too large. There is considerable fading associated with tropospheric-scatter-propagation links, so some form of diversity is desirable for high reliability links. The typical distance involved in a tropospheric scatter link is a few hundred miles, usually not more than 400. At heights greater than 10 km the troposphere is too rarefied to produce sufficient scattering. If we assume an effective earth radius equal to four-thirds of the actual radius, then the maximum line-of-sight distance to a scattering point 20,000 ft above the earth (6 km) is 200 mi. The maximum horizontal range is 400 mi for this case.

There was considerable interest in tropospheric scatter propagation during the decade 1950–1960. With the development of satellite communication systems there is now less need for tropospheric scatter systems. A considerable amount of research has gone into the development of the theory and also the gathering of operational performance data for tropospheric scatter links. A special issue of the *IRE Proceedings* was devoted to this topic, and the reader is

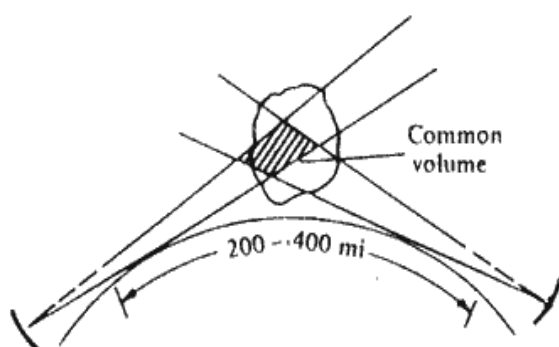
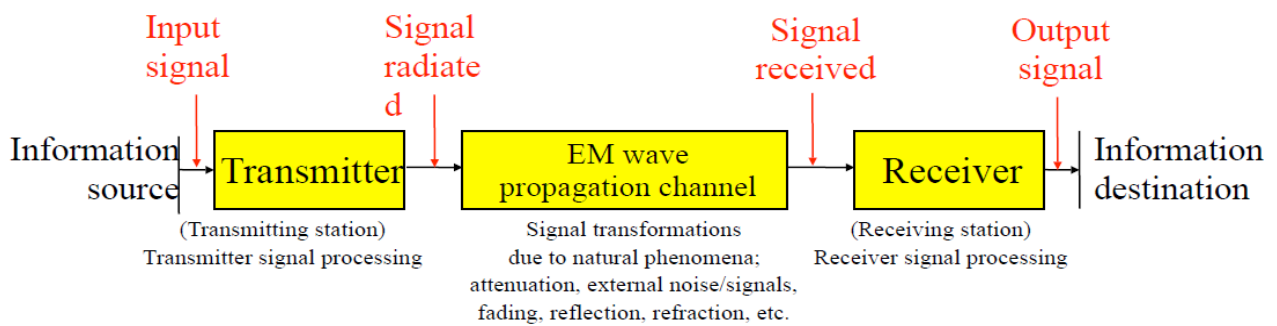
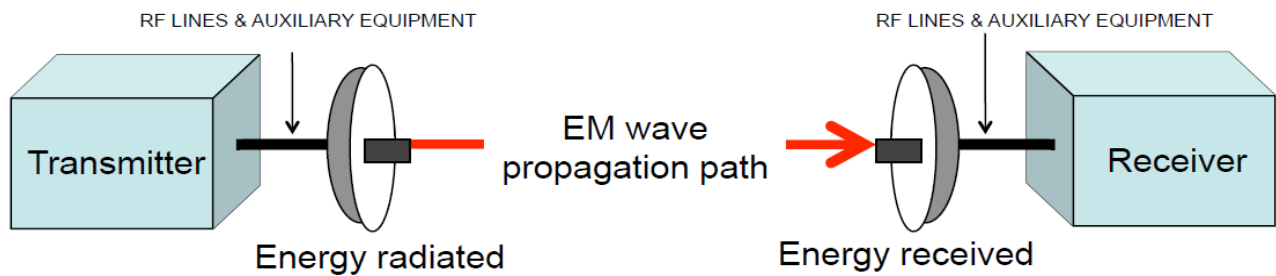


Figure 6.52 A tropospheric-scatter-propagation communication link for over-the-horizon transmission.

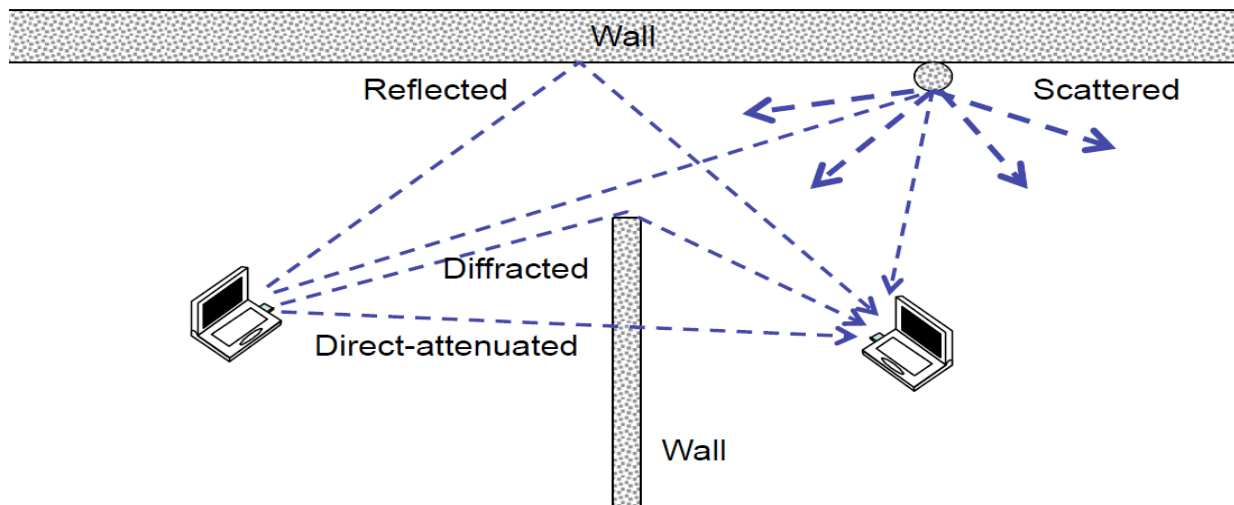
# Radio transmission: 2 viewpoints



Property of R. Struzak

34

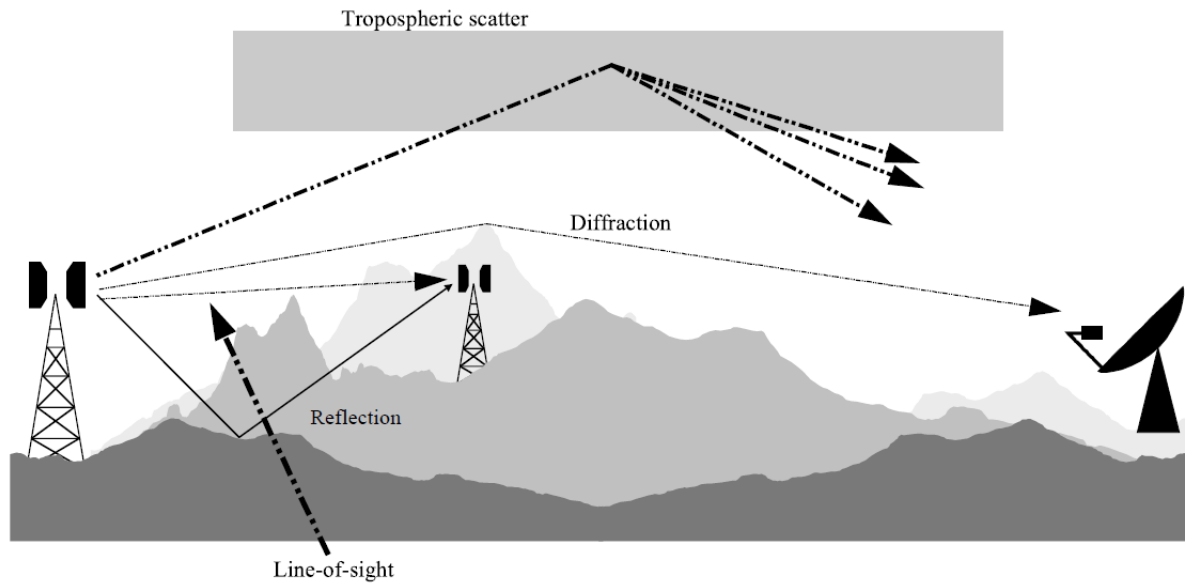
# Indoor propagation



Property of R. Struzak

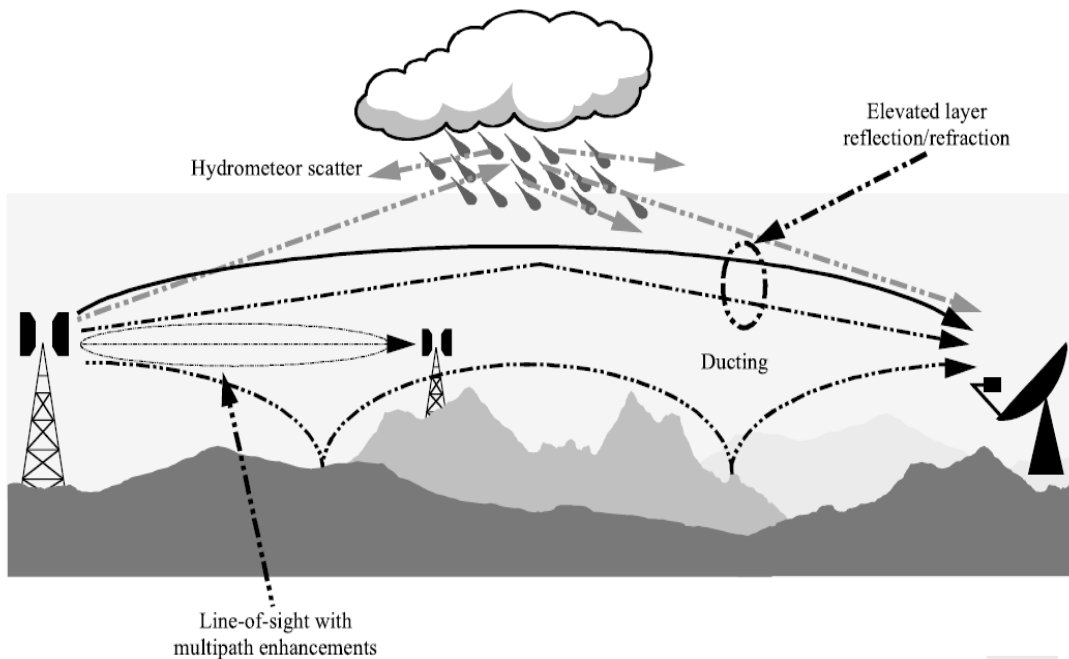
39

# Outdoor propagation: long-term modes



# Outdoor propagation: short-term modes

Anomalous (short-term) interference propagation mechanisms



0452-02

# Radio Wave Components

<i>Component</i>	<i>Comments</i>
Direct wave	Free-space/ LOS propagation
Attenuated wave	Through walls etc. in buildings, atmospheric attenuation (>~10 GHz)
Reflected wave	Reflection from a wall, passive antenna, ground, ionosphere (<~100MHz), etc.
Refracted wave	Standard, Sub-, and Super-refraction, ducting, ionized layer refraction (<~100MHz)
Diffraction wave	Ground-, mountain-, spherical earth- diffraction (<~5GHz)
Surface wave	(<~30 MHz)
Scatter wave	Troposcatter wave, precipitation-scatter wave, ionized-layer scatter wave

Property of R. Struzak

44

**Reflection:** the abrupt change in direction of a wave front at an interface between two dissimilar media so that the wave front returns into the medium from which it originated. Reflecting object is large compared to the wavelength.

**Scattering:** A phenomenon where the direction (or polarization) of the wave is changed when the wave encounters propagation medium, discontinuities smaller than the wavelength (e.g. foliage, ...). The result is a disordered or random change in the energy distribution.

**Diffraction:** The mechanism the waves spread as they pass barriers in obstructed radio path (through openings or around barriers). Diffraction is important when evaluating potential interference between terrestrial/stations sharing the same frequency.

**Absorption:** The conversion of the transmitted EM energy into another form, usually thermal. The conversion happens as a result of interaction between the incident energy and the material medium, at

the molecular or atomic level. One cause of signal attenuation due to walls, precipitations (rain, snow, sand) and atmospheric gases.

**Refraction:** The redirection of a wavefront passing through a medium having a refractive index that is a continuous function of position (e.g., a graded-index optical fibre, or earth atmosphere) or through a boundary between two dissimilar media.

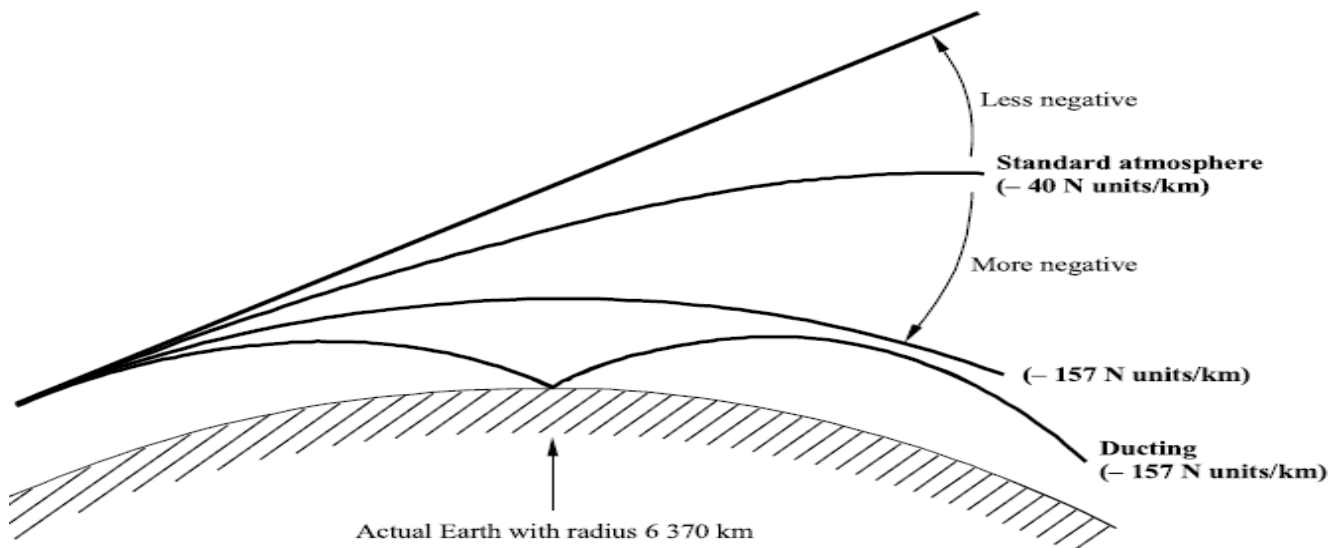
– For two media of different refractive indices, the angle of refraction is approximated by Snell's Law known from optics.

### Super-refraction and ducting

It is important when evaluating potential interference between terrestrial / earth stations sharing the same frequency.

- coupling losses into duct/layer
- geometry – nature of path (sea/land)
- propagation loss associated with duct/ layer
- frequency, • refractivity gradient, • nature of path (sea, land, coastal)
- terrain roughness

Atmospheric refraction effects on radio signal propagation



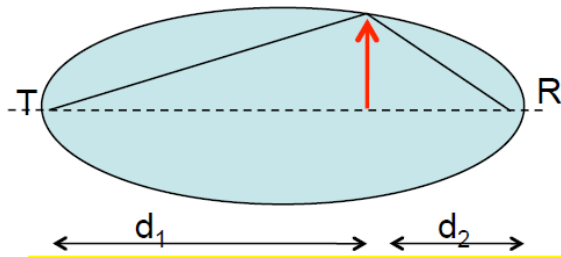
In

*Standard atmosphere:* -40 N units/km (median), temperate climates

*Super-refractive atmosphere:* < -40 N units/km, warm maritime regions

*Ducting:* < -157 N units/km (fata morgana, mirage).

# Fresnel Zone



$$r_1 = \sqrt{\frac{\lambda d_1 d_2}{d}} \leq \frac{1}{2} \sqrt{\lambda d}$$

$r_1$  : radius of the 1st Fresnel zone, m

$d = d_1 + d_2$  : distance T-R, m

$\lambda$  : wavelength, m

$d_1, d_2$  : distance to R and to T, m

Example: max. radius of the 1st Fresnel zone at 3 GHz ( $\lambda = 0.1\text{m}$ ) with T – R distance of 4 km:  
 $= (1/2)\text{sqrt}(0.1 \cdot 4000) = 10\text{m}$

- Fresnel zones are loci of points of constant path-length difference of  $\lambda/2$  ( $180^\circ$  phase difference )
  - The n-th zone is the region enclosed between the 2 ellipsoids giving path-length differences  $n(\lambda/2)$  and  $(n-1)(\lambda/2)$
- The 1<sup>st</sup> Fresnel zone corresponds to  $n = 1$

Property of R. Struzak

54

The relation between received power and transmitted one is given by Friis transmission formula:

$$P_R = P_T \times G_{TR} \times G_{RT} \times \left( \frac{\lambda}{4\pi d_{TR}} \right)^2$$

$$P_{RdB} = P_{TdB} + G_{TRdB} + G_{RTdB} + 10 \log_{10} \left( \frac{\lambda}{4\pi d_{TR}} \right)^2$$

$P_T$  = transmitted power [W]

$d$  = distance between antennas Tx and Rx [m]

$P_R$  = received power [W]

$G_T$  = transmitting antenna power gain

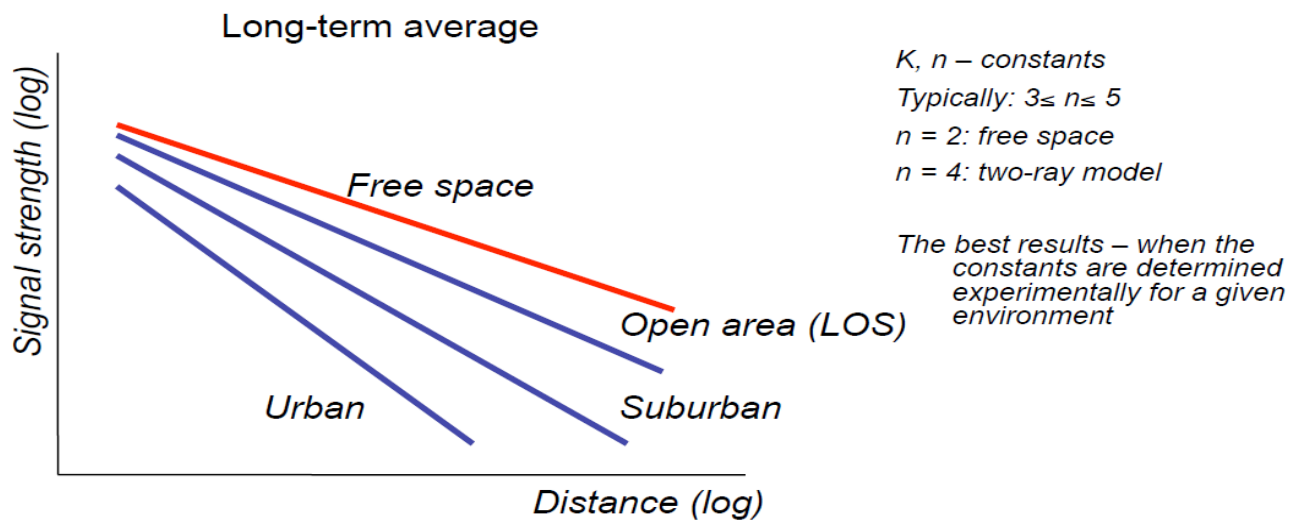
$G_R$  = receiving antenna power gain

$P_R/P_T$  = free-space propagation (transmission) loss (gain).

This formula is applicable to free-space propagation, where the exponent in the last term is equal to 2.

In practical situations where there, more than one path due to reflection, diffraction, refraction and absorption, the Friis formula is modified to some other empirical formulas using values for the exponent ( n ) other than 2. Thus, the last term of the relation is written in the following form to represent the change of signal strength with distance, as it was suggested by the **Okumura-Hata model**:

$$G_{avg} = Kd^n$$



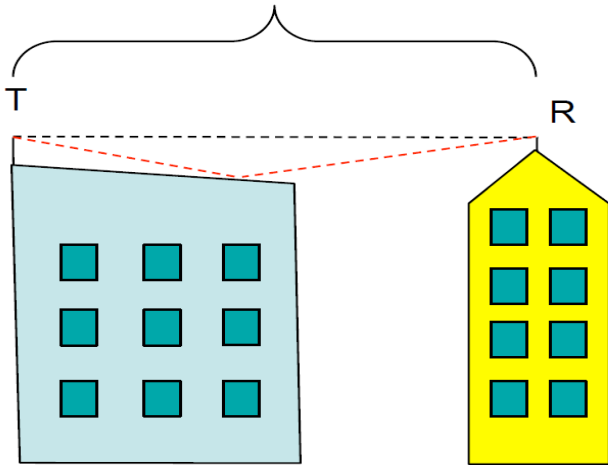
The signal level decreases with distance. Free-space propagation has the slowest decrease (n=2). Urban regions (مناطق حضرية/مدن) have the fastest decrease ( n>2).

### MAPL & max range

n	P <sub>TdBm</sub>	P <sub>RdBm</sub>	MAPL dB	2.4 GHz range m	5 GHz range m
2	0	-80	80	100	45
2	+20	-80	100	1000	450
4	0	-80	80	6	4
4	+20	-80	100	32	21

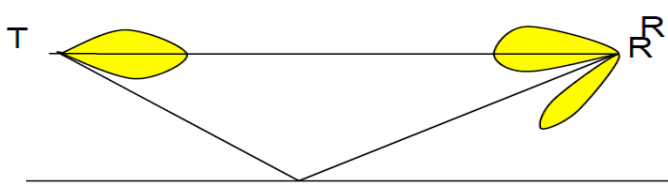
# Non-LOS propagation

- – when the 1st Fresnel zone is obstructed and/ or the signal reached the receiver due to reflection, refraction, diffraction, scattering, etc.
- An obstruction may lie to the side, above, or below the path.
- » Examples: buildings, trees, bridges, cliffs, etc.
- » Obstructions that do not enter in the 1st Fresnel zone can be ignored. Often one ignores obstructions up to 1/2 of the zone.



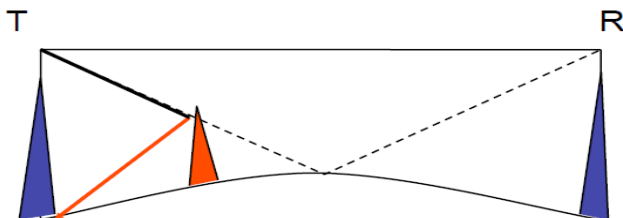
- A LOS link shown in the figure was designed with positive link budget. After deployment, no signal was received
- Why?

- At what distance difference the phase of the direct ray differ from that of the reflected ray by 180 deg at frequency of
  - 3 MHz?
  - 300 MHz?
  - 3 GHz?



- Controlling the directive antenna gain at the transmitter and/or receiver

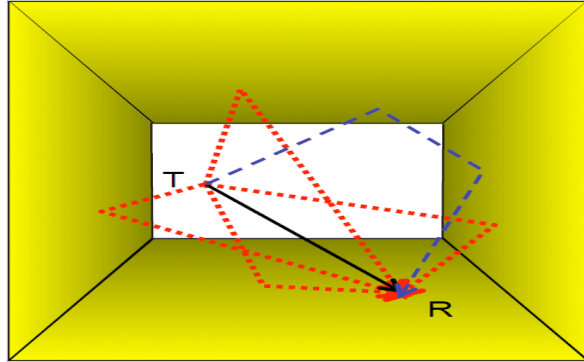
- Blocking the reflected ray at the transmitter-reflector path and/or reflector – receiver path



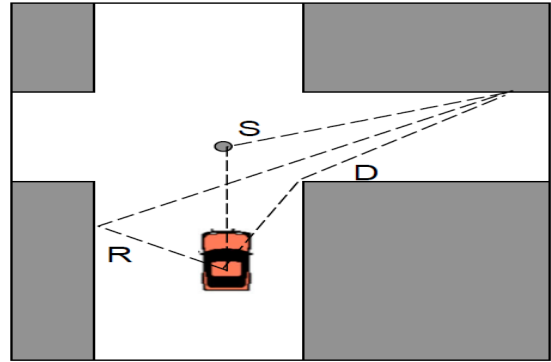
- Combine constructively the signals using correlation-type receiver
  - Antenna diversity (~10 dB)
  - Dual antennas placed at  $\lambda/2$  separation

Methods to avoid the reflected ray at the receiving antenna.

# Multipath propagation



Indoor



Outdoor: reflection (R),  
diffraction (D), scattering (S)

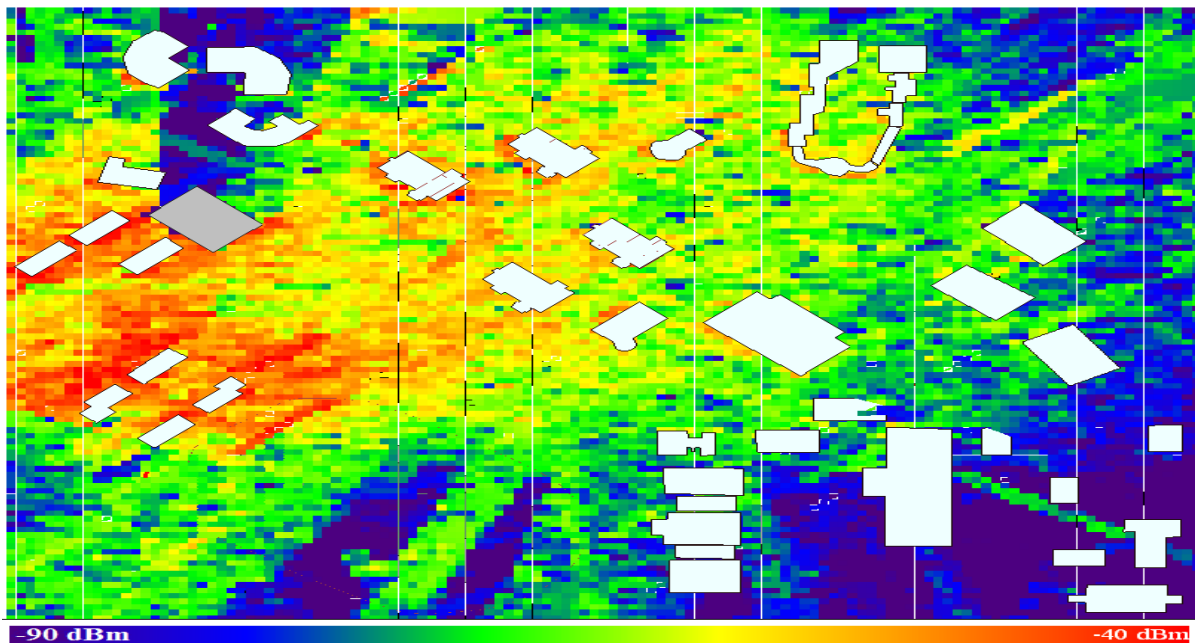
The effects of multipath include constructive and destructive **interference**, and **phase** shifting of the **signal**. This causes *Rayleigh fading*, with standard statistical distribution known as the

***Rayleigh distribution***.

- Rayleigh fading with a strong **line of sight** content is said to have a ***Rician distribution***, or to be *Rician fading*.

» [http://en.wikipedia.org/wiki/Rayleigh\\_fading](http://en.wikipedia.org/wiki/Rayleigh_fading);

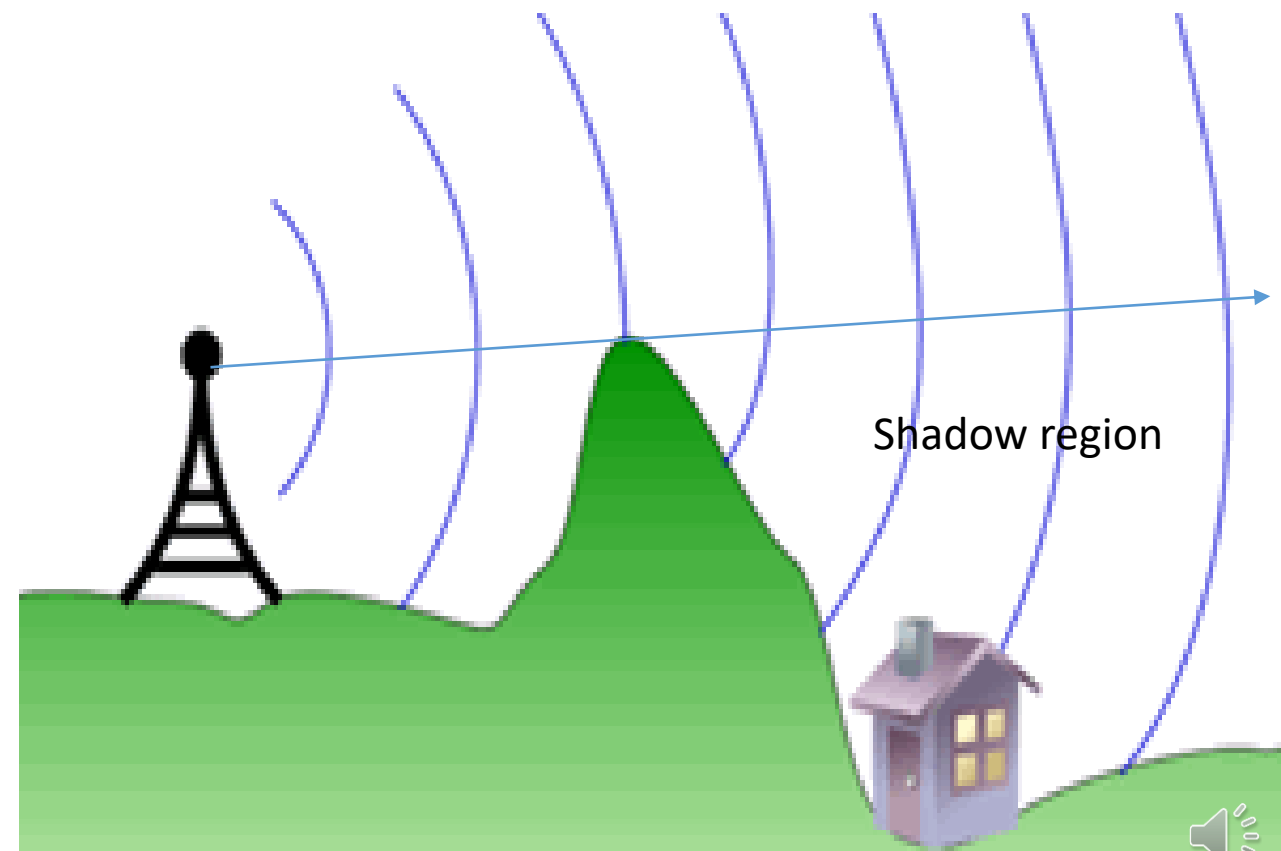
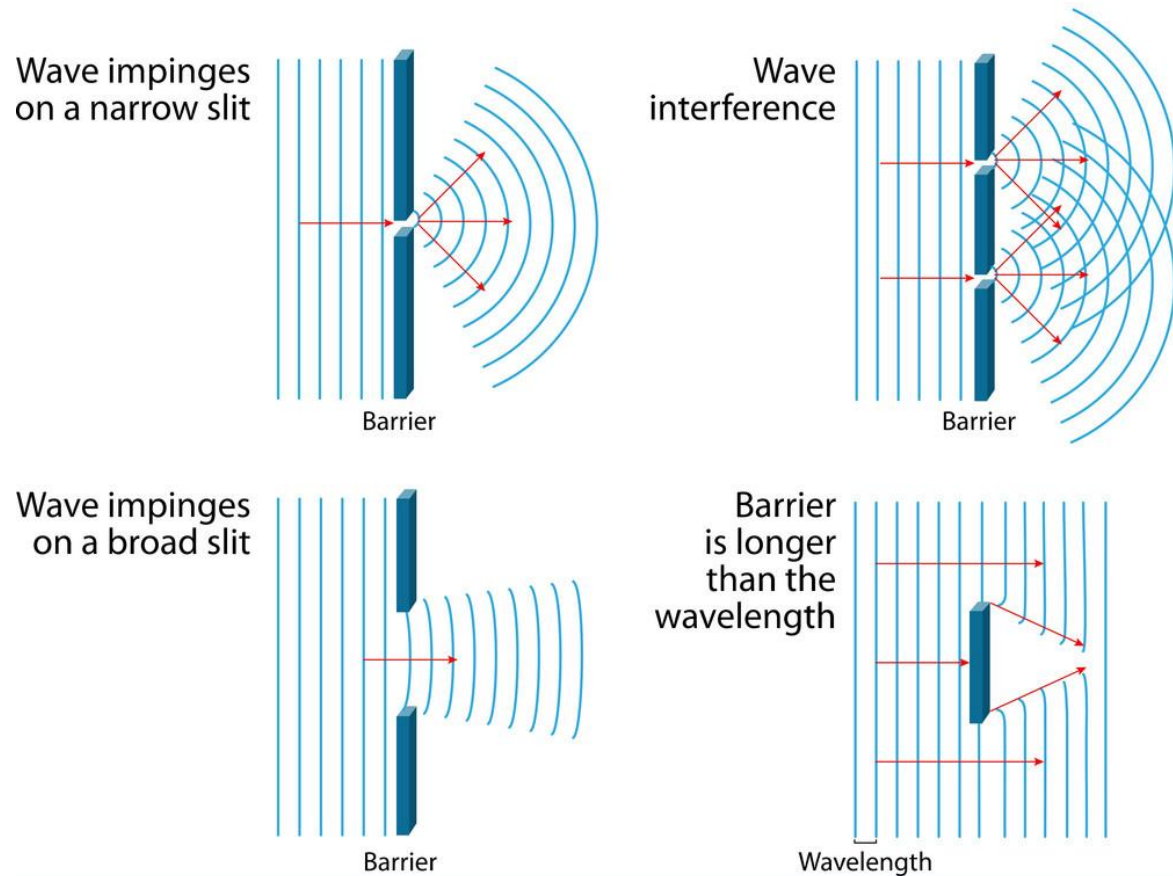
[http://en.wikipedia.org/wiki/Lord\\_Rayleigh](http://en.wikipedia.org/wiki/Lord_Rayleigh);



Received power coverage in the region around the college of Electronics Eng. due to sector-1 of the base station near the stadium. Mohammed Sameer dissertation.

# Diffraction

## DIFFRACTION OF WAVES



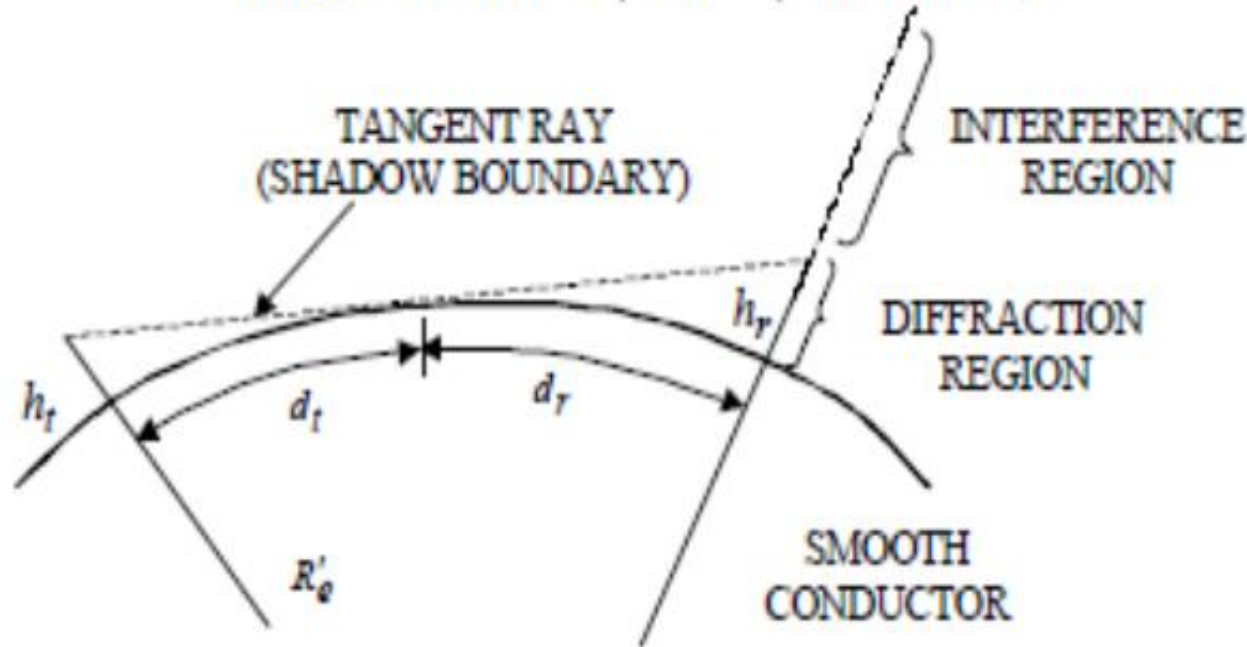
When the transmitter to receiver distance becomes too large the flat Earth approximation is no longer accurate. The curvature of the surface causes:

1. divergence of the power in the reflected wave in the interference region
2. diffracted wave in the shadow region (note that this is not the same as a ground wave)

The distance to the horizon is  $d_t = R_{RH} \approx \sqrt{2R_e' h_t}$  or, if  $h_t$  is in feet,  $d_t \approx \sqrt{2h_t}$  miles.

The maximum LOS distance between the transmit and receive antennas is

$$d_{\max} = d_t + d_r \approx \sqrt{2h_t} + \sqrt{2h_r} \text{ (miles)}$$



$$d_t^2 + R^2 = (R + h_t)^2$$

$$d_t \approx \sqrt{2R h_t}$$

$$R = 6370 \text{ km}$$

$$d_t \approx 3.57 \sqrt{h_t}$$

$h_t$  in meters

$d_t$  in km

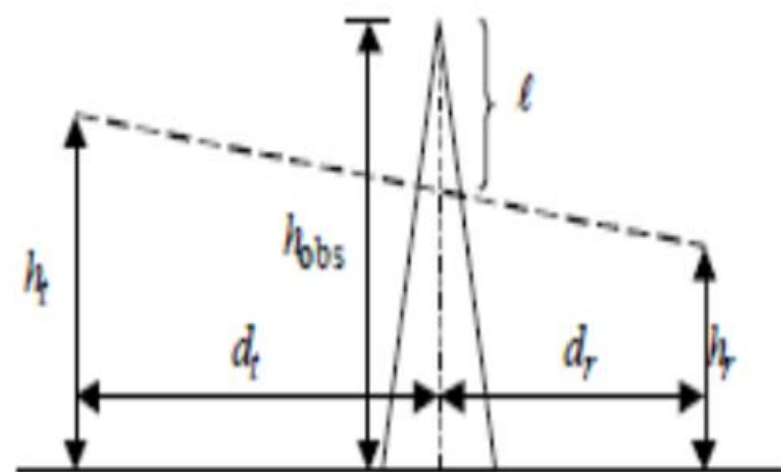
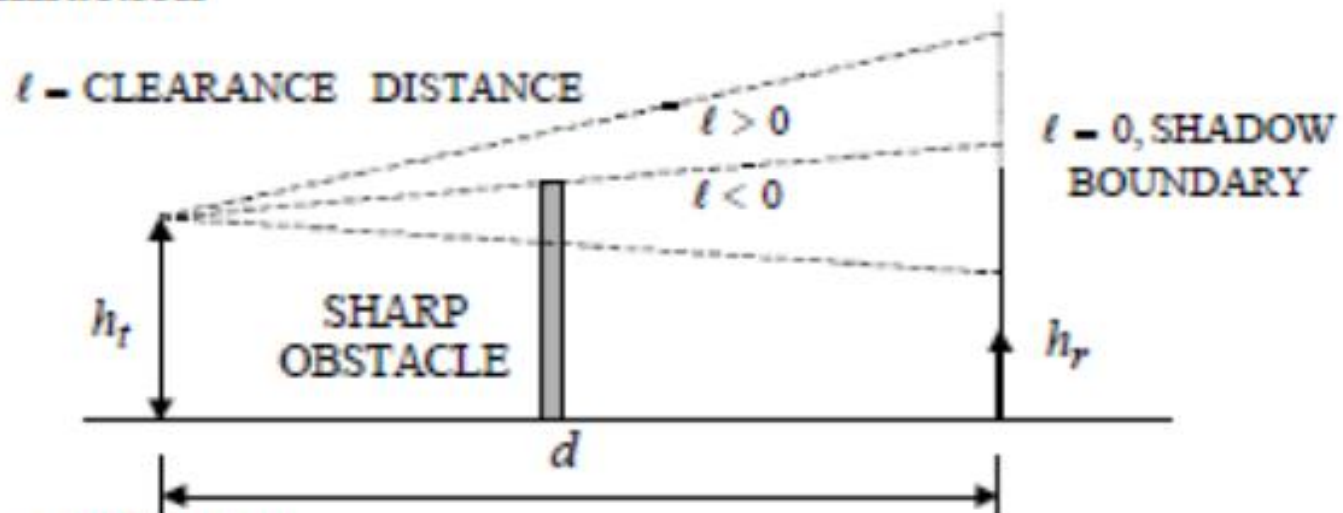
$d_t$  is called the  
**Radio Horizon**

If refraction is considered

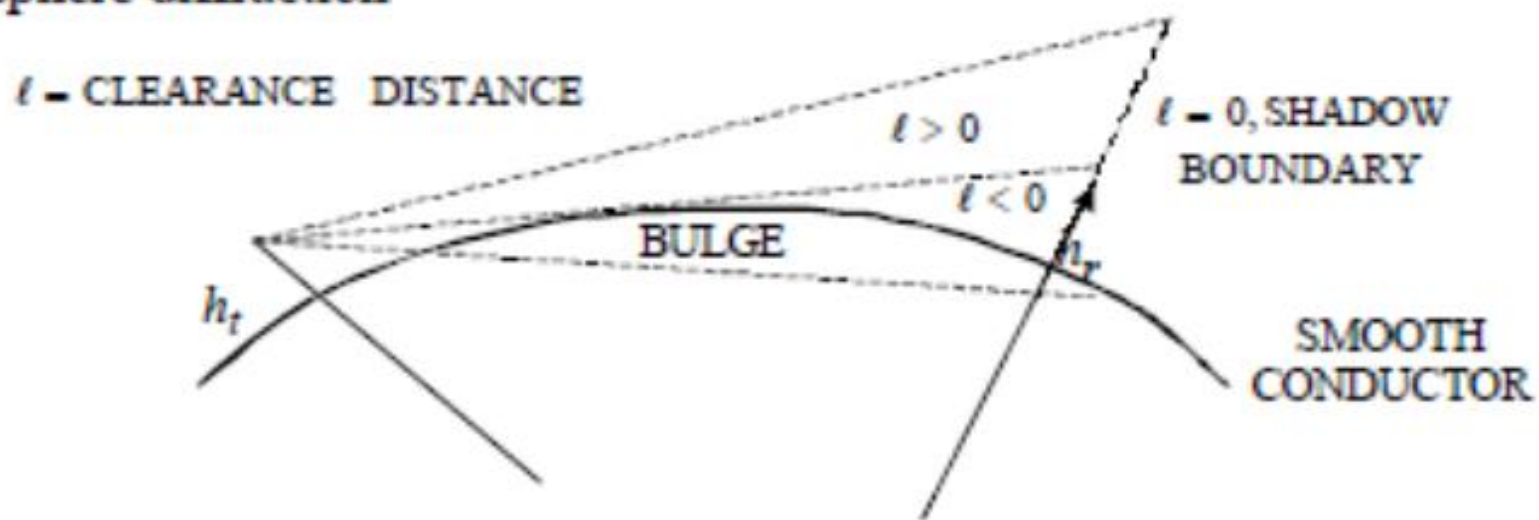
$$d_t \approx 4.11 \sqrt{h_t}$$



## Knife edge diffraction

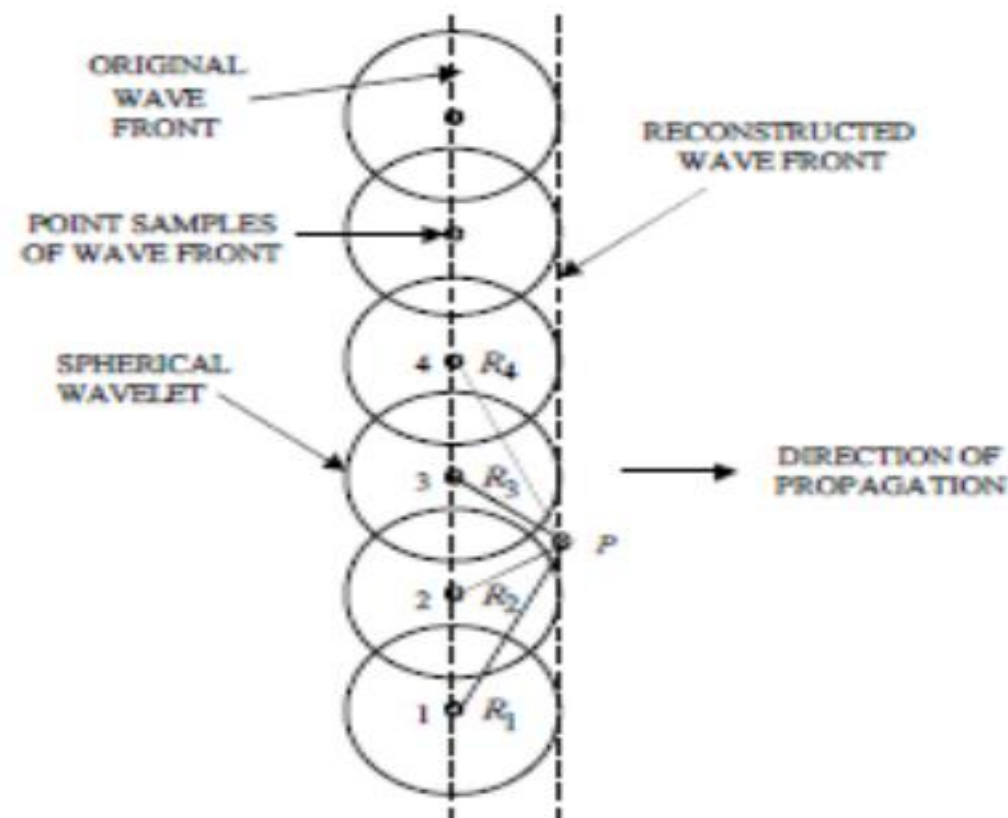


## Smooth sphere diffraction



# Huygen's Principle (1)

Huygen's principle states that any wavefront can be decomposed into a collection of point sources. New wavefronts can be constructed from the combined "spherical wavelets" from the point sources of the old wavefront.

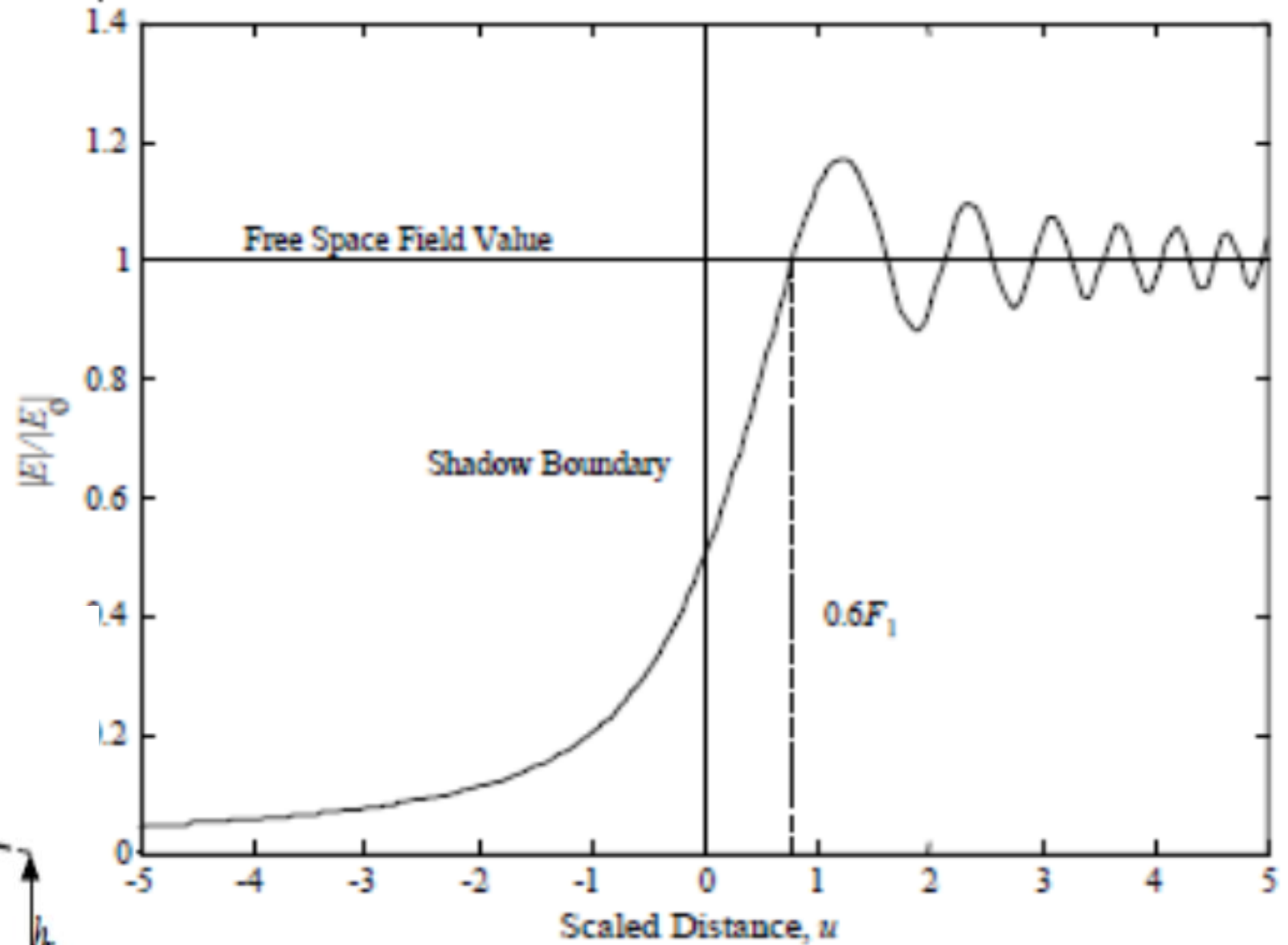
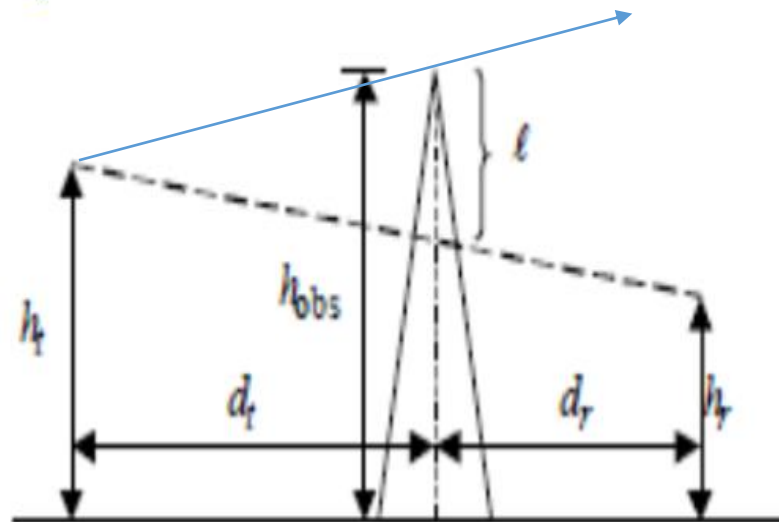


$$E(P) \sim \sum_{n=-\infty}^{\infty} \frac{e^{-jkR_n}}{R_n} \rightarrow \int_{-\infty}^{\infty} \frac{e^{-jkR_P}}{R_P}$$

where  $R$  is the distance from a wavelet source to the observation point,  $P$ . Sources closest to  $P$  will contribute most to the field

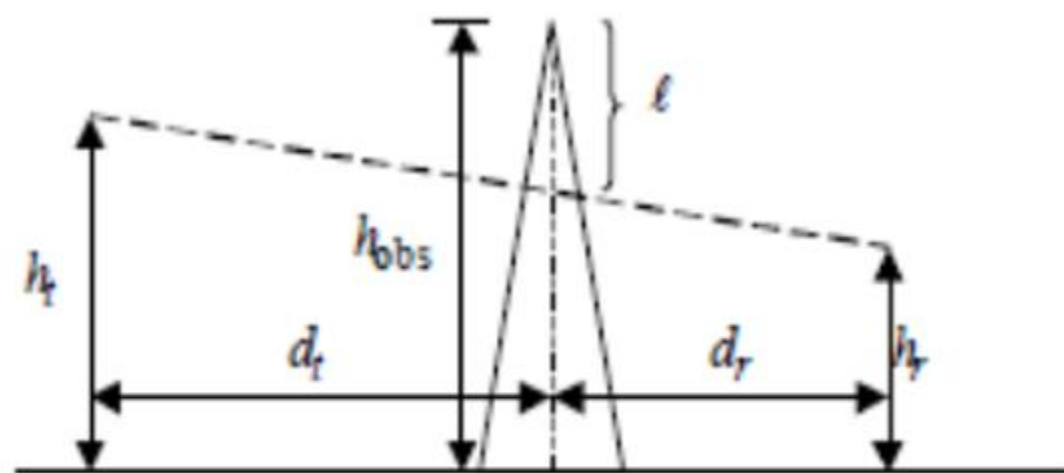
A plot of  $|E/E_0|$  shows that at  $0.6F_1$  the free space (direct path) value is obtained

$$u = \ell \sqrt{\frac{2d}{\lambda d_t d_r}}$$



The received power is reduced by a factor of 4 (6dB) when the knife-edge is situated exactly on the LOS line.



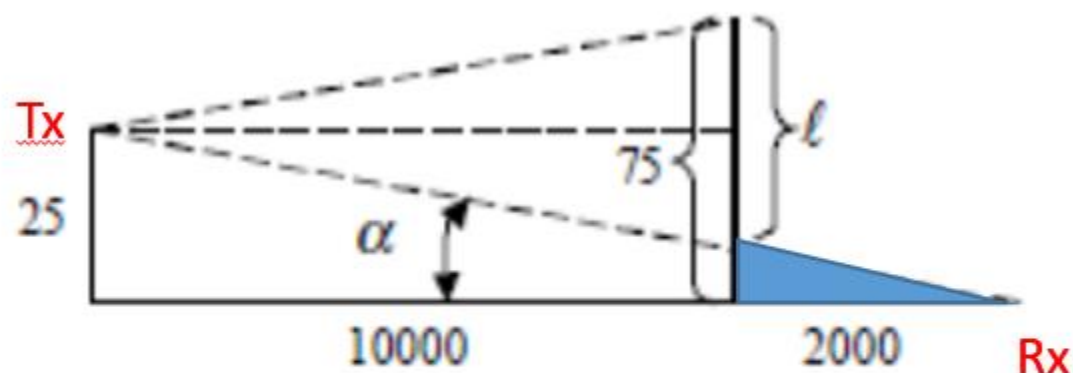


Scaled distance parameter:

$$u = \ell \sqrt{\frac{2d}{\lambda d_t d_r}}$$

where  $\ell < 0$  (i.e.,  $u$  negative) when the obstacle extends above the direct path.

Example:  $h_t = 50$  m,  $h_r = 25$  m,  $d_t = 10$  km,  $d_r = 2$  km,  $h_{obs} = 100$  m,  $f = 900$  MHz



$$\frac{75 - \ell}{2000} = \frac{25}{12000} \rightarrow \ell = 75 - 4.167 = 70.8 \text{ m}$$

$$u = -70.8 \sqrt{\frac{24 \times 10^3}{(0.33) 24 \times 10^6}} = -4.27$$

From the diffraction plot for  $u = -4.27$ ,  $|E/E_0| \approx 0.053 \rightarrow 25.5$  dB loss

$$20 \log (E/E_0) = 20 \log(0.053) = 25.5 \text{ dB}$$

Q1] A microwave link is to be deployed in an urban area at 17 GHz. The transmitter antenna is to be located on a rooftop at 15 m. The receiver antenna is to be installed at 5 m above ground level. Determine the maximum height of a building at the centre of the path if transmitter and receiver antennas are separated by 5 km.

Q2] A UHF television broadcast antenna is mounted at a height of 100 m. Assuming flat terrain and receive antennas which are very close to the ground, what is the maximum effective range of this antenna?

